

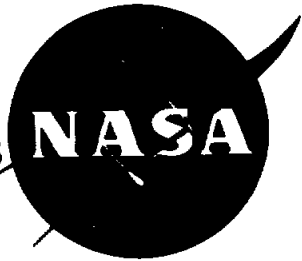
GL

83

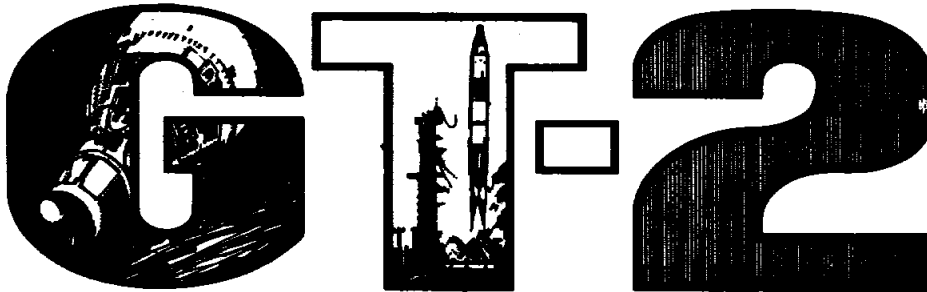
~~CONFIDENTIAL~~

4350-108-1

NATIONAL AERONAUTICS AND SPACE ADMINISTRATION
MANNED SPACECRAFT CENTER • HOUSTON, TEXAS



GEMINI PROGRAM MISSION REPORT



GEMINI 2

(U)

FEBRUARY 1965

GROUP 4
DOWNGRADED
AT 3 YEAR INTERVALS;
DECLASSIFIED
AFTER 12 YEARS

CLASSIFIED DOCUMENT— This material contains information affecting the National Defense of the United States within the meaning of the espionage laws, Title 18, U.S.C., Secs. 793 and 794, the transmission or revelation of which in any manner to an unauthorized person is prohibited by law

~~CONFIDENTIAL~~

UNCLASSIFIED

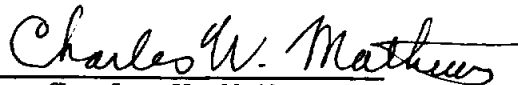
MSC-G-R-65-1

GEMINI PROGRAM MISSION REPORT GT-2

Gemini 2

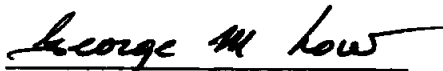
Prepared by: Gemini Mission Evaluation Team

Approved by:



Charles W. Mathews
Manager, Gemini Program

Authorized for Distribution:



George M. Low
Deputy Director

NATIONAL AERONAUTICS AND SPACE ADMINISTRATION

Manned Spacecraft Center

Houston, Texas

February 1965

UNCLASSIFIED

UNCLASSIFIED

iii

CONTENTS

Section		Page
	TABLES	x
	FIGURES	xiii
1.0	<u>MISSION SUMMARY</u>	1-1
2.0	<u>INTRODUCTION</u>	2-1
3.0	<u>VEHICLE DESCRIPTION</u>	3-1
3.1	GEMINI SPACECRAFT DESCRIPTION	3-1
3.1.1	Structure	3-1
3.1.1.1	Reentry assembly	3-1
3.1.1.2	Adapter assembly	3-3
3.1.2	Major Systems	3-4
3.1.2.1	Communications	3-4
3.1.2.2	Instrumentation and recording	3-8
3.1.2.3	Environmental control	3-10
3.1.2.4	Guidance and control	3-12
3.1.2.5	Time reference	3-15
3.1.2.6	Electrical	3-15
3.1.2.7	Propulsion	3-16
3.1.2.8	Pyrotechnics	3-18
3.1.2.9	Crew station furnishings and equipment	3-20
3.1.2.10	Landing	3-21
3.1.2.11	Postlanding and recovery	3-22
3.2	GEMINI LAUNCH VEHICLE DESCRIPTION	3-23
3.2.1	Structure	3-24
3.2.1.1	Stage I	3-24
3.2.1.2	Stage II	3-25
3.2.2	Major Systems	3-25
3.2.2.1	Propulsion	3-25

UNCLASSIFIED

UNCLASSIFIED

Section		Page
	3.2.2.2 Flight control	3-26
	3.2.2.3 Radio guidance	3-28
	3.2.2.4 Hydraulic	3-28
	3.2.2.5 Electrical	3-28
	3.2.2.6 Malfunction detection	3-29
	3.2.2.7 Instrumentation	3-29
	3.2.2.8 Range safety	3-30
	3.2.2.9 Ordnance separation	3-31
	3.3 GT-2 WEIGHT AND BALANCE DATA	3-33
4.0	<u>MISSION DESCRIPTION</u>	4-1
	4.1 ACTUAL MISSION	4-2
	4.2 SEQUENCE OF EVENTS	4-3
	4.3 FLIGHT TRAJECTORIES	4-3
	4.3.1 Launch	4-4
	4.3.2 Reentry	4-4
5.0	<u>VEHICLE PERFORMANCE</u>	5-1
	5.1 SPACECRAFT PERFORMANCE	5-1
	5.1.1 Spacecraft Structure	5-1
	5.1.1.1 General	5-1
	5.1.1.2 Thermal environment	5-1
	5.1.1.3 Vibratory environment	5-11
	5.1.1.4 Compartment pressures	5-13
	5.1.1.5 Reentry angle of attack	5-14
	5.1.2 Communications System	5-14
	5.1.2.1 Radar transponders	5-15
	5.1.2.2 Telemetry transmitters and acquisition aid beacon	5-15
	5.1.2.3 HF and UHF voice trans- mitters	5-16
	5.1.2.4 Digital command system	5-16
	5.1.2.5 Recovery beacon and flashing light	5-16

UNCLASSIFIED

UNCLASSIFIED

v

Section	Page
5.1.3 Instrumentation and Recording System . . .	5-17
5.1.4 Environmental Control System	5-18
5.1.5 Guidance and Control Systems	5-20
5.1.5.1 IGS performance summary	5-20
5.1.5.2 Evaluation of IGS	5-21
5.1.5.3 IGS steering	5-22
5.1.5.4 IVAR performance	5-24
5.1.5.5 Orbit velocity-change measure- ments	5-25
5.1.5.6 IGS component performance	5-26
5.1.5.7 Control system evaluation	5-26
5.1.5.8 Special areas	5-31
5.1.5.9 IGS flight problems	5-32
5.1.6 Time Reference System	5-35
5.1.6.1 Electronic timer	5-35
5.1.6.2 G.m.t. clock	5-35
5.1.6.3 Event timer	5-36
5.1.7 Electrical System	5-36
5.1.7.1 Electrical power system	5-36
5.1.7.2 Fuel cells	5-37
5.1.7.3 Reactant supply system	5-37
5.1.7.4 Sequential system	5-39
5.1.8 Propulsion System	5-39
5.1.8.1 Orbital attitude and maneuver system	5-39
5.1.8.2 Reentry control system	5-41
5.1.8.3 Retrograde rockets	5-43
5.1.9 Pyrotechnic System	5-44
5.1.10 Crew Station Furnishings and Equipment	5-45
5.1.10.1 Controls and displays	5-45
5.1.10.2 Out-the-window view	5-45
5.1.10.3 Crew station furnishings	5-47

UNCLASSIFIED

UNCLASSIFIED

Section	Page
5.1.11 Landing System	5-47
5.1.12 Postlanding Systems	5-47
5.2 LAUNCH VEHICLE PERFORMANCE	5-155
5.2.1 Airframe	5-155
5.2.1.1 Longitudinal oscillation	5-155
5.2.1.2 Structural loads	5-156
5.2.1.3 Vibration environment	5-157
5.2.1.4 Forward skirt heating	5-157
5.2.1.5 Post-SECO pulse	5-158
5.2.2 Propulsion	5-158
5.2.2.1 Summary	5-158
5.2.2.2 Propulsion system configuration	5-158
5.2.2.3 Stage I engine performance	5-158
5.2.2.4 Stage II engine performance	5-160
5.2.2.5 Pressurization system	5-161
5.2.2.6 Propellant system	5-161
5.2.3 Flight Control System	5-162
5.2.3.1 Lift-off and hold-down transients	5-162
5.2.3.2 Roll and pitch programs	5-162
5.2.3.3 Stage I flight	5-163
5.2.3.4 Stage separation	5-163
5.2.3.5 Control system biases	5-163
5.2.3.6 Radio guidance initiate	5-164
5.2.3.7 Post-SECO transients	5-164
5.2.4 Hydraulic System	5-164
5.2.4.1 Stage I - primary system	5-164
5.2.4.2 Stage I - secondary system	5-165
5.2.4.3 Stage II	5-166
5.2.4.4 Resume of primary system anomaly	5-166
5.2.5 Guidance System	5-166
5.2.5.1 Programed guidance	5-167

UNCLASSIFIED

UNCLASSIFIED

vii

Section	Page
5.2.5.2	Closed-loop guidance 5-167
5.2.6	Electrical Power System 5-169
5.2.6.1	Preflight 5-169
5.2.6.2	Umbilical drops 5-169
5.2.6.3	Flight 5-169
5.2.7	Instrumentation 5-170
5.2.7.1	Airborne 5-170
5.2.7.2	Ground instrumentation 5-171
5.2.8	Malfunction Detection System 5-171
5.2.8.1	Engine MDS 5-171
5.2.8.2	Vehicle MDS 5-172
5.2.8.3	Ground slow malfunction detection 5-173
5.2.9	Range Safety and Ordnance 5-173
5.2.9.1	Range safety 5-173
5.2.9.2	Ordnance system 5-176
5.3	LAUNCH VEHICLE INTERFACE 5-209
6.0	<u>MISSION SUPPORT PERFORMANCE</u> 6-1
6.1	PRELAUNCH OPERATIONS 6-1
6.1.1	Gemini Spacecraft 6-1
6.1.2	Gemini Launch Vehicle 6-2
6.2	FLIGHT CONTROL 6-3
6.2.1	Prepermission Operations 6-4
6.2.2	Mission Operations Summary 6-5
6.3	NETWORK PERFORMANCE 6-9
6.3.1	MCC and Remote Facilities 6-10
6.3.2	Network Facilities 6-11

UNCLASSIFIED

UNCLASSIFIED

Section	Page
6.4 RECOVERY OPERATIONS	6-16
6.4.1 Recovery Force Deployment	6-16
6.4.2 Location and Retrieval	6-17
6.4.3 Recovery Aids	6-19
6.4.4 Postretrieval Procedures	6-20
6.4.5 Spacecraft RCS Deactivation	6-21
7.0 Not required in this report	
8.0 Not required in this report	
9.0 <u>CONCLUSIONS</u>	9-1
10.0 <u>RECOMMENDATIONS</u>	10-1
11.0 <u>REFERENCES</u>	11-1
12.0 <u>APPENDIX A</u>	12-1
12.1 VEHICLE HISTORIES	12-1
12.1.1 Spacecraft	12-1
12.1.2 Gemini Launch Vehicle	12-9
12.2 WEATHER CONDITIONS	12-18
12.3 FLIGHT SAFETY REVIEWS	12-19
12.3.1 Spacecraft	12-19
12.3.2 Launch Vehicle	12-20
12.3.3 Flight Safety Review Board	12-20
12.4 SUPPLEMENTAL REPORTS	12-21
12.5 DATA AVAILABILITY	12-21
12.5.1 Telemetry Data	12-21

UNCLASSIFIED

UNCLASSIFIED

ix

Section	Page
12.5.2	Trajectory Data 12-22
12.5.3	Reduced Telemetry Data 12-23
12.5.4	Photographic Coverage 12-24
12.6	POSTFLIGHT INSPECTION 12-27
12.6.1	Chronology 12-29
12.6.2	Spacecraft Systems 12-31
12.6.3	Continuing Evaluation 12-34
13.0	<u>APPENDIX B -- GT-2 LAUNCH ATTEMPT</u> 13-1
13.1	SUMMARY 13-1
13.2	GLV PERFORMANCE 13-1
13.2.1	Hydraulic System Operation 13-1
13.2.2	Other Systems 13-4
13.3	SPACECRAFT PERFORMANCE 13-5
13.3.1	Fuel Cell 13-5
13.3.2	Propulsion 13-7
13.4	OPERATIONS 13-8
13.4.1	Countdown 13-8
13.4.2	Mission Control Operations 13-10
14.0	DISTRIBUTION 14-1

UNCLASSIFIED

UNCLASSIFIED

TABLES

Table		Page
3-I	SPACECRAFT MODIFICATIONS	3-34
3-II	COMMUNICATIONS EQUIPMENT	3-35
3-III	SPACECRAFT INSTRUMENTATION MEASUREMENTS FOR GT-2	3-36
3-IV	GUIDANCE AND CONTROL SWITCHES	3-54
3-V	GLV-2 MODIFICATIONS	3-55
3-VI	LAUNCH-VEHICLE INSTRUMENTATION MEASUREMENTS FOR GT-2	3-56
4-I	SEQUENCE OF EVENTS	4-6
4-II	COMPARISON OF PLANNED AND ACTUAL TRAJECTORY PARAMETERS	4-8
5.1-I	CABIN SECTION PEAK STRUCTURAL TEMPERATURES DURING REENTRY	5-48
5.1-II	MAXIMUM VALUES OF g_{rms}	5-49
5.1-III	REAL AND DELAYED TIME DATA ACQUISITION	5-50
5.1-IV	USABLE PCM DATA	5-51
5.1-V	LAUNCH GUIDANCE AND CONTROL EVENTS	5-52
5.1-VI	INSERTION CONDITION COMPARISON AT SPACECRAFT SEPARATION	5-53
5.1-VII	IGS MEASURED VELOCITY CHANGES	5-54
5.1-VIII	IGS REENTRY EVENT SEQUENCE	5-55
5.1-IX	INDICATED INERTIAL GUIDANCE SYSTEM ERRORS	5-56
5.1-X	GUIDANCE SYSTEM ERRORS	5-57
5.1-XI	CONTROL SYSTEM EVENTS	5-58

UNCLASSIFIED

UNCLASSIFIED

xi

Table		Page
5.1-XII	CONTROL SYSTEM PERFORMANCE	
	(a) Control System Measured Torques	5-59
	(b) Retrorocket Disturbance Torques	5-60
5.1-XIII	SPACECRAFT MOMENTS OF INERTIA	5-61
5.1-XIV	MAIN BUS VOLTAGE LEVELS	5-62
5.1-XV	SEQUENCE OF EVENTS	5-63
5.1-XVI	CONDITION OF THE OAMS AT LIFT-OFF AND EQUIPMENT SECTION SEPARATION	5-67
5.1-XVII	RCS CONDITION AT LIFT-OFF AND TOUCHDOWN	5-68
5.1-XVIII	BURN TIME FOR ROCKET MOTORS	5-69
5.2-I	PROPULSION SYSTEM ELAPSED TIME	5-177
5.2-II	AVERAGE STAGE I PERFORMANCE	5-177
5.2-III	STAGE I PERFORMANCE - STANDARD INLET CONDITIONS	5-178
5.2-IV	AVERAGE STAGE II PERFORMANCE	5-178
5.2-V	STAGE II PERFORMANCE - STANDARD INLET CONDITION	5-179
5.2-VI	PROPELLANT LOADING	5-179
5.2-VII	AVERAGE PROPELLANT TEMPERATURES	5-180
5.2-VIII	OUTAGE AND BURN-TIME MARGIN	5-180
5.2-IX	HOLD-DOWN TRANSIENTS	5-181
5.2-X	MAXIMUM RATES AND ATTITUDE ERRORS	5-182
5.2-XI	GYRO DISPLACEMENT BIAS	5-183
5.2-XII	PLANNED AND ACTUAL EVENT TIMES AND VEHICLE RATES	5-184

UNCLASSIFIED

UNCLASSIFIED

Table		Page
5.2-XIII	SUMMARY OF INSTRUMENTATION SYSTEM DATA	5-185
5.2-XIV	MALFUNCTION DETECTION SYSTEM SWITCHOVER	5-186
6-I	TELEMETRY COVERAGE	6-24
6-II	RADAR COVERAGE	6-25
6-III	ACQUISITION AID COVERAGE	6-25
6-IV	RECOVERY SUPPORT	6-26
12-I	LAUNCH-AREA ATMOSPHERIC CONDITIONS AT 9:21 a.m. e.s.t.	12-36
12-II	RECOVERY-AREA ATMOSPHERIC CONDITIONS AT 1:37 p.m. e.s.t.	12-37
12-III	SUPPLEMENTAL REPORTS	12-38
12-IV	STILL AND MOTION PICTURE CAMERA COVERAGE	12-39
12-V	ENGINEERING SEQUENTIAL CAMERA DATA	12-40
12-VI	INSTRUMENTS FOR WHICH PANEL FILM WAS TABULATED	12-42
12-VII	CAMERAS USED DURING RECOVERY OPERATIONS	12-43
12-VIII	SPACECRAFT BATTERY LIFE	12-44
13-I	EVENT SUMMARY	13-13

UNCLASSIFIED

UNCLASSIFIED

xiii

FIGURES

Figure		Page
3-1	GT-2 space vehicle lift-off configuration	3-73
3-2	Spacecraft arrangement and nomenclature	3-74
3-3	Launch vehicle - spacecraft relationships	3-75
3-4	Reentry assembly - right-hand equipment bay	3-76
3-5	Spacecraft 2 instrument panels	3-77
3-6	Adapter electronic module, and left-hand landing gear well installation	3-78
3-7	Spacecraft antenna locations	3-79
3-8	Special instrumentation pallet assemblies	3-80
3-9	Reentry assembly ECS package and adapter primary oxygen supply	3-81
3-10	Adapter-equipment section - ECS coolant module and space radiator	3-82
3-11	Block diagram of guidance and control system equipment	3-83
3-12	Reentry assembly - left-hand equipment bay	3-84
3-13	Fuel-cell module	3-85
3-14	Orbital attitude and maneuver system	3-86
3-15	Reentry control system	3-87
3-16	Pyrotechnic separation assemblies and devices	3-88
4-1	Ground track	4-9
4-2	Time histories of trajectory parameters	
	(a) Altitude and range	4-10
	(b) Latitude and longitude	4-11

UNCLASSIFIED

UNCLASSIFIED

Figure		Page
	(c) Space-fixed velocity and flight-path angle . . .	4-12
	(d) Earth-fixed velocity and flight-path angle . . .	4-13
	(e) Mach number and dynamic pressure	4-14
	(f) Longitudinal acceleration	4-15
5.1-1	Distribution of peak measured reentry temperatures	
	(a) Leeward side	5-70
	(b) Windward side	5-71
5.1-2	Comparison of pressure distribution during the launch phase as obtained during flight and in wind-tunnel tests	5-72
5.1-3	Aerodynamic environment	5-73
5.1-4	Comparison of pressure distributions during the reentry phase as obtained during flight and in wind-tunnel tests	
	(a) Windward side	5-74
	(b) Leeward side	5-75
5.1-5	Distribution of peak heating rates	
	(a) Windward side	5-76
	(b) Leeward side	5-77
5.1-6	Typical heating rates	
	(a) Windward side of cabin	5-78
	(b) Localized heating in wake of windward adapter interconnect firing	5-79
	(c) Leeward side of cabin	5-80

UNCLASSIFIED

UNCLASSIFIED

xv

Figure		Page
5.1-7	Typical heating rates	
	(a) Windward side, RCS and R and R section	5-81
	(b) Leeward side, RCS and R and R section	5-82
5.1-8	Heat shield instrumentation	5-83
5.1-9	Heat shield temperature distribution during reentry	5-84
5.1-10	Heat shield after reentry	5-85
5.1-11	Cabin section outer skin temperatures during reentry	5-86
5.1-12	Most windward adapter interconnect fairing	5-87
5.1-13	Cabin section temperature distribution through the ECS door	5-88
5.1-14	Region of damage in wake of most windward interconnect fairing	5-89
5.1-15	Damage in wake of most windward adapter interconnect fairing	5-90
5.1-16	RCS section outer skin temperatures during reentry	5-92
5.1-17	RCS section structural temperature distribution during reentry	5-93
5.1-18	R and R section outer skin temperatures during reentry	5-94
5.1-19	Comparison of flight data with equipment vibration qualification spectrum	5-95
5.1-20	Adapter to ambient differential pressure	5-96
5.1-21	Reentry assembly compartment to ambient differential pressures	5-97
5.1-22	Reentry angle of attack	5-98

UNCLASSIFIED

UNCLASSIFIED

Figure		Page
5.1-23	Spacecraft communications usable signal strength time history	5-99
5.1-24	S-band and C-band radar coverage	5-100
5.1-25	Usable PCM data	5-101
5.1-26	Cabin pressure control during launch and reentry	5-102
5.1-27	Crew compartment gas temperatures	5-103
5.1-28	ECS oxygen storage pressures	5-104
5.1-29	Comparison of steering commands during launch with preflight values	5-105
5.1-30	Comparison of flight steering errors during reentry with preflight nominal values	5-106
5.1-31	IMU sensed acceleration	5-107
5.1-32	IGS velocity comparisons with ground tracking	5-108
5.1-33	Attitude errors	5-109
5.1-34	Inertial measuring unit gimbal angles during incremental velocity adjust routine	5-110
5.1-35	Incremental velocity indicator computer sample and window set routine	5-111
5.1-36	Inertial velocity changes due to thrust tail-off	5-112
5.1-37	Spacecraft - launch vehicle separation accelerations	5-113
5.1-38	Accelerations during retrofire	5-114
5.1-39	Spacecraft attitude compared to 3 sigma limits	5-115
5.1-40	Reentry control parameter comparison	5-116

UNCLASSIFIED

UNCLASSIFIED

xvii

Figure		Page
5.1-41	Spacecraft - launch-vehicle separation transients	5-118
5.1-42	Relative positions of GLV and spacecraft after separation	5-119
5.1-43	Retrofire transients	5-120
5.1-44	Rate summations	
	(a) Pitch rates	5-121
	(b) Yaw rates	5-122
5.1-45	Selected spacecraft rate time histories	
	(a) Pitch rate	5-123
	(b) Roll and yaw rates	5-124
5.1-46	Attitude display performance	5-125
5.1-47	Horizon sensor performance	
	(a) Pitch	5-126
	(b) Roll	5-127
5.1-48	Comparison of measured camera angles and camera angles computed from measured platform gimbal angles	5-128
5.1-49	Comparison of airborne computer parameters with preflight nominal values	5-129
5.1-50	Main electrical power system characteristics	5-130
5.1-51	Isolated electrical power system characteristics	5-131
5.1-52	Pressure and mass-quantity, cryogenic vessels	5-132
5.1-53	OAMS attitude TCA mission duty cycle	5-133
5.1-54	Orbital attitude and maneuver system, propellant quantity	5-134

UNCLASSIFIED

UNCLASSIFIED

Figure		Page
5.1-55	RCS ring A and B TCA mission duty cycle	
	(a) Pitch-up	5-135
	(b) Pitch-down	5-136
	(c) Yaw-right	5-137
	(d) Yaw-left	5-138
	(e) Roll-right	5-139
	(f) Roll-left	5-140
5.1-56	RCS A ring performance	5-141
5.1-57	RCS B ring performance	5-142
5.1-58	Wire bundle guillotine	5-143
5.1-59	Command pilot's instrument panel	5-144
5.1-60	Center instrument panel	5-145
5.1-61	Pilot's instrument panel (right)	5-146
5.1-62	Window view - spacecraft separation from the launch vehicle at IO + 352 seconds	5-147
5.1-63	Window view - retrograde maneuver at IO + 414 seconds	5-148
5.1-64	Window view - typical ionization effects during constant roll reentry	5-149
5.1-65	Window view - commencement of maximum lift reentry at IO + 717 seconds	5-150
5.1-66	Window view - rendezvous and recovery section separation from the spacecraft at IO + 876 seconds	5-151
5.1-67	Window view - parachute deployed and starting two point suspension	5-152
5.1-68	Landing system performance	5-153

UNCLASSIFIED

UNCLASSIFIED

xix

Figure		Page
5.2-1	Comparison of launch vehicle longitudinal oscillation for GT-1 and GT-2 (Sta. 280)	5-187
5.2-2	Comparison of spacecraft and launch vehicle longitudinal oscillations	5-188
5.2-3	Launch day wind profile	5-189
5.2-4	Modal moments at maximum $q\alpha$	5-190
5.2-5	Gemini launch vehicle peak modal moments from stage I flight	5-191
5.2-6	Gemini launch vehicle vibration modes for stage I flights	5-192
5.2-7	Peak modal bending moment response to transonic buffet	5-193
5.2-8	Launch-vehicle forward skirt skin temperature	5-194
5.2-9	Stage I engine flight performance	5-195
5.2-10	Stage II engine flight performance	5-196
5.2-11	Pitch flight displacement	5-197
5.2-12	Yaw flight displacement	5-198
5.2-13	Roll flight displacement	5-199
5.2-14	GT-2 post-SECO oscillations	5-200
5.2-15	Time history of stage I hydraulic pressure	5-201
5.2-16	Hydraulic pump cross-section, stage I primary and secondary systems	5-202
5.2-17	Space-fixed velocity and flight-path angle in the region of cutoff using launch vehicle guidance data	
	(a) Space-fixed velocity	5-203
	(b) Space-fixed flight-path angle	5-204

UNCLASSIFIED

UNCLASSIFIED

Figure		Page
5.2-18	Space-fixed velocity and flight-path angle in the region of cutoff using MISTRAM I Range Safety computer (IP-3600) data	
	(a) Space-fixed velocity	5-205
	(b) Space-fixed flight-path angle	5-206
5.2-19	Range Safety IP plotboard	5-207
6-1	Spacecraft 2 countdown sequence on January 19, 1965	6-27
6-2	Cape Kennedy Air Force Eastern Test Range network stations	6-28
6-3	Mainland Air Force Eastern Test Range instrumentation facilities	6-29
6-4	Network remote stations	6-30
6-5	Recovery force deployment	6-31
6-6	Detailed recovery area	6-32
6-7	Swimmers after installing flotation collar	6-33
6-8	R and R section being delivered to carrier	6-34
6-9	Spacecraft being lifted from water	6-35
6-10	Condensation on spacecraft window	6-36
12-1	Spacecraft 2 test history at contractor facility	12-45
12-2	Spacecraft 2 test history at Cape Kennedy	12-46
12-3	GLV-2 test history at Cape Kennedy	12-48
12-4	Variation of wind direction and velocity with altitude for launch area	12-50
12-5	Variation of wind direction and velocity with altitude for recovery area	12-51

UNCLASSIFIED

UNCLASSIFIED

xxi

Figure		Page
12-6	Data availability	12-52
12-7	Data selection for composite spacecraft instrumentation	12-56
12-8	Engineering sequential fixed camera locations	12-57
12-9	Engineering sequential tracking camera locations	12-58
12-10	Engineering sequential tracking camera coverage	12-59
12-11	Helicopter camera coverage	12-60
12-12	Holes in shingles of reentry assembly	12-61
12-13	R and R section and bent stub antenna	12-63
12-14	Inertial guidance system components after flight	12-64
12-15	Damaged umbilical seal	12-65
13-1	GLV start transients	13-14
13-2	Failed servovalve body showing fractures of the mounting lugs	13-15
13-3	GLV tandem actuator with part of the case removed	13-16
13-4	Hydraulic actuator used on GLV-2 launch attempt	13-17
13-5	Impulse energy capability of modified and unmodified actuators	13-18
13-6	Stage I tandem actuator vibration	13-19
13-7	GT-2 countdown sequence on attempted launch on December 9, 1964	13-20

UNCLASSIFIED

UNCLASSIFIED

1-1

1.0 MISSION SUMMARY

The second mission of the Gemini Program, the United States' second program of manned space exploration, was successfully launched from Complex 19 at Cape Kennedy, Florida, at 9:03:59 a.m. e.s.t. on January 19, 1965. The flight was suborbital and unmanned and used the second production Gemini spacecraft and launch vehicle. The combined vehicle was designated GT-2. Recovery of the spacecraft was accomplished by the primary recovery ship, the aircraft carrier Lake Champlain, at 16°31.9' North latitude, 49°46.8' West longitude at 10:52 a.m. e.s.t.

The major objectives of this mission for the spacecraft were to demonstrate the basic structural integrity of the unit throughout the flight environment and to verify the adequacy of the reentry heat protection under the most severe conditions. In addition, the satisfactory performance of vital flight control systems, life support systems, retrograde rocket system, recovery and landing systems, and other systems critical to flight safety and mission success was required. With minor exceptions these objectives were accomplished, and the performance of the spacecraft was satisfactory. Corrective action is required to improve the performance of the inertial guidance system and to alleviate excessive heating in a localized area on the spacecraft skin. The launch vehicle successfully demonstrated its primary objective of the mission which was to reaffirm its capability to insert the spacecraft into a prescribed trajectory. The countdown of the space vehicle was completed with no delays caused by the launch vehicle and one minor delay caused by the spacecraft. The flight was well within the allowable dispersions. The insertion of the spacecraft into the required high heating rate trajectory was accomplished with precision. All launch vehicle systems performed satisfactorily in flight, but there was an indication of abnormal operation in the primary hydraulic system prior to lift-off which will be the subject of corrective action. All mission support and flight control operations were adequate, and the GT-2 mission served to enhance the readiness of these functions for the support of manned operations. The GT-2 mission served as the final flight qualification of the total Gemini-space system prior to manned flight.

UNCLASSIFIED

UNCLASSIFIED

THIS PAGE LEFT BLANK INTENTIONALLY

UNCLASSIFIED

UNCLASSIFIED

2-1

2.0 INTRODUCTION

The first-order mission objectives of the GT-2 mission were as follows:

(a) Demonstrate the adequacy of the reentry assembly heat protection equipment during a maximum heating-rate reentry.

(b) Demonstrate the structural integrity and capability of the spacecraft from lift-off through landing.

(c) Demonstrate satisfactory performance of the following spacecraft systems:

- (1) Environmental control system
- (2) Reentry control system
- (3) Retrograde rocket system
- (4) Parachute recovery system (partial)
- (5) Pyrotechnics (partial)
- (6) Electrical system (partial)
- (7) Sequential (partial)
- (8) Spacecraft displays (partial)
- (9) Orbital attitude and maneuver system (during separation from the launch vehicle) (partial)
- (10) Inertial measuring unit (during launch and reentry)
- (11) Attitude control maneuver electronics (from spacecraft separation through reentry)
- (12) Inertial guidance system (during turnaround and retrograde maneuvers)
- (13) Spacecraft recovery aids
- (14) Communications (partial)
- (15) Tracking

UNCLASSIFIED

UNCLASSIFIED

(16) Data transmission

- (d) Demonstrate systems checkout and launch procedures.
- (e) Evaluate backup guidance steering signals throughout launch.

The second-order mission objectives of the GT-2 mission were the following:

- (a) Obtain test results on the following systems:
 - (1) Cryogenics
 - (2) Fuel cell and reactant supply system
 - (3) Communications
- (b) Further flight qualify the launch vehicle and demonstrate its ability to insert the spacecraft into a prescribed trajectory.
- (c) Demonstrate the compatibility of the launch vehicle and spacecraft through the countdown and launch sequence.
- (d) Provide training for flight controllers.
- (e) Further qualify ground communications and tracking systems in support of future manned missions.

All of the first-order objectives were met, and all of the second-order objectives were met with the exception of obtaining test results on the fuel cell. The fuel cell was deactivated prior to lift-off due to a system malfunction, and a discussion of this malfunction is contained in this report.

All spacecraft and Gemini launch vehicle transmitted telemetry data, spacecraft onboard data, ground-based radar data, and engineering photographic data obtained during the mission were used by the Mission Evaluation Team in determining the results of the mission. The evaluation consisted of analyzing the flight data and comparing these data with the ground-test results obtained from the various test programs conducted on the spacecraft, its systems, and the launch vehicle. Also, analyses were made of the flight data with respect to the design specification requirements and the predicted operating conditions for this mission. The results of these analyses are presented in this report.

UNCLASSIFIED

UNCLASSIFIED

2-3

More detailed analyses of the data are continuing as this report is being published. These analyses for the launch vehicle are overall performance, radio guidance system performance, and the launch vehicle primary hydraulic system anomaly prior to lift-off. Analyses of spacecraft performance are being continued in the areas of aerodynamic performance and heating, reactant supply system pressure anomaly, and guidance and control system performance and anomalies. The results of these analyses will be published in supplemental reports to this document. A complete list of these supplemental reports including the responsible organizations is shown in section 12.4.

Section 13.0 of this report contains an analysis of the Gemini launch vehicle and spacecraft performance during the attempted launch on December 9, 1964.

UNCLASSIFIED

UNCLASSIFIED

THIS PAGE LEFT BLANK INTENTIONALLY

UNCLASSIFIED

3.0 VEHICLE DESCRIPTION

Gemini launch vehicle 2 (GLV-2) and Gemini spacecraft 2 constituted the space vehicle for the second Gemini mission (GT-2). The GT-2 space vehicle at lift-off is shown in figure 3-1. The configurations of the spacecraft and launch vehicle which existed at lift-off are described in sections 3.1 and 3.2 of this report. Section 3.3 provides GT-2 weight and balance data.

3.1 GEMINI SPACECRAFT DESCRIPTION

This section provides a general description of the structure and major systems of spacecraft 2. Since spacecraft 2 contained production units of virtually all equipment which will be used on later manned missions, with the exception of the rendezvous radar and the drogue parachute, the following description is also intended to serve as a reference for subsequent mission reports. The major differences between spacecraft 1 and spacecraft 2 are indicated in table 3-I, and a description of spacecraft 1 is given in reference 1.

3.1.1 Spacecraft Structure

The Gemini spacecraft lift-off configuration was a conical structure consisting of two major assemblies: the reentry assembly and the adapter assembly (fig. 3-2). The primary materials used in the spacecraft structure were titanium, magnesium, and aluminum. The overall dimensions of the spacecraft were as follows: length, 226.09 inches (18.8 feet); diameter at the heat shield, 90.0 inches (7.5 feet); and diameter at the adapter - launch-vehicle interface, 120.0 inches (10.0 feet). The following paragraphs provide descriptions of the major structural assemblies of spacecraft 2. Additional information may be obtained from references 2 and 3.

3.1.1.1 Reentry assembly. - The reentry assembly consisted of the cabin section, the reentry control system (RCS) section, and the rendezvous and recovery (R and R) section, as shown in figure 3-2. Also included in the reentry assembly were a heat shield attached to the aft end of the cabin section, a nose fairing attached to the forward end of the R and R section, and a horizon-sensor fairing attached to the left side at the mating point of the cabin and RCS sections.

3.1.1.1.1 Cabin section: The basic cabin structure was an internal pressure vessel having a titanium frame assembly to which side panels

UNCLASSIFIED

and two bulkheads of double-skin titanium were seam welded. Space was provided between the vessel and the outer conical shell for an equipment bay on each side and an equipment compartment underneath the floor.

Two access doors were provided on each side of the cabin to enclose components installed in the side equipment bays. Although landing gear was not installed in spacecraft 2, two main landing-gear doors covered the landing-gear wells located below the side equipment bays. Two additional access doors were installed on the bottom of the cabin between the main landing-gear doors. The forward door provided access to the lower equipment bay, and the aft door provided access to the environmental control system (ECS) compartment.

Two hatches sealed the openings and provided for ingress and egress. Each hatch is normally operated manually; however, if the seat-ejection sequence is initiated, the hatches are automatically opened by pyrotechnic operated actuators. See paragraph 3.1.2.8.5. Each hatch had an observation window which consisted of a sealed double-glass-pane inner assembly and a vented single-pane outer assembly. The conical surface of the reentry assembly was covered with beaded shingles of Rene 41 for thermal protection.

One horizon sensor was mounted on the left side of the cabin near the junction of the cabin and the RCS section. The sensor was protected during the initial phase of powered flight by a plastic laminate fairing. The fairing was jettisoned approximately 45 seconds after ignition of the launch-vehicle second stage engine. The sensor head and mount were jettisoned after the retrograde sequence in order to provide an aerodynamically clean mold line for reentry.

3.1.1.1.2 RCS section: The RCS section was located between the R and R section and the cabin section, as shown in figure 3-2. The RCS section was cylindrical and consisted of a titanium supporting structure with taper-machined and formed beryllium shingles used for the outer skin. The structure housed the reentry control system, which provided thrust for stabilization and control during retrorocket firing and reentry. The forward face of the RCS section contained a structural assembly to which the main parachute bridle was attached.

3.1.1.1.3 R and R section: The truncated cone-shaped R and R section was mated to the RCS section, as shown in figure 3-2. Titanium was used as the primary structural material. The external surface consisted of beryllium shingles, except for the nose fairing which was made from fiber-glass reinforced plastic laminate. The nose fairing provided thermal protection for equipment in the R and R section during the initial portion of powered flight and was jettisoned approximately 45 seconds after ignition of the launch-vehicle second stage engine.

UNCLASSIFIED

On future rendezvous missions, the R and R section will contain rendezvous radar and docking equipment, a high-altitude drogue parachute assembly, a pilot parachute, and a main parachute. The rendezvous radar and docking equipment and the drogue parachute were not installed in spacecraft 2.

3.1.1.1.4 Heat protection structure: The heat protection structure of spacecraft 2 consisted primarily of the following types of materials. The afterbody (cabin section, RCS section, and R and R section) was protected by Rene 41 or beryllium shingles. The forebody (heat shield) protection consisted of a silicone elastomer ablative compound that was filled into a fiber-glass honeycomb. In addition to these structures, insulating material was installed outside the large bulkhead of the pressure vessel and inside the afterbody shingles to impede the transfer of heat to the pressure vessel and equipment.

The spacecraft 2 heat-shield ablative material was approximately one-half the thickness of the production design. The modified heat shield was used to demonstrate the adequacy of the heat protection materials used in the Gemini spacecraft design.

3.1.1.2 Adapter assembly. - The adapter assembly was a truncated cone, and its structure consisted of circumferential aluminum rings, extruded magnesium-alloy stringers, and magnesium skin. The stringers were designed to provide a flow path for the liquid coolant which transferred heat to the adapter skin for radiation into space.

The adapter assembly consisted of three sections: the retrograde section, the equipment section, and the launch-vehicle mating section. The forward end of the adapter assembly was attached to the aft end of the reentry assembly, as shown in figure 3-2. Pyrotechnic separation rings were provided between the retrograde and the equipment sections, and between the equipment and the launch-vehicle mating sections.

The adapter assembly contained equipment which was not necessary to the reentry and landing phases of the mission. The thrust chamber assemblies (TCA's) of the orbital attitude and maneuver system (OAMS) were mounted in positions around the adapter assembly which permitted the spacecraft to be rotated about its three axes (roll, pitch, and yaw), and provided the capability for translation in any direction.

3.1.1.2.1 Retrograde section: The retrograde section was mated to the aft end of the reentry assembly and was held in place by three titanium interconnects which contained the necessary pyrotechnics to separate the section from the reentry assembly. The primary function of the retrograde section was to support four retrograde rockets and six of the OAMS TCA's. Figure 3-2 shows the location of the two crossed aluminum "I" beams used to support the retrograde rockets.

UNCLASSIFIED

3.1.1.2.2 Equipment section: On spacecraft 2, the equipment section contained a fuel cell module; OAMS pressurant, fuel, and oxidizer tanks, lines, and components; water storage tanks; the primary oxygen supply tank; cooling system components; and an electrical and electronic module. A honeycomb blast shield was attached to the forward end of the equipment section to prevent the OAMS propellant tanks and the launch-vehicle second stage from receiving excessive heat during retrorocket firing. The large-diameter end of the equipment section provided for mounting of 10 additional OAMS TCA's.

3.1.1.2.3 Spacecraft - launch-vehicle mating section: Spacecraft 2 was mated to the launch-vehicle in the same manner as that which was successfully demonstrated on the GT-1 mission. The access doors, thrusters, and scupper cutouts in both the spacecraft equipment section and the launch vehicle upper skirt were the same as the GT-1 configuration. The relationship of the spacecraft and launch-vehicle axes is illustrated in figure 3-3. Reference 1 contains a more complete description of the structural interface of the Gemini space vehicle.

3.1.2 Major Systems

3.1.2.1 Communications.- The following paragraphs are a general description of the subsystems which comprised the communications equipment installed in spacecraft 2. Table 3-II lists the spacecraft 2 communications equipment and gives a comparison between the spacecraft 2 equipment and that to be installed in subsequent manned spacecraft. Communications equipment locations are shown in figures 3-4 to 3-7.

3.1.2.1.1 Voice communications: HF and UHF modes of voice communications were provided on spacecraft 2.

(a) HF transmitter-receiver: A single high-frequency amplitude-modulated transmitter-receiver unit was provided, and was installed in the reentry assembly equipment bay. The transmitter operated on a frequency of 15.016 megacycles and had a 5.0 watt RF output. The transmitter was amplitude modulated by a CW tone generated in the voice control center unit. Provisions were incorporated for automatically energizing the equipment in the DF mode for recovery purposes after landing.

(b) UHF transmitter-receiver: A single ultra-high-frequency amplitude-modulated transmitter-receiver unit was installed in the reentry assembly equipment bay. The transmitter operated on a frequency of 296.8 megacycles and had a 3.0 watt RF output. The output was modulated with a 1000-cycle tone. The UHF transmitter-receiver was set to operate from launch until R and R section separation and was turned on again after two-point suspension on the main parachute.

UNCLASSIFIED

(c) Voice control center (VCC): A voice control center was provided in the cabin section. The unit was set to provide a CW tone for modulating the HF transmitter during recovery operations. The unit was switched to the direction finding (DF) mode during the prelaunch check of the spacecraft systems. In this mode, when the transmitter was keyed, the voice control center generated a CW pulse of 1000 cps through an integral tone generator.

3.1.2.1.2 Telemetry transmitter: Two 2.0-watt solid-state UHF telemetry transmitters were located in the reentry assembly equipment bay. The real-time transmitter was set to operate throughout the mission. The delayed time transmitter was sequenced to operate in parallel with the real-time transmitter until 0.05g +200 seconds, and then to switch to the delayed time mode for playback of tape recorder data.

3.1.2.1.3 Tracking subsystem: The tracking subsystem consisted of a C-band radar transponder, an S-band radar transponder, a CW acquisition aid beacon, and the associated circuitry which was installed for this mission.

(a) C-band transponder: A 1 kW C-band double-pulse-coded transponder was installed in the reentry assembly equipment bay. The transponder operated throughout this mission.

(b) S-band transponder: A 1.5 kW S-band double-pulse-coded transponder was installed in the equipment section. The transponder operated continuously from lift-off until equipment section separation.

(c) Acquisition aid beacon: An acquisition aid beacon was installed in the equipment section. The transmitter was designed to transmit a CW-modulated RF signal on a frequency of 246.3 megacycles with a 0.25-watt output. The beacon was sequenced to operate from spacecraft separation until equipment section jettison.

3.1.2.1.4 Recovery subsystem: The recovery subsystem consisted of a UHF recovery beacon installed in the reentry assembly. The unit was compatible with existing ARA-25 and SARAH receivers. The recovery beacon was sequenced to turn on after R and R section separation and operate until spacecraft recovery.

3.1.2.1.5 Command subsystem: The digital command system (DCS) was a digital, phase-shift keyed system installed in the equipment section of the adapter, which consisted of two receivers, single decoding circuits, and externally packaged relays. The DCS was operated from prelaunch until equipment section separation. The purpose of the DCS was to update the guidance and control system during launch and provide backup to the sequential system.

UNCLASSIFIED

Provisions were made to transmit guidance commands via the DCS link to spacecraft 2 immediately prior to launch and twice during powered flight. No real-time commands were transmitted during the mission; however, spacecraft 2 was equipped to receive real-time commands for the following functions:

- Relay 1 - Real-time telemetry mode, on-off (not planned for use).
- Relay 2 - Tape dump, on-off (not planned for use).
- Relay 3 - Real-time telemetry (not planned for use).
- Relay 4 - Acquisition aid, on-off (not planned for use).
- Relay 5 - Tape playback (not planned for use).
- Relay 6 - Calibration, on-off (not planned for use).
- Relay 7 - Abort command.
- Relay 8 - C-band transponder, on-off (not planned for use).
- Relay 9 - S-band transponder, on-off (not planned for use).
- Relay 10 - Manual guidance switchover.
- Relay 11 - Spacecraft separation backup.
- Relay 12 - Abort backup.
- Relay 13 - Retro-jettison abort (for use below 70 000 feet and simultaneously with abort command and/or abort backup).

These real-time commands with the exception of relays 6, 8, and 9 were unique to spacecraft 2 as a result of its being unmanned.

3.1.2.1.6 Antenna subsystem: The antenna subsystem consisted of antennas, multiplexing and switching networks, and associated installation circuitry and components. (See fig. 3-7.)

(a) Recovery antenna: A UHF whip antenna of gold-plated spring steel was installed in the spacecraft to radiate signals generated by the UHF recovery beacon. The antenna was stowed in the main parachute cable trough and was extended after the parachute bridle suspension cables pulled through the cable trough cover.

(b) Stub antenna: The UHF stub antenna installed on the forward end of the R and R section of the spacecraft provided the capability

UNCLASSIFIED

for receiving commands and transmitting telemetry data. This antenna operated in conjunction with the UHF whip antenna on the retrograde section. However, on the GT-2 mission, switchover to the UHF whip antenna did not occur.

(c) Descent antenna: This antenna, similar to the recovery antenna, was installed in the spacecraft for UHF voice communications in conjunction with the telemetry transmitters. The antenna was switched into operation during the main parachute system deployment sequence and radiated telemetry and UHF transceiver signals until after landing.

(d) C-band helices: A C-band antenna array installed on the reentry assembly consisted of three circularly polarized helices spaced equally around the cabin section. The antennas were used for C-band radar tracking of the spacecraft throughout the mission. The lower right helix was connected to a phase shifter to reduce the effect of deep nulls in the antenna pattern.

(e) C-band slot: This annular slot antenna, located in the adapter assembly, was linearly polarized and was designed to optimize the antenna pattern for ground tracking during the orbital phase of a mission; however, it was not used on spacecraft 2.

(f) S-band slot: This annular slot antenna, located in the adapter assembly, was linearly polarized and was used from launch until equipment section separation.

(g) HF whip antenna: An extendible-retractable, motor-operated HF whip antenna was installed in the reentry assembly for HF communications in conjunction with the HF transmitter-receiver and voice control center. For this mission, the antenna was extended only after landing and remained in the extended position until recovery.

(h) UHF forward whip antenna: This antenna was located on the retrograde section and was extended by a solenoid-actuated spring after SECO. On manned flights, the astronaut may select this antenna or the UHF stub antenna for use with the PCM standby and real-time telemetry transmitters, UHF transmitter-receiver, and DCS receiver 2. (See fig. 3-7.) However, during GT-2, this antenna was not used, and all reception and transmission by the above systems was accomplished by the UHF stub antenna until R and R section separation.

(i) UHF aft whip antenna: This antenna was located on the equipment section and was extended after SECO by a solenoid-actuated spring. The antenna was used by the acquisition aid beacon and DCS receiver 1. (See fig. 3-7.)

UNCLASSIFIED

(j) Quadriplexer, diplexer, and coaxial switches: The quadriplexer and diplexer were used to reduce the number of radiating devices necessary for the UHF spacecraft communications system. The coaxial switches provided the means for connecting the various communications subsystems to the appropriate antennas.

3.1.2.2 Instrumentation and recording. - The basic function of the instrumentation and recording system was to measure or sense conditions and events onboard the spacecraft and to transmit these data to ground stations. The data received by selected ground stations were visually displayed for mission monitoring purposes and/or recorded on magnetic tape for analysis and evaluation. In addition to the production instrumentation required for PCM telemetry, special instrumentation was installed in spacecraft 2 to record data and to photograph instrument panel displays and the view through the left-hand window. References 2 and 4 contain detailed descriptions of the production instrumentation system installed in all Gemini spacecraft. References 3 and 5 provide additional information on the production and special instrumentation installed in spacecraft 2.

3.1.2.2.1 Production instrumentation and recording: The components described in the following paragraphs comprise the major elements of the production instrumentation and recording system installed in spacecraft 2. Component locations are shown in figures 3-4 and 3-6.

(a) Sensors: Several different types of sensors were used to indicate whether spacecraft conditions and events were within prescribed parameters. Typical sensors included pressure transducers, thermocouples, and accelerometers. The spacecraft parameters measured on the GT-2 mission are listed in table 3-III.

(b) Signal conditioners: A number of signals derived from sensors or other sources were not compatible with the PCM telemetry system inputs of 0 to 20 millivolts or 0 to 5 volts. Before these signals were applied to the telemetry system, they were changed in amplitude and/or characteristic by routing them through signal conditioning packages. These packages are identified as "instrumentation packages 1 and 2" in figures 3-4 and 3-6.

(c) PCM-FM telemetry system: The major types of components which make up the telemetry system were the following:

- (1) Telemetry transmitters¹

¹Descriptions of the telemetry transmitters have been included in the discussion of the communications system (paragraph 3.1.2.1.2); however, the telemetry transmitters are also considered to be part of the PCM-FM telemetry system.

UNCLASSIFIED

- (2) Programmer
- (3) Low-level multiplexers (0 to 20 millivolts)
- (4) High-level multiplexers (0 to 5 volts)
- (5) Dc-to-dc converters

The programmer and multiplexers comprised a "multiplexer-encoder" which converted signals from various sensors, signal conditioners, the computer, and other monitoring points into two serial, binary-coded, digital signals for output to the real-time telemetry transmitter and to the tape recorder-reproducer. The output to the telemetry transmitter was a 51.2K bit-per-second, NRZ signal, and the output to the tape recorder was a 5.12K bit-per-second NRZ signal. The programmer was located in the reentry assembly along with one high-level and two low-level multiplexers and the dc-to-dc converter. One low-level multiplexer and one high-level multiplexer were also located in the equipment section.

Two dc-to-dc converters (fig. 3-4) were furnished as production spacecraft instrumentation to provide regulated dc power to the instrumentation system. These converters provided highly regulated output voltages of +5, +24, and -24 V dc.

(d) PCM tape recorder: The tape recorder-reproducer was located in the instrument panel pedestal in the spacecraft cabin, as shown in figure 3-8. For the GT-2 mission, data were recorded at a tape speed of 41.25 in./sec from lift-off until the playback signal was given (0.05g +200 sec). The PCM data were played back at the same speed during spacecraft descent and were transmitted to prevent the loss of significant reentry data in the event that recovery of the spacecraft was not effected.

3.1.2.2.2 Special instrumentation: In addition to the production instrumentation installed in spacecraft 2, special instrumentation was mounted on the two pallet assemblies which were fitted to the ejection seats (fig. 3-8) or in the left-hand landing-gear well (fig. 3-6). The major special instrumentation components were as follows:

(a) One additional dc-to-dc converter was mounted on the left-hand pallet to provide regulated dc power for the special instrumentation.

(b) One additional signal conditioning package was mounted on the left-hand pallet. This package is identified as "instrumentation package 1A" in figure 3-8.

(c) A low-level commutator (multicoder) was installed in the left-hand landing-gear well.

UNCLASSIFIED

(d) A high-level commutator (multicoder) was mounted on the left-hand pallet.

(e) Three instrumentation assemblies, consisting of amplifiers and/or voltage controlled oscillators (VCO's), were mounted on the left-hand pallet assembly.

(f) A special tape recorder (PAM-FM) was mounted on the right-hand pallet assembly. This device recorded seven channels of data on magnetic tape. See reference 5 for the purpose of these seven channels.

(g) Two 16-mm cameras were mounted on the left-hand pallet, one 16-mm camera was mounted on the right-hand pallet, and one 16-mm camera was mounted between the pallets. Three of the cameras were used to monitor the instrument panel displays at a frame speed of approximately 4 frames per second in order to obtain pictures from lift-off through several minutes after touchdown.

(h) One of the 16-mm cameras mounted on the left-hand pallet photographed the view through the left-hand window. The camera was actuated at the spacecraft separation, and the frame speed was set at approximately 6 frames per second to obtain approximately 12 minutes of pictures.

3.1.2.3 Environmental control. - The spacecraft 2 environmental control system (ECS) was essentially operational, and differed from the configuration for manned missions in only a few minor respects.

3.1.2.3.1 Oxygen supply: Primary, secondary, and egress oxygen supplies were installed in spacecraft 2. The primary supply furnished oxygen during the launch and coast phases of the flight. The secondary supply furnished oxygen during the retrograde and reentry phases. An egress oxygen container was installed in each of the two egress kit packets.

The primary supply was liquid oxygen stored supercritically in a container located in the equipment section. The secondary supply was in gaseous form stored in one of two bottles located inside the cabin (fig. 3-9). (The secondary oxygen supply normally provides suit circuit oxygen and maintains cabin pressure at 5.1 psia after the equipment section is jettisoned.)

3.1.2.3.2 Cooling: The coolant system consisted of two identical loops that functioned independently of each other. Each loop contained a pump package, cold plate loops, heat exchanger loops, a radiator, filter, and necessary plumbing and controls. Liquid coolant flowing through the cold plates and heat exchangers provided the means to absorb heat from the spacecraft cabin and various heat-generating components. On orbital flights, the heat will be dissipated into space by the space

UNCLASSIFIED

radiator (see fig. 3-10). However, due to the short duration of this flight, the space radiator was operable but could not be evaluated.

During launch countdown, an external supply of coolant fluid was circulated through the ground cooling heat exchanger to cool the spacecraft equipment and cabin. During powered flight, the water evaporator heat exchanger was used for heat dissipation.

The spacecraft cooling system was disabled prior to the firing of the retrograde rockets since the pump packages, radiator, and various heat exchangers were jettisoned with the equipment section.

3.1.2.3.3 Cabin circuit: The cabin circuit was provided to maintain the cabin pressure and temperature at the required levels. The cabin circuit included the following components: cabin pressure regulator, cabin repressurization valve, cabin pressure relief valve, cabin outflow valve, cabin heat exchanger, and cabin fan.

The purpose of the cabin pressure regulator was to control cabin pressure to a nominal 5.1 psia. To conserve oxygen in the event of spacecraft depressurization, the cabin pressure regulator was designed to close if cabin pressure decreased to 4 psia.

The cabin pressure relief valve prevented excessive positive or negative buildup between cabin and ambient pressures. This valve also incorporated a manually operated water shutoff valve to prevent inflow of water during postlanding operations. On spacecraft 2, the water shutoff valve remained closed throughout the mission.

The cabin outflow valve provided a means of depressurizing the cabin. Cabin temperature was controlled by circulation of the atmosphere through the cabin heat exchanger.

3.1.2.3.4 Pressure suit circuit: The pressure suit circuit of the ECS was designed to provide temperature control, pressure control, ventilation, and atmospheric purification independently of the cabin circuit. On manned flights, a single suit circuit will serve both crew members with the two pressure suits connected to the circuit in parallel. The spacecraft 2 circuit included an ECS package, shown in figure 3-9, a snorkel inlet valve, a cabin inflow valve, and a cabin air circulation valve. The ECS package, located in the environmental system equipment bay, consisted of CO₂ and odor absorber canister upon which was mounted various other suit circuit components including suit compressors, demand regulators, and a suit heat exchanger.

Demand regulators will be used on manned flights to supply oxygen to maintain a minimum suit pressure of 3.5 psia. In the event suit

UNCLASSIFIED

pressure drops to between 3.0 and 3.3 psia during the launch or orbital phases of a mission, the suit circuit automatically switches to an oxygen high-rate (open-loop) mode of operation in which the suit recirculating system and compressor are turned off and oxygen flows directly from the oxygen supply at a high-rate flow of 0.1 lb/min to each suit. The oxygen high-rate mode is the normal mode employed during the reentry phase of flight. On manned flights, switching to the oxygen high-rate mode supply prior to reentry will be performed manually; however, the sequencer provided this signal on the GT-2 mission.

3.1.2.3.5 Water management: The water management system to be installed for manned flights consists of one drinking water tank in the cabin, two tanks in the equipment section, a water-transfer line, and a water management panel. (The cabin water tank was not installed in spacecraft 2.) The water-transfer line will connect the cabin tank to the tank in the adapter so that the cabin tank may be replenished when its water level becomes low. The water management panel, which was mounted in the cabin between the two ejection seats, normally provides manual controls for operating the system. (See fig. 3-5.)

The water management system on spacecraft 2 also included a temporary fuel-cell water pressure system which was designed to prevent fuel-cell water pressure from exceeding 20 ± 0.5 psia. Because the fuel cell water is highly corrosive, the system was designed to allow regulation of the water pressure indirectly. A water collection tank identical to the cabin water tank was installed in the adapter. The gas side of the water tank was charged with nitrogen and the regulator was to have controlled the nitrogen pressure.

3.1.2.4 Guidance and control. - The relationships of the major components included in the guidance and control system are illustrated by the block diagram in figure 3-11. Guidance and control system equipment installed in the left-hand equipment bay is shown in figure 3-12. The spacecraft 2 guidance and control system equipment was essentially identical to that planned for use on manned Gemini flights except for deletion of the radar range and range-rate indicator, and one of two redundant horizon sensors. A description of this system, which is more complete than the following, is given in reference 6.

3.1.2.4.1 Control system: The spacecraft 2 control system consisted of attitude control and maneuver electronics (ACME), one horizon sensor, and the associated controls and displays. The functions of the ACME components are described in the following paragraphs.

(a) Attitude control electronics (ACE): The ACE accepted signals from the guidance subsystems and rate gyros. These signals were, in turn, converted by the ACE into drive commands to the RCS solenoids and into on-off logic commands to the orbital attitude and maneuver electronics (OAME) subsystem.

UNCLASSIFIED

(b) Orbital attitude and maneuver electronics: The OAME converted signals accepted from the ACE into drive commands to the orbital attitude and maneuver system (OAMS) solenoids (see paragraph 3.1.2.7.1).

(c) Power inverter: The power inverter converted spacecraft dc voltage into ac voltage for use by the ACME, when not powered by the IGS power supply.

(d) Rate gyro packages: The rate gyro packages sensed angular rates about the pitch, roll, and yaw axes of the spacecraft.

The function of the horizon sensor was to sense spacecraft pitch and roll attitude variations with respect to the local vertical by receiving an input from the earth-space infrared radiation gradient. The sensor provided outputs proportional to the spacecraft attitude variations. The horizon sensor outputs will normally be applied to the ACME for orbit stabilization, or they will be used to align the inertial measuring unit (IMU) automatically. On this mission, the horizon-sensor signals were not used by the ACME or the IMU; however, the horizon sensor installed in spacecraft 2 was operated continuously to obtain performance data.

Command inputs to control the spacecraft will also be provided on manned flights by manual displacement of attitude and maneuver hand controllers located in the crew station (see paragraph 3.1.2.4.3). The controllers were installed for this mission, but they were not operated.

3.1.2.4.2 Inertial guidance system (IGS): The functions of the IGS were to provide known reference coordinates, to measure acceleration in this reference system, and to perform the necessary computations to convert these measurements into position information and into the required corrective maneuvers during all phases of the mission. The IGS also provided information to and received information from the digital command system (DCS) and the guidance and control display system. The IGS included the IMU, a digital computer system, and an auxiliary computer power unit (ACPU), with associated controls and displays.

The basic function of the IMU was to provide attitude reference and incremental velocity data. The IMU electronic circuits also provided the capability for detecting malfunctions in attitude reference and accelerometer output signals. The major components of the IMU were the following:

(a) Inertial platform: This unit consisted of a stable element (pitch block) suspended in a 4-axis gimbal structure. The assembly contained three gyros and three pendulous accelerometers.

UNCLASSIFIED

(b) Platform electronics package: Circuits were provided for gyro torque control, timing logic, spin motor power, accelerometer logic, accelerometer rebalance, and malfunction detection.

(c) IGS power supply: The IGS power supply unit converted spacecraft dc power into ac power for the IGS. It also provided dc power for the IGS, and in the event of a malfunction, it provided standby ac power for selected components normally supplied by the ACME power supply.

The digital computer provided parameter storage and performed computations necessary to develop guidance and control outputs. On manned flights, the type of computation to be performed will be determined by a computer mode selector, and a manual data insertion unit (MDIU) will provide a means for loading information into the computer memory and reading information out from the computer. However, information can also be inserted in the computer by the digital command system from ground stations.

The ACPU protects the computer in the event of spacecraft bus voltage variation. If the bus voltage drops for short periods (up to 100 milliseconds), the ACPU supplies temporary computer power. If the bus voltage remains low for longer periods, the ACPU automatically shuts the computer down.

3.1.2.4.3 Controls and displays: The functions of the major controls and displays associated with the guidance and control system were as follows (see fig. 3-5):

(a) Attitude display group (ADG):

(1) Flight director indicators (FDI's) - Two FDI's were mounted on the right-hand and left-hand instrument panels to display spacecraft quantities such as attitude measured by the IMU; spacecraft attitude rates determined by the ACME rate gyros; steering commands, range errors, and attitude errors determined by the computer.

(2) Flight director controllers (FDC's) - FDC's were mounted on the instrument panels adjacent to the FDI's to allow selection of the source and type of information to be displayed by the FDI's.

(b) Incremental velocity indicator (IVI): The IVI, which was mounted on the left-hand instrument panel, provided visual indications of computed velocity increments along each spacecraft translational axis required for or resulting from a specific maneuver. On manned missions, displays will be used during orbit insertion, orbit correction, rendezvous, and retrograde maneuvers.

UNCLASSIFIED

(c) Radar range and range-rate indicator: This instrument will normally be mounted on the left-hand instrument panel to display rendezvous radar range information; however, it was not installed for this mission.

(d) Manual data insertion unit (MDIU): As stated previously, the MDIU allows insertion, and read-out of computer data. It was mounted on the right-hand instrument panel and consisted of a keyboard and a read-out display.

(e) Attitude hand controller: This controller provides "rate," "pulse," or "direct" command signals when the handle is manually displaced. In the direct command mode, firing commands are applied directly to the RCS or OAME attitude solenoid valve drivers. In the pulse command mode, handle movements trigger a pulse generator in the ACE which supplies attitude commands to the RCS or OAME solenoid valve drivers. In the rate command mode, angular rates about each of the three spacecraft axes are controlled by the attitude hand controller. On this mission, the pulse and direct modes were not operated. Automatic attitude control modes were used for turnaround, attitude stabilization, retrograde attitude hold, and reentry requirements.

(f) Maneuver hand controller: When manually displaced, this controller provides translational command signals to the OAMS.

Table 3-IV identifies the switches associated with the guidance and control system and gives the positions in which they were placed prior to the GT-2 flight.

3.1.2.5 Time reference. - The time reference system consisted of an electronic timer, an event timer, and a Greenwich mean time (G.m.t.) clock. The electronic timer, which was mounted behind the instrument panel, provided time correlation for the PCM telemetry system and a record of elapsed time relative to lift-off for the computer. The event timer, mounted on the left-hand instrument panel (see fig. 3-5), provided a visual display for timing various short-term functions such as elapsed time during the ascent phase of the mission. The mechanical clock mounted on the right-hand instrument panel (see fig. 3-5), displayed Greenwich mean time and the calendar date. The clock also has a stop watch capability which will provide an emergency method of performing the functions of the event timer on manned flights. On GT-2, the time reference system operated from lift-off until after landing with the event timer and G.m.t. clock providing time correlation for the cameras.

3.1.2.6 Electrical. - The function of the electrical system was to supply and distribute electrical power at a nominal voltage of 24 V dc to all spacecraft devices which required electrical power for

UNCLASSIFIED

operation. Since this was primarily a dc system, any system which required ac power was supplied by a system inverter designed to meet the requirements of the particular system.

3.1.2.6.1 Power sources: Electrical power for spacecraft 2 was supplied by four silver-zinc main batteries, three silver-zinc squib batteries, and four silver-zinc special pallet batteries. A fuel cell was also installed in spacecraft 2; however, it was not used to supply spacecraft power.

The fuel cell, illustrated in figure 3-13, consisted of two sections, and each section contained three stacks, with 32 cells per stack. The fuel-cell reactants were stored in containers mounted adjacent to the fuel-cell sections.

The spacecraft 2 main batteries and squib batteries were installed in the right-hand equipment bay of the reentry assembly, as shown in figure 3-4. The four main batteries were 45 A-hr, 16-cell, silver-zinc batteries having a nominal terminal voltage of 25 V dc with no load applied. The three squib silver-zinc batteries were 16-cell, high-discharge-rate batteries which were designed to maintain a 15-V terminal voltage under a 100-A load for 1 second. The squib batteries also had a nominal 25 V dc terminal voltage with no load applied.

Four special pallet batteries were identical to the main batteries and were installed on the seat pallets in the crew station, as shown in figure 3-8.

3.1.2.6.2 Power distribution: Power was distributed throughout spacecraft 2 by a main bus, an isolated bus system, and two special pallet buses. The main bus serviced such major systems as the guidance and control system, the instrumentation system, and the communications system. The isolated bus system, consisting of two squib buses and a common control bus, supplied power to noise generating devices such as solenoids or relays in the OAMS, the RCS, the ECS, and the pyrotechnic system.

The two special pallet buses supplied all electrical power required by the equipment mounted on the seat pallets, and special pallet bus 2 (right-hand) also supplied power for the UHF tone generator.

3.1.2.7 Propulsion. - Spacecraft attitude and maneuver control was provided by three rocket engine systems. The OAMS provided the capability for translational maneuvering and control of spacecraft attitude during the period from spacecraft - launch-vehicle separation until initiation of the retrograde sequence. The RCS provided the means for controlling the reentry assembly attitude during the retrograde rocket firing and reentry phases of the flight. The retrograde rocket system

UNCLASSIFIED

has two functions. It is normally used to retard spacecraft velocity for reentry; however, in the event of an abort early in the launch phase, the retrorockets would have been used to propel the spacecraft away from the launch vehicle. Reference 7 provides descriptive information concerning the spacecraft propulsion systems in addition to that which follows.

3.1.2.7.1 Orbital attitude and maneuver system: The OAMS employed hypergolic propellants (nitrogen tetroxide and monomethylhydrazine), and a cold-gas helium pressure fed system. This system contained 16 fixed-mount thrust chamber assemblies (TCA's) mounted at various points around the adapter assembly, providing the capability for rotating the spacecraft about its three attitude control axes, and controlling translation in any direction. The system was used for normal separation of the spacecraft from the launch vehicle and would have been used to separate the spacecraft from the launch vehicle in the event that abort had become necessary late in the launch phase. The OAMS was also used for spacecraft turnaround and for attitude control between spacecraft separation and initiation of the retrograde sequence.

The pressurant, fuel, and oxidizer tanks were mounted in the equipment section as shown in figure 3-14. The TCA's were constructed to fire singly or in groups upon command from the automatic or manual controls. When commanded to fire, signals were transmitted through the ACME to selected TCA fuel and oxidizer solenoid valves.

Eight of the OAMS TCA's were used for attitude control and each thruster produced a nominal 23 pounds of thrust. The other eight OAMS TCA's will normally be used for translational maneuvers as follows: two 95-pound rated thrusters fire aft, two 79-pound rated thrusters fire forward, two 95-pound rated thrusters fire horizontally (one right and one left), and two 95-pound rated thrusters fire vertically (one up and one down). The two aft-firing TCA's were the only translational TCA's used on the GT-2 mission.

3.1.2.7.2 Reentry control system: The RCS employed the same propellants as the OAMS and was also a pressure fed system, but it employed nitrogen as a pressurant rather than helium. The RCS consisted of two identical, completely redundant systems designed to operate individually or simultaneously. These systems were designated A and B. Each system contained eight 23-pound TCA's arranged about the RCS section of the reentry assembly. Attitude control was maintained by firing the TCA's in pairs or in larger groups. Figure 3-15 shows the location of the TCA's, the propellant tanks, and the pressurant tank in the RCS section.

3.1.2.7.3 Retrograde rocket system: The retrograde rocket system consisted primarily of four solid-propellant rocket-motor assemblies symmetrically mounted in the retrograde section of the adapter assembly,

UNCLASSIFIED

as shown in figure 3-2. The solid propellant was a polysulphide ammonium perchlorate composition which was cast into the motor cases. Two pyrogen igniter assemblies were mounted 180° apart on the nozzle bulkhead of each motor case to ignite the propellant grain.

The normal mode of operation was used for GT-2. In this mode, the retrograde rockets were used to initiate spacecraft reentry, and the rocket motors were fired at nominal 5.5-second intervals. Each motor burned for approximately 5.4 seconds and produced approximately 2500 pounds of thrust. In the abort mode of operation, the retrograde rockets would be fired in salvo and would produce approximately 10 000 pounds of thrust.

On GT-2, the actual performance of the retrograde rockets was not monitored; however, the electrical signals resulting from the operation of relays which actuated the ignition devices were monitored, as well as the spacecraft accelerations. The acceleration data were used to determine the ignition time of each engine.

3.1.2.8 Pyrotechnic. - Various types of pyrotechnic devices were installed throughout the spacecraft to perform the following functions:

- (a) Separate major structural assemblies.
- (b) Open electrical circuits.
- (c) Release the horizon sensor fairing, the horizon sensors, and the nose fairing.
- (d) Actuate valves.
- (e) Actuate sequential functions in the parachute landing system.

Almost all of the pyrotechnic devices installed in spacecraft 2 were of the same configuration as those to be installed for manned missions; however, some of the devices, primarily in the ejection seat escape system, were not operational. The principal types of pyrotechnic devices installed in spacecraft 2 and their uses are described in the following paragraphs.

3.1.2.8.1 Flexible linear-shaped charge (FLSC): This material consisted of V-shaped flexible lead sheathing which contained a high-explosive core. Detonation of the core resulted in a cutting jet composed of explosive products and minute metal particles. The FLSC was used in the following separation assemblies of the spacecraft. (See fig. 3-16 for assembly locations.)

- (a) Spacecraft - launch vehicle separation assembly.

UNCLASSIFIED

(b) Equipment section - retrograde section separation assembly (Z-70).

(c) Retrograde section - reentry assembly separation assembly (Z-100).

3.1.2.8.2 Mild detonating fuse (MDF): This material was used to separate the R and R section from the RCS section of the reentry assembly. It was also used as an explosive interconnect to actuate operations in the parachute landing system, the ejection-seat escape system, and in the Z-70 and Z-100 separation assemblies.

When MDF was used as a separation device, it consisted of a strand of high explosive encased in lead sheathing and placed in grooves milled in a magnesium ring. The R and R section was attached to the RCS section by bolts with the MDF ring fastened to the R and R section at the mating surface. Detonation of the MDF broke the bolts, thus separating the sections.

When used as explosive interconnects, the MDF was enclosed in either flexible woven steel mesh hose or in rigid stainless-steel tubing.

3.1.2.8.3 Guillotines: These devices were used throughout the spacecraft to sever bundles of electrical wire and twisted steel cables. The body of the guillotine contained a piston-cutter, a cartridge installation, and an anvil attachment.

When initiated by an electrical signal, the cartridges produced gas pressure which exerted force on the piston-cutter. When sufficient force was applied, a shear pin broke and the piston-cutter struck against the anvil and severed the wire bundle or cable.

3.1.2.8.4 Tubing cutter-sealers: Devices of this type were employed to cut and seal steel tubes which contained OAMS propellants and oxidizer when the equipment section was jettisoned. The operation of the tubing cutter-sealers was similar to that of wire-bundle guillotines except for the addition of a crimper which sealed the tube ends.

3.1.2.8.5 Other pyrotechnic devices: The following additional types of pyrotechnic devices were installed:

(a) Pyrotechnic switches: These devices provided a positive means of opening electrical circuits. The switches were located in various places throughout the reentry assembly.

(b) Horizon-sensor fairing release assembly: This device secured the fairing to the spacecraft and released it when initiated by an electrical signal.

UNCLASSIFIED

(c) Horizon-sensor release assembly: This device was used to secure the horizon-sensor assembly to the spacecraft and to jettison it when initiated by the appropriate electrical signal.

(d) Pyrotechnic valves: These devices were one-time actuating valves installed in OAMS and RCS packages to provide positive control of fluids. Two types of valves were employed, normally open and normally closed.

(e) Parachute landing system pyrotechnic devices: The pyrotechnic portion of this system, as installed in spacecraft 2, consisted of a pilot parachute mortar, pilot parachute cutters, main parachute reefing cutters, and main parachute disconnects. Descriptions of these devices are given in reference 2.

(f) Ejection seat escape system pyrotechnic devices: The pyrotechnic portion of the ejection seat escape system consisted of the following:

- (1) Hatch actuator initiation system.
- (2) Hatch actuator assemblies.
- (3) Seat ejectors.
- (4) Harness release actuator assemblies.
- (5) Thruster assembly - seat/man separators.
- (6) Ballute deployment and release systems.
- (7) Drogue mortar - personnel parachutes.

These devices are also described in reference 2. The spacecraft 2 ejection seat escape system pyrotechnics were installed but not completely connected. MDF interconnects which propagate detonation waves to the hatch actuator assemblies were not connected, as well as the gas interconnects which conduct gas pressure to initiate the firing mechanisms of the seat ejectors.

3.1.2.9 Crew station furnishings and equipment. - The equipment installed in the crew station of spacecraft 2 was essentially the same as that to be used for later manned flights. It consisted basically of two ejection seats, controls, instrument panel displays, and switch panels. All controls, displays, and switch panels (except those required for rendezvous with an Agena target vehicle) were incorporated as shown in figure 3-5.

UNCLASSIFIED

On manned flights, the ejection seats will provide the crew with escape capability in the event of a launch-vehicle malfunction during the initial phase of launch, or a landing system malfunction during the final phase of reentry. In addition to the basic seat structure, the ejection seats will normally include personalized contours, restraint systems, egress kits (containing oxygen), survival kits, ballutes, and associated pyrotechnics.

Atop the ejection seats installed in spacecraft 2 were mounted pallets upon which were installed special instrumentation and crewman simulator sequencers as shown in figure 3-8. Mounting of the pallets necessitated the removal of certain ejection seat components including personalized contours, arm restraints, leg straps, foot stirrups, and backboard and egress-kit jettisoning equipment.

Since seat ejection capability was not required for this mission, both seats were clamped to the seat rails to minimize the possibility of vibration damage to the pallet instrumentation and equipment.

In addition to the provisions for mounting the seat pallets, other items omitted from the crew station equipment of spacecraft 2 were survival kits, drinking water dispenser, waste disposal system, personal hygiene system, and biomedical tape recorder.

3.1.2.10 Landing. - The spacecraft 2 landing system consisted of a pilot parachute and a main parachute.

3.1.2.10.1 Pilot parachute: The pilot parachute was an 18.3 foot-diameter ringsail parachute. It was installed in a mortar located in the forward end of the R and R section of the reentry assembly. A function of the pilot parachute was to separate the R and R section from the reentry assembly, thus deploying the main parachute. Another function of the pilot parachute was to prevent recontact of the R and R section with the main-parachute canopy.

3.1.2.10.2 Main parachute: The main parachute was an 84.2-foot-diameter ringsail parachute designed to provide stable descent of the reentry assembly at a nominal vertical velocity of 29.8 ft/sec at touchdown.

3.1.2.10.3 Landing system sequence: The planned GT-2 landing system sequence is described as follows. The sequence began with the arming of the landing squib bus at 5.5 seconds after separation of the retrograde section from the reentry assembly. Operation of a barostat at an altitude of 10 600 feet energized the pilot parachute mortar squibs, which in turn initiated several time delay sequences. After barostat operation, the pilot parachute was mortared and remained in a reefed

UNCLASSIFIED

condition for 6 seconds after deployment. At the conclusion of a 2.0-second delay after barostat operation, the R and R section separated from the reentry assembly. As the pilot parachute pulled the R and R section away from the reentry assembly, the main parachute deployed from the open end of the R and R section in a reefed condition and supported the reentry assembly from a single-point attachment. The main parachute was disreefed 10 seconds after line stretch.

Beginning with the pilot parachute mortar, a period of 22 seconds was allowed for the reentry assembly to become stabilized on the fully opened main parachute. At the end of this period, the single-point attachment was released, repositioning the reentry assembly to the proper attitude for water landing (nose, 35° above the horizon) by means of a two-point bridle support. A 10-minute delay, beginning at pilot parachute deployment, was allowed for the spacecraft to land. At the end of this period, a timer switch initiated the bridle disconnect squibs which released the main parachute from the reentry assembly.

3.1.2.11 Postlanding and recovery. - Provisions incorporated in the spacecraft to aid in its recovery included the UHF recovery beacon¹, recovery flashing light, fluorescent dye marker, and hoist loop.

The UHF recovery beacon was provided to transmit homing signals on the international distress frequency of 243 megacycles. The UHF recovery beacon was compatible with existing ARA-25 and SARAH receivers. The beacon, which was mounted in the right-hand equipment bay of the reentry assembly, was sequenced to activate 30 seconds after pilot parachute mortar.

The recovery flashing light and fluorescent dye marker were provided to aid in the visual location of the spacecraft during postlanding operations. The recovery flashing light was mounted on a retractable assembly located near the aft end of the reentry assembly between the hatches, as shown in figure 3-7. The light was designed to extend automatically by means of a torsion spring mechanism at the same time the main parachute was released; after extension, the light was to receive power from its own power supply. The dye marker container, located in the RCS section of the reentry module, was constructed with openings covered with water soluble film. The film dissolved upon immersion, allowing the dye to disperse and provide a marker for visual location of the reentry assembly.

¹The UHF and HF voice transceivers were also planned for use as recovery aids by providing direction finding signals. Descriptions of these devices are given in paragraph 3.1.2.1.1.

UNCLASSIFIED

A spring-loaded hoist loop was provided to facilitate the engagement of a hoisting hook. It was located near the heat shield between the hatches. The hoist loop was designed to extend automatically at the time of main parachute release.

On manned missions, one UHF survival radio beacon will be included in each crew member's survival kit in case the reentry assembly must be abandoned. These beacons were not included in the spacecraft 2 equipment.

3.2 GEMINI LAUNCH VEHICLE DESCRIPTION

This section describes the Gemini launch vehicle (GLV) for the GT-2 mission. The description is intended to serve as the basic description of all launch vehicles to be used for future Gemini missions and will not be repeated in the mission reports subsequent to GT-2. Only modifications to the GLV incorporated in vehicles used for future missions will be described in the reports of those missions, and the modifications will be referenced to the GLV description contained in this report. The major differences between the launch vehicles used for the GT-1 and GT-2 missions are noted in table 3-V.

The launch vehicle was a two-stage intercontinental ballistic missile (Titan II) which had been modified and "man rated" for use in the Gemini Program. The propulsion system in each stage used hypergolic propellants. Modifications made to the basic Titan II vehicle to achieve the "man rated" GLV are as follows:

- (a) Addition of a completely redundant malfunction detection system (MDS).
- (b) Replacement of the Titan II inertial guidance system with the Mod III-G radio guidance system (RGS).
- (c) Addition of a three-axis reference system (TARS) to provide attitude reference and also to provide open-loop programming to the autopilot.
- (d) Addition of a secondary flight control system (FCS).
- (e) Addition of a secondary stage I hydraulic system.
- (f) Addition of the capability of switchover to the secondary guidance, flight control, and hydraulic system.

UNCLASSIFIED

- (g) Provision of redundancy in electrical sequencing by accessory power supply (APS) and instrumentation power supply (IPS).
- (h) Provision of an engine shutdown capability from the spacecraft.
- (i) Provision of a 120-inch-diameter cylindrical skirt forward of the stage II oxidizer tank for mating the spacecraft to the launch vehicle.
- (j) Removal of the retrorockets, vernier rockets, and allied equipment.
- (k) Addition of fuel line spring-piston accumulators and oxidizer line tuned standpipes to suppress longitudinal oscillations.

3.2.1 Structure

The launch vehicle was primarily of semi-monocoque shell construction (stage II tank barrels are monocoque) with fuel and oxidizer tanks integral with the structure. The basic diameter of the structural vehicle was 10 feet, and the length was 89.27 feet. Stage I, which included the interstage transportation section, the fuel tank, and the oxidizer tank, was 70.67 feet long. The transportation section was attached to the tank assembly by a manufacturing splice located at vehicle station 621. (See fig. 3-3.)

Stage II, consisting of the fuel tank assembly and the oxidizer tank assembly, was 28.27 feet long. The two stages were joined together at vehicle station 500 by four studs employing eight explosive nuts, the latter being used for staging. On both stage I and stage II, external conduits were provided along the fuel and oxidizer tanks to house and support the propulsion and electrical lines which led into the various vehicle compartments. (See fig. 3-3.)

3.2.1.1 Stage I. - The stage I structure consisted of a fuel tank, an oxidizer tank, skirts at each end of the tanks, an interstage structure, and external conduits. Channel-shaped, high-strength longerons, mounted externally on the fuel-tank aft skirt, provided separate interfaces for engine-truss attachment and launch-stand tiedown. The propellant tanks were capable of withstanding ground and prelaunch loads with no internal pressure applied.

The fuel tank was completely welded aluminum alloy structure. It consisted of an ellipsoidal-shaped forward dome, a cylindrical barrel section, and the aft-cone assembly. An internal conduit, welded to the forward and aft domes, provided for passage of a single oxidizer line from the oxidizer tank through the fuel tank to the engine assembly.

UNCLASSIFIED

The oxidizer tank consisted of two end domes welded to a cylindrical section. During staging, the forward dome and the surrounding skirt structure were protected from the heat and blast of the stage II engine exhaust by an ablative coating material. Aluminum alloy welded trusses were installed within this structure to support subassembly components.

The interstage section consisted of the structure between the stage separation plane and the oxidizer-tank forward skirt. Approximately 7100 sq in. of blast port area were provided at the aft end of the interstage section for venting of the stage II exhaust during staging.

3.2.1.2 Stage II.- The stage II structure included an oxidizer tank, a fuel tank, skirts at the forward and aft ends of each tank, and external conduits. The tanks were capable of withstanding ground and prelaunch loads with no internal pressure applied.

The fuel tank consisted of two ellipsoidal-shaped domes, each welded to an extruded aluminum-alloy ring frame which formed the juncture of the dome, tank wall, and skirt. The cap in the forward dome had a hole to accommodate the passage of the oxidizer line through this tank. The aft dome had provisions for passage of the oxidizer line and for a single fuel outlet. The aft skirt extended to the stage separation plane.

The between-tanks compartment consisted of the forward section which was welded to the oxidizer-tank aft-dome ring frame and the aft section which was welded to the fuel-tank forward-dome ring frame. Aluminum-alloy welded trusses were installed within this structure to support subassembly components.

The oxidizer tank was similar to the fuel tank. It consisted of two ellipsoidal-shaped domes, each welded to an extruded aluminum-alloy ring frame which formed the juncture of the dome, tank wall, and skirt. The aft dome contained the outlet for the oxidizer line. The forward skirt formed the interface between the spacecraft and the launch vehicle. Tension bolts were used in 20 external lugs, which were machined as part of the interface frame to attach the spacecraft to the launch vehicle. An external 0.05-inch-thick insulating coating was applied to the forward skirt to protect it in event of protuberance heating.

3.2.2 Major Systems

3.2.2.1 Propulsion system.- The two-stage propulsion system for the Gemini launch vehicle was adapted from the system used on the Titan II missile. Minor changes were made to eliminate the elements of the Titan II system not required for the Gemini mission and to "man rate" it for use in a spacecraft launch vehicle.

UNCLASSIFIED

3.2.2.1.1 Stage I: The stage I engine consisted of two independently operated subassemblies mounted on a single engine frame and designed to operate simultaneously. Each subassembly contained a thrust chamber, a turbopump and a gas generator. The thrust chambers were gimbaled to permit control and stabilization of the vehicle in flight. Gimbal action was provided by tandem hydraulic actuators which operated in response to signals from the flight control system.

Propellants were fed to the thrust chamber by turbopumps. Gas generators, used to drive the turbopumps, used the same propellants discharged by the pumps thus allowing the engine to "bootstrap" during steady-state operations. Propellants consisted of fuel, which was 50-percent hydrazine combined with 50-percent unsymmetrical-dimethyl hydrazine, and oxidizer (nitrogen tetroxide). This hypergolic mixture eliminated the need for combustion chamber igniters. Engine start was initiated by solid propellant cartridges which provided hot gas to start and drive the turbopumps during the engine start period. The thrust chambers were regeneratively cooled by circulating fuel through coolant tubes within the chamber walls. A dry-jacket start was employed.

In-flight propellant tank pressurization was provided by an auto-genous (self-generating) pressurization system. The fuel tank was pressurized by small portions of the gas-generator exhaust-gas output. A heat exchanger was provided to cool the gas generator exhaust before supplying it to the fuel tank for pressurization. The oxidizer tank was pressurized by oxidizer which had been heated to a gaseous state. Liquid oxidizer, supplied under pressure from the turbopump, was directed through a superheater where it was vaporized by the heat from the turbine exhaust.

3.2.2.1.2 Stage II: The stage II engine was a single-chamber unit similar in operation to the stage I engine. However, this engine was designed for operation at high altitude. An ablative skirt was attached to the regeneratively cooled thrust chamber to increase the nozzle expansion ratio for high-altitude performance improvement.

Like stage I, the thrust chamber was gimbaled. Since only pitch and yaw control was provided with the one engine, a roll nozzle was incorporated to permit roll control. This nozzle directed gas generator exhaust gas overboard, and roll control was obtained through swivel action of the nozzle. An autogenous pressurization system was provided to pressurize the fuel tank in a manner similar to that of stage I. The oxidizer tank was pressurized before launch, and no additional pressurization was required.

3.2.2.2 Flight control system. - The redundant flight control system (FCS) consisted of three systems designated as the primary guidance

UNCLASSIFIED

and control system, the secondary guidance and control system, and the switchover system.

The primary system consisted of a three-axis-reference system (TARS), an adapter package, a stage I rate gyro package, an autopilot, the primary servo valves in the stage I tandem actuators, and the stage II hydraulic actuators. The TARS was used to establish angular reference along the pitch, roll, and yaw axes; to provide roll and pitch programmed rates during stage I flight; to accept pitch and yaw radio guidance steering signals during stage II closed-loop guidance operation; and to provide discrete timing functions. The main function of the adapter package was to condition attitude outputs from the TARS for inputs to the autopilot. The package also housed the FCS switchover relays. The Mod III-G radio guidance system provided steering commands to the primary control system during stage II flight.

The secondary system consisted of a duplicate stage I rate gyro package, a duplicate autopilot, the secondary servo valve in the stage I tandem actuators, and the stage II hydraulic actuators. The spacecraft inertial guidance system provided stabilization and steering commands to the secondary control system.

The switchover system consisted of the redundant power amplifiers located in the malfunction detection package (MDP), the flight control system switchover relays located in the adapter package, the stage I tandem actuator switchover valve, pressure switches and hardover sensors, and the MDS rate switches.

Two sets of rate gyros were used for launch vehicle stabilization - the stage I rate gyro package (one each for the primary and secondary systems) and the stage II rate gyros located within the redundant autopilot assemblies. During stage I flight, signals from both the stage I and stage II pitch and yaw rate gyros were summed in a given proportion.

The autopilot contained an 800-cps static inverter, stage II rate gyros, gain switching module, channel amplifiers, and valve drive amplifiers. The rate and displacement gyro signals were suitably amplified, demodulated, mixed, and dynamically compensated, with filtering, in the autopilot to provide vehicle stability. The autopilot output signals were used to drive the servo valves.

Both the primary and secondary flight control systems operated at all times during flight, and during stage I flight, each servo valve coil in the stage I tandem actuators received control signals. At switchover, control of the tandem actuator is switched from the primary to the secondary servo valve.

UNCLASSIFIED

3.2.2.3 Radio guidance system.- The Mod III-G RGS was used to guide the GLV stage II and spacecraft combination in the proper trajectory. The RGS accomplished this by using steering commands to torque the pitch and yaw attitude gyros in the TARS. The RGS also supplied the stage II shutdown signal (SECO) in the primary mode. The airborne components of the RGS were the pulse beacon unit, the rate beacon unit, decoder unit, and antenna system.

Vehicle rates were derived by means of the Doppler principle, and position tracking radar was used to derive the vehicle position as a function of range, elevation, and azimuth. The vehicle position and rate information were used by the ground-based guidance computer to generate the steering commands. The messages that contained the steering commands and SECO discrete were monitored by the decoder for validity. If the message is found to be valid, the steering commands are supplied to the control system as pitch and yaw corrections; and the SECO command, when present, is supplied to the engine shutdown circuitry.

3.2.2.4 Hydraulic system.- The stage I hydraulic system was redundant. Separate primary and secondary hydraulic circuits powered the four tandem actuators for positioning the two thrust chambers in response to signals from the FCS. The system contained two engine-driven pumps, two accumulator-reservoirs, four tandem actuators, one electrical motor pump (used during prelaunch checkout), one test selector valve, one in-line filter, two coaxial disconnects, and instrumentation transducers. Each tandem actuator contained two hydraulically and electrically separated servo loops which could be switched from primary to secondary by external command or by a pressure loss in the primary system. Each circuit was powered during engine operation by a variable-displacement pressure-compensated pump driven through the accessory gearbox of each subassembly. For tests and during the launch countdown, the electric motor pump powered the system.

The stage II hydraulic system contained an engine-driven pump, two engine actuators, a roll-nozzle actuator, an accumulator-reservoir, an electric motor pump, an in-line filter, a coaxial disconnect, and instrumentation transducers. The system was not redundant, and operation was the same as that for a single system on stage I.

3.2.2.5 Electrical system.- The GLV electrical system was divided into a power distribution system and a sequencing system. The power distribution system consisted of the accessory power supply (APS) and the instrumentation power supply (IPS). The APS and IPS buses were provided with airborne power from separate 28 V dc silver-zinc rechargeable batteries.

The APS provided power to the static inverter, the MDS, the APS-command receiver, the APS-shutdown circuitry for shutdown of stage I and

UNCLASSIFIED

stage II and destruct of stage II, the RGS, the FCS, the sequencing system, and the stage II engine-start circuitry. Static inverter output was 115/200 volts, 400 cps, at 750 V A.

The IPS provided power to the MDS, MISTRAM, the IPS-command receiver, the IPS-shutdown circuitry for shutdown of stage I and stage II and destruct of stage II, the FCS, the sequencing system, stage II engine-start circuitry, and the airborne instrumentation system.

The sequencing system provided the proper sequencing of events from stage I engine start to stage II engine shutdown. Major functions were: reset stage I prevalues switch, actuate APS and IPS staging switches, shut down stage I engine, fire staging nuts, start stage II engine, and arm stage II shutdown relays.

Redundancy in the form of dual power supplies, relays, motorized switches, diodes, and wiring was used throughout the GLV electrical system. A separate battery was provided in stage I to supply power to the engine shutdown and destruct system if inadvertent separation occurred.

3.2.2.6 Malfunction detection system (MDS). - The malfunction detection system was provided to monitor launch-vehicle performance and to supply indications of potentially catastrophic malfunctions and certain significant flight events to the spacecraft. An automatic function was provided for switching from the primary stage I flight control-guidance-hydraulic combination to the secondary system in the event of a failure in the primary system. Switchover could be initiated by pitch, yaw, or roll overrate; stage I engine hardover; loss of primary system hydraulic pressure; or ground command through the spacecraft digital command system (DCS). The last function, as well as switch back to the primary system, will be a pilot function on future manned missions.

Main components of the MDS were the malfunction detection package (MDP), the rate switch package (RSP), and the various bilevel and analog sensors located throughout the launch vehicle. All circuits, components, and wiring of the MDS were redundant to provide high reliability.

Functions monitored by the MDS include the following: stage I engine chamber pressure, stage II fuel injector pressure, propellant tank pressures, excessive angular rates, staging, loss of stage I primary hydraulic pressure, engine hardover, and switchover.

3.2.2.7 Instrumentation system. - The airborne instrumentation system was composed of various transducers or measuring points (see table 3-VI), signal conditioners, program board, PCM multiplexer, PCM-FM telemetry unit, tape recorder-reproducer, and an antenna system.

UNCLASSIFIED

The PCM telemetry was a time-multiplexed data system with an input capacity of 196 analog and 48 bilevel channels. The output was a serial pulse train. Samples of input data were as follows:

Number of channels	Rate, samples/sec
Analog	
85	20
35	40
36	100
20	200
20	400
Bilevel	
40	20
8	100

The major components of the FM telemetry were an FM multiplexer subcarrier oscillator assembly, an RF transmitter, and a separate power amplifier. The system had a seven-channel data capacity.

Prior to staging, the seven FM channels were switched to monitor staging functions, and these signals were transmitted in real time and paralleled on the tape recorder. The recorder was programmed to play back its recording after completion of the staging event.

3.2.2.8 Range safety system - The GLV range safety system was comprised of the MISTRAM system, command control system, and ordnance destruct systems.

The primary tracking and impact prediction system employed in the GLV was the MISTRAM system. The system consisted of an airborne transponder, antenna, and ground stations located at Valkaria, Florida, and Eleuthera. In operation, the airborne transponder received two CW signals from the ground station and displaced and retransmitted them back

UNCLASSIFIED

to the ground station for computation of accurate position, velocity, and impact prediction information. Since line-of-sight transmission between the GLV and Valkaria was impossible before lift-off and during the first few seconds after lift-off, MISTRAM could not lock on until the launch vehicle had attained an altitude of approximately 8000 feet. A beacon system in the spacecraft combined with an AN/FPS-16 radar was used to supply backup tracking information.

The command control system consisted of two ACI receivers, four flush-mounted antennas, a six-port junction, and interconnecting cable. The redundant receivers each contained a decoder unit which was capable of receiving a coded frequency-modulated signal from the ground station and converting this signal (tones) into commands for (1) engine shutdown and warning to the spacecraft, (2) destruct (command 1 must be received before command 2 can take effect), and (3) auxiliary second-stage cut-off (ASCO) which was a backup to RGS/IGS stage II engine shutdown. The ASCO command originated at the Burroughs ground guidance computer.

The ordnance destruct system components consisted of destruct initiators, primacord, and bidirectional destruct charges. The initiators were basically out-of-line explosive trains which were armed by aerospace ground equipment (AGE) prior to lift-off. Each of the initiators was connected to two bidirectional destruct charges which were located 180° apart, midway between the fuel and oxidizer tanks in each stage. Upon receipt of command 2, the IPS and APS electrical signals would have caused the initiators to ignite the primacord, thus setting off the destruct charges which would have ruptured the tanks.

The stage I inadvertent separation destruct system was designed to function up to the time of staging enable (approximately LO + 145 sec). This system consisted of a separate destruct battery; lanyard switches between stages I and II; and the same stage I initiators, primacord, and destruct charges used in the command control ordnance destruct system. Should stage I have inadvertently separated from stage II prior to staging enable, the lanyard switches would have routed the output of the stage I destruct battery to stage I engine shutdown and through a 5.5-second delay timer to the initiators, causing the destruct charges to explode.

3.2.2.9 Ordnance separation system.- The launch separation system used ordnance devices at the four vehicle-to-pad attachment points. Each attachment point had one interconnecting stud with an explosive nut on each end. Each nut assembly contained a gas pressure cartridge with two independent bridgewires mounted internally. The circuits for these bridgewires were activated by a master operations control system (MOCS) signal to the launch release control set 2 seconds after the thrust chamber pressure switches (TCPS) made contact.

UNCLASSIFIED

The airborne separation system used ordnance devices at the four stage I and stage II attachment points located at vehicle station 500. Each attachment point had one interconnecting stud with an explosive nut on either end. Each nut assembly was similar to that of the launch separation system. The cartridges were ignited electrically by the staging command (initiated by TCPS).

UNCLASSIFIED

~~CONFIDENTIAL~~

3.3 GT-2 WEIGHT AND BALANCE DATA

Weight data for the GT-2 space vehicle is shown in the following table:

Condition	Weight (including spacecraft), lb (a)
Ignition	343 626
Lift-off	340 072
BECO	83 813
Stage II, start of steady-state combustion	72 617
Stage II burnout	13 504

^aPostflight trajectory weights obtained from Aerospace Corporation, as measured during the flight.

Spacecraft weight and balance data are as follows:

Condition	Weight, lb	Center of gravity location, in. (a)		
		X	Y	Z
Launch, gross weight	6882.88	-1.52	-1.99	114.01
Retrograde	5439.03	0.12	-1.92	130.46
Reentry	4776.58	0.07	-1.96	136.16
Main parachute deployment	4450.77	0.07	-2.08	130.48
Touchdown (no parachute)	4340.89	0.07	-2.15	128.44

^aZ-axis reference was located 13.44 inches aft of the launch vehicle-spacecraft mating plane (GLV station 290.265). The X- and Y-axes were referenced to the centerline of the vehicle.

~~CONFIDENTIAL~~

UNCLASSIFIED

TABLE 3-I.- SPACECRAFT MODIFICATIONS

System	Significant differences from manned configuration	
	Spacecraft 1 ^a	Spacecraft 2
Reentry assembly structure	(a) Heat shield counter-bored to insure complete destruction during reentry (b) Ballasted to simulate weight and center of gravity of production configuration	Heat shield ablative material reduced to approximately $\frac{1}{2}$ thickness of production design
Adapter assembly structure	Dummy equipment mounted on aluminum alloy truss beam bolted to primary structure	None
Communications	Not installed, with the exception of one C-band radar transponder, three telemetry transmitters, and associated equipment	(a) One of two UHF voice transceivers deleted (b) One of two HF voice transceivers deleted (c) Mid-frequency telemetry transmitter deleted (d) Two of two UHF survival beacons deleted (e) Microphones and headsets deleted
Instrumentation	Not installed. Special instrumentation system used.	Special instrumentation system installed. Special hi-speed production PCM tape recorder installed.
Environmental control	Not installed, with the exception of a cabin pressure relief valve and a special prelaunch cooling system	Secondary O ₂ high-rate flow set at 0.1 pound/minute
Guidance and control	Not installed	(a) One of two horizon sensors deleted (dummy installed in place of secondary sensor) (b) Range and range rate indicator deleted (c) Rendezvous radar deleted
Time reference	Not installed	None
Electrical	(a) Power source consisted of one 24 volt dc 45 ampere-hour, silver-zinc battery installed on left-hand pallet (b) Electrical umbilical to adapter was connected only to test umbilical ejection system	(a) Power source consisted of four silver-zinc main batteries and three silver-zinc squib batteries installed in right-hand equipment bay of reentry module, and four silver-zinc batteries installed on seat pallets. (b) Fuel cell module was installed in the adapter equipment section, but was not connected to a load.
Propulsion	Not installed	None
Pyrotechnic	Not installed	None
Crew station furnishings and equipment	(a) Pallets installed on ejection seat rails for mounting special instrumentation and communications equipment (b) Pressure, temperature and vibration sensors installed in cabin (c) Ballast weights installed on ejection seat rails	(a) Pallets containing crewman simulators and special instrumentation installed on ejection seats (b) Food, water, and waste management system components deleted (c) Some ejection seat parts removed
Landing	Not installed	High altitude drogue parachute not installed
Postlanding and recovery	Not installed	Survival kits containing UHF survival beacons and other recovery aids deleted

^aSee reference 1 for description of spacecraft 1

UNCLASSIFIED

TABLE 3-II.- COMMUNICATIONS EQUIPMENT

Equipment	Spacecraft 2	Spacecraft 3 and subsequent spacecraft
Voice communications:		
HF voice transmitter receiver (HF/TR)	1	2
UHF voice transmitter receiver (UHF/TR)	1	2
Voice control center (VCC)	1	1
Telemetry transmitters:		
Low frequency - real time	1	1
Mid frequency - delayed time	0	1
High frequency - standby	1 (used as delayed time XMTR)	1
Tracking subsystem:		
C-band transponder	1	1
S-band transponder	1	1
Acquisition aid beacon	1	1
Recovery subsystem:		
UHF recovery beacon	1	1
UHF survival beacon	0	2
Flashing light	1	1
Digital command system (DCS)	1	1
Antenna subsystem:		
Recovery antenna (UHF)	1	1
UHF stub antenna	1	1
Descent antenna (UHF)	1	1
C-band helices	3	3
Phase shifter	1	1
Power divider	1	1
HF whip antenna	1	1
C-band slot	1	1
S-band slot	1	1
UHF whip antenna	2	2
Quadriplexer	1	1
Diplexer	1	1
Coaxial switches	6	6

UNCLASSIFIED

TABLE 3-III. - SPACECRAFT INSTRUMENTATION MEASUREMENTS FOR GT-2

Measurement	Description	Instrumentation range	Type of data
AA01	Time since lift-off	LSB = 1/8 sec	Delayed time
AA02	Time since lift-off	LSB = 1/8 sec	Delayed time
AA03	Time to T _R	LSB = 1/8 sec	Delayed time
AB01	Stage II cut-off (IGS command)	1 = cut-off	Delayed time
AB02	Spacecraft shaped charge fire	1 = fire	Delayed time
AB03	Launch vehicle - space- craft separation	1 = separation	Delayed time
AB04	Launch vehicle cut-off command	1 = cut-off	Delayed time
AB06	Autopilot switch command	1 = command	Delayed time
AB07	Nose fairing jettison	1 = jettison	Delayed time
AB08	Scanner fairing jettison	1 = jettison	Delayed time
AD01	Adapter shaped charge fire	1 = fire	Delayed time
AD02	Equipment section separation	1 = separation	Delayed time
AD03	Automatic retrofire initiation	1 = fire	Delayed time
AD04	Retrograde section separation	1 = separation	Delayed time
AD05	Retrograde shaped charge fire	1 = fire	Delayed time
AD06	Manual retrofire initiate	1 = fire	Delayed time
AD08	Retrorocket 3 fire	1 = fire	Delayed time
AD09	Retrorocket 2 fire	1 = fire	Delayed time
AD10	Retrorocket 4 fire	1 = fire	Delayed time
AE01	R and R section separation	1 = separation	Delayed time
AE02	Pilot parachute deployed	1 = deploy	Delayed time
AE13	Parachute jettisoned	1 = jettison	Delayed time
AF01	Astronaut actuated abort	1 = abort	Delayed time
AF02	Right ejection seat gone	1 = gone	Delayed time
AF03	Left ejection seat gone	1 = gone	Delayed time
AF04	Emergency retrofire salvo relay	1 = fire	Delayed time
AG02	Pitch rate gyro, primary, on/off	1 = on	Delayed time
AG03	Roll rate gyro, primary, on/off	1 = on	Delayed time

UNCLASSIFIED

TABLE 3-III. - SPACECRAFT INSTRUMENTATION MEASUREMENTS FOR GT-2 - Continued

Measurement	Description	Instrumentation range	Type of data
AG04	Yaw rate gyro, primary, on/off	1 = on	Delayed time
AG05	Platform, on/off	1 = on	Delayed time
AG09	ACME rate command mode, on/off	1 = on	Delayed time
AG10	Pitch rate scale factor	1 = ± 2.5 deg/sec	Delayed time
AG11	Roll rate scale factor	1 = ± 2.5 deg/sec	Delayed time
AG12	Yaw rate scale factor	1 = ± 2.5 deg/sec	Delayed time
AG13	Pitch rate gyro (secondary), on/off	1 = on	Delayed time
AG14	Roll rate gyro (secondary), on/off	1 = on	Delayed time
AG15	Yaw rate gyro (secondary), on/off	1 = on	Delayed time
AG16	Horizon sensor (primary), on/off	1 = on	Delayed time
BA01	Oxygen mass quantity	0 to 100 percent	Delayed time
BA02	Oxygen tank pressure	0 to 1000 psia	Delayed time
BA03	Hydrogen mass quantity	0 to 100 percent	Delayed time
BA04	Hydrogen tank pressure	0 to 350 psia	Delayed time
BBO3	O ₂ to H ₂ O differential pressure, section 1	1.23 to 3.1 psid	Delayed time
BBO4	O ₂ to H ₂ O differential pressure, section 2	1.23 to 3.1 psid	Delayed time
BBO5	Temperature at heat exchanger outlet	50 to 150° F	Delayed time
BC01	H ₂ to O ₂ differential pressure, section 1	0.03 to 1.37 psid	Delayed time
BC02	H ₂ to O ₂ differential pressure, section 2	0.03 to 1.37 psid	Delayed time
BC03	Temperature at heat exchanger outlet	50 to 150° F	Delayed time
BD10	Current, dummy load	0 to 20 A	Delayed time
BE10	Current, dummy load	0 to 20 A	Delayed time
BF01	Main battery 1 temperature	0 to 200° F	Delayed time
BFO5	Squib battery 1 temperature	0 to 200° F	Delayed time
BF07	Main battery 1, on/off	1 = on	Delayed time

UNCLASSIFIED

TABLE 3-III.- SPACECRAFT INSTRUMENTATION MEASUREMENTS FOR GT-2 - Continued

Measurement	Description	Instrumentation range	Type of data
BF08	Main battery 2, on/off	1 = on	Delayed time
BF09	Main battery 3, on/off	1 = on	Delayed time
BF10	Main battery 4, on/off	1 = on	Delayed time
BG01	Main bus voltage	15 to 35 V	Delayed time
BG02	Squib bus 1 voltage (armed)	15 to 35 V	Delayed time
BG03	Squib bus 2 voltage (armed)	15 to 35 V	Delayed time
BG04	Control bus voltage	15 to 35 V	Delayed time
BH01	Battery and FC, section 1	0 to 50 A	Delayed time
BH02	Battery and FC, section 2	0 to 50 A	Delayed time
CA01	O ₂ mass quantity, primary system	0 to 100 percent	Delayed time
CA02	O ₂ tank pressure, primary system	0 to 1000 psia	Delayed time
CA03	O ₂ supply pressure 1, secondary system	0 to 6000 psia	Delayed time
CA04	O ₂ supply pressure 2, secondary system	0 to 6000 psia	Delayed time
CB01	Cabin pressure (to forward compartment)	0 to 6 psid	Delayed time
CB02	Cabin air temperature	40 to 200° F	Delayed time
CB03	Inner skin temperature	0 to 200° F	Delayed time
CB07	Forward compartment absolute pressure (reference)	0 to 15 psia	Delayed time
CC01	Suit pressure, left (to cabin)	0 to 6 psid	Delayed time
CC02	Suit pressure, right (to cabin)	0 to 6 psid	Delayed time
CC03	Suit inlet air temperature, left	50 to 100° F	Delayed time
CC04	Suit inlet air temperature, right	50 to 100° F	Delayed time
CC05	Oxygen high rate	1 = high rate	Delayed time
CD01	Inlet to FC section 1, primary	90 to 140° F	Delayed time
CD02	Inlet to FC section 2, secondary	90 to 140° F	Delayed time

UNCLASSIFIED

TABLE 3-III.- SPACECRAFT INSTRUMENTATION MEASUREMENTS FOR GT-2 - Continued

Measurement	Description	Instrumentation range	Type of data
CD03	Outlet of radiator control, primary	20 to 80° F	Delayed time
CD04	Outlet of radiator control, secondary	20 to 80° F	Delayed time
CD07	Inlet to FC/battery control, primary	90 to 140° F	Delayed time
CD08	Inlet to FC/battery control, secondary	90 to 140° F	Delayed time
CD09	Inlet - radiator bypass valve, primary	-20 to 160° F	Tape recorded
CD10	Inlet - radiator bypass valve, secondary	-20 to 160° F	Delayed time
CD11	Inlet - radiator control valve, primary	-80 to 80° F	Delayed time
CD12	Inlet - radiator control valve, secondary	-80 to 80° F	Delayed time
CE01	Pump A, primary loop	1 = pump failure	Delayed time
CE02	Pump B, primary loop	1 = pump failure	Delayed time
CE03	Pump A, secondary loop	1 = pump failure	Delayed time
CE04	Pump B, secondary loop	1 = pump failure	Delayed time
CF03	Section 2 outlet temperature	80 to 180° F	Delayed time
CF04	Section 1 outlet temperature	80 to 180° F	Delayed time
CJ01	Inlet pressure, primary loop	0 to 100 psia	Delayed time
CJ02	Inlet pressure, secondary loop	0 to 100 psia	Delayed time
CJ03	Differential pressure, pump, primary loop	0 to 230 psid	Delayed time
CJ04	Differential pressure, pump, secondary loop	0 to 230 psid	Delayed time
CJ05	Reservoir, low-level indicator, primary	1 = low	Delayed time
CJ06	Reservoir, low-level indicator, secondary	1 = low	Delayed time
CL01	Water pressure (FC mod)	0 to 22 psia	Delayed time
DB03	IMU TCA output, X-axis accelerometer	0 to 40 volts	Delayed time
DB06	IMU TCA output, X-axis gyro	0 to 40 volts	Delayed time
DC01	Accelerometer malfunction	1 = malfunction	Delayed time

UNCLASSIFIED

TABLE 3-III.- SPACECRAFT INSTRUMENTATION MEASUREMENTS FOR GT-2 - Continued

Measurement	Description	Instrumentation range	Type of data
DC02	Attitude malfunction	1 = malfunction	Delayed time
DC03	Computer malfunction	1 = malfunction	Delayed time
DD01	Pitch error (launch) or down range error (reentry)	$\pm 6^\circ$ or ± 20 n. mi.	Delayed time
DD02	Roll error (launch) or bank angle (reentry)	$\pm 6^\circ$ or $\pm 20^\circ$	Delayed time
DD03	Yaw error (launch) or cross range error (reentry)	$\pm 6^\circ$ or ± 20 n. mi.	Delayed time
DE01	35 V dc	32 to 38 V dc	Delayed time
DE02	28.9 V dc	15 to 35 V dc	Delayed time
DE05	10.2 V dc	5.5 to 12.5 V dc	Delayed time
DF01	Computer case temperature	0 to 300° F	Delayed time
DF02	Platform case temperature	0 to 200° F	Delayed time
DF03	Electronics case temperature	0 to 300° F	Delayed time
DF04	Power supply case temperature	0 to 300° F	Delayed time
DG01	Prelaunch	(binary 001)	Delayed time
DG02	Ascent	(binary 010)	Delayed time
DG05	Reentry	(binary 101)	Delayed time
DH01	Pitch gimbal position	rev (scaling 15) ^a	Delayed time
DH02	Yaw gimbal position	rev (scaling 15) ^a	Delayed time
DH03	Roll gimbal position	rev (scaling 15) ^a	Delayed time
DH04	Sum of X-axis acceleration (F-X)	ft/sec (scaling 15) ^a	Delayed time
DH05	Sum of Y-axis acceleration (F-Y)	ft/sec (scaling 15) ^a	Delayed time
DH06	Sum of Z-axis acceleration (F-Z)	ft/sec (scaling 15) ^a	Delayed time
DH07	Accumulation of X-axis acceleration (SFXP)	Quanta (scaling 20) ^a	Delayed time
DH08	Accumulation of Y-axis acceleration (SFYP)	Quanta (scaling 20) ^a	Delayed time

^aEach computer word is a 24 bit binary word, consisting of a sign bit and 23 data bits. Scaling indicates the position of the binary point. Bits to the left of the binary point represent the whole number portion of the data word, bits to the right represent the fractional portion. For example, a scaling of 17 indicates that the binary point is located 17 places to the right of the sign bit or between the 17th and 18th data bits. The possible range of this number would be $\pm 2^{17}$ or $\pm 131\ 072$.

UNCLASSIFIED

TABLE 3-III.- SPACECRAFT INSTRUMENTATION MEASUREMENTS FOR GT-2 - Continued

Measurement	Description	Instrumentation range	Type of data
DH09	Accumulation of Z-axis acceleration (SFZP)	Quanta (scaling 20) ^a	Delayed time
DH10	Pitch error	Quanta (scaling 13) ^a	Delayed time
DH11	Yaw error	Quanta (scaling 13) ^a	Delayed time
DH12	Roll error	Quanta (scaling 13) ^a	Delayed time
DH13	Time in mode	23 sec (scaling 17) ^a	Delayed time
DH14	Flow tag	Quanta (scaling 23) ^a	Delayed time
DH15	Multiplex frame (13 frames)		Delayed time
DH16	MDIU, DCS multiplex word 1	} (Not applicable computer word in different units for different times)	Delayed time
DH17	MDIU, DCS multiplex word 2		Delayed time
DH18	MDIU, DCS multiplex word 3		Delayed time
DH19	MDIU, DCS multiplex word 4		Delayed time
DH20	MDIU, DCS multiplex word 5		Delayed time
DH21	MDIU, DCS multiplex word 6		Delayed time
DJ01	Pitch gimbal position	0.0001 rev (scaling 14) ^a	Delayed time
DJ02	Yaw gimbal position	.0001 rev (scaling 14) ^a	Delayed time
DJ03	Roll gimbal position	.0001 rev (scaling 14) ^a	Delayed time
DJ04	Accumulation of X-axis acceleration (SFXP)	Quanta (scaling 20) ^a	Delayed time
DJ05	Accumulation of Y-axis acceleration (SFYP)	Quanta (scaling 20) ^a	Delayed time
DJ06	Accumulation of Z-axis acceleration (SFZP)	Quanta (scaling 20) ^a	Delayed time
DJ07	Velocity, X-axis	ft/sec (scaling 15) ^a	Delayed time
DJ08	Velocity, Y-axis	ft/sec (scaling 15) ^a	Delayed time
DJ09	Velocity, Z-axis	ft/sec (scaling 15) ^a	Delayed time

^a Each computer word is a 24 bit binary word, consisting of a sign bit and 23 data bits. Scaling indicates the position of the binary point. Bits to the left of the binary point represent the whole number portion of the data word, bits to the right represent the fractional portion. For example, a scaling of 17 indicates that the binary point is located 17 places to the right of the sign bit or between the 17th and 18th data bits. The possible range of this number would be $\pm 2^{17}$ or $\pm 131\ 072$.

UNCLASSIFIED

TABLE 3-III.- SPACECRAFT INSTRUMENTATION MEASUREMENTS FOR GT-2 - Continued

Measurement	Description	Instrumentation range	Type of data
DJ10	Pitch error	rad (scaling 3) ^a	Delayed time
DJ11	Yaw error	rad (scaling 3) ^a	Delayed time
DJ12	Roll error	rad (scaling 3) ^a	Delayed time
DJ13	Time in mode	sec (scaling 17) ^a	Delayed time
DJ14	Flow tag	Quanta (scaling 23) ^a	Delayed time
DJ15	Z-axis velocity update	ft/sec (scaling 15) ^a	Delayed time
DJ16	Pitch rate	- rad/sec (scaling 5) ^a	Delayed time
DJ17	Yaw rate	- rad/sec (scaling 5) ^a	Delayed time
DJ18	Position, X-axis	ft (scaling 25) ^a	Delayed time
DJ19	Position, Y-axis	ft (scaling 25) ^a	Delayed time
DJ20	Position, Z-axis	ft (scaling 25) ^a	Delayed time
DJ21	Time to go to SECO	sec (scaling 10) ^a	Delayed time
DM01	Pitch gimbal position	0.0001 rev (scaling 14) ^a	Delayed time
DM02	Yaw gimbal position	.0001 rev (scaling 14) ^a	Delayed time
DM03	Roll gimbal position	.0001 rev (scaling 14) ^a	Delayed time
DM04	Accumulation of X-axis acceleration (SFXP)	Quanta (scaling 20) ^a	Delayed time
DM05	Accumulation of Y-axis acceleration (SFYP)	Quanta (scaling 20) ^a	Delayed time
DM06	Accumulation of Z-axis acceleration (SFZP)	Quanta (scaling 20) ^a	Delayed time
DM07	Distance to center of earth	ft (scaling 25) ^a	Delayed time
DM08	Spacecraft velocity	ft/sec (scaling 15) ^a	Delayed time
DM09	Flight-path angle	rad (scaling 3) ^a	Delayed time
DM10	Down-range error	n. mi. (scaling 14) ^a	Delayed time
DM11	Cross-range error	n. mi. (scaling 14) ^a	Delayed time
DM12	Commanded bank	rad (scaling 3) ^a	Delayed time
DM13	Time in mode	sec (scaling 17) ^a	Delayed time
DM14	Flow tag	Quanta (scaling 23) ^a	Delayed time
DM15	Longitude	rad (scaling 3) ^a	Delayed time

^aEach computer word is a 24 bit binary word, consisting of a sign bit and 23 data bits. Scaling indicates the position of the binary point. Bits to the left of the binary point represent the whole number portion of the data word, bits to the right represent the fractional portion. For example, a scaling of 17 indicates that the binary point is located 17 places to the right of the sign bit or between the 17th and 18th data bits. The possible range of this number would be $\pm 2^{17}$ or $\pm 131\ 072$.

UNCLASSIFIED

TABLE 3-III.- SPACECRAFT INSTRUMENTATION MEASUREMENTS FOR GT-2 - Continued

Measurement	Description	Instrumentation range	Type of data
DM16	Latitude	rad (scaling 3) ^a	Delayed time
DM17	Predicted zero-lift range	n. mi. (scaling 14) ^a	Delayed time
DM18	Spacecraft heading	rad (scaling 3) ^a	Delayed time
DM19	Density altitude	Quanta (scaling 4) ^a	Delayed time
DM20	Heading to target	rad (scaling 3) ^a	Delayed time
DM21	Range to target	n. mi. (scaling 13) ^a	Delayed time
EA01	Pitch rate	±2.5 or ±20 deg/sec (see AG10) ^a	Delayed time
EA02	Roll rate	±2.5 or ±30 deg/sec (see AG11) ^a	Delayed time
EA03	Yaw rate	±2.5 or ±20 deg/sec (see AG12) ^a	Delayed time
EBO1	Horizon sensor pitch output	±20°	Delayed time
EBO2	Horizon sensor roll output	±20°	Delayed time
EBO3	Sensor search mode	1 = search	Delayed time
ECO1	ac voltage	23 to 29 V ac	Delayed time
ECO2	ac frequency	380 to 420 cps	Delayed time
ECO3	20 V dc B +	0 to 25 V dc	Delayed time
ECO4	10 V dc bias	7.5 to 12.5 V dc	Delayed time
ECO5	-10 V dc bias	-7.5 to -12.5 V dc	Delayed time
GB01	Fuel feed temperature	-20 to 150° F	Delayed time
GB02	Oxidizer feed temperature	-20 to 150° F	Delayed time
GC01	Pressure, source helium	0 to 5000 psia	Delayed time
GC02	Temperature, source helium	-100 to 200° F	Delayed time
GC03	Temperature, regulated helium at fuel tank	-100 to 200° F	Delayed time
GC04	Temperature, regulated helium at oxidizer tank	-100 to 200° F	Delayed time
GC05	Pressure, regulated helium	0 to 500 psia	Delayed time
GD01	Injector head temperature, TCA No. 9	0 to 400° F	Delayed time
GB01	TCA 1, left-hand, fires down	1 = fire	Delayed time

^aEach computer word is a 24 bit binary word, consisting of a sign bit and 23 data bits. Scaling indicates the position of the binary point. Bits to the left of the binary point represent the whole number portion of the data word, bits to the right represent the fractional portion. For example, a scaling of 17 indicates that the binary point is located 17 places to the right of the sign bit or between the 17th and 18th data bits. The possible range of this number would be $\pm 2^{17}$ or $\pm 131\ 072$.

UNCLASSIFIED

TABLE 3-III.- SPACECRAFT INSTRUMENTATION MEASUREMENTS FOR GT-2 - Continued

Measurement	Description	Instrumentation range	Type of data
GEO2	TCA 2, right-hand, fires down	1 = fire	Delayed time
GEO3	TCA 3, bottom, fires right	1 = fire	Delayed time
GEO4	TCA 4, top, fires right	1 = fire	Delayed time
GEO5	TCA 5, right-hand, fires up	1 = fire	Delayed time
GEO6	TCA 6, left-hand, fires up	1 = fire	Delayed time
GEO7	TCA 7, top, fires left	1 = fire	Delayed time
GEO8	TCA 8, bottom, fires left	1 = fire	Delayed time
GEO9	TCA 9 and 10, TYBY, fires aft	1 = fire	Delayed time
GE11	TCA 11 and 12, LXRK, fires forward	1 = fire	Delayed time
GE13	TCA 13, left-hand, fires left	1 = fire	Delayed time
GE14	TCA 14, right-hand, fires right	1 = fire	Delayed time
GE15	TCA 15, bottom, fires down	1 = fire	Delayed time
GE16	TCA 16, top, fires up	1 = fire	Delayed time
HA02	Oxidizer feed temperature	-20 to 150° F	Delayed time
HBO2	Oxidizer feed temperature	-20 to 150° F	Delayed time
HC01	Pressure, source nitrogen (system A)	0 to 5000 psia	Delayed time
HC02	Pressure, source nitrogen (system B)	0 to 5000 psia	Delayed time
HC03	Pressure, regulated nitrogen (system A)	0 to 500 psia	Delayed time
HC04	Pressure, regulated nitrogen (system B)	0 to 500 psia	Delayed time
HC05	Temperature, source nitrogen (system A)	-100 to 200° F	Delayed time
HC06	Temperature, source nitrogen (system B)	-100 to 200° F	Delayed time
HD01	Injector head temperature, TCA 8	0 to 400° F	Delayed time
HD02	Nozzle temperature, TCA 7	^b Referenced to MA28 reference +1300° F	Tape recorded
HE01	TCA 1, right-hand, fires up	1 = fire	Delayed time
HE02	TCA 2, left-hand, fires up	1 = fire	Delayed time

^bReference temperature determined by reference junction temperature MA24, MA28, or MA29.

UNCLASSIFIED

TABLE 3-III.- SPACECRAFT INSTRUMENTATION MEASUREMENTS FOR GT-2 - Continued

Measurement	Description	Instrumentation range	Type of data
HE05	TCA 3, top, fires left	1 = fire	Delayed time
HE04	TCA 4, bottom, fires left	1 = fire	Delayed time
HE05	TCA 5, left-hand, fires down	1 = fire	Delayed time
HE06	TCA 6, right-hand, fires down	1 = fire	Delayed time
HE07	TCA 7, bottom, fires right	1 = fire	Delayed time
HE08	TCA 8, top, fires right	1 = fire	Delayed time
HF01	TCA 1, right-hand, fires up	1 = fire	Delayed time
HF02	TCA 2, left-hand, fires up	1 = fire	Delayed time
HF03	TCA 3, top, fires left	1 = fire	Delayed time
HF04	TCA 4, bottom, fires left	1 = fire	Delayed time
HF05	TCA 5, left-hand, fires down	1 = fire	Delayed time
HF06	TCA 6, right-hand, fires down	1 = fire	Delayed time
HF07	TCA 7, bottom, fires right	1 = fire	Delayed time
HF08	TCA 8, top, fires right	1 = fire	Delayed time
HG01	Fuel inlet at TCA 2	-50 to 300° F	Tape recorded
HG02	Fuel inlet at TCA 5	-50 to 300° F	Tape recorded
HG03	Fuel inlet at TCA 6	-50 to 300° F	Tape recorded
HG04	Fuel inlet at TCA 8	-50 to 300° F	Tape recorded
HG05	Oxidizer inlet at TCA 2	-50 to 300° F	Tape recorded
HG06	Oxidizer inlet at TCA 5	-50 to 300° F	Tape recorded
HG07	Oxidizer inlet at TCA 6	-50 to 300° F	Tape recorded
HG08	Oxidizer inlet at TCA 8	-50 to 300° F	Tape recorded
HH07	Retrorocket package temperature 2	-150 to 500° F	Delayed time
KA01	Longitudinal acceleration (Z)	-3 to 19g	Delayed time
KA02	Lateral acceleration (X)	±3g	Delayed time
KA03	Vertical acceleration (Y)	±3g	Delayed time
KB02	Static pressure	0 to 15 psia	Delayed time
KC01	Local static pressure, top Z123	0 to 10 mm Hg	Delayed time
KC02	Local static pressure, top Z163	0 to 10 mm Hg	Delayed time

UNCLASSIFIED

TABLE 3-III.- SPACECRAFT INSTRUMENTATION MEASUREMENTS FOR GT-2 - Continued

Measurement	Description	Instrumentation range	Type of data
KC03	Local static pressure, top Z179	0 to 10 mm Hg	Delayed time
KC04	Local static pressure, top Z189	0 to 10 mm Hg	Delayed time
KC05	Local static pressure, bottom Z123	0 to 40 mm Hg	Delayed time
KC06	Local static pressure, bottom Z163	0 to 40 mm Hg	Delayed time
KC07	Local static pressure, bottom Z179	0 to 40 mm Hg	Delayed time
KC08	Local static pressure, bottom Z189	0 to 40 mm Hg	Delayed time
LA01	DCS system verification	8 zeros = verify	Real time
LA02	6 V dc regulated power	0 to 6 V	Delayed time
LA03	Receiver signal strength, QUADX (2 or B)	-50 to -100 dbm	Delayed time
LA04	Receiver signal strength, DIPX (1 or A)	-50 to -100 dbm	Delayed time
LA05	Package temperature	0 to 200° F	Delayed time
LA06	28 V dc regulated power	+27 to +29 volts	Delayed time
LA07	-18 V dc regulated power	-17 to -19 volts	Delayed time
LA08	23 V dc regulated power	+22 to +24 volts	Delayed time
LA09	-6 V dc regulated power	-5 to -7 volts	Delayed time
LB01	Output-power (RF)	1 to 2 kW	Delayed time
LB03	Receiver PRF	0 to 2000 pps	Delayed time
LB04	Package temperature	0 to 200° F	Delayed time
LC03	Receiver PRF	0 to 600 pps	Delayed time
LC04	Package temperature	0 to 300° F	Tape recorded
LD01	Package temperature	0 to 200° F	Delayed time
LE05	Package temperature (R-V)	0 to 300° F	Delayed time
MA17	High-level zero reference (PAM + PCM)	0.0 V	Delayed time
MA18	High-level full-scale (PAM)	5.0 V	Tape recorded
MA20	Low-level zero reference (PAM)	0.0 mV	Tape recorded
MA21	Low-level full scale (PCM)	15.0 mV	Delayed time
MA22	Calibrate	0 or 28 V	Delayed time
MA24	Reference junction temperature	-55 to 200° F	Delayed time

UNCLASSIFIED

UNCLASSIFIED

3-47

TABLE 3-III.- SPACECRAFT INSTRUMENTATION MEASUREMENTS FOR GT-2 - Continued

Measurement	Description	Instrumentation range	Type of data
MA26	Low-level full-scale (PAM)	20.0 mV	Tape recorded
MA28	Reference junction temperature no. 1	-55 to 200° F	Tape recorded
MA29	Reference junction temperature no. 2	-55 to 200° F	Delayed time
MA34	25 kc reference oscillator	25 kc	Tape recorded
MA37	High-level full-scale (PCM)	4.50 V	Delayed time
MA38	Low-level zero reference (PCM)	3.0 mV	Delayed time
MA95	PCM tape motion monitor	1 = run	Delayed time
MA96	Tape motion monitor TR 1		Delayed time
MB01	High-level full-scale (PCM)	4.50 V	Delayed time
MB02	Low-level zero PCM reference	3.0 mV	Delayed time
MB03	Low-level full-scale (PCM)	15 mV	Delayed time
MD04	Time synchronization (TR cameras - PCM)	2.4 sec	Tape recorded
PB01	Inner skin	0 to 600° F	Delayed time
PB02	Outer skin (top)	^b Referenced to MA29 reference +1300° F	Delayed time
PB03	Outer skin	^b Referenced to MA28 reference +1900° F	Tape recorded
PB04	Outer skin	^b Referenced to MA24 reference +1900° F	Delayed time
PB05	Outer skin	^b Referenced to MA24 reference +1900° F	Delayed time
PB06	Outer skin	^b Referenced to MA28 reference +1900° F	Tape recorded
PB07	Separation joint magnesium strip	0 to 500° F	Delayed time
PB08	Parachute compartment inner skin	0 to 700° F	Tape recorded
PB10	Inner skin	0 to 600° F	Tape recorded
PB11	Outer skin	^b Referenced to MA29 reference +1900° F	Delayed time
PB12	Outer skin	^b Referenced to MA28 reference +1900° F	Tape recorded

^bReference temperature determined by reference junction temperature MA24, MA28, or MA29.

UNCLASSIFIED

UNCLASSIFIED

TABLE 3-III.- SPACECRAFT INSTRUMENTATION MEASUREMENTS FOR GT-2 - Continued

Measurement	Description	Instrumentation range	Type of data
PB13	Outer skin	^b Referenced to MA29 reference +1900° F	Delayed time
PB17	Outer skin	^b Referenced to MA29 reference +1900° F	Delayed time
PC01	Inner skin	0 to 400° F	Tape recorded
PC03	Outer skin	^b Referenced to MA24 reference +1900° F	Delayed time
PC04	Outer skin	^b Referenced to MA24 reference +1900° F	Delayed time
PC05	Outer skin	^b Referenced to MA29 reference +1900° F	Delayed time
PC06	Outer skin	^b Referenced to MA28 reference +1900° F	Tape recorded
PC07	Outer skin	^b Referenced to MA28 reference +1900° F	Tape recorded
PC09	Stringer (point 1)	^b Referenced to MA29 reference +1300° F	Delayed time
PC10	Stringer (point 2)	0 to 400° F	Delayed time
PC11	Stringer	0 to 400° F	Tape recorded
PC12	TCA 8 - Support	^b Referenced to MA28 reference 1300° F	Tape recorded
PC13	TCA 8 - Support	^b Reference to MA28 reference 1300° F	Tape recorded
PC14	Stringer	0 to 700° F	Tape recorded
PD01	Inner skin	0 to 700° F	Tape recorded
PD03	Outer skin	^b Referenced to MA24 reference +1900° F	Delayed time
PD04	Outer skin	^b Referenced to MA24 reference +1900° F	Delayed time
PD05	Outer skin	^b Referenced to MA24 reference +1300° F	Delayed time
PD06	Outer skin	^b Referenced to MA24 reference +1900° F	Delayed time
PD07	Outer skin	^b Referenced to MA24 reference +1900° F	Delayed time
PD08	Outer skin	^b Referenced to MA24 reference +1300° F	Delayed time
PD09	Outer skin	^b Referenced to MA28 reference +1900° F	Tape recorded
PD10	Outer skin	^b Referenced to MA29 reference +1900° F	Delayed time

^bReference temperature determined by reference junction temperature MA24, MA28, or MA29.

UNCLASSIFIED

TABLE 3-III.- SPACECRAFT INSTRUMENTATION MEASUREMENTS FOR GT-2 - Continued

Measurement	Description	Instrumentation range	Type of data
PD11	Outer skin	^b Referenced to MA28 reference +1900° F	Tape recorded
PD12	Cabin wall	0 to 300° F	Tape recorded
PD13	Cabin wall	0 to 300° F	Tape recorded
PD16	Cabin wall	0 to 300° F	Tape recorded
PD17	Stringer (point 1)	^b Referenced to MA29 reference +1300° F	Delayed time
PD18	Stringer (point 2)	0 to 700° F	Delayed time
PD22	Adapter clamp influence	^b Referenced to MA28 reference +1900° F	Tape recorded
PD23	Adapter clamp influence	^b Referenced to MA28 reference +1900° F	Tape recorded
PD25	Adapter clamp influence	^b Referenced to MA28 reference +1900° F	Tape recorded
PD26	Adapter clamp influence	^b Referenced to MA28 reference +1900° F	Tape recorded
PD27	Adapter clamp influence	^b Referenced to MA28 reference +1900° F	Tape recorded
PD28	Window (right-hand) inside outer pane	^b Referenced to MA29 reference +950° F	Delayed time
PD29	Window (right-hand) inside inner pane	0 to 300° F	Delayed time
PD30	Window (left-hand) inside outer pane	^b Referenced to MA28 reference +950° F	Tape recorded
PD33	Trough compartment (roll)	0 to 600° F	Tape recorded
PD34	Landing gear door	^b Referenced to MA28 reference +1300° F	Tape recorded
PD35	ECS RIB	^b Referenced to MA28 reference +950° F	Tape recorded
PD36	Equipment access door	^b Referenced to MA28 reference +1300° F	Tape recorded
PD37	Ring center line	^b Referenced to MA29 reference +950° F	Delayed time
PD39	Stringer	^b Referenced to MA28 reference +1300° F	Tape recorded
PD40	Landing gear door pyro	^b Referenced to MA29 reference +950° F	Delayed time
PD41	Landing gear door pyro	^b Referenced to MA28 reference +950° F	Tape recorded
PD53	Cone to cylinder tiedown	^b Referenced to MA29 reference +950° F	Delayed time

^bReference temperature determined by reference junction temperature MA24, MA28, or MA29.

UNCLASSIFIED

TABLE 3-III.- SPACECRAFT INSTRUMENTATION MEASUREMENTS FOR GT-2 - Continued

Measurement	Description	Instrumentation range	Type of data
PD54	Outer skin	^b Referenced to MA29 reference +1900° F	Delayed time
PD55	Umbilical disconnect	^b Referenced to MA28 reference +1300° F	Tape recorded
PD58	Window (right-hand) inside- outer pane	^b Referenced to MA28 reference +950° F	Tape recorded
PD59	Window (right-hand) inside- inner pane	0 to 300° F	Tape recorded
PE01	Ablation material backface	^b Referenced to MA29 reference +950° F	Delayed time
PE03	Ablation material backface	^b referenced to MA28 reference +950° F	Tape recorded
PE06	Ablation material backface	^b referenced to MA28 reference +950° F	Tape recorded
PE07	Ablation material backface	^b Referenced to MA29 reference +950° F	Delayed time
PE11	Ablation material backface	-55 to 1000° F	Delayed time
PE12	Ablation material backface	-55 to 1000° F	Tape recorded
PE13	Ablation material backface	^b Referenced to MA29 reference +2300° F	Delayed time
PE14	Ablation material backface	^b Referenced to MA28 reference +950° F	Tape recorded
PE15	Ablation material backface	^b Referenced to MA28 reference +950° F	Tape recorded
PE16	Ablation material backface	^b Referenced to MA29 reference +950° F	Delayed time
PE17	Ablation material backface	^b Referenced to MA29 reference +2300° F	Delayed time
PE18	Ablation material backface	^b Referenced to MA29 reference +2300° F	Delayed time
PE19	Honeycomb backface	^b Referenced to MA29 reference +950° F	Delayed time
PE20	Honeycomb backface	^b Referenced to MA29 reference +950° F	Tape recorded
QA09	X-axis vibration Z106	1 to 30 cps	Tape recorded
QA10	Y-axis vibration Z106	1 to 30 cps	Tape recorded
QA11	Z-axis vibration Z106	1 to 30 cps	Tape recorded
QA12	X-axis vibration Z132.5	20 to 600 cps	Tape recorded
QA13	Y-axis vibration Z132.5	20 cps to 2 kcps	Tape recorded
QA14	Z-axis vibration Z132.5	20 cps to 2 kcps	Tape recorded

^bReference temperature determined by reference junction temperature MA24, MA28, or MA29.

UNCLASSIFIED

UNCLASSIFIED

3-51

TABLE 3-III.- SPACECRAFT INSTRUMENTATION MEASUREMENTS FOR GT-2 - Continued

Measurement	Description	Instrumentation range	Type of data
QB04	Equipment compartment absolute pressure (right hand)	0 to 15 psia	Delayed time
QB09	Landing gear compartment absolute pressure	0 to 15 psia	Delayed time
QB10	Equipment compartment absolute pressure (left hand)	0 to 15 psia	Delayed time
QB13	Y-axis vibration Z113.8	20 cps to 2 kcps	Tape recorded
QB14	Z-axis vibration Z117.8	20 cps to 2 kcps	Tape recorded
QC14	Retro compartment absolute pressure	0 to 15 psia	Delayed time
QC15	Equipment compartment absolute pressure	0 to 15 psia	Delayed time
QD06	Cover cavity absolute pressure	0 to 15 psia	Delayed time
QD07	X-axis vibration	20 cps to 2 kcps	Tape recorded
QD08	Y-axis vibration	20 cps to 2 kcps	Tape recorded
QD09	Z-axis vibration	20 to 600 cps	Tape recorded
QD10	X-axis vibration	1 to 30 cps	Tape recorded
QD11	Y-axis vibration	1 to 30 cps	Tape recorded
SA01	Fairing jettison	1 = jettison	Tape recorded
SA02	Antenna extend	1 = extend	Tape recorded
SA03	Separate spacecraft (sequence)	1 = separate	Tape recorded
SA04	Separate spacecraft DCS command	1 = separate	Tape recorded
SA05	HF-DF key on	1 = key on	Tape recorded
SA06	Attitude control parachute and HS off	1 = command	Tape recorded
SA07	Select adapter antenna and event TR-5	1 = command	Tape recorded
SA08	Event timer TR-30	1 = command	Tape recorded
SA09	Retro squib bus arm	1 = arm	Tape recorded
SA10	Indicate retroattitude (IGS abort)	1 = command	Tape recorded
SA11	Indicate retroattitude on	1 = on	Tape recorded
SA12	SA11 off and roll command on	1 = command	Tape recorded
SA13	Oxygen high rate	1 = command	Tape recorded
SA15	BIA squib bus safe	D = safe	Tape recorded

UNCLASSIFIED

UNCLASSIFIED

TABLE 3-III.- SPACECRAFT INSTRUMENTATION MEASUREMENTS FOR GT-2 - Continued

Measurement	Description	Instrumentation range	Type of data
SA16	Separate OAMS lines	1 = command	Tape recorded
SA17	Separate electrical	1 = command	Tape recorded
SA18	Separate adapter and automatic retrofire	1 = command	Tape recorded
SA19	Manual retrofire	1 = command	Tape recorded
SA20	Jettison retro section	1 = jettison	Tape recorded
SA21	Landing squib bus arm	1 = arm	Tape recorded
SA22	Pilot parachute deploy	1 = deploy	Tape recorded
SA23	Cabin air valves	1 = command	Tape recorded
SA24	UHF rescue beacon on	1 = on	Tape recorded
SA25	Water seal closed	1 = close	Tape recorded
SA26	Parachute jettison	1 = jettison	Tape recorded
SA27	IGS power off	1 = on	Tape recorded
SA28	Platform malfunction reset	1 = reset	Tape recorded
SA29	Computer malfunction reset	1 = reset	Tape recorded
SA30	Secondary guidance on	1 = on	Tape recorded
SA31	Abort (launch vehicle shutdown command)	1 = command	Tape recorded
SA32	Abort (abort sequence start)	1 = command	Tape recorded
SA33	OAMS on/manual and attitude mode	1 = command	Tape recorded
SA34	Reentry mode at spacecraft separation +2.0 sec	1 = command	Tape recorded
SA35	Horizontal mode (SEF)/OAMS off	1 = command	Tape recorded
SA36	Simulated right yaw /rate command/ RCS actuate	1 = command	Tape recorded
SA38	Automatic retrograde mode + RCS B select	1 = command	Tape recorded
SA39	RCS A to ACME + ground RCS A & B	1 = command	Tape recorded
SA40	Horizontal mode (BEF)	1 = command	Tape recorded
SA41	Reentry mode (0.05g relay)	1 = command	Tape recorded
SA42	RCS A & B off	1 = off	Tape recorded
SA43	HS HTR off & RCS pulse mode	1 = command	Tape recorded
SA44	Retrojettison abort command	1 = command	Tape recorded
SA45	C-band beacon off	2nd 1 = off	Tape recorded

UNCLASSIFIED

TABLE 3-III.- SPACECRAFT INSTRUMENTATION MEASUREMENTS FOR GT-2 - Concluded

Measurement	Description	Instrumentation range	Type of data
SA46	Kinetic switch actuate	1 = command	Tape recorded
SA47	Abort command (DCS)	1 = command	Tape recorded
SA48	PCM tape playback command	1 = command	Tape recorded
SA49	PCM mode select (real time or delayed time)	1 = command	Tape recorded
SA50	UHF key	1 = on	Tape recorded
SA51	RCS off (abort)	1 = off (abort)	Tape recorded
SA52	Tone generator off	1 = off	Tape recorded
SA53	Maximum lift command	1 = command	Tape recorded
SC01	Simulator 1 battery voltage	15 to 35 V	Delayed time
SC02	Simulator 2 battery voltage	15 to 35 V	Delayed time
SC03	Simulator 1 battery current	0 to 20 A	Real time
SC04	Simulator 2 battery current	0 to 20 A	Real time

UNCLASSIFIED

TABLE 3-IV.- GUIDANCE AND CONTROL SWITCHES

Switch identification ^a	Position prior to launch of spacecraft 2
Center instrument panel	
Platform (mode selector)	Free
Computer (mode selector)	Ascent
Start comp.	Off
Malfunction reset (momentary)	Not operated
Radar	Off
Attitude control (mode selector)	Rate command
Scanner	Primary
Rate gyros	
Yaw	Primary
Pitch	Primary
Roll	Primary
ACME logic	
Yaw	Primary (momentarily on)
Pitch	Primary (momentarily on)
Roll	Primary (momentarily on)
Right-hand instrument panel	
MDIU	On
FDC - mode	Attitude
FDC - ref.	Computer

^aSwitches associated with the guidance and control system on the right-hand switch-circuit breaker panel, the overhead panel, and the right-hand sequencer control panel are not listed.

UNCLASSIFIED

TABLE 3-V. - GLV-2 MODIFICATIONS

System	Significant changes incorporated in GLV-2 from GT-1 configuration
Stage I structure	None
Stage II structure	(a) External insulation on oxidizer tank forward skirt (for protection against protruberance heating) reduced in thickness from 0.10 inch to 0.05 inch. (b) Scupper life increased from 2 seconds to minimum of 6 seconds.
Propulsion	(a) Actuating mechanism and electrical connections of position potentiometer on stage I fuel accumulators revised from friction drive to direct drive and from soldered connections to pigtail leads and crimped splices. (b) Shield assembly incorporated on one-half of fuel-tank level sensors to inhibit deposits on sensing prism from fuel tank autogenous pressurization gases. (c) Stage I and stage II engine start cartridges temperature conditioned to a range of 45° F to 70° F.
Flight control	(a) Relay circuit which directed primary guidance (RGS) to secondary system removed so that IGS inputs can be used for secondary guidance. (b) Pitch program in TARS changed to suit unique GT-2 mission requirements.
Radio guidance	None
Hydraulic	(a) Stage I engine-driven pump compensator changed to lessen pump pressure start transients. (b) Stage II pitch actuator rigged null length shortened by 0.038 inch to correct for attitude error offset on GT-1 flight. (c) Tandem actuator piston velocity limits increased. (d) Stage I tandem actuators redesigned.
Electrical	AFS power to TCPS jumpered through umbilical DIE to prevent feedback causing premature staging due to APS bus failure.
Malfunction detection	(a) Rate switch settings revised to ± 2.5 deg/sec in yaw and +2.5 to -3.0 deg/sec in pitch. (b) Stage II engine sensor changed from thrust chamber pressure (MDTCPS) to fuel injector pressure (MDFJPS).
Instrumentation	(a) Telemetry antenna system changed from 4 antennas plus 5 port junctions to two antennas plus 3 port junctions. (b) Program board removed.
Range safety	(a) Command control receivers changed from AVCO MK III to ACI R423A type. (b) Stage I destruct initiator relocated from inside the stage I fuel tank conduit to inside compartment IV. (c) Titan II type destruct initiator replaced with new GLV type initiator.
Ordnance separation	None

UNCLASSIFIED

TABLE 3-VI.- LAUNCH-VEHICLE INSTRUMENTATION MEASUREMENTS FOR GT-2

Measurement	Description	Instrumentation range
0001	Thrust chamber valve position, subassembly 1	0 to 100 percent open
0002	Thrust chamber valve position, subassembly 2	0 to 100 percent open
0003	Thrust chamber pressure, subassembly 1	0 to 1 000 psia
0004	Thrust chamber pressure, subassembly 2	0 to 1 000 psia
0005	Gas-generator chamber pressure, subassembly 1	0 to 750 psia
0006	Gas-generator chamber pressure, subassembly 2	0 to 1 000 psia
0007	Turbine speed, subassembly 1	0 to 40 000 rpm
0008	Turbine speed, subassembly 2	0 to 40 000 rpm
0009	Turbine inlet temperature, subassembly 1	0 to 2 500° F
0010	Fuel-pump discharge pressure, subassembly 1	0 to 1 500 psia
0011	Fuel-pump discharge pressure, subassembly 2	0 to 1 500 psia
0012	Turbine inlet temperature, subassembly 2	0 to 2 500° F
0013	Fuel-pump inlet temperature, subassembly 1	0 to 200° F
0014	Fuel-pump inlet pressure, subassembly 1	0 to 100 psia
0015	Oxidizer-pump discharge pressure, subassembly 1	0 to 1 500 psia
0016	Oxidizer-pump discharge pressure, subassembly 2	0 to 1 500 psia
0017	Oxidizer-pump inlet pressure, subassembly 2	0 to 200 psia

UNCLASSIFIED

UNCLASSIFIED

3-57

TABLE 3-VI.- LAUNCH-VEHICLE INSTRUMENTATION MEASUREMENTS
FOR GT-2 - Continued

Measurement	Description	Instrumentation range
0021	Fuel-pressurant-orifice inlet pressure, subassembly 2	0 to 500 psia
0022	Fuel-pressurant-orifice inlet temperature, subassembly 2	0 to 500° F
0023	Oxidizer-pump inlet temperature, subassembly 2	0 to 200° F
0024	Oxidizer-pump inlet temperature, subassembly 2	0 to 300° F
0026	Oxidizer-pressurant-orifice inlet, subassembly 2	0 to 1 000 psia
0027	Oxidizer-pressurant-orifice inlet temperature, subassembly 2	0 to 500° F
0028	Bootstrap fuel venturi inlet pressure, subassembly 1	0 to 1 500 psia
0029	Bootstrap fuel venturi inlet pressure, subassembly 2	0 to 1 500 psia
0030	Bootstrap oxidizer venturi inlet pressure, subassembly 1	0 to 1 500 psia
0031	Bootstrap oxidizer venturi inlet pressure, subassembly 2	0 to 1 500 psia
0032	Power-on TCVPSVORS (87FS2) stage I	Bilevel
0033	Pressure, oxidizer standpipe, subassembly 1	0 to 200 psia
0034	Pressure, oxidizer standpipe, subassembly 2	0 to 200 psia
0035	Piston motion, fuel surge chamber, subassembly 1	0 to 8.6 in.
0036	Piston motion, fuel surge chamber, subassembly 2	0 to 8.6 in.
0037	Pressure, fuel surge chamber, subassembly 1	0 to 100 psia

UNCLASSIFIED

UNCLASSIFIED

TABLE 3-VI.- LAUNCH-VEHICLE INSTRUMENTATION MEASUREMENTS
FOR GT-2 - Continued

Measurement	Description	Instrumentation range
0038	Pressure, fuel surge chamber, subassembly 2	0 to 100 psia
0050	Fuel sensor shutdown, stage I	Bilevel
0052	Fuel sensor outage, stage I	Bilevel
0053	Fuel sensor outage, stage I	Bilevel
0054	Fuel sensor high, stage I	Bilevel
0055	Fuel sensor high, stage I	Bilevel
0056	Oxidizer sensor high, stage I	Bilevel
0057	Oxidizer sensor high, stage I	Bilevel
0058	Oxidizer sensor outage, stage I	Bilevel
0059	Oxidizer sensor outage, stage I	Bilevel
0060	Fuel sensor shutdown, stage I	Bilevel
0150	Travel actuator 1, pitch, stage I	± 1.25 in.
0151	Travel actuator 2, yaw-roll, stage I	± 1.25 in.
0152	Travel actuator 3, yaw-roll, stage I	± 1.25 in.
0153	Travel actuator 4, pitch, stage I	± 1.25 in.
0154	Pressure, hydraulic system (primary), stage I	0 to 4 500 psia
0155	Fluid-level, hydraulic reservoir (primary), stage I	0 to 100 percent
0156	Hydraulic fluid temperature (primary), stage I	0 to 300° F
0157	Pressure, hydraulic system (secondary system), stage I	0 to 4 500 psia
0158	Fluid-level, hydraulic reservoir (secondary system), stage I	0 to 100 percent

UNCLASSIFIED

UNCLASSIFIED

3-59

TABLE 3-VI.- LAUNCH-VEHICLE INSTRUMENTATION MEASUREMENTS
FOR GT-2 - Continued

Measurement	Description	Instrumentation range
0159	Hydraulic fluid temperature (secondary system), stage I	0 to 300° F
0169	Acceleration, axial, vehicle compartment 5	± 10g
0171	Acceleration, lateral, vehicle compartment 5	± 2g
0172	Acceleration, vertical, vehicle compartment 5	± 2g
0173	Strain gage on stringer 13	0 to 0.005 in./in.
0174	Strain gage on stringer 1	0 to 0.005 in./in.
0175	Skin temperature, stringers 1 and 2	0 to 600° F
0176	Calorimeter	0 to 600° F
0177	Skin temperature, stringers 1 and 36	0 to 600° F
0178	Strain gage on stringer 19	0 to 0.006 in./in.
0179	Strain gage on stringer 11	0 to 0.006 in./in.
0180	Strain gage on stringer 1	0 to 0.006 in./in.
0181	Strain gage on stringer 28	0 to 0.006 in./in.
0230	Rate gyro output, pitch, stage I (primary)	± 12.5 deg/sec
0231	Rate gyro output, yaw, stage I (primary)	± 12.5 deg/sec
0232	Rate gyro output, roll, stage I (primary)	± 12.5 deg/sec
0233	Rate gyro output, pitch, stage I (secondary system)	± 12.5 deg/sec pitch
0234	Rate gyro output, yaw, stage I (secondary system)	± 12.5 deg/sec yaw
0235	Rate gyro output, roll, stage I (secondary system)	± 12.5 deg/sec roll

UNCLASSIFIED

UNCLASSIFIED

TABLE 3-VI.- LAUNCH-VEHICLE INSTRUMENTATION MEASUREMENTS
FOR GT-2 - Continued

Measurement	Description	Instrumentation range
0355	APS/IPS (Comp. 4)	0 to 35 V dc
0356	Subassembly 1, MDTCPs A and B (B.C.)	Step voltage
0357	Subassembly 2, MDTCPs A and B (B.C.)	Step voltage
0358	Subassembly 1, MDTCPs A and B	Bilevel
0359	Subassembly 2, MDTCPs A and B	Bilevel
0364	Fuel tank pressure (A), stage I	0 to 50 psia
0365	Fuel tank pressure (B), stage I	0 to 50 psia
0366	Oxidizer tank pressure (A), stage I	0 to 50 psia
0367	Oxidizer tank pressure (B), stage I	0 to 50 psia
0501	Thrust-chamber valve position, subassembly 3	0 to 100 percent (open)
0502	Thrust-chamber pressure, subassembly 3	0 to 1 000 psia
0503	Turbine-inlet pressure, subassembly 3	0 to 1 000 psia
0504	Turbine speed, subassembly 3	0 to 30 000 rpm
0505	Turbine-inlet temperature, subassembly 3	32° to 2 500° F
0506	Fuel-pump discharge pressure, subassembly 3	0 to 1 500 psia
0507	Fuel-pump inlet pressure, subassembly 3	0 to 100 psia
0508	Fuel-pump inlet temperature, subassembly 3	0 to 300° F
0509	Oxidizer-pump discharge pressure, subassembly 3	0 to 1 500 psia

UNCLASSIFIED

TABLE 3-VI.- LAUNCH-VEHICLE INSTRUMENTATION MEASUREMENTS
FOR GT-2 - Continued

Measurement	Description	Instrumentation range
0510	Oxidizer-pump inlet pressure, subassembly 3	0 to 100 psia
0512	Fuel-pressurant-orifice inlet pressure, subassembly 3	0 to 500 psia
0513	Fuel-pressurant-orifice inlet temperature, subassembly 3	0 to 500° F
0514	Oxidizer-pump inlet temperature, subassembly 3	0 to 300° F
0517	Bootstrap fuel venturi inlet pressure, subassembly 3	0 to 1 500 psia
0518	Bootstrap oxidizer venturi inlet pressure, subassembly 3	0 to 1 500 psia
0519	Power on TCVP SVORS (91FS2), stage II	Bilevel
0520	Pressure oxidizer injector gas generator, subassembly 3	0 to 1 500 psia
0521	Shutdown squib actuation, stage II	Bilevel
0522	Shutdown valve relay actuation, stage II	Bilevel
0540	Fuel sensor, high, stage II	Bilevel
0541	Fuel sensor, high, stage II	Bilevel
0542	Oxidizer sensor, high, stage II	Bilevel
0543	Oxidizer sensor, high, stage II	Bilevel
0544	Fuel sensor shutdown, stage II	Bilevel
0545	Oxidizer sensor shutdown, stage II	Bilevel
0546	Fuel sensor outage, stage II	Bilevel
0547	Fuel sensor outage, stage II	Bilevel
0548	Oxidizer sensor outage, stage II	Bilevel

UNCLASSIFIED

TABLE 3-VI.- LAUNCH-VEHICLE INSTRUMENTATION MEASUREMENTS
FOR GT-2 - Continued

Measurement	Description	Instrumentation range
0549	Oxidizer sensor outage, stage II	Bilevel
0550	Oxidizer sensor shutdown, stage II	Bilevel
0551	Fuel sensor shutdown, stage II	Bilevel
0650	Travel actuator 5, yaw, stage II	± 0.522 in.
0651	Travel actuator 6, pitch, stage II	± 0.522 in.
0652	Travel actuator 7, roll, stage II	± 1.50 in.
0653	Pressure, hydraulic system, stage II	0 to 4 500 psia
0654	Fluid-level, hydraulic reservoir, stage II	0 to 100 percent
0655	Hydraulic fluid temperature, stage II	0 to 300° F
0660	Skin temperature, stringers 13 and 14	0 to 600° F
0661	Skin temperature, stringers 18 and 19	0 to 600° F
0662	Skin temperature, stringers 2 and 3	0 to 600° F
0665	Strain gage on stringer 13	0 to 0.005 in./in.
0666	Strain gage on stringer 1	0 to 0.005 in./in.
0667	Strain gage on stringer 6	0 to 0.005 in./in.
0668	Strain gage on stringer 18	0 to 0.005 in./in.
0670	Acceleration, axial, vehicle compartment 1	$\pm 10g$
0671	Acceleration, lateral, vehicle compartment 1	$\pm 2g$

UNCLASSIFIED

UNCLASSIFIED

3-63

TABLE 3-VI.- LAUNCH-VEHICLE INSTRUMENTATION MEASUREMENTS
FOR GT-2 - Continued

Measurement	Description	Instrumentation range
0672	Acceleration, vertical, vehicle compartment 1	$\pm 2g$
0673	Skin temperature	0 to 600° F
0674	Skin temperature	0 to 600° F
0675	Skin temperature	0 to 600° F
0676	Skin temperature	0 to 600° F
0677	Skin temperature	0 to 600° F
0678	Skin temperature	0 to 600° F
0679	Skin temperature	0 to 600° F
0680	Skin temperature	0 to 600° F
0681	Skin temperature	0 to 600° F
0682	Skin temperature	0 to 600° F
0683	Calorimeter slug temperature	0 to 600° F
0684	Calorimeter slug temperature	0 to 600° F
0685	Calorimeter slug temperature	0 to 600° F
0686	Calorimeter slug temperature	0 to 600° F
0687	Calorimeter slug temperature	0 to 600° F
0699	Acceleration, axial, low range	$\pm 0.5g$
0720	TARS attitude error, pitch, stage II	$\pm 6^\circ$
0721	TARS attitude error, yaw, stage II	$\pm 6^\circ$
0722	TARS attitude error, roll, stage II	$\pm 6^\circ$
0723	Rate gyro output, pitch, stage II (primary)	± 12.5 deg/sec
0724	Rate gyro output, yaw, stage II (primary)	± 12.5 deg/sec

UNCLASSIFIED

UNCLASSIFIED

TABLE 3-VI.- LAUNCH-VEHICLE INSTRUMENTATION MEASUREMENTS
FOR GT-2 - Continued

Measurement	Description	Instrumentation range
0725	Rate gyro output, roll, stage II (primary)	± 12.5 deg/sec
0726	25 V dc power supply voltage	0 to 39.4 V dc
0727	800 cps power supply voltage (primary or secondary)	20 to 30 V ac
0728	TARS discrete (stage I gain change)	Bilevel
0729	Autopilot output pitch sub-assembly 3 (primary or secondary)	± 0.7 V dc
0730	Autopilot output, yaw, sub-assembly 3 (primary or secondary)	± 0.7 V dc
0731	Autopilot output, roll, secondary assembly 1 (primary or secondary)	± 1.2 V dc
0732	Displacement gyro torquer monitor, pitch	± 0.80 V dc
0733	Displacement gyro torquer monitor, yaw	± 0.80 V dc
0734	Displacement gyro torquer monitor, roll	± 0.80 V dc
0735	TARS discrete (arm stage I shutdown sensor)	Bilevel
0736	Rate gyro output, pitch, stage II (secondary system)	± 12.5 deg/sec
0737	Rate gyro output, yaw, stage II (secondary system)	± 12.5 deg/sec
0738	Rate gyro output, roll, stage II (secondary system)	± 12.5 deg/sec
0739	TARS discrete (arm stage II shutdown sensors)	Bilevel
0740	TARS discrete (guidance initiate)	Bilevel
0741	IPS staging arm timer actuation	Bilevel

UNCLASSIFIED

UNCLASSIFIED

3-65

TABLE 3-VI.- LAUNCH-VEHICLE INSTRUMENTATION MEASUREMENTS
FOR GT-2 - Continued

Measurement	Description	Instrumentation range
0743	IGS pitch attitude error output	$\pm 6^\circ$
0744	IGS yaw attitude error output	$\pm 6^\circ$
0745	IGS roll attitude error output	$\pm 6^\circ$
0746	Rate beacon guidance, 30 volt supply	0 to 5 V dc
0747	Pulse beacon guidance, 15 volt supply	0 to 5 V dc
0748	Decoder guidance, 10 volt supply	0 to 5 V dc
0749	Rate beacon guidance, received signal 2	0 to 5 V dc
0750	Rate beacon guidance, received signal 1	50 to 85 dbm
0751	Rate beacon guidance, PH detect	Step voltage
0752	Rate beacon guidance, power output	Step voltage
0753	Pulse beacon guidance, MAG current	Step voltage
0754	Pulse beacon guidance, AGC	-10 to -65 dbm
0755	Pitch output, guidance	± 100 percent
0756	Yaw output, guidance	± 100 percent
0757	Decoder, discrete, binary 8	Bilevel
0758	Decoder, discrete, binary 4	Bilevel
0759	Decoder, discrete, binary 2	Bilevel
0760	Decoder, discrete, binary 1	Bilevel
0762	Autopilot output, pitch, subassembly 1 (primary)	± 1.2 V dc
0763	Autopilot output, yaw, subassembly 1 (primary)	± 1.2 V dc

UNCLASSIFIED

UNCLASSIFIED

TABLE 3-VI.- LAUNCH-VEHICLE INSTRUMENTATION MEASUREMENTS
FOR GT-2 - Continued

Measurement	Description	Instrumentation range
0764	Autopilot output, pitch, subassembly 2 (primary)	± 1.2 V dc
0765	Autopilot output, yaw, subassembly 2 (primary)	± 1.2 V dc
0766	Adapter package output, pitch	± 6.0 V dc
0767	Adapter package output, yaw	± 6.0 V dc
0768	Adapter package output, roll	± 6.0 V dc
0769	Autopilot output, yaw, subassembly 1 (secondary)	± 1.2 V dc
0770	Autopilot output, pitch, subassembly 1 (secondary)	± 1.2 V dc
0771	Autopilot output, pitch, subassembly 2 (secondary)	± 1.2 V dc
0772	Autopilot output, yaw, subassembly 2 (secondary)	± 1.2 V dc
0773	IGS stage I gain change, discrete	Bilevel
0777	RCS SECO signal	Bilevel
0780	AGC command receiver 1, RSS and burst	10 to 40 μ V
0781	AGC command receiver 2, RSS and burst	10 to 20 μ V
0782	Engine cut-off, receiver 1	Bilevel
0783	Engine cut-off, receiver 2	Bilevel
0784	AGC range channel, MISTRAM transponder	-40 to -110 dbm
0785	AGC calibration channel, MISTRAM transponder	-40 to -110 dbm

UNCLASSIFIED

UNCLASSIFIED

3-67

TABLE 3-VI.- LAUNCH-VEHICLE INSTRUMENTATION MEASUREMENTS
FOR GT-2 - Continued

Measurement	Description	Instrumentation range
0786	RF-output range channel, MISTRAM transponder	Calibration voltage
0787	RF-output calibration channel, MISTRAM transponder	Calibration voltage
0788	Phase detector calibration channel, MISTRAM transponder	Calibration voltage
0789	Phase detector range channel, MISTRAM transponder	Step voltage
0799	Auxiliary sustainer cut-off signal	Bilevel
0800	IPS bus voltage	15 to 35 V dc
0801	APS bus voltage	0 to 37.5 V dc
0802	ac bus voltage, phase A (400 cps)	105 to 125 V ac
0803	ac bus frequency, phase A	380 to 420 cps
0804	IPS battery current	0 to 150 A
0805	APS battery current	0 to 150 A
0810	Instrument voltage, compartment 2	0 to 6 V dc
0811	Temperature bridge power supply, compartment 2	35.5 to 45 V dc
0812	Signal conditioner package temperature	0 to 200° F
0813	PCM mercury cell voltage	1.35 V dc
0814	PCM mercury cell voltage	1.35 V dc
0815	PCM mercury cell voltage	1.35 V dc
0816	Signal conditioner power supply, positive regulated	29.9 to 30.1 V dc
0817	Signal conditioner power supply, negative regulated	29.9 to 30.1 V dc

UNCLASSIFIED

UNCLASSIFIED

TABLE 3-VI. LAUNCH-VEHICLE INSTRUMENTATION MEASUREMENTS
FOR GT-2 - Continued

Measurement	Description	Instrumentation range
0842	Pitch SMRD (BH bypass)	Bilevel
0843	Pitch SMRD (BL bypass)	Bilevel
0844	Yaw SMRD (BH bypass)	Bilevel
0845	Yaw SMRD (BL bypass)	Bilevel
0846	Roll SMRD (BH bypass)	Bilevel
0847	Roll SMRD (BL bypass)	Bilevel
0848	Overrate warning	Bilevel
0853	Subassembly 3, MDTCPs A and B	Bilevel
0854	Subassembly 3, MDFJPS A and B	Bilevel
0855	Subassembly 3, MDFJPS A and B (B.C.)	Bilevel
0856	Shutdown lockout, timers 1 and 2	Bilevel
0858	Shutdown switches, reset monitor	Bilevel
0859	APS-IPS compartment 2 (RSP)	15 to 30 V dc
0861	Subassembly, MDTCPs A and B (B.C.)	Step voltage
0862	IPS staging	Bilevel
0863	APS staging	Bilevel
0868	Fuel tank pressure (A) stage II	0 to 75 psia
0869	Fuel tank pressure (B) stage II	0 to 75 psia
0870	Oxidizer tank pressure (A) stage II	0 to 75 psia
0871	Oxidizer tank pressure (B) stage II	0 to 75 psia
0872	Transfer to secondary control system (A)	Bilevel

UNCLASSIFIED

UNCLASSIFIED

3-69

TABLE 3-VI. - LAUNCH-VEHICLE INSTRUMENTATION MEASUREMENTS
FOR GT-2 - Continued

Measurement	Description	Instrumentation range
0873	Transfer command to secondary control system (A)	Bilevel
0874	Transfer to secondary control system (B)	Bilevel
0875	Transfer command to secondary control system (B)	Bilevel
0876	APS to spacecraft	0 to 35 V dc
0877	Pitch SMRD-B (B.C.)	Step voltage
0878	Yaw SMRD-B (B.C.)	Step voltage
0879	Roll SMRD-B (B.C.)	Step voltage
0880	Subassembly 2 hydraulic switchover command	Bilevel
0881	Subassembly 1 hydraulic switchover command	Bilevel
0882	Spacecraft switchover command (A)	Bilevel
0883	Spacecraft switchover command (B)	Bilevel
0884	APS-IPS compartment 2 (Eng. subassembly 3)	15 to 35 V dc
0885	Spacecraft switchback command (A)	Bilevel
0886	Spacecraft switchback command (B)	Bilevel
1003	Thrust chamber pressure, subassembly 1	0 to 1 000 psia
1004	Thrust chamber pressure, subassembly 2	0 to 1 000 psia
1017	Oxidizer-pump inlet pressure (T-0 to 87FS2-5), subassembly 2	0 to 200 psia
1085	Pressure, oxidizer tank dome, 27-in. radius	0 to 100 psia

UNCLASSIFIED

UNCLASSIFIED

TABLE 3-VI. - LAUNCH-VEHICLE INSTRUMENTATION MEASUREMENTS
FOR GT-2 - Continued

Measurement	Description	Instrumentation range
1086	Pressure in oxidizer tank dome centerline, stage I (87FS2-5 to stage separation)	0 to 200 psia
1169	Acceleration, axial, compartment 5	$\pm 10g$
1170	Acceleration, axial, compartment 5	$\pm 10g$
1189	Vibration, tandem actuator (axial), stage I	$\pm 100g$
1190	Vibration, tandem actuator (lateral)	$\pm 100g$
1191	Vibration, tandem actuator (vertical), stage I	$\pm 100g$
1502	Thrust chamber pressure, subassembly 3	0 to 1 000 psia
1651	Travel, actuator 6, pitch, stage II	± 0.505 in.
1670	Acceleration, axial, compartment 1	$\pm 10g$
1671	Acceleration, lateral, vehicle compartment 1	$\pm 2g$
1672	Acceleration, vertical, vehicle compartment 1	$\pm 2g$
1692	Vibration, MOD 3 rate beacon, axial	$\pm 30g$
1695	Sound pressure level, external, compartment 2	40 to 160 dB
1696	Sound pressure level, external, compartment 1	40 to 160 dB
1697	Vibration, RGS equipment mount, lateral	$\pm 30g$
1698	Vibration, RGS equipment mount, vertical	$\pm 30g$

UNCLASSIFIED

TABLE 3-VI.- LAUNCH-VEHICLE INSTRUMENTATION MEASUREMENTS
FOR GT-2 - Continued

Measurement	Description	Instrumentation range
1723	Rate gyro output, pitch, stage II, primary	± 12.5 deg/sec
1855	Subassembly 3, MDF5PS A and B	Bilevel
1861	Subassembly 3, MDTCP5 A and B	Step voltage
1862	IPS staging	Bilevel

NASA-S-65-1515

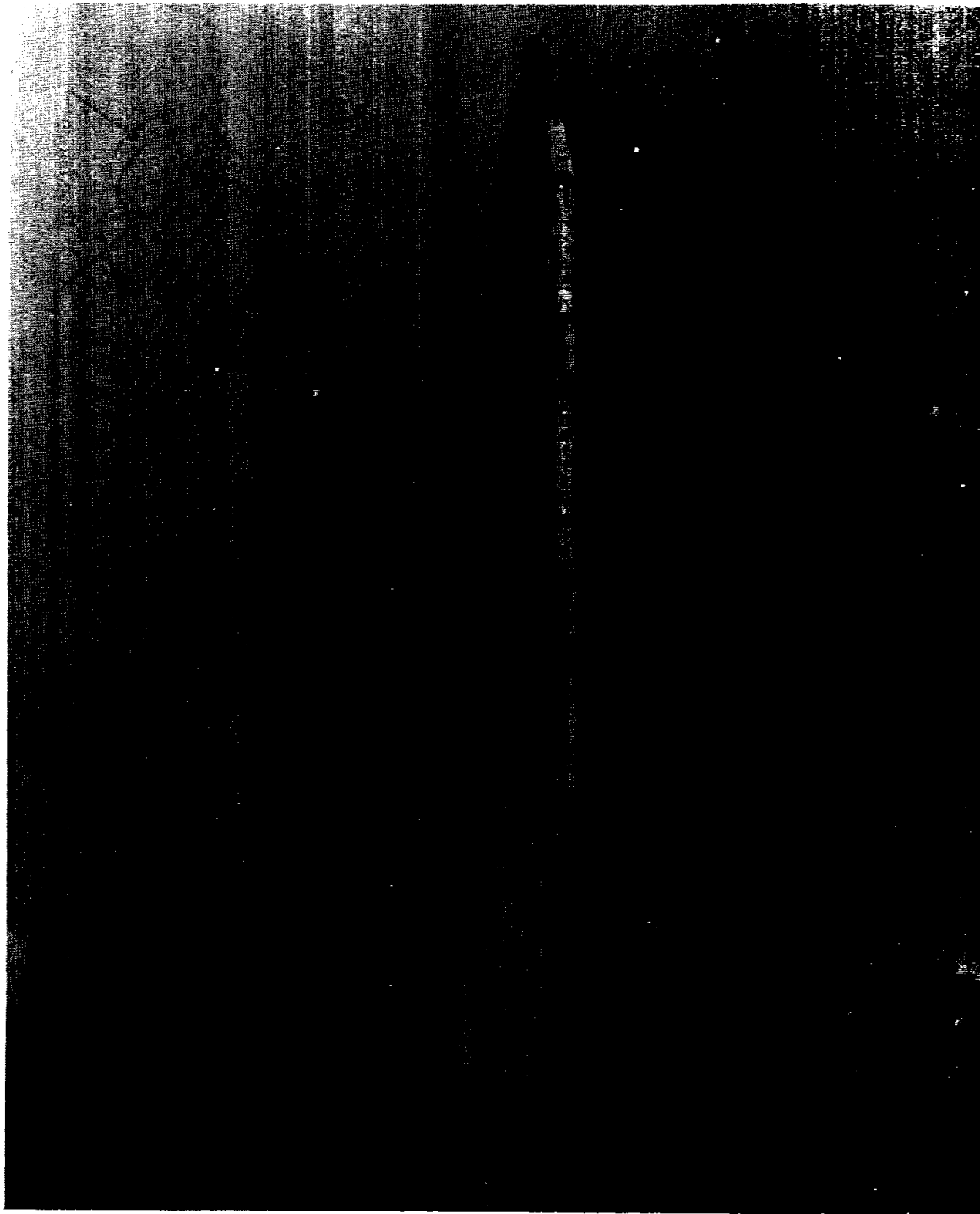


Figure 3-1 GT-2 space vehicle lift-off configuration

UNCLASSIFIED

UNCLASSIFIED

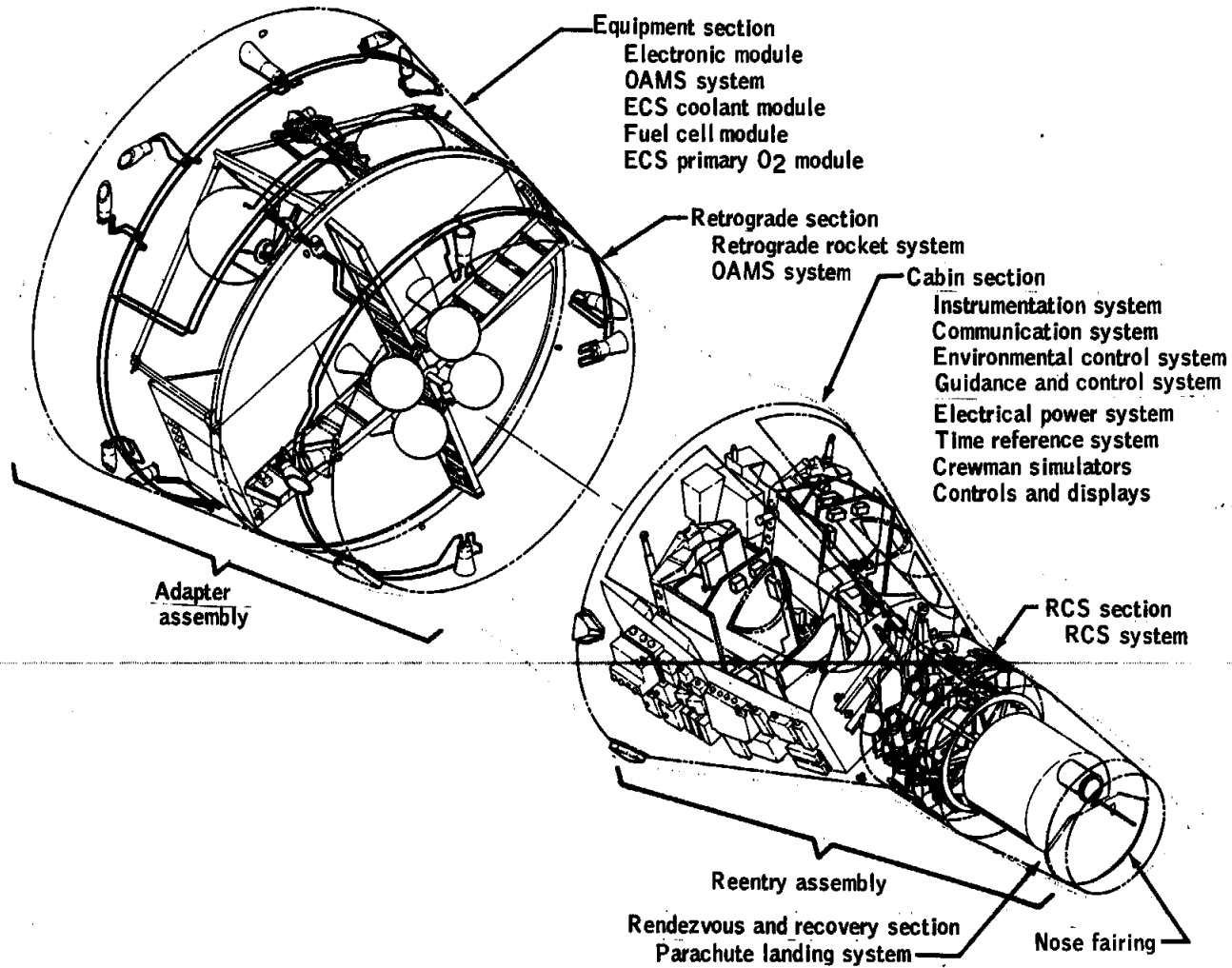
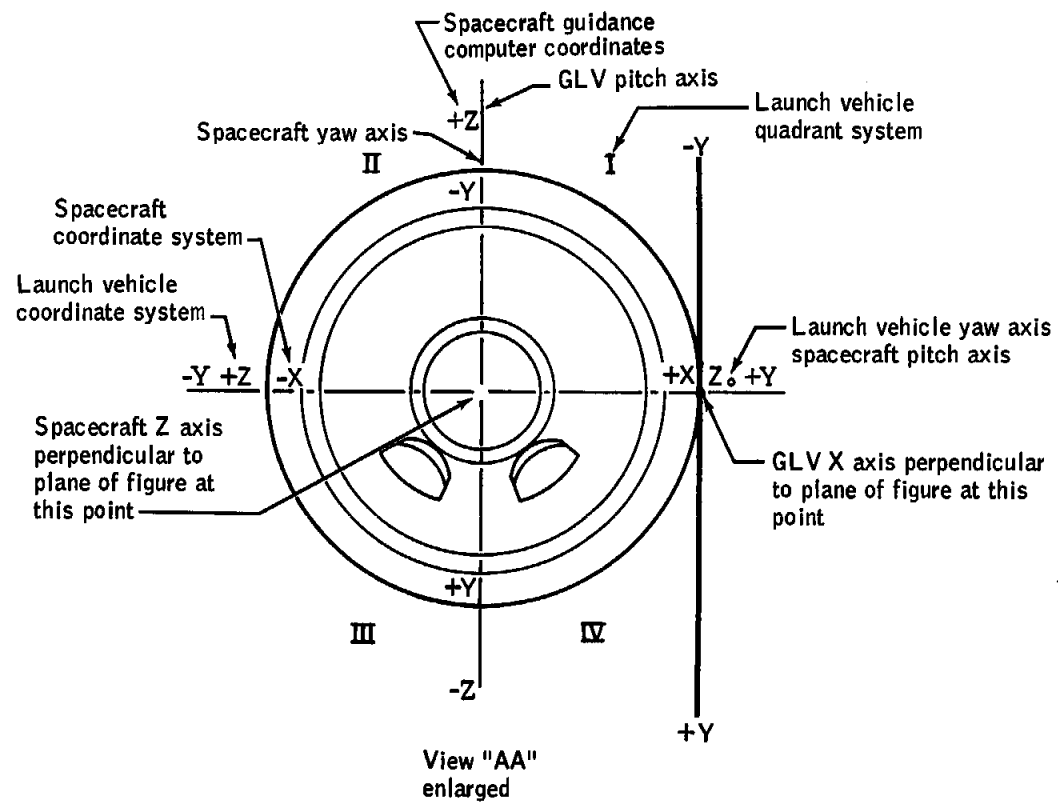
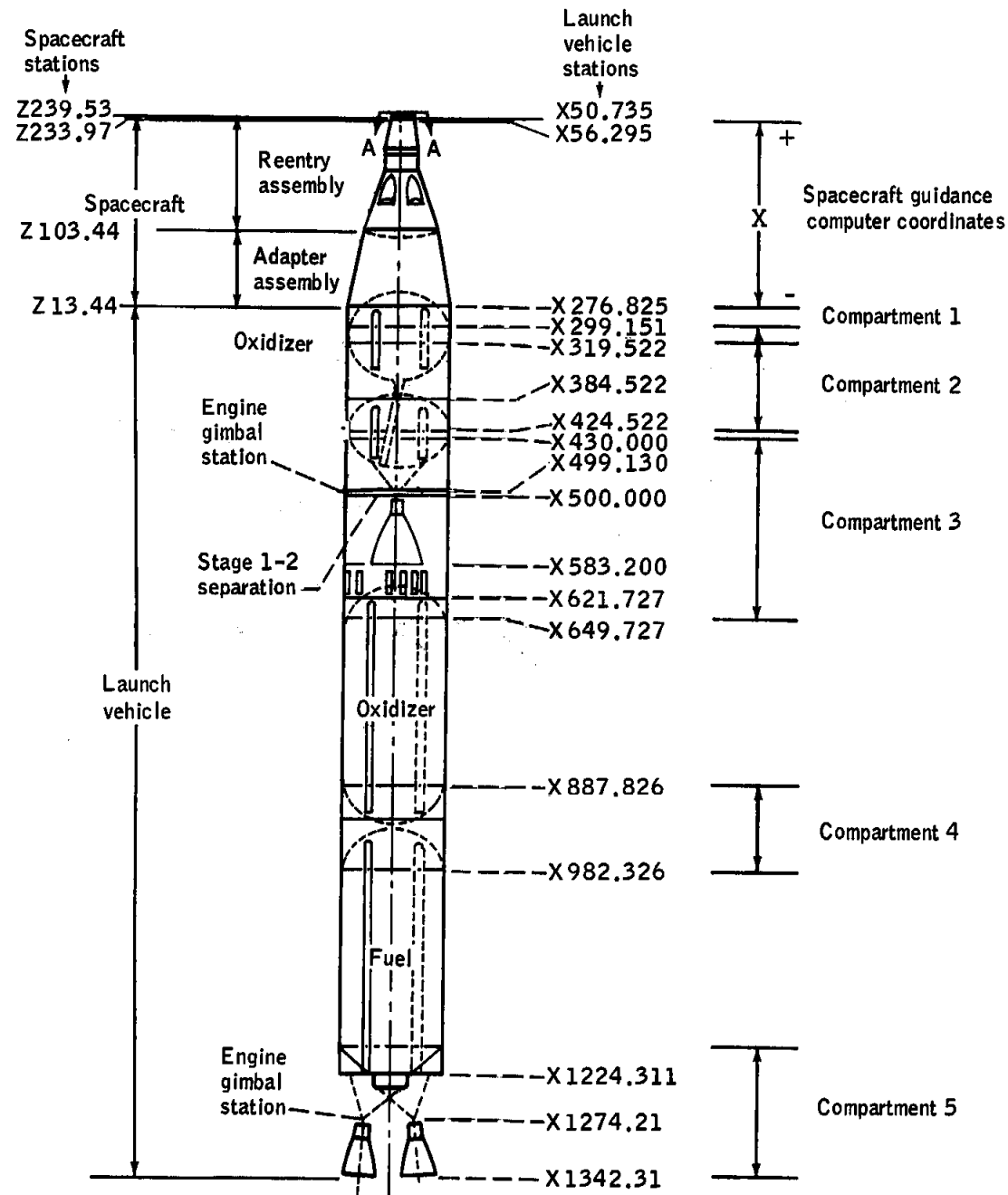


Figure 3-2 Spacecraft arrangement and nomenclature

NASA-S-65-1238



Note: Spacecraft inertial guidance coordinates remained referenced to the launch stand for GT-2 as shown below

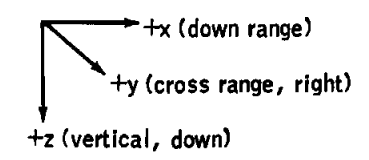


Figure 3-3 - Launch vehicle - spacecraft relationships

NASA-S-65-1231

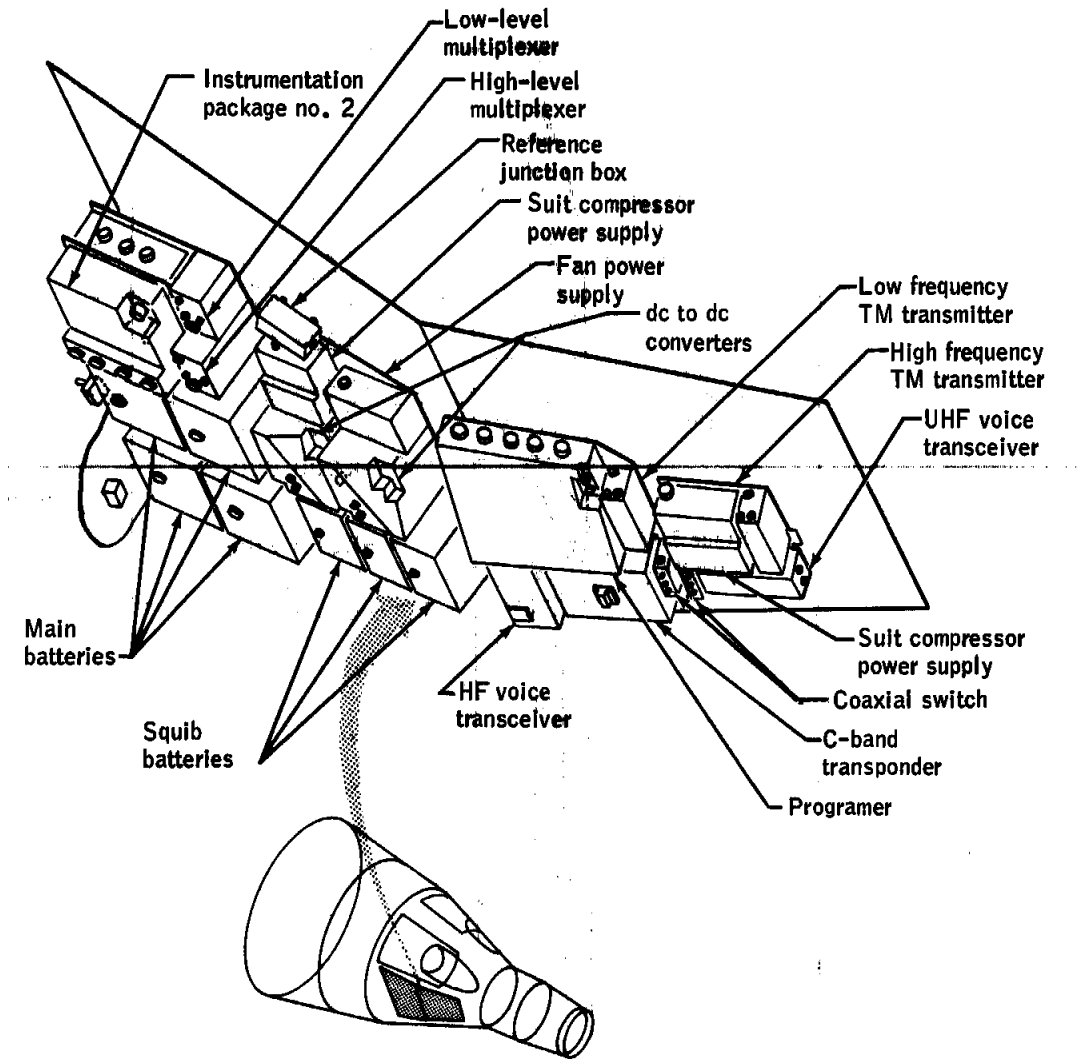
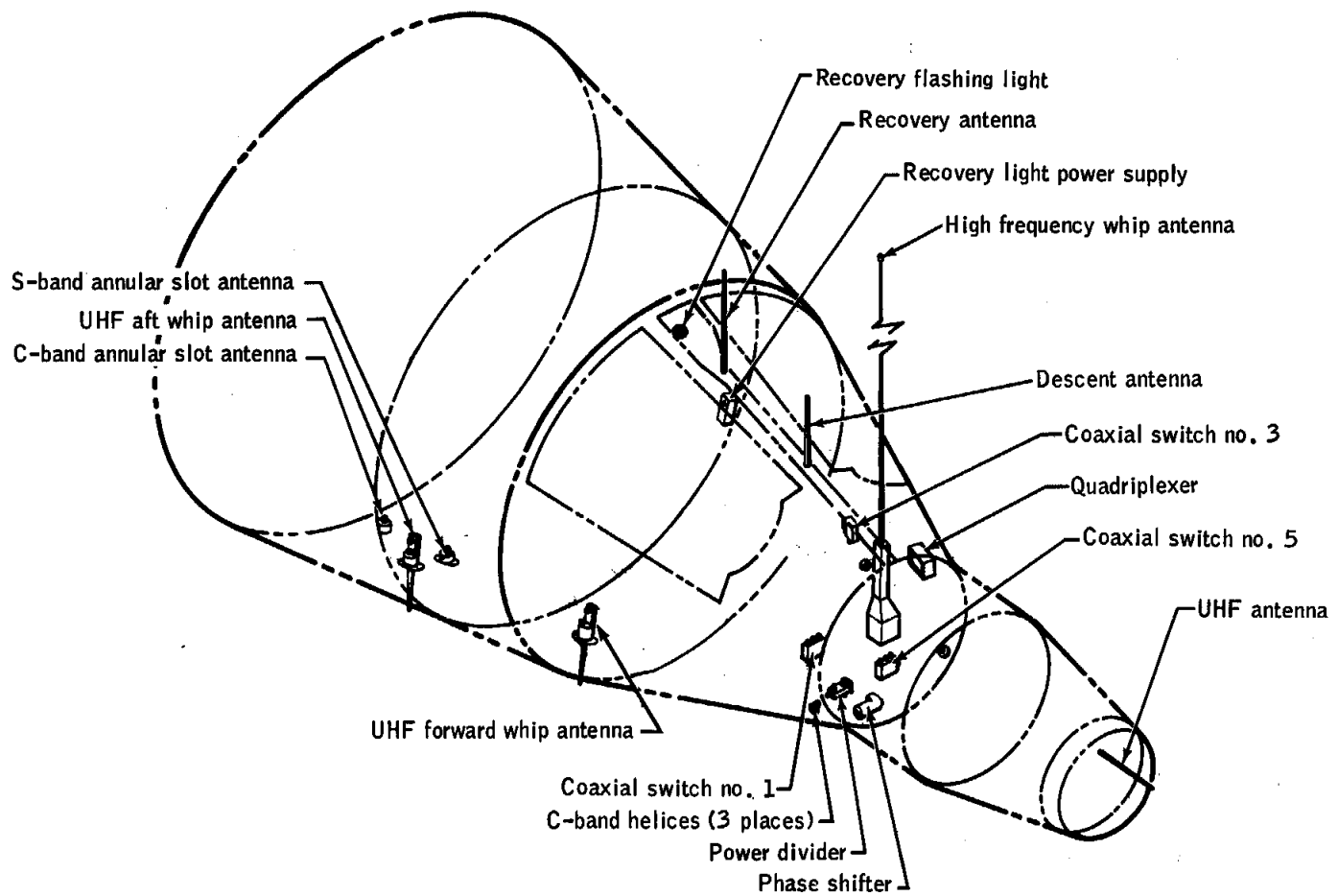


Figure 3-4 Reentry assembly - right hand equipment bay

UNCLASSIFIED



UNCLASSIFIED

Figure 3-7 Spacecraft antenna locations

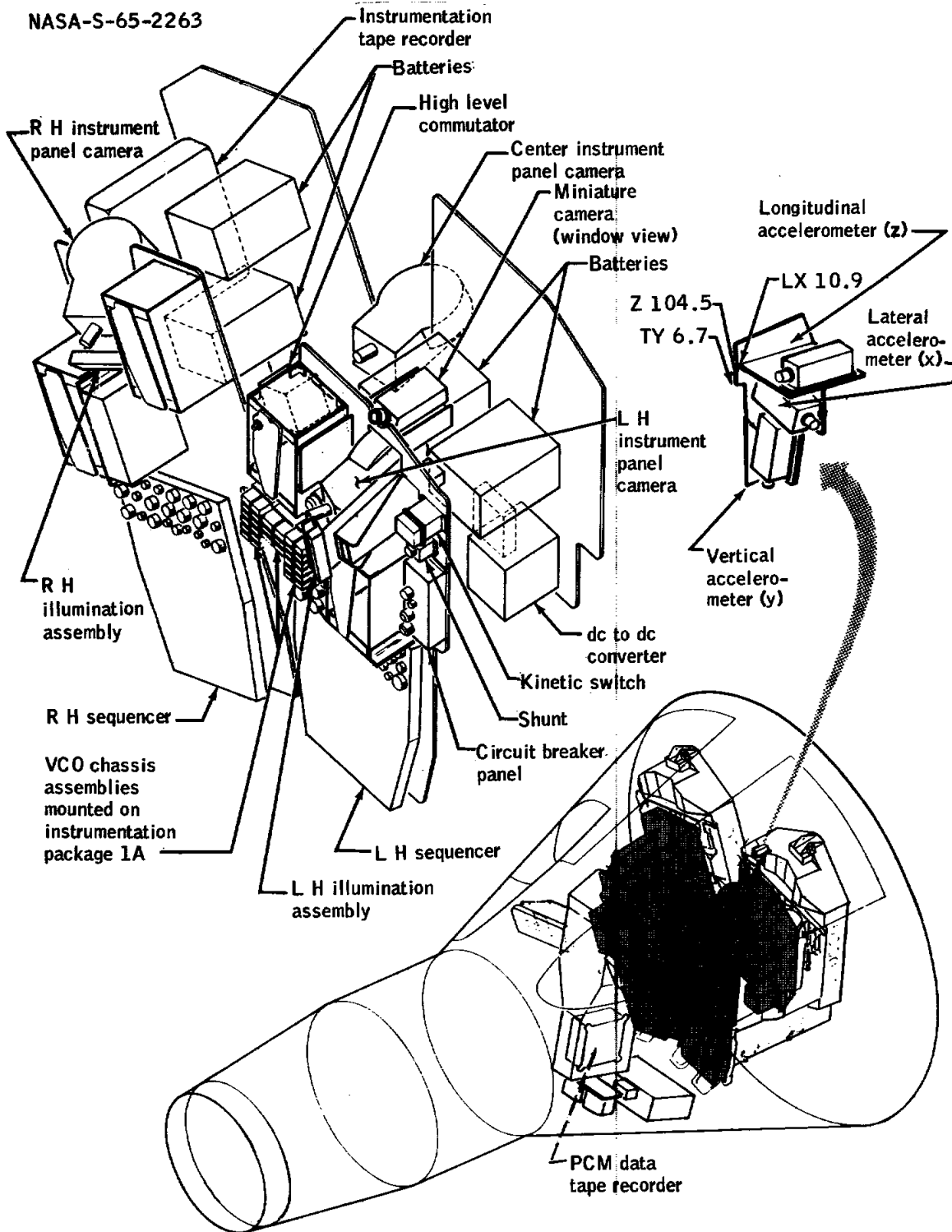


Figure 3-8. - Special instrumentation pallet assemblies

NASA-S-65-1234

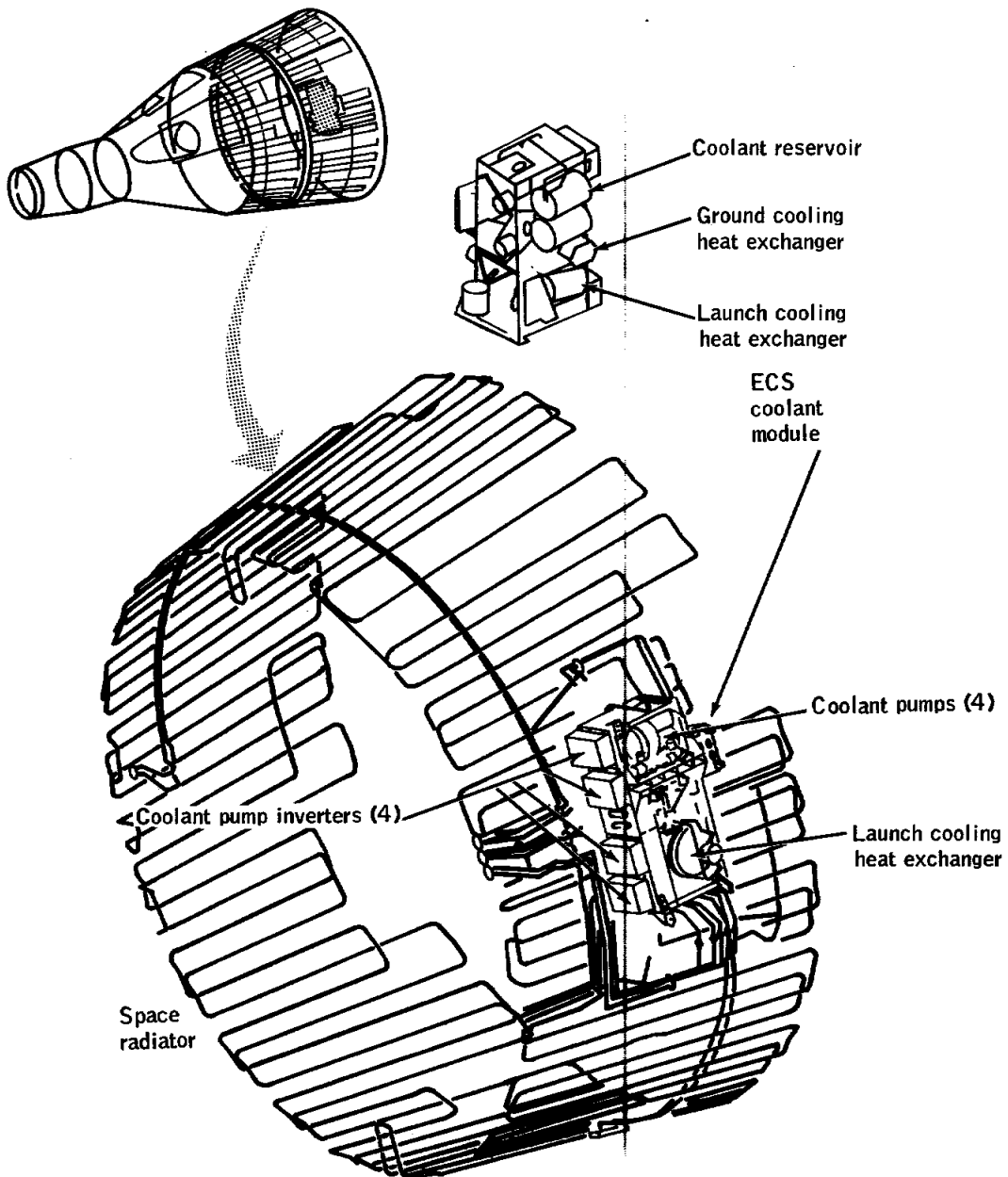


Figure 3-10 Adapter-equipment section - ECS coolant module and space radiator

UNCLASSIFIED

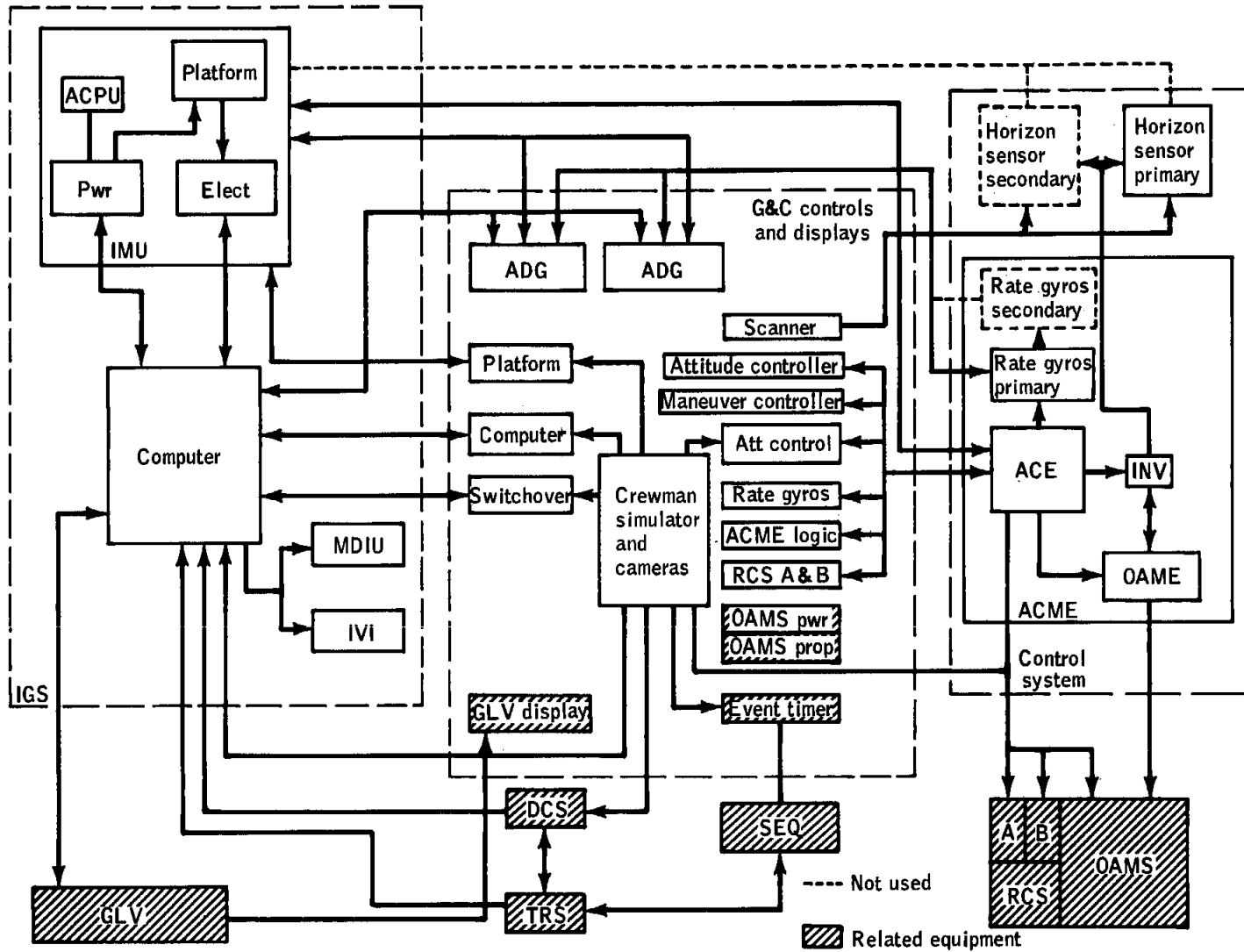


Figure 3-11 Block diagram of guidance and control system equipment

UNCLASSIFIED

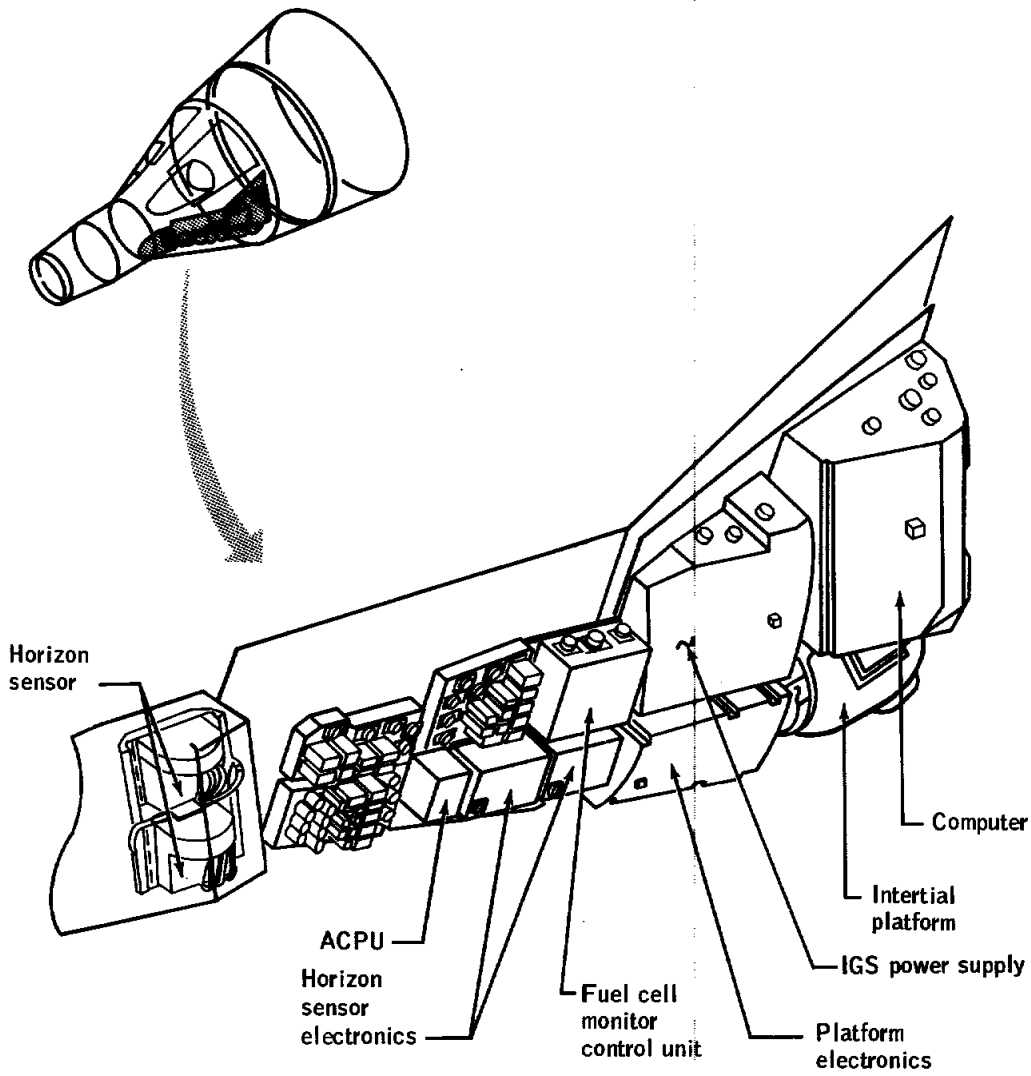


Figure 3-12 Reentry assembly - left hand equipment bay

NASA-S-65-1236

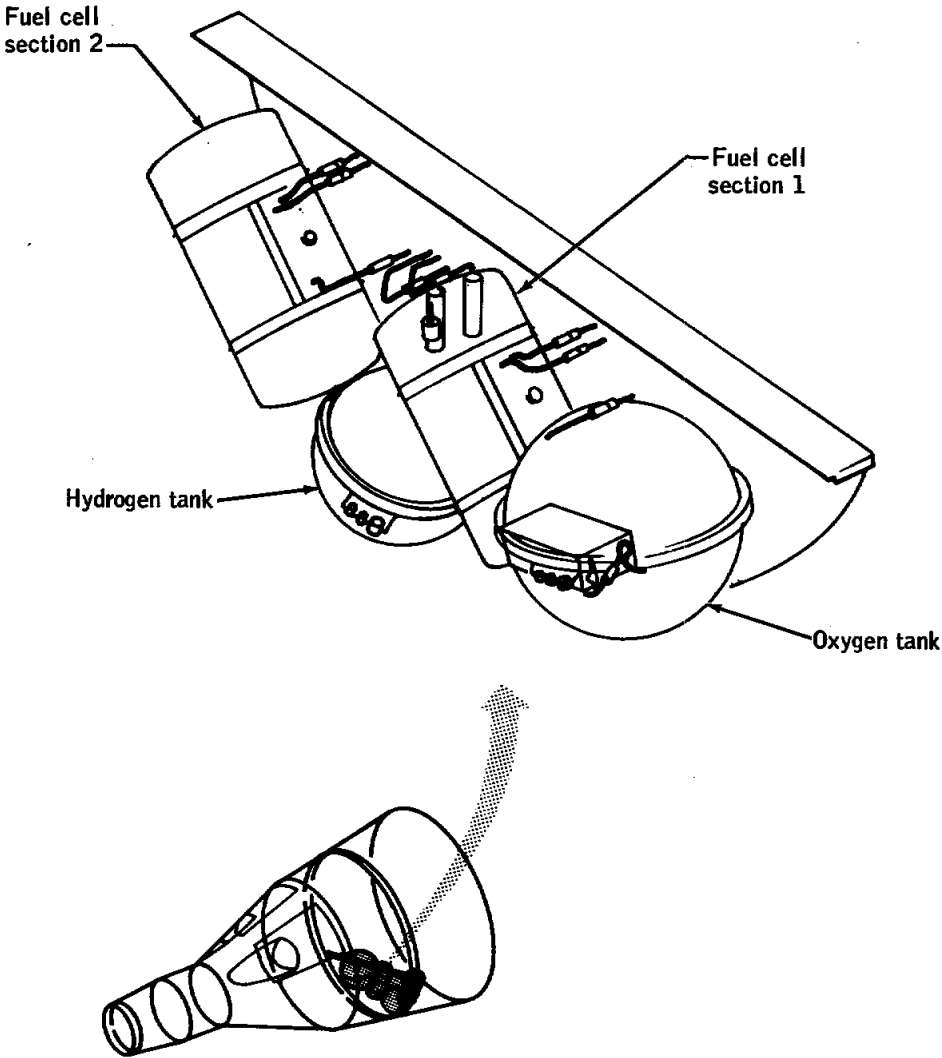


Figure 3-13 Fuel cell module

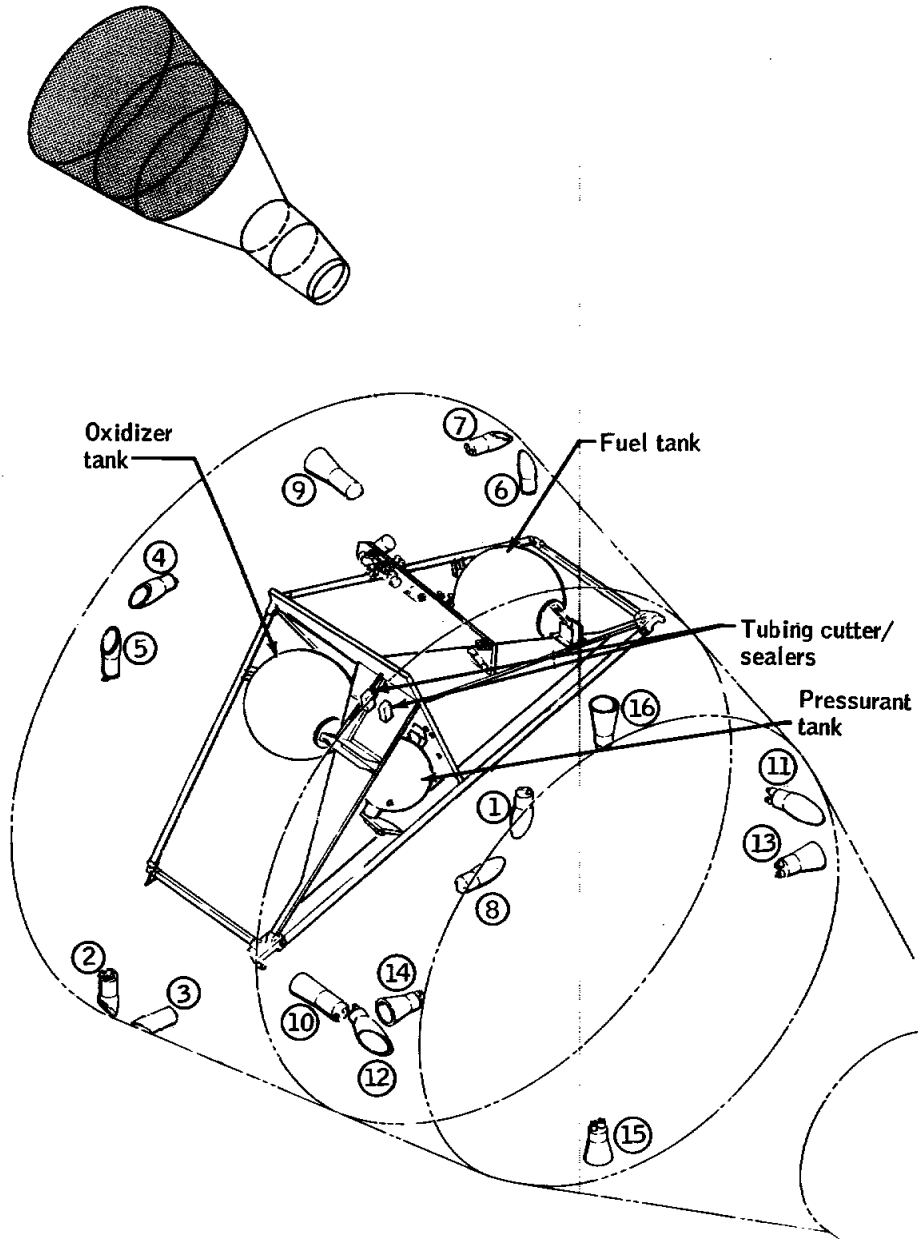
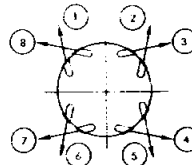


Figure 3-14 Orbital attitude and maneuver system

NASA-S-65-1608

RCS thrust chamber attitude control



- | | | |
|---|---|------------|
| 5 | 6 | Pitch up |
| 1 | 2 | Pitch down |
| 3 | 4 | Yaw right |
| 7 | 8 | Yaw left |
| 3 | 7 | Roll right |
| 4 | 8 | Roll left |

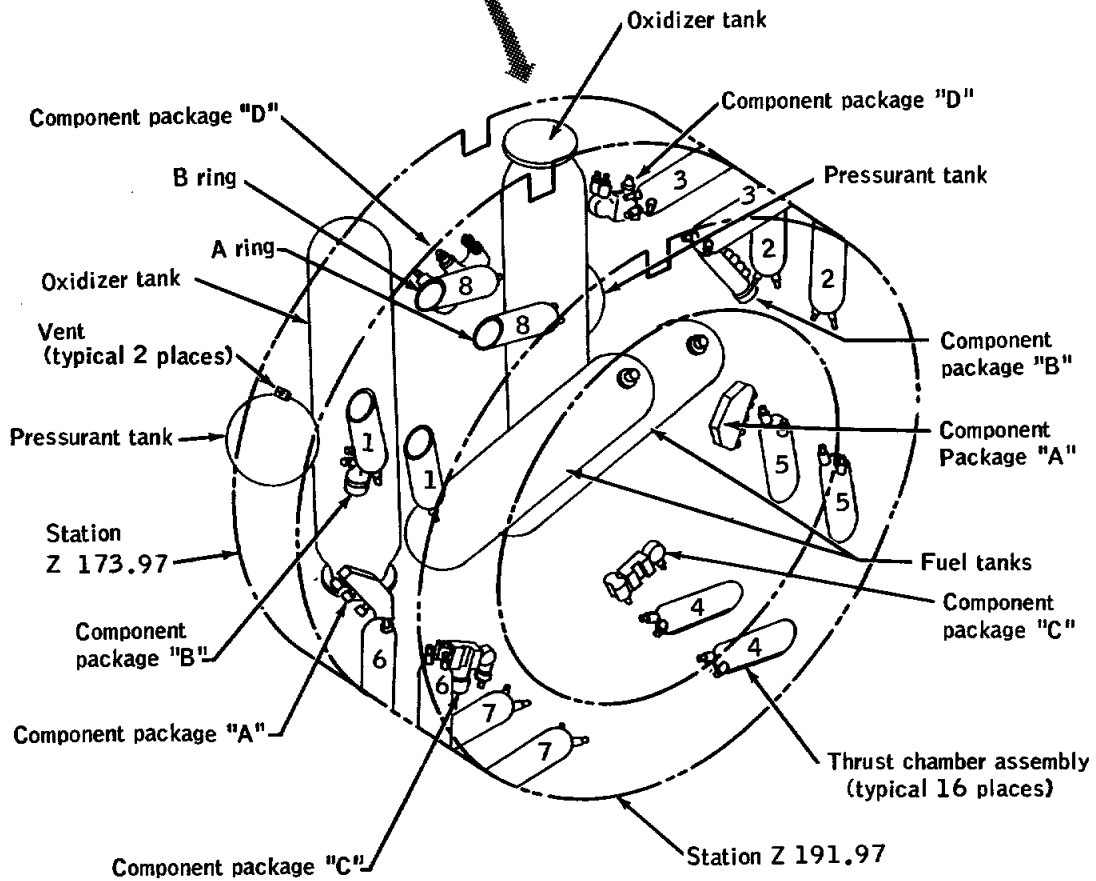


Figure 3-15 Reentry control system

UNCLASSIFIED

UNCLASSIFIED

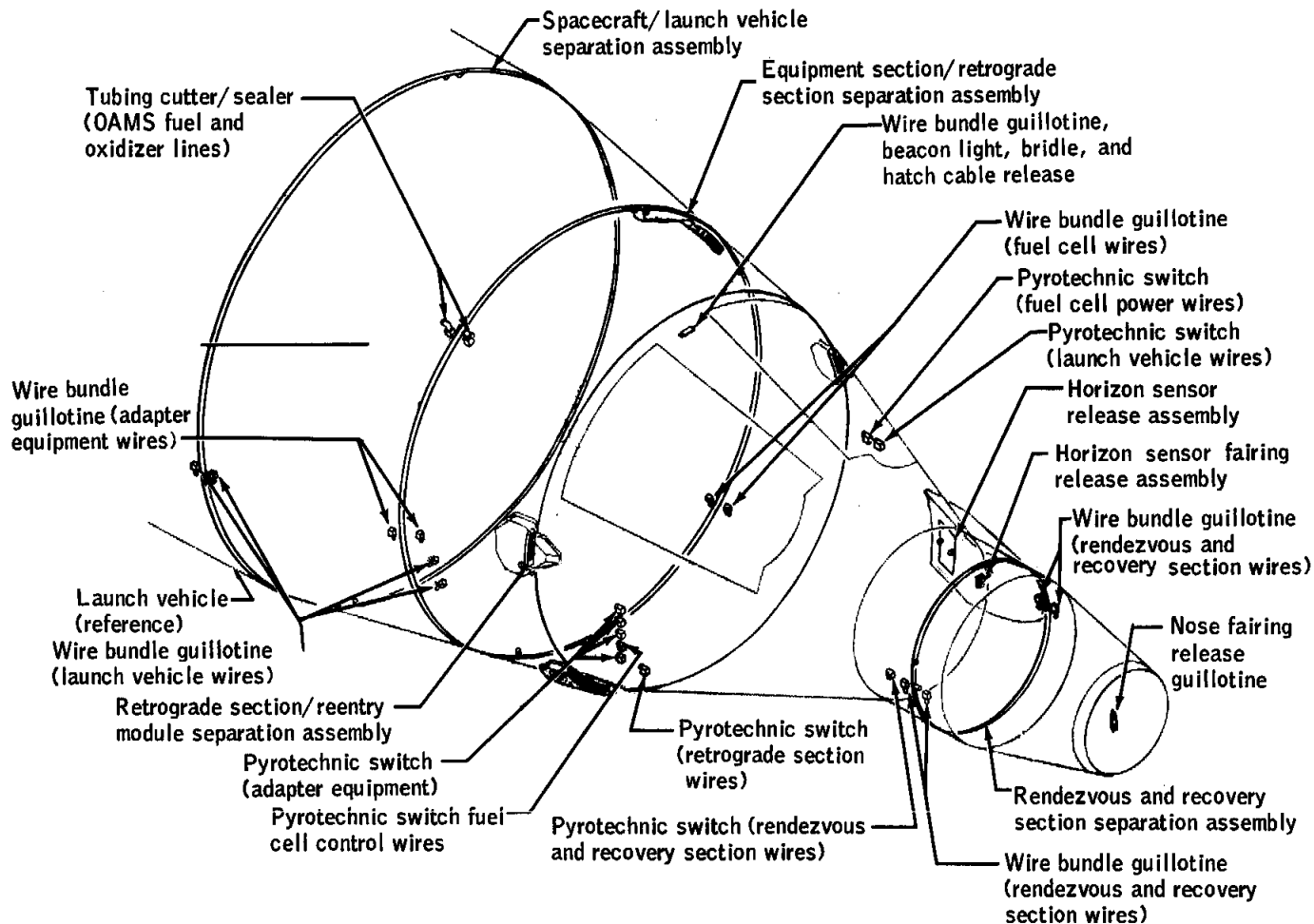


Figure 3-16 Pyrotechnic separation assemblies and devices

4.0 MISSION DESCRIPTION

The GT-2 mission was planned to demonstrate the adequacy of spacecraft reentry heat protection equipment and to qualify further, by actual flight environment, those spacecraft and launch vehicle systems necessary to support manned flight. Since heating is of prime concern, a ballistic trajectory was planned to provide a maximum design heating rate on the spacecraft reentry assembly. A launch azimuth of 105° was chosen to provide a safe flight corridor with respect to land masses, a good recovery posture, and sufficient instrumentation and tracking coverage.

The first-stage programed portion of launch-vehicle ascent guidance was programed in roll to provide the required azimuth reference plane after lifting off from a launch-stand azimuth of 85° . The second-stage closed-loop portion of the ascent guidance by the GE/Burroughs radio guidance system was to begin approximately 8 seconds after staging at 162.56 seconds and continue throughout the remainder of stage II powered flight. Steering commands were to be provided to guide the launch vehicle along a trajectory which was to result in injection of the spacecraft into the planned trajectory at an altitude of 87 nautical miles, with a space-fixed velocity of 25 731 ft/sec and a space-fixed flight-path angle of -2.28° .

Spacecraft separation from the launch vehicle was to be effected, after second stage engine tail-off, by imparting a velocity increment of 15 ft/sec with the two aft-firing orbital attitude and maneuver system (OAMS) engines. Separation was to be followed by a 90° left-roll, (spacecraft separation +2 sec) and a 180° turnaround (spacecraft separation +30 sec), and a pitch-up maneuver (spacecraft separation +45 sec), to a retroattitude of -16° (small end down), referenced to the horizontal at the launch complex, which represents an attitude of approximately -29.2° , referenced to the local horizontal at the initiation of retrofire. Equipment section jettison and the automatic retrograde rocket firing was sequenced to begin at SECO + 82 seconds followed by retrograde section jettison at SECO + 127 seconds. The reentry mode of the attitude control maneuver electronics (ACME) was programed to initiate a 15 deg/sec spacecraft roll rate when a load factor of 0.05g was sensed and to maintain that rate for 150 seconds. At the end of this time, the spacecraft was to assume the maximum lift attitude. The parachute and recovery sequence was to be initiated by a barostat at an altitude of 10 600 feet. The nominal landing point was located 1862 nautical miles downrange at $16^\circ 26'$ north latitude and $49^\circ 34'$ west longitude.

UNCLASSIFIED

4.1 ACTUAL MISSION

Lift-off (LO), defined as the launch vehicle umbilical separation, occurred at 9:03:59.861 a.m. e.s.t. As the vehicle rose vertically, the roll program was initiated at LO + 4.34 seconds and continued until the vehicle rolled to a flight azimuth of approximately 105°. For a comparison of actual times against planned times, see table 4-I. At LO + 22.9 seconds, the first of three programmed pitch rates was initiated. The pitch program continued to guide the vehicle until the radio guidance system (RGS) was enabled at LO + 162.12 seconds.

The first flight control system gain change occurred at LO + 104.67 seconds, and the second occurred during staging (BECO) at LO + 151.71 seconds. Spacecraft inertial guidance system (IGS) updates were received at LO + 103.75 and 144.55 seconds. The IGS served as back-up guidance during the entire flight but was not required to control the vehicle.

Reconstructed trajectory results indicate that the vehicle was slightly high and fast during the stage I powered flight. The GE/Burroughs, Mission Control Center, and Range Safety plotboards verified this deviation. Cause of this minor deviation in the pitch plane may be attributed to slightly high thrust due to higher than normal propellant flow rates, gyro drift, and high winds causing the vehicle to pitch up. Stage I shutdown occurred 1.81 seconds earlier than predicted.

The range safety plotboards indicate the vehicle deviated to the left of the nominal ground track. At LO + 70 seconds, the vehicle's path was observed to cross the lateral left 3σ locus of instantaneous impact points and to remain in this region until LO + 87 seconds. The major contribution to this deviation was a wind shear recorded at that time. The 3σ boundary was based on a September wind profile for the original launch date and was not updated for the December wind profile which is considerably higher in velocity. Had this updating been made, the ground track would not have exceeded the plotboard limits. (See section 5.2.9.)

Staging was complete and separation had started by 152.40 seconds. The stage II thrust was higher than nominal, and as in stage I, an earlier than predicted engine shutdown occurred when the RGS detected the programmed velocity.

The spacecraft radar and sensor fairings were jettisoned 45 seconds after BECO as planned.

UNCLASSIFIED

The RGS commands corrected the trajectory and steered the vehicle to the desired spacecraft separation conditions. At SECO + 20.32 seconds, spacecraft OAMS aft-firing thrusters were ignited to achieve spacecraft - launch-vehicle separation. A 90° roll, a 180° turnaround, and a pitch maneuver to -29.2° small end down attitude (referenced to local horizontal) followed separation. At LO + 414.22 seconds, the equipment section was separated by pyrotechnics, and the automatic retrograde rocket firing sequence was initiated. The retrorocket firing order was 1, 3, 2, 4; and the retrograde section was jettisoned at 459.12 seconds. The spacecraft entered telemetry blackout at LO + 545.0 seconds, and blackout ended at LO + 698.9 seconds. At 0.05g deceleration (LO + 560.23 sec), the ACME reentry mode initiated an average roll rate of 13.6°/sec to provide zero lift. A constant roll was maintained until LO + 710.01 seconds when the spacecraft assumed the maximum lift attitude.

The peak stagnation point ($\alpha = 0^\circ$) heating rate of 71.8 Btu/ft²/sec was reached at LO + 643 seconds. Pilot and main parachutes were deployed at LO + 871.76 and 875.38 seconds, respectively, based on telemetry acceleration and vibration data. The landing point, based on Antigua reentry tracking data, was 1848 nautical miles from Cape Kennedy at 49°46' west longitude and 16°36' north latitude. The landing time was LO + 1096 seconds.

4.2 SEQUENCE OF EVENTS

The times at which major events were planned and executed are presented in table 4-I. All events were completed as scheduled within the expected tolerances, indicating a satisfactory flight.

4.3 FLIGHT TRAJECTORIES

The trajectories referred to as planned are preflight calculated nominal trajectories contained in reference 8, and the trajectories referred to as actual are based on the Manned Space Flight Network tracking data. The Patrick Air Force Base model atmosphere was used below 25 nautical miles for the planned trajectory, and the actual atmosphere at the time of launch was used for the actual trajectory. The 1959 ARDC model atmosphere was used above 25 nautical miles in both the planned and actual trajectories. The earth model used was the Fischer Ellipsoid. A ground track of the GT-2 mission is presented in figure 4-1. Since GT-2 was a suborbital trajectory, the launch and reentry phases are shown together in figure 4-2. These figures show that the actual GT-2 mission profile was very close to the planned profile.

~~CONFIDENTIAL~~

4.3.1 Launch

The launch phase of the trajectory data shown in figure 4-2 is based on the real-time output of the range safety impact predictor computer (IP-3600) and the Guided Missile Computer Facility (GMCF). The IP-3600 had data available from the missile trajectory measurement (MISTRAM) system and FPS-16 and FPQ-6 radars, while the GMCF used data from the GE Mod III radar. The data from these tracking facilities were used during the time periods listed in the following table:

Facility	Time after lift-off, sec
IP-3600 (FPS-16)	0 to 24
GMCF (GE Mod III)	24 to 410

The actual launch trajectory as compared with the planned launch trajectory in figure 4-2 was high in velocity, altitude, and flight-path angle during stage I powered flight. After BECO, the radio guidance system (RGS) corrected the trajectory error and guided the second stage to a nominal insertion. At BECO, the actual velocity, altitude, and flight-path angle were higher than planned by 161 ft/sec, 12 863 feet, and 1.3°, respectively. At SECO there was essentially no difference from the planned velocity, and attitude and flight-path angle were low by only 40 feet and 0.04°, respectively. The velocity change during tail-off was 8.0 ft/sec greater than predicted. As a result, the velocity was 7 ft/sec higher than planned at spacecraft separation.

4.3.2 Reentry

The planned reentry phase of the trajectory shown in figure 4-2 was obtained by beginning with the nominal insertion conditions supplied by reference 11 and integrating forward through the orbital attitude and maneuver system (OAMS) for separation and retrofire to landing. The actual reentry phase of the trajectory was obtained by taking the spacecraft position and velocity vector as determined by the Goddard Space Flight Center (GSFC) computer which used the Antigua tracking data after retrofire. This vector was integrated backward through retrofire and OAMS for spacecraft separation conditions, and forward for reentry conditions.

A comparison of the actual and planned trajectory parameters is given in table 4-II. The flight parameters at spacecraft separation were in good agreement with the parameters obtained from the GMCF and

~~CONFIDENTIAL~~

~~CONFIDENTIAL~~

4-5

MISTRAM insertion vectors as obtained by the Goddard Space Flight Computing Facilities, thus confirming the validity of the backward integration method. The velocities and flight-path angles obtained from the GMCF and the MISTRAM data were 4 ft/sec and 7 ft/sec less and 0.03° and 0.01° greater (more negative), respectively, than the Antigua data at spacecraft separation. The times of communications blackout, 0.05g, and pilot parachute deployment taken from the integrated trajectory were in good agreement with the data obtained from the Gemini network station and spacecraft onboard measurements. The landing point from the integrated trajectory was within 3 miles of the retrieval point reported by the recovery ship. The agreement of these events validate the reentry phase of the integrated trajectory.

~~CONFIDENTIAL~~

~~CONFIDENTIAL~~

TABLE 4-I. - SEQUENCE OF EVENTS

Event	Planned time, sec	Actual time, sec	Difference, sec
Stage I engine ignition signal (87FS1)	-3.34	-3.36	-0.02
Lift-off (9:03:59.861 a.m. e.s.t)	0.00	0.00	0.00
Roll program start	4.40	4.34	-0.06
Roll program end	20.48	20.40	-0.08
No. 1 pitch rate start	23.04	22.99	-0.05
No. 2 pitch rate start	88.32	88.07	-0.25
No. 1 IGS update received	103.00	103.75	+0.75
No. 1 flight control gain change	104.96	104.67	-0.29
No. 3 pitch rate start	119.04	118.71	-0.33
No. 2 IGS update received	143.00	144.55	+1.55
Arm stage I engine shutdown	144.64	144.28	-0.36
BECO (stage I engine shut- down signal (87FS2)) Stage II engine ignition signal (91FS1) No. 2 flight control gain change	153.52	151.71	-1.81
Separation start	154.22	152.40	-1.82
Stage II MD FJPS make	154.42	152.37	-2.05
No. 3 pitch rate end	162.56	162.09	-0.47
RGS enable	162.56	162.12	-0.44

~~CONFIDENTIAL~~

TABLE 4-I. - SEQUENCE OF EVENTS - Concluded

Event	Planned time, sec	Actual time, sec	Difference, sec
First radio guidance command received	169.00	168.29	-0.71
Horizon sensor fairing jettison	198.52	196.64	-1.88
Nose fairing jettison	198.52	196.74	-1.78
Arm stage II engine shutdown	317.44	316.58	-0.86
SECO (stage II engine shutdown (91FS2))	336.48	332.15	-4.33
Stage II MD FJPS break	336.78	332.47	-4.31
Fire spacecraft separation device	356.48	352.45	-4.03
Separate equipment adapter section.	418.48	414.22	-4.26
Initiate automatic retrograde firing sequence	418.48	414.22	-4.26
Jettison retrograde section	463.50	459.12	-4.38
Begin communication blackout	546.5	545.0	-1.5
0.05g, initiate roll	567.10	560.23	-6.87
End communication blackout	704.8	698.9	-5.9
Initiate full lift	717.10	710.01	-7.09
Pilot parachute deployment	879.20	871.76	-7.44
Main parachute deployment	882.40	875.38	-7.02
Touchdown	1141	1096	-53

~~CONFIDENTIAL~~

TABLE 4-II.- COMPARISON OF PLANNED AND ACTUAL TRAJECTORY PARAMETERS

Condition	Planned	Actual	Difference
SECO			
Time from lift-off, sec	336.48	332.15	-4.33
Time from lift-off, min:sec	5:36.48	5:32.15	-4.33
Geodetic latitude, deg North	26.24	26.28	0.04
Longitude, deg West	72.51	72.61	0.10
Altitude, ft	546 850	546 810	-40
Altitude, n. mi.	90.0	90.0	0
Range, n. mi.	450.1	446	-4.1
Space-fixed velocity, ft/sec	25 605	25 604	-1
Space-fixed flight-path angle, deg	-2.24	-2.28	-0.04
Space-fixed heading angle, deg East of North	108.34	108.30	-0.04
Spacecraft separation			
Time from lift-off, sec	356.48	352.45	-4.03
Time from lift-off, min:sec	5:56.48	5:52.45	-4.03
Geodetic latitude, deg North	25.80	25.85	0.05
Longitude, deg West	71.15	71.21	0.06
Altitude, ft	525 971	524 867	-1104
Altitude, n. mi.	86.6	86.4	-0.2
Range, n. mi.	529.2	525.3	-3.9
Space-fixed velocity, ft/sec	25 731	25 738	7
Space-fixed flight-path angle, deg	-2.28	-2.29	-0.01
Space-fixed heading angle, deg East of North	108.98	108.95	-0.03
Maximum conditions			
Altitude, statute miles	105.6	106.3	0.7
Altitude, n. mi.	91.7	92.4	0.7
Space-fixed velocity, ft/sec	25 822	25 829	7
Earth-fixed velocity, ft/sec	24 499	24 506	7
Exit acceleration, g	7.6	7.3	-0.3
Exit dynamic pressure, lb/sq ft	743	683	-60
Reentry deceleration, g	9.6	9.9	0.3
Reentry dynamic pressure, lb/sq ft	657	657	0
Landing point			
North latitude, deg:min	16:26	^a 16:34	00:08
West longitude, deg:min	49:34	^a 49:46	00:12
Range, n. mi.	1862	1848	-14

^aLanding point reported by recovery ship:

North latitude, deg:min:sec . . . 16:31:54

West longitude, deg:min:sec . . . 49:46:48

~~CONFIDENTIAL~~

NASA-S-65-1818

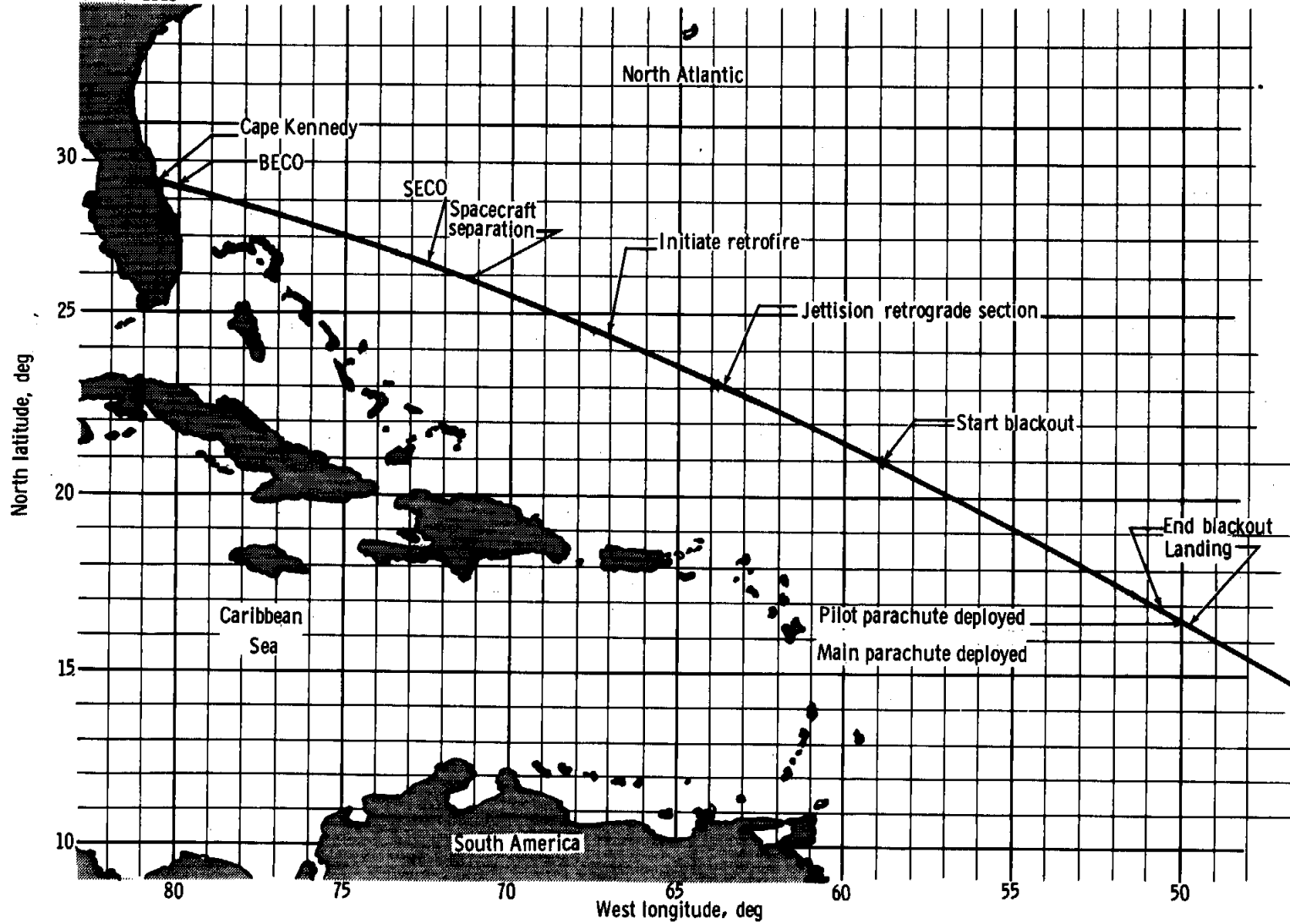


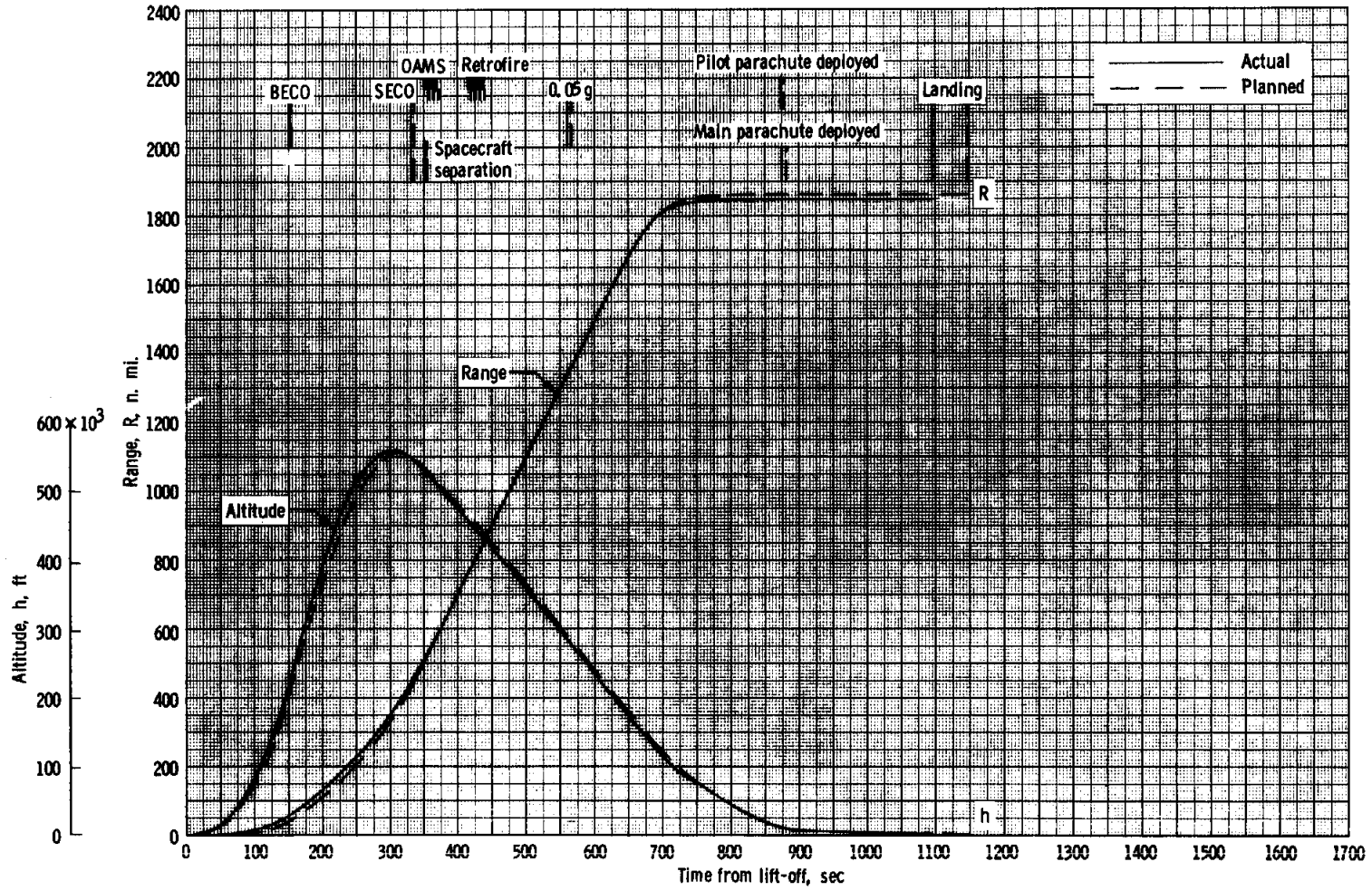
Figure 4-1 - Ground track

UNCLASSIFIED

UNCLASSIFIED

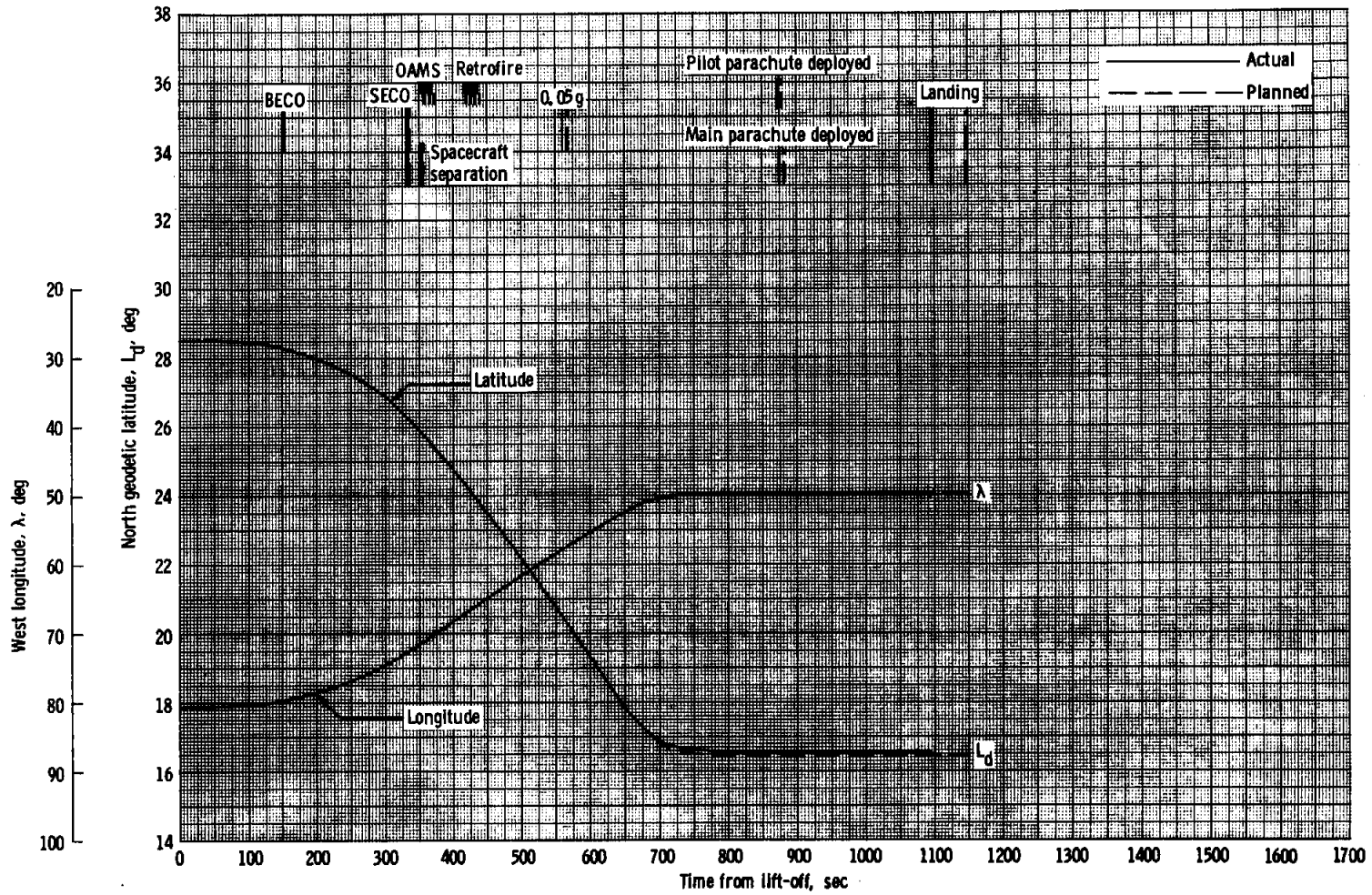
CONFIDENTIAL

CONFIDENTIAL



(a) Altitude and range.

Figure 4-2 - Time histories of trajectory parameters

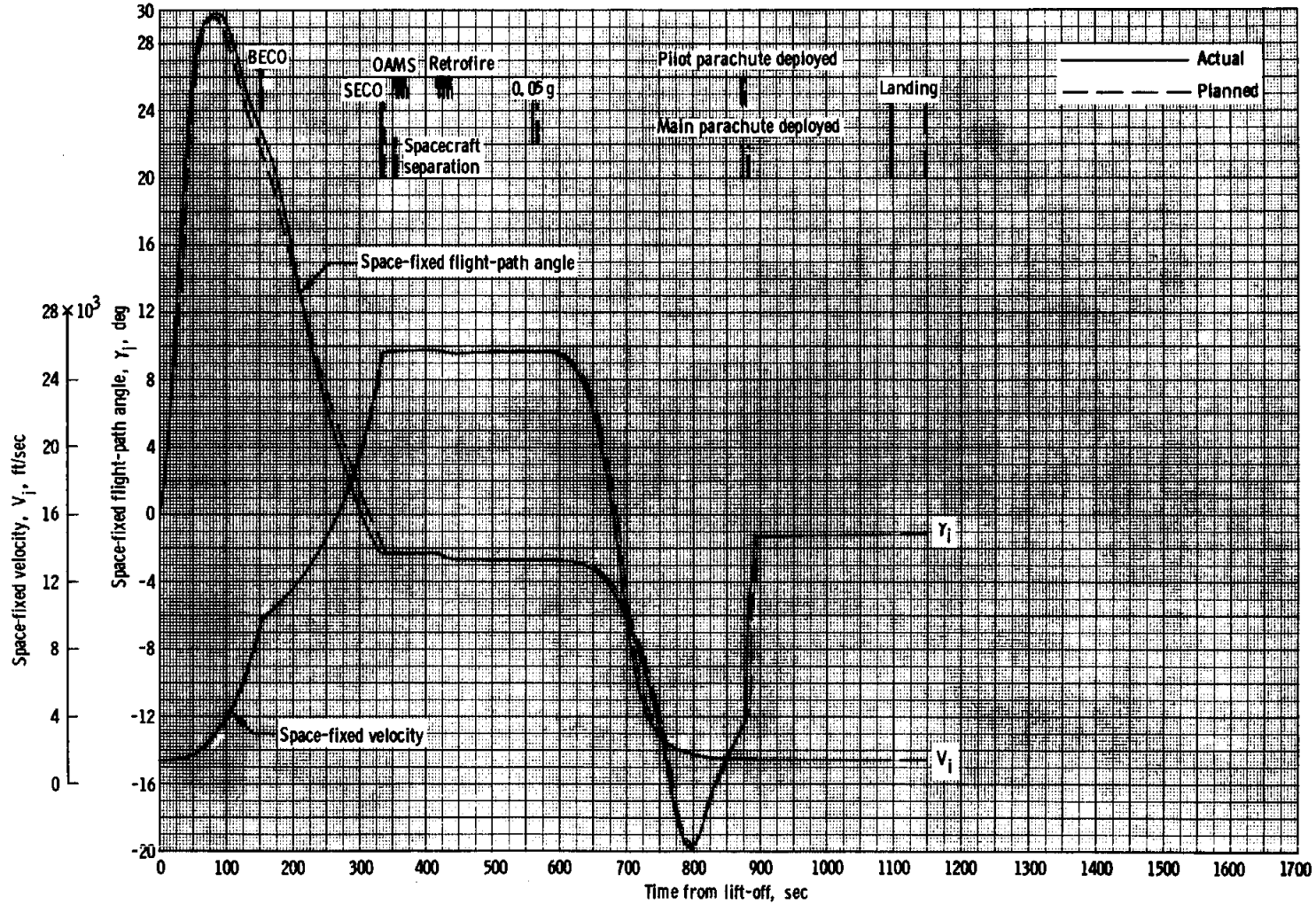


(b) Latitude and longitude.

Figure 4-2 - Continued.

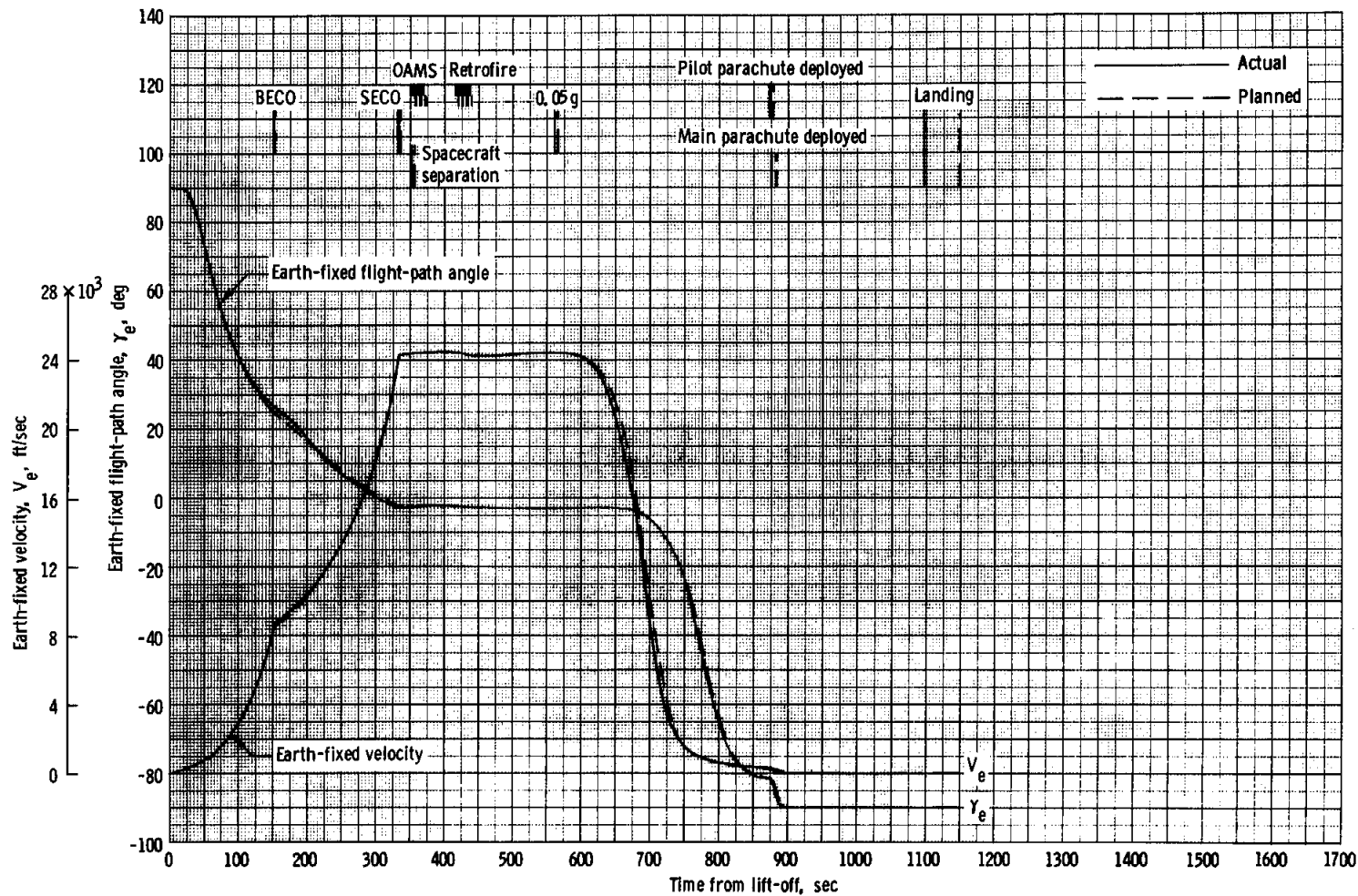
~~CONFIDENTIAL~~

~~CONFIDENTIAL~~



(c) Space-fixed velocity and flight-path angle.

Figure 4-2 - Continued.



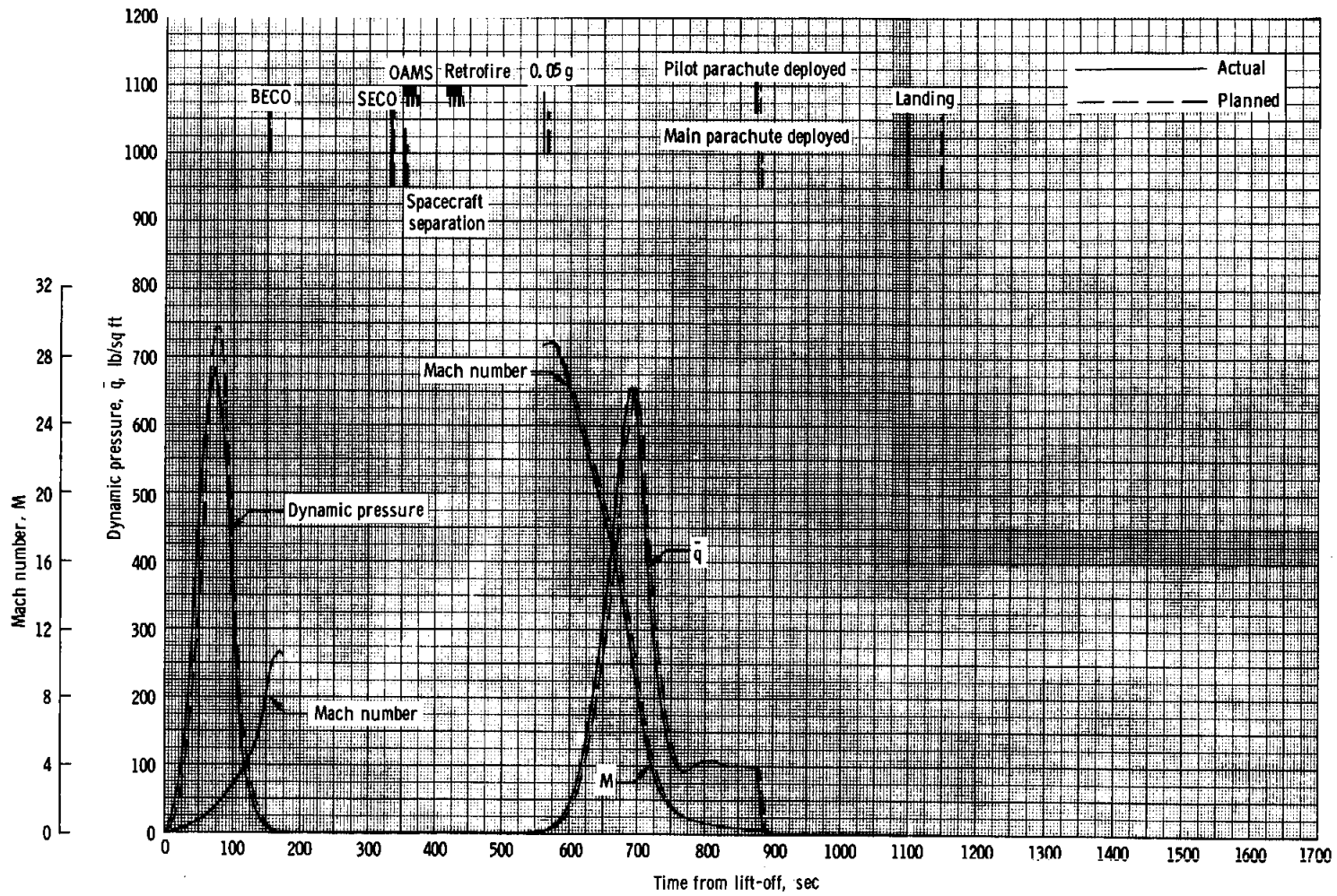
(d) Earth-fixed velocity and flight-path angle.

Figure 4-2 - Continued.

~~CONFIDENTIAL~~

~~CONFIDENTIAL~~

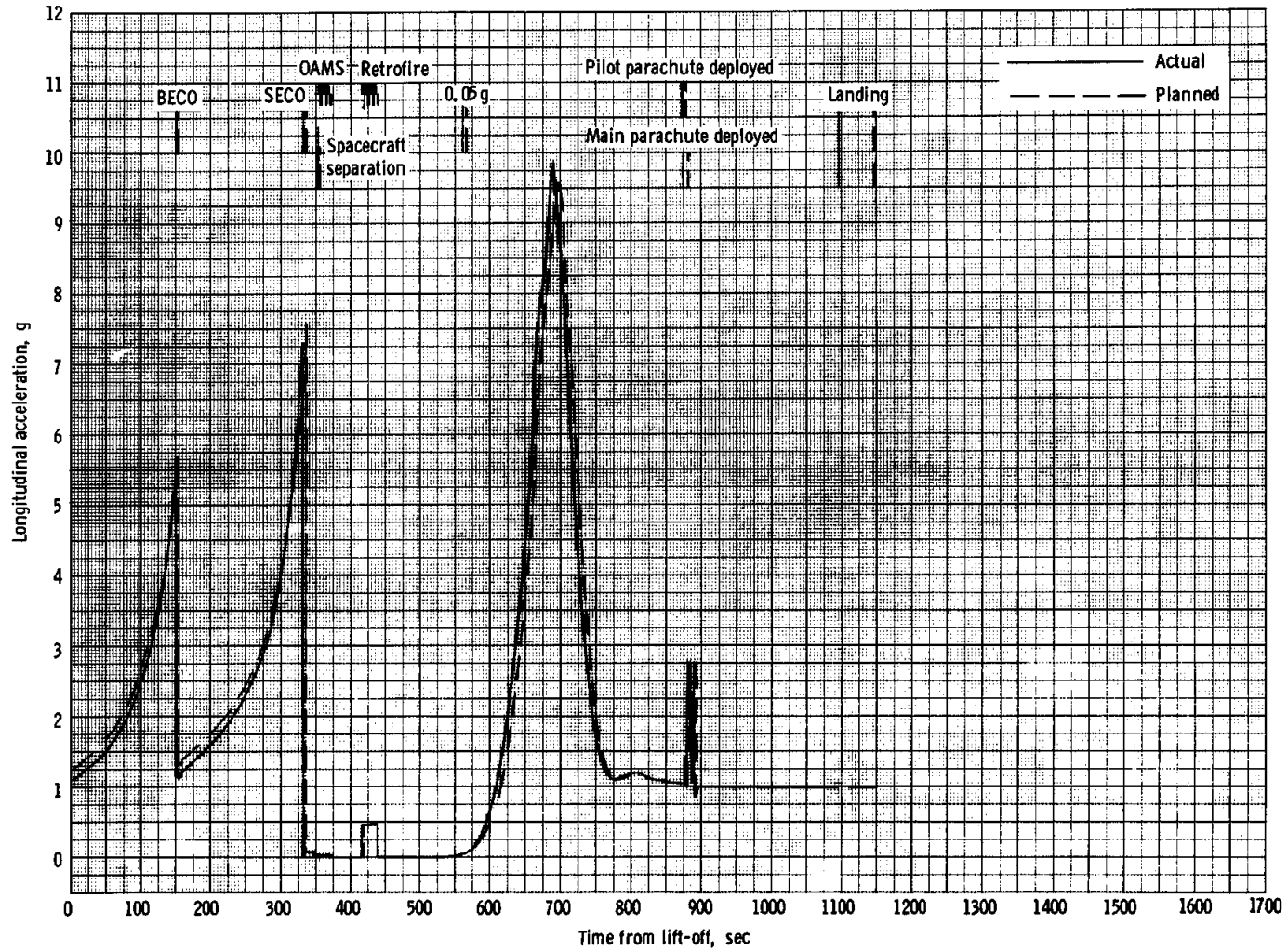
~~CONFIDENTIAL~~



(e) Mach number and dynamic pressure.

Figure 4-2 - Continued.

~~CONFIDENTIAL~~



(f) Longitudinal acceleration.

Figure 4-2 - Concluded.

~~CONFIDENTIAL~~

~~CONFIDENTIAL~~

~~CONFIDENTIAL~~

~~CONFIDENTIAL~~

~~CONFIDENTIAL~~

5-1

5.0 VEHICLE PERFORMANCE

Final engineering data have been reviewed and this review has revealed no failure to meet the first-order and second-order mission objectives, except for the requirement to flight test the fuel cell. A high heating-rate reentry trajectory was attained with maximum spacecraft lift and demonstrated the adequacy of the reentry assembly heat protection. The adequacy of the spacecraft structure was demonstrated for all phases of the mission including recovery. The Gemini launch vehicle performed within its specification limits and inserted the spacecraft into the planned reentry path. The performance of the vehicles and their systems and known anomalies are discussed and evaluated in the following paragraphs.

5.1 SPACECRAFT PERFORMANCE

5.1.1 Spacecraft Structure

5.1.1.1 General.- The primary structural objective of the GT-2 mission was to demonstrate the ability of the reentry assembly to withstand reentry heating and loads and water impact and recovery loads. The GT-2 mission again demonstrated the launch-phase structural integrity of the spacecraft and its compatibility with the launch vehicle. The mission also provided reentry vibration data which confirmed the adequacy of the vibration spectrum used to qualify the system equipment.

Local heating caused burn-through of four holes $\frac{1}{8}$ to $\frac{3}{8}$ -inch diameter in two shingles 14 to 25 inches downstream in the wake of the windward adapter interconnect fairing. Plastic flow and surface melting also occurred in this area. No damage of underlying insulation or structure occurred other than temperature discolorations.

5.1.1.2 Thermal environment.- The thermal environment encountered by the spacecraft during flight was of primary importance to this mission because final definition of aerodynamic heating constraints and structural adequacy of the spacecraft are to be based on data obtained from GT-2. The purpose of this analysis is to evaluate the actual environment as compared to that expected prior to flight.

Although the Gemini spacecraft configuration is quite similar to that of Mercury, experience gained during the Mercury program was not directly applicable since the Gemini spacecraft reenters at a finite angle of attack. Therefore, additional efforts were made to define aerodynamic heating for the predicted spacecraft attitude. Heating

~~CONFIDENTIAL~~

~~CONFIDENTIAL~~

predictions were based on correlations of wind-tunnel data obtained from facilities at NASA Langley Research Center, Arnold Engineering and Development Corporation, and Cornell University. These correlations result from data obtained at Mach numbers from 3.5 to 16.8 over a wide range of Reynolds numbers. In order to obtain structural temperature data, and to verify these heating correlations, 75 temperature and 8 static pressure sensors were installed in the spacecraft. In general, outer mold line temperature measurements were made with chromel-alumel thermocouples, while temperatures on internal structure were obtained with resistive type sensors. All thermal instrumentation appeared to function normally. External heating rates derived from these temperature data serve as the basis for refinement of wind-tunnel correlations. In addition, local pressure data obtained during the flight were obtained to allow correlation of flight and wind-tunnel pressure data which would provide a more accurate base for aerodynamic heating estimates using local flow conditions.

The GT-2 trajectory was planned to subject the spacecraft to the highest heating rates predicted for any phase of a Gemini flight, including abort. It is evident that the desired trajectory was achieved with a peak reference heating rate (zero angle-of-attack stagnation point) estimated at $71.8 \text{ Btu/ft}^2/\text{sec}$. This compares very closely to a planned value of 71.2 . The peak heating rate on the heat shield at the actual stagnation point is estimated to have reached a maximum of $76.2 \text{ Btu/ft}^2/\text{sec}$. Reentry total heating was calculated from the trajectory data to be 6670 Btu/ft^2 .

Heating estimates during mission planning were made using the Patrick Air Force Base atmosphere for launch and the 1959 ARDC atmosphere for reentry. Atmospheric data obtained the day of the flight are presented in section 4.3.2 of this report.

Angle-of-attack computations based on flight data indicate a range of 15° to 16° during peak reentry heating as compared with a planned value of 17.7° . Oscillations on the order of $\pm 1^\circ$ were recorded at this time during the flight.

5.1.1.2.1 Distribution of peak measured temperatures on reentry assembly afterbody: The distribution of peak temperatures measured on the reentry assembly afterbody outer skin temperatures is shown, for the upper and lower halves of the spacecraft, in figure 5.1-1. Temperature trends discussed are those for areas of the spacecraft which are least affected by outer skin protuberances. The extremely high temperatures recorded for sensors PD26 and PD27 on the cabin section right-hand side (fig. 5.1-1(b)) were located in an area of high heating caused by

~~CONFIDENTIAL~~

the most windward molded plastic adapter interconnect fairing and are discussed in detail in subsection 5.1.1.2.4.

Temperature variations occurred in the longitudinal direction. On the cabin section bottom centerline (BY), outer skin temperatures increased toward the heat shield as shown in figure 5.1-1(b), with the highest reentry assembly temperature (not the result of protuberance heating) occurring at station Z116. On the upper half of the cabin section, temperatures increased in the direction of the cone-cylinder junction, with the highest temperature occurring at station Z163.8. Along the bottom half of the reentry control system (RCS) and rendezvous and recovery (R and R) sections, distinct longitudinal temperature trends occurred. On the RCS section, temperatures increased toward the cone-cylinder junction, with the maximum temperature for this area occurring at station Z179.0. On the R and R section, temperatures also increased toward the cabin section, with the maximum occurring at station Z209.0 as shown in figure 5.1-1(b).

On the cabin section, the bottom half of the spacecraft experienced the higher reentry temperatures, especially along the bottom centerline. This circumferential distribution was also evident on the RCS section. Temperatures on the R and R section were highest on the top centerline, lower along the right and left sides, and increased again along the bottom centerline. Circumferential temperature variation in the beryllium areas was related to the variation in circumferential thickness in conjunction with the levels of aerodynamic heating. Individual temperature sensors are discussed in conjunction with the spacecraft sections.

5.1.1.2.2 Aerothermodynamics: Heat transfer rates generated during the launch and reentry phases of the flight were mathematically derived from the thermocouple-measured temperatures on the underneath side of the outer skin. This was accomplished by a computer program which used a series of differential equations to describe the temperature distribution through the wall of the spacecraft, and thus permitted the heating rate to be calculated. The aerodynamic heating rate was considered to be the sum of the rates at which heat was stored in the outer skin, radiated from the outer surface, radiated from the backside of the skin to the interior wall, and conducted to the interior of the spacecraft.

Maximum heating rates during launch occurred at approximately 10 + 100 seconds, or at an altitude of 100 000 feet and a velocity of 2750 feet/sec which corresponds to a Mach number of 2.9. The maximum launch heating rate measured on the spacecraft was 1.7 Btu/ft²/sec at PB06 on the R and R section. The results of the launch heating are essentially in agreement with the GT-1 flight test data and, therefore, are not discussed in further detail. Temperatures, but not surface

UNCLASSIFIED

static pressures, were measured during the flight of the GT-1 spacecraft. The pressure distribution measured during the flight of the GT-2 spacecraft is compared in figure 5.1-2 with the wind-tunnel data. Pressures measured on the cabin at the lower Mach numbers tend to fall in the upper portion of the estimated range and progress toward the lower portion of the range as the Mach number increases; therefore, the estimated and measured pressures are in better agreement at the higher Mach numbers.

The reentry aerodynamic environment in terms of velocity and altitude is shown in figure 5.1-3. The wind-tunnel test conditions are related to the flight conditions through the Mach and Reynolds number range to facilitate comparison of data from the two sources. The wind-tunnel data are not related to any point on the trajectory by a simple statement of altitude and velocity because the wind-tunnel static temperature was much lower than that found along the trajectory. As is shown, pressure and heat transfer tests were conducted over a range of Mach numbers from 3.5 to 16 and Reynolds numbers, based on the maximum body diameter, from 0.05×10^6 to 2.8×10^6 .

Analytical estimates of the heat transfer to the spacecraft depend on a knowledge of the local flow properties, which were estimated by using a pressure distribution over the body measured during wind-tunnel tests. In order to evaluate the accuracy of these pressure distributions, static pressures were measured during the flight of the GT-2 spacecraft. The static pressure sensors were arranged so that, during reentry, four sensors were on the windward side and four were on the leeward side of the spacecraft. Data at points along the trajectory where either the Mach number or the Reynolds number matched that of a particular wind-tunnel test were chosen for comparison with the wind-tunnel pressure distribution. These comparisons are shown in figure 5.1-4 for both the windward and leeward sides. The static pressures are non-dimensionalized by dividing by the total pressure behind the shock wave, and the surface dimension S/R is the distance from the center of the heat shield to the point being considered divided by the maximum radius (45 inches). Pressures along the windward side of the RCS section during flight differed measurably from the wind-tunnel measurements. The manner in which the local flow impinged on the RCS section is shown by the wind-tunnel data to be sensitive to both the Mach number and Reynolds number. The pressure distribution over the leeward side of the cabin is slightly lower than that shown by wind-tunnel tests, while measurements over the RCS section are in better agreement. The wind-tunnel pressure distributions shown were obtained at a 15° angle of attack. Calculations of the flight angle of attack, based on telemetered data from the spacecraft gyros, show that the angle of attack was fairly constant at approximately 15° during the interval from $L0 + 620$ to $L0 + 690$ seconds which

UNCLASSIFIED

was the period of maximum heating for which the measured pressures are compared. The angle-of-attack and the pressure on the afterbody further agreed in that neither indicated any sizeable oscillation about the trim angle of attack.

Peak heating rates which occurred on the afterbody during reentry are shown in figure 5.1-5 for both the windward and leeward sides. The maximum afterbody heating rate calculated at any thermocouple location was 22.4 Btu/ft²/sec, aft of the windward adapter interconnect fairing and localized melting of the surface also occurred in this area. A heating rate of 21.7 Btu/ft²/sec was measured on the windward side of the RCS section at station Z179 (PC07). As would be expected, peak heating rates over the leeward side of the spacecraft were relatively low. Since all the peaks did not occur at the same time, these figures should not be construed as a distribution of heating over the spacecraft.

Heating rate histories at representative stations over the cabin portion of the spacecraft are shown in figure 5.1-6. The four thermocouple locations along the windward side of the cabin were chosen to be in the region of most severe heating and are in satisfactory agreement with preflight estimates, except for station Z116 (PD03). The heating at this location was underestimated because of a closer than expected reattachment of the flow around the edge of the heat shield, resulting in higher heating rates in the region of reattachment. A somewhat larger area of separation was observed during wind-tunnel tests at this angle of attack.

Localized heating more severe than that along the windward ray was obtained in the area behind the most windward adapter interconnect fairing. Heating rates obtained from the measured temperature were greater by a factor of more than 3 than would have been expected had the interconnect fairing not been there. As previously mentioned, some melting of the surface was found in this region. An analysis made of the effect of conduction on the maximum heating rate in the burn-through indicates that the maximum heating rates at the various points of failure may have exceeded 40 Btu/ft²/sec. The previously mentioned wind-tunnel tests of the Gemini configuration were conducted with this adapter interconnect fairing in position but failed to indicate a significant degree of interference heating. An explanation for this discrepancy is that the adapter interconnect fairings used on the wind-tunnel model were not exactly the same configuration as those flown on spacecraft 2 because of late changes in the interconnect fairings necessitated by results of separation tests. Also, since the region of highest interference heating is confined to the very thin windward edge of the wake extending aft of the interconnect fairing, the instrumentation location would have had to have been a very fortunate choice to record this phenomena.

~~CONFIDENTIAL~~

Heating rates aft of the two other interconnect fairings were higher than would have been experienced without the interconnect fairings but were not of a level sufficient to generate temperatures such as to jeopardize the integrity of the skin. Also, the interconnect fairings were of a different size and shape than the most windward adapter interconnect fairing. Heating rates over the remainder of the upper cabin surface were relatively low. Heating rate predictions on the aft cabin area were generally higher than those which were measured during flight, and the temperatures near the small end of the cabin were slightly lower than predicted.

Heating rates at representative locations over the RCS and R and R sections are shown in figure 5.1-7. The highest rates were obtained along the windward side, particularly at station Z179 (PC07), where a maximum of 21.7 Btu/ft²/sec occurred. This measurement is in near agreement with preflight predictions, but a heating rate of 24.2 Btu/ft²/sec was estimated for station Z189 (PC03). The measured temperature at this location indicated a heating rate of 15.0 Btu/ft²/sec, which was considerably lower than predicted.

A similar disagreement between the wind-tunnel and flight pressure distributions (fig. 5.1-4) in the region of the RCS section also exists. Heating rates over the windward side of the R and R section were considerably lower than those on the RCS section and were somewhat lower than predicted.

The leeward side of the RCS section (PC05) and R and R section (PBO3) experienced maximum heating rates of 4.1 and 8.6 Btu/ft²/sec, respectively. The fact that the measured heating rate on the leeward side of the R and R section is higher than that on the windward side may be attributed to the difference in shingle thickness between the leeward and windward sides. Wind-tunnel tests have shown that flow over the leeward side of the Gemini spacecraft is strongly dependent on Mach number and Reynolds number.

Heating rates obtained from the GT-2 flight test, in most instances, substantiated the methods used to estimate reentry heating. Further analysis of the data will afford refinements in certain areas where minor discrepancies were observed. Problems brought to light by the test, such as the interference heating caused by the adapter interconnect fairing, will require additional attention to formulate a complete analysis.

5.1.1.2.3 Heat shield: The ablative thickness for the GT-2 shield was reduced to approximately one-half of that on normal production

~~CONFIDENTIAL~~

~~CONFIDENTIAL~~

5-7

shields to experience realistic structural heat-shield temperatures in combination with water landing loads and thus provide a valid test of heat shield structure. The reduced thicknesses were nominally 0.54 inch on the bottom (windward) heat shield edge and 0.39 inch on the top (leeward) edge, as compared with 1.0 inch on the bottom edge and 0.85 inch on the top edge for the production shields. Actual heat-shield ablative-material thicknesses are shown in the region of each temperature sensor in figure 5.1-8.

The GT-2 heat shield was instrumented with 12 thermocouples and 2 resistive temperature sensors to study structural temperature distribution. Locations of these sensors are shown in figure 5.1-8. Seven thermocouples and two resistive sensors were located at various positions over the shield near the interface (bondline) between the upper structural honeycomb faceplate and the fiber-glass honeycomb core. Three thermocouples were located within the ablative layer and two near the backface of the honeycomb structure. All thermocouples and resistive sensors appeared to record accurately over the entire flight.

Temperatures of the bondline thermocouples and resistive sensors began to increase from ambient after peak reentry heating and reached their maximum values near the time of landing about 400 seconds later. This slow response of bondline temperature was due to the insulative and heat-sink properties of the ablation material. Temperature in the ablation material began to rise slightly earlier and reached a maximum approximately 25 seconds before touchdown, while backface temperatures were still rising at landing. Typical temperature histories in the ablation material at the bondline and on the backface are shown for the windward (BY) shield location in figure 5.1-9. The maximum bondline temperature of 260° F was recorded near the left edge of the heat shield, while the maximum backface temperature of 160° F was recorded at the top of the heat shield. The maximum heat shield temperature recorded was 325° F at 0.14 inch from the bondline in the ablation material at the top of the heat shield.

The predicted temperatures for the heat shield are shown in figure 5.1-8. The ablation program used to predict the heating response was essentially derived from a correlation of char depth and temperature gradient obtained in plasma jet testing at varying heat rate, pressure and enthalpy conditions. The predictions are given as a range because allowance is made for possible swelling of the ablation material in the local areas. All other input conditions, such as trajectory and the resulting local heating rates, were considered nominal. Estimated local heating rates were obtained as a percentage of the reference stagnation-point heating rate at zero angle of attack. Measured values were 100° F or more below the predicted maximum temperatures. Preliminary postflight estimates of char depth are within the predicted range.

~~CONFIDENTIAL~~

~~CONFIDENTIAL~~

The predicted heat shield weight loss was 12 to 20 pounds based on the amount of predicted char thickness and average ablation material density (char and virgin material). The measured heat shield weight loss after drying was 2.97 pounds, however, this low weight loss is consistent with the measured internal low heating of the heat shield.

No apparent effect of adapter interconnect fairing interference heating was noted on the heat shield. This effect was noted on the cabin section and is described in detail in subsection 5.1.1.2.4. In general, the appearance of the heat shield was excellent and showed no evidence of thermal or structural failure such as inter-cell cracking of the honeycomb matrix (fig. 5.1-10). Gouges in the heat shield evident in the upper right and upper left portions of figure 5.1-10 were caused by the divers during recovery operations. From the focus of rays which were darker than the remainder of the shield surface, a stagnation heating point could be estimated at 17 inches from the bottom edge indicating a flight path angle of approximately 17.5° at the time this pattern was impressed on the surface.

5.1.1.2.4 Cabin section: The most severe temperature environment on the spacecraft afterbody was on the windward cabin section during reentry where temperatures as high as 2150°F were recorded. While this temperature, which was due to local heating protuberance effects discussed elsewhere in this report, exceeded all predictions by at least 400°F , the flight was planned to produce Rene' 41 shingle temperatures higher than those expected for any future flight condition. The peak launch temperature on this section of the spacecraft was 540°F at station 113.4. (See fig. 5.1-1(a) for location of PD23). In general, temperatures during launch were approximately 100°F cooler than those encountered during the GT-1 launch. A comparison of GT-2 and GT-1 launch trajectories indicates that the cooler temperature was to be expected.

Higher than predicted temperatures over the cabin section were limited to the bottom centerline of the spacecraft near the heat shield and directly behind the most windward adapter interconnect fairing. All other measured temperatures were below the 1700°F limit used for design. Typical time histories are shown in figure 5.1-11.

Spacecraft windows were quite cool with an average peak temperature of 265°F on the outer pane. A postflight inspection indicated that window installations were in excellent condition. The three molded plastic adapter interconnect fairings at the cabin section - heat shield junction were also in good condition but did reflect the anticipated stagnation point heating, as can be seen in figure 5.1-12.

~~CONFIDENTIAL~~

Peak temperatures on the internal structure are shown in table 5.1-1. All measured internal temperatures were approximately equal to or lower than preflight predictions. For example, the peak temperature on a stringer at station Z131 (PD39) was estimated to be 455° F as compared with the measured value of 320° F. On the inner skin of the left-hand equipment bay door at station Z135.9 (PD01), the prediction of 298° F was higher than the measured value of 168° F. Where internal temperatures were low, the external temperatures in the area were also lower than expected. The temperature distribution through the ECS equipment bay door during reentry is presented in figure 5.1-13.

While all measured temperatures on internal structure appear to be quite low, it should be pointed out that the GT-2 reentry trajectory was short and did not allow a significant amount of heat conduction to the interior and thus did not represent the critical heating case. A long, shallow, reentry from orbit would result in maximum internal temperatures that would be much higher than those measured during the GT-2 flight. It is significant to note, however, that predictions based on the GT-2 trajectory were not exceeded on the internal structure.

The primary problem on the cabin section was the region of high heating behind the interconnect fairing noted earlier. This area may be seen in figure 5.1-14. The severe heating caused by this interconnect fairing resulted in damage to two Rene '41 shingles, a hold-down washer, and a circumferential strap in the affected area. Two shingles covering the right-hand equipment bay sustained incipient melting with four holes ranging from $\frac{1}{8}$ to $\frac{3}{8}$ inch in diameter. The holes were located along a line of maximum heating between 12° and 16° to a cone surface slant line, 14 and 25 inches downstream from the adapter interconnect fairing. One bolt washer, 3 inches upstream from the first burn-through, showed melting on the leading edge. The strap between affected shingles buckled between two bolts due to thermal expansion and also showed a slight edge melting. The shingle under the leading edge of the strap also buckled due to the air stream flowing under the strap after it buckled. Locations of the damaged areas are pointed out in figure 5.1-14. In addition, temperatures of 2100° F and 2150° F were recorded at two thermocouple locations. Detailed photographs of the damaged areas are presented in figure 5.1-15. No damage of underlying insulation or structure was observed after removal of these shingles other than temperature discolorations of the insulation blanket and light charring of phenolic fiber-glass channels.

This high local heating is attributed to an upstream wake generated by the adapter interconnect fairing. This was evidenced by outlining the area of color change on the Rene '41 shingles. Shingle surfaces in the

~~CONFIDENTIAL~~

wake region were covered with a black deposit which was darker than regions located outside the wake. In addition, the black discoloration of underlying insulation showed a pattern similar to that on the Rene shingles. Fairings over similar adapter interconnects, located just above the horizontal centerline, produced similar wake patterns. However, these patterns were different from those in the high heating area, in that a greater billowing out toward the top centerline of the spacecraft could be traced by outlining areas of discoloration. A peak temperature of 990° F was noted in these regions.

The only other area where higher than expected temperatures were obtained was on the bottom centerline at station Z116. Although the peak temperature of 1830° F exceeded the predicted value of 1760° F, no shingle damage was noted in this area. Underlying insulation blankets were discolored in a manner similar to that described above, but the discoloration was less pronounced.

5.1.1.2.5 RCS section: With the cooler GT-2 launch trajectory, peak measured temperatures on the RCS section were approximately 10° F cooler than those obtained during the GT-1 ascent. A maximum launch temperature of 125° F was recorded on this section for GT-2.

Peak reentry temperatures noted in figure 5.1-1 ranged between 580° F and 1030° F. No particular thermal problems were encountered during the flight since measured temperatures were considerably less than preflight predictions and design limits. Postflight inspection of the spacecraft revealed no problem with RCS nozzles due to aerodynamic heating. The peak temperature on the TCA 8 nozzle support was 440° F at landing. Transient temperatures on the beryllium shingles are presented in figure 5.1-16 for one leeward and two windward locations.

As a result of low shingle temperatures, internal structure temperatures were also lower than predicted. Peak temperatures of 180° F and 76° F were measured on a stringer and inner skin, respectively. These temperatures are indicated in figure 5.1-17 which shows transient structural temperatures. Also presented are temperatures on the mild detonating fuse (MDF) separation ring at station Z192. The temperature adjacent to this pyrotechnic at the time of R and R separation was 70° F. The temperature increased only 6° F during reentry as compared with the preflight estimate of 40° F.

Structural damage on this section was limited to two cracked beryllium shingles. There was no indication of heating damage in the region of the crack; therefore, it has been assumed that this damage was incurred at the time of landing due to thermal shock or in subsequent handling during recovery.

~~CONFIDENTIAL~~

Since all measured temperatures were well below predicted values, it is concluded that no structural heating problems exist on the spacecraft RCS section. While the GT-2 flight was not intended to subject RCS beryllium shingles to maximum design temperatures, higher temperatures expected during orbital reentry should also remain well below design limits.

5.1.1.2.6 R and R section: During launch, outer skin temperatures on the conical portion of the R and R section ranged from 80° F at PB17 to 190° F at PBO3. See figure 5.1-1 for these thermocouple locations. Launch temperatures for GT-2 averaged about 40° F lower than at corresponding locations on GT-1, again due to the different trajectory.

Peak reentry temperatures and corresponding predictions for the R and R section outer skin thermocouples are shown in figure 5.1-1. The peak temperature on the conical portion of the R and R section reached 1010° F along the top centerline. The predicted temperature for this point was 1190° F. Temperatures on the R and R section ranged from this peak value of 1010° F to a low value of 440° F along the left side. Typical temperature histories along the common Z station of 217.0 are shown in figure 5.1-18. Outer skin temperatures ranged from 75° F to 600° F lower than predicted values.

There appeared to be no thermal problem from protuberances on the R and R section. The docking latch was found to be in good condition. No flow effects appeared to emanate from the shingle retainer gaps, and they appeared to be in satisfactory condition. Inspection of the nose stub antenna revealed no heating damage, although some softening of the protective teflon sleeve was noted. The stub antenna was apparently bent by the pilot parachute bridle when the pilot parachute was deployed. Rub marks on the bridle matched scrape marks on the stub antenna. The radar heat-shield fairing was slightly charred but appeared to be in satisfactory condition. A peak temperature of 1090° F was recorded on the Rene 41 outer skin adjacent to this radar fairing.

One R and R section shingle located on the top centerline was cracked. Five crack lines emanated from the Molybolt thermocouple attachment. The cracking appeared to have occurred after reentry heating, as evidenced by the sharpness of cracked edges which showed no edge melting or internal discolorations.

Internal skin temperatures were measured at three locations on the R and R section, at stations Z199, Z217, and Z227, and showed no rise during reentry.

5.1.1.3 Vibratory environment.- The vibratory environment of spacecraft 2 was measured in flight by 13 accelerometers to measure structural

~~UNCLASSIFIED~~

response and low-frequency body bending and longitudinal response of the reentry module assembly during both launch and reentry. All responses were low throughout launch and even lower, as was expected, during reentry. The equipment vibration qualification level was proved to be sufficient, the anticipated low buffet bending moment was confirmed, and the launch-vehicle induced low-frequency longitudinal oscillation was as in the GT-1 mission of no consequence. In general, the high-frequency response of GT-2 during the launch phase was lower than that of GT-1; whereas, the low frequency response was slightly higher.

During reentry the high frequency vibration began to rise at a Mach number of 19 and an altitude of 180 000 feet, increased to a maximum at a Mach number of 3.8 and an altitude of 93 000 feet, and then decreased to a minimum at a Mach number of 1.11 at an altitude of 68 000 feet. The low-frequency vibration increased rapidly at LO + 760 seconds and remained at a somewhat constant level until parachute deployment (LO + 880 sec.).

5.1.1.3.1 Equipment vibratory environment: The original Gemini vibration spectrum was derived from Project Mercury measurements. This spectrum was changed as a result of GT-1 measurements because of two pronounced differences between the Mercury and Gemini spacecraft: (a) The Mercury spacecraft response increased with dynamic pressure q up to q_{max} ; whereas, the Gemini spacecraft response increases with q up to sonic velocity, and then decreases with increasing q ; (b) Gemini maximum power spectral density is at several hundred cycles higher frequency than that of Mercury. Hence, the original 12.6 g_{rms} spectrum was reshaped to shift the high energy to higher frequencies and was reduced in accordance with the sonic-point deviation from dynamic pressure dependence. This change in the spectrum resulted in total power spectral density of 8.8 g_{rms} which was used to qualify the Gemini equipment.

Spacecraft 2 contained flight accelerometers to confirm the adequacy of this 8.8 g_{rms} test excitation spectrum.

The reference accelerometers between GT-1 and GT-2 were QB13 and QB14, located at a "hard" structural point in the left equipment bay of the spacecraft which housed the spacecraft's guidance and control equipment. The QB13 accelerometer, sensing in the radial or transverse direction, reached a maximum of 3.8 g_{rms} on GT-1 and 2.5 g_{rms} on GT-2. The QB14 accelerometer, sensing in the longitudinal direction, reached a maximum of 2.2 g_{rms} on GT-1 and 0.75 g_{rms} on GT-2. The power spectral densities of the maximum QB13 measurements for both flights are given in figure 5.1-19 to compare frequency distribution with the 8.8 g_{rms} test spectrum. As seen, the test spectrum, which is an envelope of what

~~UNCLASSIFIED~~

is believed to be 3σ excursion, is not encroached upon by the maximum response of the reference accelerometers, except in the 1100 cps region. This is not considered to be a problem because of the results of ground tests measuring high attenuation from structure to equipment in this frequency band.

Vibration measurements were made on the overhead hatch sill beam (QA12, QA13, and QA14) and the R and R section of the spacecraft (QD07, QD08, and QD09). Although the QD09 (longitudinal) accelerometer did not function properly, sufficient data were obtained from the other five accelerometers to confirm the adequacy of the $8.8 g_{rms}$ test spectrum for the launch and reentry environments. Because of limited instrumentation capacity the QB13 and QB14 accelerometers measured launch response and then were switched to QA14 and QD07 which measured reentry vibration. Table 5.1-II presents the g_{rms} maximum responses from each of the functioning accelerometers throughout the flight. As seen, the maximum high-frequency response was at $10 + 65$ seconds laterally in the radial direction in the equipment bay (QB13) and vertically in the overhead beam (QA13). The vibration at QA13 had most of the energy in the 400- to 550-cps band, with a peak power spectral density of $0.018 g^2/cps$. The maximum high-frequency vibration recorded was in the R and R section (QD07 and QD08) with energy concentrated in the 600- to 900-cps band having a peak power spectral density of $0.0003 g^2/cps$.

5.1.1.3.2 Low-frequency response: The low-frequency accelerometers provided an excellent record of spacecraft structural dynamics during all events of the flight.

To obtain the maximum buffet bending moment, the spacecraft contractor used a 1.5 cycle-wide tracking filter and isolated the first three bending modes of the "launch vehicle/spacecraft" configuration. The measured zero-to-peak values were 0.022g for the 3-cps mode, 0.084g for the 7.6-cps mode, and 0.076g for the 14.6-cps mode. When combined, these responses produce a bending moment of 76 300 inch-pounds at the interface of the spacecraft and launch vehicle.

The Manned Spacecraft Center used 20-cps, 10-cps, and 5-cps sharp cut-off filters on the data and obtained a slightly lower response. The response measured by either method resulted in a bending moment which was well within the design limit of 2.7×10^6 inch-pounds.

5.1.1.4 Compartment pressures. - The venting of compartments during launch and the pressure buildup during reentry was as expected.

UNCLASSIFIED

Figures 5.1-20 and 5.1-21 show the pressure lags in the adapter assembly and reentry assembly equipment bays, respectively.

The GT-2 adapter pressure differential was very close to that of GT-1, and well within design limits. The pressure decay tests before launch had indicated that the GT-2 adapter had about 12 square inches of vent area compared with 8 square inches in the GT-1 adapter. However, the GT-2 spacecraft ascended through the atmosphere at a faster rate, and thus, even with a greater vent area, the GT-2 adapter pressure built up nearly the same as in GT-1.

The equipment bays of the reentry assembly vented as expected during launch and repressurized during reentry with less lag than predicted. A maximum pressure lag of perhaps 1.3 psi during reentry had been predicted, but the measured maximum lag was only 0.26 psi (fig. 5.1-21).

5.1.1.5 Reentry angle of attack.- The inertial guidance system (IGS) parameters and the body-mounted accelerometer data were used to compute the inertial velocity components in the spacecraft aerodynamic coordinate system. The total angle of attack is the angle between the aerodynamic velocity vector and the longitudinal aerodynamic axis.

The angle of attack for the GT-2 mission is compared in figure 5.1-22 with the angle of attack obtained from a six-degrees-of-freedom digital simulation. It may be noted that the angle of attack was slightly higher than predicted during the early reentry period, with very close agreement during highest heating (Mach number of approximately 15) and then dropped below predicted during the final portion of the reentry trajectory.

The initial results of the lift-drag ratio analysis indicate that there are several uncertainties in the calculations which cannot be resolved during this reporting period. It is anticipated that subsequent analysis of mission data will provide useful information which will be published as a supplement to this report.

5.1.2 Communications System

All data received indicate satisfactory operation of the spacecraft communications system with the possible exception of HF tone transmission in the direction finding mode after landing. Overall operation and anomalies are further discussed in the following paragraphs. In the case of telemetry transmissions, an attempt was made to analyze certain data primarily for separating radio-frequency transmission link problems from other anomalies. The data available for this purpose consisted of recorder charts of field strength from telemetry and tracking stations and written logs indicating acquisition and loss of signal from aircraft.

UNCLASSIFIED

These data are presented in figure 5.1-23, which represents usable signal strength in the opinion of the engineers reviewing the data, and in the case of aircraft, entries in the flight log.

Considerable engineering judgment has been exercised in deciding what represents "usable" signal strength on the recorder charts since this information was not indicated by the station submitting the chart. The HF and UHF indicated in the figure were tone modulated voice transmitters. The UHF transmitter was cycled 30 seconds on and 30 seconds off until R and R section separation; however, the signal is shown as continuous in the figure. Loss of signal during reentry blackout and loss of a properly radiating antenna from parachute deployment until 2-point suspension are indicated in the figure.

The Coastal Sentry Quebec (CSQ) range instrumentation ship received usable signal strength during part of the general reentry blackout period, and the logs from the range instrumentation aircraft 630 and 491 show acquisition of signal during part of the normal blackout. The CSQ and aircraft also indicated usable signal strength during part of the time prior to two-point parachute suspension while the descent antenna was still stowed in the parachute cable trough. These peculiarities were due to the close proximity of these stations during those periods.

5.1.2.1 Radar transponders.- Nominal operation of C- and S-band radar transponders was evidenced by good results at the tracking stations. Available signal strength charts, logs, and summary messages were reviewed, and these data indicate good C-band radar transponder tracking by Patrick Air Force Base (PAT), Grand Turk Island (GTI), San Salvador Island (SSI), and Antigua (ANT). Tracking by Merritt Island Launch Area (MILA) and Grand Bahama Island (GBI) was somewhat degraded. S-band tracking was nominal at Cape Kennedy Central Control, GTI, and GBI. The tracking coverage is shown in figure 5.1-24. C- and S-band transponder case temperatures were about 90° F and rose slightly until loss of telemetry. An examination of S- and C-band pulse repetition frequency records revealed successful multiple interrogation until approximately LO + 500 seconds after which dual interrogation was impossible due to the trajectory.

5.1.2.2 Telemetry transmitters and acquisition aid beacon.- Satisfactory telemetry transmitter operation was indicated by overlapping range-station reception as shown in figure 5.1-23. The range instrumentation ship, Rose Knot Victor (RKV), signal strength was between 20 and 150 microvolts and highly variable during its tracking interval from LO + 185 to LO + 536 seconds. The RKV log indicates that this was not a usable signal and that they could not autotrack. However, during the same time period, GTI signal strength varied from 4 to 40 microvolts and

UNCLASSIFIED

ANT from 40 to 80 microvolts. Good telemetry data were received at both stations, and no tracking problems were indicated. Coastal Sentry Quebec (CSQ) and aircraft 630 received usable signals during the early part of the reentry; however, no data were on the tapes at this time. The CSQ signal strength varied between 80 and 300 microvolts. The data were usable although there were some dropouts. It cannot be determined at this time whether the data dropouts were caused by faulty operation of airborne PCM, RF link, or ground equipment. Both telemetry transmitters operated throughout the mission and after touchdown. The acquisition aid beacon was not needed during this flight since the telemetry transmitters operated continuously. It was exercised, however, and reports from MCC, GTI, and GBI indicated correct operation of this unit.

5.1.2.3 HF and UHF voice transmitters.- HF and UHF voice transmitters were 1000-cps tone modulated during this mission for evaluation and for direction finding purposes. The HF transmitter was not energized during the flight, but was sequenced on approximately 7 minutes after landing. No HF signals were received at ground stations other than those in the immediate recovery area. One of the recovery aircraft indicated proper HF reception beginning at about 3 miles from the spacecraft. A report from the CSQ ship indicates that HF was received at a distance of about 25 nautical miles.

Nominal UHF voice transmitter signal strengths were logged and recorded as indicated in figure 5.1-23. In the recovery area, the U.S.S. Lake Champlain (CVS) logged UHF reception at about the correct bearing from LO + 710 seconds until touchdown. Search aircraft BB-5 logged UHF reception at LO + 780 seconds at 30 nautical miles from the landing area. The CSQ ship received UHF from LO + 703 seconds until touchdown.

5.1.2.4 Digital command system.- Both DCS receivers were in complete command of the ground transmitters as evidenced by signal saturation from before lift-off until they were jettisoned with the equipment section at LO + 414.22 seconds. All power supply voltages were normal. Package temperature was normal at 80° F with a very gradual rise prior to loss of equipment. The only commands sent during the mission were two guidance velocity updates during the launch phase. These were received, validated, and accepted by the spacecraft computer on the first execution.

5.1.2.5 Recovery beacon and flashing light.- The UHF recovery beacon was energized at two-point parachute suspension at about LO + 901 seconds. A signal was received by a helicopter at a range of 25 nautical miles and rescue aircraft at ranges up to 145 nautical miles. The flashing light did not operate because its deployment door jammed, preventing extension and activation of the light.

UNCLASSIFIED

5.1.3 Instrumentation and Recording System

The instrumentation system provided for the monitoring of the 428 parameters listed in table 3-II. Three of these parameters (DE05, PDO6, and QD09) were not measured because of instrumentation system malfunctions. Both QD09 and DE05 sensors had been intermittent before launch; and after isolating the problem to spacecraft wiring, it was determined that these parameters were not necessary to accomplish the objectives of the mission and it would not be in the best interest of the program to correct the deficiencies. Sensor PDO6 was also intermittent or erratic during the flight; however, it has no history of trouble. Six temperature measurements (CB01, CD01, CD02, CD07, CD08, and CFO3) in the coolant system were off-scale on the low side due to the fuel-cell deactivation and resultant warmer coolant fluid. The cabin pressure was slightly over-scale during most of the period of powered flight.

The data transmission system performed exceptionally well during the mission. The PCM multiplexer-encoder had only two resets and no multiplexer lockups during the mission. These resets occurred at T - 143 seconds at the time the PCM and PAM tape recorders were turned on, and at LO + 411.6 seconds when the adapter separation sequence was initiated. Only the landing-gear-well low-level multiplexer was affected by spurious reset signals and it recovered within the 0.1-second interval or one prime subframe. The onboard PCM tape recorder was turned on at T - 143 seconds and began recording. Dumping of the stored PCM data was started at LO + 772.97 seconds. Telemetry reception of the PCM dump-data by aircraft 630 and 497, and the Coastal Sentry Quebec (CSQ) ship ended at LO + 1094 seconds when the signal was lost approximately 2 seconds before landing.

The acquisition of signal (AOS) and loss of signal (LOS) times for each telemetry receiving station for both the real-time and delayed-time data links are tabulated in table 5.1-III. The times given are those corresponding to the beginning and ending of useful data reception. The data from table 5.1-III are charted in figure 5.1-25 to illustrate actual data coverage for the mission. Table 5.1-IV presents the results of an examination of the data from the receiving station data tapes processed by the computer. The table shows total acquisition time, data losses, and usable data in both real time and delayed time. Over 99 percent of the real-time data from Cape Kennedy (Tel II), Grand Bahama Island (GBI), and Antigua (ANT) was useful. Ninety-eight percent of the data from the CSQ was useful; 95 percent of the Grand Turk Island (GTI) data was useful; and 92 percent of the data provided by aircraft 630 and 497 was useful.

UNCLASSIFIED

The MCC telemetry data recorders suffered a power loss from LO + 306 to LO + 339 seconds. Since Cape Kennedy (CNV) and GBI covered the same time, these data were not processed. The Rose Knot Victor (RKV) ship had low quality and intermittent data; and since GBI and Antigua covered that time, data from the RKV ship also were not processed.

Considering all stations from first AOS to final LOS, there were 2950.3 seconds of real-time data possible and 2583.05 seconds of usable data were recorded, or 87.6 percent. Removing the MCC power loss of 33 seconds, the RKV poor quality data, and the times lost by the receiving stations during R and R section separation when there was no telemetry antenna on the spacecraft, a total of 22.4 seconds of synchronization loss and/or dropouts out of 2531.65 seconds resulted in 99.92 percent of possible reception time at seven stations.

By using the onboard PCM recorder-reproducer to give delayed-time data coverage of the communications blackout, it can be seen in figure 5.1-25 that a composite PCM useful data coverage of 1090.1 seconds, or 99.452 percent, resulted from a possible coverage of 1096.1 seconds.

5.1.4 Environmental Control System

The environmental control system (ECS) performed normally throughout the flight. The flight configuration was one suit compressor operating, cabin fan operating, pump A in each coolant loop operating, coolant bypass lines to the fuel-cell inlet temperature-control valves shut off (fuel cells were not activated), primary oxygen bottle mass-quantity of 93 percent, right-hand secondary oxygen bottle serviced to 5000 psia, and the left-hand secondary oxygen bottle not serviced.

Coolant loop temperatures were maintained at approximately 74° F by ground cooling equipment until T-5 minutes, when ground cooling was terminated. Radiator outlet temperature rose to an indicated 80° F (off-scale, high) at launch, and generally remained off-scale until adapter separation. The highest anticipated coolant temperature was at the coolant pump outlet, which remained at 80 to 83° F throughout the flight. Instrumentation to assess launch cooling heat exchanger (water-boiler) performance was not installed; however, suit inlet gas temperature and cabin gas temperature indicated that the launch cooler was operating.

As shown by figure 5.1-26, cabin pressure increased as expected from launch, went off-scale (6.0 psid, relative to forward compartment) at approximately LO + 48 seconds, and returned within scale at LO + 125 seconds. Cabin pressure then stabilized at 5.78 psid until reentry. Accurate determination of maximum cabin pressure was not

UNCLASSIFIED

possible due to the gage limit of 6.0 psid. Tests were run on cabin pressure relief valves of the same design as that in GT-2 when it was discovered that this design did not have sufficient flow capacity to limit cabin pressure to a maximum of 6.0 psid. A comparison of these special test data with GT-2 flight data indicates that the maximum cabin pressure in GT-2 did not exceed 7.0 psid.

The cabin air temperature was stable at 75° F until approximately LO + 160 seconds, when the launch cooling heat exchanger became effective. This temperature decreased in a linear fashion to 62° F at LO + 414 seconds (adapter separation). The cabin gas temperature sensor is located at the cabin heat exchanger outlet and gives a relatively good indication of the cabin supply coolant temperature. Cabin gas temperature during reentry reached a maximum of 75° F at landing, as shown in figure 5.1-27(a).

Suit inlet temperature remained at 72 to 73° F as expected until approximately LO + 200 seconds; then it declined slowly to 67° F at initiation of O₂ high rate at LO + 382.5 seconds. At this time the temperature rose to 72° F, then showed a continual decrease to 65° F at landing. (See fig. 5.1-27(b).) The initial temperature decay was a result of launch cooling heat exchanger operation, the return to 72° F is a result of the heat exchanger being turned off, and the subsequent decrease is due to withdrawal.

The primary oxygen vessel was fully serviced approximately 23 hours prior to launch. The vessel pressure rose to the vent pressure before launch and apparently vented O₂ until there was an indicated mass-quantity of 93 percent at launch. Both quantity and pressure remained stable until LO + 382.5 seconds (initiation of O₂ high rate) when a decline of vessel pressure was noted. Pressure decayed from 985 psia to 715 psia at LO + 411.7 seconds, as shown in figure 5.1-28. The change in slope of the pressure decay curve indicates actuation of the automatic heater. Calculations show that this pressure transient is representative of a 0.214 lb/min withdrawal rate, which is normal for O₂ high rate from the primary supply using only the small automatic heater for pressure control.

The right-hand secondary oxygen subsystem was serviced to 5000 psi prior to flight. Since only one secondary oxygen bottle was required to demonstrate O₂ high rate operation during reentry, the left-hand subsystem was not serviced. As shown in figure 5.1-28, the secondary bottle pressure began to decay at adapter separation and continued to decay until it reached approximately 3000 psia at touchdown. Calculation indicates a normal secondary subsystem withdrawal rate of 0.20 lb/min.

~~CONFIDENTIAL~~

The snorkel cabin inflow valve, normally opened manually at approximately 25 000 feet, was intentionally not actuated in this mission. The cabin inflow valve is normally opened to reenergize the suit compressor which assists in crew cooling during descent and postlanding. Since this function was not checked in flight, it will be checked by special tests.

5.1.5 Guidance and Control Systems

5.1.5.1 IGS performance summary.- The inertial guidance system (IGS) is discussed in the following order: mission phases, overall system performance and anomalies, the computer performance, and inertial measurement unit (IMU) performance.

One of the objectives of the GT-2 flight was to demonstrate secondary launch guidance capability, for which the IGS performed guidance computations and supplied steering signals to the GLV secondary autopilot. Table 5.1-V summarizes the IGS events during launch. All events occurred as planned within the tolerances expected except for the second-stage engine cut-off (SECO) which occurred approximately 0.35 seconds early. Table 5.1-VI is a summary of the insertion conditions measured by the separate systems. A comparison of the preliminary Space Technology Laboratories (STL) best estimate trajectory (BET) and the IGS quantities indicate an error in the IGS x-velocity at SECO of approximately 66.5 ft/sec, which is greater than expected. An analysis of this problem has isolated the error to be in the IMU accelerometer output to the computer. A postflight simulation was run on the computer to verify that its operation was correct during the launch phase. A complete mission simulation was conducted using the reentry initial conditions that would have resulted if the IGS had controlled the GLV during launch and commanded SECO. These simulations show that all the mission objectives would have been met and that the flight would have been considered successful. Figure 5.1-29 is a comparison of the IGS steering commands with the comparable commands from the three-axis reference system (TARS) adapter to the primary autopilot. These commands indicate nominal performance in all areas, except where the pitch command was greater than the expected upper boundary near SECO. All other deviations result from off-nominal launch conditions.

The insertion velocity adjust routine (IVAR) target orbit for this flight was 90 to 141 nautical miles, and if the correction, as calculated by the IVAR routine including the accelerometer error, had been applied as an impulse, an orbit of approximately 87 to 111 nautical miles would have been achieved. In general, the IGS system, including displays, performed well during the launch phase in all respects except for the out-of-tolerance velocity performance.

~~CONFIDENTIAL~~

~~CONFIDENTIAL~~

5-21

During the coast phase of the mission, the IGS measured velocity changes and provided attitude reference to the control system. Table 5.1-VII shows the measured velocity changes for GLV tail-off, separation, and retrorocket operation.

During reentry, the IGS was navigating and computing steering commands to a target. The target location was chosen to insure that the proportional bank-angle computation-loop would be exercised. Table 5.1-VIII shows the IGS reentry sequence summary.

Figure 5.1-30 shows IGS computer down range error, cross range error, and flight-path angle as compared with preflight computed nominals. The down-range-error plot shows that the steering commands were initiated early because the mechanization of the initiation technique was sensitive. The flight-path-angle plot reveals a deviation from the expected maximum values in flight-path angle at about $10 + 800$ seconds. The ability of the IGS to compute corrective steering at the low velocities encountered this late in the reentry is highly questionable. In addition, there is no tracking or wind data available for this portion of the flight to enable a reasonable evaluation of the anomaly. It must be noted that the expected maximum values of flight-path angle shown on the figure may be in error due to the wrong choice of constants or assumptions of winds and their effects. It should be further noted that the deviations shown, even if correct, would not have a significant effect on the landing location.

5.1.5.2 Evaluation of IGS.

5.1.6.2.1 Tracking data quality: The GE Mod III data were of excellent quality and provided good velocity comparisons. The quick-look MISTRAM I data had dropouts; however, good velocity comparisons were obtained. The tracking data were adequate for a quick-look analysis and there was generally good agreement among the tracking systems.

5.1.5.2.2 Error analysis:

Position and velocity errors: Guidance system performance was estimated by comparing the on-board computation of velocity with velocity data obtained from the ground-based reference system. Table 5.1-IX shows indicated IMU and guidance system errors at BECO and SECO using final GE Mod III and quick-look MISTRAM I data as a reference.

x-axis velocity errors: The velocity comparison along the x-axis (down-range) indicates an accelerometer malfunction when the accelerometer was sensing a high acceleration. The malfunction took the form of an excessive gain in velocity when the acceleration exceeded approximately 150 ft/sec^2 . The result was a positive error in x-axis velocity

~~CONFIDENTIAL~~

~~CONFIDENTIAL~~

of approximately 20 ft/sec between IO + 148 seconds and BECO (IO + 151.71 sec) and 45 ft/sec between IO + 307 seconds and SECO (IO + 332.51 sec). Figure 5.1-31 shows the flight acceleration profiles and figure 5.1-32 shows the velocity difference from various tracking sources. The total indicated IGS error at SECO was 66.5 ft/sec.

Azimuth update: Velocity comparisons were made using a total azimuth correction of -0.298° . This number was determined by simulating the airborne computer - GE/Burroughs update procedure. It can be concluded that, since the difference in velocity was nearly zero measured at IO + 140 seconds, -0.298° was a good approximation to the initial azimuth update and tends to confirm the 3σ values used in analysis. (45 arc-min error in alignment.) The guidance system errors at SECO were estimated and are shown in table 5.1-X. Other than the malfunction in the x-accelerometer, it is concluded that the IMU errors were within specification.

Gimbal angles - preflight alignment: The gimbal angles just prior to launch were within tolerance. The following table shows the nominal values and the actual values recorded.

PRELAUNCH GIMBAL ANGLES

Parameter		Gimbal angle	
Number	Description	Expected, deg	Actual, deg
DHO1	Pitch	90.00	90.00
DHO2	Yaw	0.44	-.14
DHO3	Roll	109.07	109.08

5.1.5.3 IGS steering. - Figure 5.1-33 shows a plot of the IGS roll, pitch, and yaw attitude errors for the ascent phase of the flight. Superimposed on these plots are the outputs of the primary guidance system (RGS and TARS) adapter which are equivalent signals. A discussion of the difference between the attitude errors of the two guidance systems and possible explanations for their deviations follows.

5.1.5.3.1 **Programed flight:** At lift-off, both the IGS and TARS roll attitude errors jumped to -0.3° and remained at that level until the initiation of the roll program. During the roll program, the difference between the two attitude errors increased linearly. After the roll program

~~CONFIDENTIAL~~

~~CONFIDENTIAL~~

5-23

ended, the IGS indicated a roll error of 0.2° . The roll gimbal position reflected this error and showed a total roll movement of 19.8° instead of the planned 20° .

The constant roll offset and the shift at BECO probably reflect a thrust misalignment in the GLV first stage. The IGS roll attitude error should indicate the same offset and shift. Although the shift was of the same magnitude as that for the TARS attitude error, the total deviation between the TARS and IGS roll attitude error commands at the initiation of closed-loop guidance was about 1.2° . This deviation may be due to one or a combination of the following:

(a) A roll drift between the two systems. However, if all the deviation is a roll drift, it implies a total drift error of about 35 deg/hr, which is not likely.

(b) A cross coupling of the roll-gimbal angle with the yaw-gimbal angle during the pitch-over maneuver. This seems plausible since the IGS and TARS error deviated during a period of high wind shear that required considerable yaw stabilization.

The yaw-attitude errors from both guidance systems were nearly identical in their commands. From about LO + 40 to LO + 100 seconds, both signals reflected large, but similar, deviations from zero as a result of wind shear. The offset commands at staging were a normal reaction to the yaw moment created by the roll nozzle.

During first stage flight, both systems were issuing the same relative pitch commands. However, a pitch drift of one or both of the systems was apparent since there was a deviation that increased linearly with time to about 0.8° at BECO. This deviation implies a pitch drift of about 20 deg/hr. The STL analysis and the second-stage steering results, as explained below, tend to indicate that this drift was not caused by the IGS.

At BECO, the pitch attitude errors from both systems shifted about 0.3° . Again, this shift was probably the reaction of the moment on the GLV second stage imparted by the roll nozzle thrust.

5.1.5.3.2 Closed-loop steering: At the initiation of the closed-loop guidance (LO + 168 sec), the IGS pitch-attitude error saturated at its maximum of 6° pitchdown command. This was normal since the total pitch attitude change required after staging at guidance initiate was about 20° (the RGS limits commands to a relative 1° attitude error and was locked out by the ground computer for approximately 4 seconds after RGS initiate).

~~CONFIDENTIAL~~

~~CONFIDENTIAL~~

At about LO + 200 seconds, after the vehicle had pitched down to approximately the required attitude, both systems were issuing about a 0.4° pitch-up command. This is significant in that although the IGS cannot recognize that it is drifting, the RGS can recognize drift, and its closed-loop steering will correct for the drift. This implies that the pitch drift of about 20 deg/hr in the first stage is most probably a drift of the TARS.

A deviation in commands of only about 0.75° was predicted at LO + 300 seconds. This expected deviation is due to the subtle differences between the closed loop-guidance equations of the two guidance systems. However, most of the 3.2° error that did exist was probably the result of an altitude error of about 1200 feet at LO + 300 seconds, along with an IGS velocity error of about 25 ft/sec.

However, as the vehicle approaches the terminal condition, a significant velocity error will amplify the pitch-attitude error. By about LO + 329 seconds the IGS had accumulated a velocity error of about 65 ft/sec in the direction which would require a pitch-down command to offset. From LO + 329 seconds to SECO, the IGS stopped its closed-loop computation and commanded a constant pitch attitude of 3.1° .

After guidance initiate, the IGS yaw attitude error went to a zero command and remained there until SECO. This is significant in that the IGS is in agreement with the yaw steering of the RGS. The IGS command of zero also indicates that the velocity updates were received at LO + 100 and 140 seconds and that they were implemented correctly in the IGS computer. The command of zero also implies that the RGS equations which were added to offset the center-of-gravity shift were proper and correctly implemented.

From LO + 105 seconds to SECO, the TARS roll attitude error deviated to a $+1^\circ$ command. This deviation is most probably a roll drift of about 10 deg/hr in the TARS since an analysis of flight data shows small IGS drift values.

5.1.5.4 IVAR performance.- The incremental velocity indicators (IVI) performed as expected. All three windows displayed zero through the launch environment up to spacecraft separation (LO + 352.77). Following activation at spacecraft separation, during the velocity adjust routine, the IVI's displayed the proper magnitude and signs as commanded by the onboard computer. During this period all three windows changed at the prescribed rate of 46 ft/sec² when driving. At LO + 352.77 seconds the IVI begin to display one window at a time until the equipment section separation discrete was received at LO + 414.22 seconds.

~~CONFIDENTIAL~~

~~CONFIDENTIAL~~

5-25

The desired SECO conditions to achieve high heating rate reentry for the GT-2 mission required a large flight path angle of -2.28° and the velocity for a 90 to 141 nautical-mile orbit. In-plane incremental velocities between conditions at SECO for such an orbit and the sensed actual conditions at SECO were computed, combined with IGS computed out-of-plane velocities, and transformed into IVI readings in spacecraft coordinates for display. These computations were made during each IGS computer computation cycle over the period that the IVAR was activated.

Figure 5.1-34 shows the gimbal angles during the period of display updating. Since IVAR computes the velocity to be applied along the local horizontal, maintaining constant roll and yaw angles, these wide variations in gimbal angles cause the computed incremental velocities to change constantly and require constant updating which must be accomplished one window at a time. Figure 5.1-35 shows the actual IVI readings and the comparable computer quantities. At $10 + 352.9$ seconds the forward-aft window began to change the display at 46 ft/sec^2 toward the required incremental velocity along the X-axis computed at $10 + 352.9$ seconds. At $10 + 363.5$ seconds, the forward-aft window had reached the sampled value, and the left-right window began to change toward the required incremental velocity along the Y-axis computed at $10 + 363.5$ seconds. At $10 + 364.2$ seconds the left-right window had stopped counting, and the up-down window began to change toward the required incremental velocity along the Z-axis computed at $10 + 364.2$ seconds. The up-down stopped counting at $10 + 368.21$ seconds, and the cycle was repeated until the abort discrete sequenced the IVAR to the inactive condition. The displays, presented at that time, remained fixed until after landing.

5.1.5.5 Orbit velocity-change measurements.-

5.1.5.5.1 Tail-off velocity change: The velocity change due to GLV tail-off impulse from SECO to spacecraft separation was calculated to be 101.5 ft/sec . This velocity change does not include all changes due to the gravity effect. The IGS computer was programed to compensate for a nominal 10^4 ft/sec velocity due to the tail-off impulse by biasing the time to deliver the SECO signal. Figure 5.1-36 is a time history of the velocity change due to tail-off as measured by the inertial measuring unit on the spacecraft.

5.1.5.5.2 Separation: A 15.8 ft/sec velocity change due to the OAMS spacecraft separation impulse was calculated from the platform accelerometer data. The nominal preflight calculated velocity was 14.7 ft/sec based on a 6882-pound (preflight data) separation weight, 189-pound nominal aft-firing thrust (assumed), and a 16.7-second (flight data) firing interval. This calculated velocity indicates that the actual separation velocity change was approximately $7\frac{1}{2}$ percent higher than predicted. Flight data indicate that the system pressure was 20 psi higher than nominal at the start, which would theoretically increase

~~CONFIDENTIAL~~

~~CONFIDENTIAL~~

the thrust level 5 pounds per chamber. Hence, the normal calculated velocity should be 15.5 ft/sec, which agrees within $1\frac{1}{2}$ percent of the actual value. Figure 5.1-37 shows a time history of the separation acceleration.

5.1.5.5.3 Retrofire: From IO + 414.222 seconds to about IO + 436.220 seconds, the four retrorockets were ripple fired. The total velocity change over the interval was 334.7 ft/sec, which indicates a 1.1-percent low average thrust since the predicted velocity change, was 339.0 ft/sec. The acceleration time history during retrofire is shown in figure 5.1-38.

5.1.5.6 IGS component performance.

5.1.5.6.1 Flight status: The IMU was turned on prior to lift-off and remained on until 896.477 seconds after lift-off. Platform, attitude, and accelerometer malfunction indicators as well as IGS and platform power "on-off" functions were monitored throughout this period and no anomalies were recorded.

5.1.5.6.2 Accumulator overload check: The velocity in the guidance direction increases after the accumulator was read at 331.84 seconds. This indicates the accumulator did not overload.

5.1.5.6.3 IMU temperature control amplifiers performance: The temperature control amplifier output from the z-axis accelerometer was approximately 72 percent of full heat on, with deviations which did not exceed ± 8 percent. The temperature control amplifier output of the x-axis gyro was approximately 81 percent of full power on, with deviations which did not exceed ± 9 percent. Both parameters drifted linearly with changes of direction at BECO, SECO, and initiation of reentry roll.

5.1.5.6.4 Computer temperature and voltage levels: The computer case temperature and voltage levels remained within the prescribed limits throughout the flight. Prior to lift-off, telemetry data indicated that the 10.2 V dc regulated voltage was at the prescribed nominal value. However, at IO + 22.17 seconds, this parameter malfunctioned and data were not available until 808.58 seconds after lift-off. At this time, telemetry indicated that the voltage was still at the nominal value of 10.2 V dc and remained there until power was removed from the IGS.

5.1.5.7 Control system evaluation. - The control system became active at 2 seconds after spacecraft separation. The control-system sequence of events is tabulated in table 5.1-X. Also included in this table are the telemetered times at which each of the sequences occurred during flight.

~~CONFIDENTIAL~~

The orbit attitude data comparisons with calculated preflight data are presented in figure 5.1-39. Table 5.1-X and figure 5.1-39 show that the control system performed all operations as planned and that no significant deviations occurred, except for a slight disturbance at initiation of retrorocket 1. The disturbance was greater than expected, but the body rates still did not exceed the 3σ limits. During retrofire, the control system maintained an attitude within $\pm 4^\circ$ as indicated by the integrated attitude rates and as interpreted from the onboard camera film.

During reentry, the control system maintained control with a minimum of thruster operations. The body attitude rates during this time were very low supporting the minimum thruster operations. The combination of the two shows that the control system maintained positive control to release of pilot parachute. The control system operation during reentry is summarized in figure 5.1-40.

5.1.5.7.1 Control system mission profile: The control system, in general, performed as expected. The initiation of the first retrorocket firing was the only area where discrepancies existed after comparing the measured rates and attitudes with the expected variations of these quantities. The details of the portion of the mission during which the control system operated are reviewed for each phase.

From separation to separation +2 seconds: During this period of the flight, the aft engines were on continuously, and, with the control system inoperative, the spacecraft rates were free to change and no attitude jets were fired. The changes in rate are a measure of the aft engine disturbance torques produced by the firing of the aft engines. The nonconstant slope of the rate data shown in figure 5.1-41 could indicate (a) effects of the aft engine exhaust impingement on the launch-vehicle dome and scuppers, (b) unbalanced forces exerted by the scupper engine seals, (c) coupling present from the nonsymmetric spacecraft geometry, or (d) uneven propellant feed and resultant rough burning of the aft engines since it was the first activation of these thrusters after servicing for flight.

As seen from figure 5.1-42, the spacecraft made a continuous translation away from the launch-vehicle and no recontact occurred. In this figure, the path of the critical point as a function of time for each engine is shown as the spacecraft separates. These paths are the relative position of the engines and the launch vehicle derived from angular acceleration measurements made during this short period of time. Typical accelerations are presented in the following table:

UNCLASSIFIED

	Angular accelerations		
	Roll, deg/sec ²	Pitch, deg/sec ²	Yaw, deg/sec ²
Maximum predicted	0.5	0.9	0.4
Measured range	0.1 to 0.3	0.4 to 1.7	0.4 to 1.1

From separation +2 seconds to separation +16.5 seconds.- During this period the OAMS aft engines continued to fire, and the spacecraft was rolled by the OAMS to a roll platform angle of 0° as planned. The pitch and yaw rates stayed within the specified band of ±4 deg/sec during the roll. When the desired motion was initiated, a roll pair of attitude thrusters fired which produced a pure roll acceleration of 6.2 deg/sec². After 2.1 seconds, the roll acceleration decreased to 5.7 deg/sec². The measured yaw acceleration during this latter time was 1.1 deg/sec². This could be the result of short pulsing of the yaw thruster instead of continuous firing, or of a reduction in thrust from the engine. The instrumentation did not permit resolution of thruster activity to the pulse lengths which may have taken place during this maneuver. Vibration data tend to substantiate pulsing, but the data are not conclusive. For reduction of the roll rate to zero, only the two required roll thrusters fired, and a pure angular acceleration of 6.5 deg/sec² was measured. The difference of 0.3 deg/sec² between the pure opposite roll accelerations was very small. The difference between the measured values and the theoretical acceleration of 7.1 deg/sec² may be attributed to the aft engine disturbance torque, but this cannot be proven.

From separation +16.5 seconds to separation +30 seconds.- During this period, the spacecraft was controlled to the null of the platform in all axes by the OAMS. The angular acceleration when pitching up was 7.0 deg/sec² and when pitching down was 4.6 deg/sec². These values bracket the theoretical value of 5.7 deg/sec². The angular acceleration measured in yaw and roll were 5.6 deg/sec² and 6.8 deg/sec², respectively. The theoretical values were 5.8 deg/sec² and 7.1 deg/sec².

From separation +30 seconds to separation +45 seconds.- During this period the control system damped the rates, using OAMS thrusters, to within the rate deadband while a yaw rate command was being applied.

The acceleration toward this yaw rate command was 5.7 deg/sec², when no roll activity was present, favorably comparing with a theoretical value

UNCLASSIFIED

of 5.8 deg/sec^2 , and decreased to 5.0 deg/sec^2 when there was roll activity. This 12 percent decrease in yaw acceleration could either be pulsing or the reduction in thrust of one roll thruster. This particular thruster had been energized earlier in the flight, however, at a time when accelerations were determined and found to be nearly correct. A steady state yaw rate of 9.4 deg/sec was established. The deadbands were correct since no rates exceeded $\pm 0.2 \text{ deg/sec}$ from the quiescent value. Examination of attitude signals showed that a platform gimbal flip occurred between $10 + 391.95$ and $10 + 394.05$ seconds as expected, which further confirmed proper platform and control system operation.

From separation +45 seconds to retrofire.- At the beginning of this phase of flight, the OAMS was no longer used, and control for both rings of RCS was implemented to provide stabilization of the spacecraft for reentry down to pilot parachute deployment. The yaw maneuver was completed by firing the proper RCS thrusters to produce a yaw rate with an acceleration between 6.3 and 7.6 deg/sec^2 followed by a reduction in yaw rate to zero using the opposite thrusters which provided a reverse yaw acceleration between 6.1 and 6.3 deg/sec^2 . The theoretical acceleration for the yaw maneuver is 8.8 deg/sec^2 . To achieve the pitch down bias for the retrograde operation, the RCS thrusters provided an acceleration of 7.4 deg/sec^2 as compared with a theoretical acceleration of 9.0 deg/sec^2 .

From retrofire to retrofire +50.5 seconds.- An analysis of the disturbance torque rates indicates that torques greater than the nominal or expected occurred at retrofire. A table of the disturbance torques, control torques, nominal disturbance torques, 3σ limits, and theoretical control torques has been included (table 5.1-XI). Roll rate information during the firing of retrorockets 2, 3, and 4 unfortunately did not lend itself to the calculation of disturbance torques or control torques. A review of the disturbance torques placed all retrorocket disturbances within the 3σ limits. However, a large disturbance was observed at initiation of the retrorocket 1. This disturbance will be discussed later.

Although some of the actual control torques appeared low and the disturbance torques were larger than nominal, a margin of control torque existed which would have allowed stable operation with a malfunction in one ring of the reentry control system.

The large disturbance at retrorocket 1 firing may have been the result of the retrorocket 1 firing plume striking the interior of the adapter assembly immediately after separation. However, this disturbance will require a much more detailed study in order to definitize the cause. It should also be noted that in this discussion of control torque errors,

UNCLASSIFIED

the number and duration of thruster firings and thruster performance has been the prime concern and cross coupling moment of inertia effects were not considered. A table of the moments of inertia used in these calculations is included, together with a table of control torques and disturbance torques (table 5.1-XII). The disturbances during the firing of all four retrorockets is depicted in figure 5.1-43.

From retrofire +50.5 seconds to 0.05g.- At the initiation of this portion of the flight, the retro pitch-down bias was removed. During the resultant maneuver to platform null, the pitch rate accelerated at 14.3 deg/sec^2 . This compares with a theoretical acceleration of 15.3 deg/sec^2 . During this portion of the flight, the correlation of thruster activity did not agree with the rate data in one area where a rate change occurred without a corresponding indication of a thruster pair firing. There is no explanation for this anomaly; however, the spacecraft rates did not exceed acceptable limits.

From 0.05g to 0.05g +150 seconds.- During this period the spacecraft was programed to roll at a continuous rate between 13.1 deg/sec and 13.6 deg/sec . The acceleration applied to obtain this rate was measured at 9.4 deg/sec^2 which compares with the theoretical value of 9.5 deg/sec^2 . As the spacecraft continued in this mode, the rates oscillated with pitch rates varying from -3.8 to $+3.5 \text{ deg/sec}$, roll rates varying from -12.8 to -17.1 deg/sec , and yaw rates varying from $+1.1$ to $+7.055 \text{ deg/sec}$, except in the latter portion where the oscillations were considerably damped. The nominal 4 deg/sec damping deadbands of pitch and yaw were adequately wide, in that the thruster activity during this rolling phase was quite low. There were only five pulses in pitch and 21 pulses in yaw during this period, including the uncertainty of the $\pm 4^\circ$ deadband.

From 0.05g +150 seconds to end of controlled flight.- Except for the transient required to stop the constant roll and achieve a hatches-up condition during the roll out, the acceleration to achieve a higher rate when it went out of the low side of the deadband was 7.8 deg/sec^2 and the acceleration to reduce the roll rate was 9.6 deg/sec^2 . The theoretical acceleration is 9.5 deg/sec^2 .

5.1.5.7.2 Reentry control stability: The performance of the control system during reentry is summarized in figure 5.1-44. This figure shows the rate envelope of the oscillations during reentry. The yaw rate varied around the switching level of 4 deg/sec which caused more thruster activity in yaw than in pitch. The figures also show the frequency of the oscillations versus time and acceleration versus time portraying the disturbance torque versus control torque capability.

UNCLASSIFIED

Figure 5.1-45 shows time histories of oscillations at various times showing very little evidence of nonlinear $C_{m\alpha}$ and $C_{n\beta}$ with α and β for the periods selected. However, the vehicle was exhibiting natural frequencies requiring precise rapid and accurately timed thruster commands for effective damping.

5.1.5.8 Special areas.- Areas of special interest for this mission, in relation to the IGS system, are discussed in the following text. The performance of the attitude display system as compared to the IMU is of particular interest and is presented in detail.

Another area of interest is the verification of the horizon sensor as obtained through a frame by frame analysis of the pictures taken of the horizon with the window camera. The attitude and maneuver control electronics (ACME) system is briefly mentioned.

5.1.5.8.1 Attitude display: The control system has no active function during the launch phase; however, excellent rate information was obtained. This rate information provided the signal source for the attitude display group, which consisted of the right-hand and left-hand instrument panel attitude displays and flight director indicators. The attitudes from the flight display group were read from the film taken by the onboard instrument panel cameras. Data from all three spacecraft axes on the left-hand attitude indicators starting at lift-off were compared with the platform data from the 800 seconds of guidance system activation. The camera indicated attitude remained within 10° of the platform angle which is considered to be within the timing uncertainty and the accuracy of reading the film. Typical comparisons are shown in figure 5.1-46.

5.1.5.8.2 Horizon sensor: The horizon sensor locked on the horizon for a period of 29.3 seconds ($10 + 372.5$ to $10 + 401.8$). The horizon sensor data are presented in figure 5.1-47, together with true spacecraft attitudes. These angles were derived by resolving the platform gimbal angles to horizon sensor angles and are presented in relation to the preflight calculated 3σ limits.

A known misalignment and lag figure for the horizon sensor accounts for the displacement of the gimbal angle and horizon sensor angle. The horizon sensors remained locked on for a period greater than expected and generally indicated adequate tracking stability.

The camera angles calculated from the platform gimbal angles and calculated from the window camera film are presented in figure 5.1-48. The curves confirm the predicted horizon sensor lag and show that satisfactory performance may be expected on future flights.

~~CONFIDENTIAL~~

5.1.5.8.3 ACME components: Prior to the flight of GT-2, the nominal and 3σ limits were determined for the control system parameters to be recorded. Two of these parameters were outside of these limits during flight and are discussed briefly. These two are the ACME 26 V ac and the associated frequency (400 cps).

The 26 V ac (EC01) was indicating 24.5 V ac throughout the flight. The effect of this low voltage was relatively minor in that the rate gyro scale factor was lowered slightly. A slightly low frequency indication was present throughout the powered ACME period of flight and was also present during prelaunch tests and these had been attributed to a telemetry calibration drift. The frequency was verified to be within specification tolerance prior to flight.

The rate deadband switching line and rate-attitude switching line were verified to be within specification limits during the flight.

5.1.5.9 IGS flight problems.- Two problems were encountered during the flight of GT-2 within the inertial guidance and flight control and display systems. The following paragraphs are short discussions of these problems.

5.1.5.9.1 Improper accumulation of velocity counts: The counts of the x-accelerometer, whose sensitive axis always pointed downrange on this flight, were nominal for the first 120 seconds after lift-off. As the acceleration increased, however, the x-accelerometer count approached the upper 3σ bounds. The data then indicate that the x-accelerometer counts increased abruptly prior to BECO; however, there were no data points prior to 1.0 second before BECO showing out of tolerance gain in acceleration counts. Immediately after BECO, the accelerometer counts returned to nominal and then increased as the acceleration increased, but staying within the 3σ limits. From SECO - 1.60 seconds to SECO + 0.732 seconds the IMU indicated velocity again increased 502 ft/sec abruptly and exceeded the upper 3σ value. The x-accelerometer apparently gained excessive counts as the acceleration increased, indicating a malfunction associated with high accelerations.

The z-accelerometer (vertical of the platform) counts exceeded the upper 3σ bounds prior to BECO because the actual trajectory was higher than nominal and this value is not considered anomalous. After the initial RGS pitch correction at 168.29 seconds from lift-off, the vertical acceleration decreased to the lower 3σ value. The actual vertical acceleration was nominal after that time. The y-accelerometer (cross range) counts remained well within the 3σ envelope except at 80 seconds after lift-off when high shear winds were encountered.

The nature of the data indicates an abrupt malfunction of the x-accelerometer or associated circuitry as the acceleration approached

~~CONFIDENTIAL~~

~~CONFIDENTIAL~~

5-33

150 ft/sec² rather than a scale factor problem or calibration drift. The z-accelerometer did not measure over 80 ft/sec² during launch, and the y-accelerometer was never over 15 ft/sec². A detailed study cannot be made of reentry due to lack of tracking during that phase of the flight.

An analysis of this problem has indicated that the computer did not malfunction or compute erroneous accelerations; however, preliminary tests of the flight platform resulted in a duplication of the high counts when subjected to the same accelerations. Further analysis and tests will be conducted to formulate proper corrective action.

5.1.5.9.2 Premature initiation of reentry guidance: The reentry guidance for this mission was initiated by sensing adapter separation while in the ascent mode. Telemetry indicates that normal transfer to the reentry program was accomplished after the prescribed 30 seconds from that time. Adapter separation and automatic initiation of retro-fire occurred at 414.25 seconds after lift-off. The first of computer operations containing reentry guidance parameters are tagged 444.519 seconds after lift-off. However, most of the quantities corresponding to this time are not informative because they were obtained while in the first pass through the reentry guidance equations immediately after computing spacecraft relative velocity. All the parameters following relative velocity had not been calculated and those that were in the telemetry block were left in from the prelaunch checkout. The next block of data was tagged 2.4 seconds later and the quantities were calculated using correct data. The reentry guidance logic was entered and the correct sequence was followed.

Reentry guidance parameters are those that utilize inertial measuring unit navigation quantities and computed relative location of the spacecraft with respect to the target. This information is utilized by the computer to generate a command that will cause the spacecraft to reach the target at landing. These guidance parameters should not be computed until a threshold acceleration of 0.4 ft/sec² has been sensed by the inertial measuring unit. However, during this flight, the reentry guidance parameters were computed prematurely while in the first pass through the reentry mode. This caused a bank angle to be commanded prior to flight in the atmosphere.

The following paragraphs explain this anomaly in detail and present the correction to the problem as recommended by the spacecraft contractor. The first time through the reentry equations, the Δt , (i) is set equal to the computation cycle through the executor routine. Then the incremental velocities are computed from the last stored values of accelero-

~~CONFIDENTIAL~~

~~CONFIDENTIAL~~

meter counts. Acceleration components are computed by dividing incremental velocities by a computational cycle time increment. This time increment in the first pass through the reentry equations was a small number (estimates vary between 0.17 to 0.25 seconds) and the acceleration computed was greater than the threshold acceleration of 0.4 ft/sec^2 . The time increment used in the calculations is the time to make the last successive pass through the executor routine which was made while the computer was going through the ascent equations. The computation cycle time in the ascent mode is approximately $\frac{1}{3}$ smaller than in the abort reentry mode. This is based on an estimated time for an abort reentry mode computation cycle of 0.6 seconds.

Since the acceleration computed was greater than 0.4 ft/sec^2 , the result of the data sample initialized the reentry guidance causing the density altitude and predicted zero lift range to be computed. The density altitude parameter was 8.99 and larger than the stored value of 4.67, and the predicted range was calculated to be 579.2 nautical miles. When this situation was detected the test on downrange error (predicted less target range) was made. Due to the relative location of the target in the footprint, the result of this test caused a route through the part of the program that computes a bank angle.

The next pass through the reentry equations, the time increment was the proper value of the reentry computation cycle, and acceleration was computed properly. However, the density altitude parameter was stored from the first pass and its value was large enough to route through the logic and compute a commanded bank angle for each successive pass through the equations.

These erroneous guidance commands were computed continuously until an acceleration of 0.4 ft/sec^2 was sensed. At this time, the correct values of the guidance parameters were computed. This can be seen by noting the abrupt change in the guidance parameters plotted on figure 5.1-49. The measured values of these quantities are superimposed on plots of the predicted time histories calculated from preflight studies. This shows the abnormal behavior of these parameters during the flight.

It is planned to eliminate this problem on future missions by increasing the threshold acceleration necessary to start reentry guidance above the 0.4 ft/sec^2 used on this mission. A study is in progress to determine the optimum value for this threshold acceleration. This parameter can be loaded into the computer by the digital command system, therefore, no modification to the operational math flow is required.

~~CONFIDENTIAL~~

5.1.6 Time Reference System

All components of the time reference system operated normally, or as expected throughout the GT-2 mission.

5.1.6.1 Electronic timer.- The electronic timer was checked by comparing the PCM telemetry parameters against the recorded G.m.t. The timer started counting at LO + 0.062 seconds. Averaged over the first minute of flight, the elapsed time from lift-off T_E drifted in the fast direction at a rate of approximately 100 parts per million. Later, during a 1-minute interval beginning at about LO + 1000 seconds, the drift, and therefore the drift rate, was zero within the accuracy of the G.m.t. print-out resolution of 0.001 second. The first reading of the time-to-go to retrofire parameters T_R was 4017.250 seconds and this occurred at a T_E reading of 0.500 second. At this T_E , the T_R reading should have been 4017.375 since the T_R register was initially loaded with 4017.875. T_R counts down to zero by $\frac{1}{8}$ second counts; therefore its resolution is $\frac{1}{8}$ second. The difference is accounted for because T_R is sampled $\frac{2}{10}$ second later than T_E by the PCM telemetry system. Electronic timer operation is indicated by the following table:

Data source	LO+seconds	PCM parameter ^a
CNV Tel II	0.062	0.000
CNV Tel II	69.055	69.000
Aircraft 497	1020.178	1020.000
Aircraft 497	1094.178	1094.000

^a T_E per sensor AA01

5.1.6.2 G.m.t. clock.- The G.m.t. clock was set at 12:10 G.m.t. prior to launch. It was read at 19:45 G.m.t. and recorded as reading 19 hours, 45 minutes. Reading resolution is about $\frac{1}{2}$ minute. The calendar dial stopped operating at sometime prior to launch for reasons unknown at this time. This is not considered to be a significant

UNCLASSIFIED

anomaly since this clock contained known deficiencies and has not been fully qualified. It was permitted on the flight only to secure additional information as to its capabilities.

5.1.6.3 Event timer.- The event timer functioned properly from lift-off until it was deactivated by recovery forces. It was in the field of the instrument panel camera along with other meters. Events with known G.m.t. were observed on the meters simultaneously with event timer readings and comparisons were made. The event timer, which reads in minutes and seconds, was within $\frac{1}{2}$ second of BECO, SECO, and other events.

5.1.7 Electrical System

No major anomalies were discovered in the performance of the electrical system during the GT-2 mission. Prior to launch, a malfunction in the fuel-cell system prevented it from being activated.

5.1.7.1 Electrical power system.- The main performance characteristic of the main, squib, and common control buses are shown in figures 5.1-50 and 5.1-51. The drop in common control and squib bus voltages in the period for LO + 350 seconds to LO + 460 seconds, as shown in figure 5.1-51, corresponds to the high activity in these circuits associated with spacecraft separation, OAMS thruster firings, firings of the pyrotechnic devices necessary for separation of the adapter sections, and firing of the retrorockets. The voltage rise at the end of this period corresponds to separation of the retrograde section. Voltage perturbations in the period from LO + 690 seconds to LO + 880 seconds correspond to RCS thruster activity.

The electrical load profile for the GT-2 mission was compared with predicted performance, and GT-2 flight data were compared with simulated flight data where possible. In each case, the values corresponded and no anomalies were found.

Table 5.1-XIV shows the comparison of the main bus amperages between actual mission data, load analysis, and simulated flight data at the major changes in electrical loads during the mission.

All electrical bus voltages were within the specification limits of 22 to 30 volts throughout the mission. The main bus batteries used 10.3 A-hr from T-30 seconds to LO + 1093 seconds. This amount compares favorably with 9.85 A-hr predicted from the load analysis.

The agreement between the special pallet battery currents during the mission and the anticipated values was good, and no anomalies were

UNCLASSIFIED

found. From T-30 seconds to LO + 1093 seconds, special pallet buses 1 and 2 used 1.7 and 1.8 A-hr, respectively. In the load analysis the special pallet buses used 1.6 and 2.1 A-hr, respectively.

Since the UHF tone generator was powered from special pallet bus 2, the cyclic 30-second on and off loads were observed in the bus current traces. The short off-time of the tone generator at LO + 445 seconds is clearly identified.

The only data available for the period from spacecraft touchdown to electrical "power-down" on the aircraft carrier are from the onboard camera coverage of the main panel and postflight inspection. A review of the "onboard" camera film showed that the main bus voltmeter and ammeter readings fluctuated with a motion which seemingly corresponded to the variations in spacecraft attitude. It was possible to detect spacecraft attitude variations by changes in the water level in the zero g water bottle. All measurements made when the spacecraft was returned to Cape Kennedy indicate that the main bus, squib bus, and common control bus were not shorted at that time. Measured resistances with all necessary switches and circuit breakers closed to obtain true readings, were found to be greater than 30 000 ohms for the main, squib, and common control buses.

5.1.7.2 Fuel cells.- As is indicated in appendix A, the history of the fuel cell sections in spacecraft 2 led to the decision to activate only one of the six stacks.

5.1.7.3 Reactant supply system.- The oxygen and hydrogen cryogenic subsystems were serviced and pressurized during the prelaunch period. The oxygen vessel was operating in the venting pressure range at 980 psia with a mass quantity of 63 percent at launch. (Refer to section 6.1.1 for prelaunch events which resulted in the 63-percent mass quantity at launch.) The hydrogen-vessel pressure was between the automatic pressure-control range and vent pressure at 260 psia which indicated a mass quantity of 95 percent at launch. The high-pressure reactant shut-off valves were latched closed due to deactivation of both fuel-cell sections.

Figure 5.1-52 shows mass quantity and pressure variations from launch for the reactant supply system (RSS) oxygen and hydrogen vessels, with accompanying ECS oxygen plots for comparison. At approximately LO + 356 seconds, the RSS oxygen and hydrogen vessels each indicated a similar pressure decline which continued for approximately 40 seconds; the trend gradually leveled out at 670 and 192 psia, respectively. The indicated pressures in both vessels fell to below the minimum automatic-heater energization points of 800 psia and 210 psia. Simultaneous with the start of pressure decline, mass-quantity readouts from both RSS vessels fluctuated over a narrow range, gradually returning to original

UNCLASSIFIED

values prior to adapter separation approximately 60 seconds later. The leveling out of the quantity indication coincides with the leveling out of the pressure indication noted previously. Inflight motion pictures of the instrument panel indicate agreement between telemetered and spacecraft-displayed mass-quantity and pressure data.

The ECS primary oxygen container did not evidence similar pressure decline or mass-quantity fluctuations. The beginning of the ECS primary oxygen vessel pressure decline at LO + 382.50 seconds coincides with initiation of oxygen high flow rate and is normal for this extraction rate without manual heater energization. The indicated mass quantity shows no change over this period because the change in vessel quantity is approximately 0.07 percent, which is well below the quantity-gage resolution.

A thorough review of all telemetry data offers no satisfactory explanation of simultaneous RSS oxygen and hydrogen vessel pressure decay and indicated mass-quantity fluctuations. At present, there is no hypothesis which appears credible, but the following general statements present possibilities which will be investigated further, both analytically and by testing. Conclusions from the study will be presented in a supplemental report.

(a) Temperature stratification: Thorough mixing of a highly stratified fluid can result in a decrease in fluid pressure. For this phenomenon to be responsible for the reported anomalies, both RSS vessels would necessarily be similarly stratified and simultaneously re-mixed; however, the ECS primary oxygen vessel, though of similar design, indicated immunity to these processes.

(b) Extraction: Rapid cryogen extractions could overpower the automatic pressure-control heater and result in a decline of vessel pressure. Calculated extraction rates which would cause the indicated pressure decline exceed normal valve flow capability. Reactant temperature measurements in the supply line from the heat exchanger to system components showed no change through the mission. Extraction by sudden, nearly simultaneous leakage is not supported by apparent pressure-leveling of both oxygen and hydrogen at LO + 410 seconds, which indicates a reduction in extraction rate.

(c) Instrumentation: The nearly simultaneous indicated decay of both RSS oxygen and hydrogen pressures does not appear to have been due to instrumentation difficulties. Panel-mounted pressure indicators confirm the reported telemetry data. The panel-meter indications and TM signals originate at individual, but commonly driven, potentiometers which share a regulated 5 V dc source. The oxygen pair of potentiometers is not common with the hydrogen pair. Flight regulation of the 5 V dc

UNCLASSIFIED

supply shows no anomalies, and this supply was used for many other measurements without problems.

5.1.7.4 Sequential system. - A detailed review of telemetry data for mission sequential functions has been completed, and the applicable parameters are tabulated in table 5.1-XV.

The major sequential events are used as the reference for subsequent functions and for calculating the difference between expected and actual times. These differences appear in the right-hand column as either PAM (onboard tape) or PCM (real time) deviations in time increments. It should be noted that for the function of spacecraft separation the PCM parameter ABO3 was used as the time base line for subsequent events in PAM calculations.

The system errors encountered in this tabulation are all within the accuracy limits of the data used. The PAM commutated data have a maximum absolute error (time from lift-off) of 1 second.

The UHF voice transmitters were cycled on and off by a 30-second on-off cyclic timer. One "off" cycle was 11.1 seconds between $10 + 445.21$ and $10 + 456.31$ seconds.

The fuse block assemblies were opened during the postlaunch inspection and found to contain moisture. All fuses were checked for continuity and found to be normal.

5.1.8 Propulsion System

5.1.8.1 Orbital attitude and maneuver system. - The objectives of the OAMS for the GT-2 mission were to impart to the spacecraft, upon command, the impulse required to effect separation from the GLV, to establish and maintain proper spacecraft attitude, and to accomplish the spacecraft turnaround. The analysis of all available data shows that these objectives were satisfactorily achieved.

At T-15 minutes the system was activated by actuating the propellant isolation valves. Nineteen 0.5-second pulses of thrust chamber assemblies (TCA's) 1 and 2 were required to obtain visual confirmation of acceptable performance. Initial pulses were characterized by apparent fuel-rich indications. The latter five pulses were accumulated after proper performance was noted. To date there is no substantiated explanation for the large number of pulses. On the previous attempt to launch GT-2, less than half this number were performed which was still considerably more than required during similar spacecraft tests. The most suspect possibilities for the fuel-rich indications are excessive entrapped gas in

UNCLASSIFIED

the oxidizer lines or restricted flow through the TCA's. No anomalies associated with these TCA's were observed during the flight, nor were any abnormalities noted in the previous test histories on these pitch TCA's.

The condition of the OAMS from lift-off through the launch phase was invariant and is presented in table 5.1-XVI.

Figure 5.1-53 depicts OAMS TCA activity as indicated through bilevel instrumentation on the firing signals. The accuracy of TCA signal width relative to actual burn time is ± 0.10 second due to the nature of the instrumentation. Spacecraft rate changes show that thrust levels on all attitude TCA's were within operating performance tolerances. However, at LO + 356.8 and LO + 383.3 seconds, during intervals of yaw-roll coupling in the roll-out and yaw turnaround maneuvers, rate changes were not commensurate with the indicated TCA activity. This is attributed to short duration pulsing operation of the TCA which was not amenable to resolution by the provided instrumentation. Firing signals between data samples were recorded as single firings without regard to pulse duration. Vibration data on the X-axis (sensors QA09 and QD10), reflect a series of short duration disturbances during these time intervals rather than the continuous burning as indicated by the on-off data. (See section 5.1.5.)

The spacecraft was separated from the launch vehicle by firing the two aft engines at LO + 352.45 seconds. The firing duration was 16.7 seconds and the velocity change to the spacecraft was 15.82 ft/sec, corresponding to an average acceleration of 0.94 ft/sec^2 . This acceleration is approximately 6 percent higher than anticipated; however, most of the difference can be attributed to the increase in thrust realized from high propellant supply pressures. The regulated pressure decreased to a minimum value of 300 psia as propellant was consumed during spacecraft separation. Since the nominal regulated pressure is 295 psia, this regulator was not required to open throughout the flight.

The injector head temperature on TCA 9 (aft-firing) increased 42° F from spacecraft separation to equipment section separation at 414.25 seconds. Nineteen seconds were required to achieve a 5° F rise. All other parameters recorded remained essentially constant throughout the flight.

Propellant consumption, as determined by mass inventory of the helium pressurant, indicates that approximately two-thirds of the usable propellant load remained at retrograde. The weight of propellant used as determined by pressure-temperature calculations was 12.6 pounds. From a summation of TCA sampled "on" times and nominal flow rates, 14.3 pounds of propellant were consumed. The total serviced quantity was 48.9 pounds (20.5 lbs of fuel and 28.4 lbs of oxidizer). A time

UNCLASSIFIED

plot of propellant quantities as determined by gas laws is presented in figure 5.1-54. The actual values compare fairly well with the preflight anticipated quantity of 18.4 pounds. The anticipated overall system mixture ratio of 1.48 is almost identical to the 1.49 value determined from flight data.

5.1.8.2 Reentry control system -

5.1.8.2.1 Preflight servicing: Propellant loading of both RCS rings was performed on October 1, 1964, and they remained wetted until postrecovery deservicing at Roosevelt Roads, Puerto Rico, on January 21, 1965. Final propellant top-off occurred on December 15 and 18, 1964, and final pressurant servicing of the B ring occurred January 16, 1965. The A ring remained pressurized from November 29, 1964. Prelaunch propellant loads were estimated at 36.9 pounds and 33.5 pounds for rings A and B, respectively, from metering volumes and X-rays. The condition of the RCS at lift-off and touchdown is presented in table 5.1-XVII.

5.1.8.2.2 TCA performance: During the mission, the control demands of each ring were essentially identical, and spacecraft rate changes associated with the completion of turnaround and roll command indicate that the TCA's yielded acceptable thrust levels. The attitude-hold capability of the systems during retrofire also appeared satisfactory.

The TCA duty cycles were determined over 10-second intervals and are presented in figure 5.1-55 in terms of burn percentage and average signal width. The only measurement indicative of TCA life was the TCA 7 nozzle temperature which increased to 360° F. In ground static firings, this temperature would imply the utilization of a substantial portion of the guaranteed life of the TCA. However, since this parameter is also affected by reentry heating, postflight analysis of the char characteristics of the TCA will be required to determine the available margin.

5.1.8.2.3 Postflight deservicing: During postflight deservicing of the systems at Roosevelt Roads, essentially no propellant could be extracted from either ring, and source pressures which were 2100 and 2440 psia at touchdown had decreased to 1135 and 1365 psia in the A and B rings, respectively. Calculations show that a 760-psi decrease can be attributed to expansion of the nitrogen gas into empty propellant tanks, and an additional 36-psi decrease can be allotted to aerospace ground equipment (AGE) in the measurement of these pressures. The system temperature had increased to 81° F.

Propellant depletion is believed to have resulted from unscheduled actuation of the TCA's after touchdown. This is substantiated by the results of pressurant mass inventories at touchdown which indicated that the propellant used during the mission was 16.2 and 14.3 pounds for

UNCLASSIFIED

rings A and B, respectively. Propellant consumption based on the summation of the available bilevel "on" signals to the TCA's and nominal flow rates was determined to be 17.8 pounds from each ring. TCA firings were filmed while the spacecraft was afloat. The engine activity notably occurred in pairs, simultaneously on both rings (TCA's 1, 8, 3, 2). Intermittent vapors from TCA 3 on the B ring were also noted in the films made on the carrier deck. Of the two most probable explanations for this anomaly, that is, leakage through the systems or salt water grounding of the electrical leads (power to the solenoids is interrupted by breaking the ground circuit), unscheduled electrical actuation is believed the most likely cause. This might be expected as the attitude control electronics (ACE) package was not hermetically sealed.

Inadvertent TCA operation or leakage will not present a problem on future missions since motor-operated shutoff valves will be installed in both RCS rings and the valves will be closed after parachute deployment. Pressures downstream of these valves will be relieved by TCA actuation during the descent.

The following are details which are peculiar to each system:

5.1.8.2.4 RCS A ring: The RCS A ring was activated in flight by the simultaneous opening of the cartridge valves in component packages A, C, and D, as planned. The first indication of system activation occurred at LO + 382.245 seconds when the initial decrease in nitrogen source pressure was observed. The source pressure stabilized at 2760 psia within 2.4 seconds, and the temperature stabilized at approximately 71° F. This pressure is 153 psi lower than anticipated from preflight calculations. The error may have originated from either these calculations or a smaller quantity of propellant being loaded into the system than was stated on prelaunch logs. Although the oxidizer tank loadings were established by X-rays, the fuel tank installation prohibited this. The difference in question is equivalent to 1.9 pounds of propellant. Histories of the nitrogen source pressure and temperature are presented in figure 5.1-56. The temperature curve shows that a 15° F decrease occurred from system activation and propellant utilization until LO + 900 seconds.

Regulator performance, also presented in figure 5.1-56, resulted in a nominal 300-psi value which was measured within 4 seconds after system activation. Throughout the flight, the regulated pressure was maintained within a 6-psi band width until atmospheric pressure caused an increase in the regulator reference pressure after LO + 800 seconds.

By the conclusion of the flight the source pressurant had decayed to 2140 psia and the temperature changed to 70° F. From these data, calculations show that 16.2 pounds of propellant were consumed during the flight. This amount compares very favorably with the anticipated

UNCLASSIFIED

~~UNCLASSIFIED~~

5-43

flight utilization of 16.9 pounds. It is concluded from the source pressure data, which indicate a constant reading over 200 seconds, that the system leak rate was very low.

The temperature increase of TCA's 5 and 6 (pitch up), TCA 2 (pitch down), and TCA 8 (yaw left) due to reentry heating were well within the operational temperature limits of the system. As illustrated by figure 5.1-56, the maximum temperature rise experienced was 35° F on the fuel inlet of TCA 5. Also, the oxidizer-tank outlet temperatures showed that reentry heating caused very little increase on the bulk propellant temperatures which exhibited an incremental rise of 7° F.

5.1.8.2.5 RCS B ring: At T-15 minutes, the RCS B ring was activated by firing the cartridges in the C and D component packages. Opening of the cartridge valves in these packages was verified by a decrease in the nitrogen source pressure from 3121 psia to 3090 psia and a regulated pressure decay from 321 to 314 psia.

From visual indications of TCA operation during the static firing of TCA's 1 and 2, satisfactory performance was achieved on the second 0.5-second pulse. This is consistent with the previous static firing on December 9, 1964.

During launch, the source pressure, regulated pressure, and temperature data indicated that the system performance was satisfactory with no appreciable change occurring in any of these parameters from lift-off to SECO.

Bilevel signals and the initial decay in the regulated pressure at LO + 396.645 seconds provide the first indication of system operation. The regulator maintained propellant tank pressures at 3000 psia within the accuracy limits of the instrumentation, which is well within the design limits. During descent the regulated absolute pressure increased due to the change in regulator reference pressure.

The oxidizer feed temperature was essentially constant during reentry. The nitrogen source pressure stabilized at 2460 psia, and the source tank temperature remained constant throughout the flight at 72° F. The nitrogen source pressure and regulated pressure are presented in figure 5.1-57. From these data, calculations show that 14.3 pounds of propellant were consumed during the flight. This amount compares with the anticipated flight utilization of 16.9 pounds. The 200-second period of stabilized source pressure indicates that a low overall system leak rate was maintained.

5.1.8.3 Retrograde rockets. - The retrorocket firing sequence was initiated at LO + 414.25 seconds. The firing order was 1, 3, 2, 4 as

~~UNCLASSIFIED~~

~~CONFIDENTIAL~~

planned, with a time delay between firings of 5.47, 5.20, and 5.80 seconds, respectively. The design time delay was a constant 5.5 seconds.

The measured deceleration and total velocity decrement during retro-fire compare favorably with predicted values. The actual velocity change was 334.7 ft/sec as compared with an anticipated velocity change of 339 ft/sec, and the total rocket burn time was 21.8 seconds as determined from accelerometer data. The disturbance torques resulting from rocket misalignment were determined to be within the control capabilities of the reentry control system with one ring operative.

The burn time of each rocket motor is presented in table 5.1-XVIII. Motor temperature at time of firing is estimated at 65° F based on pre-launch readings of case temperature. The maximum case temperature recorded was 80° F which occurred at jettison.

5.1.9 Pyrotechnic System

All functions required of the pyrotechnic system during the GT-2 mission were satisfactorily achieved. Because of the lack of instrumentation on any individual pyrotechnic device, it cannot be ascertained whether all redundant elements functioned, except for those devices which were recovered. Checks of all of the bridge wires of the recovered pyrotechnics indicated that those devices had been initiated. Removal of all pyrotechnic devices from the spacecraft revealed no visual anomalies, with the exception of the guillotine used to cut the right-hand wire bundle between the R and R section and the RCS section. Since the seat devices had not been fired prior to publication of this report, it has not yet been determined whether these devices were degraded during flight.

Visual examination of the wire bundle guillotine which had malfunctioned (see fig. 5.1-58) revealed that the blade had depressed the wires in the bundle approximately $\frac{1}{2}$ to 1 inch and that none of the wires in the bundle were cut. Since recovery, attempts have been made to duplicate the failure through installation variation. These attempts were unsuccessful. Examination of the cartridge X-rays prior to launch did not reveal any suspicious areas. Failure analysis of the recovered guillotine and results of firing the seat pyrotechnics will be discussed in a supplemental report. The failure analysis will include investigation of possible under-loading of the charge.

~~CONFIDENTIAL~~

5.1.10 Crew Station Furnishings and Equipment

5.1.10.1 Controls and displays.- The evaluation of the pilots' controls was limited to a preflight and postflight inspection of the abort handle assembly and the attitude control assembly. The abort handle was electrically connected to the spacecraft abort circuits during the mission. The attitude control was isolated from the spacecraft control system circuits by use of the normal on-off switches. Neither control was operated in flight, nor were there any output signals observed from these controls. Postflight inspection and abbreviated functional testings showed that those controls had withstood the flight environment without damage or failure.

The evaluation of the pilots' displays was accomplished by analysis of photographic coverage of the most significant sections of the left, center, and right instrument panels. See figures 5.1-59, 5.1-60, and 5.1-61, respectively. The film from each of three cameras was read to obtain data from the instruments observed. The frame speed of these cameras varied between $2\frac{1}{2}$ and 6 frames per second. The time correlation of the resulting data was accurate within ± 1 second. Comparison with the telemetered data indicated that the information on the pilot's displays was accurate within the design limits for each system. Most of the data displayed was accurate within ± 2 percent.

The flight director and attitude indicators on both instrument panels were photographed. These two displays operated smoothly throughout the flight. The attitude and rate information displayed appeared to correlate well with telemetered data and the view of the horizon out of the left window.

Detailed correlation and evaluation of the attitude and rate displays are included in section 5.1.5 of this report.

All warning lights observed by the cameras operated normally. Satisfactory operation of the "Ignore Horizon Scanner" warning light was observed by the center camera. The "Acceleration" and "Attitude Malfunction" warning lights came on when the inertial guidance system platform was turned off. These lights remained on for the duration of the flight. No other warning lights were observed to come on, and examination of the telemetered data confirmed that no other lights should have come on.

5.1.10.2 Out-the-window view.- Exceptional photographic coverage was obtained of the view out of the command pilot's window (left window) from the time of spacecraft separation, LO + 352 seconds, until just before impact at LO+ 1096 seconds. This sequence, photographed in color at approximately six frames per second, gave a clear indication of the

UNCLASSIFIED

spacecraft attitude and maneuvers for this period of flight. Representative views at separation, retrograde, reentry ionization, and parachute deployment are shown in figures 5.1-62 to 5.1-67.

5.1.10.2.1 Spacecraft separation to retrograde: The attitude of the spacecraft at separation was clearly discernible as 90° right roll with the nose of the spacecraft essentially on the horizon. The left roll to the "heads-up" position and the subsequent yaw left maneuver to blunt-end-forward attitude were also readily recognizable. Thereafter, an object which was most probably the second stage of the launch vehicle passed through the field of view at the upper left. Minor variations in spacecraft attitude in pitch and yaw were apparent until the period of retrograde rocket firing. At retrograde, there were no noticeable attitude perturbations. Immediately after retrograde, an object which was most probably the equipment section passed through the field of view. See figures 5.1-62 and 5.1-63.

5.1.10.2.2 Reentry: The earth filled the upper half of the field of view during the initial part of the reentry. The horizon was clear and well defined. As the reentry progressed, the ionization effect became very noticeable in the wake of the spacecraft. At no time, however, did it obstruct the view of the horizon nor detract from the visual attitude reference provided by the horizon.

At the commencement of the constant roll rate, the attitude of the spacecraft remained stable and the visual reference to the horizon remained clear. At the maximum lift command, the rolling ceased and the earth again filled the upper portion of the field of view. The horizon then moved out of the top of the field of view as the reentry flight path became steeper. Clear indications of thruster firing were visible in the film; however, there was no evidence of flame which might interfere with visibility. In summary, the horizon view was clear and well defined throughout the reentry until the spacecraft was below 80 000 feet. See figures 5.1-64 and 5.1-65.

5.1.10.2.3 Parachute deployment sequence: The photographic coverage provided a clear record of the parachute deployment sequence although exact time correlation was not possible because of the variable film speed. Separation of the R and R section, deployment of the pilot parachute, deployment of the main parachute, disreefing of the main parachute, and release of the single-point suspension were all clearly visible. Significant oscillations were noticeable after parachute deployment, although these were within expected limits. A detailed analysis of the landing system operation is given in section 5.1.11. See figures 5.1-66 and 5.1-67. The photographic coverage terminated prior to landing in the water.

UNCLASSIFIED

5.1.10.3 Crew station furnishings.- Most crew station furnishings were omitted from spacecraft 2 because of the nature of the mission and the installation requirements for the crewman simulators. The primary items which were carried were the food boxes on either side of the crew station. These containers withstood the flight without damage or other incident.

5.1.11 Landing System

The overall performance of the parachute landing system on the GT-2 flight test was within nominal design values. All sequences occurred in the proper order and the timing of each was within established tolerances. The total time from pilot parachute deployment to spacecraft landing was 219.32 seconds which agrees with values obtained during the qualification of this system. Figure 5.1-68 depicts the performance of the GT-2 landing system. The pilot parachute was mortared out at $10 + 871.76$ seconds. A descent trajectory based on Antigua tracking data gives the corresponding altitude at which the pilot parachute was deployed as 10 491 feet. Rates of descent were nominal and resulted in approximately 30 ft/sec at touchdown. Accelerations at touchdown did not exceed $3g$ in any direction at the spacecraft center of gravity. The spacecraft was not damaged by water landing and no water leakage was evident. The flotation was approximately as predicted.

The main parachute sank before recovery forces arrived; however, the motion pictures from the onboard camera indicated that the canopy and bridle were not damaged. The R and R section with the attached pilot parachute and main parachute deployment bag were recovered. Examination of the pilot parachute, main parachute deployment bag, parachute container, pilot parachute mortar, and all other associated landing system hardware revealed no significant damage.

5.1.12 Postlanding Systems

With the exception of the recovery flashing light, all recovery aids sequentially functioned in a satisfactory manner. The door was caught at the forward edge and did not allow the recovery light to erect following parachute jettisoning. After the spacecraft was recovered, the door was manually opened. The flashing light then erected satisfactorily and began its flashing cycle.

TABLE 5.1-I.- CABIN SECTION PEAK STRUCTURAL TEMPERATURES DURING REENTRY

5-48

Parameter	Z Station	Description	Peak measured temperature, °F
PD01	135.9	Inner skin, left-hand equipment door	168
PD13	109.5	Cabin wall, ECS bay door	127
PD16	158.6	Cabin wall, small pressure bulkhead	85
PD17	116.0	Top of ECS door stringer	330
PD18	116.5	Side of ECS door stringer	178
PD29	138.3	Right-hand window, inside inner pane	99
PD33	114.9	Bottom of trough compartment	90
PD34	145.0	Side of stringer, landing gear door	345
PD35	112.1	Top of ECS door rib	174
PD36	108.0	Side of stringer, equipment access door	201
PD37	104.9	Inside flange of structural ring	163
PD39	131.0	Side of stringer, forward equipment bay door	320
PD40	123.6	Landing gear door, bottom flange of stringer	149
PD41	160.2	Landing gear door, bottom flange of stringer	148
PD53	174.0	Cabin-RCS section tie down bolt, (BY)	176
PD55	156.3	Support for umbilical disconnect	178
PD59	135.7	Right-hand window, inside inner pane	108

UNCLASSIFIED

UNCLASSIFIED

TABLE 5.1-II.- MAXIMUM VALUES OF g_{rms}

Accelerometer	QA09	QA10	QA11	QB13	QB14	QA12	QA13	QA14	QD07	QD08	QD10	QD11	
Sensing direction	X	Y	Z	Radial	Z	X	Y	Z	X	Y	X	Y	
Frequency response ^a	low	low	low	high	high	medium	high	high	high	high	low	low	
Sensing level	±2g	±2g	±4g	±16g	±16g	±16g	±16g	±16g	±16g	±16g	±4g	±4g	
Station location	Z104			Z115	Z118	Z132			Z223				
Event	LO+sec ^b	Maximum g_{rms}											
Lift-off	0	0.08	0.09	0.31	0.90	0.40	0.40	0.50			0.80	0.10	0.20
Maximum exit vibration	65	.6	.19	.10	2.50	.90	1.35	2.60			1.30	.90	.70
BECO	152	.11	.16	.46	.35	.60	.60	.35			.35	.40	.30
SECO	332	.10	.12	.24	.10	.30	.30	.10			.10	.15	.40
Spacecraft separation	352	.02	.12	.09			.45	.35			.10	.05	.05
Equipment section separation	413	.11	.28	.40			1.10	.75	.45	.15	.30	.05	.20
Retrograde section separation	459	.02	.28	.12			.80	.80	.40	.20	.35	.10	.45
Maximum reentry high frequency vibration	720	.015	.03	.02			.15	.20	.15	.80	.80	.01	.005
Maximum reentry low frequency vibration	840	.06	.06	.20			.20	.30	.80	.40	.65	.15	.15
Rendezvous & recovery section separation	871	.12	.06	.22			1.42	1.82	.78	.38	.40	.81	.85

^aFrequency response:
 Low = 1 to 30 cps
 Medium = 20 to 600 cps
 High = 20 to 2000 cps

^bTime interval under consideration centered at approximate time shown.

UNCLASSIFIED

TABLE 5.1-III.- REAL AND DELAYED TIME DATA ACQUISITION

Station	First AOS, LO+sec	First LOS, LO+sec	Second AOS, LO+sec	Final LOS, LO+sec
Real Time				
CNV (Tel II)	0	-	-	413.475
MCC (Tel III)	0	306 (Power failure to recorder)	339	422.275
GBI	50.775	-	-	441.975
GFI	195.475	383.875	386.875	411.775
ANT	322.775	-	-	544.975
RKY ^a	189.025	419.575	522.375	527.175
A/c 630	771.975	873.075	896.475	1096.475
A/c 497	786.075	872.975	896.275	1096.075
CSQ	698.775	874.275	875.425	1012.075
Composite	0	544.975	698.775	-
	-	874.275	875.425	1096.475
Delayed Time				
A/c 497 ^b	439.525	535.525	549.90	-
	-	600.275	609.90	-
A/c 630 ^b	439.525	619.375	660.275	749.150
		535.525	549.90	-
CSQ ^{b, c}	439.525	631.525	660.275	758.650
		535.525	549.90	-
Composite	-	631.525	681.90	744.275
		439.525	535.525	549.90
Composite	-	655.375	657.075	758.650
		535.525	549.90	-
Actual time				
Onboard PCM ^b Recorder	0	535.525	549.90	758.650

^a Only 75.8 seconds of usable data from LO+189.025 to LO+527.175 seconds R.F. reception was continually being lost, then regained.

^b Recorder reached end of tape recording on Track A at LO+535.525 seconds. Tape direction was reversed, and, recording on Track B started at LO+549.90 seconds.

^c CSQ received 38 seconds of usable delayed (dump) PCM data during time period LO+631.525 to LO+681.90 seconds when R and R separation was occurring.

UNCLASSIFIED

TABLE 5.1-IV.- USABLE PCM DATA

Station	Total acquisition time, sec	Synchronization loss, sec	Other losses, sec	Usable data	
				sec	percent
Real time					
CNV (Tel II)	413.475	2.625	-	410.850	99.365
MCC (Tel III)	422.275	-	33.0 (Power failure)	389.275	92.185
GBI	391.250	1.525	-	389.725	99.610
GFI	216.300	9.575	-	206.725	95.111
ANT	222.200	1.625	-	220.575	99.268
RKV	338.150	162.325	102.8 (Loss of signal)	73.025	21.6
A/C 630	324.500	1.100	23.4 (R and R sep.)	300.000	92.449
A/C 497	310.000	0.400	23.3 (R and R sep.)	286.300	92.355
CSQ	312.150	5.575	1.15 (R and R sep.)	306.575	98.207
Composite	2950.300	184.750	183.65	2583.050	87.552
Delayed time					
A/C 497	295.250	70.2	14.375 ^a	225.05	76.289
CSQ	290.375	45.725	14.375	244.650	84.253
A/C 630	276.000	9.825	14.375	266.175	96.44
Onboard PCM recorder	742.000 (on tape)	-	-	742.000	100.00

^a No data recorded. Tape turnaround.

~~CONFIDENTIAL~~

TABLE 5.1-V.- LAUNCH GUIDANCE AND CONTROL EVENTS

Event	Time from lift-off, sec ^a		
	Planned	Actual	
		Primary RGS and TARS	Secondary IGS
Switch to ascent mode	T-90 min	N/A	N/A
Update targeting	T-180	N/A	T-180
DCS verification			
Platform to target azimuth			
Stage I ignition	-3.34	-3.361	
Lift-off	-0.000	-0.000	-0.000
Roll program start	4.40	4.34	4.194
Roll program end	20.48	20.40	20.458
No. 1 pitch rate start	23.04	22.99	22.771
No. 2 pitch rate start	87.510	88.07	87.940
No. 1 IGS update verified	103		103.949
No. 1 gain change	104.96	104.67	104.667
No. 3 pitch rate start	118.231	118.71	118.755
No. 2 IGS update verified	143		143.839
No. 2 gain change	153.52	151.71	
Termination of pitch program	162.56	162.09	165.000
First RGS command received	169.000	168.29	168.000
SECO	336.48	332.151	331.807
Initiation of IVAR	SECO+20	SECO+20.3	SECO+20.3
Adapter separation	418.48		414.22

^aUnless otherwise specified~~CONFIDENTIAL~~

TABLE 5.1-VI.- INSERTION CONDITION COMPARISON AT SPACECRAFT SEPARATION

System	Inertial velocity ft/sec	Inertial flight-path angle, deg	Platform axis inertial velocity, ft/sec		
			x	y	z
Nominal (preflight)	25 731	-2.28	25 139	5 484	8
IGS STL estimate	25 798	-2.20	25 217	5 435	-115
STL preliminary BET	25 736	-2.23	25 145	5 485	-109
STL MISTRAM I	25 729	-2.20	25 140	5 474	-110
STL GE Mod III	25 738	-2.34	25 141	5 500	-109
Goddard GE Mod III	25 733	-2.39			
Impact prediction (MISTRAM)	25 731	-2.30			
Reconstructed from Antigua reentry tracking	25 738	-2.29			

CONFIDENTIAL

CONFIDENTIAL

TABLE 5.1-VII.- IGS MEASURED VELOCITY CHANGES^a

5-54

Event	Time, LO+sec	Sensed velocity change ft/sec	Nominal velocity change, ft/sec	Nominal determination
GLV tail-off	332.15 to 351.06	101.6	104.0	Imperial value of IGS computer used to bias the velocity to deliver the SECO discrete
Separation	352.45 to 378.10	15.8	14.8	Assumed, 189 lb thrust
Retrofire	414.22 to 436.22	334.7	339.0	Preflight computed value from total thrust and weight

^aThese sensed velocity changes were determined by using the accelerometer outputs, biasing them, and transforming through the misalignment and scale factor matrix, as determined from preflight data. These velocity changes are those resulting from the applied thrusts only and do not include the velocity changes due to gravity.

~~CONFIDENTIAL~~

~~CONFIDENTIAL~~

TABLE 5.1-VIII.- IGS REENTRY EVENT SEQUENCE

Event	Time	
	Planned, sec	Actual, LO+sec
Spacecraft separation	SECO+20	352.45 (SECO+20.3)(t_s)
Adapter separation	t_s +62	414.22 (t_s +62.5)(t_r)
Retrorocket 1 fire	t_s +62	414.25 (t_s +62.5)(t_r)
Retrorocket 3 fire	t_r +5.5	419.72 (t_r +5.5)
Retrorocket 2 fire	t_r +11.0	424.92 (t_r +10.7)
Retrorocket 4 fire	t_r +16.5	430.72 (t_r +16.5)
Initiate abort reentry mode	t_r +30.0	444.83 (t_r +30.0)
Reentry .05g	at .05g	560.2
Maximum lift spacecraft sequence	.05g +150.0	710.0 (.05g +148.8)
IGS maximum lift command displayed	Max. lift +30.0	739.0 (max. lift +29.0)
IGS turn-off	10 600 ft (barostat)	871.8

Key:

 t_s time of spacecraft/GLV separation t_r time of retrofire

TABLE 5.1-IX.- INDICATED INERTIAL GUIDANCE SYSTEM ERRORS

Compared to	IMU errors					
	Position, ft			Velocity, ft/sec		
	Δx	Δy	Δz	Δx	Δy	Δz
GE Mod III (at BECO)				20	-2	^a 0
MISTRAM (at BECO)				20.5	-2.4	^a 0
GE Mod III (at SECO)				66	-15	^a 5
MISTRAM (at SECO)				66.5	-7.0	^a 4.5
	IMU errors including computational errors					
GE Mod III (at BECO)	1500	-180	200	21	-2	0
MISTRAM (at BECO)				22.5	-2.3	-0.5
GE Mod III (at SECO)	6500	-1000	-100	71	-15	4
MISTRAM (at SECO)				72.0	-7.0	4.5

^aContains -0.298° azimuth alinement correction

~~CONFIDENTIAL~~

TABLE 5.1-X.- GUIDANCE SYSTEM ERRORS

(a) Errors

Computer axis (guidance coordinate)	Velocity error, ft/sec	Position error, ft
X	72	1500
Y	-10	-180
Z	4.5	-200

(b) Error sources

Platform axis	Error source	Actual value	Specification value
x	Accelerometer malfunction under high g condition	660 counts	--
x	Accelerometer scale factor error	^a 110 ppm	360 ppm
x	Gravity approximation error	~0.02 ft/sec	--
x	Gyro constant drift	0.38 deg/hr	3.00 deg/hr
y	Gyro constant drift	-0.27 deg/hr	3.00 deg/hr
y	Accelerometer mis-alinement toward X	-30 sec	-100 sec

^aExcept during intermittent malfunction periods.

TABLE 5.1-XI.- CONTROL SYSTEM EVENTS

5-58

Time		Control mode or significant change	Primary events
Design, sec	Measured LO+sec		
t_s	352.45	Inactive	Separate from GLV
t_s+2	354.70	Reentry	Remove insertion roll attitude, continue separation
$t_s+16.5$	369.00	Horizontal	Null spacecraft attitude to platform reference
t_s+30	382.50	Rate command	Yaw toward a BEF attitude
t_s+45	395.99	Retrofire	Establish retroattitude
$t_s+62.5(t_r)$	414.25	Fire retrorocket	Fire retrorockets
$t_r+50.5$	464.26	Horizontal	Remove pitch retrograde bias
0.05g	560.23	Reentry roll	Begin continuous roll
0.05g+150	710.01	Reentry, maximum lift	Achieve maximum lift attitude
R and R separate	871.76	Inverter shut off	End of controlled flight

Key:

t_s time of spacecraft - GLV separation
 t_r time of retrofire

~~CONFIDENTIAL~~~~CONFIDENTIAL~~

TABLE 5.1-XII. - CONTROL SYSTEM PERFORMANCE

(a) Control system measured torques

Propulsion system	Time interval, sec	Roll		Pitch		Yaw	
		Theoretical, deg/sec ²	Measured, deg/sec ²	Theoretical, deg/sec ²	Measured, deg/sec ²	Theoretical, deg/sec ²	Measured, deg/sec ²
OAMS	Spacecraft separation + 2 to spacecraft separation + 16.5	7.12	6.3 (ccw) 6.5 (cw)	5.71	5.6 (up) 6.2 (down)	5.80	5.9 (right) 5.7 (left)
	Spacecraft separation + 16.5 to spacecraft separation + 30			5.71	5.6 (up) 5.6 (down)	5.80	5.6 (right) 5.6 (left)
	Spacecraft separation + 30 to spacecraft separation + 45			5.71		5.80	
RCS	Spacecraft separation + 45 to spacecraft separation + 62			8.99	7.9 (up) 6.40 (down)	8.84	6.34 (right) 7.64 (right) 6.1 (left) 6.4 (left)
	Retrograde sequence	7.93		13.30	12.8 (up) 12.5 (down)	14.0	
	Retrograde + 50.5 to 0.05g			15.35	14.3 (up)		
	0.05g to 0.05g to 150	9.55	9.43 (ccw)				
	0.05g + 150 to end of controlled flight	9.55	7.8 (ccw) 9.6 (cw)				

UNCLASSIFIED

UNCLASSIFIED

TABLE 5.1-XII. - CONTROL SYSTEM PERFORMANCE - Concluded

(b) Retrorocket disturbance torques

Attitude		Retrorocket 1, ft-lb	Retrorocket 2, ft-lb	Retrorocket 3, ft-lb	Retrorocket 4, ft-lb
Roll	Actual disturbance torque	13			
	Actual control torque	65 (1 jet)			
	Nominal disturbance torque ^a	-5.7			
	3 σ disturbance torque ^a	± 20.0	± 14.6	± 18.3	± 16.3
	Control torque ^a	114			
Pitch	Actual disturbance torque	45.1	13.8	25.2	24.6
	Actual control torque	223.2	223.2	223.2	276.6
	Nominal disturbance torque ^a	-12.4	-4.6	-5.9	-6.1
	3 σ disturbance torque ^a	± 64.3	± 65.9	± 65.9	± 66.8
	Control torque ^a	425	429	433	438
Yaw	Actual disturbance torque	25.9	24.2	25.1	22.7
	Actual control torque	150.9	266.2	171.3	167.7
	Nominal disturbance torque ^a	23.9	20.9	5.2	5.0
	3 σ disturbance torque ^a	± 65.3	± 66.4	± 65.4	± 66
	Control torque ^a	425	429	433	438

^aPreflight calculations

UNCLASSIFIED

UNCLASSIFIED

TABLE 5.1-XIII. - SPACECRAFT MOMENTS OF INERTIA

	Pitch, slug-ft ²	Yaw, slug-ft ²	Roll, slug-ft ²
At coast	3624.5	3568.8	1362.4
At start of retrofire	1803.0	1736.7	829.4
At end of retrofire	1705.1	1638.9	821.3
At reentry	1426.7	1349.8	684.3

UNCLASSIFIED

UNCLASSIFIED

UNCLASSIFIED

TABLE 5.1-XIV.- MAIN BUS AMPERAGE LEVELS

Data Source	Lift-off, A	Equipment section separation, A		R and R section separation +30 sec, A	
		Before	After	Before	After
GT-2 mission	47.1	46.6	29.2	28.6	7.4
Load analysis	48.2	45.2	30.0	30.0	8.3
Simulated flight	45.7	48.9	—	—	—

UNCLASSIFIED

TABLE 5.1-XV.- SEQUENCE OF EVENTS

Event	Actual time from lift-off, sec	Planned event time, sec	Actual event time, sec	Error, sec
Lift-off	0.0	0.0		
BECO	151.7	--	Stage I propellant depletion	--
Horizon sensor fairing jettison	196.6	BECO + 45.0	BECO + 44.9	-0.1
Nose fairing jettison	196.7	BECO + 45.0	BECO + 45.0	0.0
SECO	332.2	--	RGS velocity cut-off	--
Spacecraft separation command	352.4	SECO + 20.0	SECO + 20.2	+0.2
OAMS on and attitude mode select	352.3	SECO + 20.0	SECO + 20.1	+0.1
Aft thrusters on	352.3	SECO + 20.0	SECO + 20.1	+0.1
Spacecraft separation command	352.7	SECO + 20.0	SECO + 20.3	+0.3
OAMS roll rate start command	354.7	Spacecraft separation + 2.0	--	--
Reentry mode A select	354.7	Spacecraft separation + 2.0	Spacecraft separation + 2.1	+0.1
Aft thrusters off	369.0	Spacecraft separation + 16.5	--	--
OAMS horizontal mode select	369.0	Spacecraft separation + 16.5	--	--
Select adapter antenna	369.0	Spacecraft separation + 16.5	Spacecraft separation + 16.4	-0.1
RCS isolation valve open	382.5	Spacecraft separation + 30.0	Spacecraft separation + 29.9	-0.1
OAMS yaw rate start command	382.5	Spacecraft separation + 30.0	Spacecraft separation + 29.9	-0.1
Retrograde squib bus arm	382.5	Spacecraft separation + 30.0	Spacecraft separation + 29.9	-0.1
Arm indicator for retro attitude	382.5	Spacecraft separation + 30.0	Spacecraft separation + 29.9	-0.1
O ₂ high rate	382.5	Spacecraft separation + 30.0	Spacecraft separation + 29.9	-0.1
OAMS off	396.0	Spacecraft separation + 45.0	--	--

UNCLASSIFIED

UNCLASSIFIED

TABLE 5.1-XV.- SEQUENCE OF EVENTS - Continued

Events	Actual time from lift-off, sec	Planned event time, sec	Actual event time, sec	Error, sec
RCS ring A and B on	396.0	Spacecraft separation + 45.0	--	--
Automatic retroattitude mode	396.0	Spacecraft separation + 45.0	Spacecraft separation + 43.3	-1.7
Event time TR-30	396.8	--	--	--
Separate OAMS	411.9	Spacecraft separation + 60	Spacecraft separation + 59.1	-0.9
Boost, insert, and abort squib bus safe	412.7	--	--	--
Fire guillotines	413.5	Separate OAMS + 1	--	--
Equipment section separation auto retrograde command	414.2	Separate OAMS + 2	Separate OAMS + 2.3	+0.3
Equipment section shape charge	414.2	--	--	--
Equipment section separation	414.2	--	--	--
Automatic retrofire	414.2	--	--	--
Manual retrofire	415.1	Separate OAMS + 3	Separate OAMS + 3.2	+0.2
Retrorocket 3 fire	419.7	Automatic retrofire + 5.5	Automatic retrofire + 5.5	0.0
Retrorocket 2 fire	424.9	Automatic retrofire + 11.0	Automatic retrofire + 10.7	-0.3
Retrorocket 4 fire	430.7	Automatic retrofire + 16.5	Automatic retrofire + 16.5	0.0
Initiate abort reentry mode	444.8	Automatic retrofire + 30.0	Automatic retrofire + 30.6	+0.6
Retrograde section jettison command	458.7	Automatic retrofire + 45.0	Automatic retrofire + 44.5	-0.5
Retrograde shape charge fire	459.1	--	--	--
Landing squib bus arm	464.3	Retrograde section jettison + 5.5	Retrograde section jettison + 5.6	+0.1

UNCLASSIFIED

UNCLASSIFIED

TABLE 5.1-XV.- SEQUENCE OF EVENTS - Continued

Events	Actual time from lift-off, sec	Planned event time, sec	Actual event time, sec	Error, sec
Horizontal mode (BEF)	464.3	Retrograde section jettison + 5.5	Retrograde section jettison + 5.6	+0.1
Reentry mode (.05G relay)	560.2	--	--	--
Indicate retroattitude off, roll command on	560.2	--	--	--
Maximum lift command	710.0	0.05g + 150	0.05g + 149.8	-0.2
Maximum lift command displayed	739.0	Maximum lift + 30.0	Maximum lift + 29.0	-1.0
PCM mode select delayed time	759.2	0.05g + 200	0.05g + 198.9	-1.1
PCM playback command	759.2	0.05g + 200	0.05g + 198.9	-1.1
Cabin air valves	843.2	21 000 ft	--	--
Pilot parachute deploy	871.8	10 600 ft	--	--
RCS A and B off	871.8	10 600 ft	--	--
Horizon sensor heater off and attitude control pulse mode	871.8	10 600 ft	--	--
Tone generator on	871.8	10 600 ft	--	--
Attitude control off	871.8	10 600 ft	--	--
Parachute deploy	871.8	10 600 ft	--	--
Horizon sensor off	871.8	10 600 ft	--	--

UNCLASSIFIED

UNCLASSIFIED

TABLE 5.1-XV.- SEQUENCE OF EVENTS - Concluded

Events	Actual time from lift-off, sec	Planned event time, sec	Actual event time, sec	Error, sec
UHF rescue beacon on	901.1	10 600 ft + 30	10 600 ft + 29.4	-0.6
Touchdown	1096.2			
Extend antenna (HF)	1488.6	10 600 ft + 600	10 600 ft + 616.7	+16.7
Parachute jettison	1488.6	10 600 ft + 600	10 600 ft + 616.7	+16.7
C-band beacon off	1488.6	10 600 ft + 600	10 600 ft + 616.7	+16.7
HF-DF key on	1509.3	Extend antenna + 20	Extend antenna + 20.7	+0.7

UNCLASSIFIED

UNCLASSIFIED

UNCLASSIFIED

5-67

TABLE 5.1-XVI.- CONDITION OF THE OAMS AT LIFT-OFF AND
EQUIPMENT SECTION SEPARATION

System component	Lift-off	Equipment Separation
"A" package squib valve	Fired and open	
"C" package squib valve	Fired and open	
Oxidizer quantity (serviced Oct. 1, 1964 and topped-off Dec. 15, 1964), lb	28.4	20.9
Fuel quantity (serviced Oct. 1, 1964 and topped-off Dec. 18, 1964), lb	20.5	15.4
Source pressure (serviced Jan. 14, 1964), psia	2490	2490
Source temperature, °F	65.5	65.5
Regulated pressure, psia	312	300
Pressurant temperature at fuel tank, °F	64.5	64.5
Pressurant temperature at oxidizer tank, °F	62	58
Fuel feed temperature, °F	65	65
Oxidizer feed temperature, °F	65	65
TCA 9 injector temperature, °F	61	103

UNCLASSIFIED

TABLE 5.1-XVII.- RCS CONDITION AT LIFT-OFF AND TOUCHDOWN

	Lift-off	Touchdown
A ring - unactivated, no pressure downstream of the A package		
B ring - completely activated		
Source pressure, A ring, psia	3080	2130
Source pressure, B ring, psia	3080	2490
Regulated pressure, A ring, psia	15	314
Regulated pressure, B ring, psia	316	312
Oxidizer feed temperature, A ring, °F .	71	75
Oxidizer feed temperature, B ring, °F .	76	78
Source temperature, A ring, °F	77	70
Source temperature, B ring, °F	73	72
TCA 8 injector head temperature, °F . . .	72	325
TCA 7 nozzle temperature, °F	72	360
TCA 2 fuel temperature, °F	67	90
TCA 2 oxidizer temperature, °F	68	83
TCA 5 fuel temperature, °F	60	95
TCA 5 oxidizer temperature, °F	64	95
TCA 6 fuel temperature, °F	71	95
TCA 6 oxidizer temperature, °F	67	90
TCA 8 fuel temperature, °F	73	95
TCA 8 oxidizer temperature, °F	75	95

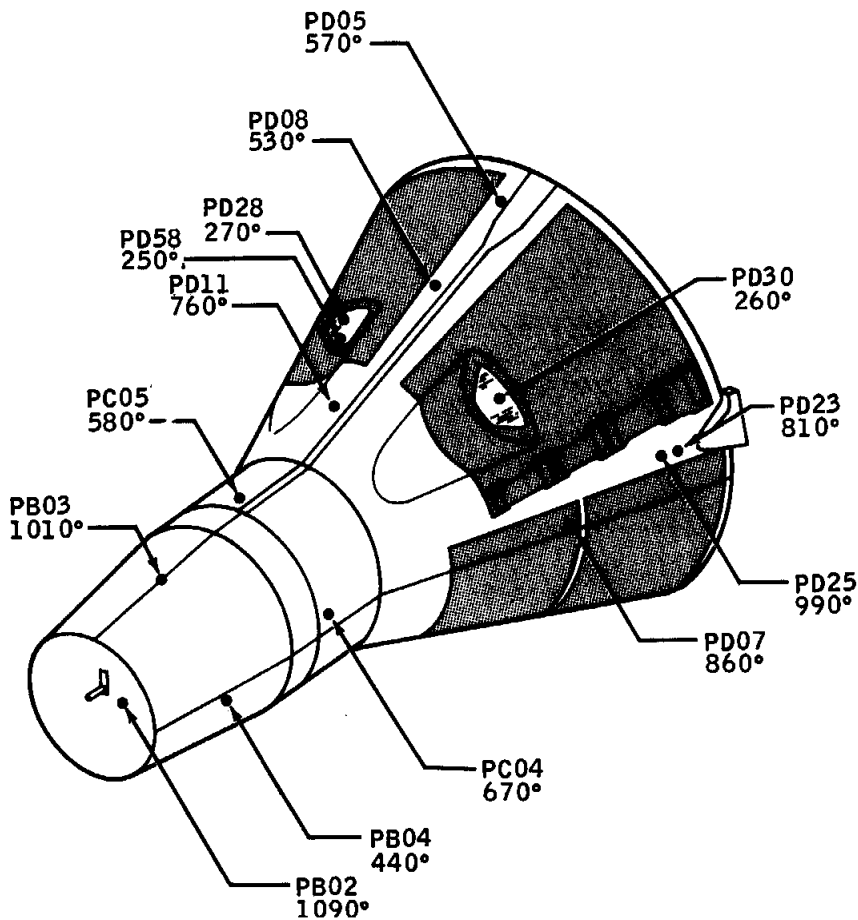
UNCLASSIFIED

TABLE 5.1-XVIII.- BURN TIME FOR ROCKET MOTORS

Rocket number	Time from lift off, (sec)	Web burn time, (sec)	Total burn time, (sec)	Time interval, (sec)
1	414.25	5.34	> 5.41	
3	419.72	> 5.20	> 5.20	5.47
2	424.92	5.32	5.50	5.20
4	430.72	5.37	5.55	5.80

CONFIDENTIAL

CONFIDENTIAL



Access doors

(a) Leeward side

Parameter	Z station	Skin thickness in.	Maximum temperature	
			Measured, °F	Predicted, °F
PB02	234.0	.016	1090	(a)
PB03	217.0	.090	1010	1186
PB04	217.0	.160	440	683
PC04	189.0	.140	670	946
PC05	189.0	.090	580	802
PD05	112.8	.016	570	1190
PD07	135.9	.016	860	1274
PD08	133.4	.016	530	820
PD11	163.8	.016	760	1130
PD23	113.4	.016	810	(a)
PD25	116.4	.016	990	(a)
PD28	137.5	-	270	441
PD30	137.5	-	260	441
PD58	141.0	-	250	441

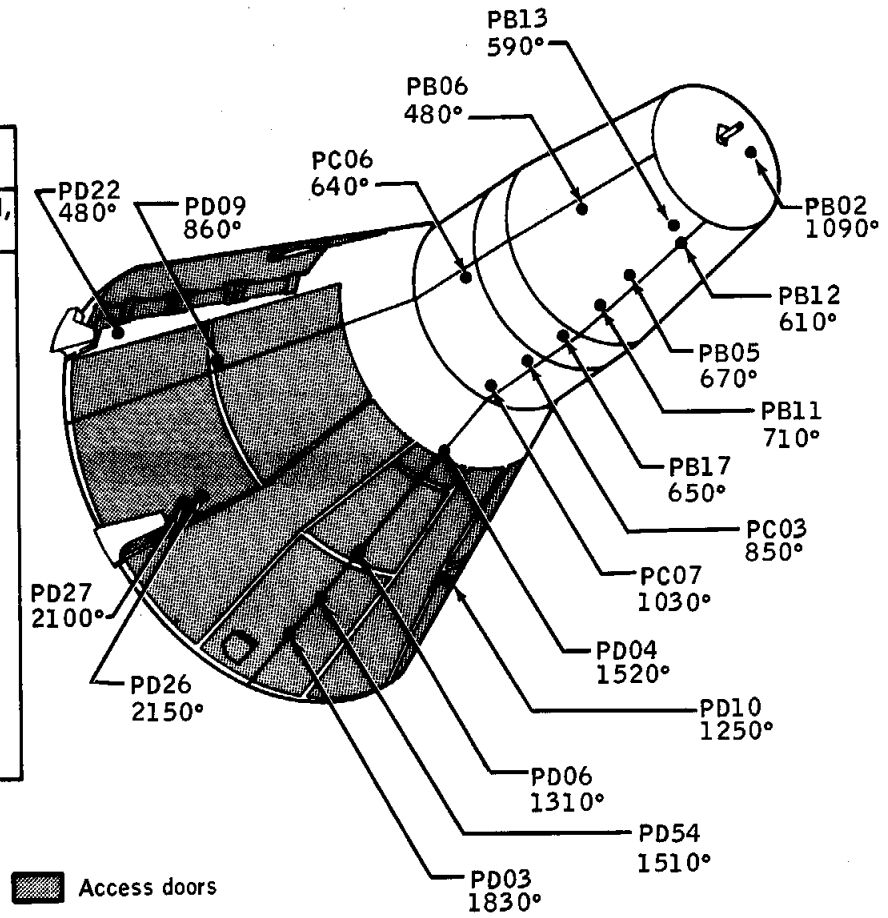
(a) No prediction

Figure 5.1-1. - Distribution of peak measured reentry temperatures

CONFIDENTIAL

Parameter	Z station	Skin thickness in.	Maximum temperature	
			Measured, °F	Predicted, °F
PB05	217.0	.20	670	1124
PB06	217.0	.16	480	683
PB11	209.0	.20	710	1190
PB12	227.0	.20	610	1171
PB13	230.0	.20	590	1104
PB17	199.0	.28	650	1251
PC03	189.0	.28	850	1318
PC06	189.0	.19	640	802
PC07	179.0	.28	1030	1109
PD03	116.0	.016	1830	1760
PD04	163.4	.016	1520	1606
PD06	131.0	.016	1310	1728
PD09	135.9	.016	860	1274
PD10	130.7	.016	1250	1589
PD22	113.4	.016	480	(a)
PD26	123.4	.016	2150	(a)
PD27	120.0	.016	2100	(a)
PD54	123.4	.016	1510	1742

(a) No prediction



(b) Windward side

Figure 5.1-1. - Concluded

CONFIDENTIAL

UNCLASSIFIED

UNCLASSIFIED

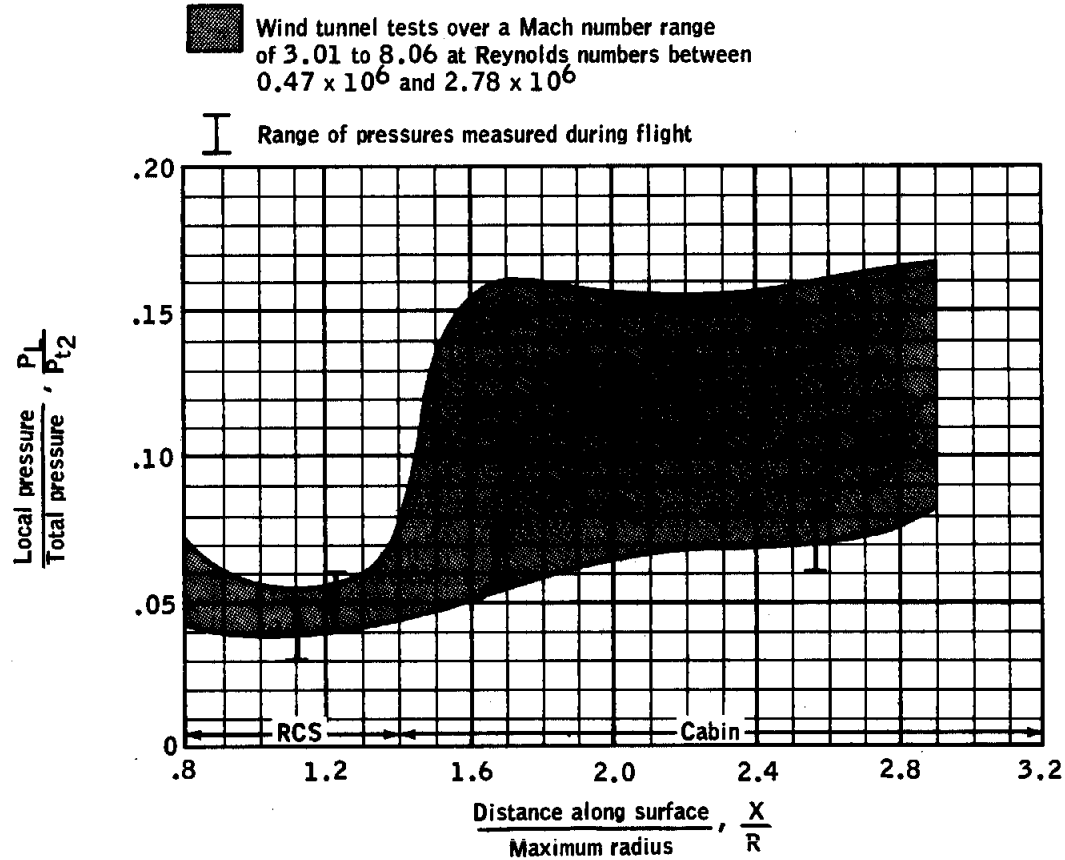
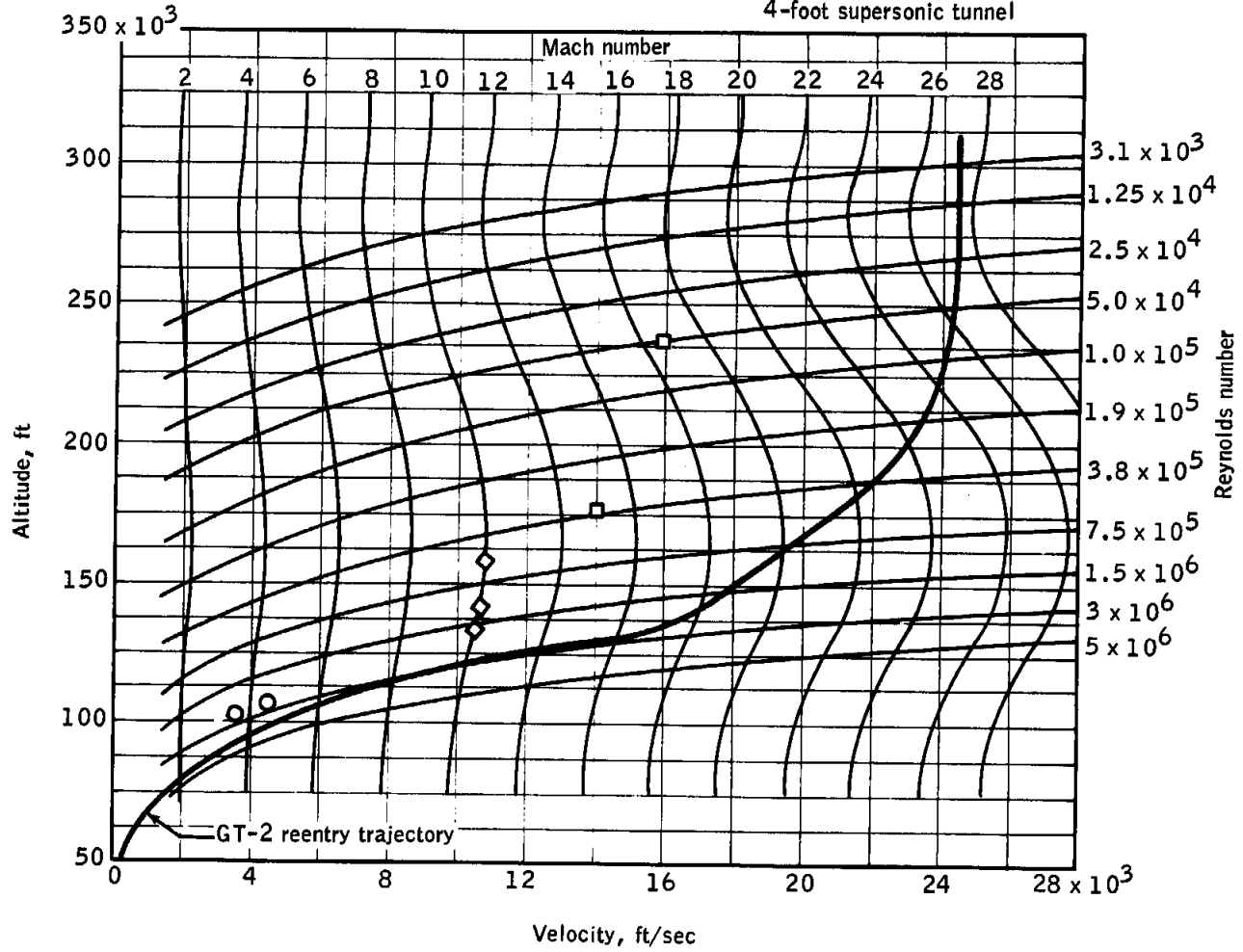


Figure 5.1-2. - Comparison of pressure distributions during the launch phase as obtained during flight and in wind tunnel tests

- LRC, variable density wind tunnel
- ◇ AEDC, wind tunnel "C"
- Cornell Aeronautical Laboratory, 4-foot supersonic tunnel

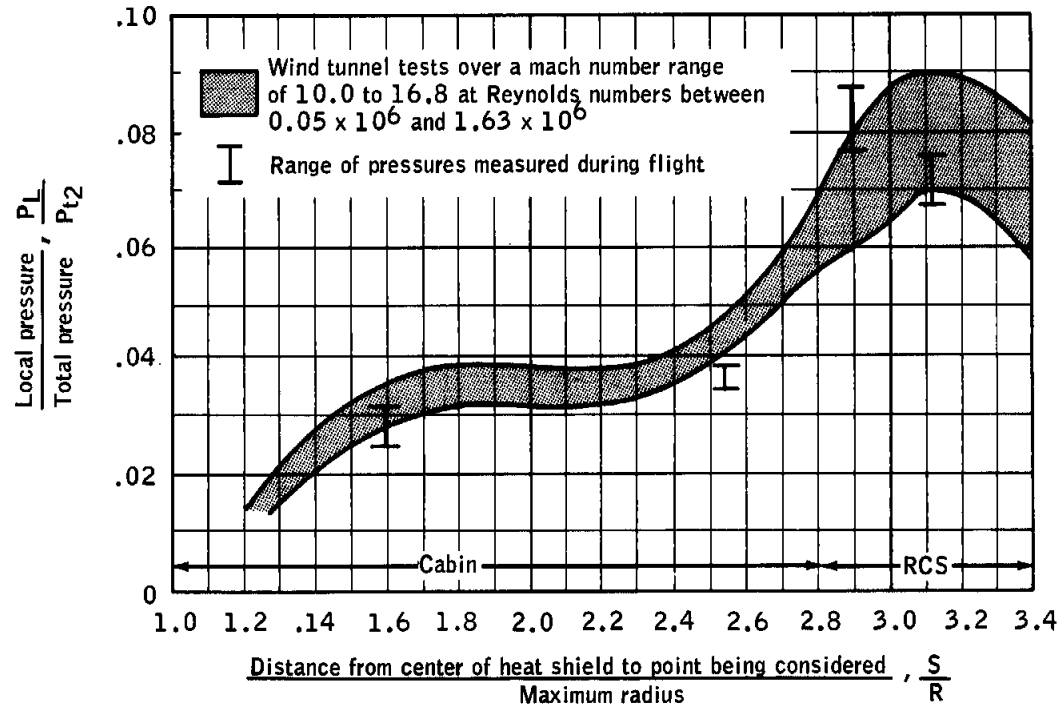
UNCLASSIFIED



UNCLASSIFIED

Figure 5.1-3. - Aerodynamic environment

UNCLASSIFIED



(a) Windward side

Figure 5.1-4. - Comparison of pressure distributions during the reentry phase as obtained during flight and in wind tunnel tests

UNCLASSIFIED

UNCLASSIFIED

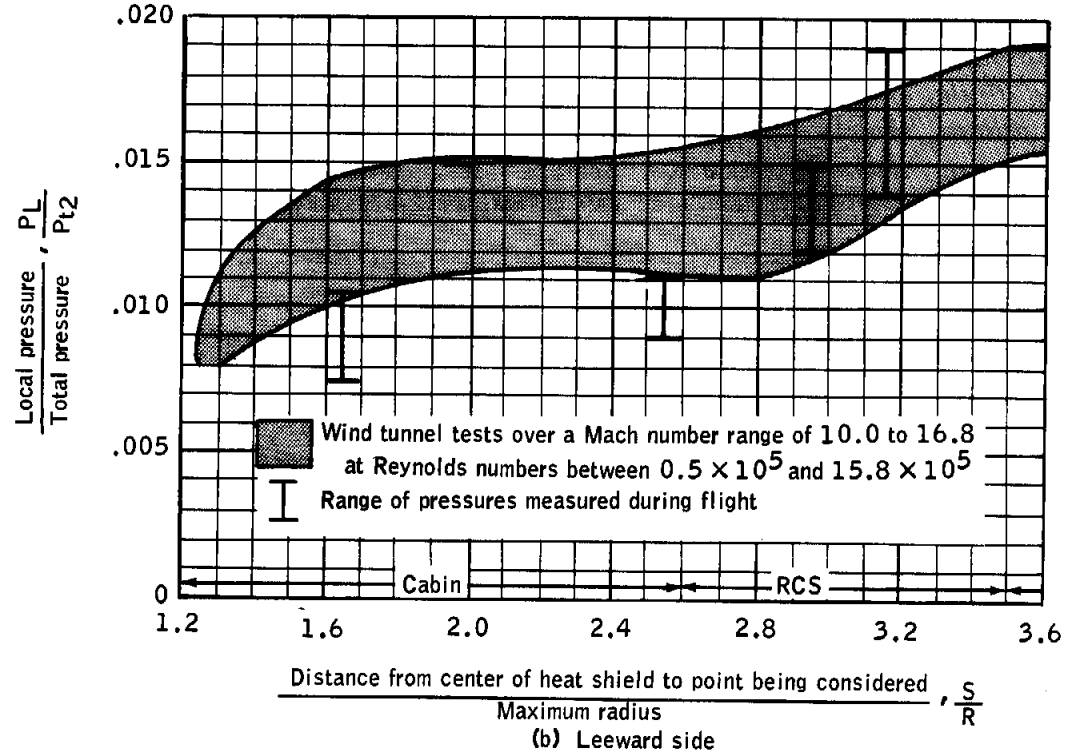
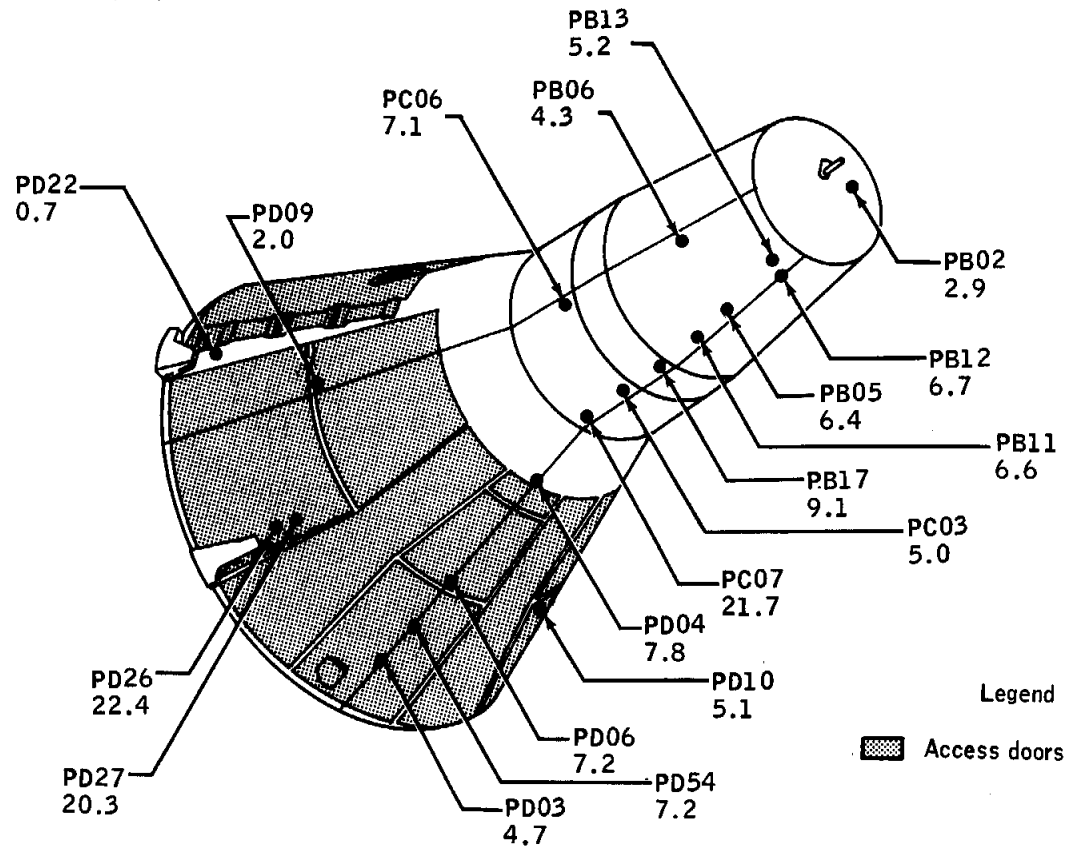


Figure 5.1-4. - Concluded

UNCLASSIFIED

Note: Number under sensor
callout indicates Btu/ft²/sec



(a) Windward side

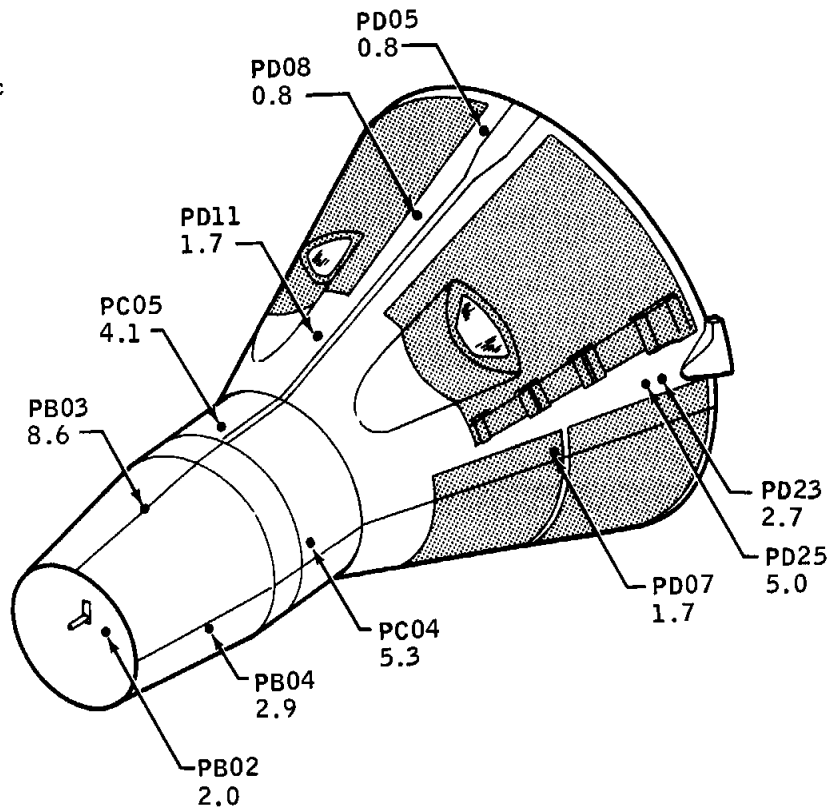
Figure 5.1-5. - Distribution of peak heating rates

UNCLASSIFIED

UNCLASSIFIED

NASA-S-65-1703

Note: Number under sensor
callout indicates Btu/ft²/sec



Legend

 Access doors

(b) Leeward side

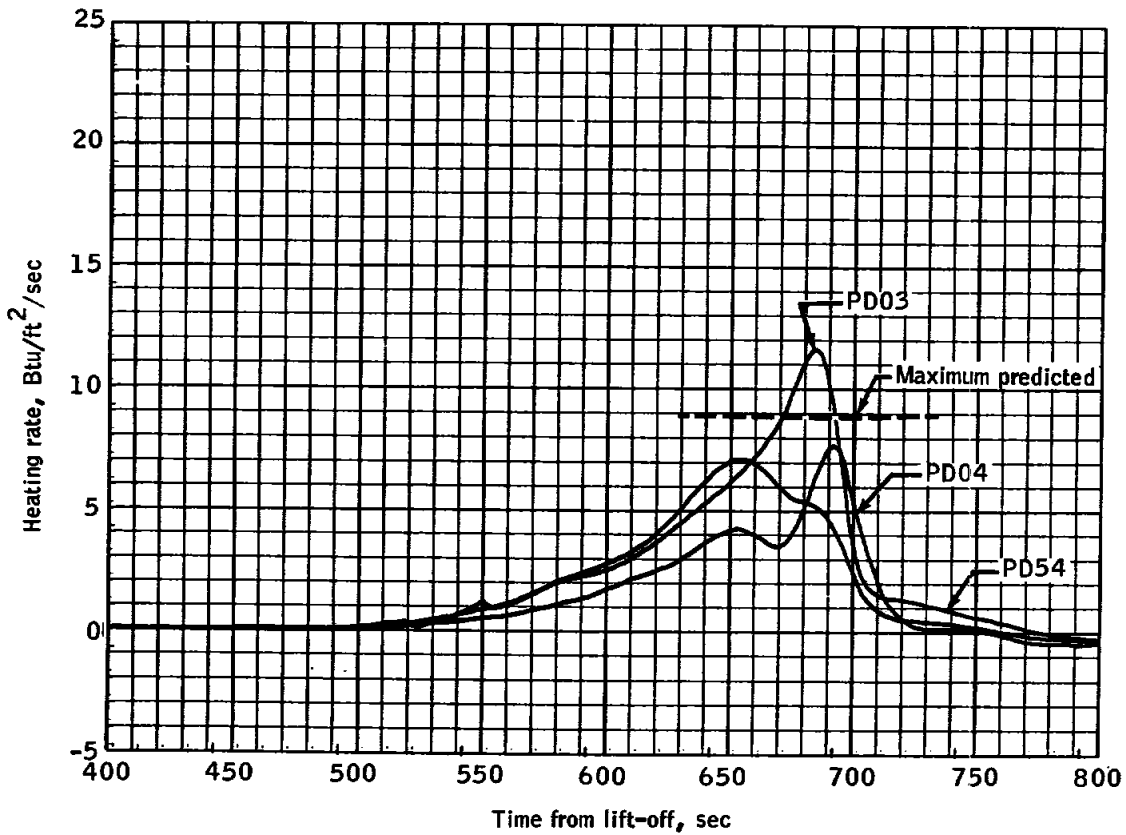
Figure 5.1-5. - Concluded

UNCLASSIFIED

UNCLASSIFIED

~~CONFIDENTIAL~~

NASA-S-65-1946

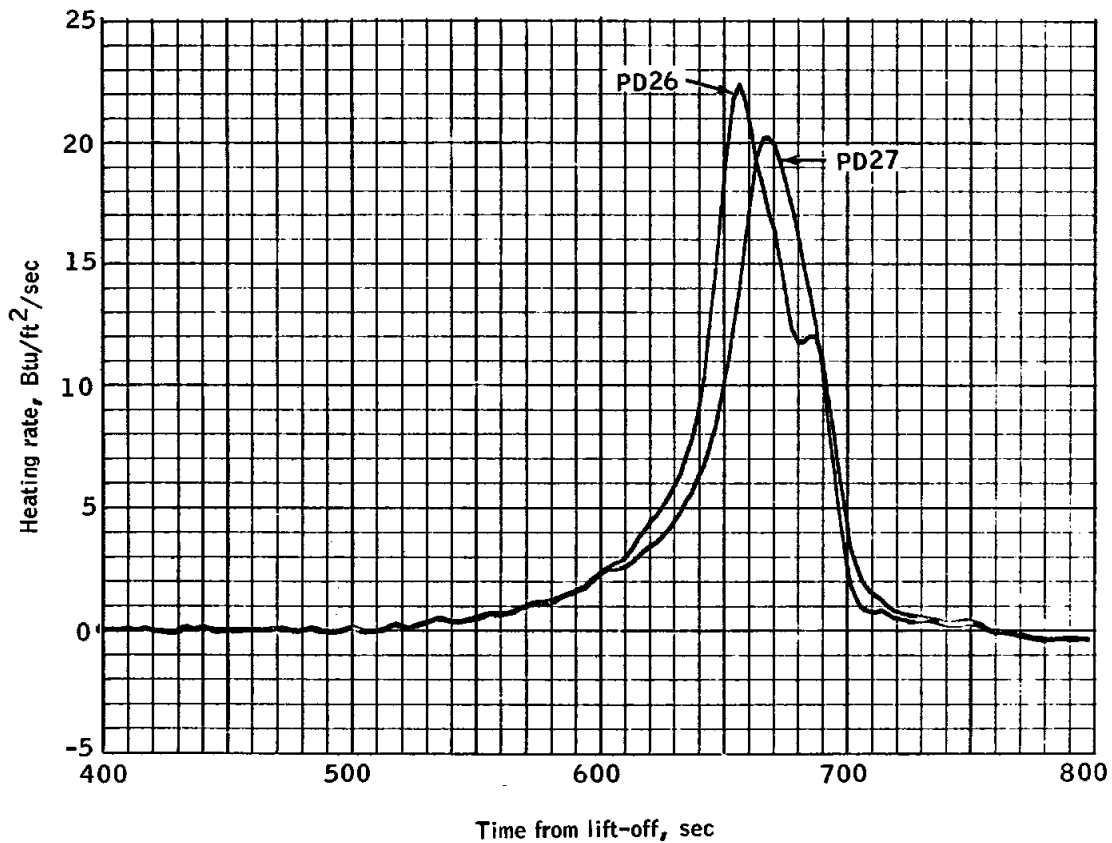


(a) Windward side of cabin

Figure 5.1-6. - Typical heating rates

~~CONFIDENTIAL~~

NASA-S-65-1945

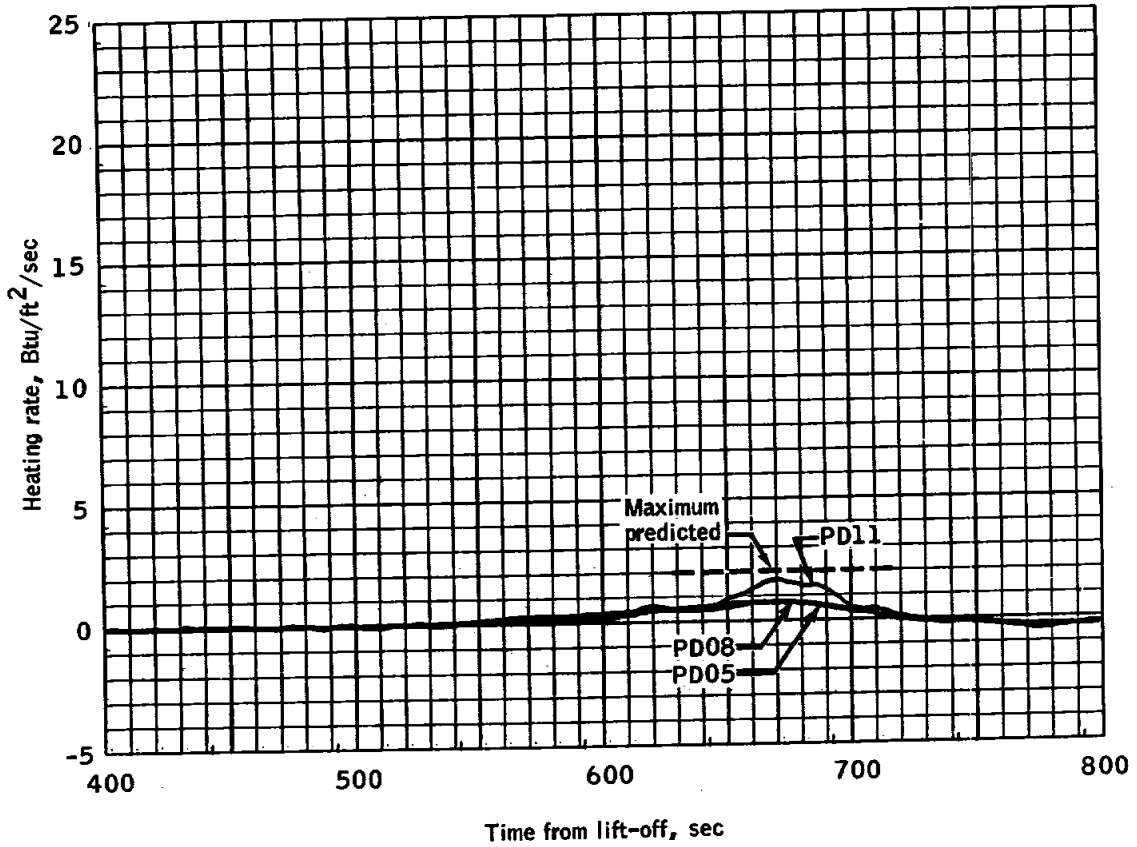


(b) Localized heating in wake of windward adapter interconnect fairing

Figure 5.1-6. - Continued

~~CONFIDENTIAL~~

NASA-S-65-1947

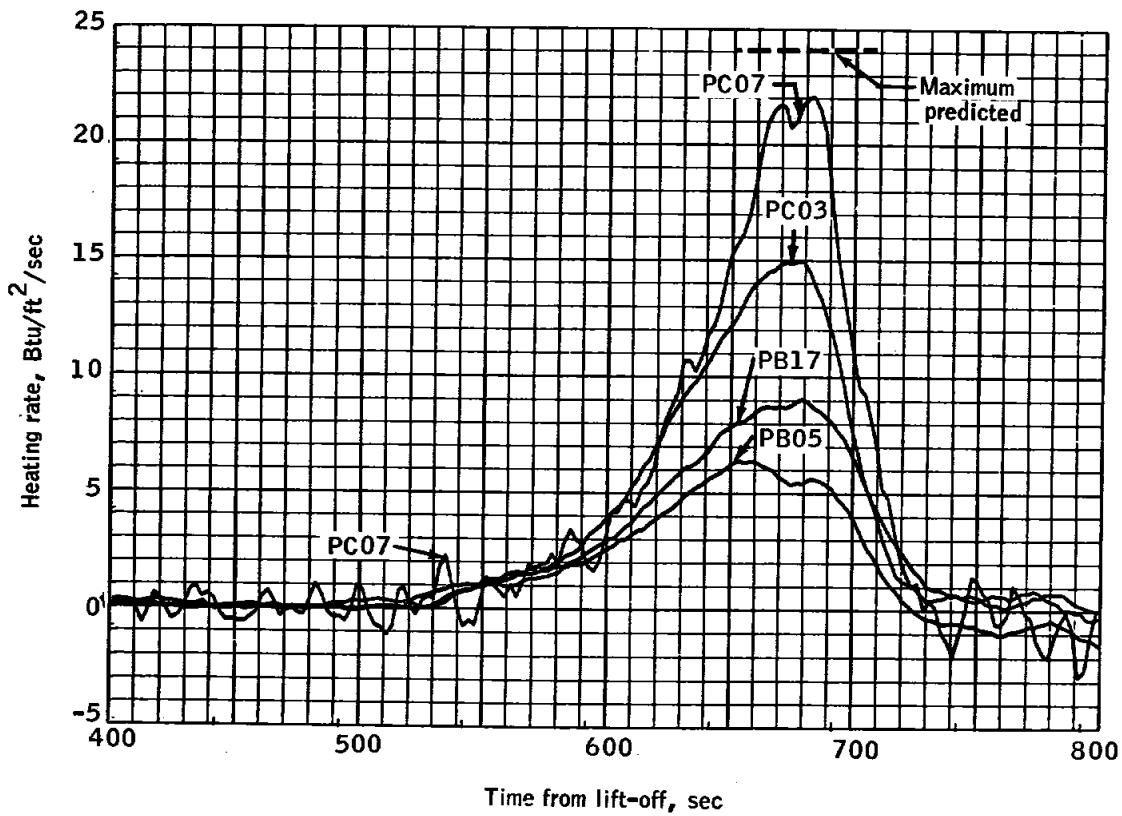


(c) Leeward side of cabin

Figure 5.1-6.- Concluded

~~CONFIDENTIAL~~

NASA-S-65-1948

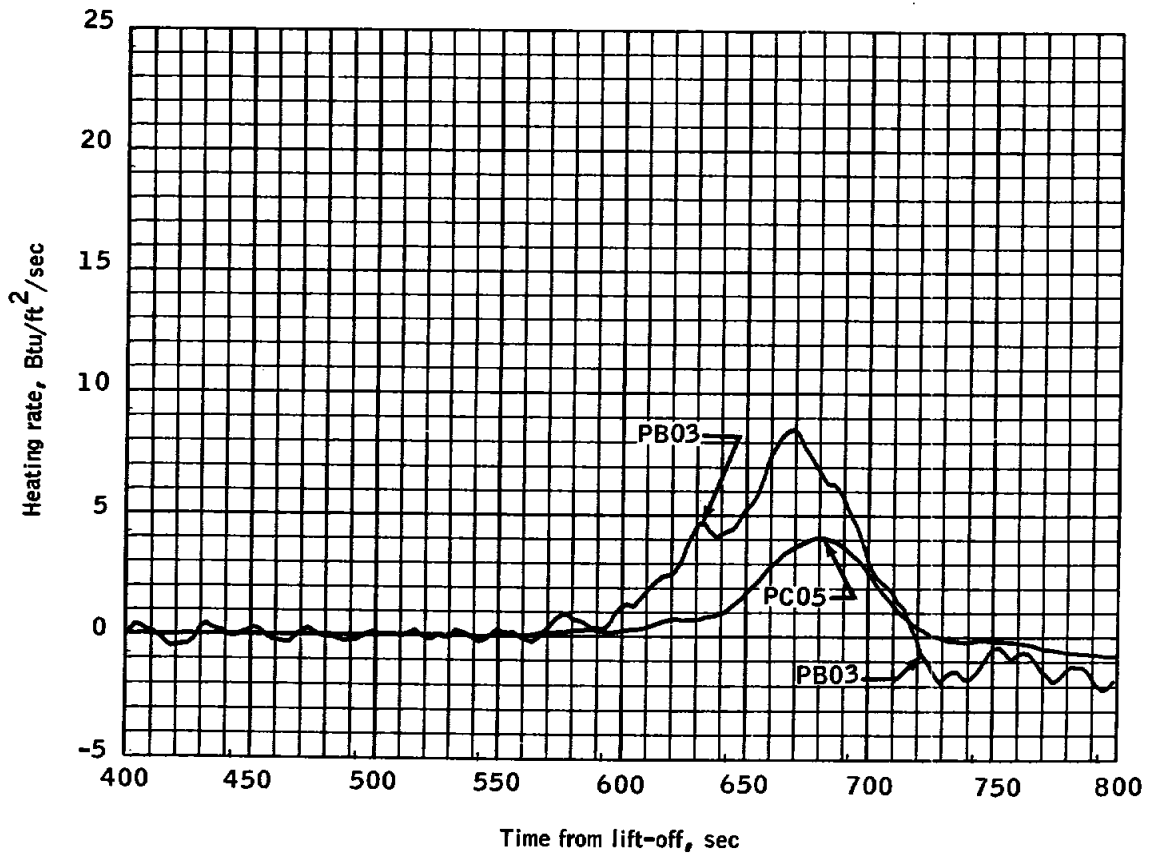


(a) Windward side, RCS, and R and R section

Figure 5.1-7. - Typical heating rates

~~CONFIDENTIAL~~

NASA-S-65-1944



(b) Leeward side, RCS, and R and R section

Figure 5.1-7. - Concluded

~~CONFIDENTIAL~~

NASA-S-65-1610

Parameter	X Distance, in.	Ablative material thickness in.	Maximum temperature	
			Measured, °F	Predicted, °F
PE01	.060	.573	205	375 to 425
PE03	.057	.570	255	347 to 397
PE06	.050	.538	260	364 to 420
PE07	.048	.597	235	336 to 385
PE11	.047	.462	225	380 to 448
PE12	.071	.613	185	344 to 393
PE14	.025	.512	255	371 to 433
PE15	.066	.563	255	368 to 423
PE16	.057	.549	240	375 to 432
PE13	-.210	.573	205	610 to 800
PE17	-.093	.455	325	536 to 700
PE18	-.140	.573	235	524 to 653
PE19	.740	.573	110	246 to 296
PE20	.737	.463	160	263 to 310

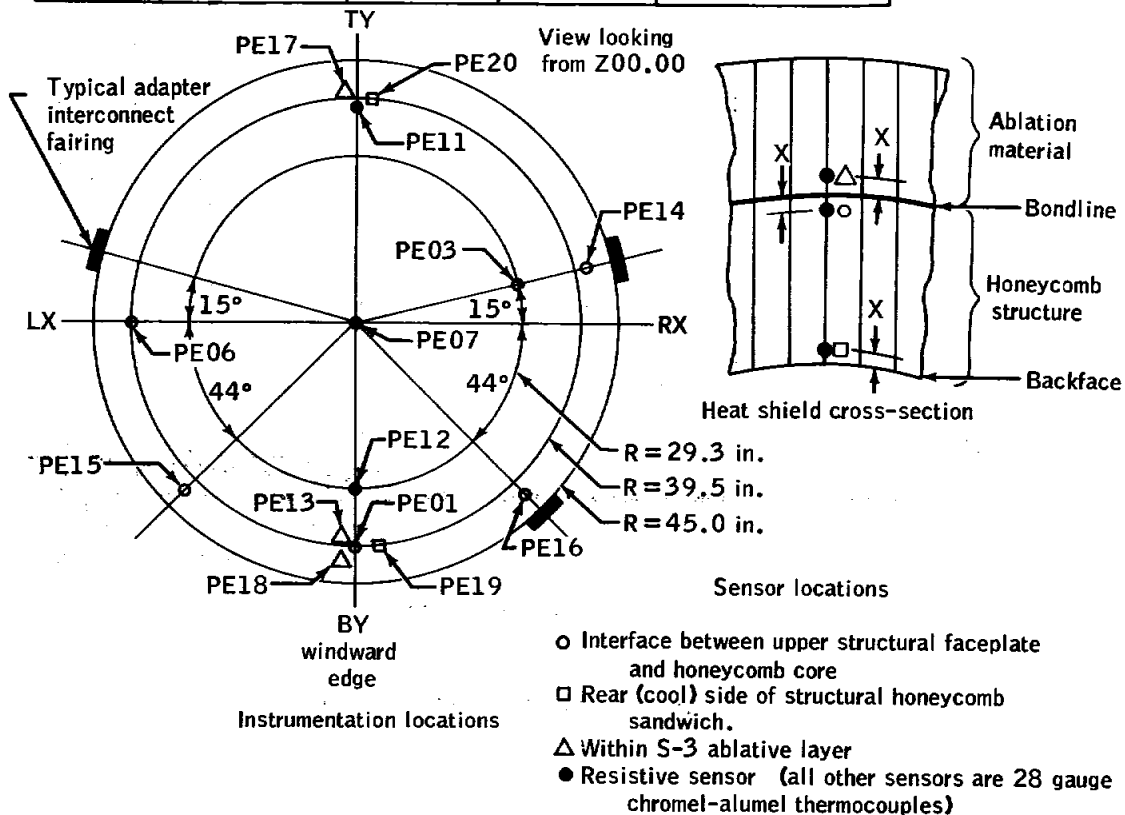


Figure 5.1-8. - Heat shield instrumentation

~~CONFIDENTIAL~~

NASA-S-65-1942

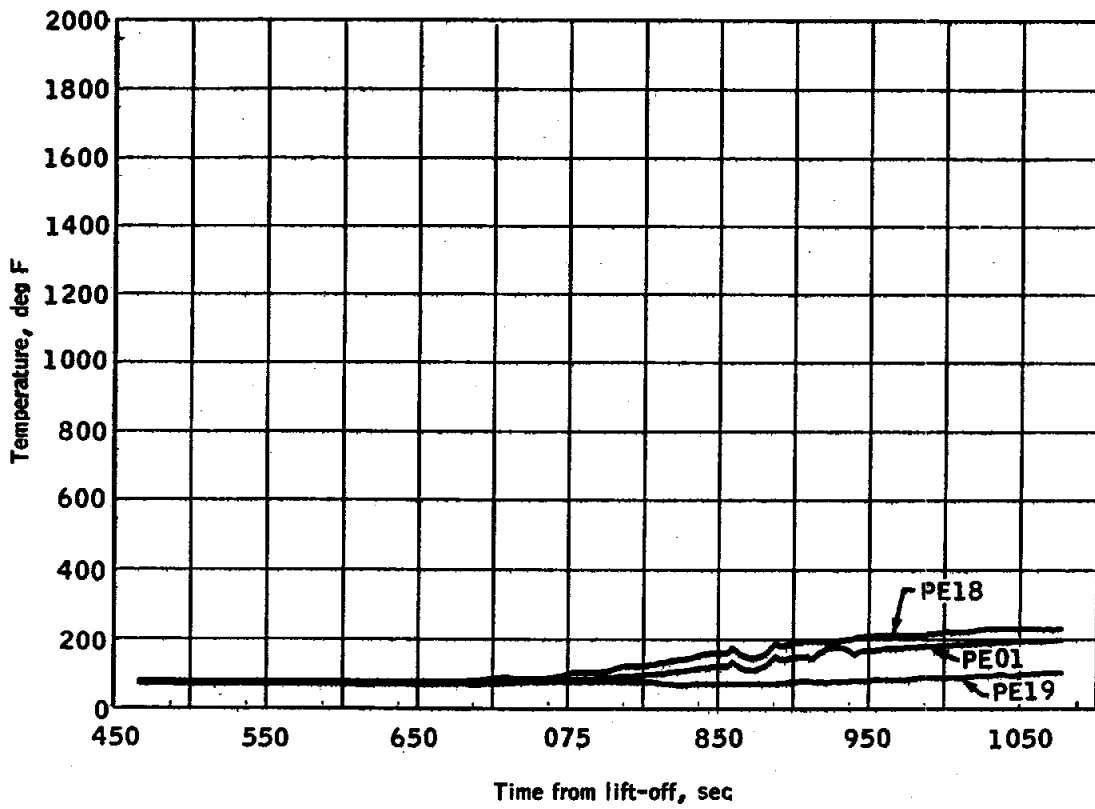


Figure 5.1-9.- Heat shield temperature distribution during reentry

~~CONFIDENTIAL~~

~~UNCLASSIFIED~~

5-85

NASA-S-65-1706

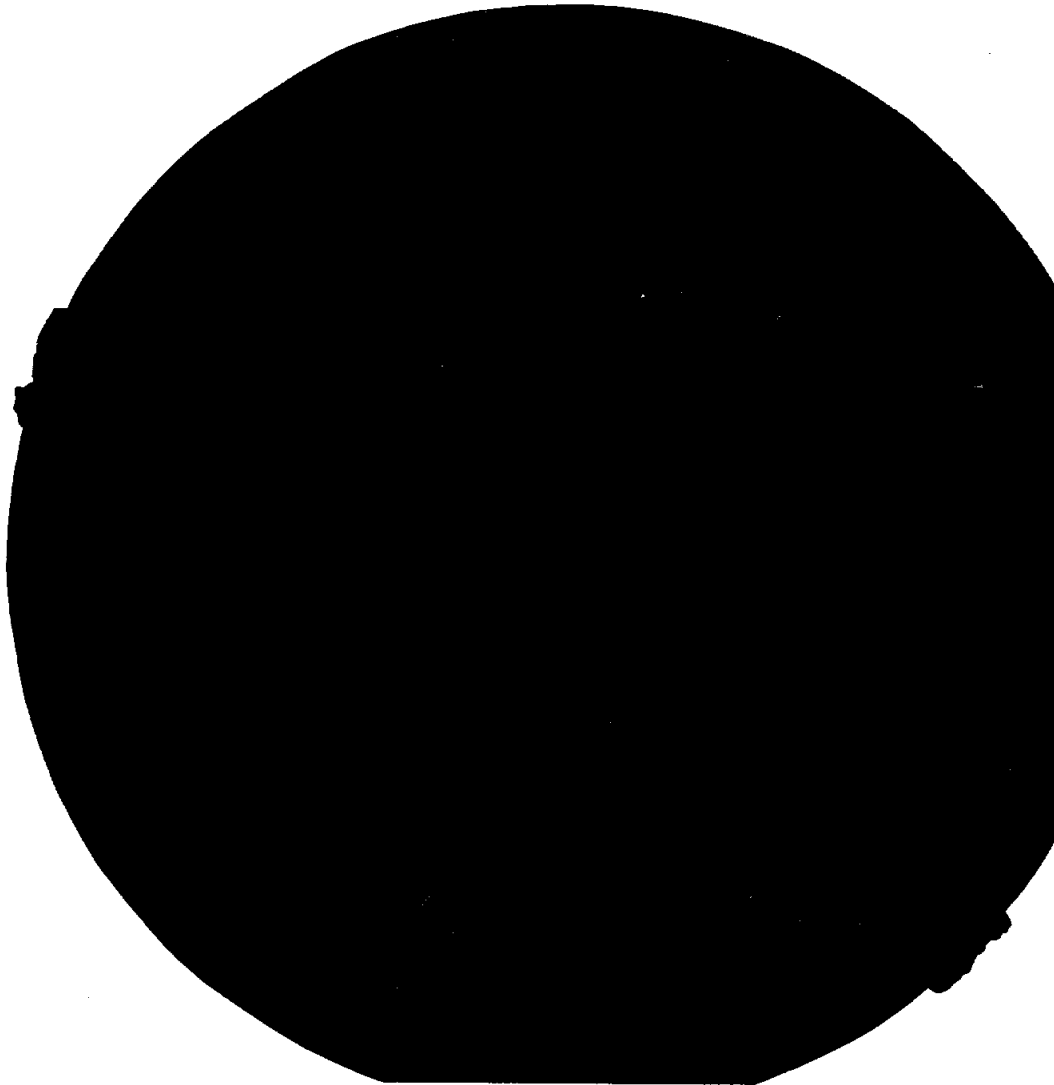


Figure 5.1-10. - Heat shield after reentry

~~UNCLASSIFIED~~

NASA-S-65-1938

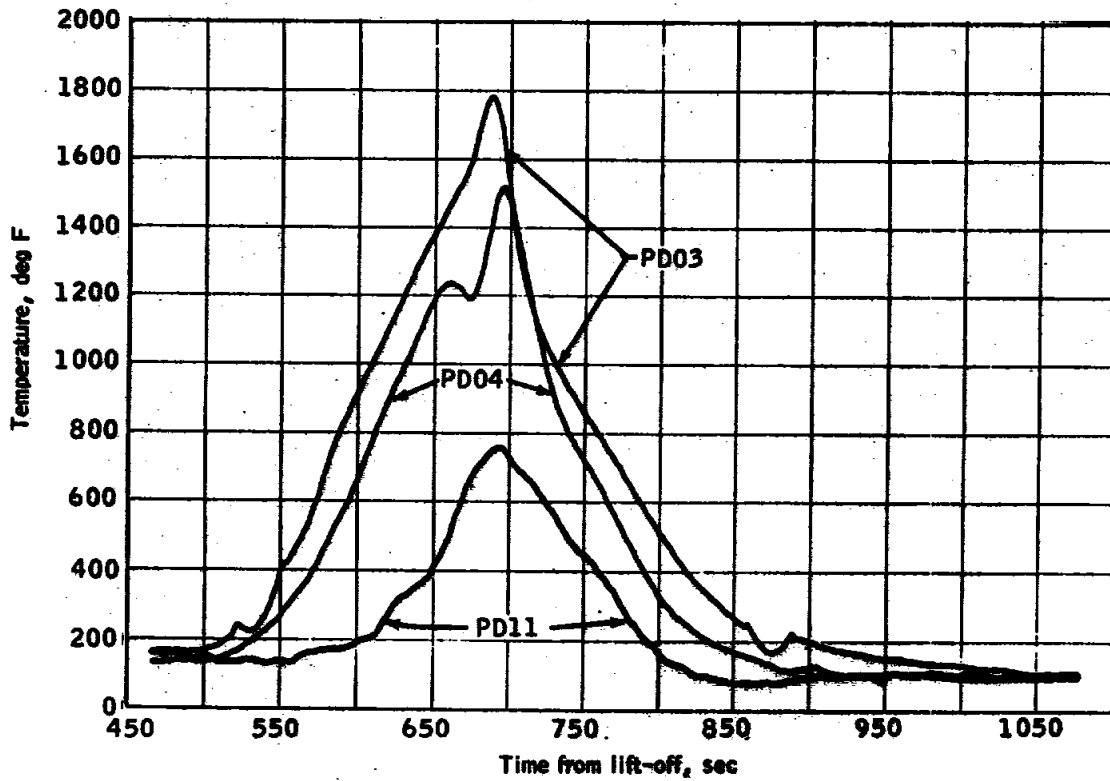


Figure 5.1-11. - Cabin section outer skin temperatures during reentry

NASA-S-65-1705

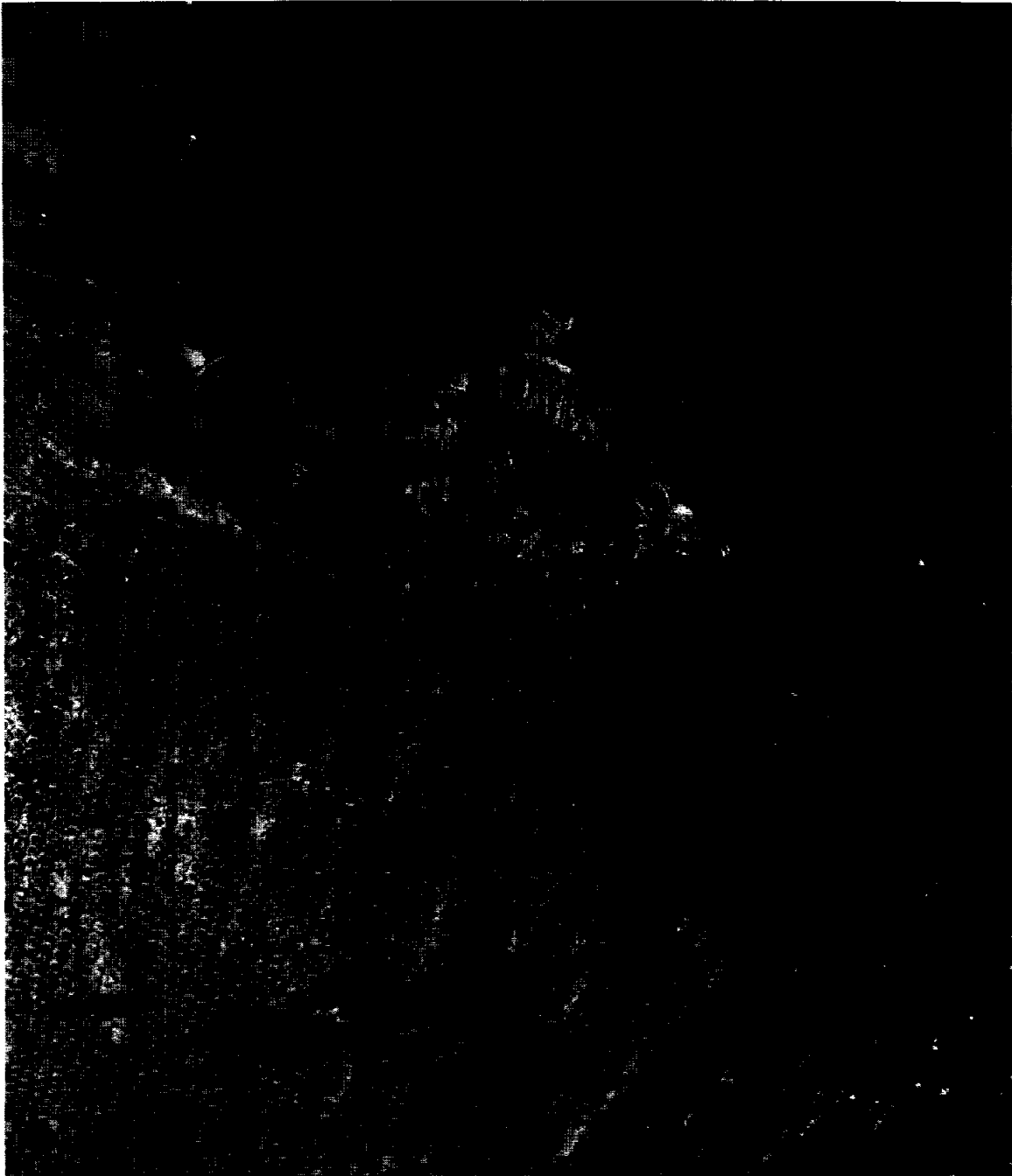


Figure 5.1-12. - Most windward adapter interconnect fairing

~~CONFIDENTIAL~~

NASA-S-65-1940

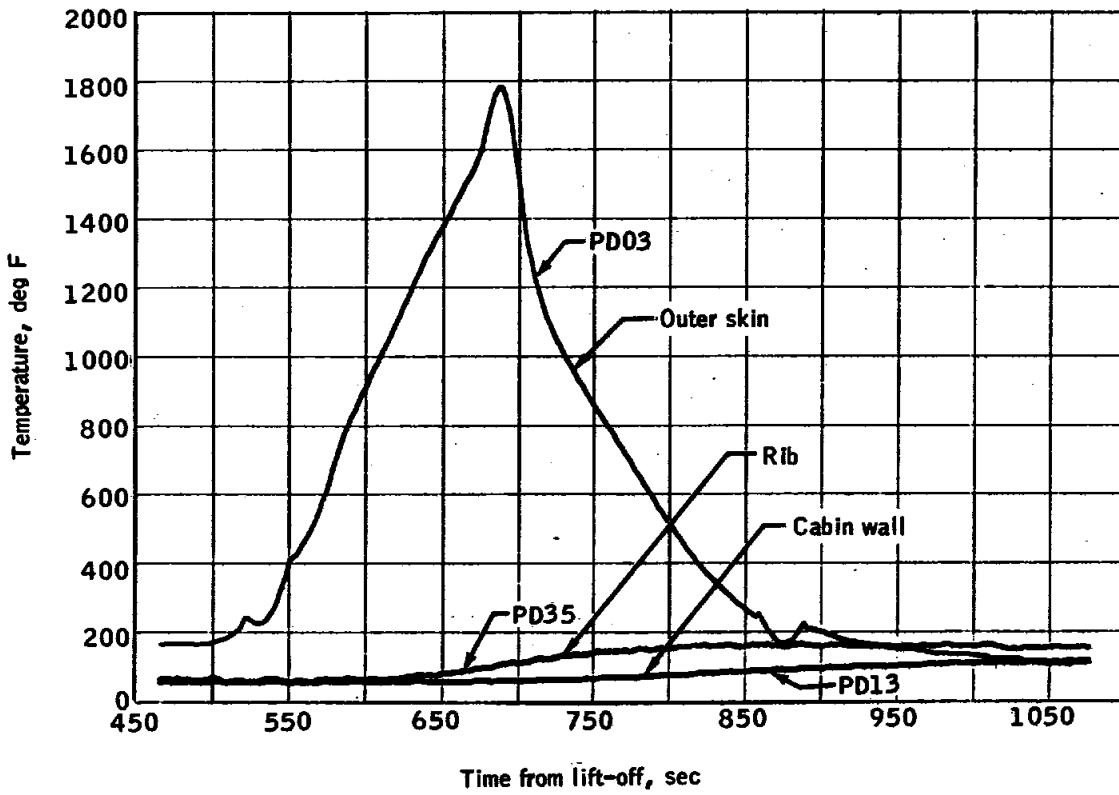


Figure 5.1-13 - Cabin section temperature distribution through the ECS door

~~CONFIDENTIAL~~

NASA-S-65-1704

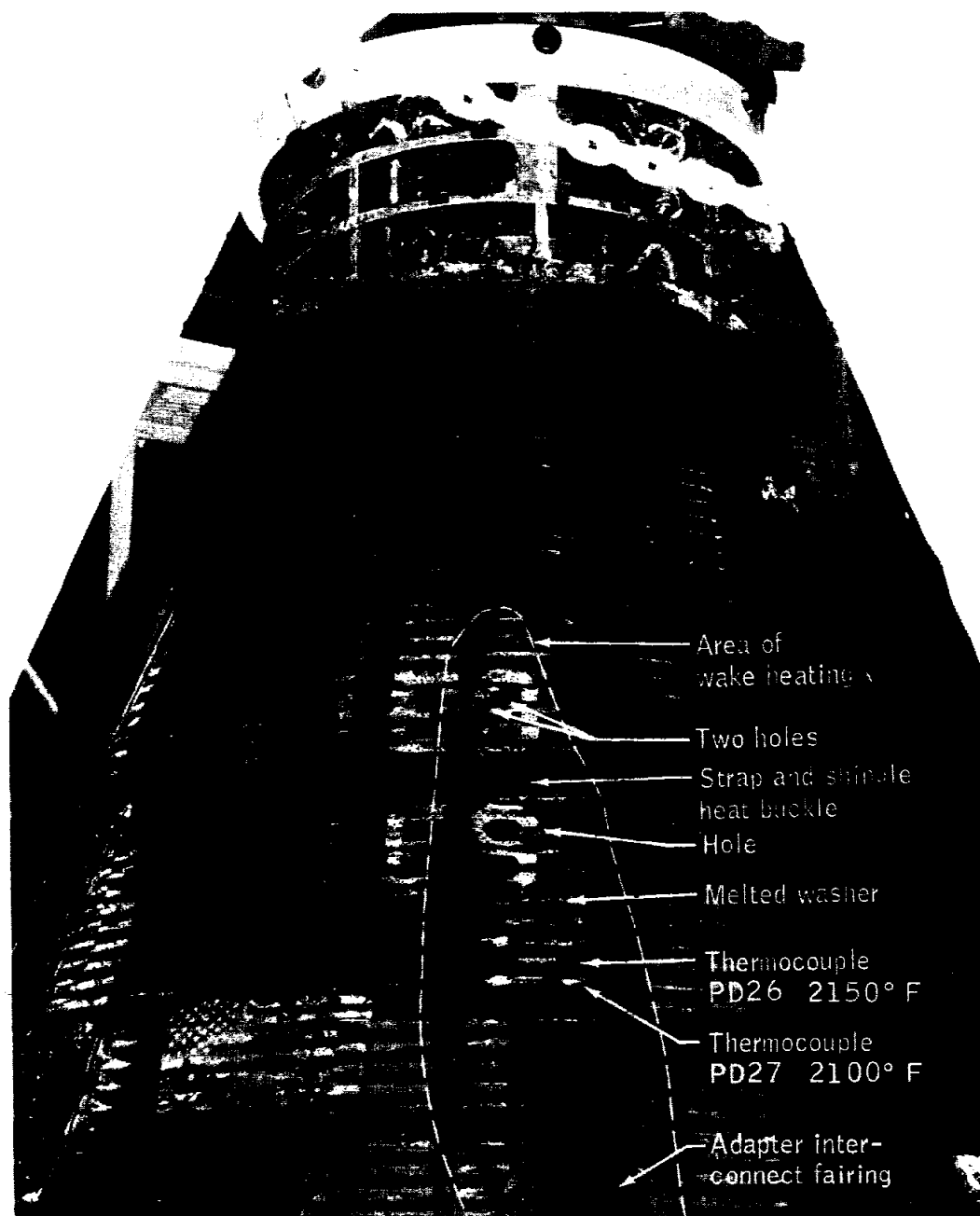


Figure 5.1-14. - Region of damage in wake of most windward interconnect fairing

NASA-S-65-1596



Figure 5.1-15. - Damage in wake of most windward adapter interconnect fairing

~~CONFIDENTIAL~~

NASA-S-65-1941

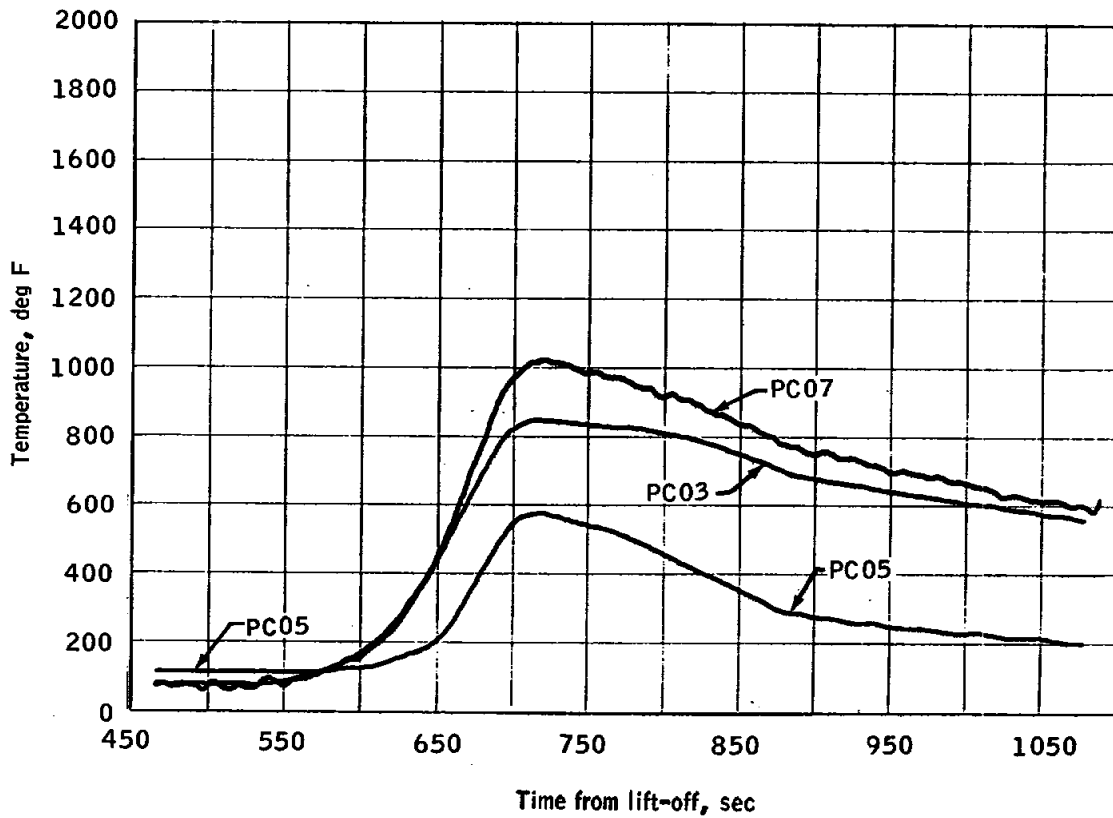


Figure 5.1-16. - RCS section outer skin temperatures during reentry

~~CONFIDENTIAL~~

~~CONFIDENTIAL~~

NASA-S-65-1943

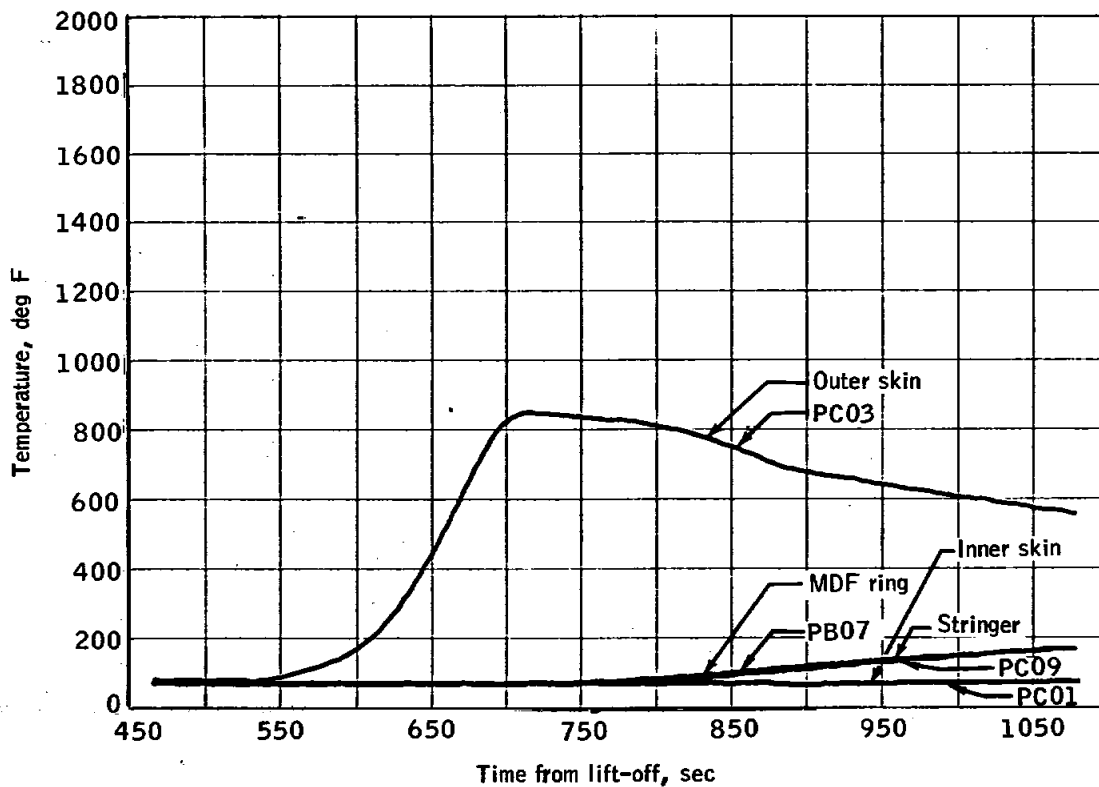


Figure 5.1-17. - RCS section structural temperature distribution during reentry

~~CONFIDENTIAL~~

~~CONFIDENTIAL~~

NASA-S-65-1939

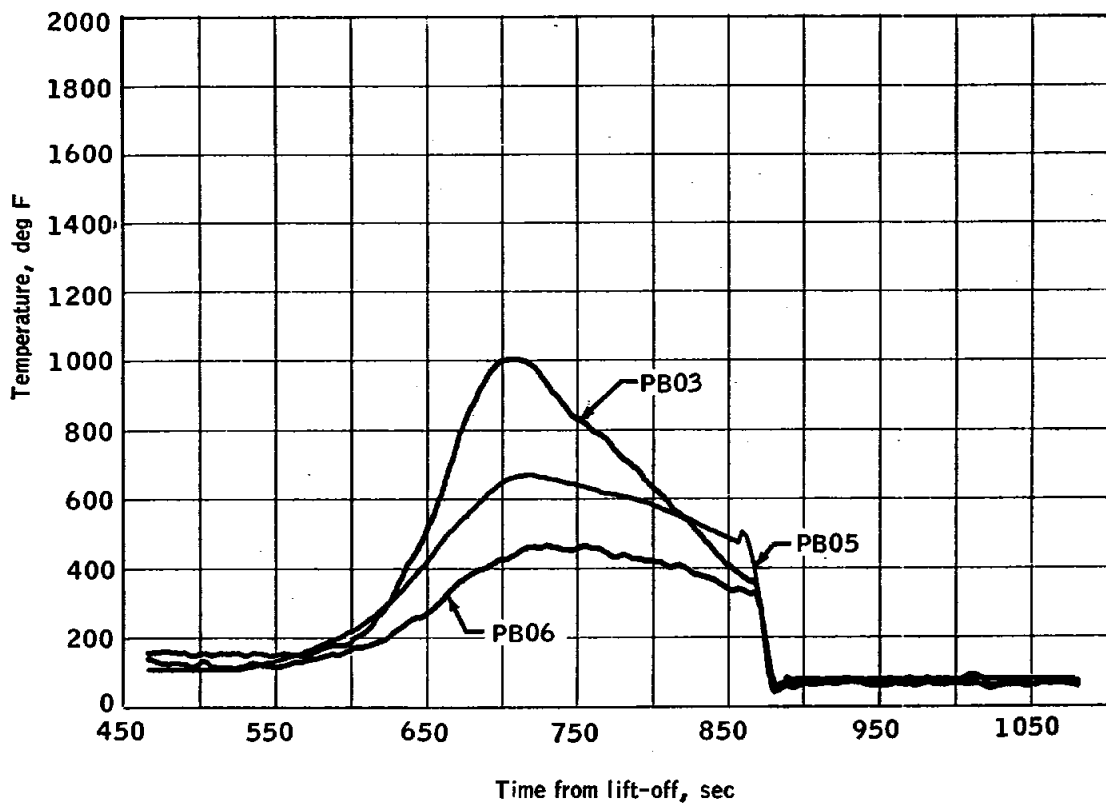


Figure 5.1-18. - R and R section outer skin temperatures during reentry

~~CONFIDENTIAL~~

UNCLASSIFIED

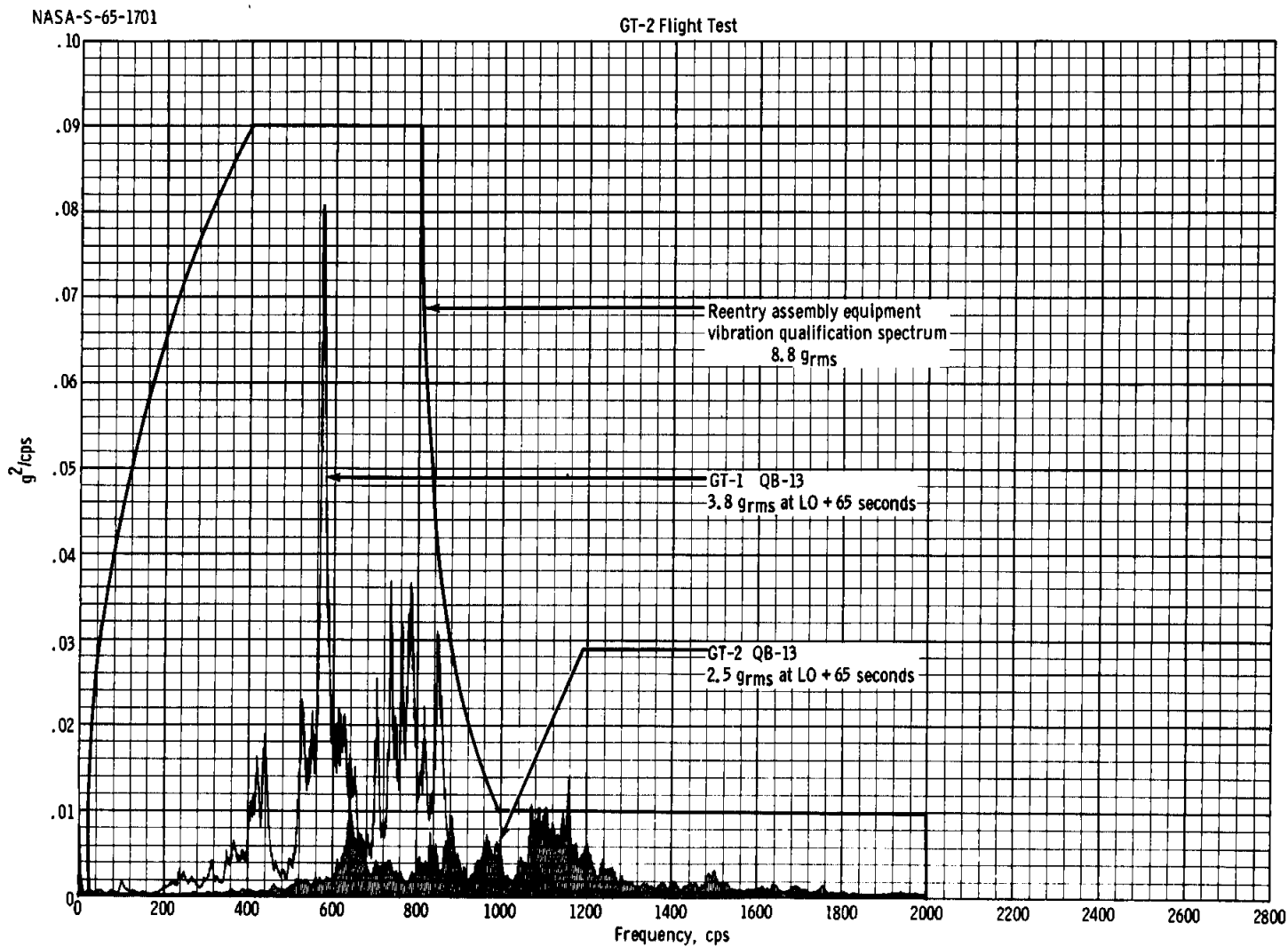


Figure 5.1-19. - Comparison of flight data with equipment vibration qualification spectrum

UNCLASSIFIED

NASA-S-65-1609

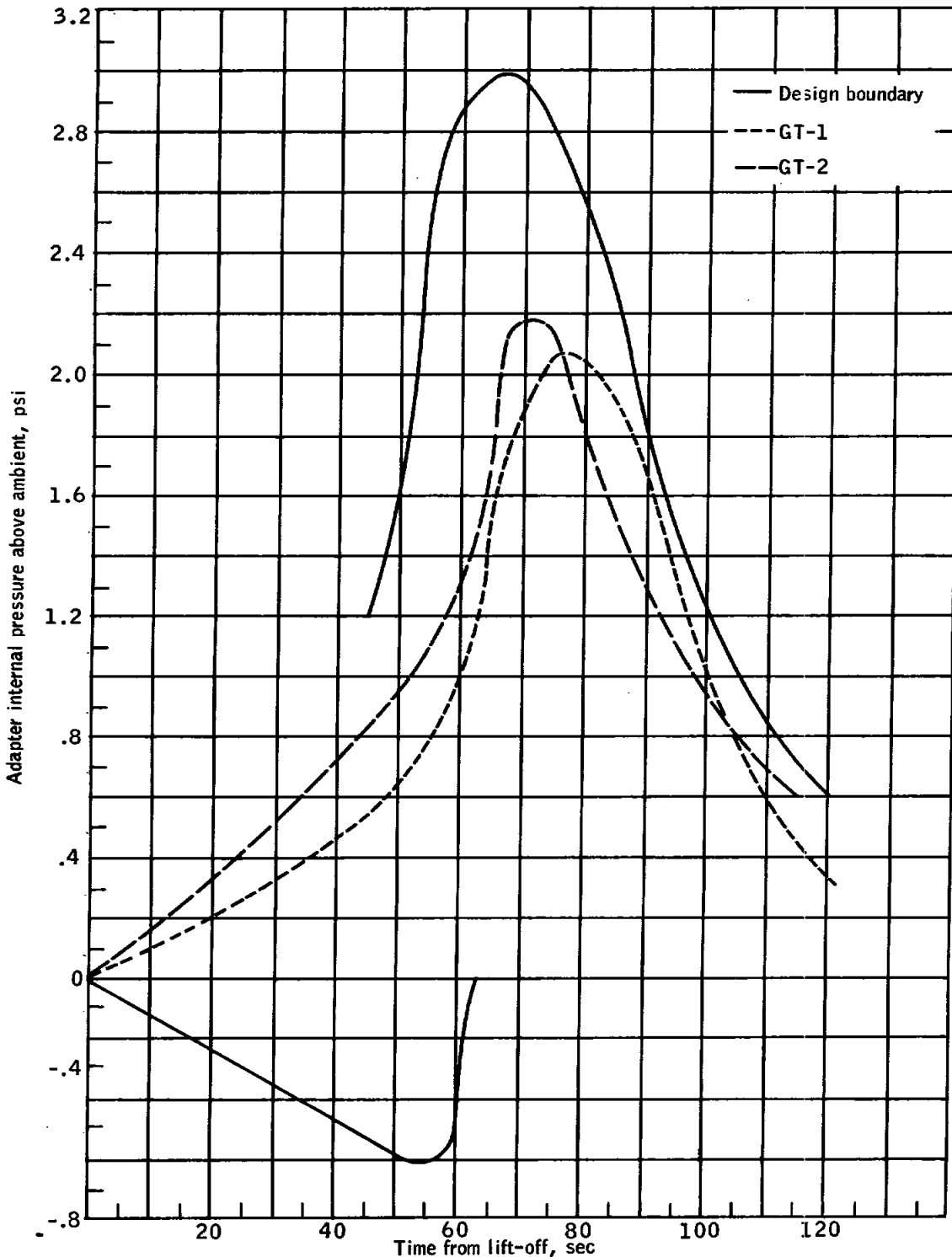
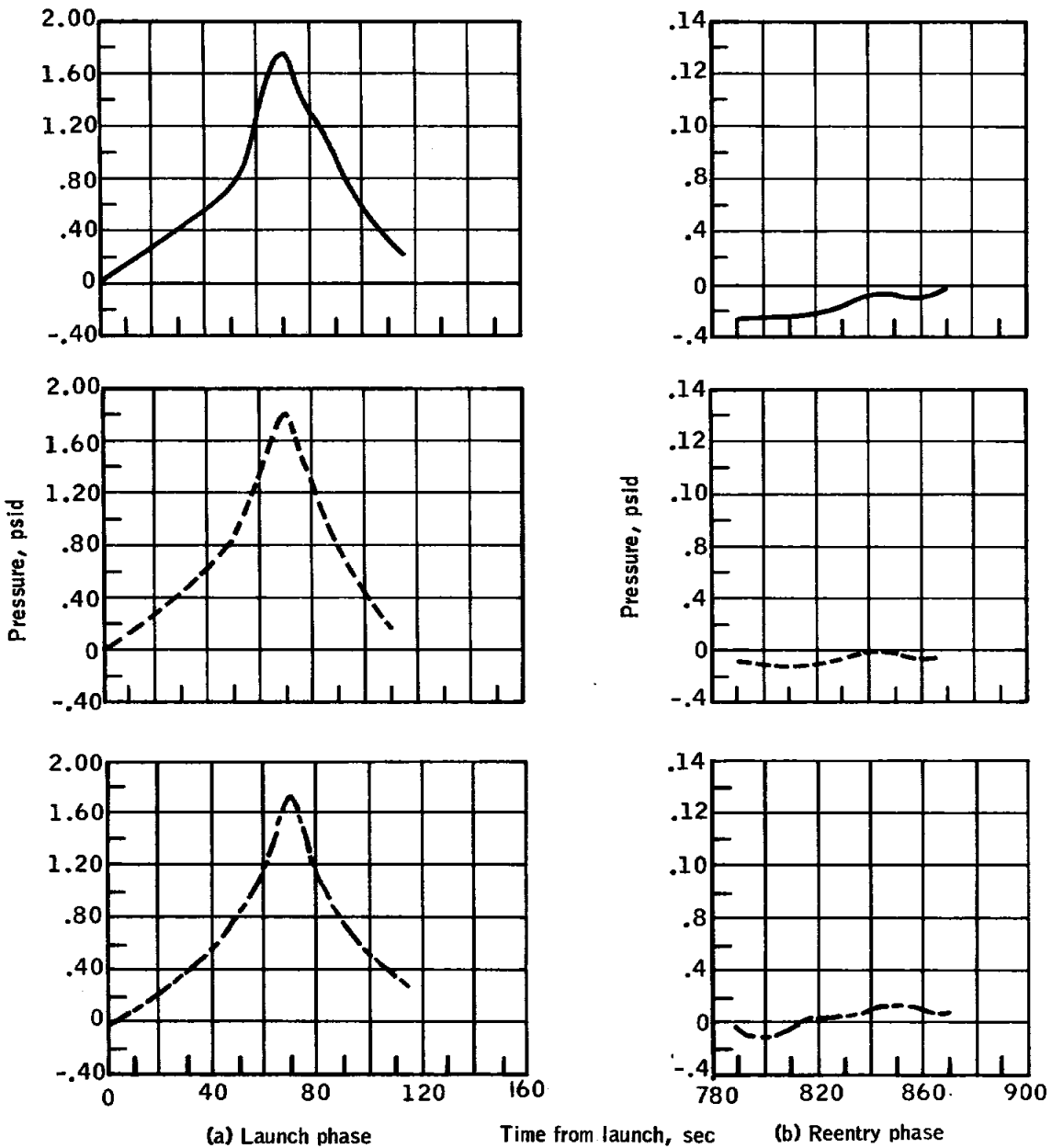


Figure 5.1-20. - Adapter internal pressure

NASA-S-65-1607



Legend:
 ——— QB04, right-hand equipment bay
 - - - - QB10, left-hand equipment bay
 - · - · QB09, landing gear well

Figure 5.1-21. - Reentry assembly compartment to ambient differential pressures

UNCLASSIFIED

UNCLASSIFIED

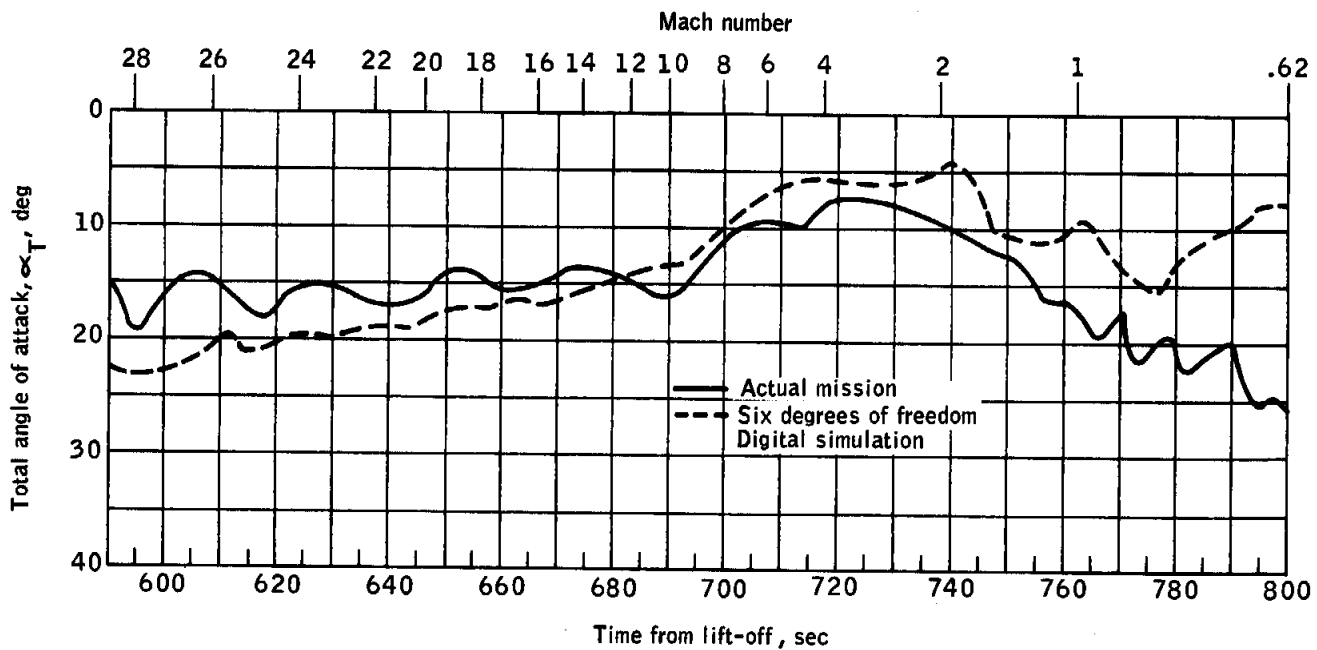


Figure 5.1-22. - Reentry angle of attack

UNCLASSIFIED

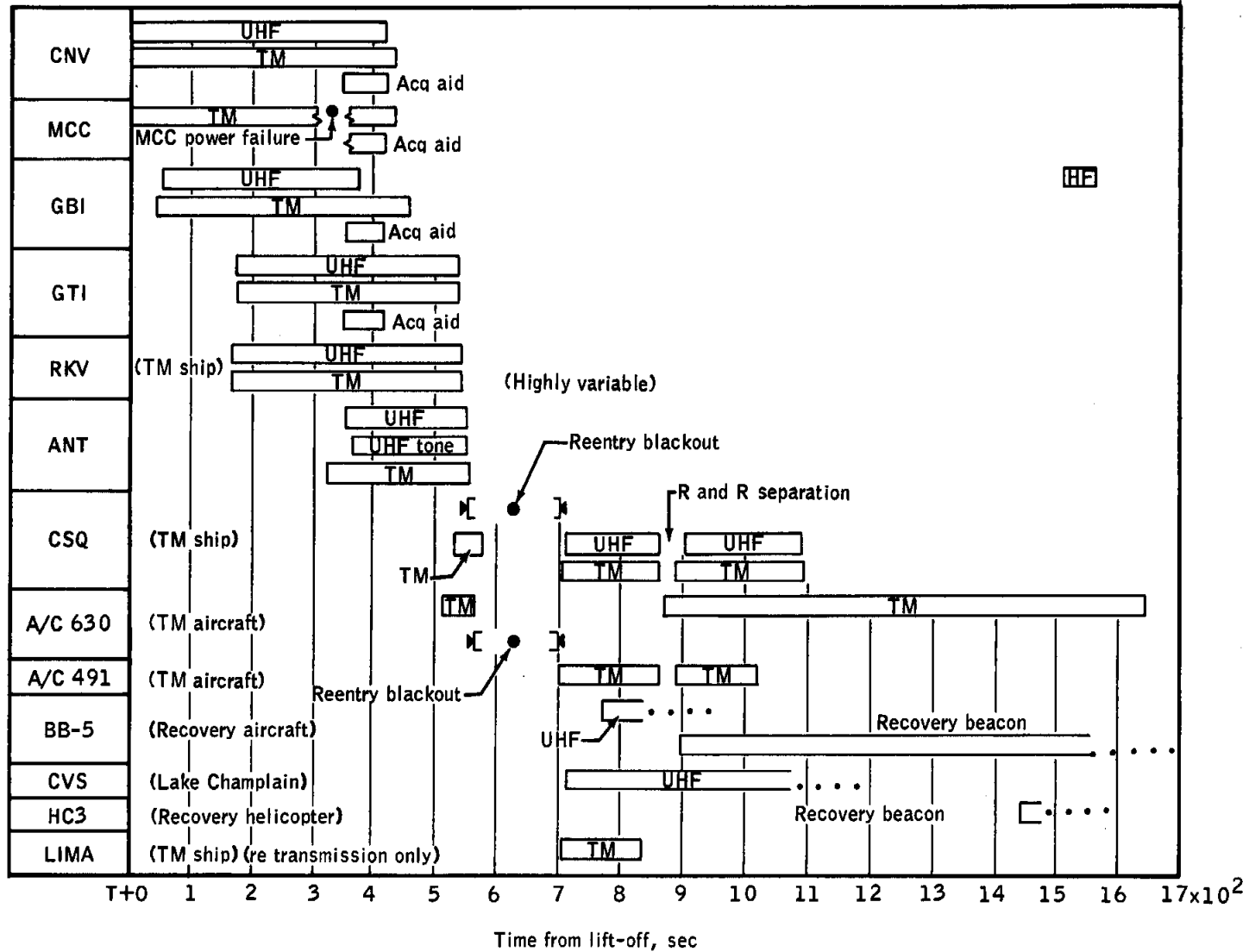


Figure 5.1-23. - Spacecraft communications useable signal strength time history

UNCLASSIFIED

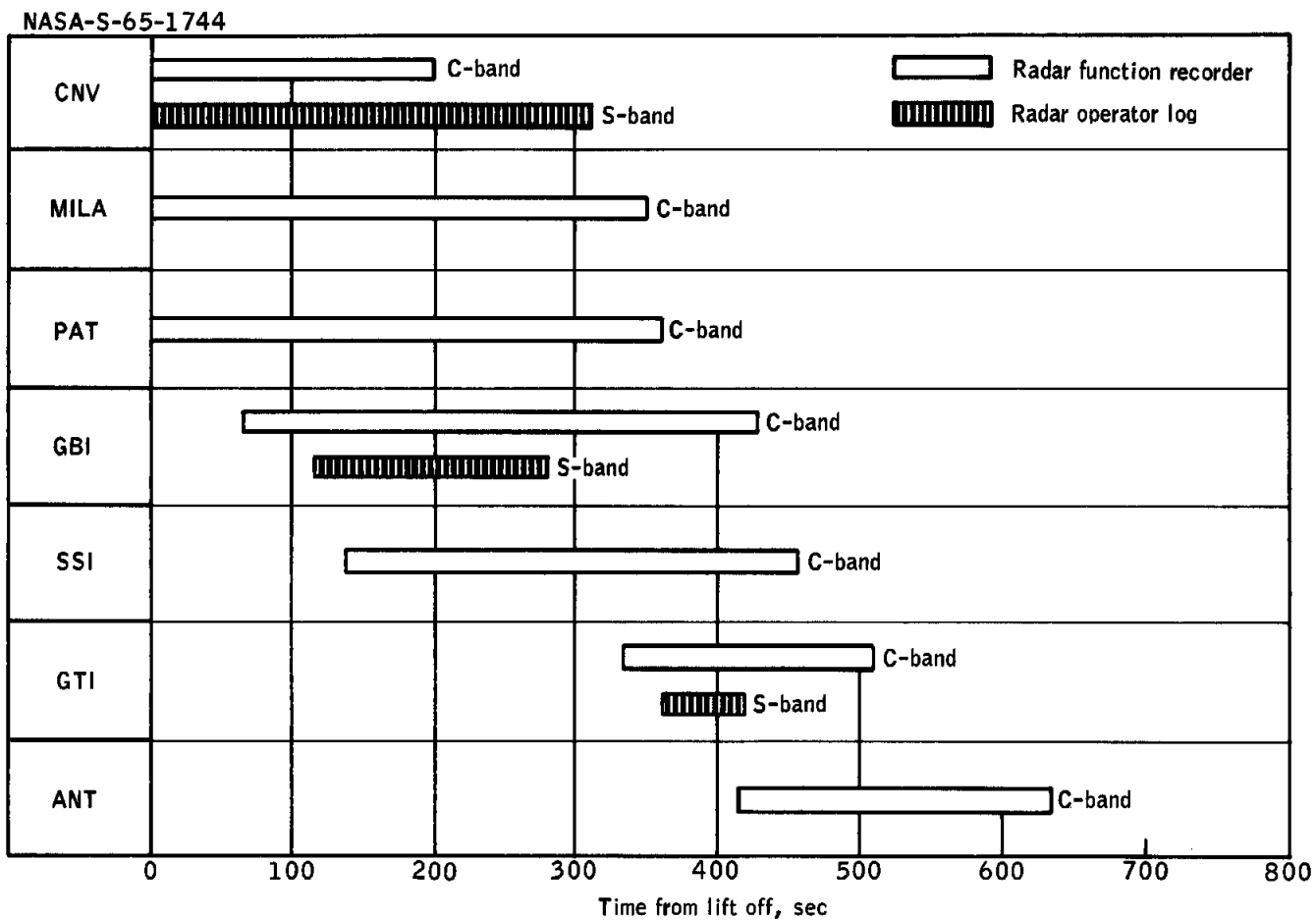
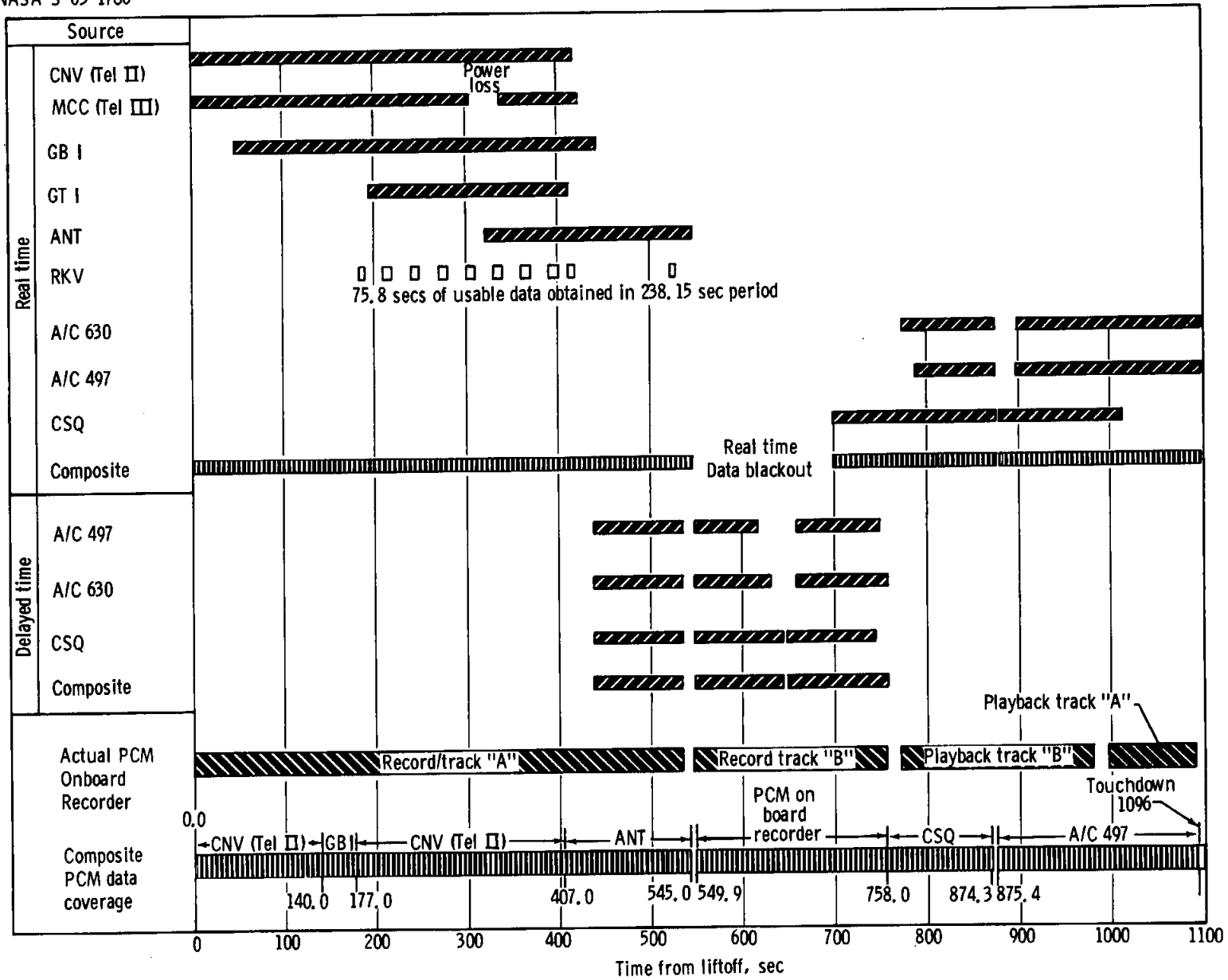


Figure 5.1-24. - S-band and C-band radar coverage

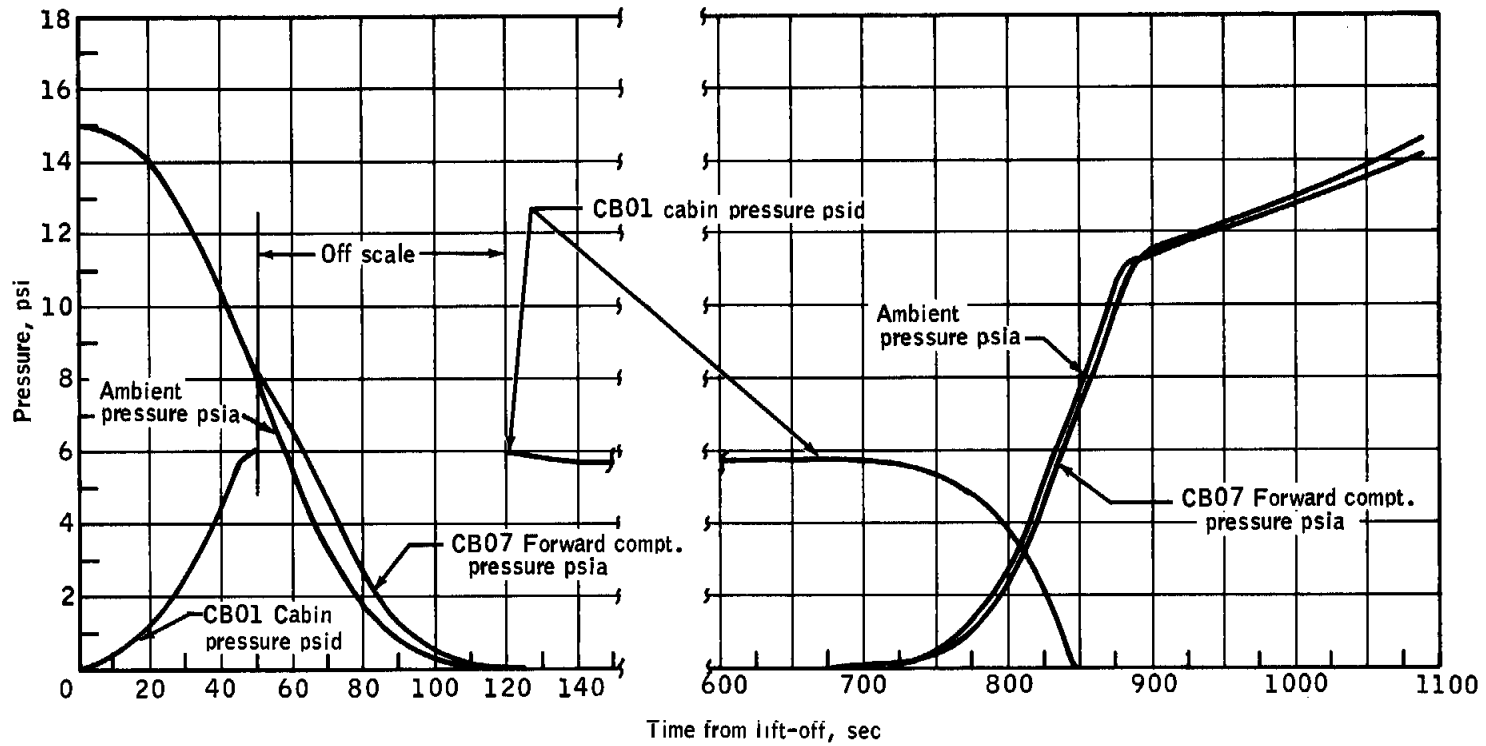
UNCLASSIFIED



UNCLASSIFIED

Figure 5.1-25. - Usable PCM data

UNCLASSIFIED



UNCLASSIFIED

Figure 5.1-26.- Cabin pressure control during launch and reentry

NASA-S-65-1605

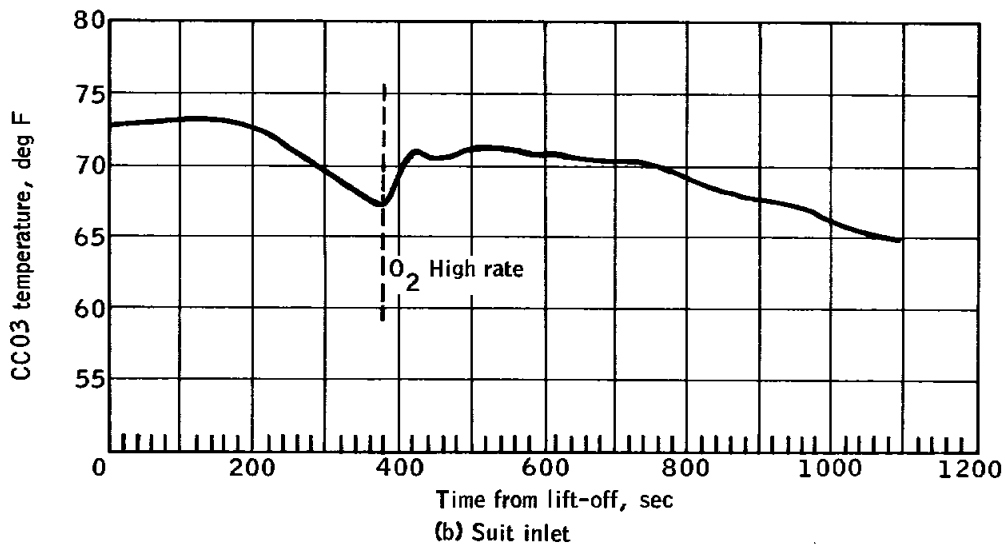
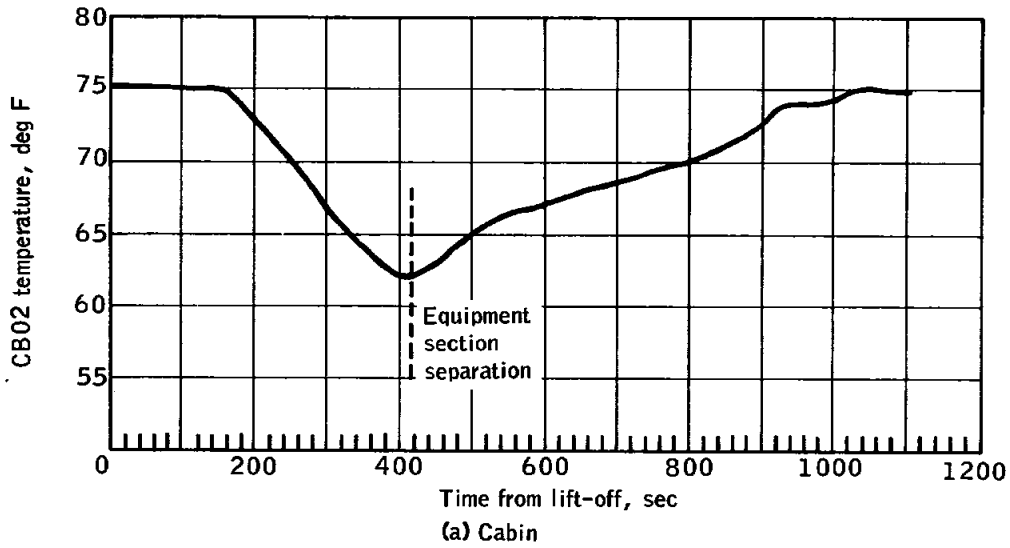
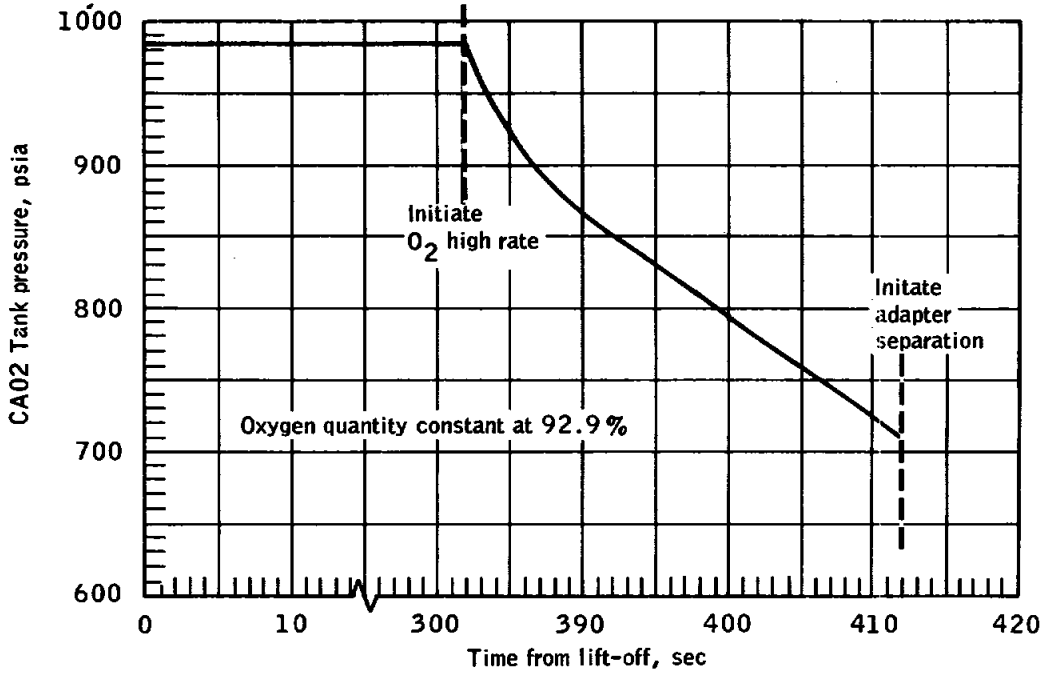
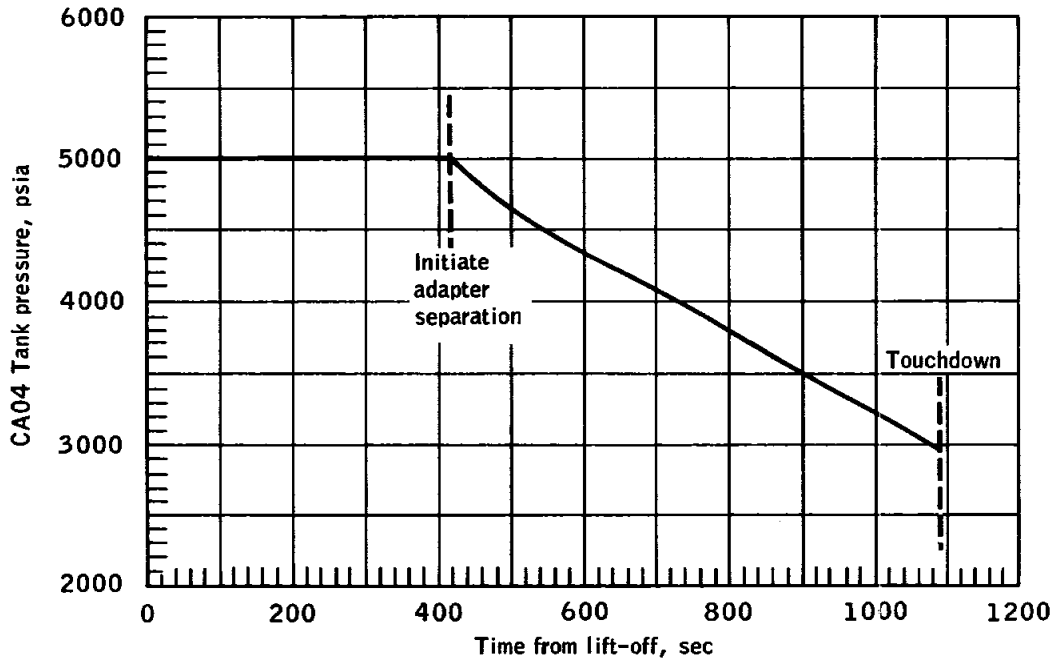


Figure 5.1-27. - Crew compartment gas temperatures

NASA-S-65-1603



(a) Primary oxygen bottle



(b) Secondary oxygen bottle

Figure 5.1-28.- ECS oxygen storage pressures

NASA-S-65-1951

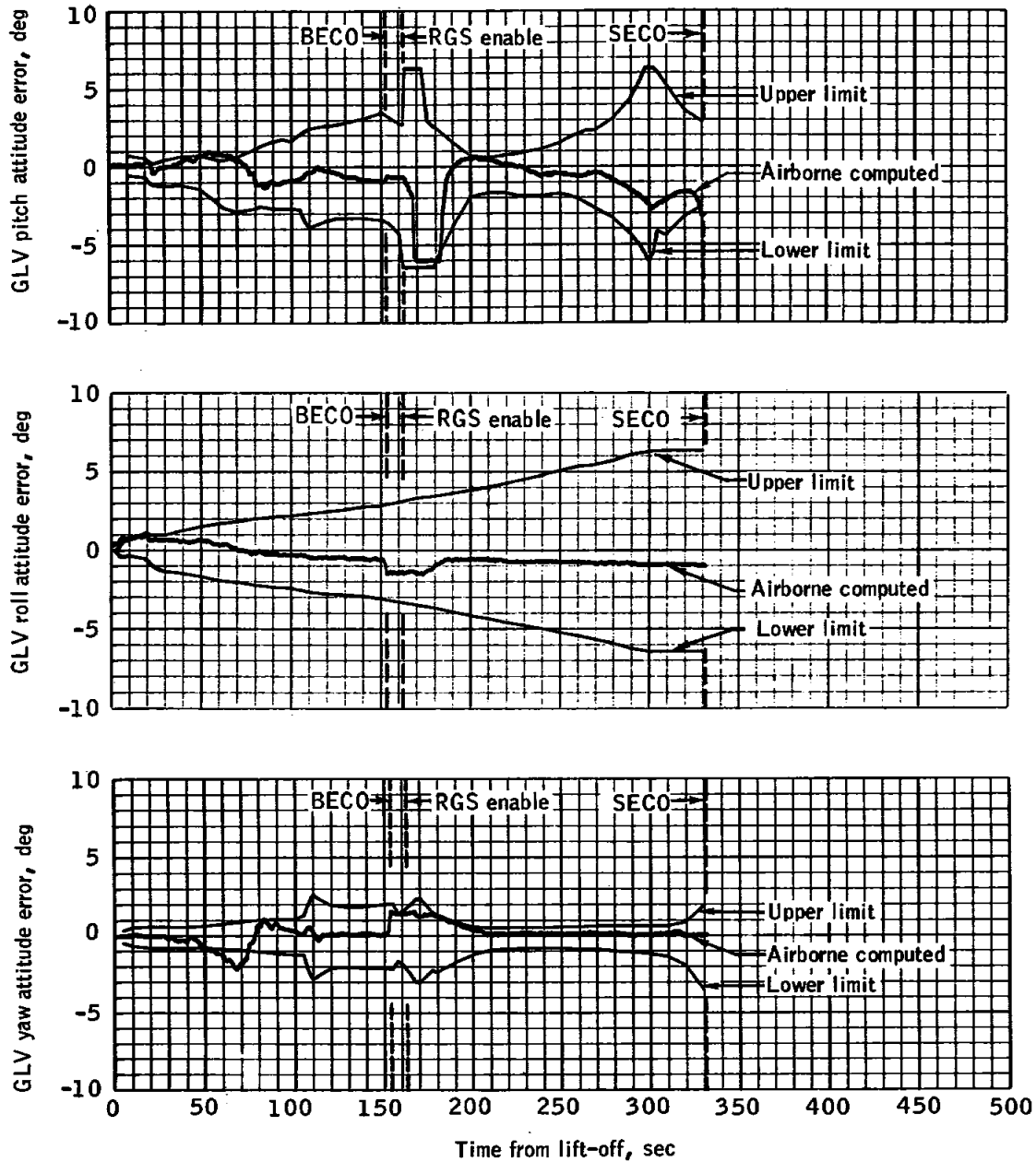


Figure 5.1-29. - Comparison of steering commands during launch with preflight value

~~CONFIDENTIAL~~

NASA-S-65-1961

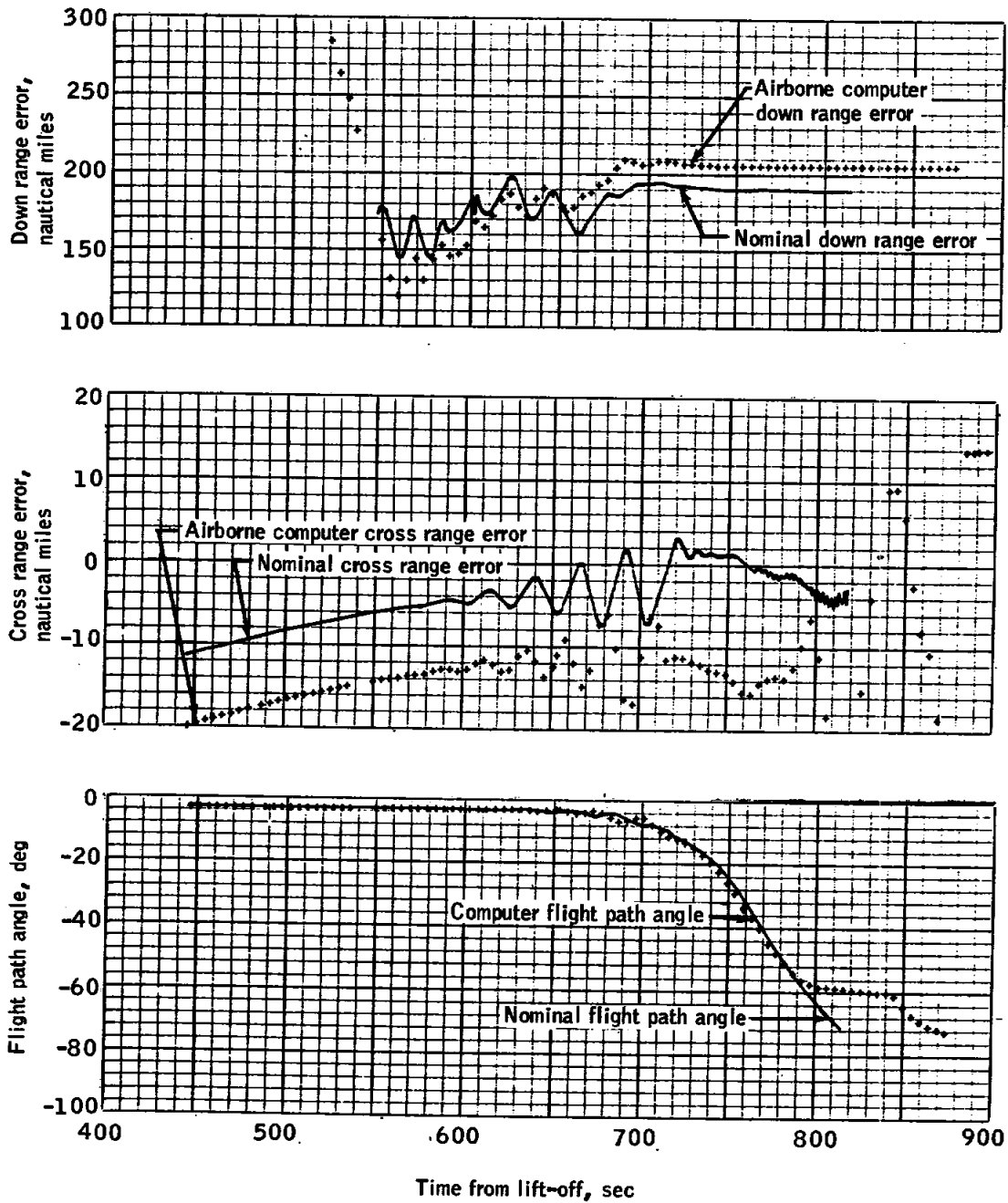
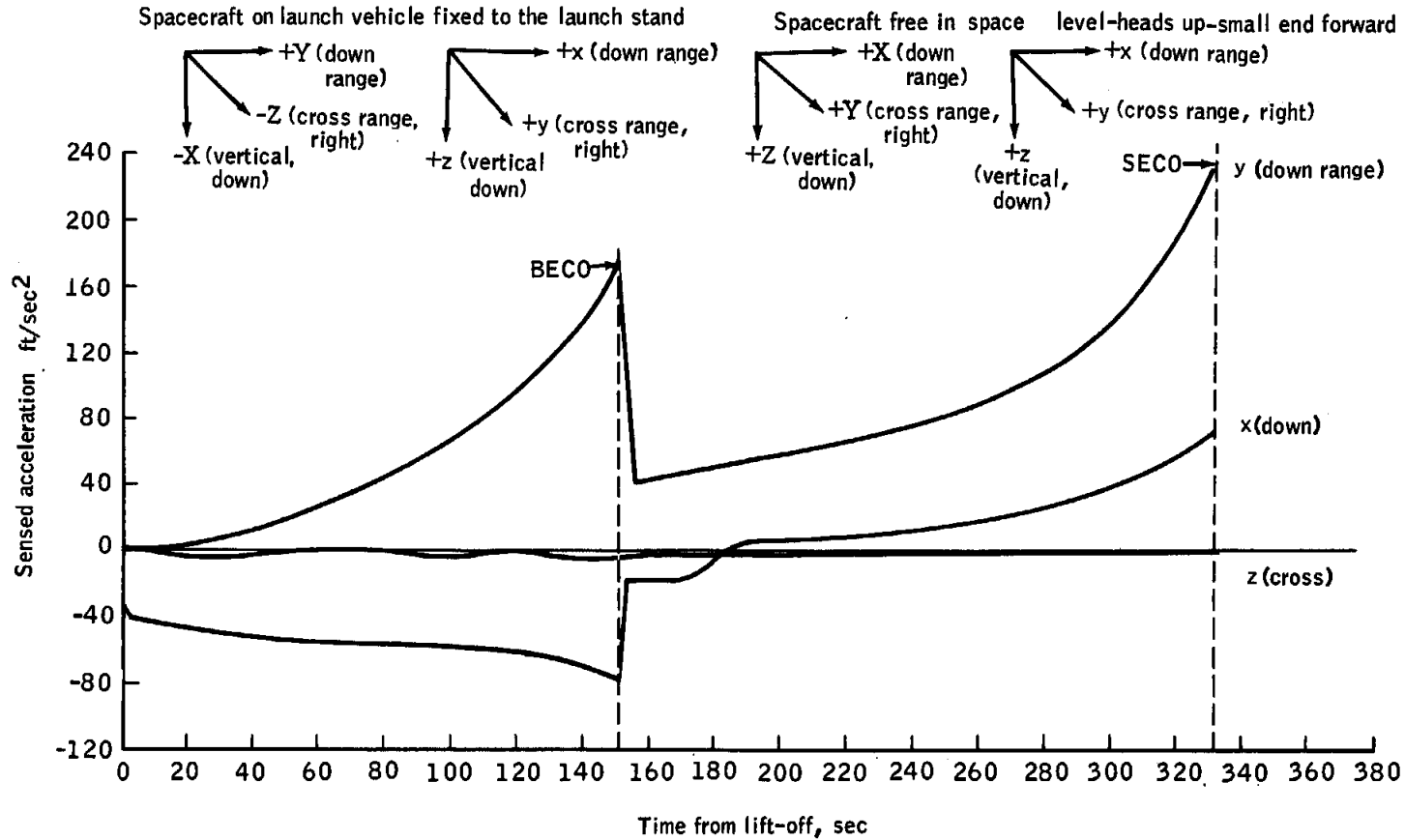


Figure 5.1-30. - Comparison of flight steering errors during reentry with preflight nominal values

~~CONFIDENTIAL~~

x, y, z: Inertial measuring unit coordinates
 X, Y, Z: Computer coordinates



Title 5.1-31. - IMU sensed acceleration

~~CONFIDENTIAL~~

~~CONFIDENTIAL~~

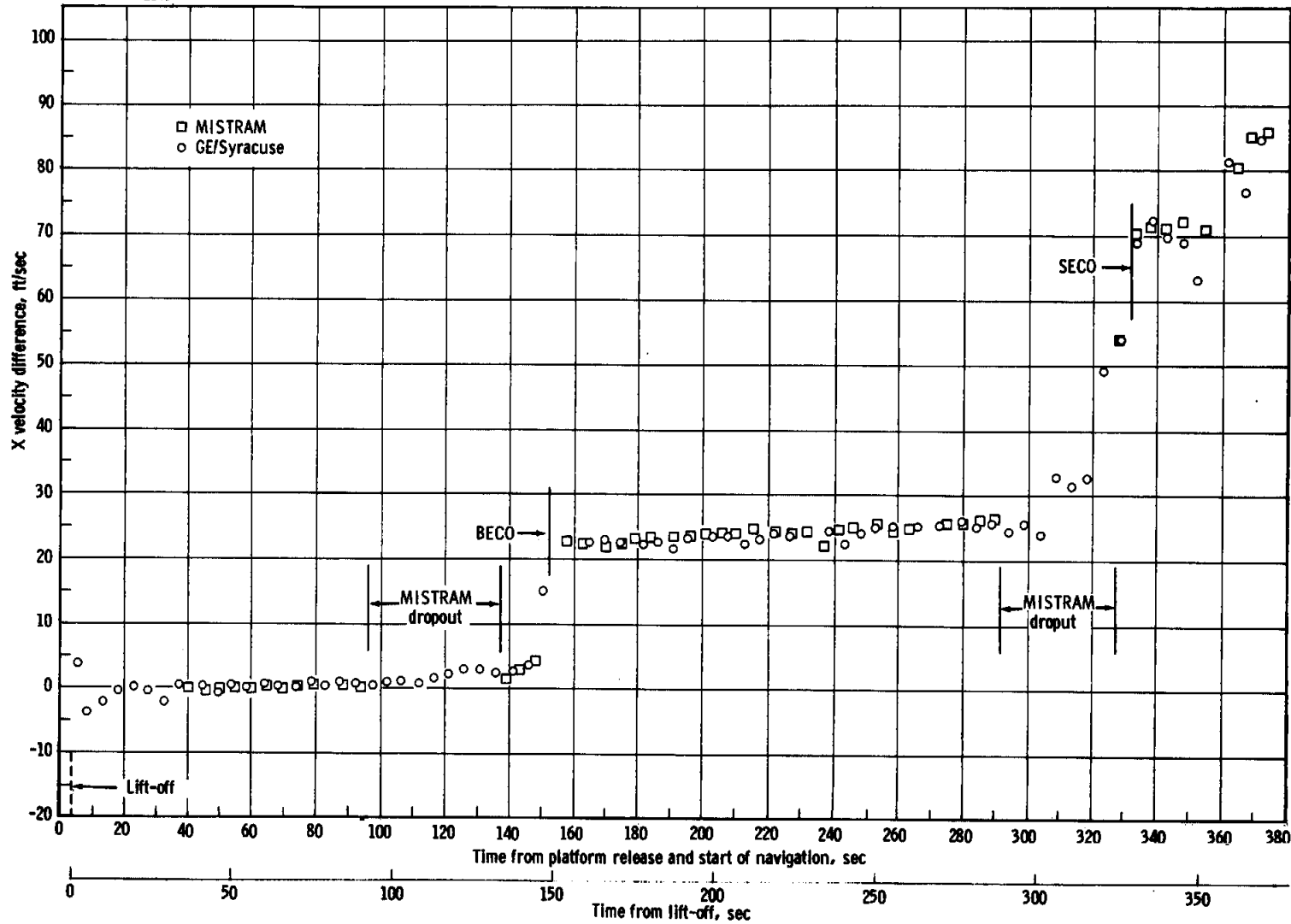
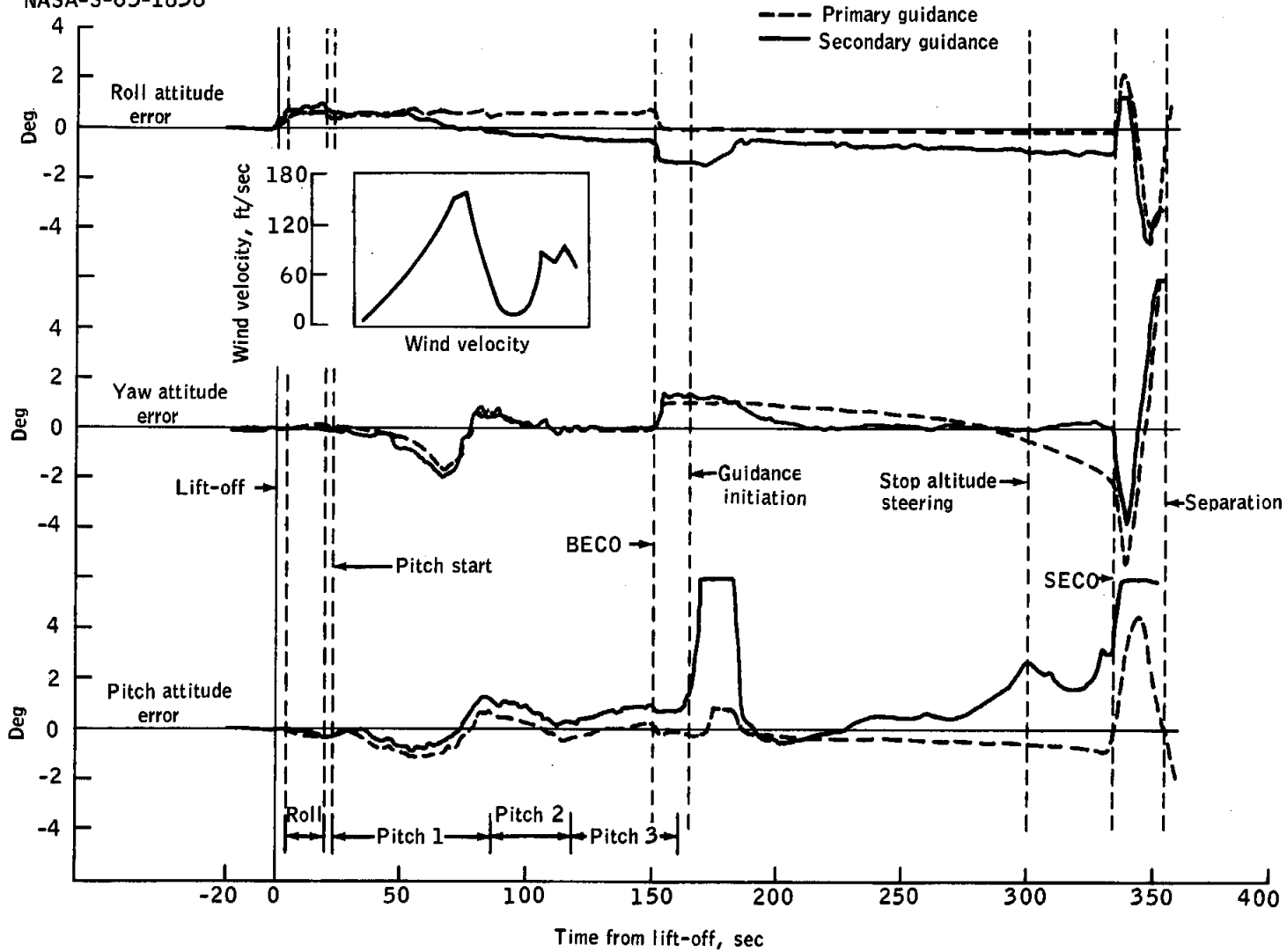


Figure 5.1-32. - IGS velocity comparisons with ground tracking

NASA-S-65-1838



CONFIDENTIAL

CONFIDENTIAL

Figure 5.1-33. - Attitude errors

UNCLASSIFIED

UNCLASSIFIED

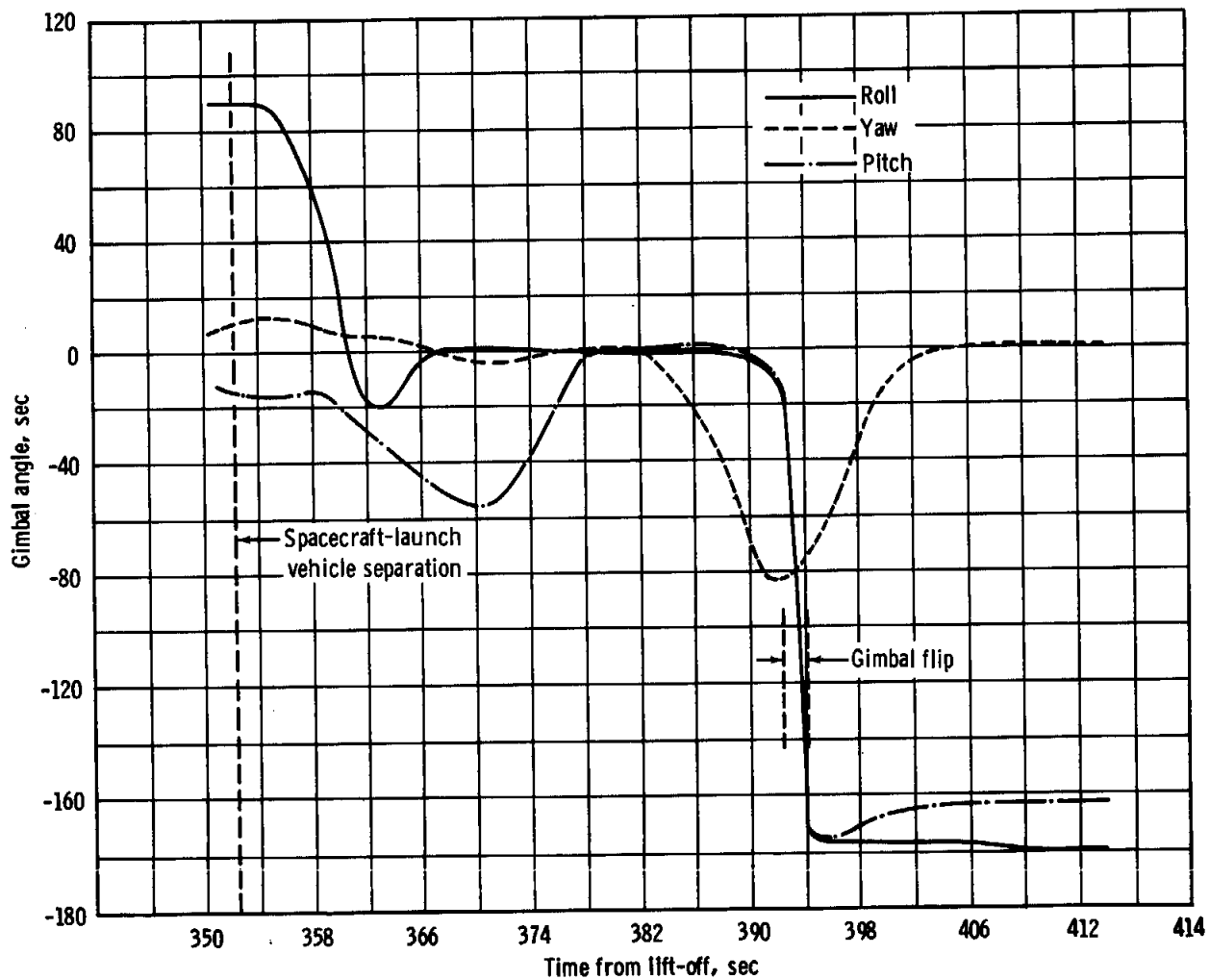


Figure 5.1-34. - Inertial measuring unit gimbals angles during incremental velocity adjust routine

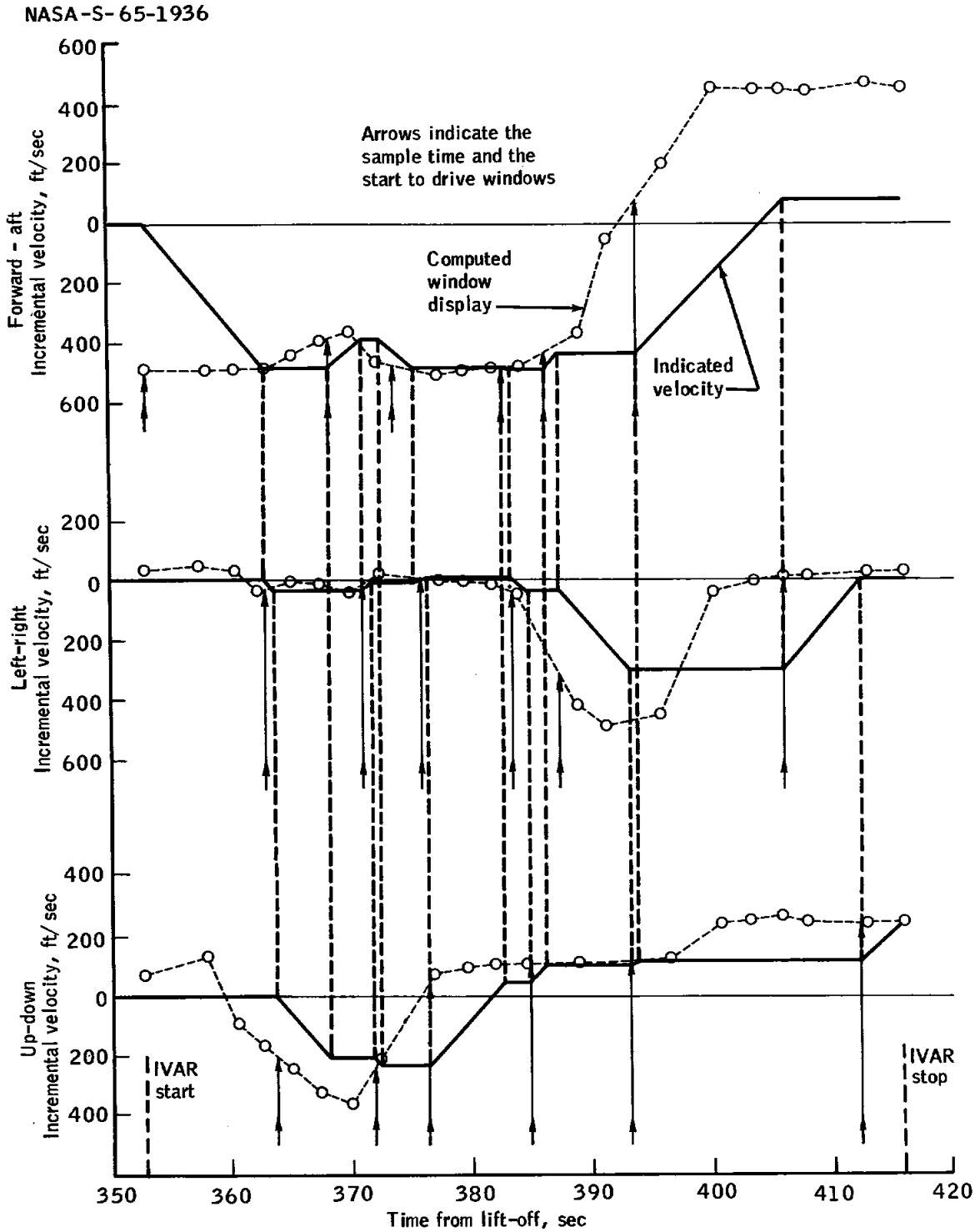


Figure 5.1-35. - Incremental velocity indicator computer sample and window set routine

UNCLASSIFIED

UNCLASSIFIED

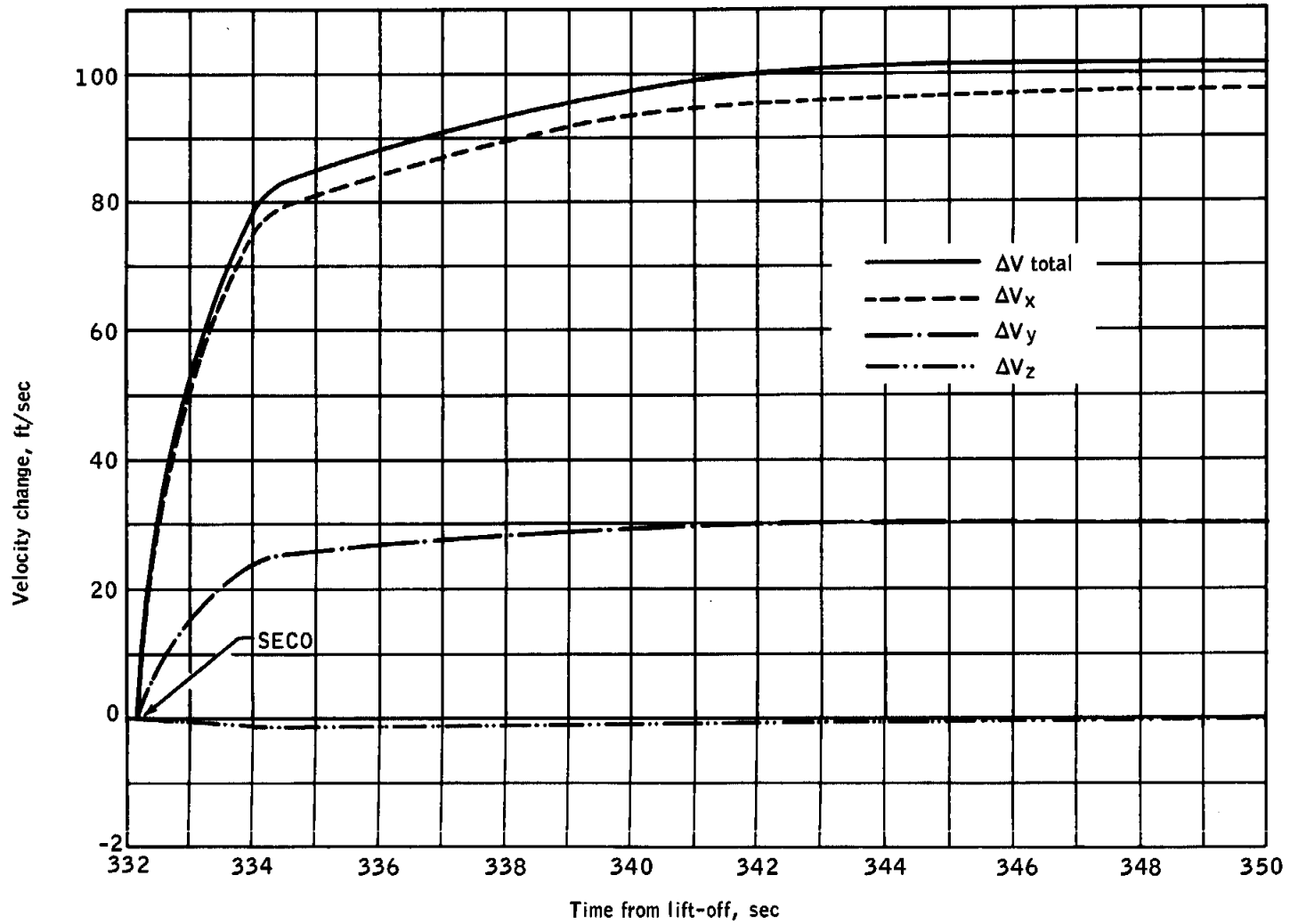
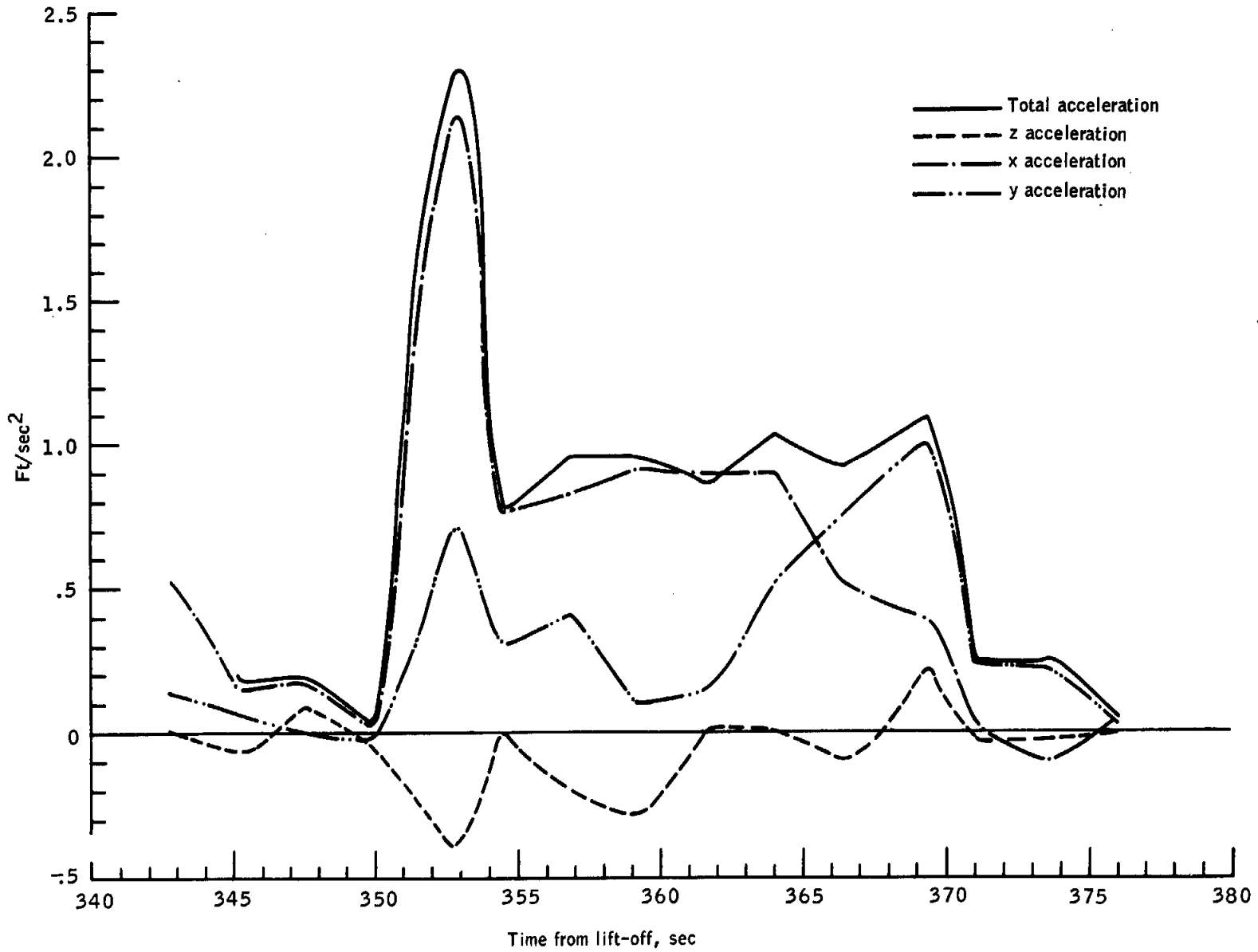


Figure 5.1-36. - Inertial velocity changes due to thrust tail off

UNCLASSIFIED



UNCLASSIFIED

Figure 5.1-37.- Spacecraft - launch vehicle separation accelerations

UNCLASSIFIED

UNCLASSIFIED

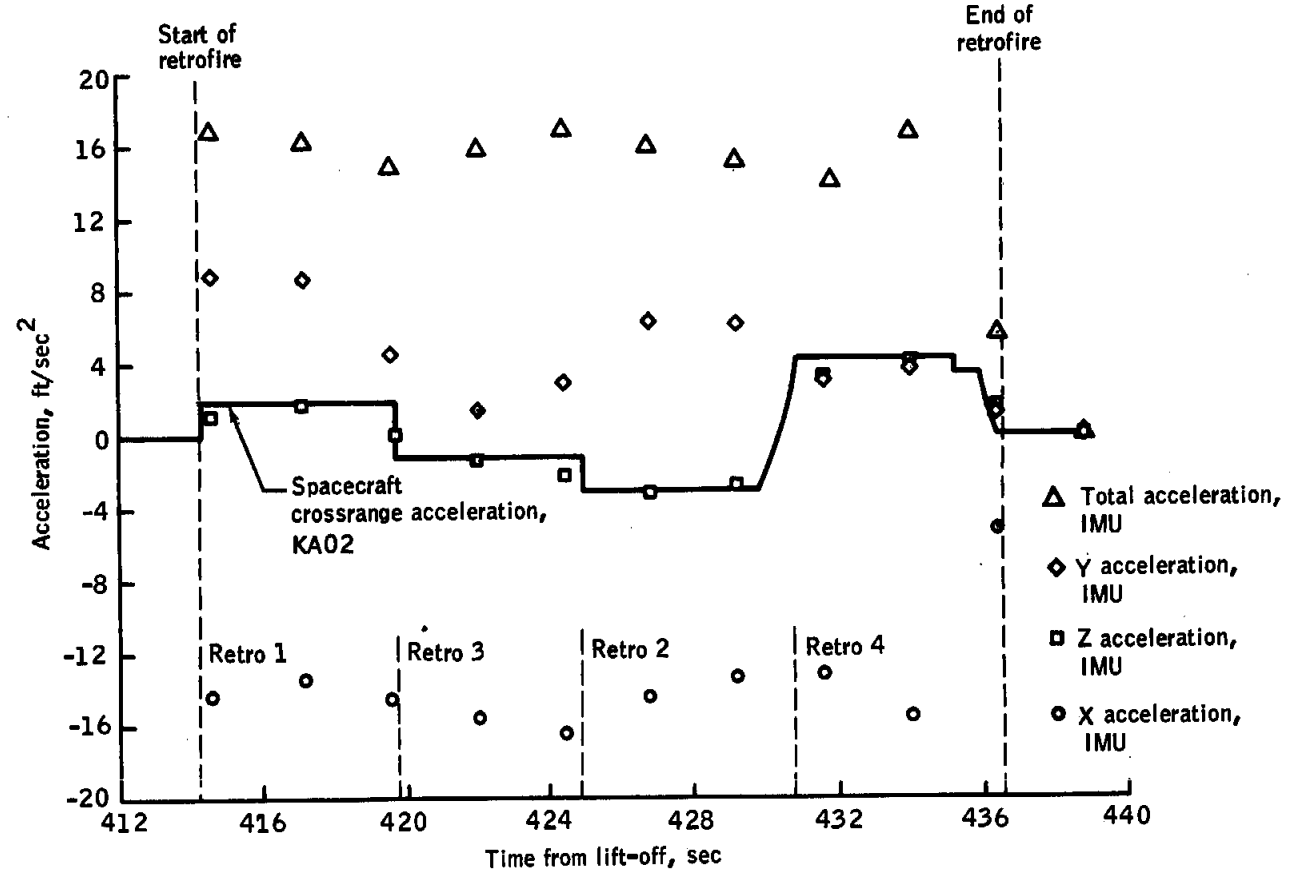


Figure 5.1-38 Accelerations during retrofire

NASA-S-65-2184

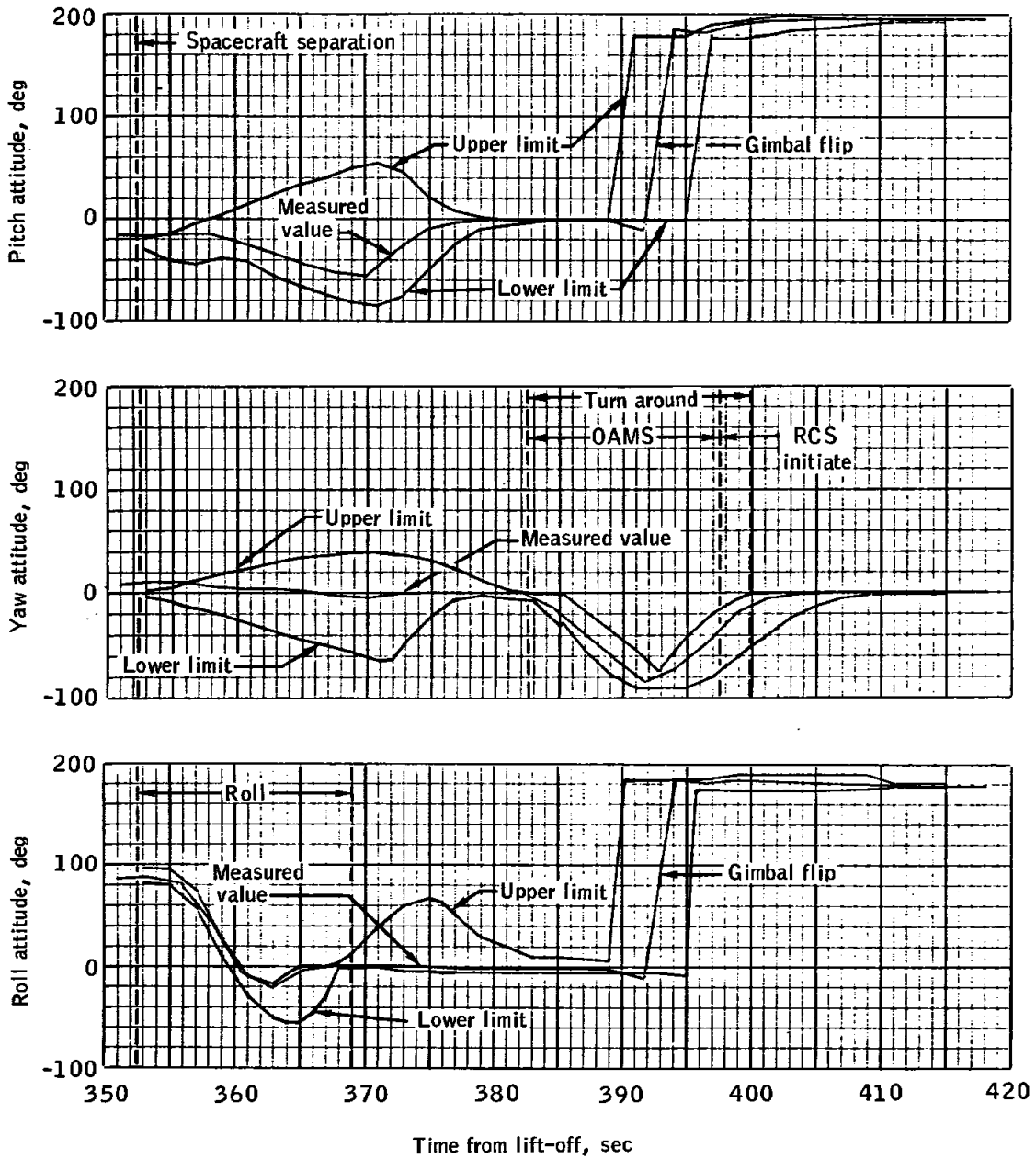


Figure 5.1-39.- Spacecraft attitude compared to 3 sigma limits

~~CONFIDENTIAL~~

NASA-S-65-2182

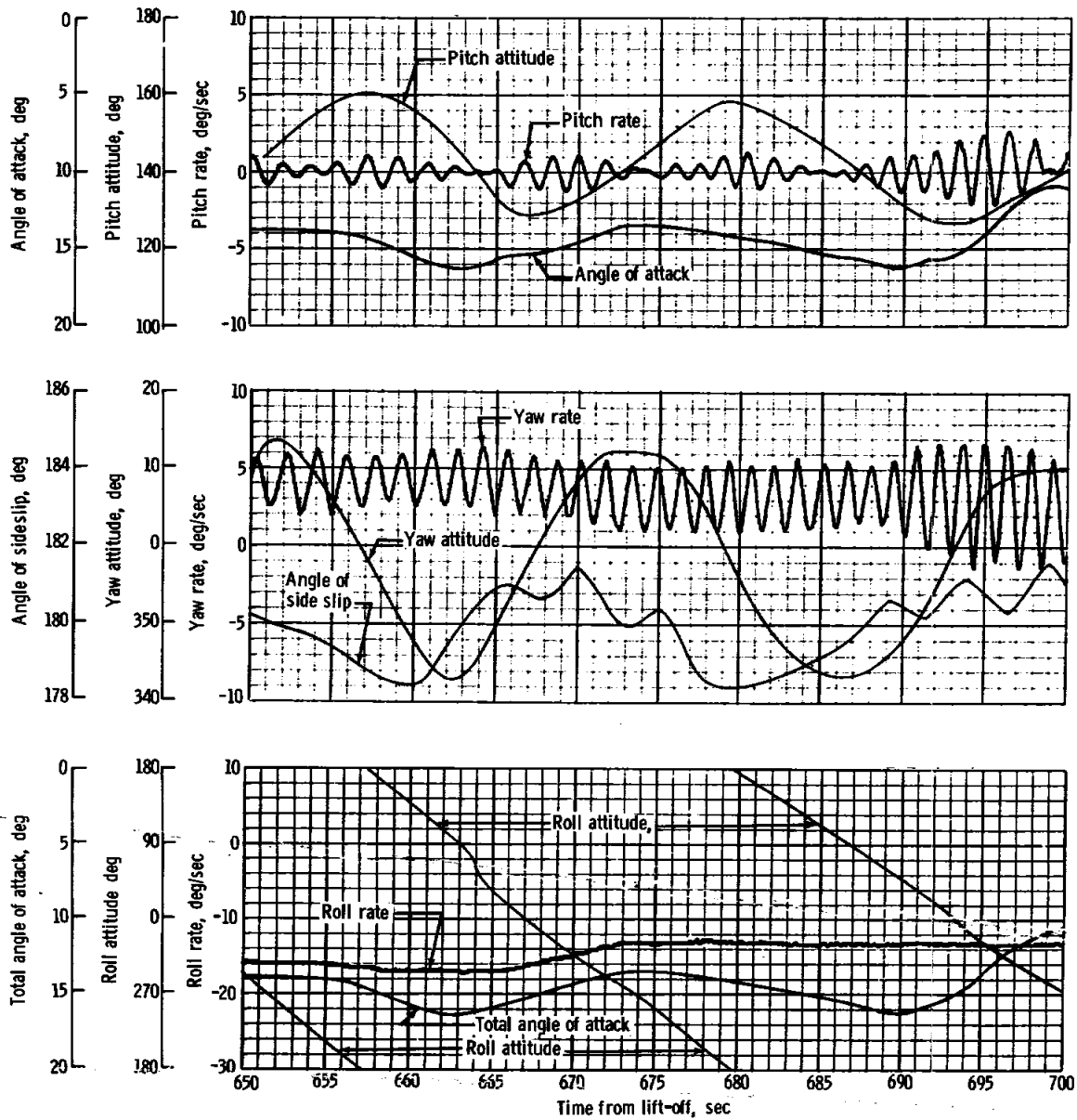
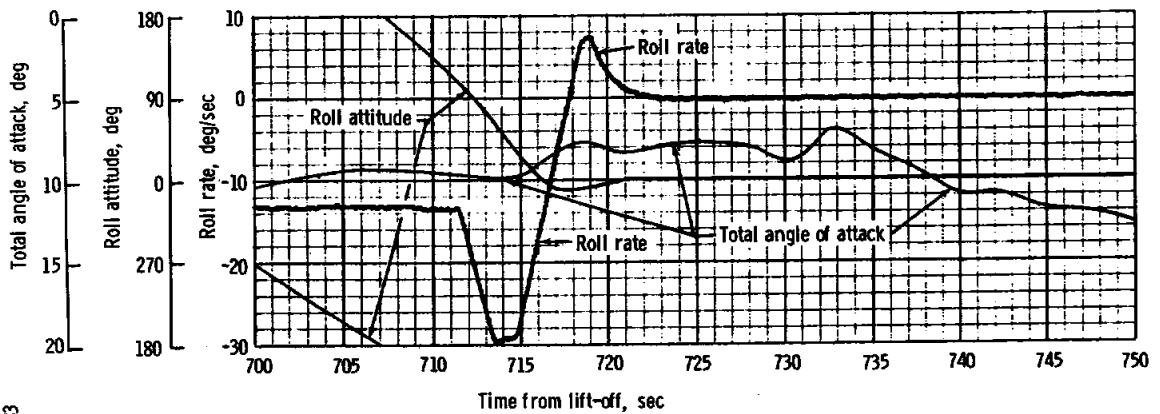
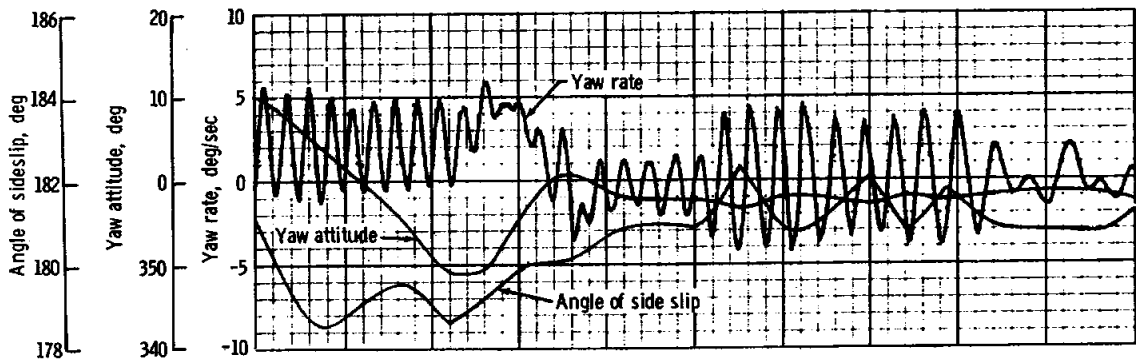
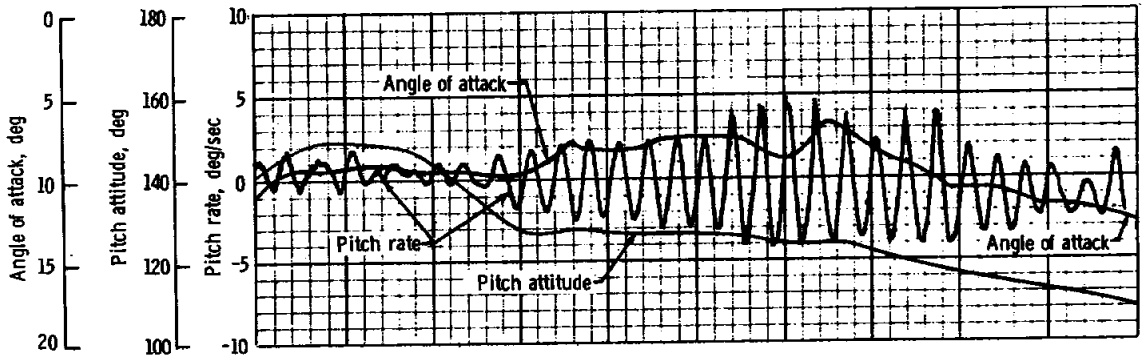


Figure 5.1-40.- Reentry control parameter comparison

~~CONFIDENTIAL~~



NASA-S-65-2183

Figure 5.1-40.- Concluded

NASA-S-65-1950

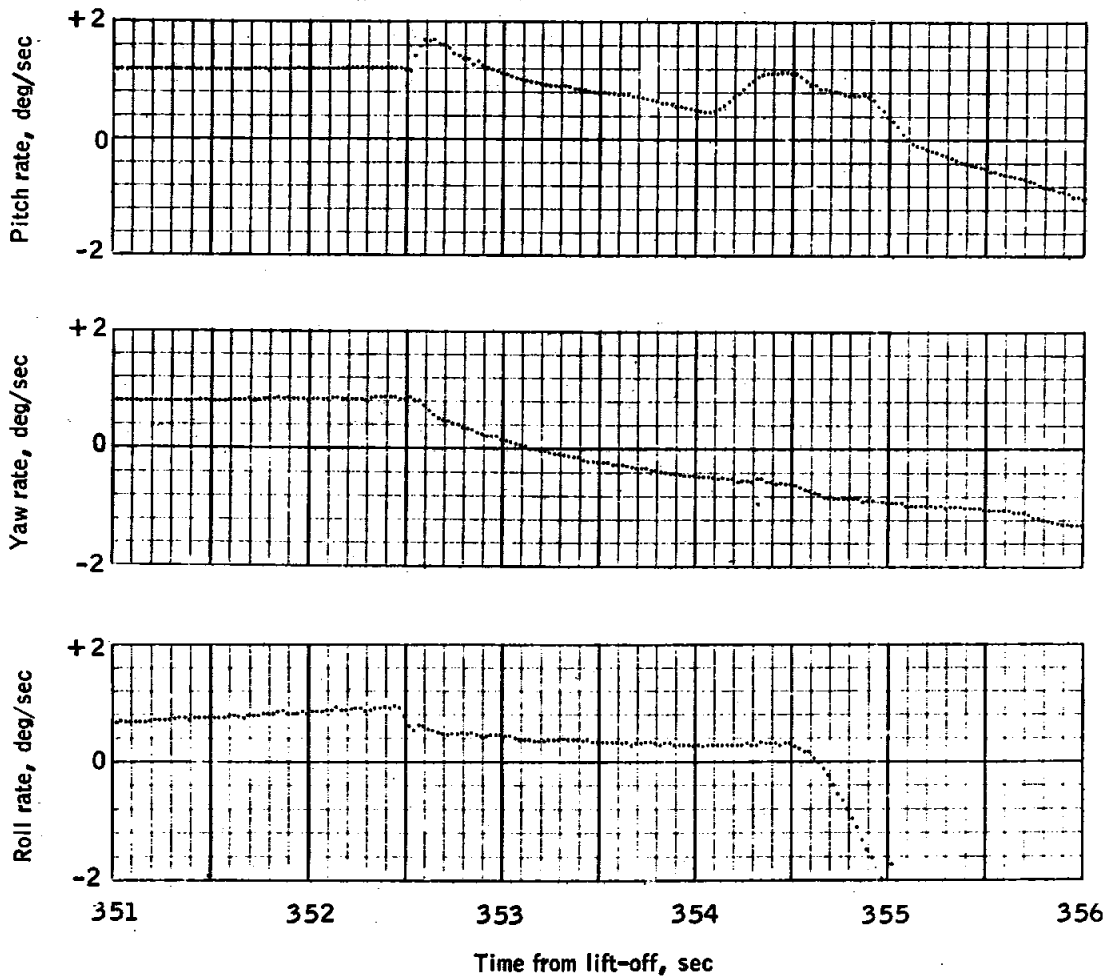


Figure 5.1-41. - Spacecraft-Launch vehicle separation transients

NASA-S-65-1949

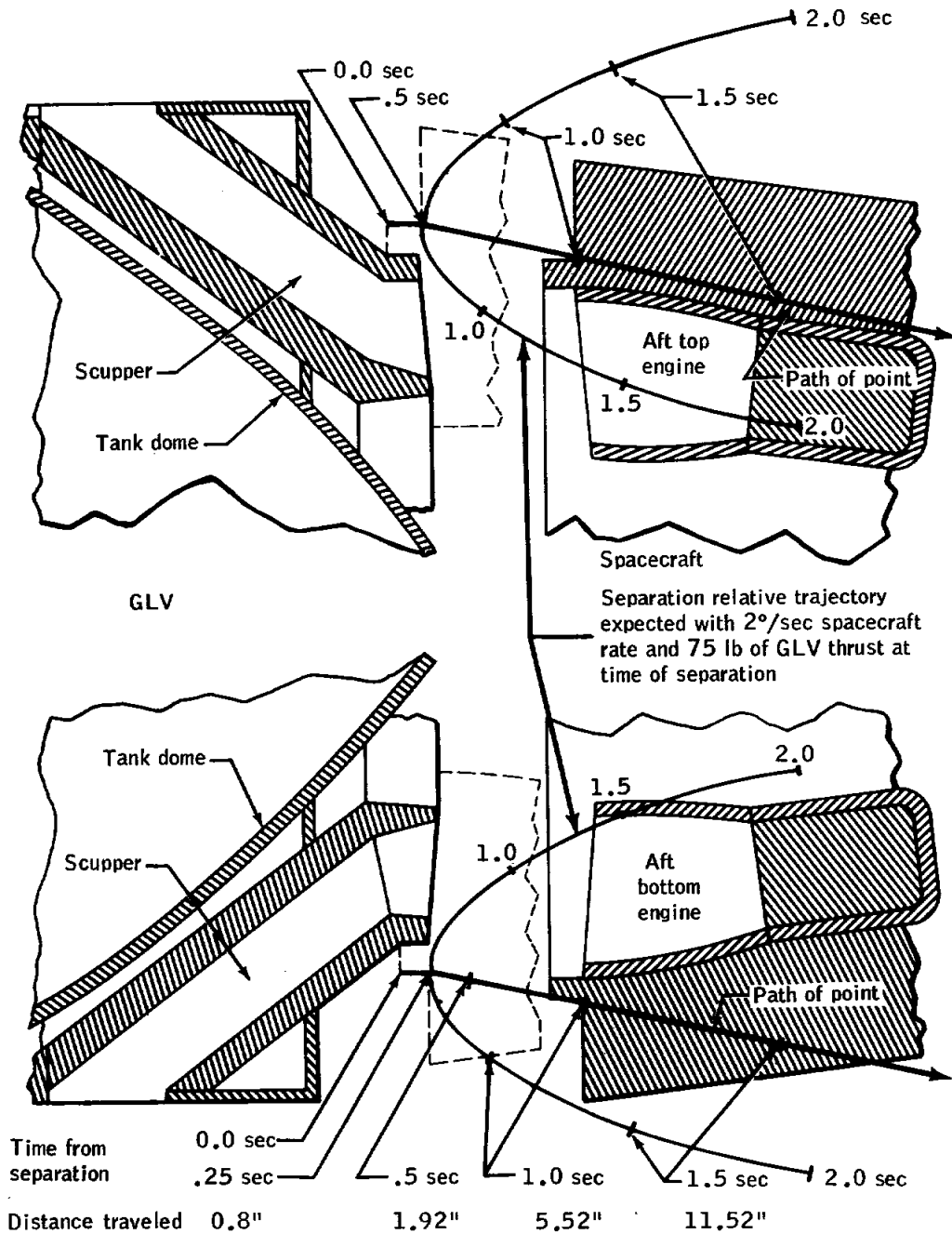


Figure 5.1-42. Relative positions of GLV and spacecraft after separation

NASA-S-65-1959

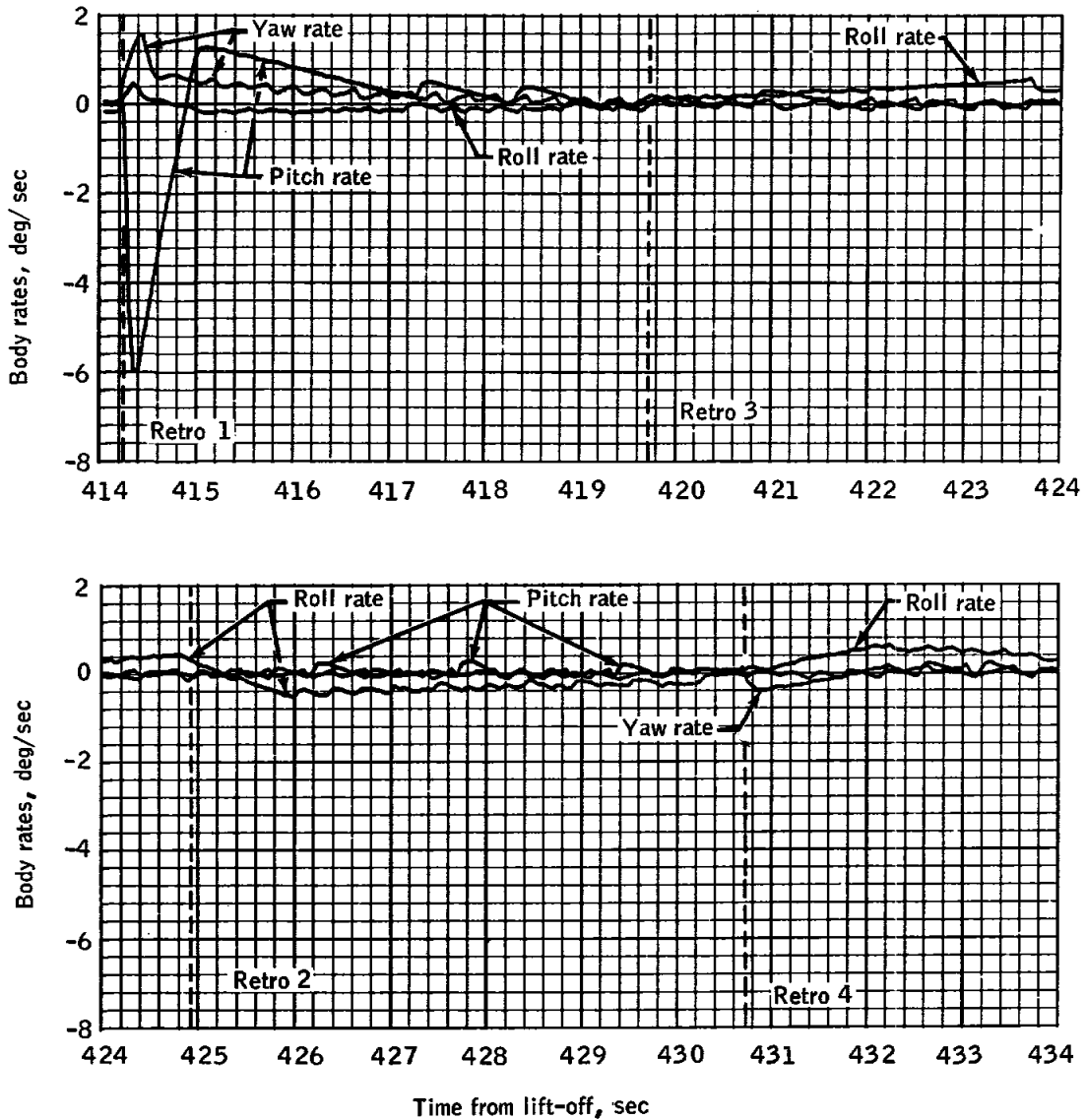
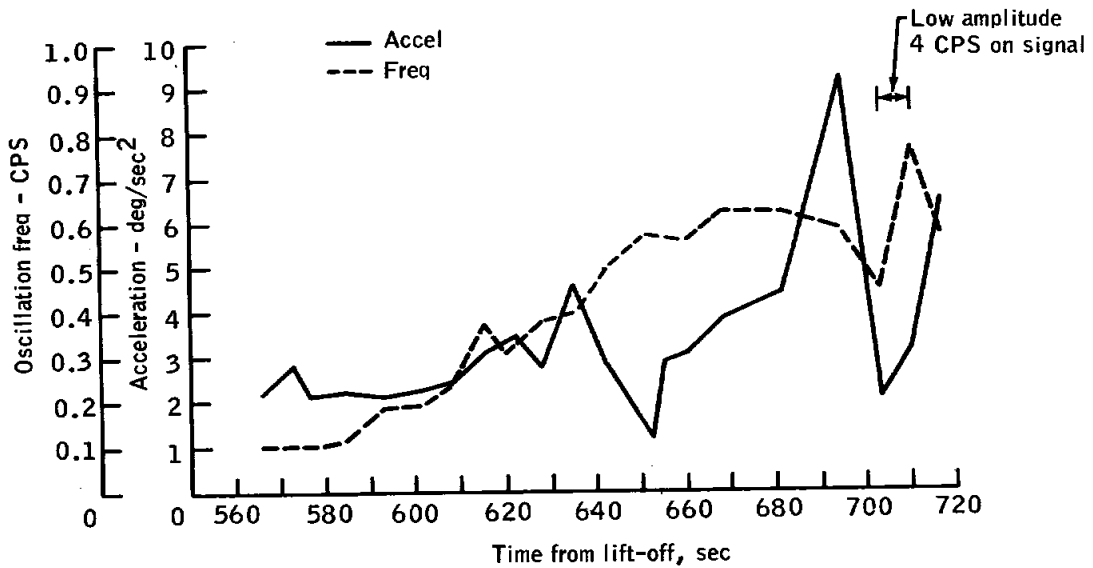
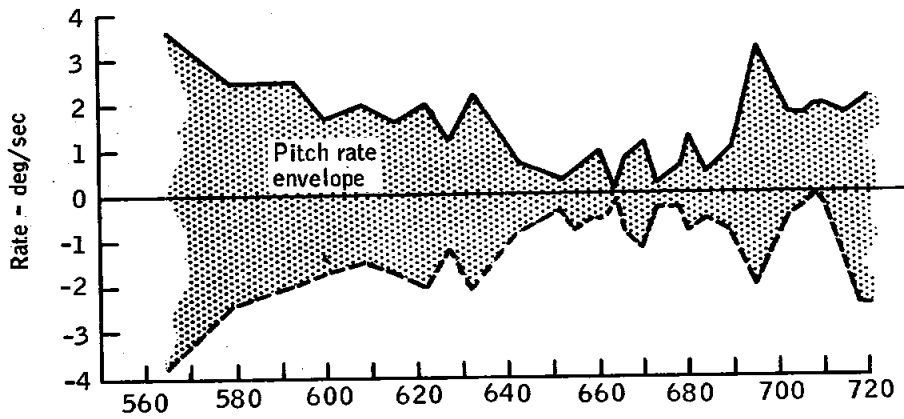


Figure 5.1-43. - Retrofire transients

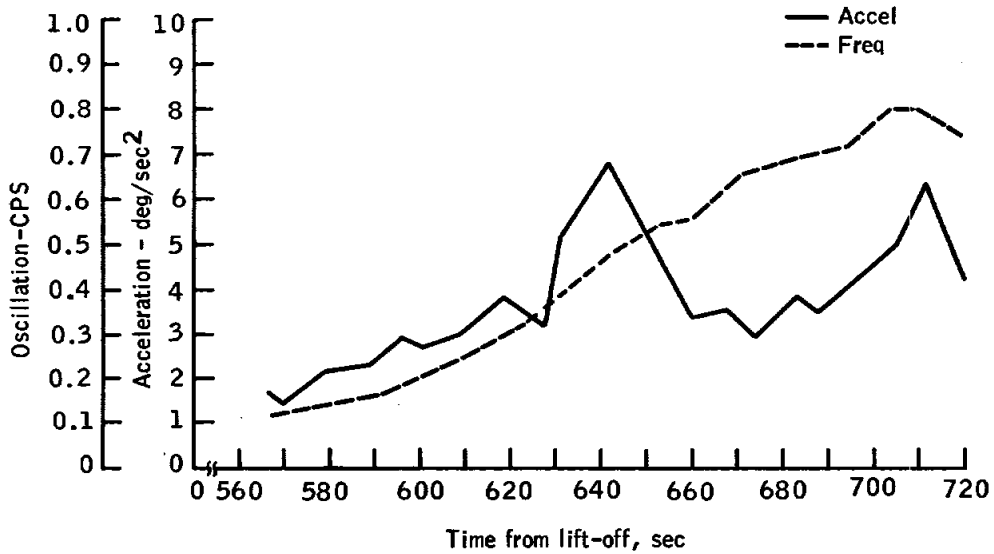
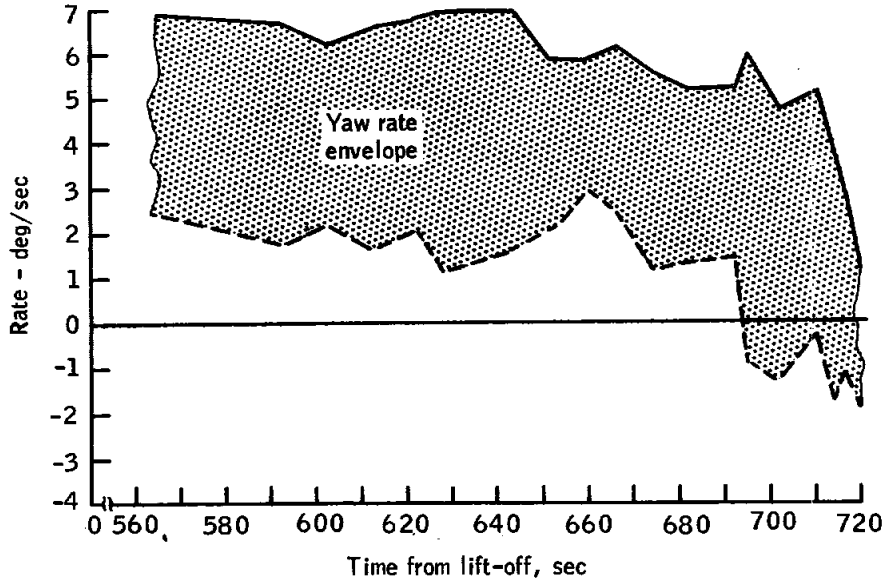
NASA-S-65-1833



(a) Pitch rates

Figure 5.1-44. - Rate summations

NASA-S-65-1834



(b) Yaw rates

Figure 5.1-44. - Concluded

NASA-S-65-1836

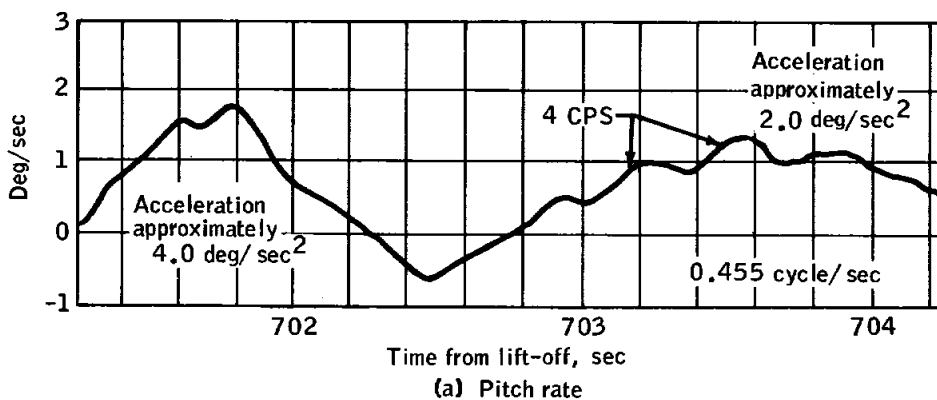
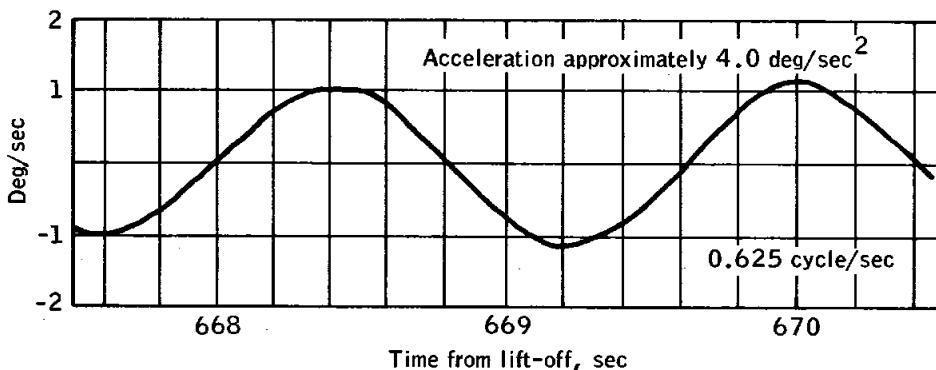
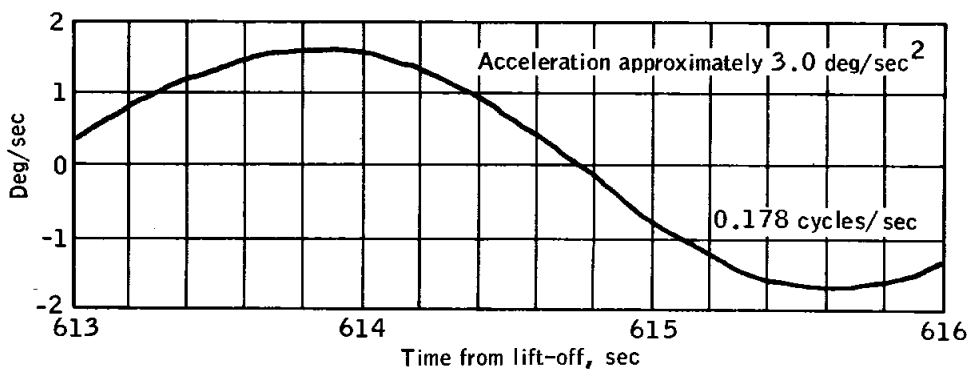
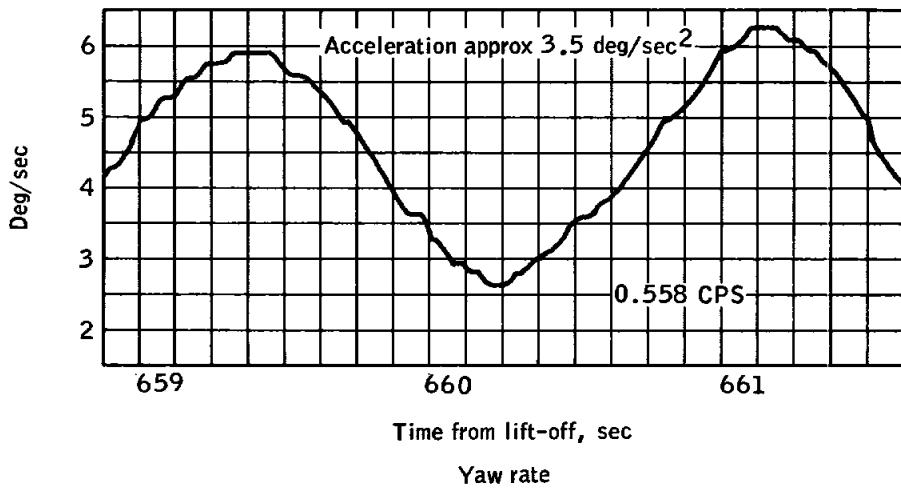
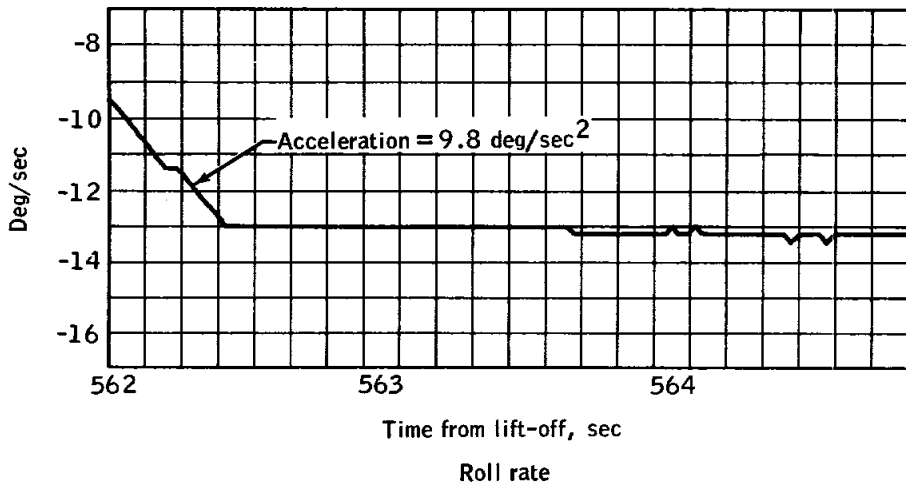


Figure 5.1-45. - Selected spacecraft rate time histories

NASA-S-65-1843



(b) Roll and yaw rates

Figure 5.1-45. - Concluded

NASA-S-65-2035

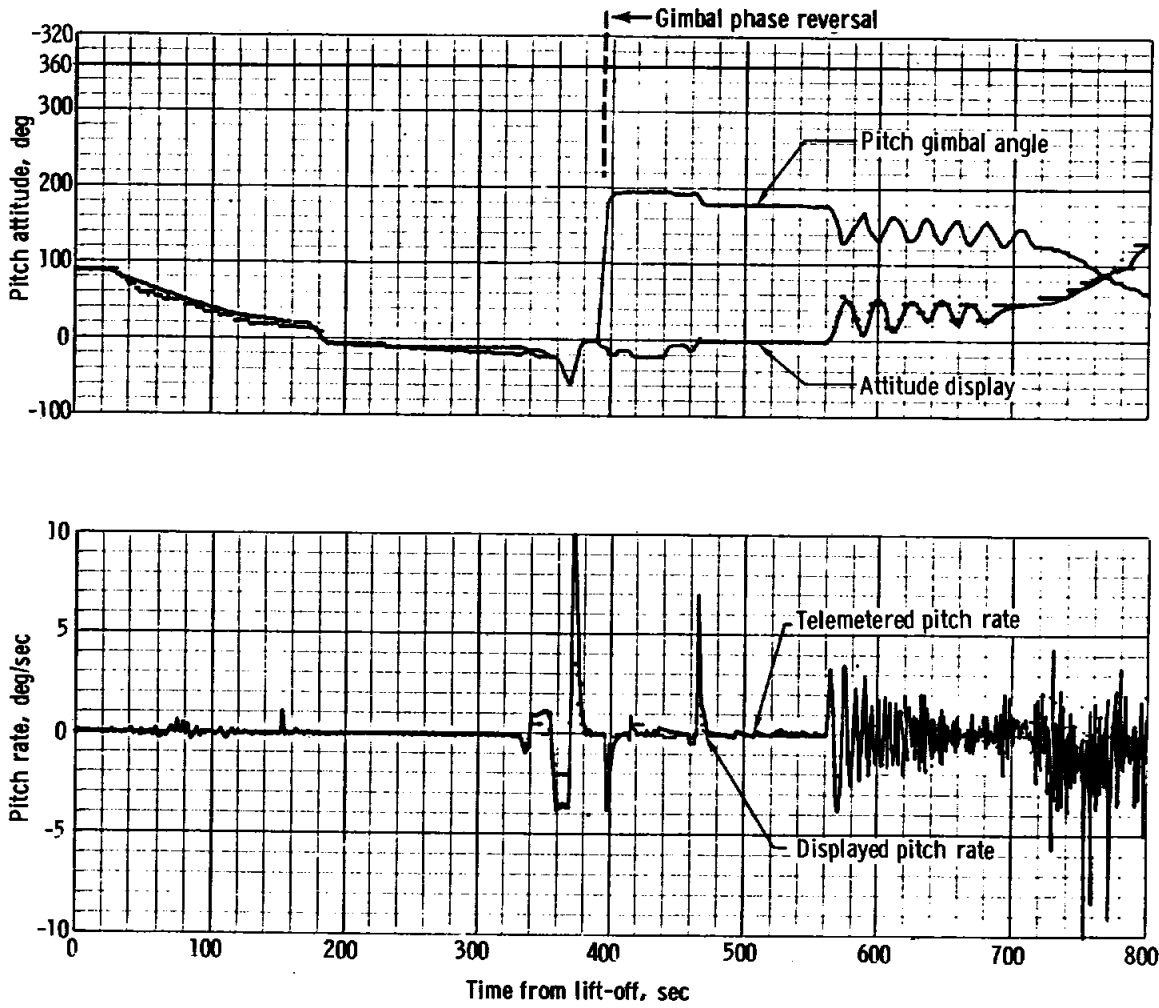


Figure 5.1-46. - Attitude display performance

~~UNCLASSIFIED~~

NASA-S-65-1957

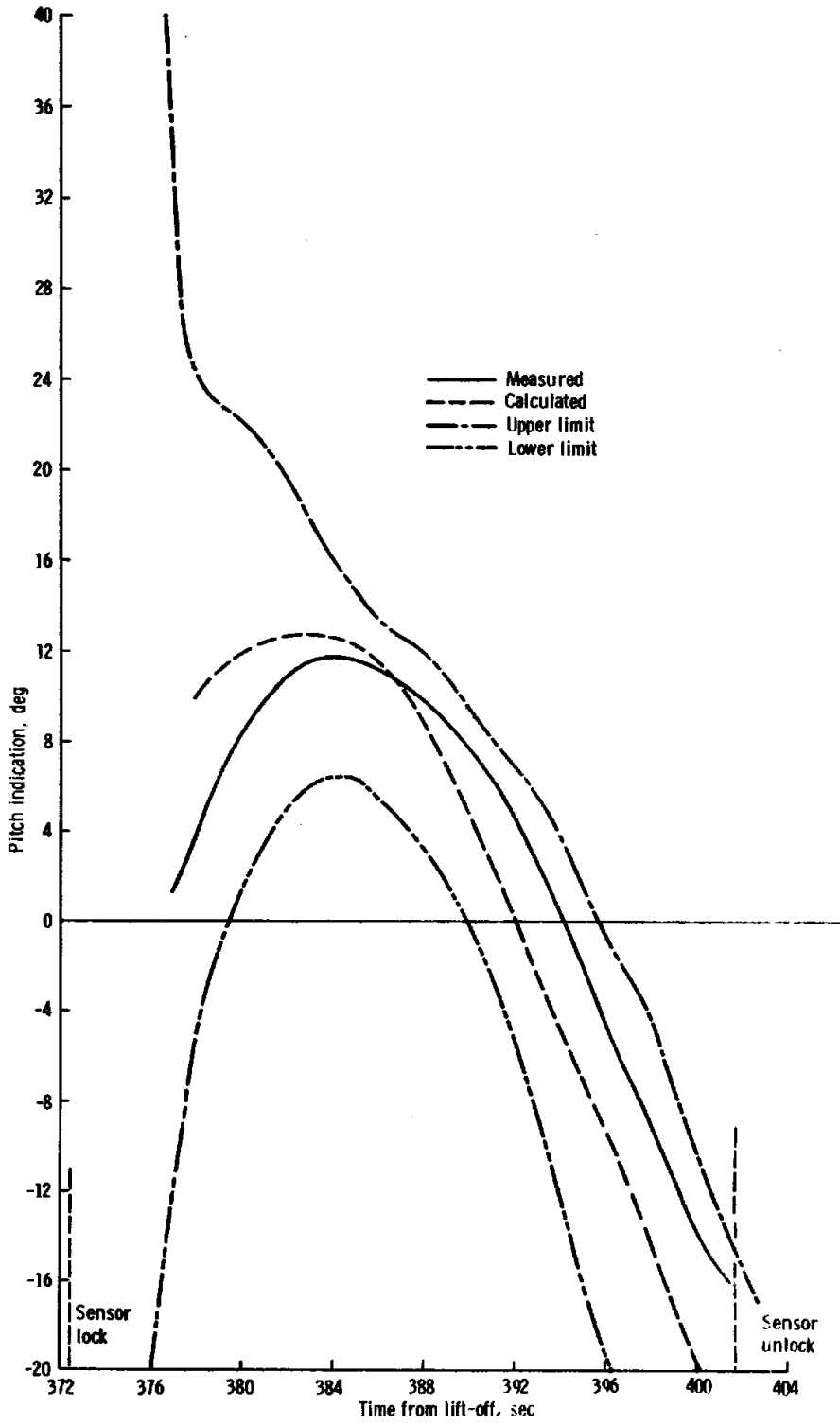


Figure 5.1-47. - Horizon sensor performance

~~UNCLASSIFIED~~

NASA-S-65-1955

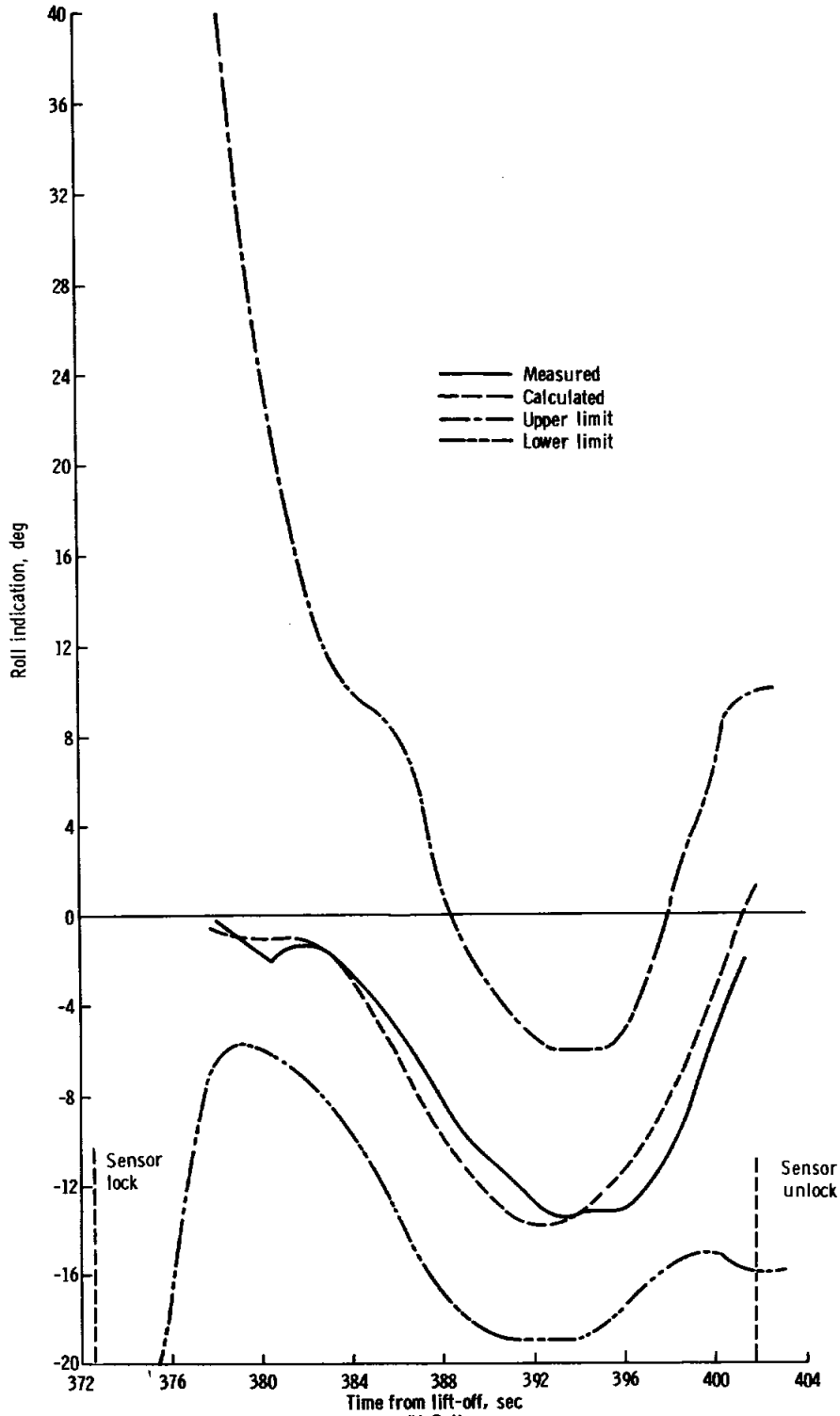


Figure 5.1-47. - Concluded

NASA-S-65-1956

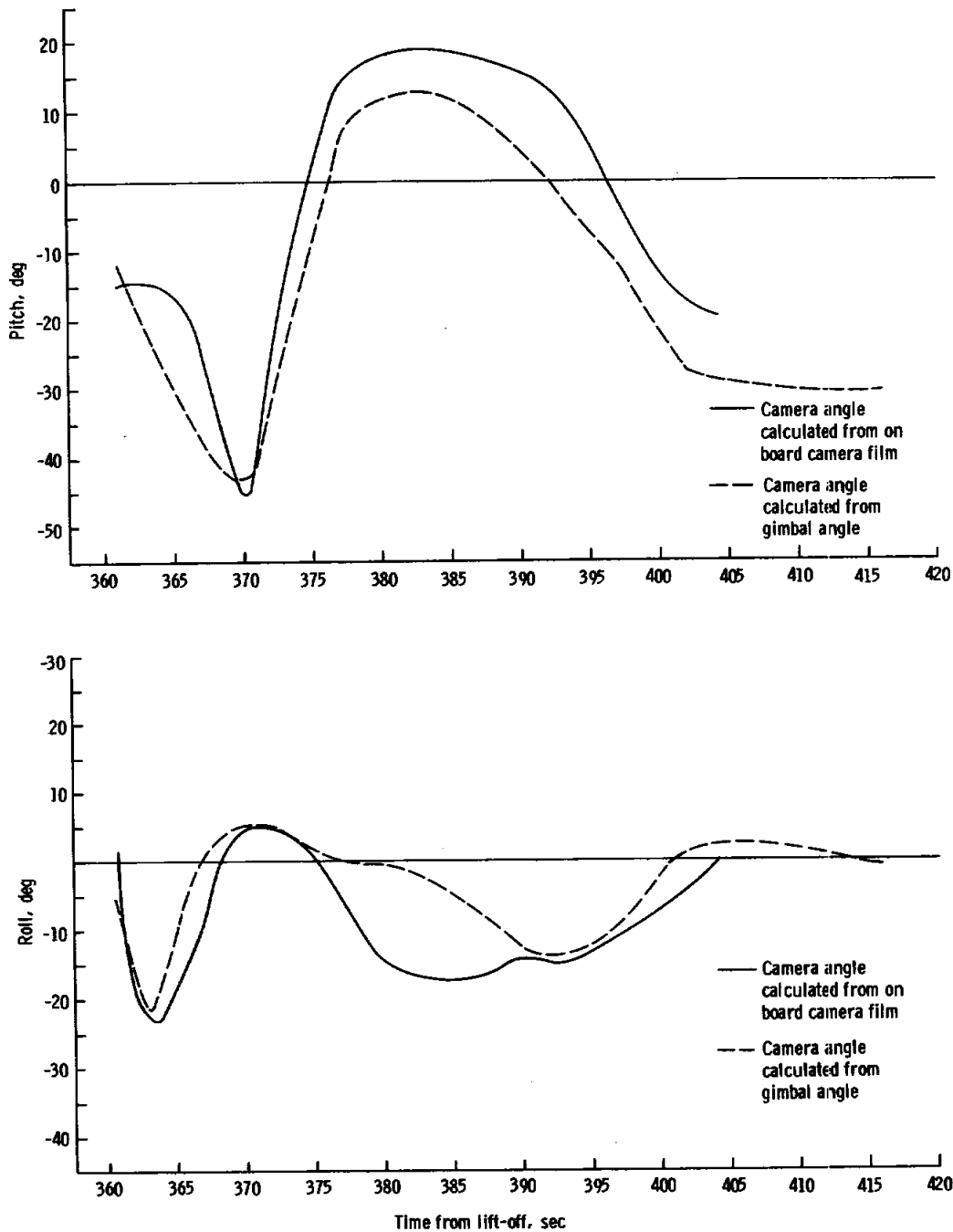


Figure 5.1-48. - Comparison of measured camera angles and camera angles computed from measured platform gimbal angles

NASA-S-65-1960

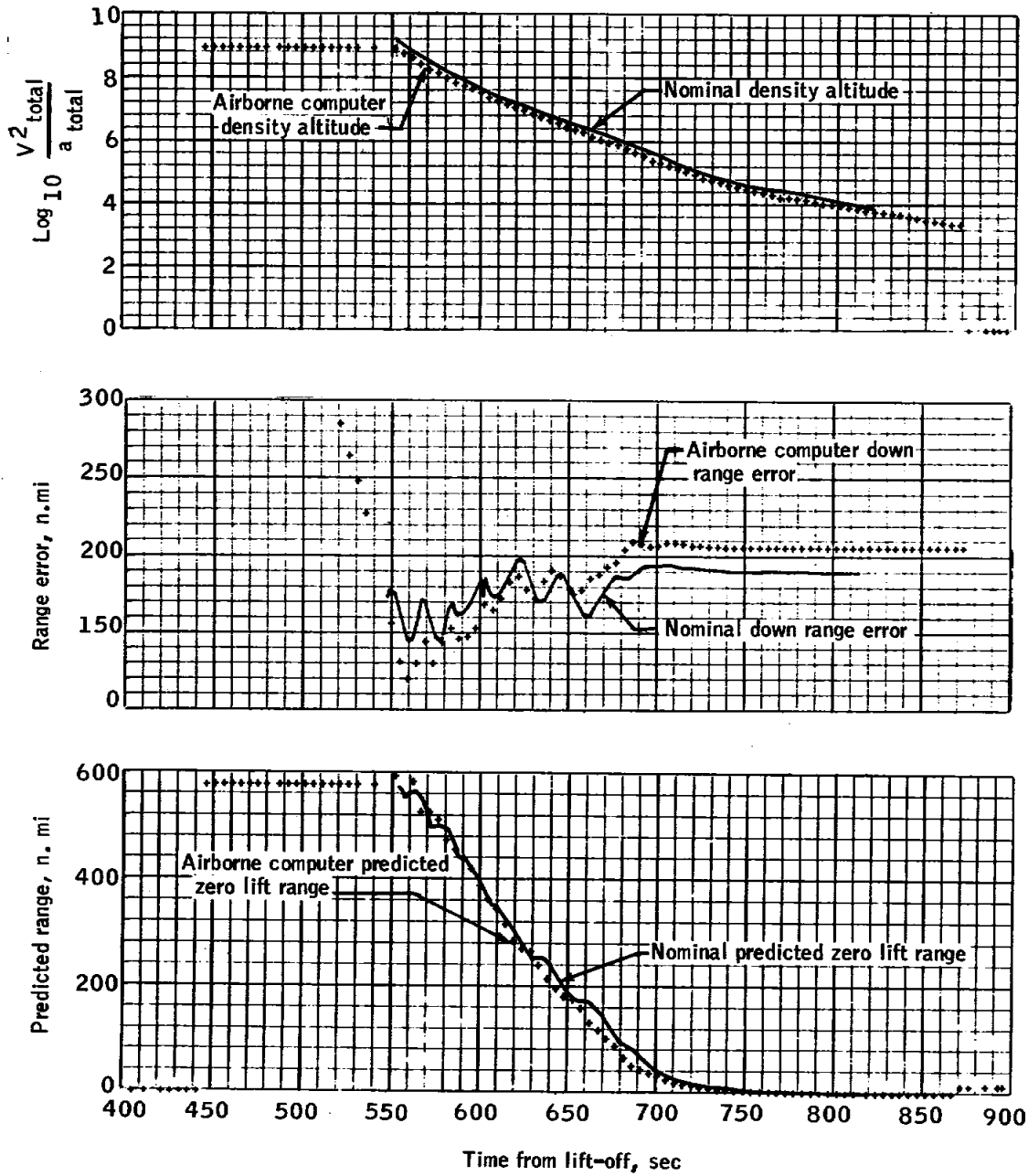


Figure 5.1-49. - Comparison of airborne computer parameters with preflight nominal values

~~UNCLASSIFIED~~

NASA-S-65-1952

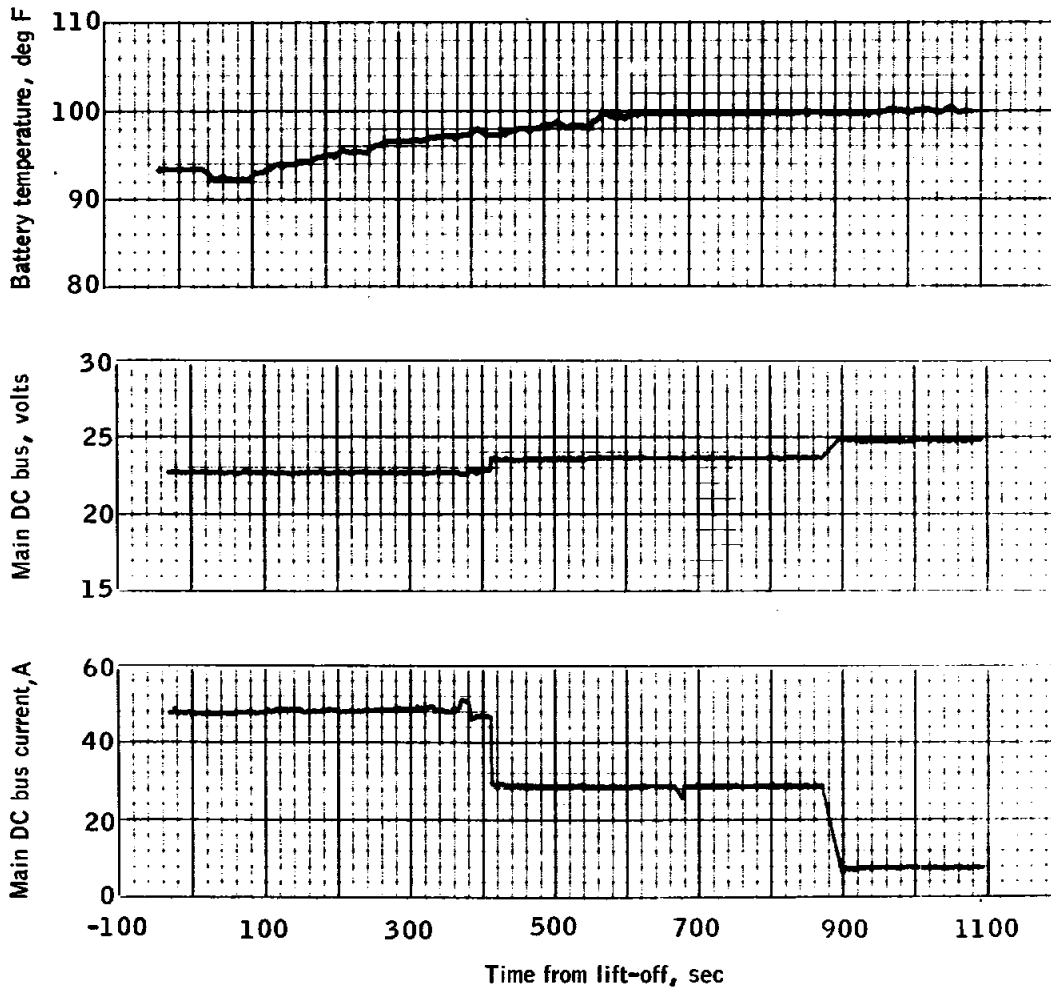


Figure 5.1-50. - Main electrical power system characteristics

~~UNCLASSIFIED~~

NASA-S-65-1954

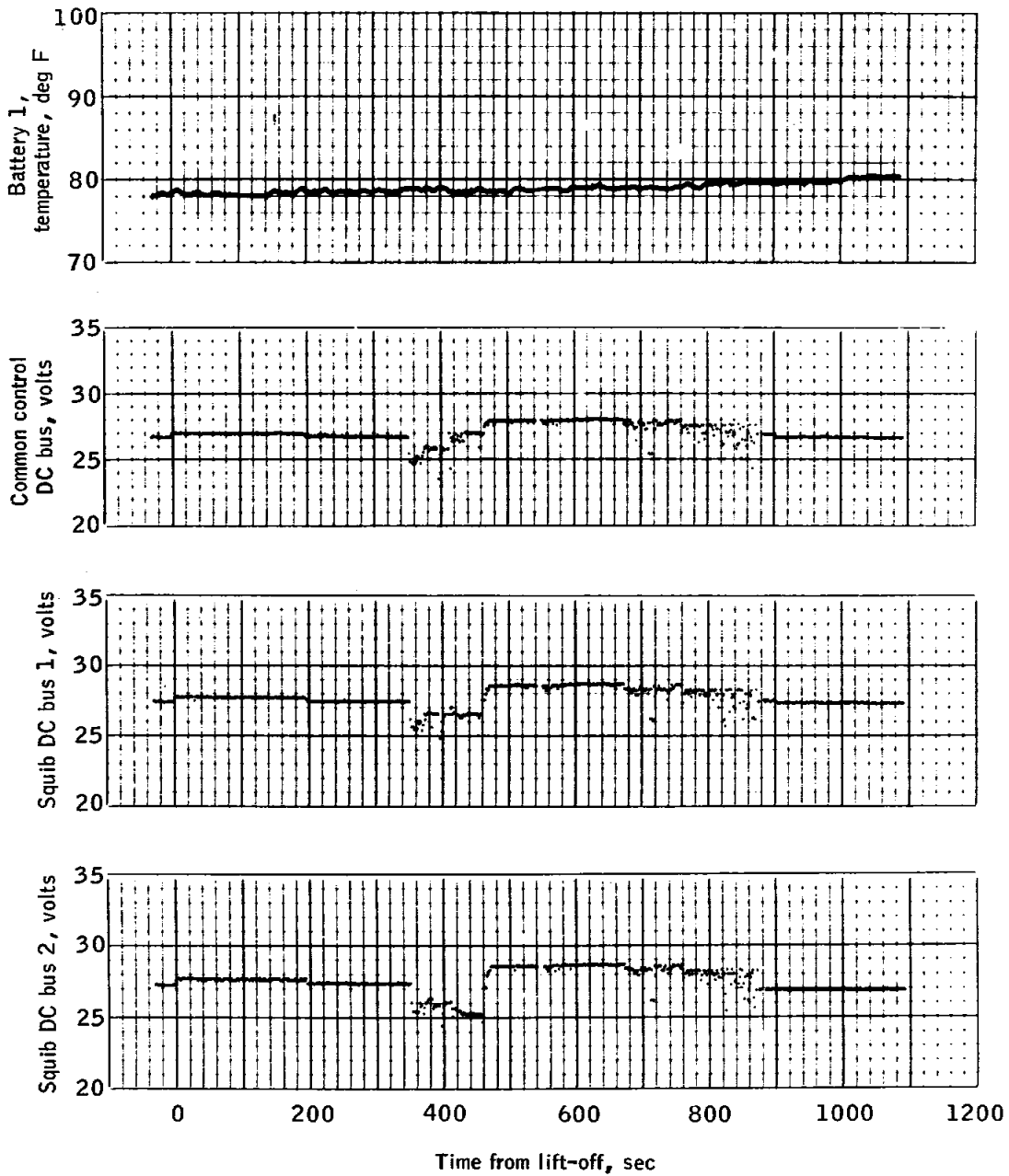


Figure 5.1-51. - Isolated electrical power system characteristics

UNCLASSIFIED

NASA-S-65-1962

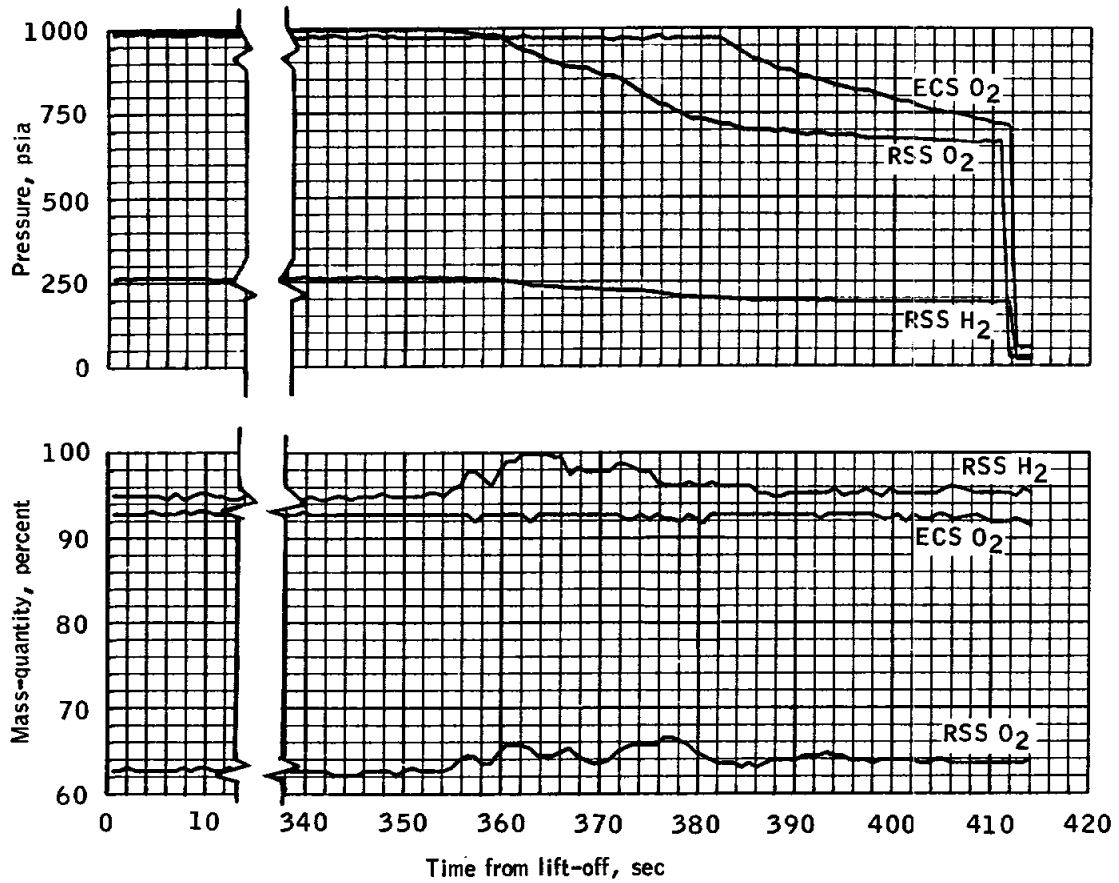


Figure 5.1-52. - Pressure and mass-quantity, cryogenic vessels

UNCLASSIFIED

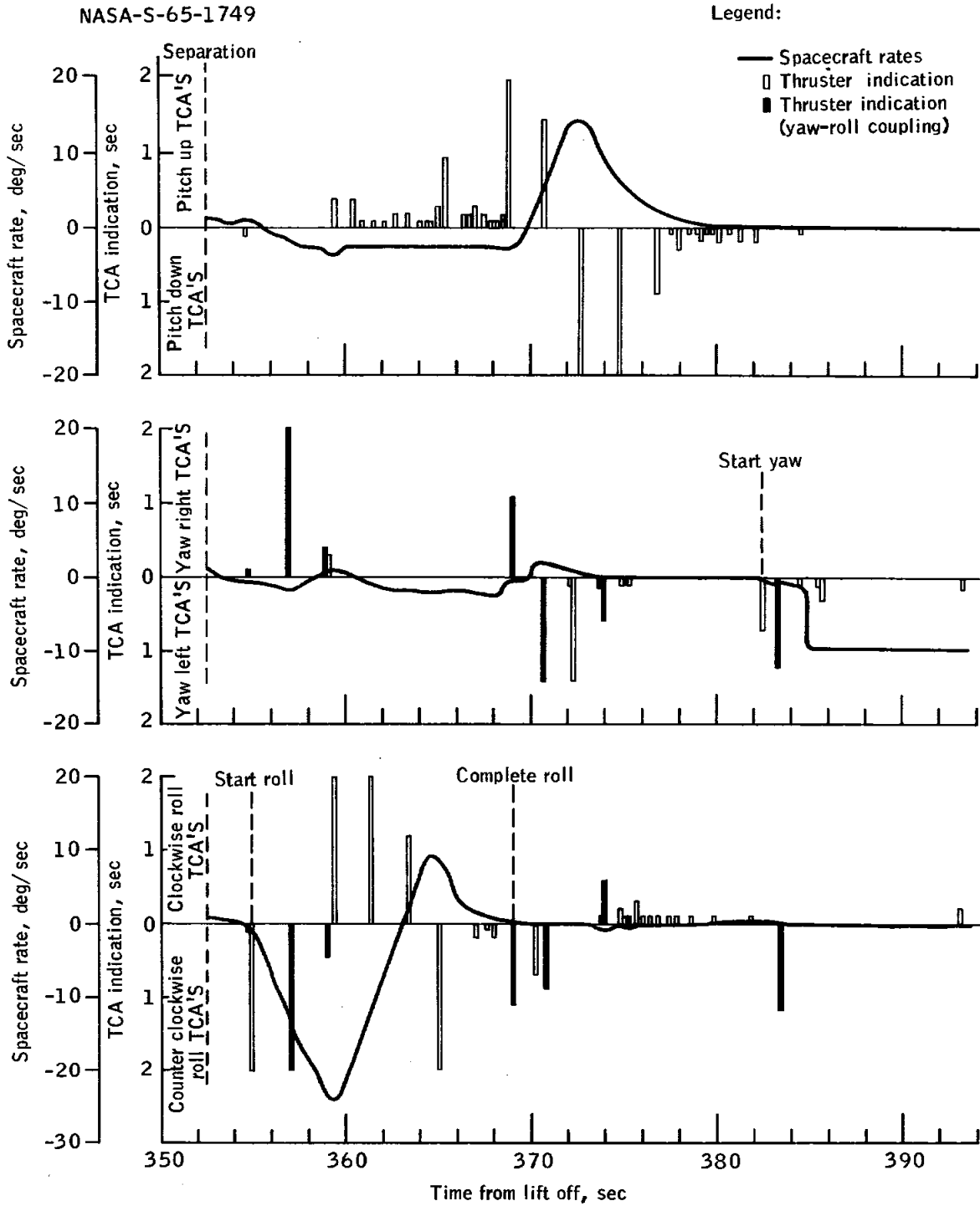


Figure 5.1-53.-OAMS attitude TCA mission duty cycle

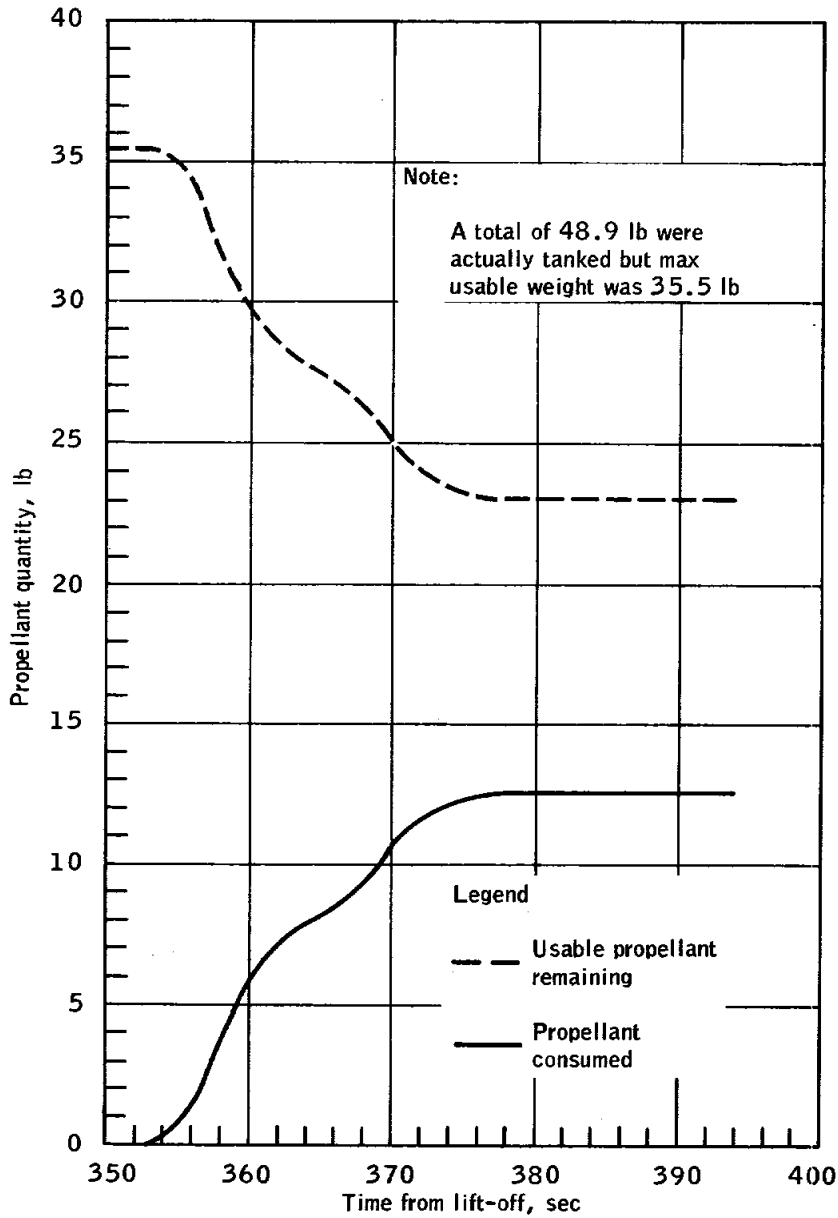
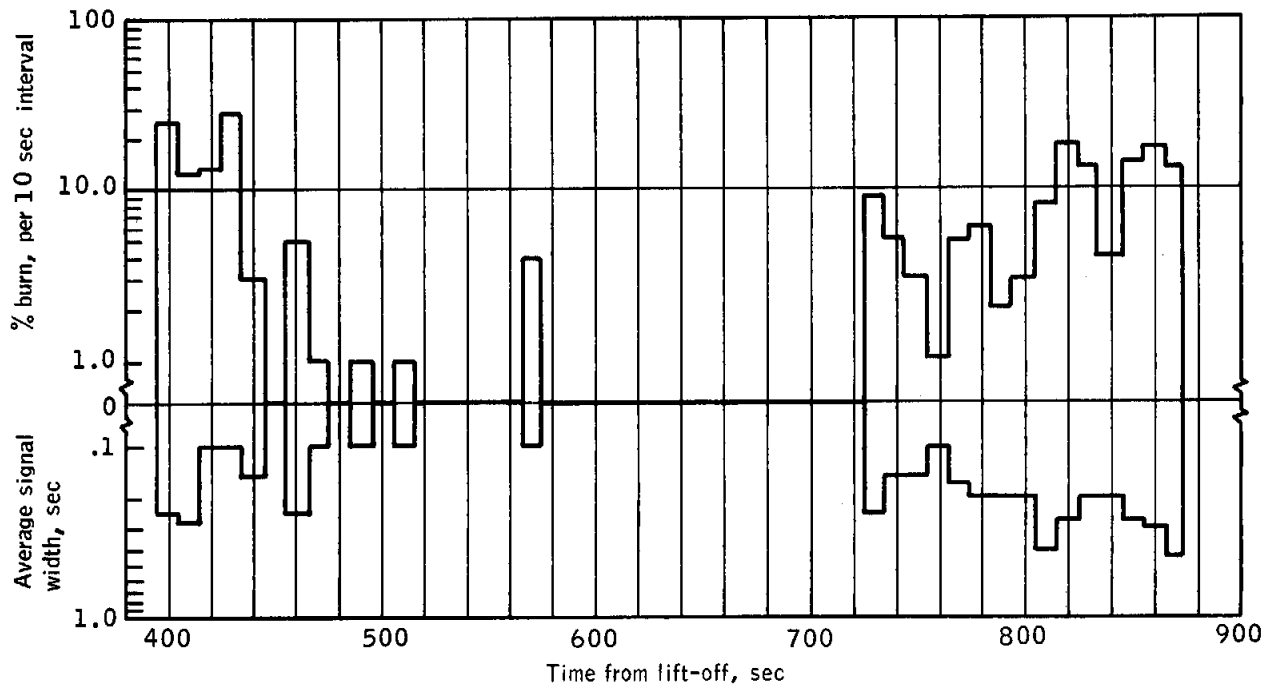


Figure 5.1-54.- Orbital attitude and maneuver system, propellant quantity

UNCLASSIFIED



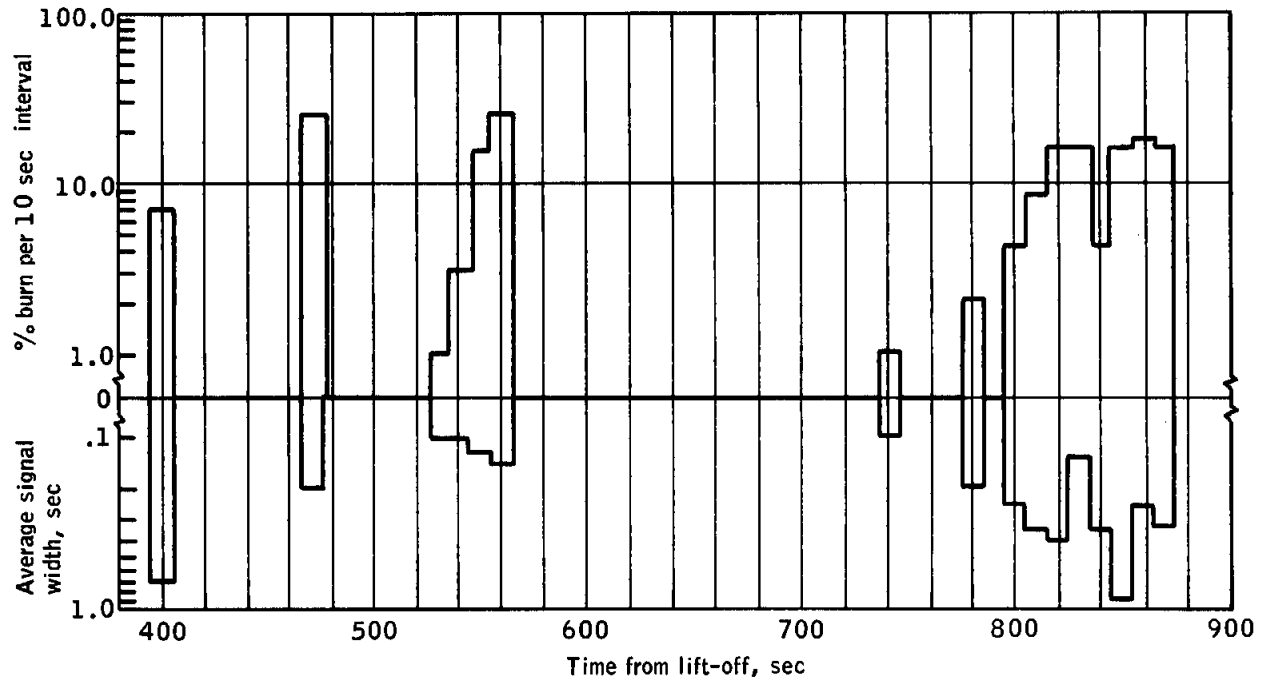
(a) Pitch up

Figure 5.1-55. - RCS ring A and B TCA mission duty cycle

UNCLASSIFIED

UNCLASSIFIED

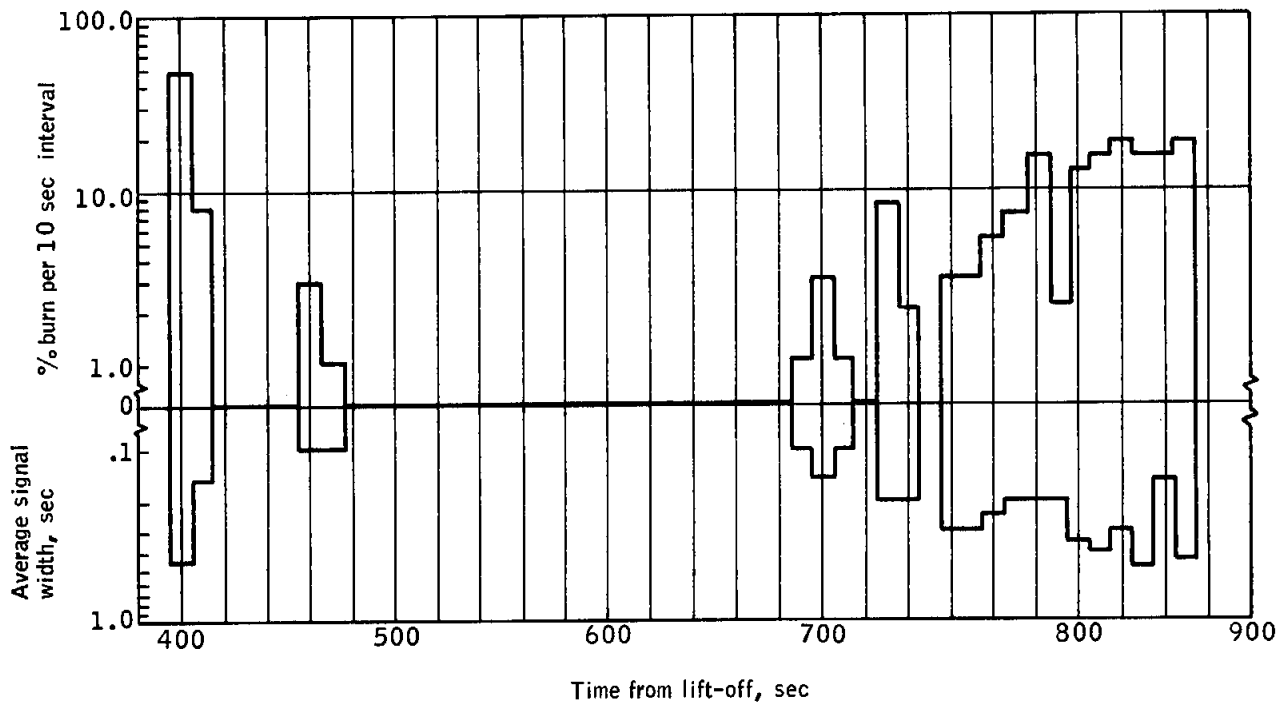
UNCLASSIFIED



(b) Pitch down

Figure 5.1-55. - RCS ring A and B TCA mission duty cycle
(Continued)

UNCLASSIFIED



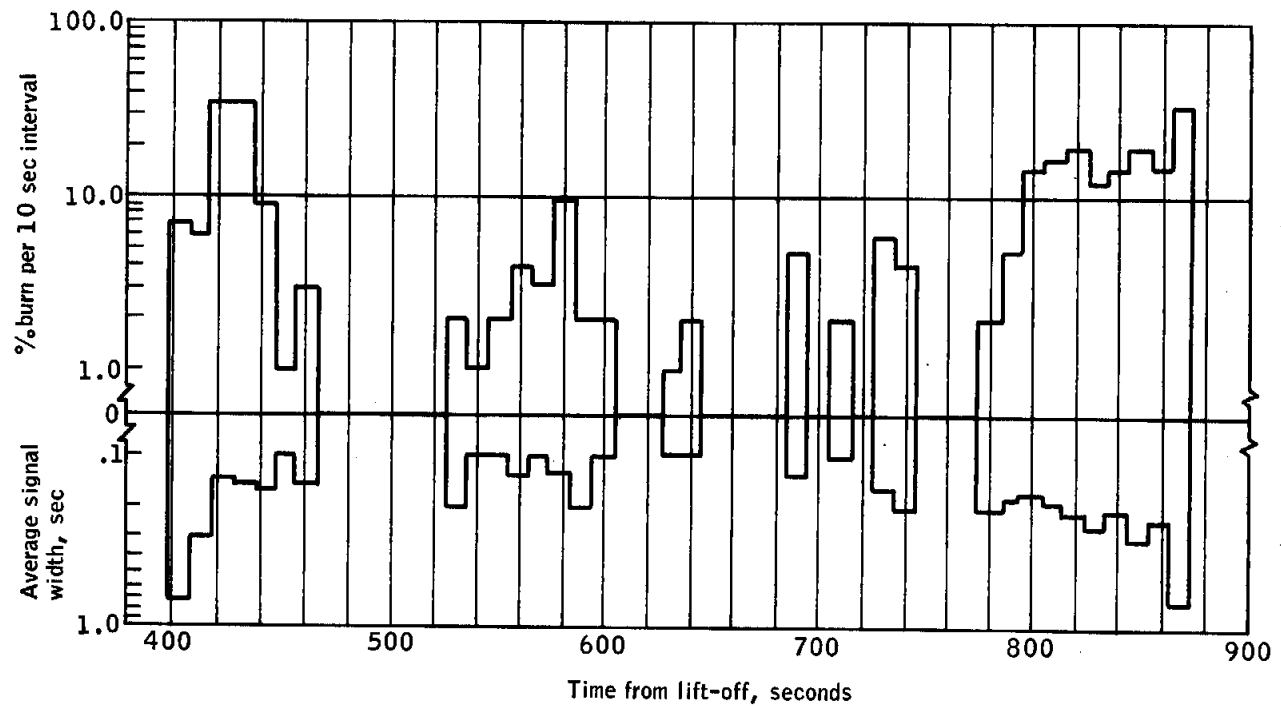
(c) Yaw right

Figure 5.1 - 55.- RCS ring A and B TCA mission duty cycle
(Continued)

UNCLASSIFIED

UNCLASSIFIED

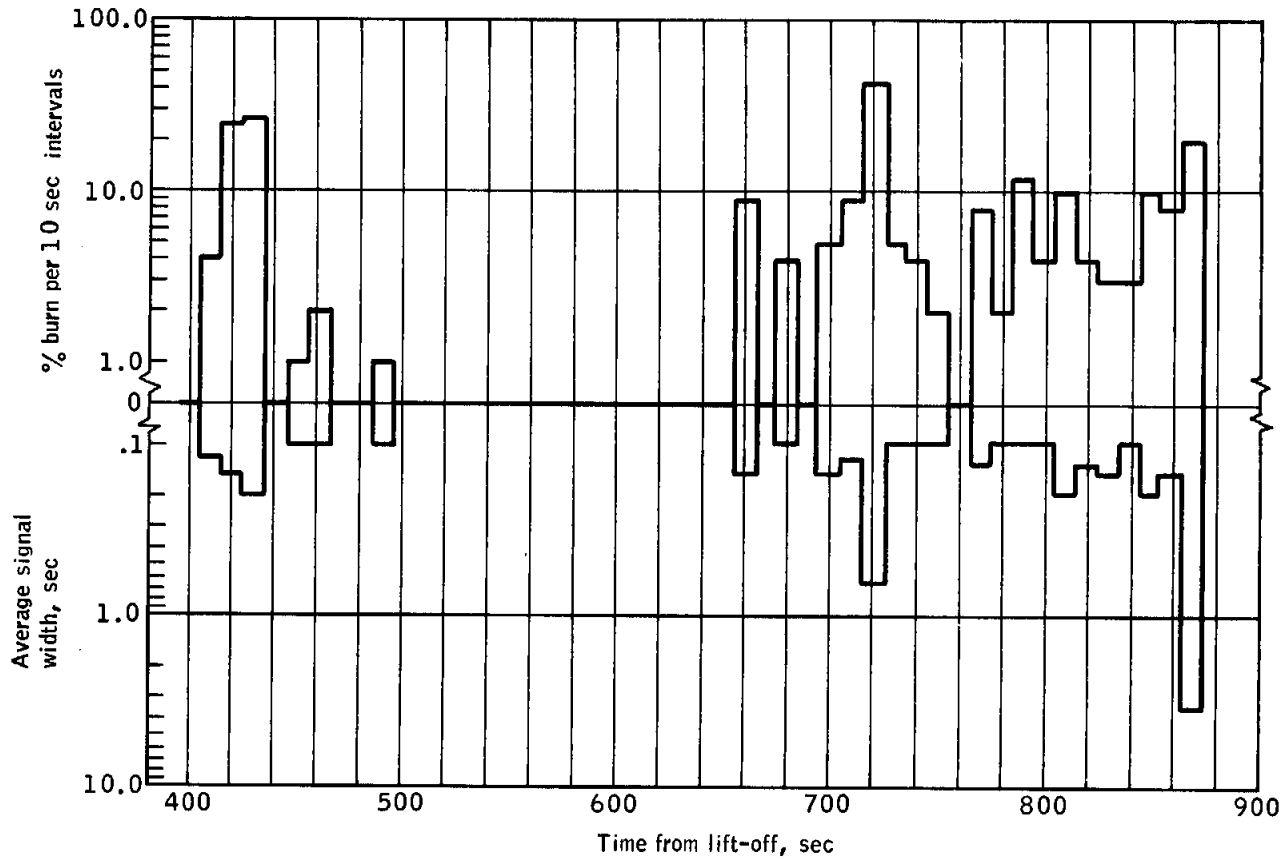
UNCLASSIFIED



(d) Yaw left

Figure 5.1 -55 - RCS ring A and B TCA mission duty cycle
(Continued)

UNCLASSIFIED



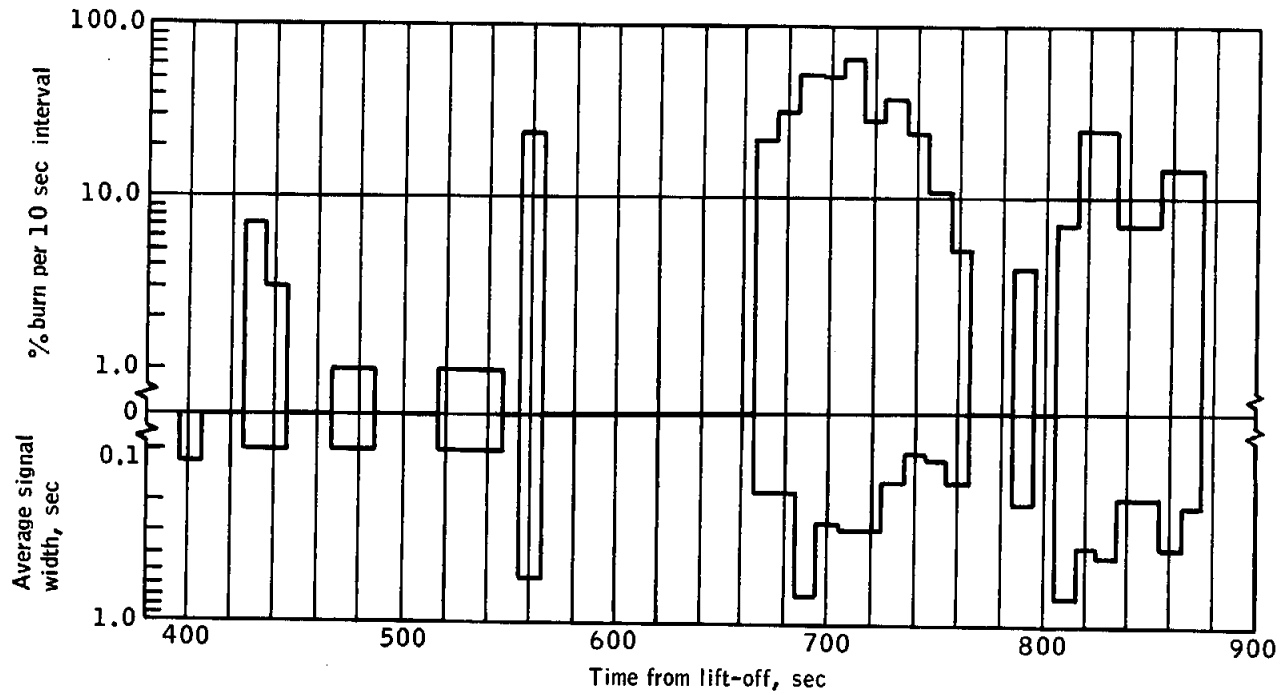
(e) Roll right

Figure 5.1-55. - RCS ring A and B TCA mission duty cycle
(Continued)

UNCLASSIFIED

UNCLASSIFIED

UNCLASSIFIED



(f) Roll left

Figure 5.1-55. - RCS ring A and B TCA mission duty cycle
(Concluded)

UNCLASSIFIED

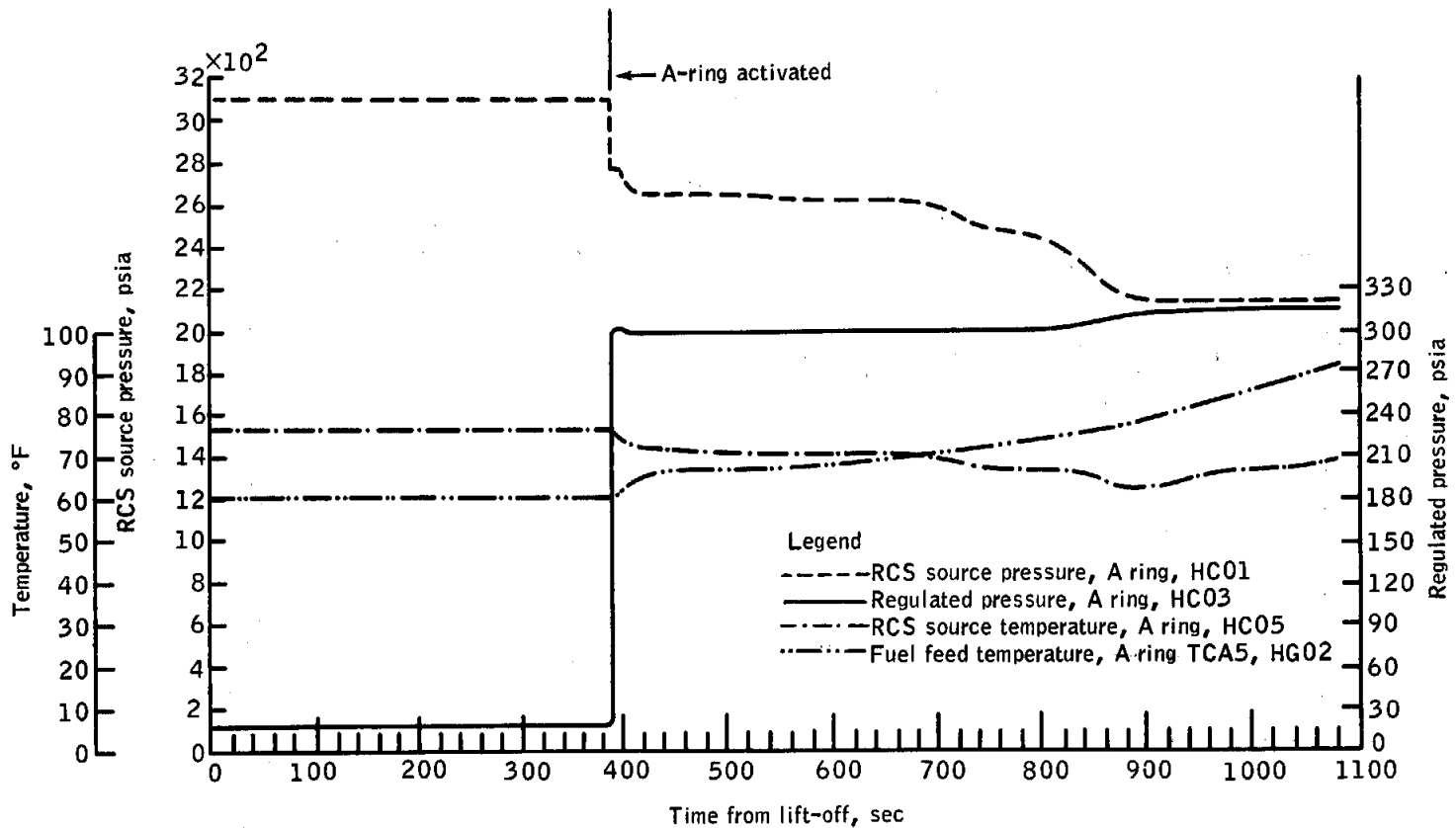


Figure 5.1-56.- RCS A ring performance

UNCLASSIFIED

UNCLASSIFIED

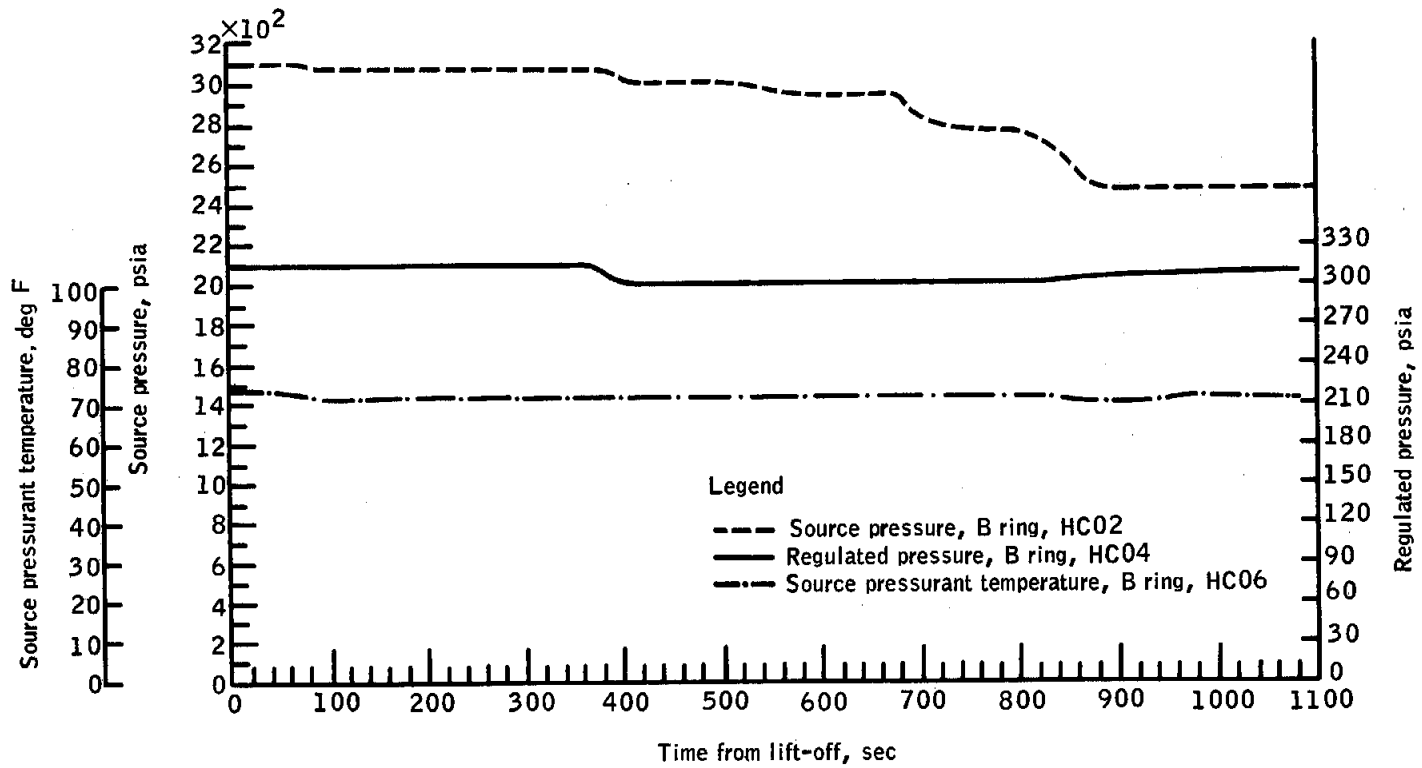


Figure 5.1-57. - RCS B ring performance

UNCLASSIFIED

NASA-S-65-1801



Figure 5.1-58.- Wire bundle guillotine

UNCLASSIFIED

NASA-S-65-1804

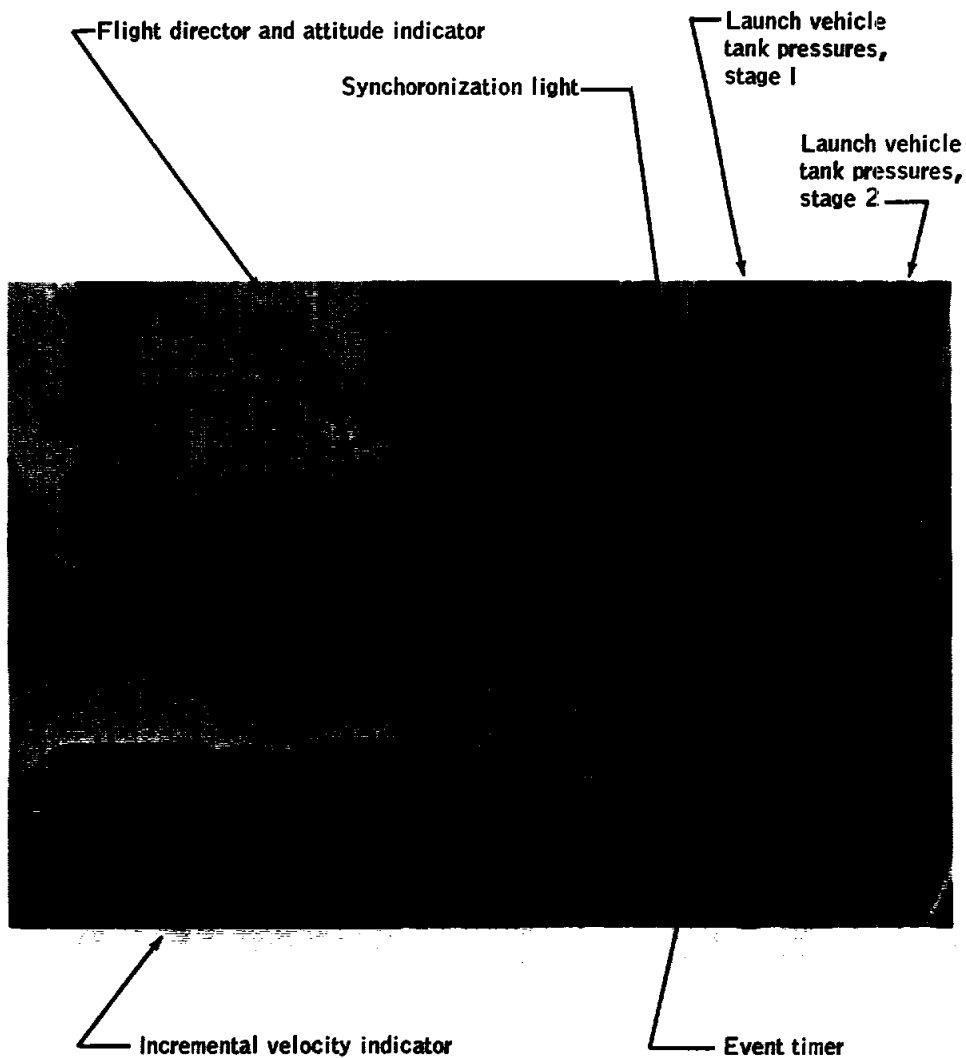


Figure 5.1-59. - Command pilot's instrument panel

NASA-S-65-1826

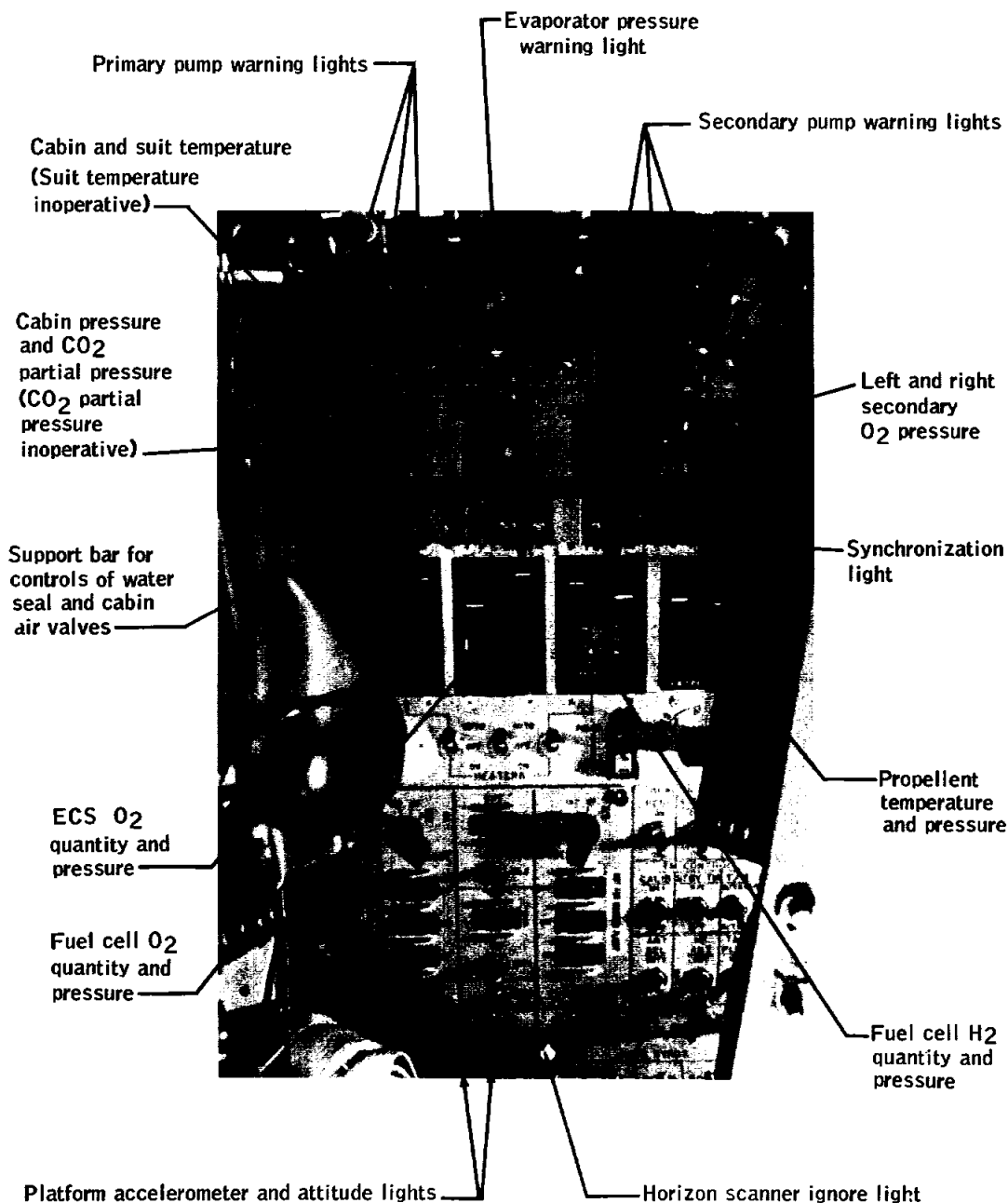


Figure 5.1-60. - Center instrument panel

NASA-S-65-1827

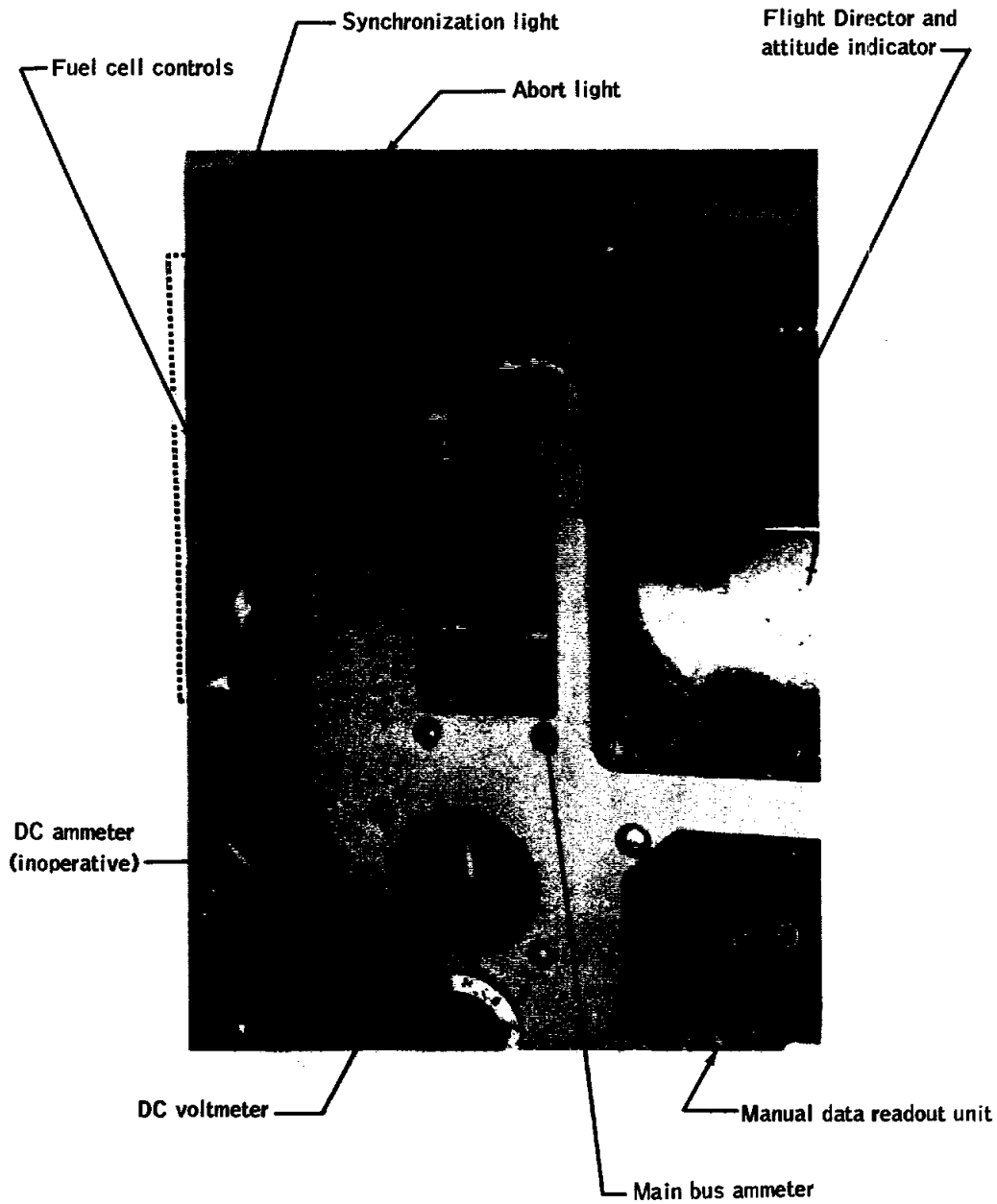


Figure 5.1-61. - Pilot's instrument panel

UNCLASSIFIED

5-147

NASA-S-65- 2285

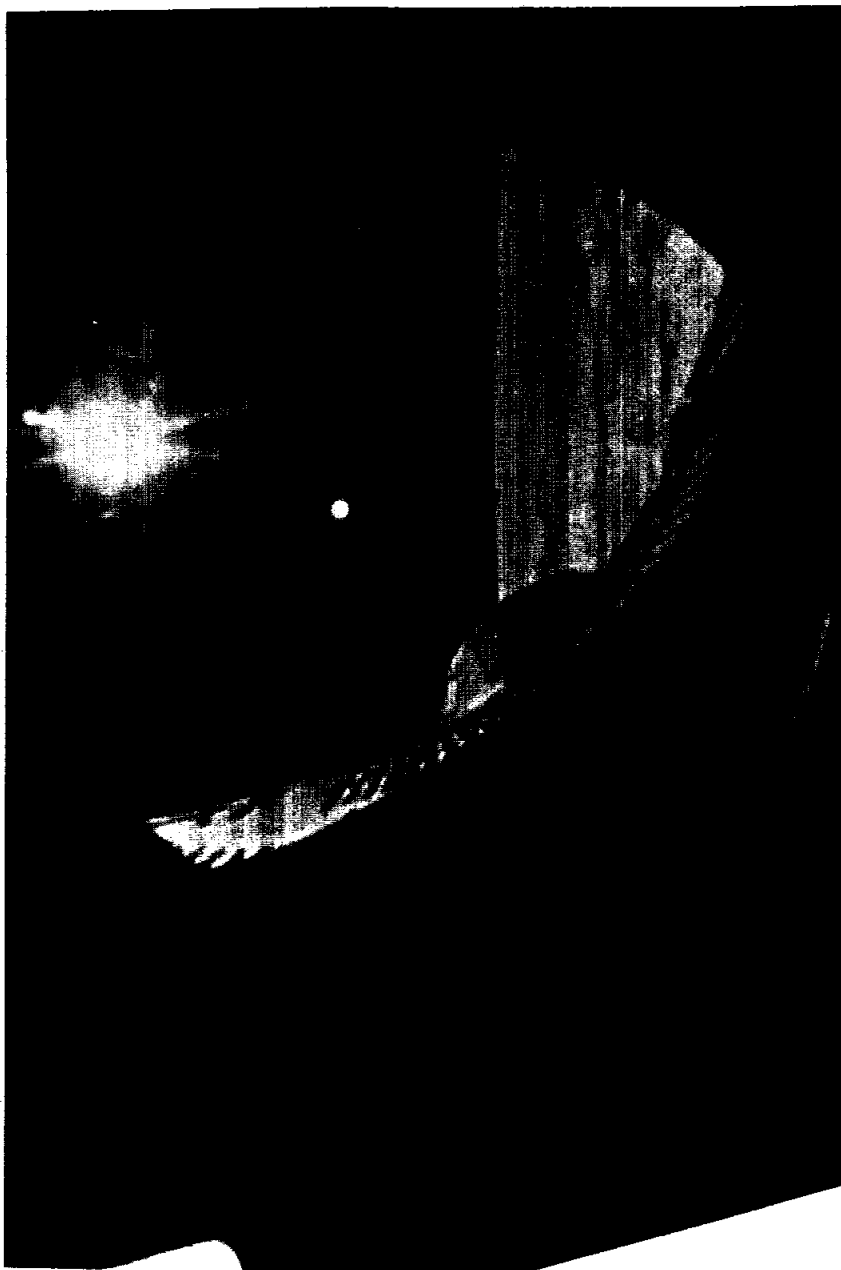


Figure 5.1-62. - Window view - spacecraft separation from the launch vehicle at lift-off +352 sec

UNCLASSIFIED

NASA-S-65-2286

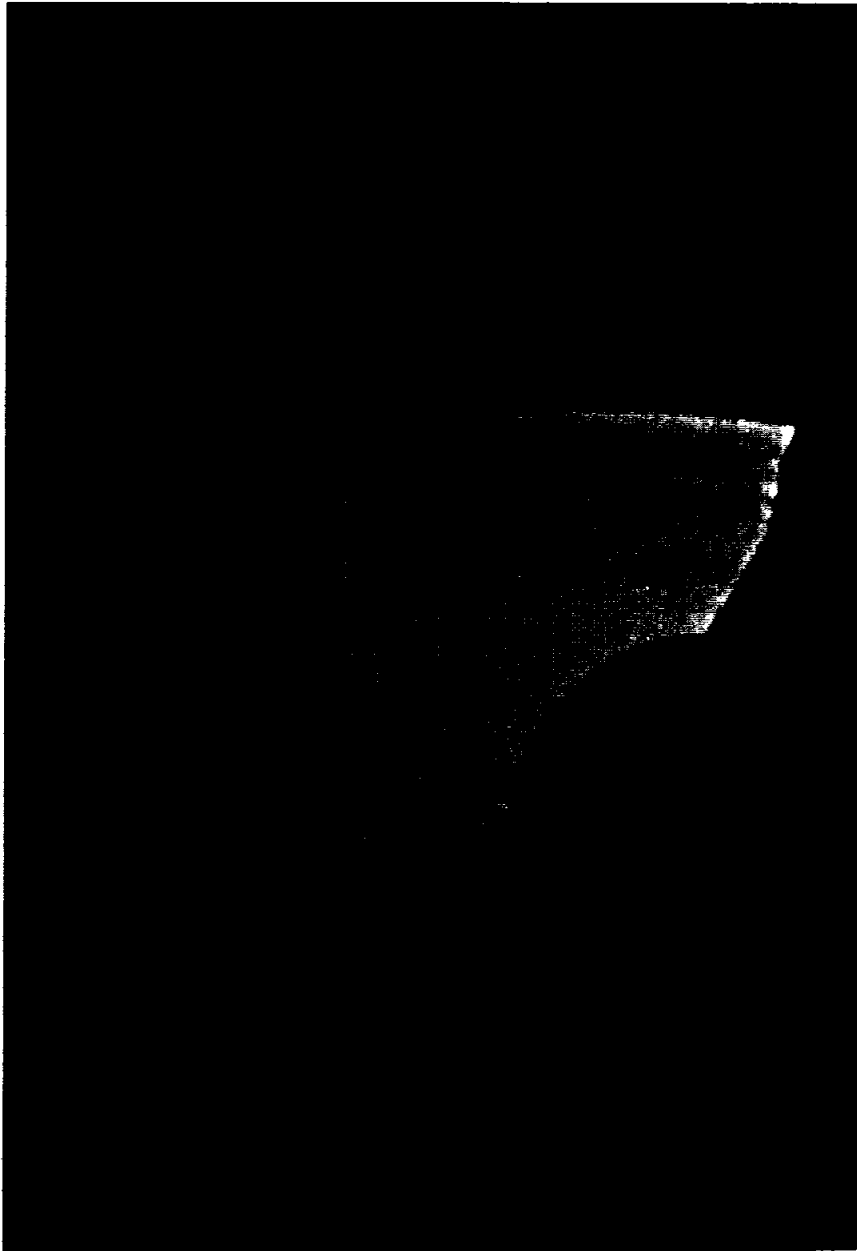


Figure 5.1-63. - Window view - Retrograde maneuver at lift-off +414 sec

NASA-S-65- 2287

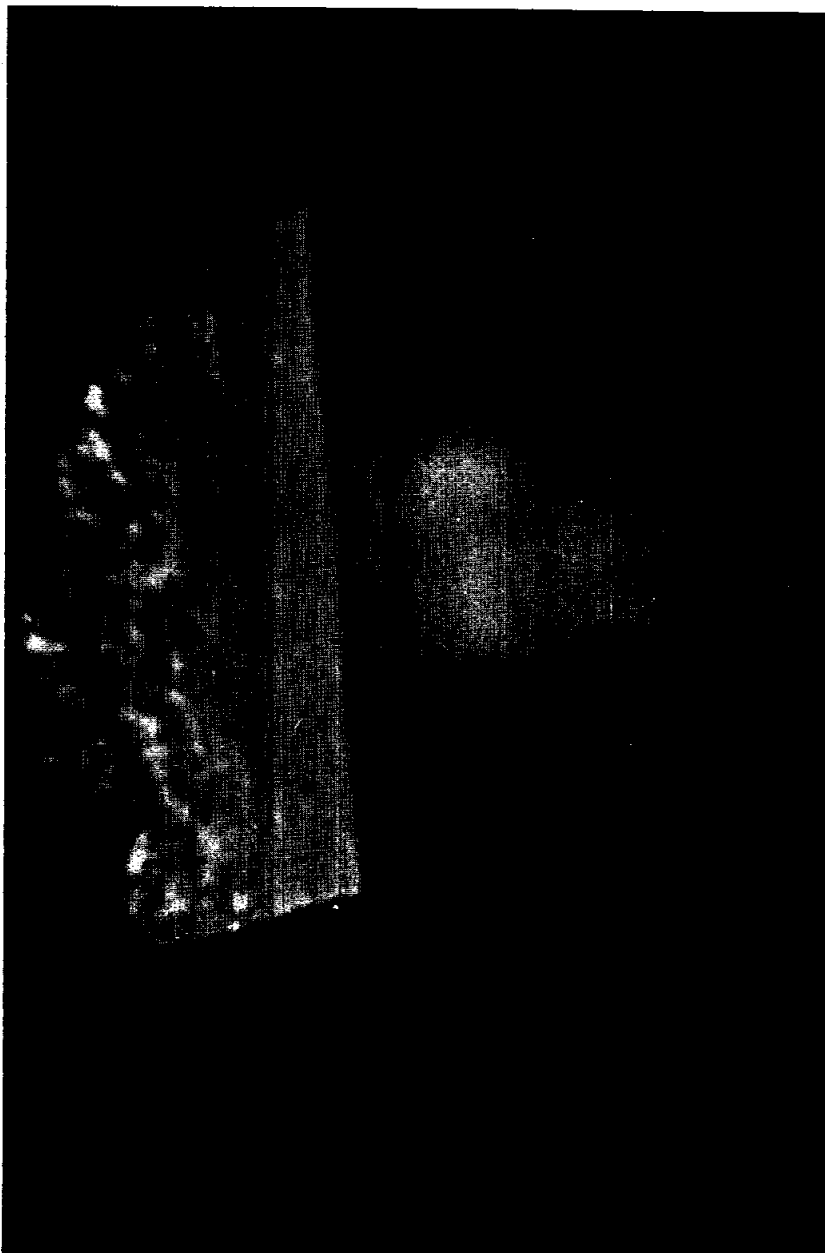


Figure 5.1-64. - Window view - typical ionization effects during constant roll reentry

NASA-S-65-2288

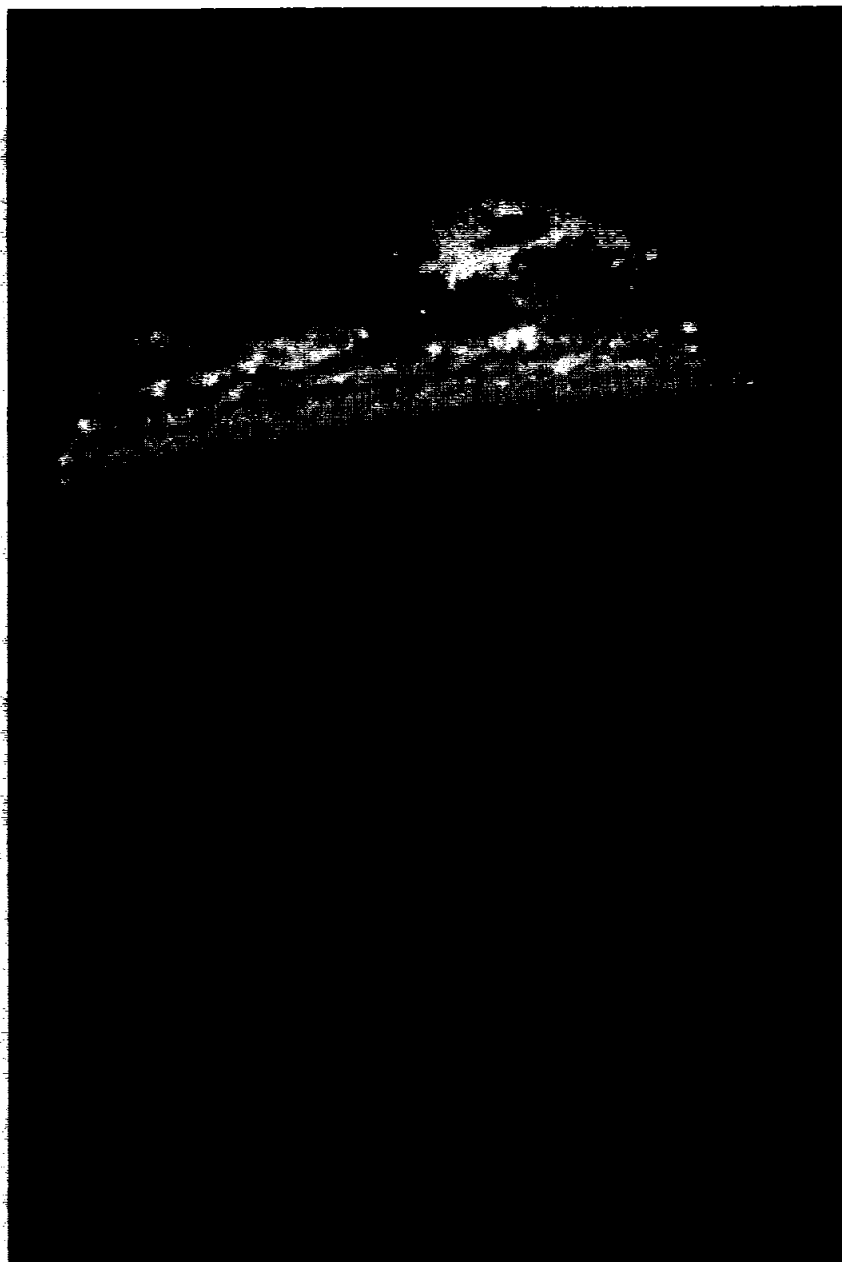


Figure 5.1-65. - Window view - commencement of maximum lift reentry at lift-off +717 sec

UNCLASSIFIED

5-151

NASA-S-65-2289

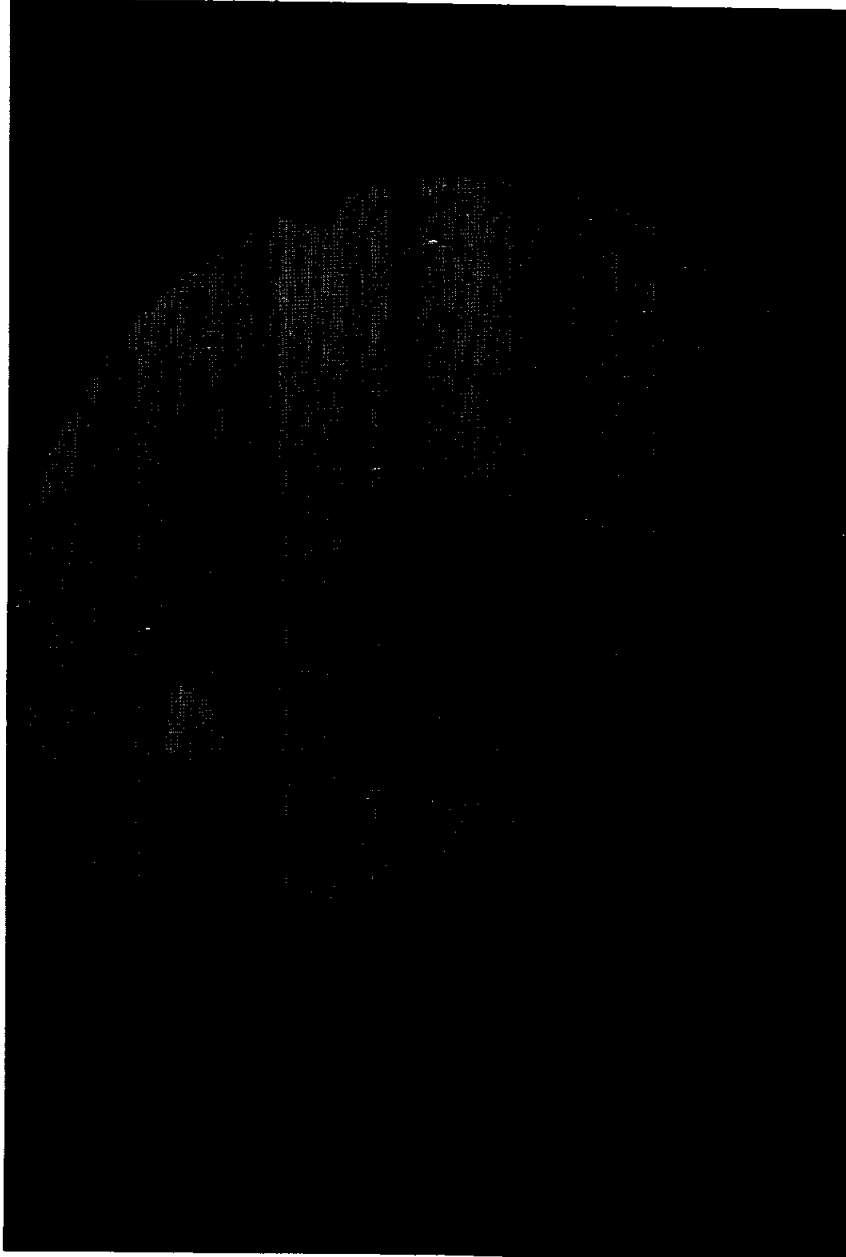


Figure 5.1-66. - Window view - rendezvous and recovery section separation from the spacecraft at lift-off +876 sec

UNCLASSIFIED

NASA-S-65-2290



Figure 5.1-67. - Window view - parachute deployed and starting two point suspension

UNCLASSIFIED

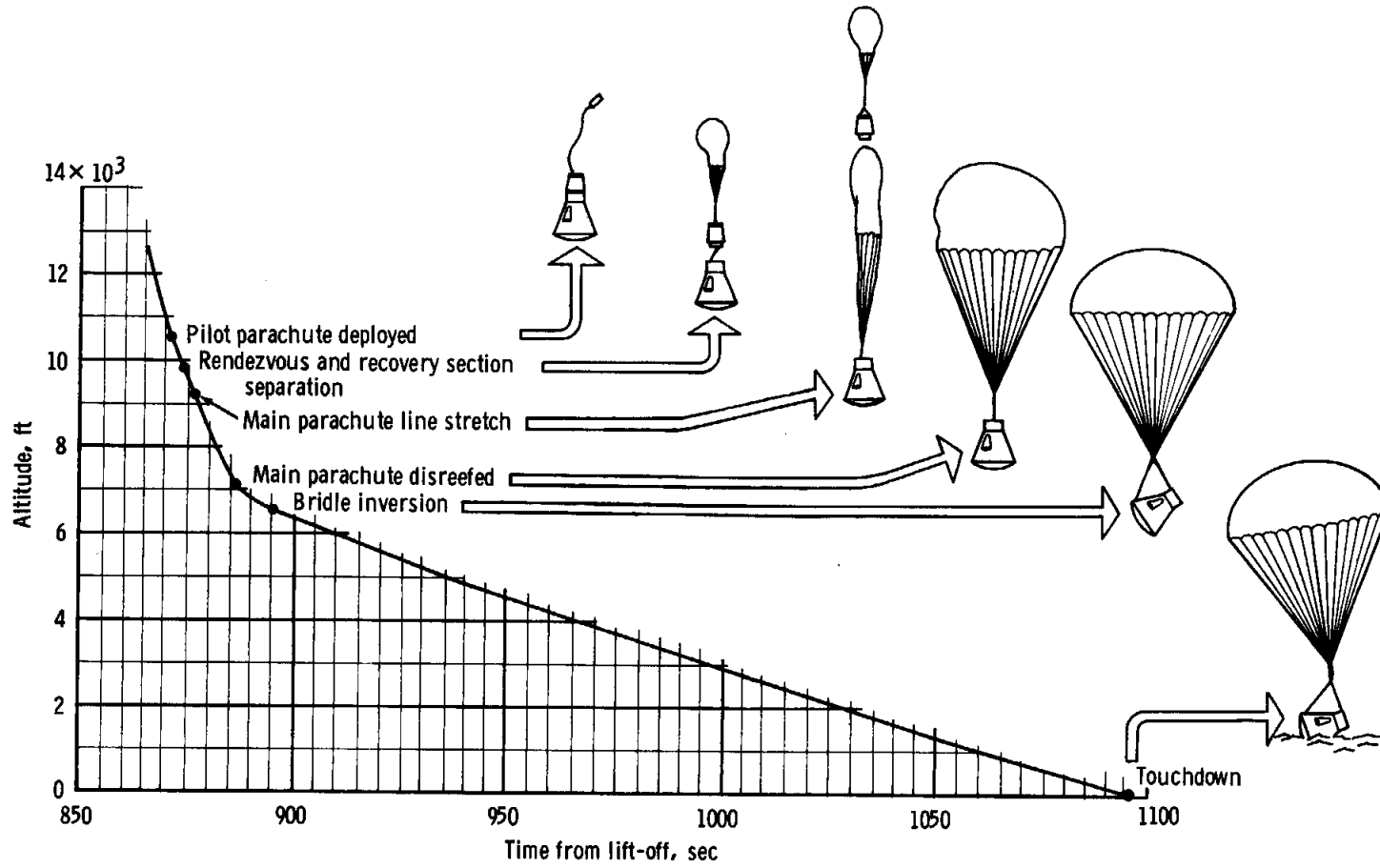


Figure 5.1-68. - Landing system performance

UNCLASSIFIED

5.2 LAUNCH VEHICLE PERFORMANCE

On the GT-2 mission the performance of the launch vehicle was satisfactory and served to further demonstrate the ability of the vehicle to place the spacecraft into a prescribed trajectory. The achieved payload capability was 10⁴2 pounds greater than the weight of the spacecraft which it carried aloft.

In the following subsections the performance of the individual launch vehicle systems is discussed and deviations from normal performance are noted and evaluated.

5.2.1 Airframe

Time periods of primary concern for the launch-vehicle structure occur at engine ignition, maximum airload ($\max \alpha C_N$), and first stage cut-off (BECO). Analysis of available GT-2 data indicates that the flight environment was within vehicle design requirements, and that flight loading was well within structural capabilities of the launch vehicle. Specific areas of interest are discussed in detail in the following paragraphs.

5.2.1.1 Longitudinal oscillation. - A longitudinal oscillation instability, characterized by a sustained 11 cps oscillation, was observed on Titan II flights during stage I operation. GT-2 was equipped with the same surge suppression devices on the propellant feedlines that were successful in damping these oscillations on GT-1. The response was similar to GT-1. The maximum longitudinal oscillation at the spacecraft - launch-vehicle interface was $\pm 0.165g$ at 11.5 cps (fig. 5.2-1).

Longitudinal oscillations were measured on the spacecraft bulkhead where crew seats were attached (QA11) and at launch vehicle station 280 (0670). Figure 5.2-2 presents a comparison of these spacecraft and launch-vehicle measurements. The trend in the values shown are in fair agreement except in the pre-BECO area where spacecraft accelerations peaked at $\pm 0.27g$ and launch-vehicle accelerations peaked at $\pm 0.165g$. Response frequencies for both locations were 18 cps. Spacecraft acceleration amplitudes are expected to be somewhat larger than those in compartment 1 of the launch vehicle because of the longitudinal mode shape. The variation of amplitude ratios (the ratio of spacecraft measurement QA11 to launch vehicle measurement 0670) shown in figure 5.2-2 indicates an amplification factor of two through the spacecraft structure. This factor was also shown in the results of spacecraft 2 vibration tests performed by the spacecraft contractor and is of significance since

~~UNCLASSIFIED~~

future Gemini flights will have longitudinal acceleration measurements only in the launch vehicle.

5.2.1.2 Structural loads.- Ground winds were approximately 9 mph during countdown of GT-2, resulting in small amplitude response of wind-induced oscillation and only 100 000 in.-lb bending moment at launch vehicle station 1224. (The allowable bending moment is 6 790 000 in.-lb.) Structural transients at ignition were approximately the same as those observed on GT-1. Accelerations in compartment 5 were approximately $\pm 0.80g$ and $\pm 0.90g$ in the lateral and vertical planes, respectively. Maximum quasi-steady loads of the maximum α flight condition occurred at 70 seconds after lift-off and reached a value of approximately 50 percent of ultimate design load. Normally, loading of this magnitude would not be encountered; however, winds aloft during the GT-2 flight caused relatively high aerodynamic loads. Wind profiles for GT-1 and GT-2 are shown in figure 5.2-3 for comparison. GT-1 experienced only 32-percent loading.

Filtered responses of spacecraft accelerometers (measurement numbers QA09, QA10, QD10, and QD11) and transfer functions developed from lateral vibration modal parameters were used to determine the vehicle lateral vibratory bending moments shown in figure 5.2-4. The resulting transient responses which occurred during boost flight were primarily associated with the first two structural bending modes (fig. 5.2-5). Responses in higher frequencies (12 cps to 25 cps) were apparent; however, additional data analysis is required in order to identify these responses with specific vehicle modes. Peak modal moments shown in figure 5.2-6, with reference to flight time, and again in figure 5.2-7, with reference to Mach number, show that maximum response occurred in the transonic region. These data indicate that peak bending moments resulting from the transients occurred prior to the maximum quasi-steady load condition. A dynamic bending moment of only 165 000 in.-lb was produced at station 935 (critical launch vehicle station), shown in figure 5.2-4, during the maximum α condition as compared with 290 000 in.-lb predicted from wind-tunnel data.

Structural loading for the BECO condition was primarily the result of direct axial acceleration, longitudinal oscillations, and lateral structural responses. Axial acceleration was 5.7g which is about 1.7 percent below the maximum dispersed value of 5.8g. Longitudinal oscillations were $\pm 0.27g$ at spacecraft station 104 (measurement QA11) at 18 cps. Lateral structural response, associated primarily with the engine mode, was $\pm 0.23g$ at 17.8 cps. The combined effects of these loads produced 276 400 pounds equivalent axial compression load at station 320 (critical launch vehicle station). A margin of safety, based on the tested strength of 380 000 pounds, is 37 percent.

~~UNCLASSIFIED~~

5.2.1.3 Vibration environment. - Two high-frequency vibration measurements were made on the GT-2 launch vehicle:

(a) Measurement 1190

location - tandem actuator 2-1
sensitive axis - actuator axial
frequency range - 20 cps to 1200 cps

(b) Measurement 1697

location - RGS mounting
sensitive axis - lateral
frequency range - 20 cps to 2000 cps

Measurement 1190 had been oriented laterally with reference to the actuator axis on the GT-2 launch attempt; however, it was reoriented to the actuator axial direction to support actuator travel data at ignition because of the previous failure.

The acceleration spectral density analyses performed at various times in the boost flight have shown that the GT-2 vibration environment was well within qualification requirements for both of these measurements. The resulting maximum g_{rms} values for these measurements were $1.96g_{rms}$ at the radio guidance system (RGS) mounting as compared with $14.3g_{rms}$ of the qualification spectrum, and $8.54g_{rms}$ on the tandem actuator as compared with $54g_{rms}$ of the qualification spectrum.

5.2.1.4 Forward skirt heating. - The outer surface of the launch-vehicle forward skirt was protected from excessive aerodynamic heating, caused by spacecraft protuberances, by an ablative coating of 0.05-inch sprayed-on silicone rubber. The ablative coating thickness was reduced from 0.10 inch used on GT-1 so that a trend of increasing temperatures could be established and the thermal protection could be removed if protuberance heating did not exist. Thermocouples on the inner surface of the skin of the launch-vehicle forward skirt, aft of the fairings over interface lugs and attitude control nozzles, measured a maximum temperature of 150° F. Figure 5.2-8 compares the highest measured temperature with predicted temperatures with and without protuberance heating. Calorimeters, located on the forward skirt, measured a maximum temperature of 190° F as compared with a predicted calorimeter temperature of 186° F without protuberance heating. It is evident from these data that

~~CONFIDENTIAL~~

protuberances on the spacecraft adapter will not cause excessive heating of the launch-vehicle forward skirt and that consideration should be given to the complete removal of insulation in this area.

5.2.1.5 Post-SECO pulse.- A pulse occurred during tail-off transient of the stage II engine at SECO + 6.6 seconds. Engine actuators, rate gyro outputs, and accelerometers exhibited transients which damped in approximately 0.5 second. Yaw actuator displacement fluctuated from 0.25 inch to 0.1 inch, and pitch actuator displacement fluctuated from 0.16 inch to 0.11 inch. Lateral acceleration at spacecraft station 104 was $\pm 0.3g$, and longitudinal acceleration was $\pm 0.5g$.

The post-SECO pulse phenomena have occurred on approximately one-third of the Titan II flights, and GT-1 exhibited a similar pulse at 11 seconds after SECO. Since the first observation of this phenomena on Titan II, considerable effort has been expended to determine the cause. However, as of this time, a detailed understanding of the cause is not available.

5.2.2 Propulsion

5.2.2.1 Summary.- A review of available data indicates that first and second stage propulsion system performance was well within specification limits. No anomalies occurred that had any effect on mission success. A thrust overshoot at stage II ignition occurred, but the magnitude and duration are in question because of the characteristics of the particular chamber pressure transducer used on this vehicle. Data from measurement 0699 ($\pm 0.5g$ axial accelerometer) indicate that a post-SECO disturbance, as discussed in section 5.2.1, occurred between LO + 338.75 and LO + 339.10 seconds; but a review of pertinent second-stage engine parameters shows that no corresponding disturbance occurred within the thrust chamber or turbopump assembly (TPA) - gas generator assembly. Table 5.2-I presents some elapsed times pertinent to engine performance.

5.2.2.2 Propulsion system configuration.- The GT-2 launch vehicle employed first-stage engine model number YLR 87-AJ-7 (serial number GLV1003) and second-stage engine model number YLR 91-AJ-7 (serial number GLV2002).

5.2.2.3 Stage I engine performance.- A review of all stage I engine parameters indicates that the overall system performance was close to predicted and that no major engine anomalies occurred. Table 5.2-II provides a comparison of significant flight average propulsion parameters with preflight predicted values. Analysis of these data indicates excellent correlation between specific impulse and mixture ratio.

~~CONFIDENTIAL~~

~~CONFIDENTIAL~~

5-159

Examination of the thrust chamber pressures at engine ignition indicates that both subassemblies experienced starts which were fast, but still within the range of previous experience. Revisions in the start cartridge flow rates were made prior to this flight and are being examined as a possible cause of this situation.

Figure 5.9-2 provides the steady-state engine performance from lift-off to 87FS2 and, as given in table 5.2-II, shows that thrust, oxidizer flow rate, and fuel flow rate were approximately 2 percent higher than predicted (10 500 pounds thrust) throughout stage I operation. Individually, subassembly 1 was approximately 3 percent higher than predicted, and subassembly 2 was approximately 1 percent higher than predicted. An examination of turbopump inlet conditions and the effects of the trajectory indicates that 3800 pounds of the 10 500 pounds is attributable to lower than predicted propellant temperatures and flight ambient pressures and the higher than predicted pump-suction pressures.

An examination of the measured turbine speed, gas generator pressure, propellant pump discharge pressure, and chamber pressure indicates excellent correlation with predicted conditions for subassembly 2; subassembly 1 shows good correlation for turbine speed and gas generator pressure, but measured thrust chamber pressure and propellant pump discharge pressures were slightly higher than predicted. The increase in these parameters on subassembly 1, in conjunction with the inlet condition changes mentioned previously, can account for the higher than anticipated thrust level.

Table 5.2-III presents a comparison of flight engine performance corrected to standard inlet conditions with engine acceptance data at the nominal 87FS1+57-second point. These data indicate that a thrust growth and associated flow rate increase occurred between the final acceptance test and flight. This thrust growth was not associated with shifts in I_{spe} or MR_e .

Traces for fuel-pump discharge pressure for both subassembly 1 and subassembly 2 show a cyclic, pulsating pressure. The gas generator pressure for subassembly 1 also exhibits this characteristic, but to a slightly lesser degree. Pressure fluctuation on subassembly 2 fuel pump discharge pressure $2-P_{pd}$ (the most extreme) reached 250 psi peak-to-peak, while gas-generator pressure fluctuation reached 160 psi peak-to-peak. The cause of these excessive fluctuations and the reasons for their cyclic nature are still being investigated. Neither subassembly 1 nor subassembly 2 chamber pressure nor oxidizer pump discharge pressures exhibited these characteristics.

~~CONFIDENTIAL~~

~~CONFIDENTIAL~~

Engine shutdown transient was normal, with a residual thrust of approximately 19 000 pounds at stage separation. An analysis of the pump discharge and thrust chamber shutdown transients indicates that the planned oxidizer exhaustion shutdown occurred.

5.2.2.4 Stage II engine performance.- The comparison of average preflight predicted with average flight performance parameters presented in table 5.2-IV indicates that the overall engine system performance was close to predicted. A review of the data showed that no major engine anomalies occurred that had any detrimental effect on mission success.

An examination of the stage II engine start transient shows that the chamber pressure did not follow the anticipated form. The initial, expected, chamber-pressure spike is not evident, and the duration of the chamber-pressure overshoot (corresponding to a thrust overshoot) is considerably longer than any that have previously been experienced. A chamber pressure transducer that is known to have poor transient response was used on GT-2, and it is believed that the transient start data for stage II are not accurate. This is supported by the fact that the long thrust overshoot indicated in the chamber-pressure plot is not supported by either oxidizer or fuel-pump discharge pressure or turbine speed.

Steady-state engine performance is shown in figure 5.2-10 and indicates good agreement with preflight predictions. A detailed review of all available engine data indicates that no anomalies occurred during steady-state operation.

Table 5.2-V compares engine flight performance corrected to standard inlet conditions with acceptance data at the nominal 91FS1+57-second point. A review of the data presented in this table shows that engine performance was within the expected range of run-to-run repeatability.

Engine shutdown was effected by guidance command, and integration of the shutdown transient from SECO to SECO+20 seconds yields a shutdown impulse of 44 685 lb-sec. This value compares quite favorably with the launch vehicle contractor's preflight prediction of 43 500±6300 lb-sec. Measurement 0699 shows essentially zero-thrust at SECO+14.55 seconds.

An evaluation of measurement 0699 ($\pm 0.5g$ axial acceleration) indicates that a post-SECO transient occurred at SECO+6.6 seconds. To determine if this disturbance occurred within the thrust chamber or turbopump - gas-generator assembly, the TM parameters monitoring these components were carefully evaluated. This evaluation showed no corresponding disturbances on these channels. Therefore, it is concluded that the post-SECO disturbance did not originate within these components.

~~CONFIDENTIAL~~

This does not, however, preclude the possibility that the disturbance occurred within the engine bell.

5.2.2.5 Pressurization system.- Preflight tank lock-up pressures were as required. In-flight autogeneous system performance was within specification and all vehicle structural requirements and pump net positive suction head (NPSH) requirements were satisfied for both stages.

Actual tank pressures for both stages compared well with the predicted variation with flight time. The stage I fuel tank pressure was approximately 2 psia higher than predicted as a result of a slightly high pressurant gas flow.

5.2.2.6 Propellant system.- Tables 5.2-VI to 5.2-VIII provide pertinent data pertaining to propellant system performance and indicate satisfactory agreement with preflight predictions. Propellant loading data show excellent correlation between requested propellant load and measured flow-meter propellant load.

Good agreement was obtained between all predicted and actual temperatures except the stage I fuel temperature. The low stage I fuel temperature resulted from the propellant in-tank temperature rise rates having been based on a hot September day. Colder than anticipated weather conditions allowed matching only one fuel tank temperature to predictions. Stage II was selected for temperature match.

During the GT-1 flight, stage I and II fuel-tank level sensors showed a false recovered condition in the uncovered mode. Postflight analysis indicated that the most probable cause of this condition was a filming over of the sensor optical prism by autogenous gas. The corrective action proposed for this problem was the use of a shield over the sensor prisms. Of the 12 stage I and II fuel-tank level sensors employed on GT-2, 6 were equipped with the proposed shield. All of these sensors functioned properly. Of the 6 unshielded sensors, 5 uncovered during flight; and of these, 3 displayed erratic operation after uncovering.

Analysis of the stage I shutdown transient indicates that the planned oxidizer depletion shutdown occurred. The actual burn-time margin shown in table 5.2-VIII is in close agreement with the predicted value and indicates that the overall propulsion system performance was in good agreement with preflight predictions.

UNCLASSIFIED

5.2.3 Flight Control System

Analysis of the launch-vehicle flight control system revealed satisfactory operation during stage I and stage II flight. A combination of high engine thrust, gyro drift, and high winds aloft during stage I flight resulted in higher than nominal altitude and velocity at BECO. GT-2 was guided to the desired conditions at SECO. The primary flight control system was in command throughout the flight, and no switchover to the secondary system was required.

5.2.3.1 Lift-off and hold-down transients.- A small roll transient of 0.5 deg/sec was noted approximately $\frac{1}{2}$ second after lift-off and is considered negligible. This transient was caused by thrust misalignment, and induced a $+0.6^\circ$ roll attitude bias through stage I flight. No pitch or yaw transients of significant magnitude were recorded at lift-off. The peak actuator travel, null checks, and rate gyro disturbances recorded during the hold-down period are presented in table 5.2-IX.

5.2.3.2 Roll and pitch programs.- The roll program was initiated and terminated at the proper times, and the correct vehicle roll rate was indicated by the rate gyro.

Start, sec	LO + 4.352
Stop, sec	LO + 20.404
Roll rate, deg/sec	-1.16
Roll transient overshoot, deg/sec . . .	-1.55

The pitch program was initiated and rate changes occurred at the proper times, and the correct vehicle pitch rates were indicated by the rate gyros.

Step	Start time, sec	Pitch rate, deg/sec
1	22.99	-0.66
2	88.07	-0.47
3	118.71	-0.26
4	162.09	End program

UNCLASSIFIED

5.2.3.3 Stage I flight.- During stage I flight, the vehicle experienced wind disturbances with peaks at 10 + 78 and 10 + 114 seconds. Maximum rates and attitude errors recorded during this time are given in table 5.2-X.

Figures 5.2-11, 5.2-12, and 5.2-13 show the effect of the wind disturbances on the vehicle attitude. The flight control system responded normally to these disturbances. Close correlation between the primary and secondary flight control systems were noted during stage I flight.

5.2.3.4 Stage separation.- During the staging sequence, normal transients were encountered as expected due to ignition of the second stage engine. Telemetered data showed proper flight control system operation during this period of flight. The maximum rates recorded at BECO plus 2.7 seconds were as follows:

Pitch, deg/sec	-0.68
Yaw, deg/sec	+1.21
Roll, deg/sec	-0.50

All separation transients were over before BECO + 3 seconds. The maximum vehicle attitudes recorded after the staging sequence were as follows:

Pitch (at BECO + 3.29 sec), deg . . .	-0.23
Yaw (at BECO + 4.0 sec), deg	+1.25
Roll (at BECO + 4.0 sec), deg	-0.21

5.2.3.5 Control system biases.- Just prior to radio guidance initiate, the flight control system indicated gyro displacement bias in both pitch and yaw. These biases, caused by the second stage thrust misalignment, were expected and were similar to the biases recorded during GT-1 flight except they were of lower amplitude. The biases had no effect on guidance or flight control system performance during stage II flight. As the flight progressed, the pitch and yaw biases tended to drift because of the center-of-gravity shift during stage II flight, and because of the structure deformation of the second-stage engine gimbal assembly which, in effect, changed the pitch and yaw actuator null lengths. The contribution of the center-of-gravity offset, the actuator bias error, and actuator correction in pitch and yaw per degree of missile displacement are shown in table 5.2-XI for GT-1 and GT-2.

~~CONFIDENTIAL~~

5.2.3.6 Radio guidance initiate.- The transients from the initial radio guidance commands were normal, and the correct rate was observed during the full 2 deg/sec pitch-down command. This command corrected the high stage I altitude error previously mentioned. Thereafter, small pitch and yaw commands were sent to the launch vehicle to steer for correct velocity, attitude, and flight-path angle at SECO. During the last 45 seconds of radio guidance prior to SECO-2.5 seconds, a plus $2\frac{2}{3}$ -percent yaw-right and -4-percent pitch-down command was set by the GE Mod III to guide the spacecraft to the desired cut-off conditions.

5.2.3.7 Post-SECO transients.- During the period between SECO and spacecraft separation, a slight disturbance was recorded by the flight controls. This disturbance was also recorded during GT-1. The net effect on the vehicle stability and control was negligible. The rates observed during the period from SECO to spacecraft separation were as expected and were not excessive at separation. Figure 5.2-14 shows the pitch, yaw, and roll rates during this period. The rates during this period were:

Attitude	Peak rates from SECO to spacecraft separation, deg/sec	Rates at separation, deg/sec
Pitch	-0.81	-0.81
Yaw	+1.02	+1.02
Roll	-0.96	+0.79

5.2.4 Hydraulic System

5.2.4.1 Stage I - primary system.- The final stage I hydraulic system pressure and level check in the countdown was performed automatically by the sequencer. The motor-driven pump was initiated at T-110 seconds, pressurizing the secondary system. Approximately 11 seconds later, aerospace ground equipment (AGE) automatically selected, and the motor pump pressurized the primary system. During this period, accumulator precharge pressure indicated 1720 psia, and the primary system, 3160 psia.

At T-0 the current to the electrically driven pump was turned off. In the next 0.85-second, in which the turbine driven pump startup occurs, the pressure had dropped to a normal value of 3090 psia. At this point

~~CONFIDENTIAL~~

the normal drop in pressure occurred except that the drop to 2210 psia was greater than that previously experienced. At this point the pressure slowly continued its downward trend for 2 seconds to 1800 psia before the turbine gave any indication of output. The failure of the turbine pump to provide system pressure during this 2-second time constituted a potentially serious malfunction. However, a rapid buildup in pressure followed, and the system reached a maximum peak of 3700 psia at T+3.25 seconds before stabilizing at 3045 psia. See figure 5.2-15.

It should be noted that, had the pressure continued to decrease to 1500 ± 50 psia, a hydraulic switchover would have been initiated. If switchover had occurred before the shutdown circuits were disabled, the stage I engines would have shut down, as demonstrated by the first launch attempt of this vehicle. This problem is further discussed in section 5.2.4.4.

After lift-off, there were no indications of any excessive demands or any further anomalies. The pressure decreased to 2830 psia at staging, a change that is attributable to the effect of hydraulic fluid temperature changes on the pump compensator spring.

The fluid level was normal, at 57 percent full, before application of pressure. It was stabilized after engine start at 34 percent. A gradual increase in level resulted from the increasing fluid temperature and reached 45 percent at staging.

The fluid temperature increased from 55° F to 148° F, which is well below the design limit of 275° F.

5.2.4.2 Stage I - secondary system. - The final stage I secondary hydraulic system pressure and level check was performed at T-110 seconds. Thereafter, the secondary system remained unpressurized until engine start.

The system was 54 percent full (unpressurized) and stabilized at 32 percent after engine start and pressurization. The accumulator pre-charged pressure indicated 1740 psia, and the system pressure reached 3465 psia before stabilizing at 3090 psia. See figure 5.2-15.

It is noteworthy the record that the pressure buildup in the secondary system occurred without high overshoot, as evidenced on GT-1. The revised compensator employed in the turbine-driven pumps significantly reduced the pressure buildup overshoot, which exceeded 4500 psia for GT-1.

The secondary system could have fulfilled the hydraulic requirements, had it been necessary in the event of a sustained malfunction in the primary system.

~~CONFIDENTIAL~~

5.2.4.3 Stage II. - The final stage II hydraulic system pressure and level check was performed from T-240 to T-180 seconds. Thereafter, the system remained unpressurized until the staging was initiated.

The stage II system level indicated 60 percent full (unpressurized) and stabilized at 37 percent after engine start and pressurization. The accumulator precharge pressure indicated 1600 psia, and the system pressure reached 3780 psia 1.8 seconds after the staging sequence began. After the engine was centered, there were no significant hydraulic demands, and the pressure stabilized at 2880 psia.

At SECO, through gradual changes, pressure had decreased to 2750 psia, level increased to 39 percent, and the fluid temperature reached 96° F from 54° F at staging. Here, again, the reasons for the pressure and level changes was the fluid temperature rise.

At SECO+6.6 seconds, a hydraulic demand was observed by a decrease in pressure to 60 psia when the post-SECO engine disturbance occurred. The pressure rose again to 3060 psia because there were no demands on the pump, and residual fuel was obviously being supplied to the gas generator. During the last few seconds of telemetry coverage, the pressure was gradually decreasing, indicating a normal depletion of fuel. A similar pressure fluctuation was observed on GT-1.

5.2.4.4 Resume of primary system anomaly. - A definite cause of the pressure drop in the primary system has not been determined, but the data indicate that the primary pump compensator was in the fully compensated no-flow condition and continued in that position for 2 seconds even though a system demand existed. Several possible causes for this malfunction have been advanced. They include pump cavitation, contamination plugging and orifice, pump compensator sticking, and high transient pressure in the pump inlet due to engine start. A cross-section of the primary system hydraulic pump is shown in figure 5.2-16 to assist in identifying the pertinent pump components.

As of the writing of this report, the investigation has not been completed, and recommendations for corrective action or changes in operation procedure to insure proper functioning of the primary hydraulic system are not available. A supplemental report will be requested on this subject.

5.2.5 Guidance System

The vehicle was guided by the primary Mod III radio guidance system (RGS) which performed satisfactorily throughout the countdown and flight. All tests objectives were achieved. A minor procedural error late in the countdown produced a small time-bias in the remoted data, but it did

~~CONFIDENTIAL~~

~~CONFIDENTIAL~~

5-167

not affect the flight performance of the computer. The following Mod III interfaces were exercised:

- (a) Complex 19 launch azimuth link.
- (b) IGS targeting and update line (through DCS)
- (c) Trajectory remoting link to Houston (through DCU).
- (d) Trajectory data to Goddard.
- (e) Transmission of ASCO.
- (f) Trajectory data to MCC.

The power failure at the Mission Control Center (MCC) disrupted the Mod III data on display there and the data being transmitted to Goddard. However, the trajectory data transmitted to Houston remained valid, as well as computer functions on display in the flight monitor recorder console. This function, though planned as backup to the Guidance Monitor at MCC, served to apprise the Guidance Monitor and Flight Dynamics Officer that guidance was continuing satisfactorily during the blackout at MCC.

5.2.5.1 Programed guidance. - The programed guidance system for the first 162.09 seconds after lift-off consisted of sequenced events in the roll, pitch, and yaw channels provided by the primary flight control system. The sequenced events, as shown in table 5.2-XII, occurred within the acceptable limits.

As discussed in section 4.0, a lofted (dispersed) first-stage trajectory was flown. The errors at BECO, which were approximately 2σ , were 161.0 ft/sec high in velocity, 12 863.0 feet high in altitude, and 1.3° high in flight-path angle.

5.2.5.2 Closed-loop guidance. - The guidance system acquired the track beacon of the launch vehicle, tracked in the monopulse automatic mode, and was locked on continuously from lift-off to IO + 389.7 seconds. At this time, track went into a period of intermittent lock until final loss of signal at IO + 412.6 seconds (80.45 seconds after SECO). Track was maintained to an evaluation angle of 1.0° above the horizon. The average received signal strength during second stage operation was -60 dbm.

Rate lock was continuous, with no interruption at staging, from IO + 26.9 seconds to IO + 379.8 seconds (47.7 sec after SECO). Rate was maintained to an elevation angle of 2.1° . The average received signal strength during second-stage operation was -81 dbm.

~~CONFIDENTIAL~~

~~CONFIDENTIAL~~

Steering commands were transmitted as planned at LO + 168 seconds when an initial 10 percent pitch-down steering command (0.2 deg/sec) was given for 4 seconds, followed by a 100-percent pitch-down steering command (2.0 deg/sec) for 10.8 seconds. After 15 seconds, the steering gradually returned to a relatively small and constant pitch-down command of 3.0 percent. This produced a continuous pitch rate of 0.06 deg/sec until SECO -2.5 seconds.

Yaw steering started at LO + 172.8 seconds. The initial yaw commands were of small magnitude, with the command over the first 38 seconds of steering amounting to a positive yaw rate of 0.04 deg/sec. After 40 seconds, a continuous yaw right command of 2.67 percent (0.0534 deg/sec) Occurred until SECO -2.5 seconds.

SECO occurred at LO + 332.15 seconds, which was 4.33 seconds earlier than planned, and at an elevation angle of 7.64° as compared with a planned 7.38° . At SECO +20 seconds, tumbling velocities were 0.81 deg/sec pitch-down, 1.02 deg/sec yaw-right, and 0.96 deg/sec roll-clockwise (CW).

The computing system, in conjunction with the RGS track, rate, and airborne systems, completed all launch operations in a normal and satisfactory manner. A minor problem did occur during the countdown, in that an operational error resulted in a bias of 0.182 second on the Greenwich mean time (G.m.t.) data computed by the Mod III (A-1) computer. This was caused by synchronizing to G.m.t. before switching the computer to the "Flight Ready" mode.

The inertial guidance system (IGS) updates were sent and verified as follows:

Update sent LO + sec	Update verified LO + sec	Value, ft/sec
100	103.95	245.75
140	143.84	282.25

These transmission times provided the 3-second delay required by the inertial guidance system.

In figures 5.2-17 and 5.2-18, the velocity and flight-path angle are shown in the region of SECO and tail-off (SECO +20 seconds). The launch-vehicle radio guidance system data and the Range Safety computer (IP 3600) data are shown to illustrate the quality of the post-SECO data used for the orbital determination (go-no-go). As planned, the negative flight-path angle at insertion (SECO +20 seconds) caused the launch

~~CONFIDENTIAL~~

vehicle data sources used for the Goddard redundant orbital determination to indicate a no-go condition. The Mod III (A-1) computer also indicated a no-go indication. It is seen that the real-time MISTRAM I data compared quite favorably with the real-time launch-vehicle guidance data in the area of SECO and tail-off (SECO + 20 seconds).

5.2.6 Electrical Power System

The electrical power system performed nominally throughout the flight with no apparent anomalies.

5.2.6.1 Preflight.- Both the accessory power system (APS) and instrumentation power system (IPS) power transfers were normal with usual preload indications noted on the APS and IPS voltage traces. The IPS bus was subjected to some 40 percent heavier loading than the APS, which is normal.

The APS voltage rose approximately 1 volt at power transfer and came within a few tenths of a volt of the upper no-go APS voltage limit of 31.0 volt. Elimination of battery heaters and the subsequent reduction of battery voltage could possibly result in a more median value of battery voltage.

5.2.6.2 Umbilical drops.- Evidence of the first electrical plug (pad disconnect) to disconnect from the vehicle was seen at lift-off by an indicated drop of 3 amperes in IPS airborne current measurement.

A normal umbilical drop sequence was evidenced at the launch by the following data:

Umbilical plug	Disconnect, LO + sec
3D1M/3D2M	Lift-off
3D1E	0.130
3D2E	.385
3B1E	.625
2B1E	.755
2B2E	.770

5.2.6.3 Flight.- The APS battery supplied power at a nominal 29 volts associated with normal variations in current above a base load of 22 amperes during first-stage flight, and above a base load of 19 amperes during

UNCLASSIFIED

second stage flight. The variations in load were caused by three independently cycling TARS heaters. Each heater drained about 3.6 amperes which would contribute to a maximum load change of approximately 10 amperes.

The IPS battery supplied power at 29 volts for a normal load of 37 amperes during the first-stage flight, except for changes in load associated with the "gain change" event at LO + 104.6 seconds, and the tape recorder "on" event at LO + 143.7 seconds. During second-stage flight, the nominal IPS bus load was 33 amperes, except for a lower load which occurred between staging at LO + 156.8 seconds, which was the period of time before the playback tape recorder mode was initiated. Additional large variations in both the APS and IPS power occurred at staging and at spacecraft separation. (Staging variations in load are normal and result from the staging sequencing events.) Variation of load at spacecraft separation was a result of the spacecraft pyro-cutter, which cut the interfacing wiring harnesses, shorting certain APS and IPS signal leads to the spacecraft. The shorting also resulted in a momentarily false "switch over" signal from the spacecraft. The spacecraft interfacing circuitry was protected from shorting at this time by "dead facing" on the spacecraft side of the pyro-cutter.

The 400-cycle power supply frequency remained constant at 399.6 cps, which was well within the ± 4 -cps tolerance required for the TARS programmer timing. The 25 V dc regulated power used by the flight controls, the 5 V dc instrument power, and the 26 V ac 800-cycle power for the gyros all remained constant and within specification limits.

Based on an average IPS current of 37 amperes, and an average APS current of 27 amperes, as estimated for telemetry tapes, the following battery capacities were consumed from power transfer (T-85.7 seconds) to the end of the tape (LO + 388 seconds).

Power system	Battery capacity consumed
IPS	4.9 A-hr
APS	3.58 A-hr

5.2.7 Instrumentation

5.2.7.1 Airborne.- The airborne system performed satisfactorily. This system consisted of one PCM-FM link and one FM-FM link with an associated airborne tape recorder. A two-antenna configuration was

UNCLASSIFIED

~~CONFIDENTIAL~~

5-171

used instead of the four antennas (one in each quadrant) flown on GT-1 and Titan II. The two antennas were located in quadrants II and IV at azimuths of 115° and 295° . A total of 242 parameters were programed for the PCM-FM system, and 12 additional parameters were assigned to the FM-FM system. One PCM signal (0036 - fuel surge chamber piston motion for subassembly 2) was lost approximately 112.5 seconds after lift-off.

All telemetry signals were lost temporarily for 450 milliseconds during RF blackout at staging. The tape recorder operated properly during blackout and in the playback mode after staging.

Instrumentation system voltages are summarized in table 5.2-XIII.

5.2.7.2 Ground instrumentation.-

5.2.7.2.1 Complex 19: The performance of all land-line instrumentation was satisfactory. There were 44 measurements programed for the launch and no anomalies were observed.

5.2.7.2.2 Telemetry Building II at the Cape Kennedy Missile Test Annex: The Tel II range record indicated poor tracking at various times throughout flight; however, the only data loss occurred at staging. The Tel III range record indicated better data acquisition than Tel II for most of the tracking period.

Numerous dropouts were noted in the oscillograph recordings of the Tel II PCM flight data. Postflight evaluation of these occurrences showed the dropouts were not contained in the telemetered data from the vehicle and were apparently generated during data reduction. Good telemetry data were received from lift-off through LO + 415 seconds.

5.2.8 Malfunction Detection System

Performance of the malfunction detection system (MDS) during pre-flight checkout and flight was satisfactory. Analysis of flight data indicated that all MDS hardware functioned properly, with the exception of stage II oxidizer tank pressure sensor B (measurement 0871) which exhibited intermittent output between LO + 190 and LO + 218 seconds. Switchover parameters are given in table 5.2-XIV.

5.2.8.1 Engine MDS.- The malfunction detection thrust chamber pressure switch (MDTCPS) actuation times have been evaluated and are tabulated below. Allowance must be made for PCM telemetry channel sampling rate, which makes it possible to have a variance of 90 psia from the actual chamber pressures at the times of actuation of the switches. The subassembly 1 and subassembly 2 switches actuated at 570 psia and

~~CONFIDENTIAL~~

~~CONFIDENTIAL~~

574 psia, respectively. Stage II malfunction detection fuel injector pressure switch (MDFJPS) pressure cannot be determined, because there is no analog telemetry channel of injector pressure.

The switch actuation times and corresponding pressures were as follows:

Switch	Condition	Actuation time, LO ± seconds	Pressure, psia
Subassembly 1 MDTCPs	Make	-2.376	570
	Break	+151.667	563
Subassembly 2 MDTCPs	Make	-2.345	574
	Break	+151.667	580
Subassembly 3 MDTCPs	Make	+152.370	
	Break	+332.472	

5.2.8.2 Vehicle MDS.- MDS rate switch package (RSP) performed properly throughout the flight. No vehicle overrates occurred from lift-off through SECO+20 seconds. Subsequent to spacecraft separation, the tumbling launch vehicle exceeded the RSP low-rate settings in yaw and pitch. These actuations were verified by comparison with stage II rate gyro outputs. This event substantiates that the RSP was capable of proper performance, had it been required during the flight.

The tank pressure transducers performed satisfactorily throughout countdown and flight. With the exception of the stage II oxidizer B transducer, all fuel and oxidizer transducer A and B outputs were within 50 millivolts (less than 1 percent of full scale) of each other. (One-percent full scale equals 0.5 psia on stage I and 0.75 psia on stage II.)

A minor discrepancy was noted in the stage II oxidizer B transducer output, which exhibited negative voltage (increasing pressure) excursions from LO + 190 seconds to LO + 218 seconds, with a maximum excursion of 0.5 volt (7.5 psia). The excursions were observed as 2 to 3 psia fluctuations on the monitoring meters at the Mission Control Center (MCC). Since the general level of the B transducer compared closely with the A transducer, no concern was exhibited by MCC personnel.

~~CONFIDENTIAL~~

5.2.8.3 Ground slow malfunction detection.- In general, the performance of the guidance monitors (slow malfunction detection) was satisfactory for all phases of GT-2 prelaunch and launch activities. Primary monitor status at the MCC and backup monitor status in the GE/Burroughs were acceptable. Data reception and presentation in real time to the MCC guidance facility were satisfactory from engine ignition through SECO-26 seconds, at which time MCC experienced a power failure. The guidance monitors in GE/Burroughs furnished adequate information to the MCC monitors from that time through SECO.

MCC guidance trajectory plotboards 3 and 5, used for slow malfunction detection, were in position with T-12 and T-5 hour wind biased trajectories and constraints applied at T-65 minutes. Wind biased trajectory and constraint update procedures were implemented according to plan, and the data were satisfactorily transmitted to MCC where they were applied to the plotboards for launch. Satisfactory slow malfunction constraint lines (no wind bias) were available at GE/Burroughs for use on the plotboards during the launch.

5.2.9 Range Safety and Ordnance

5.2.9.1 Range safety.- The range safety system functioned as planned. No operational or equipment discrepancies occurred.

5.2.9.1.1 Performance of airborne equipment: The airborne system utilized two new lightweight solid-state command receivers in lieu of the type flown on GT-1. Both receivers operated satisfactorily throughout powered flight. Receiver loss of signal (LOS) occurred at approximately 62 seconds after spacecraft separation. The telemetered airborne-receiver automatic-gain-control (AGC) traces and the Air Force Eastern Test Range (AFETR) command-station signal-strength recordings agreed on the following events:

(a) At LO + 91.139 seconds, transfer from the 600-watt transmitter to the 10-kW transmitter at Cape Kennedy.

(b) At LO + 121.739 seconds, transfer from the 10-kW transmitter at Cape Kennedy to the 10-kW transmitter at Grand Bahama Island (GBI).

(c) At LO + 152.339 seconds, staging-event telemetry dropout of 0.5 second.

(d) At LO + 204.539 seconds, antenna transfer at GBI from the Sterling I to the Sterling II.

(e) At LO + 244.739 seconds, transfer from the 10-kW transmitter at GBI to the 10-kW transmitter at Grand Turk Island (GTI).

UNCLASSIFIED

(f) At IO + 332.209 seconds, receipt of the auxiliary second-stage engine cut-off (ASCO) signal at the command receivers.

(g) At IO + 359.339 seconds, antenna transfer at GTI from the up-range Sterling antenna to the single helix antenna.

(h) At IO + 389.339 seconds, antenna transfer from the single helix to the downrange Sterling antenna at GTI.

The engine cut-off bilevel telemetry channels from the receivers showed no anomalies.

5.2.9.1.2 Ground complex performance: The Range Safety Officer's (RSO) displays for real-time flight evaluation were as follows:

(a) Redundant plotboard displays of real-time radar, impact prediction, and vertical flight-path profile.

(b) Real-time telemetry of GLV attitude.

(c) Closed-circuit television.

A postflight evaluation of the range safety plotboard data indicates that the impact ground track exceeded the 3σ IP limits in yaw at IO + 70 seconds. At IO + 85 seconds, the plotted IP returned within the IP 3σ limits. Reference figure 5.2-19.

An analysis of the anomaly found that the data transmitted to ETR Range Safety consisted of (1) Martin Document ER 12717, Revision B and an errata TWX called "Appendix C," and (2) trajectory set consisting of a nominal, 3σ right, 3σ high-performance, and 3σ low-performance trajectories.

The trajectory set was generated by using the Cape Kennedy 3σ wind profile for August and September. The lateral 3σ used the wind profile from an azimuth of 15° . This profile is shown in figure 5.2-3 plotted with GT-1 and GT-2 actual wind profiles. As seen, the winds encountered were greatly in excess of those used in generating the lateral dispersed trajectory. This was due to the fact that the Cape Kennedy 3σ December wind profile was not used in the trajectory set.

The expanded scale vertical plotboards used X, Y, Z position data submitted in table form in ER 12717, Revision B. These data were submitted in November and did use the proper Cape Kennedy 3σ December wind profile. The launch-vehicle contractor has compared its 3σ lateral trajectory with the GE Mod III actual trajectory data for GT-2 and found that the launch vehicle did not exceed the 3σ boundary at any

UNCLASSIFIED

time. The point of closest approach was 250 feet. Had the proper December Cape Kennedy 3σ wind profile been used for the GT-2 trajectory set, the actual plotted impact would have been within 3σ IP boundaries.

Preflight checkout of the MISTRAM transponder was normal; however, some unlocks were experienced due to multipath on the microwave sub-system. This problem cleared up prior to launch time, and during powered flight, the system performed according to preflight predictions. Tracking functions occurred as follows:

- (a) MISTRAM I lock - 9:04:06.25 a.m. e.s.t. (I0 + 6.3 sec)
- (b) Calibrate channel sweep - 9:04:17.95 a.m. e.s.t. (I0 + 18.1 sec)
- (c) Transponder unlock, both channels at staging event - 9:06:32.5 a.m. e.s.t. (normal) (I0 + 152.6 sec)
- (d) Reacquisition and lock - 9:06:33.7 a.m. e.s.t. (I0 + 153.8 sec)
- (e) Transponder calibrate channel unlock just prior to handover to station 2 - 9:10:20.25 a.m. e.s.t. (I0 + 380.3 sec)
- (f) Station 1 handover to station 2 - 9:10:26.95 a.m. e.s.t. (I0 + 387 sec)
- (g) Lost telemetry data - 9:10:55.1 a.m. e.s.t. (I0 + 415.2 sec)
- (h) MISTRAM II loss of lock - 9:11:15.5 a.m. e.s.t. (I0 + 435.4 sec)
- (i) MISTRAM II loss of signal - 9:11:42.4 a.m. e.s.t. (I0 + 462.5 sec)

Data were obtained during the following periods:

Station	Track mode	Time, I0 + sec
I	Active	14.5 to 380.3
I	Passive	Not obtained due to low elevation angle
II	Passive	97.4 to 387.4
II	Active	387.9 to 435.4

UNCLASSIFIED

MISTRAM data were selected by the automatic data and selection program (ADSAP) for impact prediction during the following periods:

Seconds from lift-off	Time, a.m. e.s.t.	Duration, sec
30.5	9:04:30.40	
31.9	9:04:31.80	1.4
48.0	9:04:47.90	
93.5	9:05:33.40	45.5
96.8	9:05:36.70	
98.5	9:05:38.40	1.7
102.9	9:05:42.80	
103.1	9:05:43.00	0.2
107.5	9:05:47.40	
107.6	9:05:47.50	0.1
135.0	9:06:14.90	
152.6	9:06:32.50	17.6
164.0	9:06:43.90	
271.8	9:08:31.70	107.8
282.4	9:08:42.30	
368.8	9:10:08.70	86.4

The performance of the MISTRAM transponder was nominal throughout the flight, and telemetry data on its operation extended to IO + 415 seconds. Operational mode changes, station handover, and loss of lock were clearly discernable on the telemetry signal. The use of the velocity memory program to reacquire after dropout proved to be extremely successful. Loss of lock at staging was only 1.2 seconds, and at handover, the loss was held to approximately 0.5 second.

5.2.9.2 Ordnance system.-

- (a) Airborne: All flight ordnance was normal.
- (b) Launch nuts: All launch nuts fired.

UNCLASSIFIED

TABLE 5.2-I. - PROPULSION SYSTEM ELAPSED TIME

Event	Time, sec	
	Predicted (a)	Actual
87FS1 to lift-off	3.2	3.361
Stage I burn time (87FS1 to 87FS2) . . .	158.15	155.073
Stage II burn time (91FS1 to 91FS2) . . .	182.96	180.439
Stage II burn time margin	2.83	2.87

^aLaunch Vehicle Contractor predicted burn times are quoted to provide consistency with loaded propellant quantities. It should be noted that these times differ slightly from those predicted in reference 8 which was used to prepare the predicted event times quoted in other sections of this report.

TABLE 5.2-II. - AVERAGE STAGE I PERFORMANCE

Parameter	Predicted (a)	Flight	Difference, percent
Thrust, lb	456 050	466 525	+2.30
Engine specific impulse, $\frac{\text{lb-sec}}{\text{lb}}$. . .	276.28	276.87	+0.21
Engine mixture ratio	1.9022	1.8946	-0.40
Oxidizer overboard flow rate, $\frac{\text{lb}}{\text{sec}}$. .	1081.52	1102.56	+1.95
Fuel overboard flow rate, $\frac{\text{lb}}{\text{sec}}$	569.11	582.45	+2.34
Burn time (87FS1 to 87FS2), sec . . .	158.15	155.073	-1.95

^aLaunch Vehicle Contractor predicted burn times are quoted to provide consistency with loaded propellant quantities. It should be noted that these times differ slightly from those predicted in reference 8 which was used to prepare the predicted event times quoted in other sections of this report.

~~CONFIDENTIAL~~

TABLE 5.2-III.- STAGE I PERFORMANCE - STANDARD INLET CONDITIONS

Parameter	Standard inlet conditions	
	Acceptance test	Flight performance
Thrust, lb	435 389	439 985
Specific impulse, $\frac{\text{lb-sec}}{\text{lb}}$	259.54	259.87
Engine mixture ratio	1.9166	1.9205
Oxidizer overboard flow rate, $\frac{\text{lb}}{\text{sec}}$	1102.01	1113.06
Fuel overboard flow rate, $\frac{\text{lb}}{\text{sec}}$	575.51	580.05

TABLE 5.2-IV.- AVERAGE STAGE II PERFORMANCE

Parameter	Predicted	Flight	Difference, percent
Thrust (chamber), lb	100 903	102 396	+1.48
Specific impulse (engine), $\frac{\text{lb-sec}}{\text{lb}}$	311.30	311.68	+0.12
Engine mixture ratio	1.7848	1.7632	-1.20
Oxidizer overboard flow rate, $\frac{\text{lb}}{\text{sec}}$	207.90	209.79	+0.97
Fuel overboard flow rate, $\frac{\text{lb}}{\text{sec}}$	116.23	118.74	+2.16

~~CONFIDENTIAL~~

TABLE 5.2-V.- STAGE II PERFORMANCE - STANDARD INLET CONDITION

Parameter	Standard inlet conditions	
	Acceptance test	Flight performance
Thrust (chamber), lb	101 029	102 503
Specific impulse (engine), $\frac{\text{lb-sec}}{\text{lb}}$. .	310.67	311.03
Engine mixture ratio	1.8173	1.7950
Oxidizer overboard flow rate, $\frac{\text{lb}}{\text{sec}}$. .	209.93	211.81
Fuel overboard flow rate, $\frac{\text{lb}}{\text{sec}}$	115.27	117.75

TABLE 5.2-VI.- PROPELLANT LOADING

Stage	Tank	Requested load, lb	Measured load, lb
I	Oxidizer	170 639	170 659
	Fuel	90 236	90 308
II	Oxidizer	38 801	38 801
	Fuel	21 872	21 872

~~UNCLASSIFIED~~

TABLE 5.2-VII.- AVERAGE PROPELLANT TEMPERATURES

Stage	Propellant	Temperature, °F	
		Predicted	Actual
I	Oxidizer	46.6	44.1
	Fuel	45.2	36.9
II	Oxidizer	48.7	48.8
	Fuel	42.1	41.3

TABLE 5.2-VIII.- OUTAGE AND BURN-TIME MARGIN

	Predicted	Actual
Stage I outage, lb	560 (mean)	12 (fuel)
Stage II outage, lb	226 (mean)	359 (oxidizer)
Stage II burn- time margin, sec	2.83	2.87

~~UNCLASSIFIED~~

TABLE 5.2-IX.- HOLD-DOWN TRANSIENTS

Actuator designation	Max. engine displacement, in.	Position at null check, in.	Rate gyro designation	Peak rate, deg/sec
Pitch, 1 ₁	-0.12	-0.03	Pitch, stage II	+0.30
Yaw/roll, 2 ₁	+0.23	+0.02	Yaw, stage II	+0.54
Yaw, roll, 3 ₁	+0.16	-.04	Roll, stage I	-.10
Pitch, 4 ₁	-.11	-.01		

UNCLASSIFIED

TABLE 5.2-X.- MAXIMUM RATES AND ATTITUDE ERRORS

Gyro designation	Rates and attitudes	IO + sec
Pitch stage I rate gyro	-0.9 deg/sec	78
	-0.9 deg/sec	86
Yaw stage I rate gyro	+0.62 deg/sec	74
	+0.62 deg/sec	78
Roll stage I rate gyro	+0.48 deg/sec	54
Pitch attitude	-1.36 deg	56
	+1.03 deg	85
Yaw attitude	-1.81 deg	67.6
	+1.16 deg	83
Roll attitude	+0.86 deg	49
	+0.86 deg	55

UNCLASSIFIED

TABLE 5.2-XI.- GYRO DISPLACEMENT BIAS

	GT-1		GT-2	
	Pitch, deg	Yaw, deg	Pitch, deg	Yaw, deg
After staging transients				
Center-of-gravity offset contribution	-0.103	-0.430	-0.034	-0.689
Actuator correction	None	None	+1.0	None
Actuator offset (initial)	-1.92	+2.55	-.23	+1.83
Displacement error	-2.02	+2.12	-.26	+1.14
At SECO				
Center-of-gravity offset contribution	-0.331	-1.788	-0.18	-2.9
Actuator correction	None	None	+1.0	None
Actuator offset (initial)	-2.75	1.39	-.72	+9
Displacement error	-3.08	-.40	-.90	-2.0

TABLE 5.2-XII.- PLANNED AND ACTUAL EVENT TIMES AND VEHICLE RATES

Event	Planned time after lift-off, sec	Actual time after lift-off, sec	Difference, sec	Planned rate, deg/sec	Actual rate, deg/sec	Difference, deg/sec
Roll program start	4.40	4.34	-0.06	1.25	1.14	-0.11
Roll program end	20.48	20.40	-.08	1.25	1.14	-.11
Pitch program 1 start	23.04	22.99	-.05	-.67	-.66	-.01
Pitch program 1 end	88.32	88.07	-.25	-.67	-.66	-.01
Pitch program 2 start	88.32	88.07	-.25	-.48	-.47	-.01
Pitch program 2 end	119.04	118.71	-.33	-.48	-.47	-.01
Pitch program 3 start	119.04	118.71	-.33	-.25	-.26	.01
Pitch program 3 end	162.56	162.09	-.47	-.25	-.26	.01

UNCLASSIFIED

UNCLASSIFIED

TABLE 5.2-XIII.- SUMMARY OF INSTRUMENTATION SYSTEM DATA

Measurement	Nomenclature	Required value	Value before T=0	Value at 87FS1	Value at 87FS2	Value at 91FS1	Value at 91FS2	Value at end of data
810	5-V power supply	5.000 ± 0.022	4.98	4.98	4.98	4.98	4.98	4.98
811	40-V power supply, V dc	40 ± 0.400	40.37	40.37	40.19	40.19	40.37	40.19
812	Signal conditioner package temperature, °F	105 to 125	116.0	116.0	115.3	115.3	116.0	116.0
813	PCM mercury battery, V dc	1.33 to 1.35	1.34	1.34	1.34	1.34	1.34	1.34
814	PCM mercury battery, V dc	1.33 to 1.35	1.34	1.34	1.34	1.34	1.34	1.34
815	PCM mercury battery, V dc	1.33 to 1.35	1.35	1.35	1.35	1.35	1.35	1.35
816	+30-V power supply, V dc	+30 ± 0.100	29.99	29.99	30.00	30.00	30.00	30.00
817	-30-V power supply V dc	-30 ± 0.100	30.00	30.00	30.00	29.99	29.99	29.99

~~UNCLASSIFIED~~

~~UNCLASSIFIED~~

TABLE 5.2-XIV.- MALFUNCTION DETECTION SYSTEM SWITCHOVER PARAMETERS^a

Parameter	Switchover setting	Maximum or positive	Time from LO, sec	Minimum or negative	Time from LO, sec	Comments
Stage I primary hydraulics (0154)	Shuttle spring 1500 psia	3640 psia	-0.04	1780 psia	-0.45	Unusually large pressure decay at engine start
Stage I tandem actuators						
1 subassembly 2 pitch	±4.0°	+0.92°	+55.3	-0.39°	+85.3	
2 subassembly 2 yaw-roll	±4.0°	+0.62°	+82.8	-1.32°	+68.4	
3 subassembly 1 yaw-roll	±4.0°	+1.03°	+68.3	-0.92°	+82.8	
4 subassembly 1 pitch	±4.0°	+0.28°	+85	-1.16°	+55.6	
Stage I pitch rate	+2.5 deg/sec -3.0 deg/sec	+0.15 deg/sec	+23.3	-0.8 deg/sec	+86.2	
Stage I yaw rate	±2.5 deg/sec	+0.55 deg/sec	+74.1	-0.38 deg/sec	+90.8	
Stage I roll rate	±20.0 deg/sec	+0.35 deg/sec	Lift-off transient	-1.2 deg/sec	+4.7 to +21.0	Roll program
Stage II pitch rate	±10 deg/sec	+0.6 deg/sec	SECO+3.0	-2.1 deg/sec	+175 to +183	
Stage II yaw rate	±10 deg/sec	+1.1 deg/sec	+153.4	-0.85 deg/sec	SECO+4.0	
Stage II roll rate	±20 deg/sec	+0.65 deg/sec	SECO+3.0	-0.9 deg/sec	SECO+10	The roll program (stage I) was also correctly sensed

^aActual readings~~CONFIDENTIAL~~~~CONFIDENTIAL~~

NASA-S-65-1785

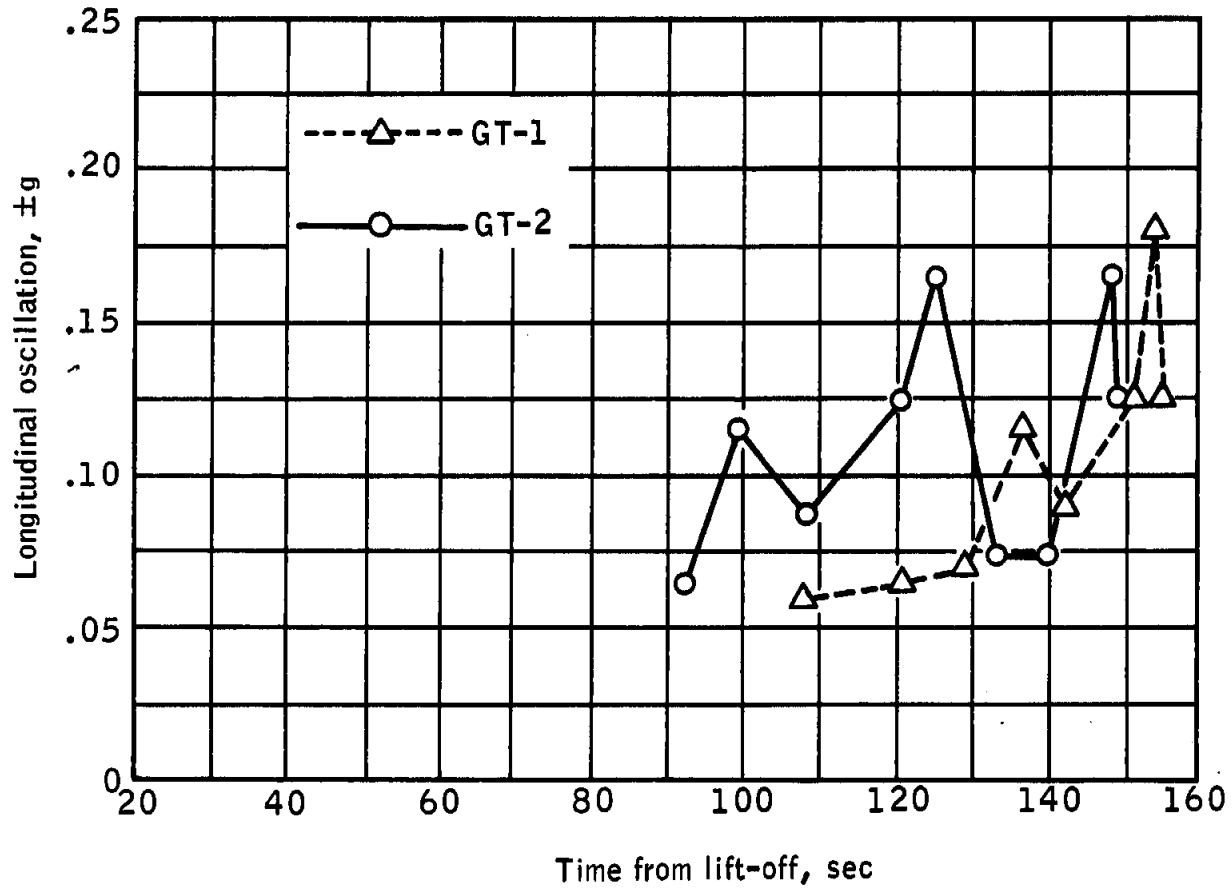


Figure 5.2-1. - Comparison of launch vehicle longitudinal oscillation for GT-1 and GT-2 (Sta. 280)

UNCLASSIFIED

UNCLASSIFIED

NASA-S-65-1783

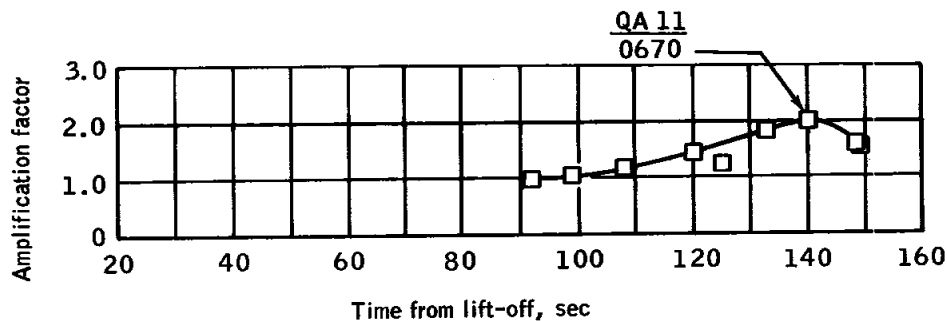
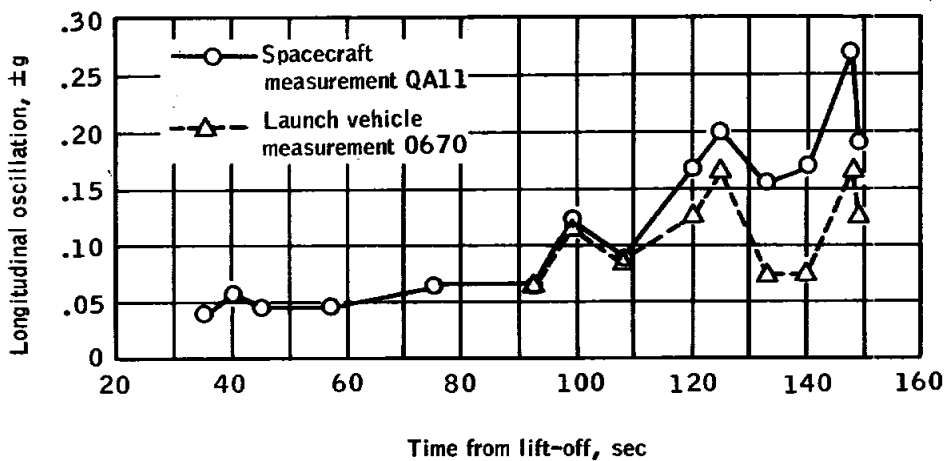


Figure 5.2-2. - Comparison of spacecraft and launch vehicle longitudinal oscillations

NASA-S-65-1835

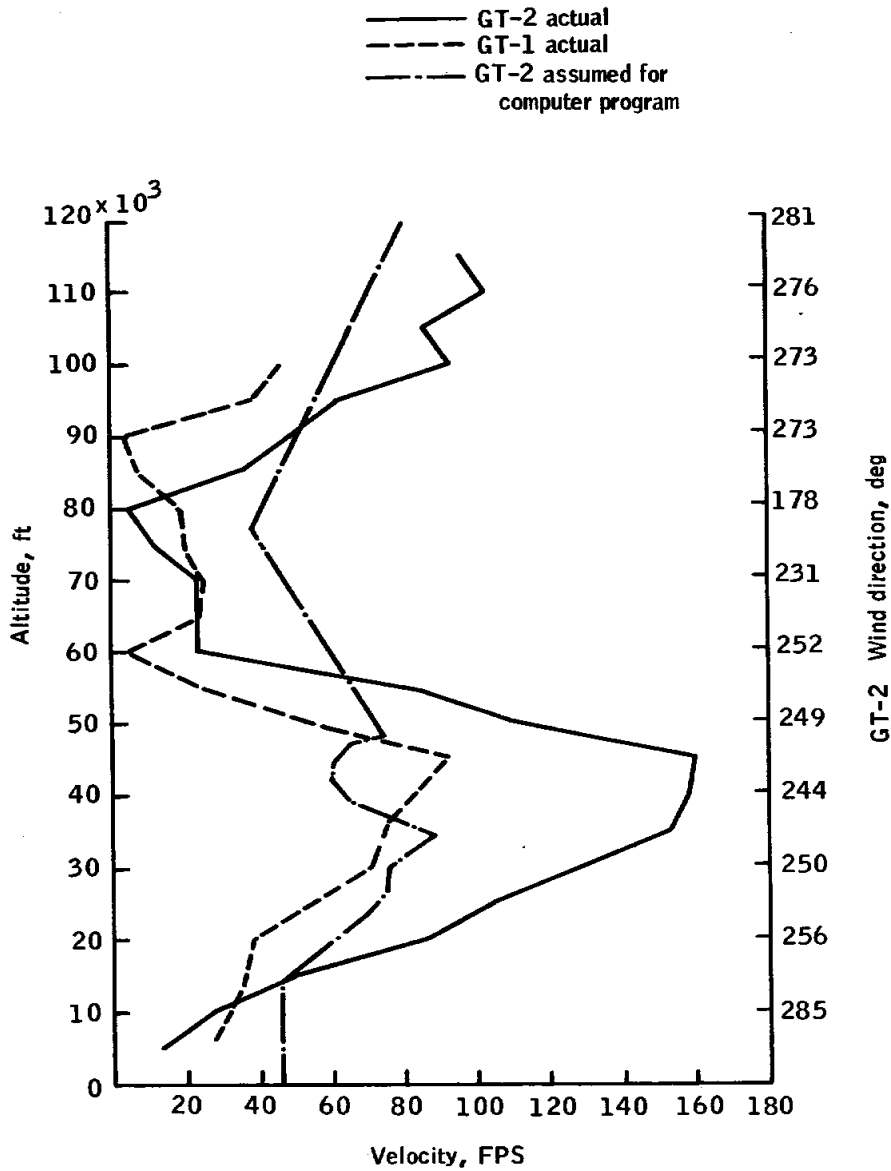


Figure 5.2-3. - Launch day wind profile

NASA-S-65-1781

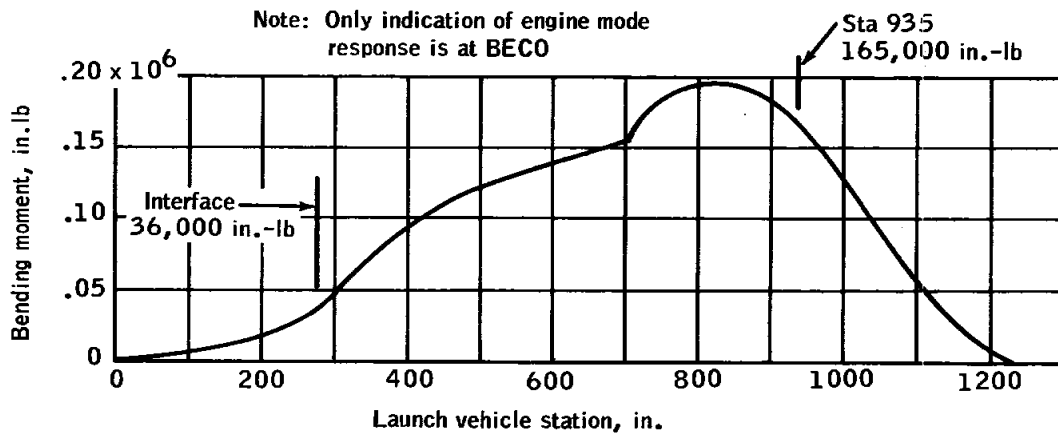
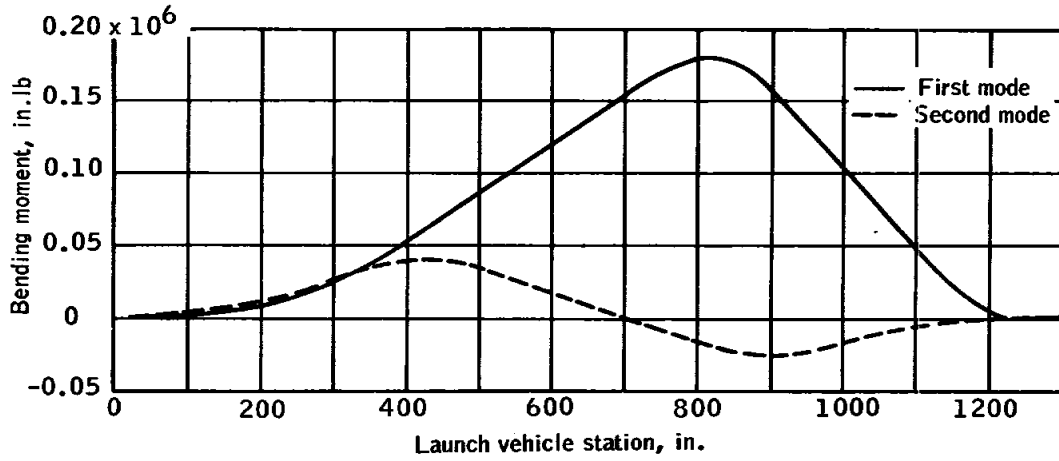
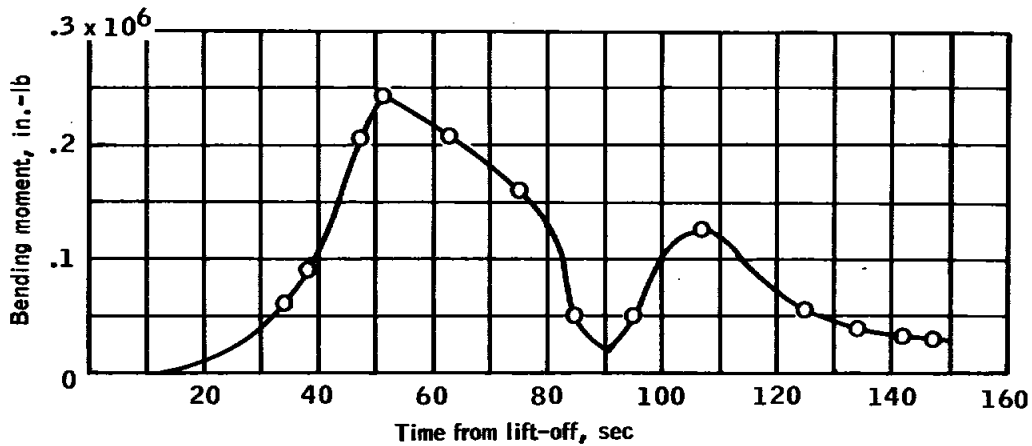
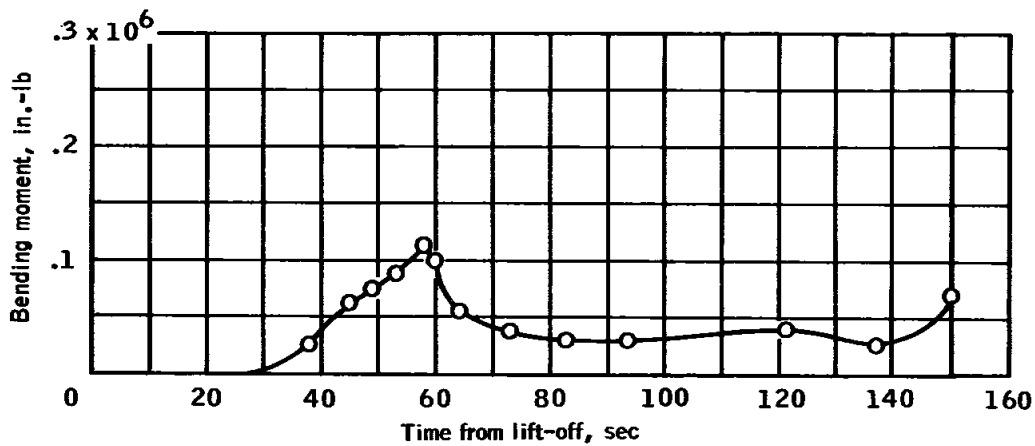


Figure 5.2-4. - Modal moments at maximum $q \alpha$

NASA-S-65-1780



(a) Peak mode 1 moment (station 800)



(b) Peak mode 2 moment (station 430)

Figure 5.2-5. - Gemini launch vehicle peak modal moments from stage I flight

NASA-S-65-1787

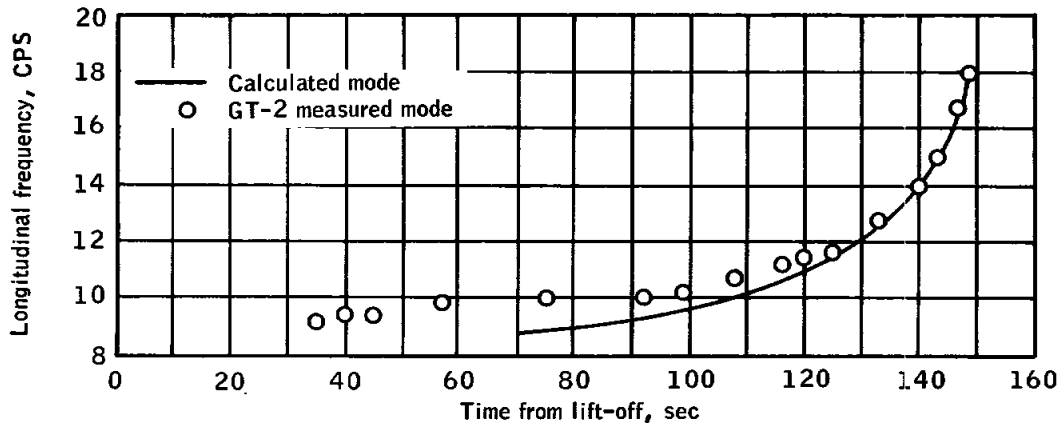
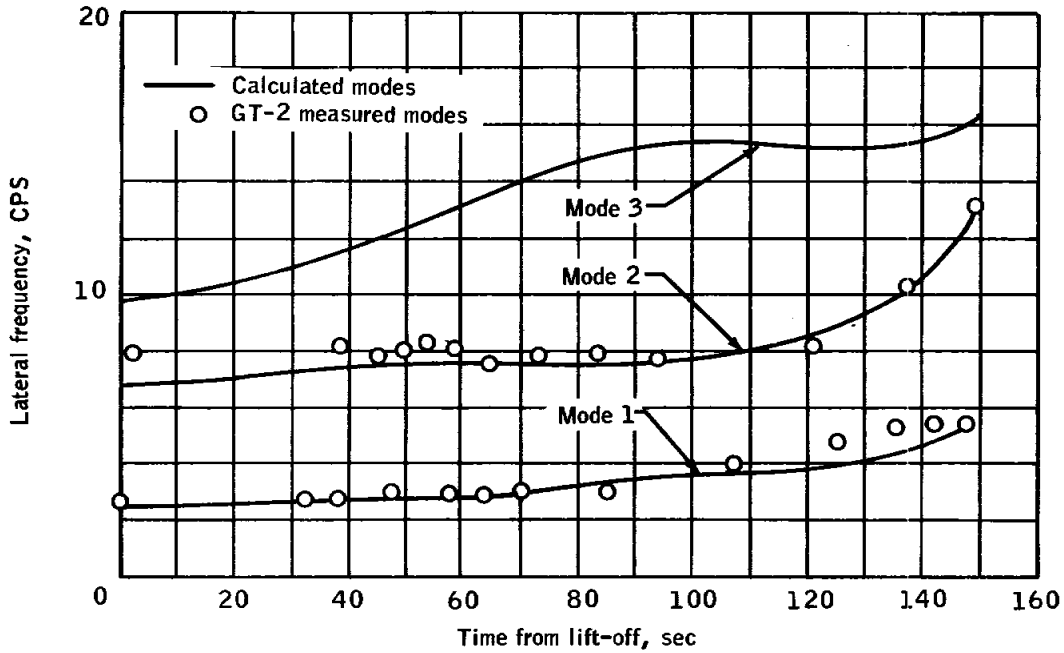


Figure 5.2-6, - Gemini launch vehicle vibration modes for stage I flight

NASA-S-65-1755

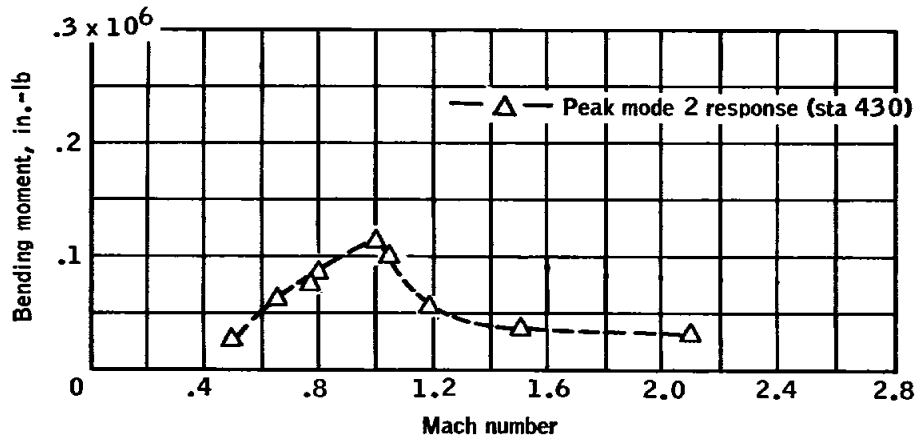
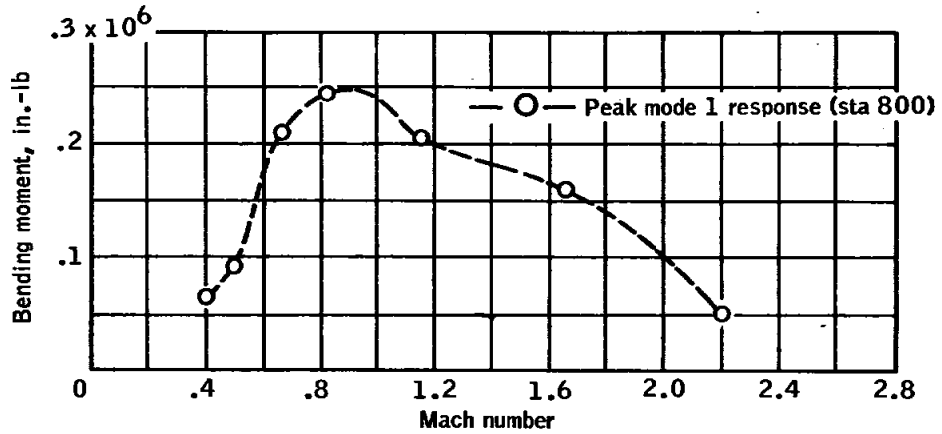


Figure 5.2-7. - Peak modal bending moment response to transonic buffet

~~CONFIDENTIAL~~

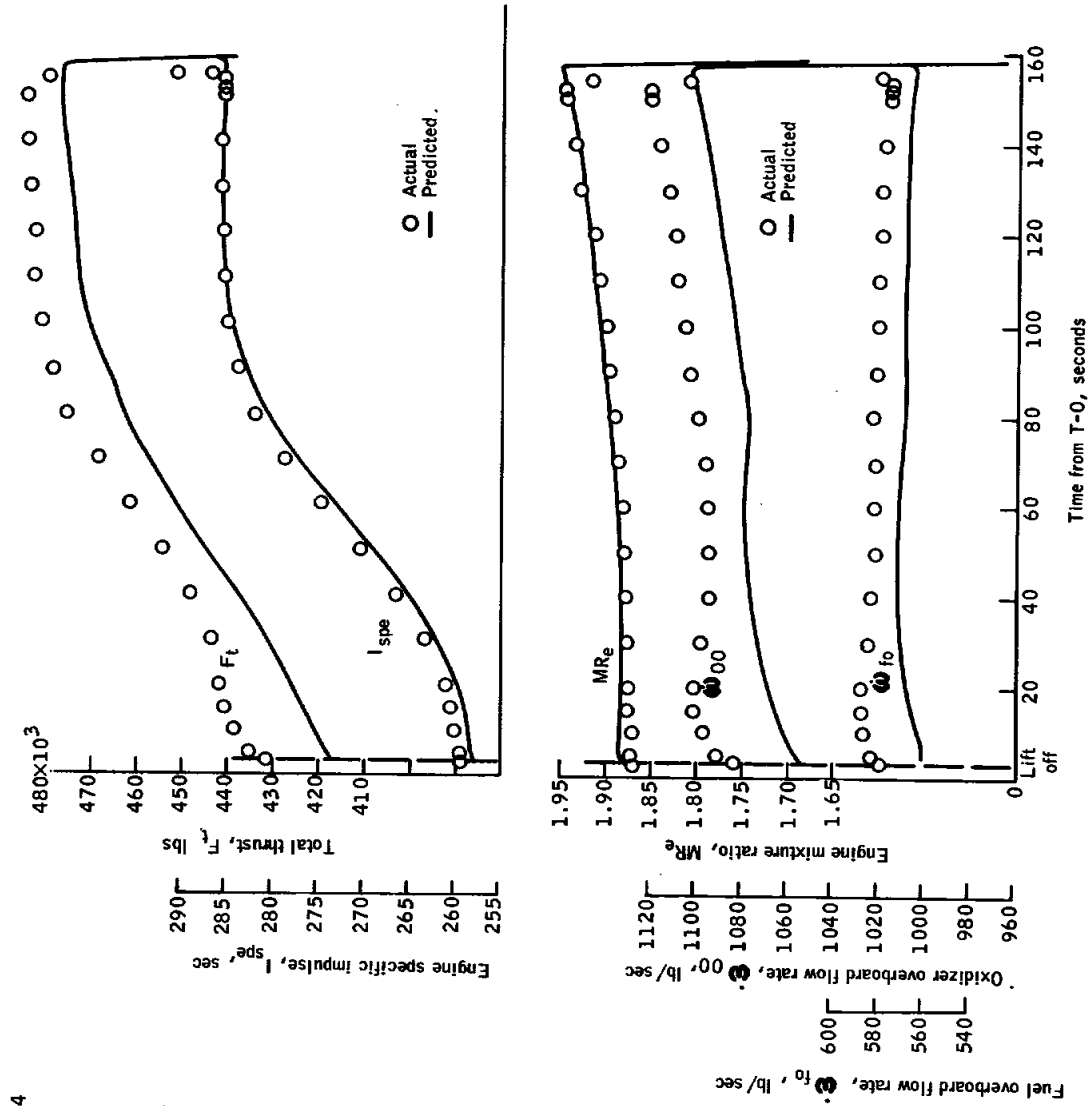


Figure 5.2-9. - Stage I engine flight performance

~~CONFIDENTIAL~~

~~CONFIDENTIAL~~

~~CONFIDENTIAL~~

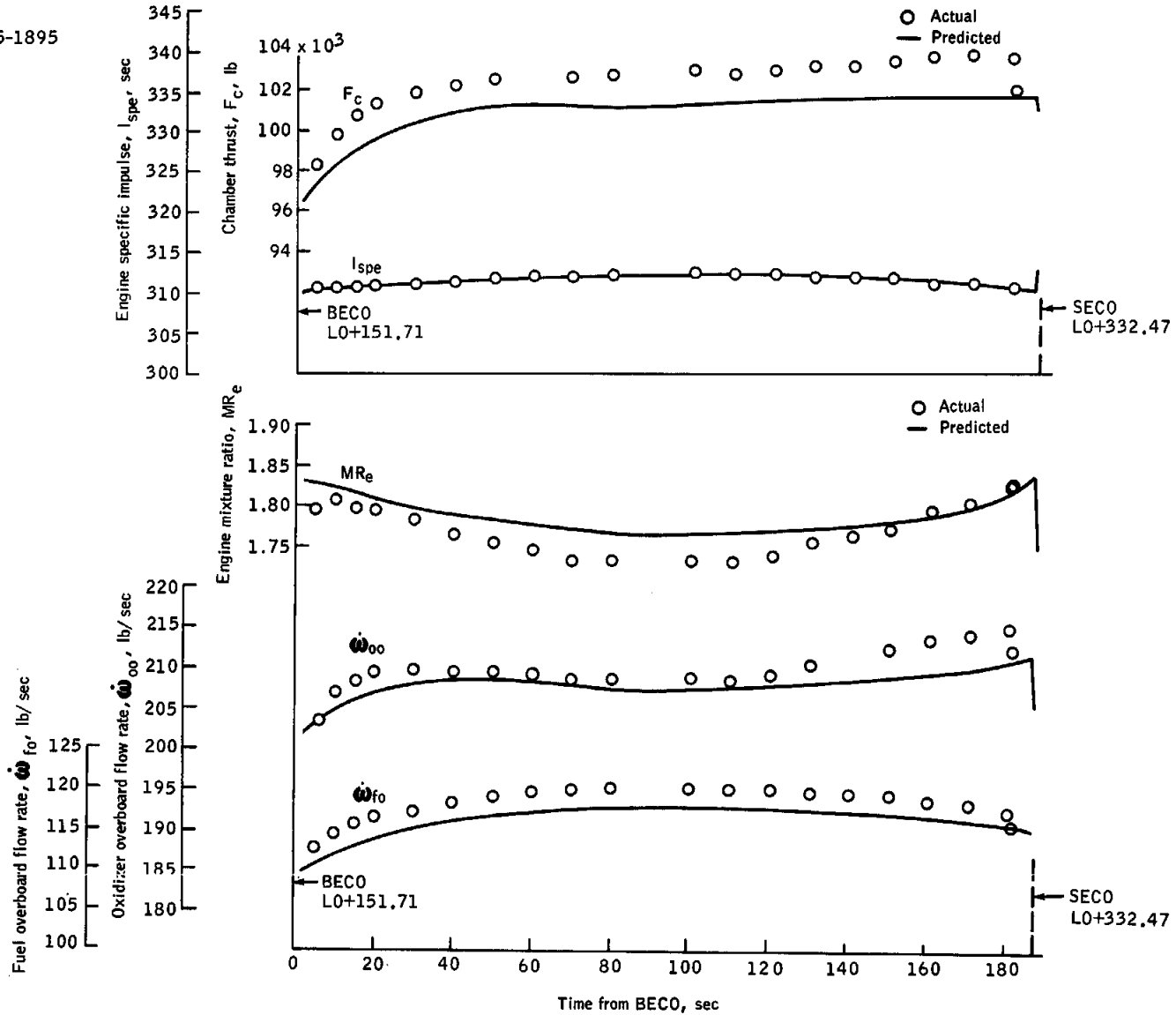
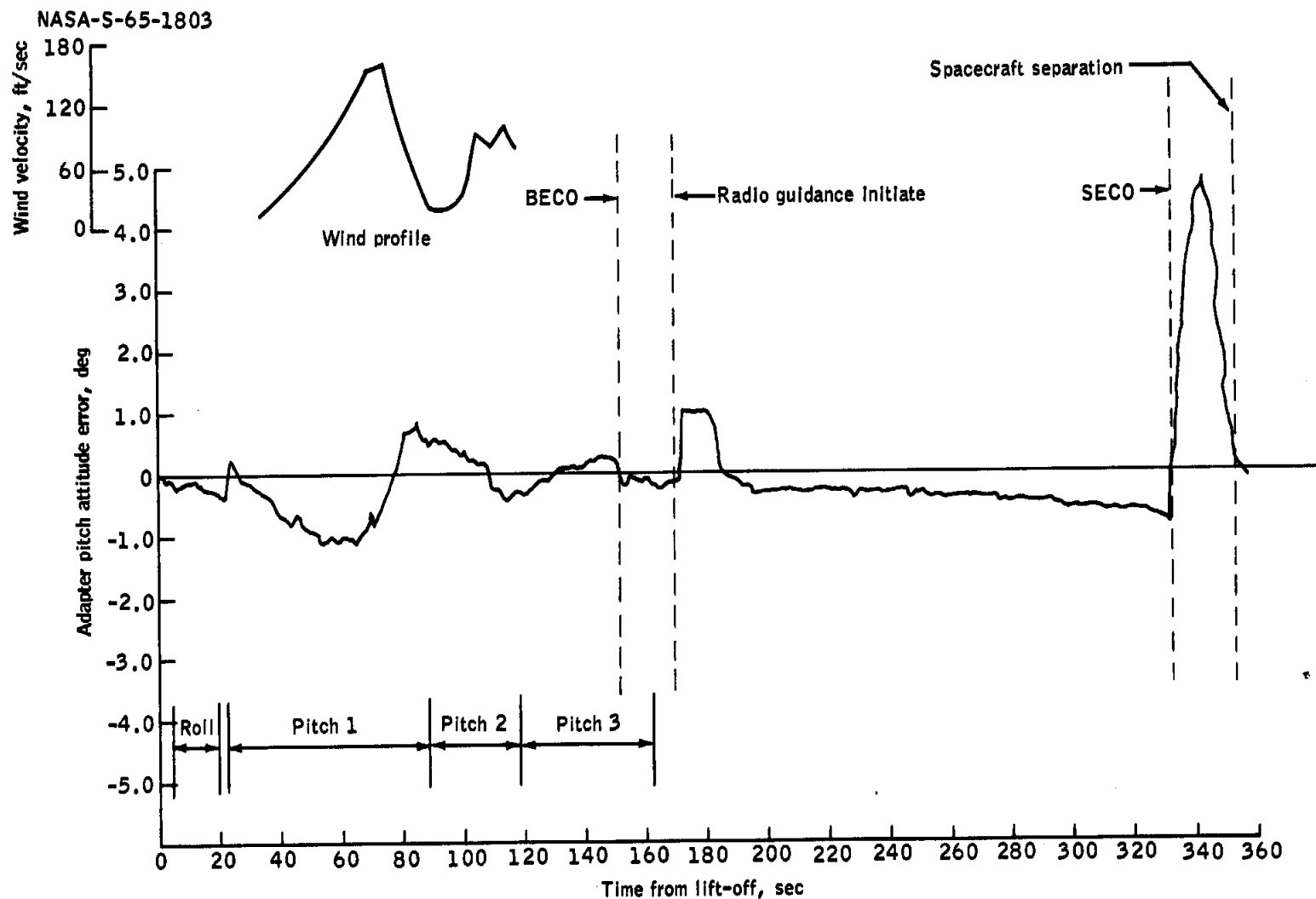


Figure 5.2-10. - Stage II engine flight performance

UNCLASSIFIED



UNCLASSIFIED

Figure 5.2-11. - Pitch flight displacement

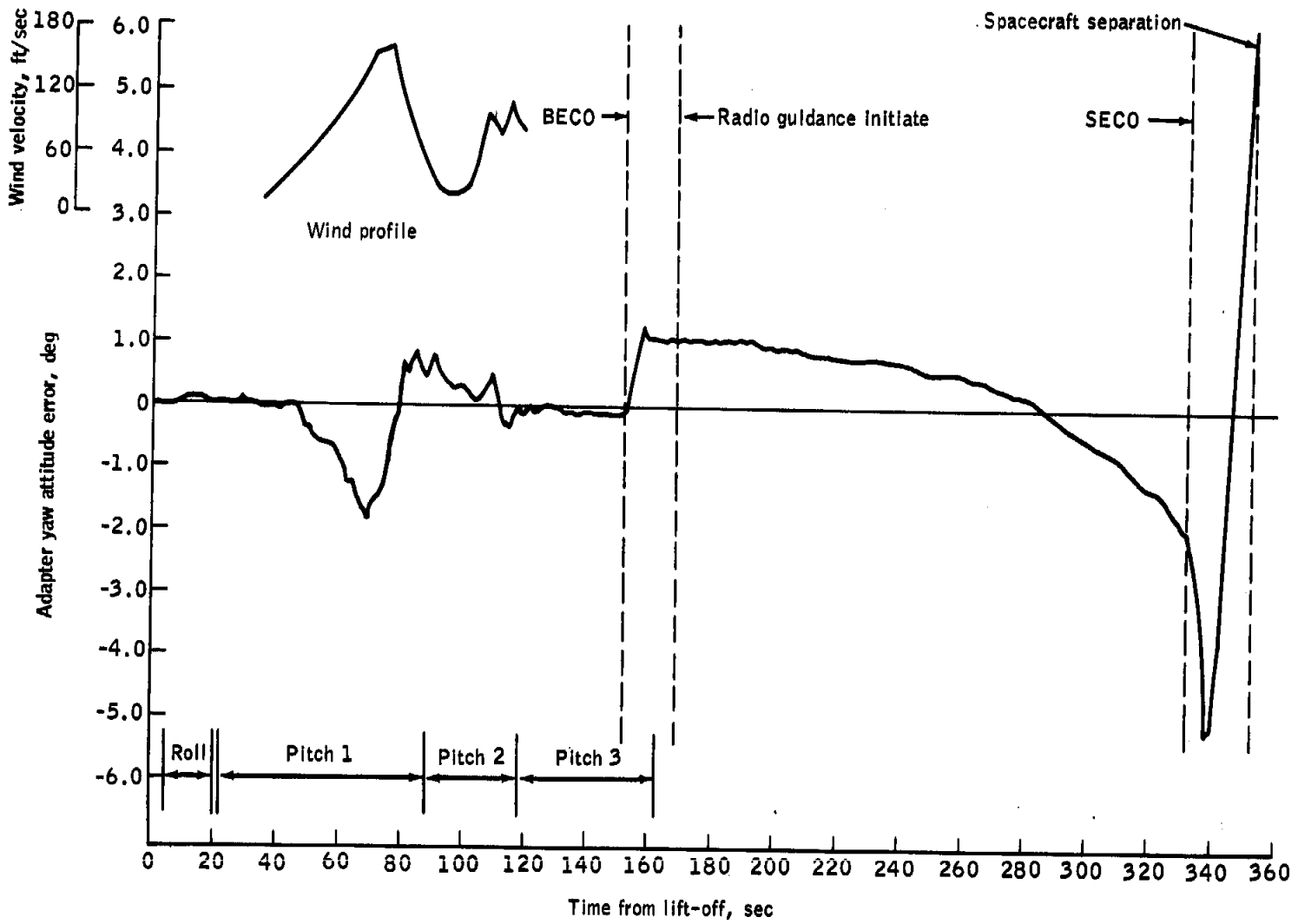
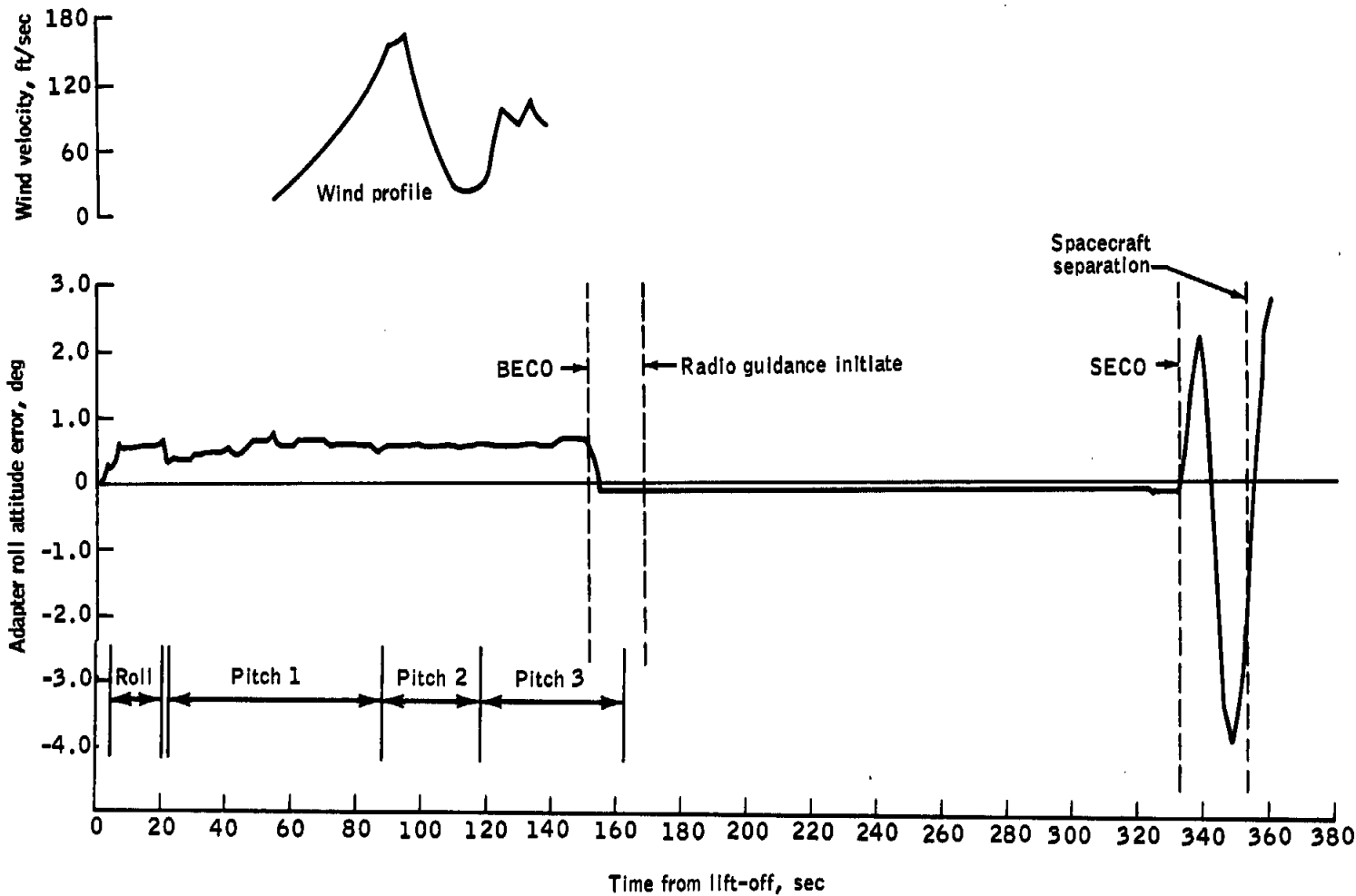


Figure 5.2-12. - Yaw flight displacement

UNCLASSIFIED

UNCLASSIFIED



UNCLASSIFIED

UNCLASSIFIED

Figure 5.2-13. - Roll flight displacement

UNCLASSIFIED

UNCLASSIFIED

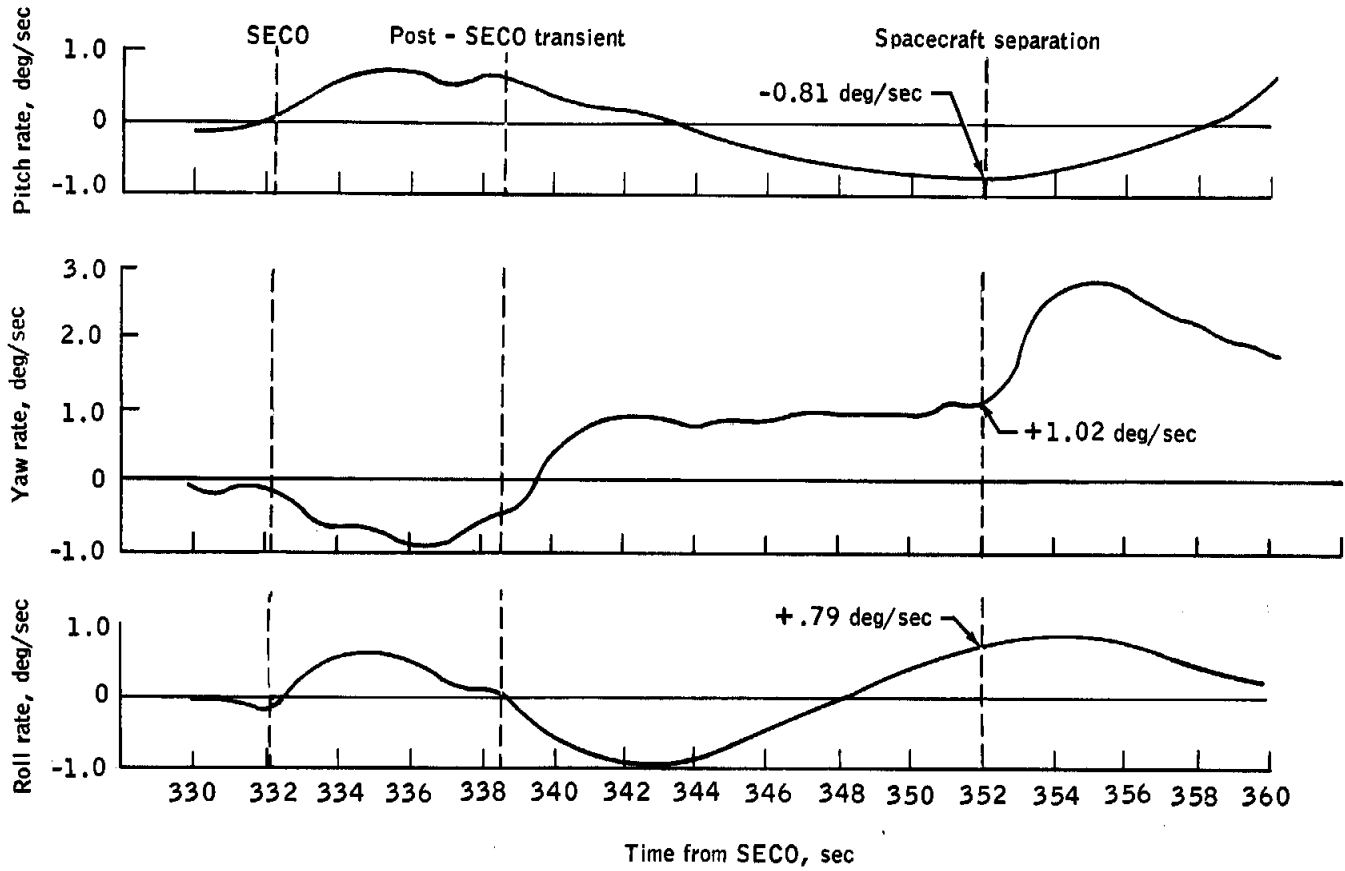


Figure 5.2-14. - GT-2 post - SECO oscillations

NASA-S-65-1830

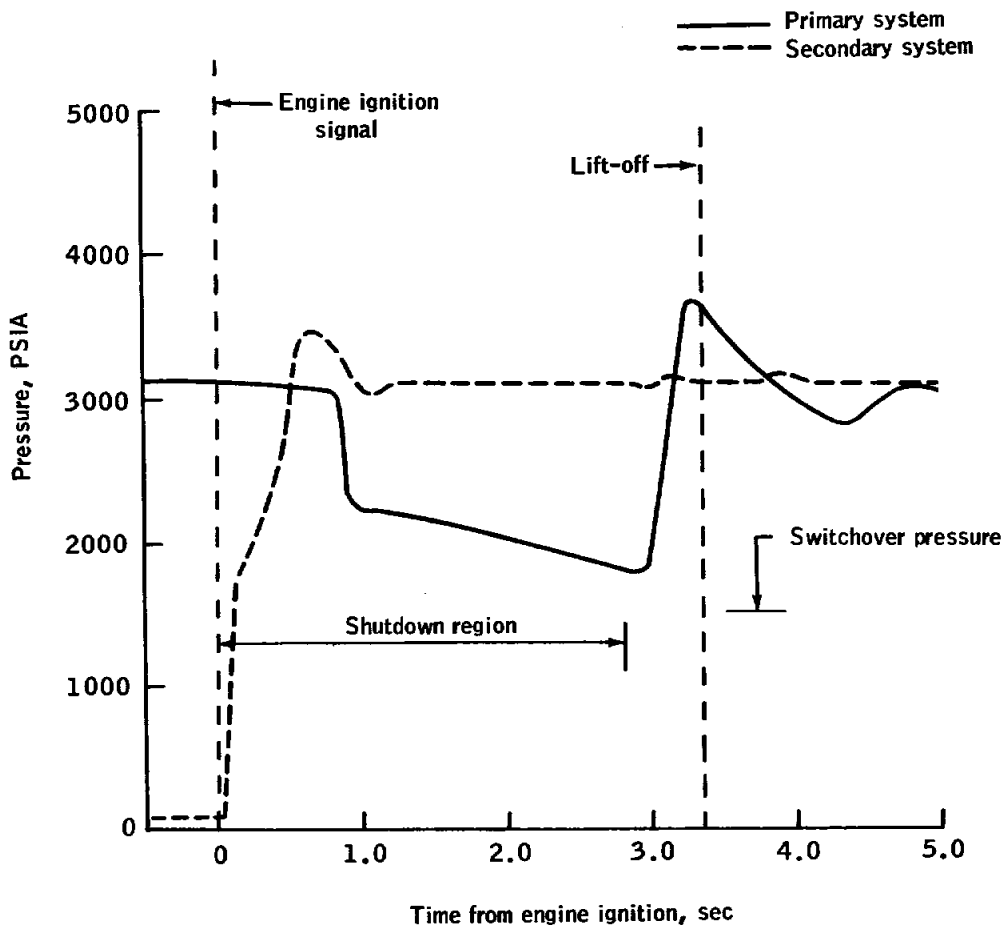
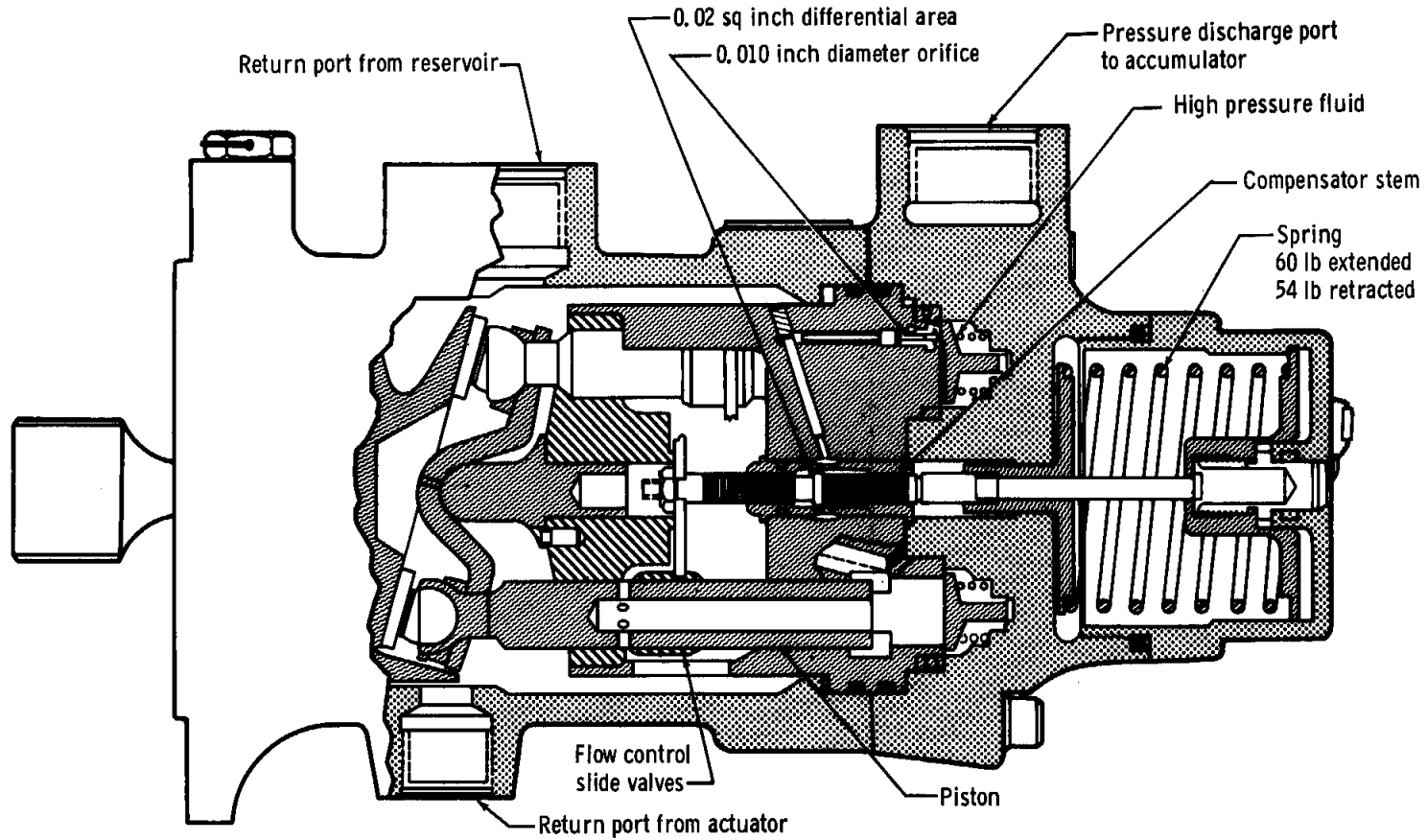


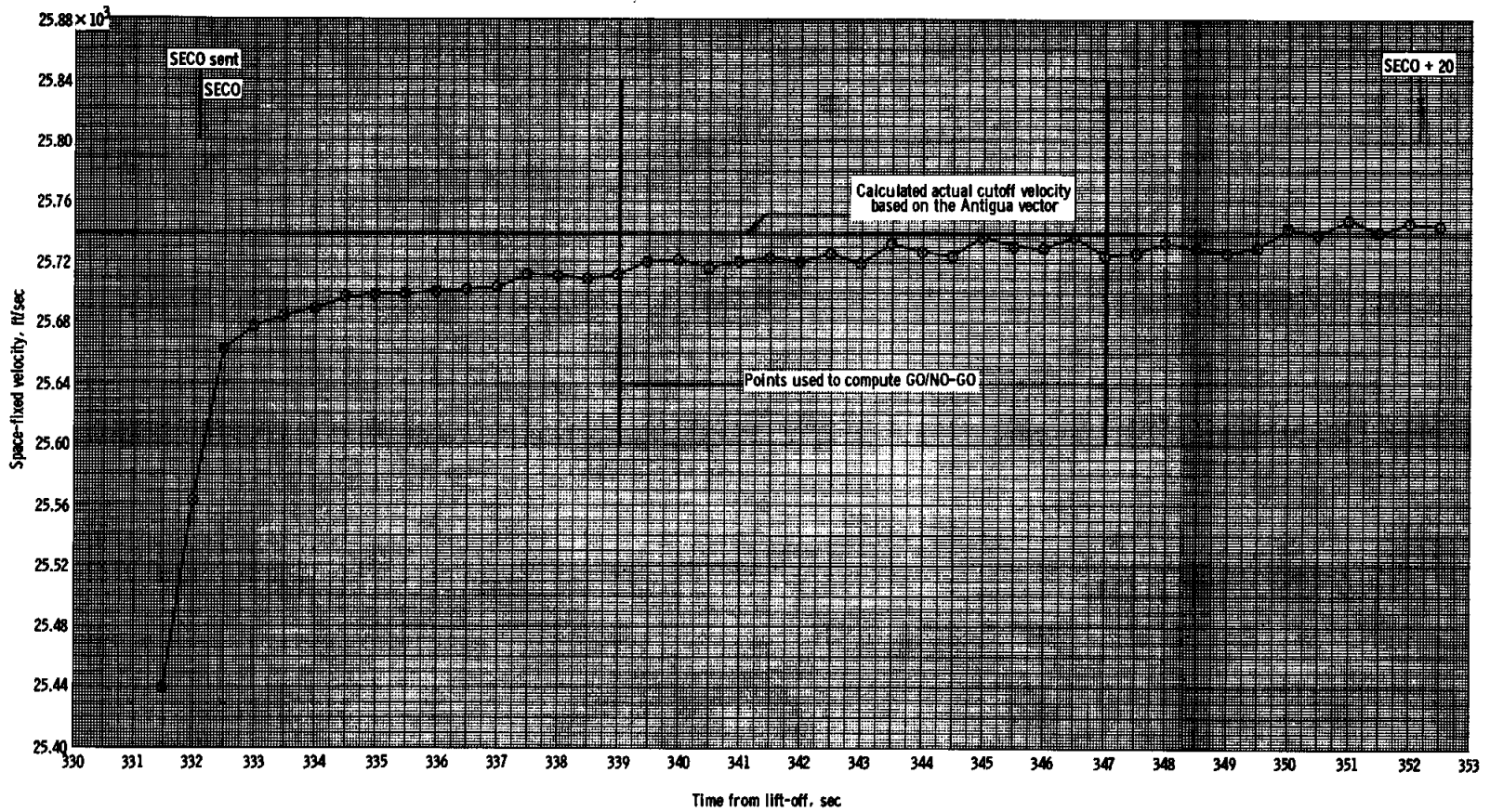
Figure 5.2-15. - Time history of stage I hydraulic pressure

~~UNCLASSIFIED~~



~~UNCLASSIFIED~~

Figure 5.2-16. - Hydraulic pump cross-section, stage I primary and secondary systems

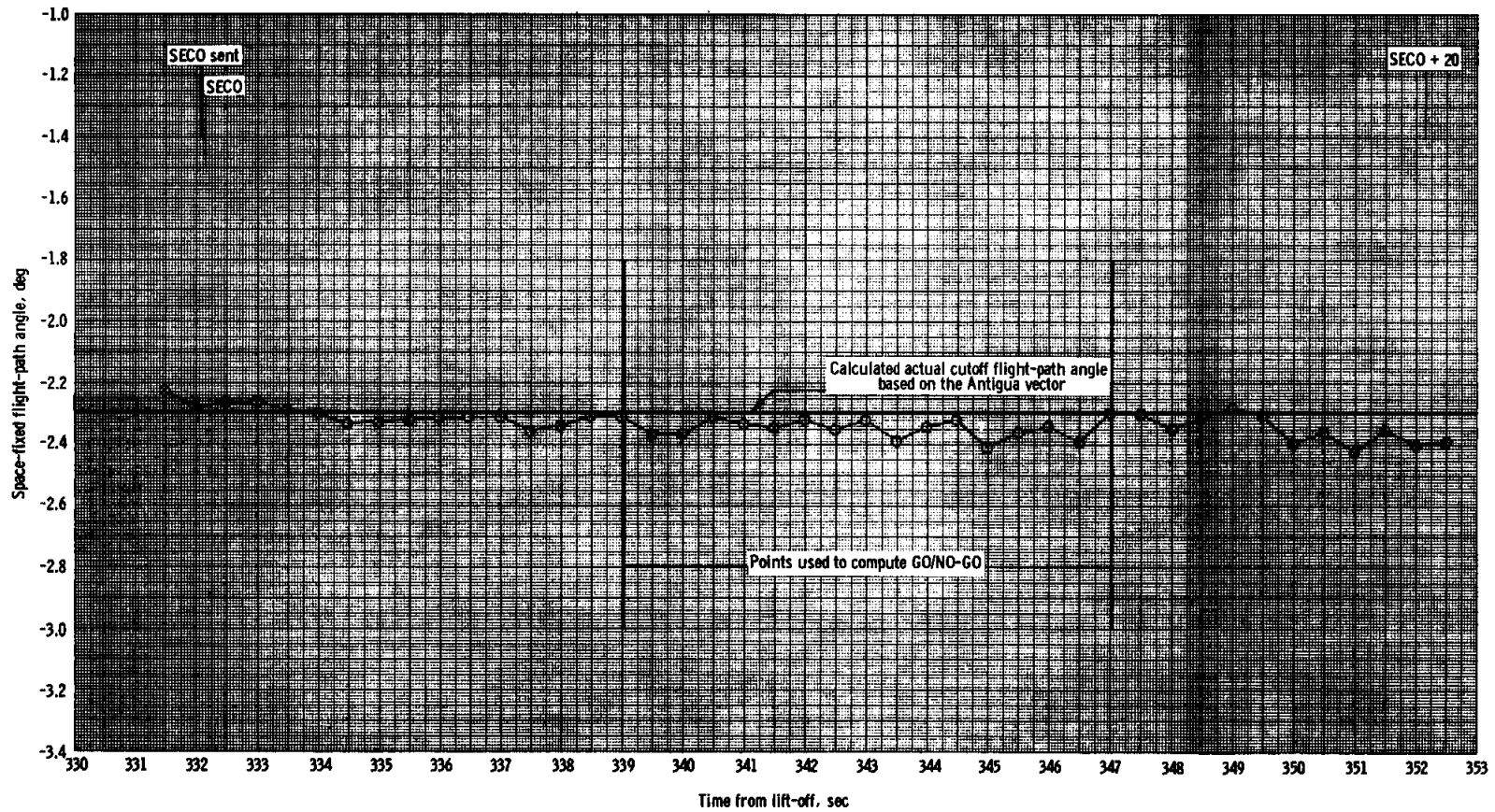


(a) Space-fixed velocity.

Figure 5.2-17. - Space-fixed velocity and flight-path angle in the region of cutoff using launch vehicle guidance data.

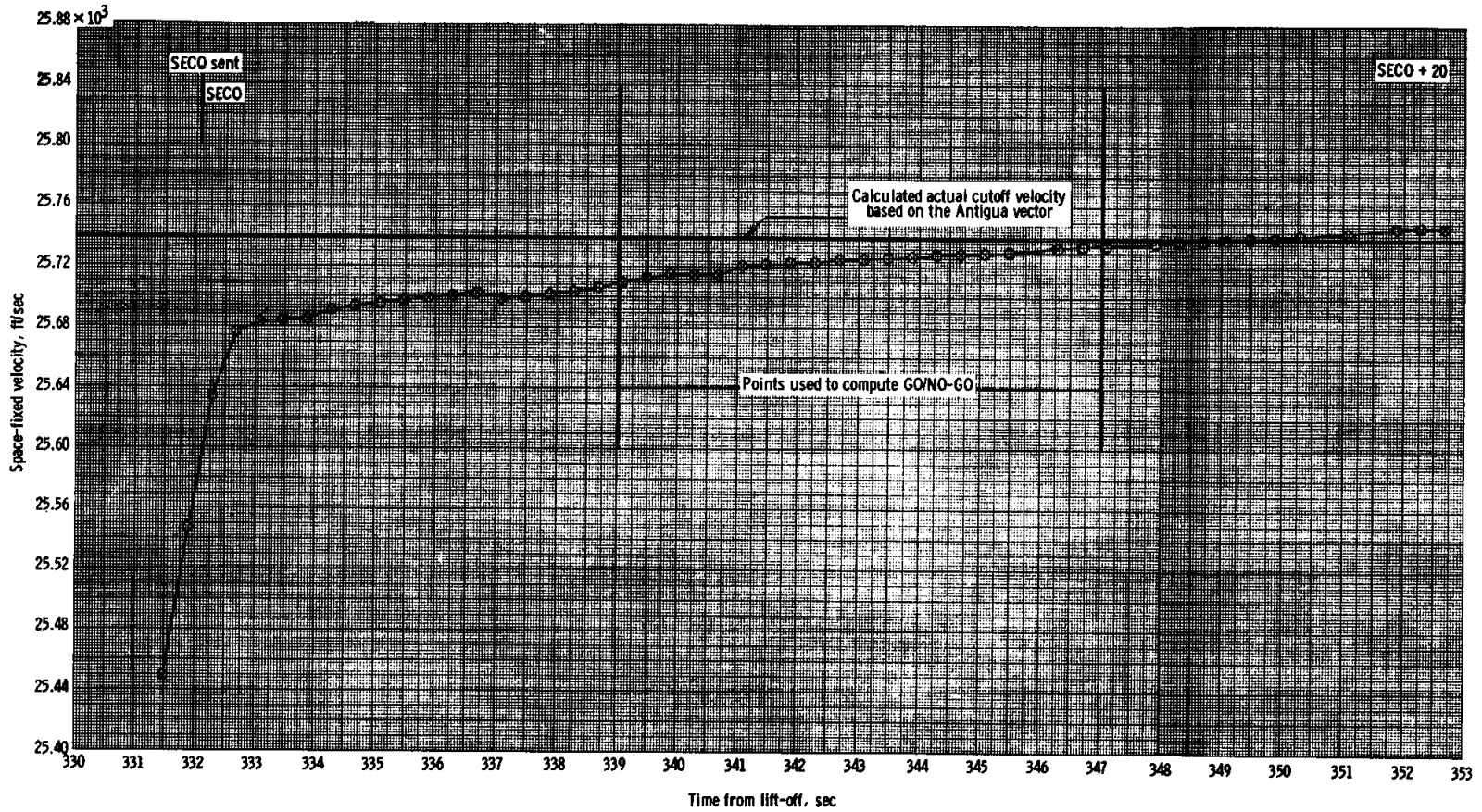
~~CONFIDENTIAL~~

~~CONFIDENTIAL~~



(b) Space-fixed flight-path angle.

Figure 5.2-17 - Concluded.

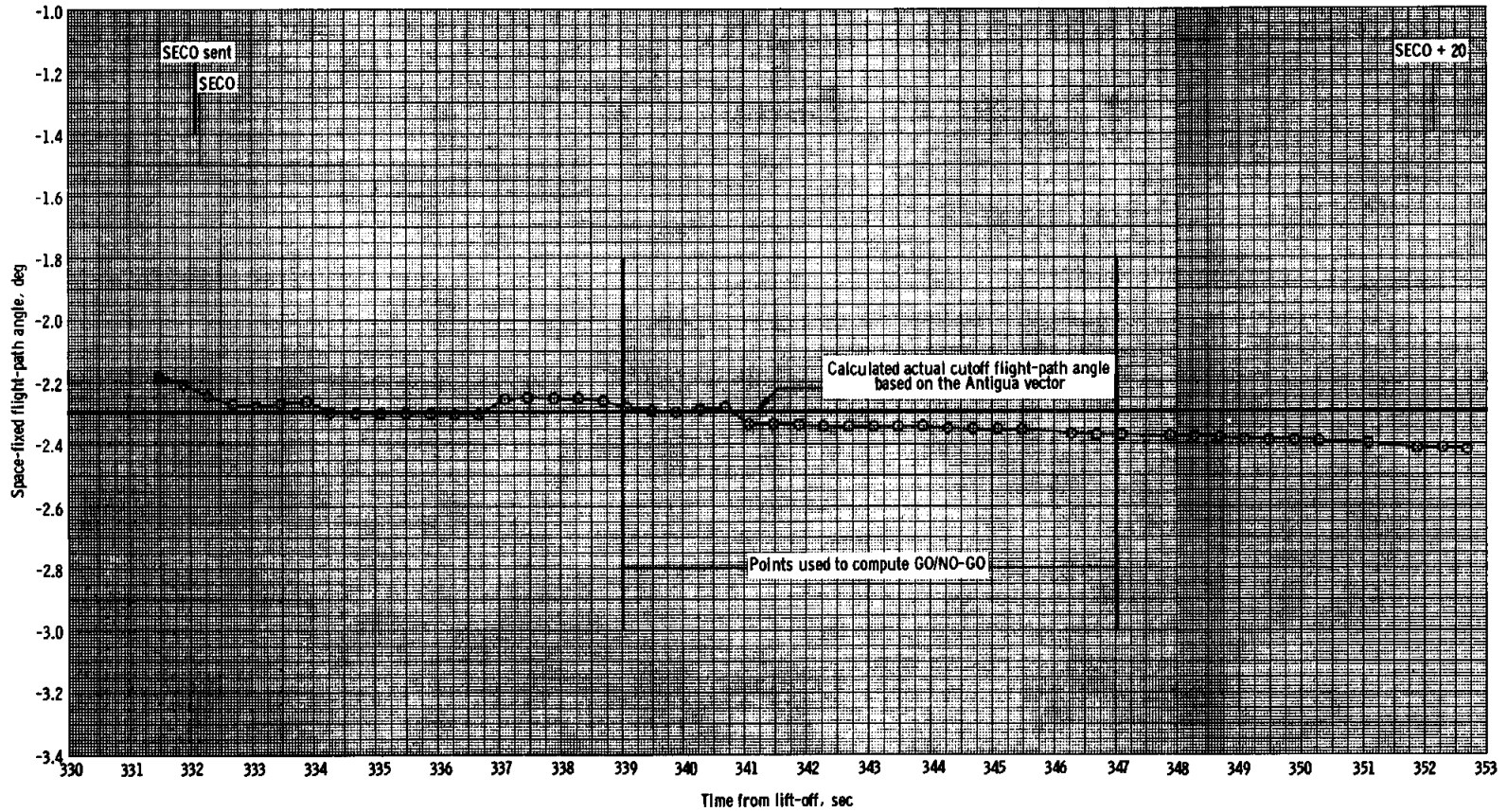


(a) Space-fixed velocity.

Figure 5.2-18 - Space-fixed velocity and flight-path angle in the region of cutoff using MISTRAM I Range safety computer (IP-3600) data.

CONFIDENTIAL

CONFIDENTIAL



~~CONFIDENTIAL~~

~~CONFIDENTIAL~~

(b) Space-fixed flight-path angle.

Figure 5.2-18 - Concluded.

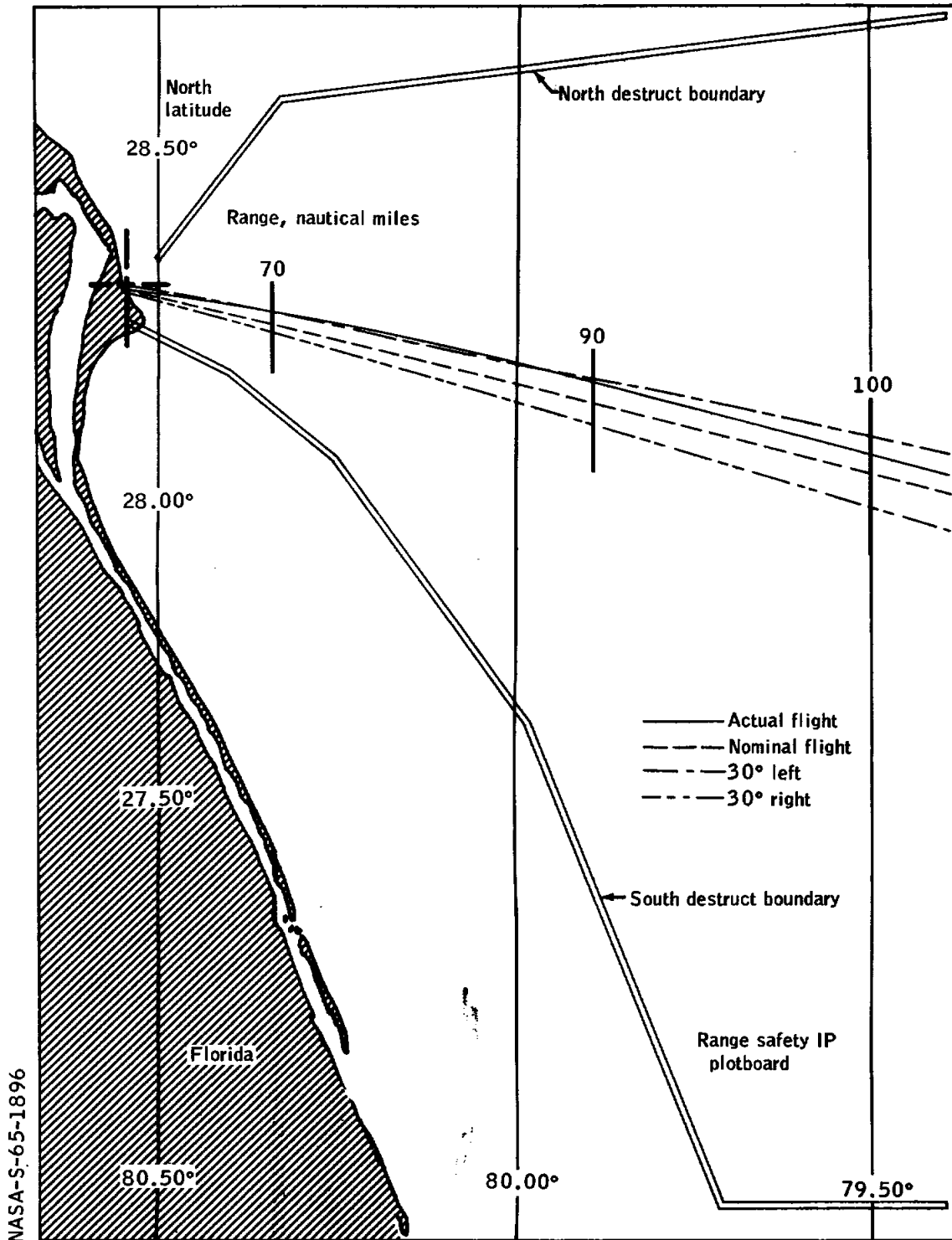


Figure 5.2-19. - Range safety IP plotboard

5-208

~~UNCLASSIFIED~~

THIS PAGE LEFT BLANK INTENTIONALLY

~~UNCLASSIFIED~~

5.3 GEMINI LAUNCH VEHICLE - SPACECRAFT INTERFACE PERFORMANCE

The various aspects of the Gemini launch vehicle - spacecraft interface, as defined in reference 9, performed within specification limits. The performance of the electrically and mechanically interfacing systems were derived from the overall performance of the launch vehicle and the spacecraft as determined from telemetry measurements of specific parameters made on both sides of the interface.

The interface structural loading conditions were such that maximum αq was approximately 50 percent of launch-vehicle design loading. In comparison, the GT-1 mission experienced about 32 percent of launch-vehicle design loading. Interface vibration measurements indicate an environment equivalent to that of the GT-1 flight. The differential pressure of the interface compartment area reached 66 percent of the design value. The measured venting area which controls the differential pressure was about 13 square inches, which is well within the permissible limits.

An inspection of the mechanical interface prior to and during the launch-vehicle - spacecraft mating showed no major discrepancies between the actual hardware and the mechanical-interface and venting-interface specification drawing. The thermal curtains usually located at the spacecraft adapter - launch vehicle interface were not installed for the GT-2 mission.

The electrical interfacing circuitry on both sides of the interface performed without any anomalies in regard to opens, shorts, or transients. Signals generated for the malfunction detection system (MDS) and sequence of events were on time and correct for the normal mission flown. A known discrepancy existed in the spacecraft stage II fuel pressure meter (unit A) prior to the launch day. This meter was not required for the flight since the redundant MDS fuel pressure meter was operating satisfactorily and was further backed up by the telemetry measurements of the tank pressures. During the count, the stage II fuel pressure meter indicated correct pressures but failed about 1 second after lift-off.

5-210

UNCLASSIFIED

THIS PAGE LEFT BLANK INTENTIONALLY

UNCLASSIFIED

6.0 MISSION SUPPORT PERFORMANCE

This section contains a discussion of the spacecraft and launch-vehicle countdown, flight-control operations, network performance, and recovery operations.

6.1 PRELAUNCH OPERATIONS

6.1.1 Gemini Spacecraft

Spacecraft precount preparation started at 10:30 p.m. e.s.t., January 14, 1965, following the successful completion of the final simulated flight. A pyrotechnic shielding check was started at 4:00 a.m. e.s.t., January 15, 1965, to allow time in the precount activities to change the RCS B-ring pressure regulator. Liquid oxygen servicing was completed by 7:00 a.m. e.s.t., January 16, 1965; however, liquid hydrogen servicing was delayed pending completion of the regulator change. Replacement of the regulator and pressurization of the RCS B-ring pressure tank were completed by 4:00 p.m. e.s.t. on January 16. Liquid hydrogen servicing was then completed, and the precount started on schedule at 9:00 p.m. e.s.t. on January 16, 1965.

The following spacecraft activities were implemented in an attempt to avoid delays to the final countdown.

- (a) Installation of the horizon sensor fairing at T-23 hours rather than T-15 hours.
- (b) Removal of the reentry control system (RCS) and orbital attitude and maneuver system (OAMS) emergency dump systems immediately following final connection of the spacecraft pyrotechnics (T-51 hours).
- (c) Placement of temporary plastic covers over access doors so that erector white room disassembly could begin early in the countdown.
- (d) Setting up of spacecraft switches prior to launch-vehicle propellant loading.
- (e) Elimination of the use of a force gage to fit shingle retention washers.

Before starting the count, it was known that the reactant supply system (RSS) oxygen was 64 percent loaded rather than the nominal 98 percent. On January 18, the blockhouse oxygen pressure indicator

UNCLASSIFIED

was hard over the full-scale reading of 1000 psi and was believed to be inoperative since it should have been indicating 80 to 90 psi. Access to the erector white room to verify this supposition was not allowed because of launch stand personnel restrictions at that time. The oxygen heaters were turned on as part of the required procedure; and as a result the oxygen temperature rose, and the tank pressure apparently reached the relief valve setting and vented oxygen to the atmosphere. After midnight on F-day, the oxygen quantity was determined to be 64 percent. This amount was acceptable for a single fuel-cell stack, and it was decided that launch preparations should not be delayed to reload the RSS oxygen.

The servicing and mechanical work during the precount period were satisfactorily completed. Final spacecraft preparations were then made for the countdown. The final countdown was started at 2:01 a.m. e.s.t. and continued uninterrupted until T-5 minutes (8:56 a.m. e.s.t.), at which time a 2-minute hold was called to obtain a satisfactory proof firing of one of the orbital attitude and maneuver system (OAMS) thrusters. The countdown was recycled to T-6 minutes, restarted at 8:58 a.m. e.s.t., and continued uninterrupted to lift-off. A schedule of the countdown is given in figure 6-1.

A minor problem occurred during activation of the fuel cell at T-329 minutes when helium-hydrogen flow could not be obtained through the hydrogen purge valve. Troubleshooting of this problem was continued until T-223 minutes when it was determined that further trouble isolation would have required disconnecting the spacecraft wire bundles. A decision was made at that time not to activate the fuel cell for the flight.

At T-85 minutes, personnel in the white room had some temporary difficulty in closing and securing the spacecraft left-hand hatch. The inside handle was not remaining in the neutral position so that the gears could be engaged to set the latches. The problem was solved in less than 5 minutes and a hold was not required. Design and assembly procedures have been changed for the latching mechanism, and this difficulty should not occur with future spacecraft.

6.1.2 Gemini Launch Vehicle

6.1.2.1 Propellant loading operations. - Propellant loading operations were initiated at 4:00 p.m. e.s.t. on F-1 day, some 2 hours earlier than originally planned. The total loading time was 6 hours and 20 minutes. Cold ambient weather conditions, forecasted through the planned T-0, indicated that an earlier start was possible and would allow time for troubleshooting if necessary. Operations were exceptionally smooth,

UNCLASSIFIED

and only three significant hardware anomalies were noted:

(a) Cut-out of the stage II oxidizer loading pump at the start of pre-chill. The primary cause of this condition was overloading of the pump motors.

(b) Failure of the stage I fuel secondary counter to record propellant flow properly led to non-standard procedures. Failure analysis of the counter mechanism is underway.

(c) Failure of the stage I fuel preset counter to shut off the loading pump upon reaching zero caused a minor overload condition in that tank. Pump cut-off was accomplished after observing the failure.

Indicated final loading accuracies based on the flowmeter readouts compared with desired mission loads and were within ± 0.10 percent as shown in table 5.2-VI.

6.1.2.2 Countdown. - The countdown began at 2:01 a.m. e.s.t. January 19, 1965, and progressed to a successful lift-off with no launch-vehicle holds. For approximately the first 3 hours in the count, intermittent communications were experienced between the Complex 19 Test Conductor and the Superintendent of Range Operations (SRO), and Mod III and the Mission Control Center (MCC). This problem was rectified before automatic sequencing was initiated.

Countdown clock synchronization between the blockhouse, SRO, and the GE/Burroughs complex was not finalized before starting the count.

At T-266 minutes an azimuth update of 108.1° , instead of the proper 104.1° signal, was sent by Mod III. This update was corrected, and the Mod III interface checks were completed successfully.

The countdown proceeded to T-4 minutes 59 seconds when a hold was called to conduct an additional firing of the spacecraft thrusters. The count was recycled approximately 2 minutes later to T-6 minutes and then proceeded smoothly to lift-off.

6.2 FLIGHT CONTROL

In this section, the events which occurred during prelaunch, powered flight, and reentry phases of the flight are reported in real time as they appeared to the flight controllers during the mission. Consequently, there are certain inconsistencies between this section and other sections of the report which are the result of extensive postflight analysis.

UNCLASSIFIED

6.2.1 Premission Operations

6.2.1.1 Premission schedule.- Flight controllers departed for their stations on November 22, 1964, and participated in prelaunch activities. On December 9, 1964, a malfunction in the hydraulic system of the launch vehicle resulted in the launch being postponed, and the flight controllers returned to Houston. The mission was rescheduled for January 19, 1965, and flight controllers returned to their stations on January 10, 1965. The Mission Control Center (MCC) flight control team schedule included the documentation review on F-8 day, abbreviated systems test on F-7 day, launch-abort simulations on F-6 and F-4 days, spacecraft simulated flight on F-5 day, confidence test and precount on F-3 day, final ground-station checkout and Flight Dynamics Officer (FIDO) exercises on F-1 day, and launch on F-0 day.

6.2.1.2 Documentation.- The documentation generated for this mission was adequate. The major documentation problem was the difficult coordination of spacecraft TM calibration data between MCC, Goddard Space Flight Center (GSFC), and the Gemini Program Office (GPO). A total of 53 Instrumentation Support Instructions (ISI's) were generated from the start of mission operation in November 1964 through launch in January 1965. Two revisions were made to the Mission Rules, primarily to simplify procedures as a result of changes to the abort interface agreements made with the Range Safety Officer (RSO). Revisions were made to the overall mission countdown to facilitate digital command system (DCS) testing, move the confidence testing to F-1 day, and accommodate changes in spacecraft testing and in range safety procedures.

6.2.1.3 MCC network flight control operations.- The flight control team participated in all launch-complex support operations requiring MCC support. The MCC, Coastal Sentry Quebec (CSQ), and Rose Knot Victor (RKV) participated in 5 days of simulation exercises for a total of 25 simulations during the two periods of activity. The simulations included full countdowns for the entire network on 2 days and short counts on the remaining days. Final ground systems checkout was scheduled for F-1 day to reduce the probability of holds in the final F-0 day count.

6.2.1.4 Countdown.- The operations room at the MCC was initially manned by the Operations and Procedures monitor (O and P) and the booster systems engineer (BSE) at 4:05 a.m. e.s.t. (T-295 min). The range safety inhibit check was completed at T-230 minutes. All flight control positions were manned at 5:25 a.m. e.s.t. (T-218 min). At 6:16 a.m. e.s.t. (T-164 min) all power except that for the DCS and intercom failed as a result of a fail-over of an industrial lighting circuit to critical power. This power failure disabled the 1218 computer. Power was restored and the fail-over feature was disabled on this circuit. Minor crosstalk and low-level circuits occurred on the intercom but presented

UNCLASSIFIED

no significant problems. At T-130 minutes the preinsertion status appeared satisfactory. Trajectories based on T-300-minute wind data were available and in place at T-70 minutes. Little difference was indicated by the T-60 minute report. Erector lowering status check at T-46 minutes was satisfactory. Internal power was turned on at T-33 minutes, and the internal power check was completed. Status check was GO by MCC at T-26 minutes, and the final MCC GO was given at T-6 minutes. A hold was called for spacecraft orbital attitude and maneuver system (OAMS) static firing at 8:55 a.m. e.s.t. (T-5 min), and the count was recycled to T-6 minutes. The count began again at 8:58 a.m. e.s.t. The IGS update was enabled at T-4 minutes 30 seconds, and target parameters were verified at T-2 minutes 40 seconds. Ignition occurred at 9:03:55 a.m. e.s.t., and lift-off occurred at 9:03:59 a.m. e.s.t. The countdown was performed satisfactorily and functions were often completed ahead of or on schedule.

6.2.2 Mission Operations Summary

6.2.2.1 Powered flight.- At lift-off, the spacecraft and ground clocks were in sync, and all spacecraft and launch-vehicle systems were functioning normally. The launch-vehicle primary and secondary hydraulic pressures fluctuated considerably more than normal during engine start, but stabilized at 3000 psi, and remained steady throughout stage I flight. Telemetry data indicated that the launch-vehicle pitch and roll programs had been initiated properly, and subsequent tracking data confirmed this information. Spacecraft systems appeared normal, and data during the powered flight did not differ significantly from prelaunch values. At approximately LO + 25 seconds, the IGS 10.2 V dc regulated voltage, which had been erratic on telemetry before lift-off, dropped to zero and remained there for the duration of the mission. This was known to be a spacecraft instrumentation problem. Shortly after lift-off, cabin differential pressure began rising, reached the relief point of 5.7 psid at LO + 48 seconds, and went off scale on the meter at 6 psid. At about LO + 117 seconds, the pressure dropped slowly to 5.7 psid, indicating that the cabin pressure had relieved normally and was within the expected range. This value remained constant until the reentry phase. The electrical system main bus voltages were between 22.6 to 22.8 V dc, and the special pallet bus voltages ranged between 24.1 and 25.2 volts during the mission. The coolant loop temperatures rose as anticipated and went beyond the meter scale range at LO + 180 seconds. It was impossible to monitor operation due to the lack of water outlet temperature readings on spacecraft 2. Cabin air and suit temperatures were between 65° and 75° F throughout the flight.

The spacecraft inertial guidance system (IGS) performed extremely well, and good correlation was obtained between the RGS and IGS systems

UNCLASSIFIED

throughout the powered flight. Stage I engine cutoff and staging occurred normally at LO + 153 seconds. At staging, the stage II thrust rose to the nominal value and increased slightly, as expected, during stage II powered flight. The stage II hydraulic pressure went to 2800 psi at staging and fluctuated somewhat, which is an indication of engine gimbaling. This pressure was about 300 psi below predicted values. The stage II oxidizer tank-pressure sensor B began to fluctuate about ± 3 psi around nominal shortly after staging and continued for approximately 30 seconds; then it stabilized at nominal values. The A sensor remained stable during this period.

The thrust vector shift at staging was noted; however, the shift in the pitch axis was very small, and the shift in the yaw axis was nearly the same as that observed on the GT-1 mission. The initiation of RGS steering was delayed a few seconds since the flight-path angle flag was set by Burroughs, indicating that Burroughs was not computing steering orders. This delay and the lofted trajectory resulted in a delay of about 10 to 12 seconds before steering converged. The reason for the flag being set was not known.

The nose-fairing and horizon-sensor-fairing jettison functions were reported to be 2 seconds early by the Guidance Navigation and Control (GNC) engineer at LO + 195 seconds. The final status check was started by the Flight Director at LO + 213 seconds, and the MCC reported GO for the flight at LO + 225 seconds. The RKV ship had acquired the spacecraft at the nominal time of LO + 200 seconds and was reporting all events and status data to the procedures monitor.

Immediately prior to a velocity ratio of $V/V_r = .8$, another electrical power failure occurred in the MCC, at approximately LO + 306 seconds. As a result, all displays, certain lighting, all MCC recordings, and the 1218 computer telemetry outputs were lost. The intercom continued to function on battery power; the DCS and computer were functioning on the Gemini mission simulator (GMS) uninterrupted power supply. Lighting in the operations room was provided by critical power. The Flight Director advised the RKV of the power failure, and the ship's flight control team began briefing the MCC on the separation sequence. SECO occurred at approximately LO + 333 seconds, and a voice report of the SECO transmission was monitored at LO + 336 seconds, enabling the Assistant Flight Director to start the manual timers. These timers were planned to be used as a reference for transmitting a backup spacecraft separation command and for transmitting the abort command to backup spacecraft separation sequence and start the retrofire sequence. These functions were not sent because of the uncertainty in SECO time and because the spacecraft was sequencing normally. Power was restored in the MCC at approximately LO + 339 seconds, and all systems with the exception of the 1218 computer were functioning within 60 seconds of power restoration.

UNCLASSIFIED

The separation sequence was normal and occurred at LO + 353 seconds. The RKV ship reported a rise in the aft-firing thruster temperature from 60° to 100° F in a 30-second period commencing approximately 15 seconds after separation. This temperature rise was useful in confirming OAMS separation thrusting. No detectable decrease in OAMS propellant quantity was noted as a result of separation burn. During the period from GLV-spacecraft separation to retrograde section separation, it was reported that the horizon sensor did not appear to acquire a solid lock, and the search mode dropped in and out continuously. After power restoration at the MCC, the GSFC computers received the SECO discrete, and started the go-no-go computation. The real-time go-no-go was as follows:

Source	Velocity, ft/sec	Flight-path angle, deg
GE/Burroughs	25759	-2.48
IP	25753	-2.46

Based on the go-no-go vector obtained from GSFC and the GE/Burroughs source, an initial impact point of 16°51' N. latitude, 50°18' W. longitude was relayed to the recovery forces at LO + 565 seconds. Spacecraft turnaround started at approximately LO + 384 seconds, and the turnaround was normal. Several telemetry display dropouts occurred during the spacecraft pass over the RKV; these dropouts were also noted on the data at MCC via the Grand Turk Island (GTI) station. Both stations were able to monitor and evaluate the retrofire. At LO + 384 seconds, the initiation of oxygen high-rate flow was noted, and the attitudes and rates appeared normal.

The anticipated pressure drop in primary oxygen tank pressure after the initiation of high-rate flow was noted. Subsequent computations based on secondary oxygen usage showed the rate to be nominal. However, an anomaly was observed in the decrease in tank pressures on the fuel-cell cryogenics tanks. The decrease apparently began at spacecraft separation, and by the time of adapter jettison, the pressure had dropped to 70 percent of normal.

6.2.2.2 Reentry. - The adapter flexible linear shaped charge (FLSC) firing, automatic retrorocket initiation, and equipment section separation occurred at LO + 415 seconds. The retrorocket firing sequence was normal, and no significant deviations were noted in attitudes and rates. Gimbal angles at retrofire were nominal within the readability tolerances monitored at MCC from Grand Turk data. Retrograde section FLSC firing

UNCLASSIFIED

occurred at LO + 460 seconds. Because of the TM dropouts reported previously, neither the RKV nor the MCC was able to confirm retrograde section jettison; however, the pitch to reentry maneuver was used to confirm retrograde section jettison. Although this maneuver was not confirmed in real time, post-pass data analysis verified that this event occurred at LO + 467 seconds. The GTI TM loss of signal (LOS) at MCC occurred at approximately LO + 540 seconds, and RKV LOS occurred at LO + 955 seconds; both were very nearly nominal. The spacecraft subsequently entered the TM blackout region, where all sequences were assumed to have occurred normally.

The CSQ ship acquired solid telemetry at LO + 702 seconds. At CSQ the acquisition of UHF tone was accomplished, and the spacecraft roll rate was $12^{\circ}/\text{sec}$, indicating that the spacecraft was in reentry mode. The roll rate was terminated at LO + 718 seconds, and the spacecraft changed to the maximum lift attitude. The TM dropouts continued and interfered with validation of certain reentry events. PCM TM dump was initiated at LO + 762 seconds (nominal), and the signal was reported to be of good quality. The Antigua station had been tracking the spacecraft, and at LO + 820 seconds was transmitting data to GSFC.

The spacecraft cabin differential pressure went to 0 at LO + 850 seconds, indicating proper regulation. Immediately prior to R and R separation, the pitch and yaw rates were noted to exceed $15^{\circ}/\text{sec}$. R and R separation occurred at LO + 876 seconds; however, there was no indication that the pilot parachute had deployed. The TM was lost during this period until the UHF descent antenna was extended. The main parachute deployment was not verified immediately upon reacquisition of solid telemetry. The telemetry from R and R section separation to single-point release was intermittent, probably because the descent antenna was not yet extended. By monitoring the rate of change of forward compartment pressure, the CSQ verified at LO + 874 seconds that the main parachute had deployed. At approximately LO + 1020 seconds, the CSQ verified that the UHF recovery beacon was on and tone quality was good. Telemetry was lost at LO + 1098 seconds, and UHF tone was lost at LO + 1105 seconds due to the radio horizon.

The Antigua data transmitted to GSFC were processed and differentially corrected. These data resulted in an impact prediction (IP) point of $16^{\circ}36'$ N. latitude and $49^{\circ}51'$ W. longitude. This solution had converged with very small deviations, and it was decided to transmit it to the recovery forces at LO + 1170 seconds as the final IP. This answer was within approximately 4 miles of the spacecraft pickup point.

An IP was also obtained via the MCC (Houston) computer based on the MISTRAM cutoff vector. The answer was in the same general area as the other two. The CSQ reported HF beacon contact at LO + 1500 seconds; this was the first indication that the spacecraft was on the water and

UNCLASSIFIED

floating. In addition, CSQ provided a bearing at TM LOS of 287° which was in the same general direction as the IP. The flight control support of the mission terminated with a debriefing at 10:10 a.m. e.s.t.

6.3 NETWORK PERFORMANCE

The network for the GT-2 mission consisted of the Air Force Eastern Test Range (AFETR) land stations; the Mission Control Center (MCC); Merritt Island Launch Area (MILA); Bermuda (BDA); the AFETR instrumentation ships Rose Knot Victor (RKV), Coastal Sentry Quebec (CSQ), and Lima; and four AFETR telemetry aircraft. The AFETR land stations included Cape Kennedy (CNV), Patrick Air Force Base (PAT), Valkaria (VAL), Eleuthera (ELU), Grand Bahama Island (GBI), San Salvador Island (SSI), Grand Turk Island (GTI), and Antigua Island (ANT).

The CNV area is shown in figure 6-2. The mainland AFETR tracking system is shown in figure 6-3. The GT-2 network remote stations are shown in figure 6-4 along with the earth trace of the trajectory.

The network countdown was started at 2:00 a.m. e.s.t., January 19, 1965, at T-420 minutes. Initial computation and data-flow integrated subsystem (CADFISS) tests were run at T-415 minutes. The MILA TPQ-18 radar tests were successful, except for the range target test which could not be accomplished because of a defective wave-guide section and a defective 16 kV power supply. The power supply was to be replaced with an estimated time of operation (ETO) at 4:00 a.m. e.s.t. The wave-guide section was flown in, and the section was to be installed with an ETO at 6:00 a.m. e.s.t. The PAT FPQ-6 radar failed all tests except the counterclockwise slew. The GTI TPQ-18 radar passed all tests except for the counterclockwise slew. The ANT FPQ-6 passed all radar tests. The BDA FPS-16 passed all radar tests, but the Verlorrt radar failed the bore-sight test.

The MILA radar CADFISS reruns at T-110 minutes were satisfactory. The PAT radar reruns were also satisfactory. The CNV, GBI, and SSI FPS-16 radar initial CADFISS runs were satisfactory, as were the CSQ and RKV initial data-flow runs. The BDA Verlorrt reruns were satisfactory at T-110 minutes.

The MCC had two power failures during the mission. Both power failures were caused by an overloaded circuit breaker on the secondary critical power bus. Instrumentation had been continually added to the power system over the past months, but the buses had never been operated with all equipment on-line. The first power failure occurred at 6:15 a.m. e.s.t. when a lighting circuit on an industrial power bus in the MCC

UNCLASSIFIED

failed over to a critical power bus, overloading the bus. The second power failure occurred at 9:09 a.m. e.s.t., approximately LO + 300 seconds. An overload condition resulted from bringing oscillographs, recorders, and other equipment on line at T-300 seconds. The power was restored 39 seconds later, but the MCC dynamic displays were out for about 5 minutes, or until LO + 600 seconds.

There were several other power problems during the mission period. The RKV ship had a power failure at 5:47 a.m. e.s.t. caused by the tripping of the number four circuit breaker on the main power panel. The circuit breaker was improperly adjusted. At 8:43 a.m. e.s.t., the MILA radar experienced an industrial power fluctuation caused by a transfer in the commercial power source. The radar was operational again at 8:51 a.m. e.s.t. The CSQ experienced several power fluctuations during the mission period.

All telemetry aircraft in the terminal area were reported to be ready to support the mission at 8:54 a.m. e.s.t. At lift-off, the network was ready to support the mission, and during the 20-minute flight, no major instrumentation problems occurred except the MCC power failure at LO + 300 seconds.

6.3.1 MCC and Remote Facilities

Telemetry from both the spacecraft and the GLV was acquired and recorded at CNV, the MCC, Tel II, and Tel III.

6.3.1.1 Telemetry.- Tel II and Tel III remoted real-time GLV and spacecraft data to the MCC for display to flight controllers. Telemetry coverage for all stations is shown in table 6-I. Coverage for all stations was approximately equal to the premission nominal.

6.3.1.2 Radar.- The MILA TPQ-18, CNV FPS-16, PAT FPQ-6, and CNV S-band radars all performed satisfactorily. The acquisition of signal (AOS) and loss of signal (LOS) times and the mode of tracking are shown in table 6-II. Coverage was near nominal for all sites.

6.3.1.3 Timing.- The timing systems all operated satisfactorily.

6.3.1.4 UHF air-to-ground communications.- MCC had good UHF coverage from AOS at T-30 minutes until LOS at LO + 480 seconds.

6.3.1.5 Acquisition aids.- The acquisition aids at MCC, Tel II, and Tel III operated satisfactorily. The AOS and LOS times are listed in table 6-III.

UNCLASSIFIED

6.3.1.6 Digital command system (DCS).- Operation of the DCS, inertial guidance system (IGS) data link, data router and error detector (DRED), and down-range up-link (DRUL) systems was normal. The IGS updates at T-3 minutes, LO + 100 seconds, and LO + 140 seconds were transmitted and validated. The spacecraft separation command was not transmitted because the MCC clocks were inoperative due to the power failure at LO + 300 seconds. The MCC DCS was not affected by the power failure. However, since the G.m.t. and ground elapsed time (g.e.t.) clocks were not operating, the correct visual time reference for the initiation of the spacecraft separation command was not available. The auxiliary second stage cut-off (ASCO) signal was transmitted by GE/Burroughs at 9:09:33.5 a.m. e.s.t.

6.3.2 Network Facilities

The Network Operations Directive for Program Gemini (OD 63-1) was revised on August 1, 1964. In addition, a set of supplements pertaining specifically to the GT-2 mission was issued on October 23, 1964. These supplements comprised the Network Countdown, Radar Handover Plan, Command Function Handover Plan, Supplementary Support Plan, Ground Communications Plan, Computing Support Plan, Computer Countdown, and On-site Data Reduction Plan. The Data Acquisition Plan Supplement was issued on October 26; and Pointing Data, in the form of plotted curves, were distributed as a separate document on October 23, 1964. A revised Network Countdown was published on November 23, but it was superseded by Instrumentation Support Instruction (ISI) 2. The originally published Radar Handover and Command Handover Supplements were also superseded by ISI 32 and ISI 21, respectively. ISI 21 was subsequently changed by ISI 51. Revision No. 1 to the Data Acquisition Plan was issued on November 10 and Revision No. 2 was issued on December 31.

Fifty-seven ISI's pertaining to the following areas were issued:

Area	Number of ISI's
Flight Controller Documentation and Procedures	14
OD 63-1, Supplement 8 (Data Acquisition Plan)	17
Equipment Modifications	3
OD 63-1, Supplement 1 (Network Count)	2
OD 63-1, Supplement 2 (Radar Handover)	1
OD 63-1, Supplement 3 (Command Handover)	2
Miscellaneous (no documentation affected)	5
Deletions or changes to other ISI's	13

UNCLASSIFIED

Fifty-one queries were generated: 17 by BDA, 10 by CSQ, and 24 by RKV. Nine BDA queries, 4 CSQ queries, and 1 RKV query dealt with Supplement 8 or with one of the ISI's issued to correct Supplement 8. The others pertained to miscellaneous subjects and can not be categorized.

6.3.2.1 Remote stations.-

6.3.2.1.1 Telemetry: The remote telemetry stations included GBI; GTI; BDA; AMF; the RKV, CSQ, and Lima ships; and the four telemetry aircraft (tail numbers 497, 129, 630, 491). GTI and BDA acquired, recorded, and remoted real-time GLV and spacecraft data to the MCC for display to flight controllers. In addition, the RKV and CSQ acquired, recorded, and displayed spacecraft data to the flight controllers on board the ships. The remaining stations acquired and recorded data for post-mission analysis. All stations except the RKV and CSQ are believed to have performed satisfactorily, and coverages are shown in table 6-I. Computer checks of computer format tapes from GBI and Tel II reveal that receivers which were coupled to left-hand circularly polarized antennas produced higher quality data (fewer bit errors) than those coupled to right-hand circularly polarized antennas. Computer-format tapes showed three synchronize word errors at LO + 3 seconds. Similar noise appeared sporadically from LO + 60 seconds to LO + 74 seconds and again from LO + 141 seconds until second-stage ignition at approximately LO + 155 seconds. RF carrier attenuation caused by engine flame and staging was experienced at Tel II and GBI causing a data dropout of approximately $\frac{1}{2}$ second on all telemetry links. The real-time retransmitted data from GTI replaced MCC data to the flight controller's consoles at LO + 390 seconds. The real-time data quality was excellent.

6.3.2.1.2 Radar: Remote radar stations were GBI, BDA, SSI, GTI, and AMF. The coverage for these stations is given in table 6-II. The radar operation was good for the entire mission. The expected corona breakdown did not appear to occur. During the change from spacecraft helices to slot antennas, GTI reported track remained good with no cross polarization effect. The C-band tracking was generally good, although the GBI FPS-16 reported a drop-out about LO + 198 seconds. Several stations reported beacon modulation. The S-band tracking was good until LO + 420 seconds when the S-band transponder was jettisoned with the adapter. Antigua tracked on C-band continuously throughout the blackout region with some signal degradation. Skin echo was observed to the horizon.

6.3.2.1.3 Timing: No timing problems were reported by any of the remote stations.

6.3.2.1.4 Air-to-ground communications: UHF reports were good from lift-off until after the spacecraft landed, with the following remote

UNCLASSIFIED

stations reporting: GBI, GTI, and the CSQ ship. HF results are highly questionable since the only two reports received were at variance with the results that should have been achieved. GBI reported reception of HF signals immediately after lift-off when the spacecraft was not transmitting. The CSQ, only 14 miles away, reported pool quality reception after the spacecraft landed under circumstances in which the signal should have exceeded 1000 microvolts at the receiver input. Reports from the MCC Communications Maintenance and Operations (M and O) personnel indicate that a number of interfering signals were on the HF channel during the mission.

6.3.2.1.5 Acquisition aid: Acquisition aid coverage by the remote stations is given in table 6-III. The RKV did not report reception of the acquisition aid beacon (link 246.3 mc CW). Beacon radiation was confirmed by GBI, GTI, and BDA. The beacon was reported to have radiated from LO + 353 seconds to LO + 418 seconds. Subsequent conversations with RKV M and O personnel revealed that there were faint indications of the acquisition aid beacon being received. BDA reported that no difficulty was encountered when acquisition aid beacon 2 was auto-tracking the CW signal in the phase-lock mode. The system first acquired lock with the intermediate frequency (IF) bandwidth set for 500 kc and then switched to 250 cps. GBI reported a receiver input level of 50 mV/m. The acquisition aid systems on the CSQ performed satisfactorily.

6.3.2.1.6 Command control system: The command carrier on-off times were nominal and conformed to the following Command Function Handover Plan which is quoted from ISI 21:

(a) During the launch phase and until T(LO+)+435 seconds, the Range Safety Officer will control the command handover and power switching. This will be accomplished by the Programing and Electronic Sequencer (EGADS).

(b) The following times have been programed for NCG 605 simulations:

<u>Site</u>	<u>Time in Seconds</u>
CNV (low power)	T-0 to T+90
CNV (high power)	T+90 to T+120
GBI	T+120 to T+243
GTI	T+243 to T+450

(c) The Range Safety Officer will use SSI for back-up from T+235 to T+350 seconds. Digital Commands cannot be transmitted from this station.

UNCLASSIFIED

(d) The RKV will be in prime 1 high power carrier-off status from T+435 seconds to T+555 seconds. RF carrier will only be brought up for radiation to the spacecraft upon specific instructions from the Flight Director.

(e) The CSQ will be in low-power standby status from T+555 seconds to touchdown. RF carrier will be into the dummy load and only brought up for radiation to the spacecraft upon specific instructions from the Flight Director.

The RKV and CSQ command carriers were not radiated, and no range safety commands were transmitted. The DCS operation was normal throughout the mission. The only DCS commands to be uplinked were the IGS updates.

6.3.2.1.7 Remote site data processor: The performance of the Remote Site Data Processor (RSDP) has revealed several problems which must be eliminated if all future mission requirements are to be met. A detailed analysis of available data is required to determine the source and corrective measures of existing problems. During the MCC confidence test, the BDA PCM data were not being identified as such on the receiving only typing reperforator (ROTR) printouts. Since this was a minor error, no attempt was made to make the necessary changes for this mission.

At approximately T-3 hours, the RKV reported the computer access matrix (CAM) on the Gemini console "red." This would not affect the summary transmissions since the Agena console CAM was operative and could perform identical functions. However, the problem was resolved when it was determined that the Gemini selection bit in the CAM register was not being set.

The RKV transmitted six summary messages which were processed at GSFC and broadcasted. Analysis of the data indicated that the input data buffer in the RSDP was not updated after LO + 399 seconds, which meant that the PCM data were not being accepted by the computer. Since similar results were noted during the simulations of F-4 days, an investigation will be made to determine the exact cause of this problem. The CSQ computer support was normal and all messages transmitted were of good quality. The five summaries from the CSQ were processed and broadcasted by the Goddard computers in the normal manner.

6.3.2.1.8 MISTRAM: The two MISTRAM systems, Valkaria (VAL) and Eleuthera (ELU), operated during the mission. VAL was active (interrogated the transponder) during GLV powered flight, and ELU received data in the passive mode. VAL was selected for impact prediction (IP) for 261.2 out of a possible 373 seconds, or approximately 70 percent of the

UNCLASSIFIED

time that VAL was active. An estimated 421 seconds (from LO + 14.5 to LO + 435.4 seconds) of metric data are usable for postflight evaluation. Handover to ELU, at which time VAL goes to passive track and ELU assumes interrogation of the transponder, occurred at LO + 387.9 seconds. Handover was accomplished in $\frac{1}{2}$ second with VAL at an elevation of $1\frac{10}{2}$. Some fading was experienced before launch, but none occurred after launch.

6.3.2.2 Computing.- During the launch phase, the GSFC computers (A and B) received launch trajectory data during the powered flight phase from AFETR and BDA via the launch monitor subsystem and computed initial trajectory parameters for display at MCC. All computer systems were operational at LO + 310 seconds (about $V/V_r = 0.8$) when the power failure occurred at MCC. There was a momentary loss of all data at the GSFC computers; however, the GSFC computers were back up in time to meet a go-no-go decision. Initial impact prediction (IP) was $16^{\circ}51'$ N., $50^{\circ}18'$ W. at 9:17 a.m. e.s.t. The initial velocity and flight-path angle data, based on 20 points from the GE/Burroughs guidance system and 25 points from the computer control facility (CCF), were as follows:

Source	Velocity, ft/sec	Flight-path angle, deg
GE/Burroughs	25 279.4	-2.484
CCF	25 275.3	-2.461

During the free-flight phase, the GSFC computers updated the GT-2 trajectory from information received from the AFETR downrange stations. A new IP calculated at GSFC indicated $16^{\circ}36'$ N., $49^{\circ}51'$ W. at 9:25 a.m. e.s.t. Based on the ANF radar data, GSFC computed a refined IP at $16^{\circ}31.9'$ N., $49^{\circ}46.8'$ W.

Final velocity and flight-path angle data computed at GSFC were as follows:

Source	Velocity, ft/sec	Flight-path angle, deg
GE/Burroughs	25 759	-2.548
CCF	25 753	-2.546

~~UNCLASSIFIED~~

6.3.2.3 Communications.- Land-line circuits, both voice and teletype, were satisfactory during the mission period except for the brief interval when partial power was lost in the MCC. Approximately 10 messages were lost during this time but were recovered shortly after the power returned. HF communication with the RKV and CSQ were predictably poor due to radio propagation during the predawn periods of the mission. Teletype, particularly from the CSQ, was affected more than voice. On launch day, CSQ teletype was declared red on three separate occasions for a total outage of 1 hour 6 minutes. However, conditions became good approximately 1 hour before actual lift-off after shifting to day frequencies.

During the first GT-2 exercise in early December, CSQ experienced interference to telemetry when the ship was in the vicinity of the spacecraft landing area. This interference was believed to come from radars aboard the carrier. In order to verify and identify the problem, the CSQ rendezvoused with the carrier on F-1 day. It was determined that when the two ships were within a few miles of each other, the high power radar (upper VHF band) from the carrier interfered with the CSQ telemetry reception. A positioning plan for the two ships to allow the CSQ antenna to point away from the carrier was put into effect, and a time schedule to avoid radar transmissions during critical periods was arranged. The CSQ experienced no interference during the flight.

6.4 RECOVERY OPERATIONS

6.4.1 Recovery Force Deployment

The areas along the ground track where recovery ships and aircraft were located are shown in figure 6-5. The recovery forces were assigned positions in these areas in order to reach any point in their particular area within specified access times. This access time, which varied for the different areas, was based on the probability of the spacecraft landing within a given area and the amount of recovery support provided in that area. For this unmanned mission, access times were divided into two general categories: ship access time and aircraft access time. Ship access time is defined as the elapsed time between the preliminary establishment of the approximate spacecraft landing point and the positioning of a recovery ship alongside the spacecraft. Aircraft access time is the elapsed time between the preliminary establishment of the approximate spacecraft landing point and the installation of the flotation collar around the spacecraft by pararescuemen. It should be emphasized that access time is primarily a planning parameter and is based upon favorable operating conditions.

~~UNCLASSIFIED~~

Eight ships, 13 aircraft, 6 helicopters, and several small special vehicles were used for recovery support in the landing areas. Table 6-IV summarizes the type of support available and the access times for the various areas. Department of Defense (DOD) routine operational ships and aircraft were used for the recovery support. NASA provided the DOD with special equipment, such as retrieval cranes for use aboard destroyers, airborne UHF electronic receivers, and spacecraft flotation collars. All recovery aircraft were equipped with the UHF receivers, giving them the capability to "home" on the spacecraft UHF location aids. These aircraft carried 3-man pararescue teams equipped to parachute to the spacecraft after landing and install the flotation collar around the spacecraft. The destroyers (DD) along the ground track, with the exception of DD4 and DD5, were equipped with spacecraft retrieval cranes. Provided aboard the carrier (CVS) were twin-turbine helicopters (SH-3A) to carry two 3-man swimmer teams, flotation collars, and photographers to the spacecraft landing point within the primary landing area. Carrier fixed-wing aircraft were also available, if required, to assist the "on station" aircraft in locating the spacecraft.

As indicated in table 6-IV, the launch site recovery force consisted of helicopters, amphibious surface vehicles, special land vehicles, Navy craft, and small boats. This force, in addition to its launch-site recovery role in case of an early abort, was also capable of providing on-scene salvage support for launch vehicle and spacecraft components.

Although many of the DOD personnel and several of the ships and aircraft were changed after the launch attempt on December 9, 1964, the same number of recovery support units were deployed for the January 19, 1965, flight. During this interval, additional spacecraft retrieval cranes became available and were installed aboard DD2 and DD6, thereby increasing the spacecraft retrieval capability along the ground track.

Before the December launch attempt, as well as before the actual flight, extensive training for the recovery forces was conducted. In addition to individual unit training in specific phases of the recovery operation at home bases and enroute to "on station" positions, recovery simulations were conducted jointly with the aircraft, helicopters, ships, and the recovery control room (RCR) in the Mission Control Center (MCC), Cape Kennedy. These simulations were conducted for both the downrange and launch-site recovery forces.

6.4.2 Location and Retrieval

All recovery forces were on station at launch time and were in communication with the RCR. Weather conditions were favorable for spacecraft location and retrieval in all the planned landing areas.

UNCLASSIFIED

During the countdown, recovery forces were periodically informed of the count status. The recovery forces were informed of lift-off at 9:05 a.m. e.s.t. Throughout the early minutes of flight, recovery forces were continually informed of the flight progress. WINREP 1 (summary of flight progress and verification of lift-off time) was sent to recovery forces at LO + 5 minutes. At LO + 11 minutes CALREP 1 (calculated spacecraft landing position and time) was sent to the recovery forces as 16°51' N., latitude, 50°18' W., longitude, 9:23 a.m. e.s.t. Five minutes later DATUMREP 1 (best estimate of the position of spacecraft landing) was sent from the RCR and repeated the CALREP information. This position was approximately 50 nautical miles uprange from the planned landing point. The location and retrieval data are plotted in figure 6-6. Upon receipt of the DATUMREP, recovery forces in the primary landing area, including the carrier (U.S.S. Lake Champlain) based helicopters, proceeded towards the reported landing position. Several EYEREPs (visual sighting of spacecraft during reentry) were reported by recovery units (DD4 and CVS) at about LO + 15 minutes; however, it could not be confirmed that the object sighted was the spacecraft. (Later debriefing of the CVS observers seemed to indicate that the EYEREP was a sighting of the launch-vehicle second stage passing overhead.) Aircraft 5 began obtaining UHF signals from the spacecraft at approximately LO + 13 minutes; however, due to communication difficulties aboard the aircraft, it was not able to transmit a BARREP (report by a unit obtaining an electronic DF on signals radiating from the spacecraft). When the communications problems on aircraft 5 were corrected at LO + 31 minutes, a JIGREP (positive visual contact with spacecraft after landing), available at LO + 22 minutes, was transmitted to the CVS and the RCR. Aircraft 5 was over the spacecraft at LO + 26 minutes, or approximately 7 minutes after spacecraft landing. Pararescuemen aboard aircraft 5 were preparing to jump when approaching recovery helicopters were sighted within a few miles of the scene. The three helicopters (primary, secondary, and photography) arrived over the spacecraft at LO + 34 minutes, followed by immediate deployment of the primary 3-man swimmer team. Swimmers had no difficulty installing the flotation collar (fig. 6-7), and the secondary helicopter with the backup swimmer team was released to recover the rendezvous and recovery (R and R) section, sighted 1000 yards upwind of the spacecraft. Swimmers jumped to the R and R section at LO + 44 minutes, detached the pilot parachute, and attached a hoisting cable into a loop tied in the parachute risers. The R and R section was hoisted from the water, suspended 10 feet beneath the helicopter, and delivered to the CVS at LO + 1 hour 16 minutes (fig. 6-8). A fourth helicopter returned the backup swimmer and pilot parachute to the carrier. At LO + 1 hour 39 minutes, the U.S.S. Lake Champlain arrived at the spacecraft, 16°31.9' N. latitude, 49°46.8' W. longitude. A line was shot from the carrier to the swimmers who attached a retrieving line to the spacecraft recovery loop. The spacecraft was brought to a position under the deck-edge elevator of the carrier where it was hooked to the ship's crane, lifted from the water,

UNCLASSIFIED

and secured in the spacecraft dolly at LO + 1 hour 49 minutes (fig. 6-9). At this time, members of the recovery team began the examination of the spacecraft exterior and the postlanding procedures. Detailed photographic coverage of the spacecraft and the R and R section was also begun at this time.

Weather conditions at the immediate spacecraft landing area are described in section 12.2.

6.4.3 Recovery Aids

When the spacecraft was examined after recovery, the HF antenna, recovery antenna, and descent antenna appeared to have operated normally. According to reports received from recovery forces, all spacecraft recovery aids did operate with the exception of the recovery flashing light.

Signals from the UHF transmitter (296.8 mc) were received during spacecraft flight, first by aircraft 1 at LO + 6 minutes, and then by an electronic direction finder (DF) on DD3 at LO + 9 minutes. The U.S.S. Lake Champlain reported reception of 296.8-mc signals at the following times after lift-off (minutes:seconds): 11:50, 13:07, 14:10, 15:10, 16:00, 17:07, and 18:08. Signals were strong, and bearings were 290° to 295° true from the ship.

Aircraft 5, operating over the carrier, reported that signals had been received from the recovery beacon (243 mc) and the UHF transmitter. Recovery beacon signals were received both in the pulse and CW mode. The aircraft received a 296.8-mc signal at LO + 13 minutes at a range of 30 nautical miles; at LO + 15 minutes, a 243-mc signal was received, and the aircraft homed in on the spacecraft.

The photography helicopter reported receiving a 243-mc UHF signal at a range of 24 nautical miles while enroute to the spacecraft. Aircraft 6, at an altitude of 15 000 feet at the downrange end of the primary landing area, reported receiving the recovery beacon signal at a range of 145 nautical miles at LO + 17 minutes. While homing in on the 243-mc signal, the aircraft verified receiving a 296.8-mc signal 60 nautical miles from the spacecraft. Aircraft 4, at an altitude of 10 000 feet, uprange of the landing position, reported receiving a 243-mc signal at a range of 115 nautical miles at LO + 27 minutes and was able to home in on the spacecraft.

The only HF signal (15.016 mc) received by recovery forces was reported by aircraft 5. The aircraft received strong signals at LO + 58 minutes while flying about 3 nautical miles south of the spacecraft. The Coastal Sentry Quebec (CSQ) reported HF radio contact at

~~CONFIDENTIAL~~

10 + 25 minutes, approximately 25 nautical miles from the spacecraft. Both the worldwide Federal Communications Commission (FCC) and Navy HF-DF networks were alerted to listen for spacecraft HF signals but reported negative results the day of the mission. Several reports from network stations were subsequently received; however, the data indicate that the signals were not from the spacecraft.

As reported during the recovery operation, the spacecraft recovery flashing light did not function. Before the spacecraft was retrieved, it was apparent that the light had not erected. After the spacecraft was secured aboard the U.S.S. Lake Champlain, the light bay door was carefully removed, and the light erected and began flashing. Further examination revealed that the light bay door pyrotechnic device had actuated. After the door was removed the "floating rib" in the light bay was found to be slightly cocked. This rib could possibly have caught under the structure along the sides of the light bay and thus not have released the door.

The sea dye marker was reported sighted by the following recovery units at the following ranges: aircraft 4, 10 nautical miles; aircraft 5, 6 nautical miles; aircraft 6, 25 nautical miles; helicopters, 3 to 8 nautical miles; U.S.S. Lake Champlain, 4 nautical miles.

6.4.4 Postretrieval Procedures

The spacecraft postretrieval procedures aboard the U.S.S. Lake Champlain were performed as specified in the GP-2 Recovery Operations Manual (check-off data sheets are submitted with this report). The spacecraft exterior was examined for apparent damage and detailed photographs were taken. Visible damage other than the expected burned areas were the pitted areas in the heat shield and small holes in shingle no. 52-32090-12. (The swimmers reported that heat shield pitted areas were caused by their air tanks and equipment scraping against the heat shield.) Apparent equipment malfunctions were the recovery flashing light and a wire bundle guillotine which failed to slice through one of the wire bundles between the reentry control system (RCS) section and the R and R section. The windows were not transparent due to condensation behind the outer glass (fig. 6-10). There was also evidence of "hot spots" on the insulation tape around the right-hand hatch opening. Prior to opening the hatches, the cabin-purge valve was opened, and no exchange of pressure was noticed. Considerable time and effort were taken in attempts to safe those pyrotechnic devices which were not completely blocked by spacecraft equipment. The required instrument readings and switch positions were recorded before spacecraft shutdown. The cameras and a PAM tape recorder were then removed and packaged. During the postretrieval procedures, there were very small

~~CONFIDENTIAL~~

~~CONFIDENTIAL~~

6-21

leaks and occasional bursts of fuel and oxidizer fumes from RCS thrusters 4A, 2B, and 3B. The swimmers also reported evidence of small leaks while they were at the spacecraft. Spacecraft postretrieval procedures were completed approximately 7 hours after the spacecraft was brought aboard the U.S.S. Lake Champlain. The spacecraft onboard cameras, PAM tape recorder, and recovery film were flown from the carrier at 6:00 p.m. e.s.t. to Antigua where they were transferred to the waiting aircraft and flown to Patrick Air Force Base.

The R and R section was also examined and photographed when it was returned to the carrier. In addition to several hot spots, one shingle was cracked. (Swimmers and recovery personnel report that this damage did not occur during retrieval or handling of the R and R section.) There were several small abrasions on the main parachute bag which may have been caused when the section was placed on the deck since a portion of the bag was under the edge of the section.

On the morning of the second day after the flight, the spacecraft and R and R section were unloaded at Roosevelt Roads Naval Station, Puerto Rico, where the RCS was deactivated (see section 6.4.5) by the landing and safing team. After the RCS was deactivated, the spacecraft, R and R section, and deactivation equipment were loaded aboard an airplane and flown to the Cape Kennedy skid strip. The airplane arrived early on the morning of the third day after the flight, and the spacecraft, R and R section, and deactivation equipment were delivered to NASA-Cape Operations representatives.

6.4.5 Spacecraft RCS Deactivation

A significant portion of the spacecraft postretrieval procedures was the deactivation of the RCS at Roosevelt Roads. The primary reason for deactivation of the RCS at a downrange station was to safe the system prior to flying the spacecraft back to Cape Kennedy aboard an aircraft.

The landing and safing team that was flown to Roosevelt Roads consisted of NASA and spacecraft contractor engineers and technicians. This team, with the required equipment, was responsible for deactivating the RCS according to procedures in reference 10.

After the spacecraft was unloaded from the carrier at Roosevelt Roads, it was taken to a previously selected, well isolated, area where deactivation was begun at 1000 hours (local Puerto Rico). Normal safety procedures were observed throughout the operation. There was no indication of toxic vapors from the RCS thrust chamber assembly (TCA) when checked with a portable propellant vapor detector. The RCS shingles were then removed and packed in polyethylene bags.

~~CONFIDENTIAL~~

~~UNCLASSIFIED~~

Before the pressurant in each ring was relieved to atmospheric pressure, a slight deviation in reference 9 was performed to obtain pressure readings upstream of the B package regulator. A flexible $\frac{1}{4}$ -inch inside diameter hose (internal volume of approximately 4 cu in.) from TPI to a calibrated pressure gage was used for this operation. Pressure readings of 1120 psig and 1350 psig were obtained from A ring and B ring, respectively. The pressurants in each system were then relieved to atmospheric pressure.

After draining the oxidizer propellant from A ring, according to reference 10, into the holding container designated for that ring, the system downstream of the tank bladder was flushed with freon-mf. To perform this step, an auxiliary power supply and an electrical control box were required to open the RCS TCA solenoid valves. After the equipment was properly connected, a switch on the control box was positioned from the "off" position to the "oxidizer" position and back to the "off" position almost instantaneously because of a weak static firing in the B ring thrusters. Simultaneously with the firing of B ring thrusters, the A ring oxidizer solenoid valves opened. The team attributed this to an electrical short probably due to sea water in the spacecraft RCS electrical system. The flushing of the oxidizer A ring continued normally after the electrical connectors on B ring were disconnected from each thruster solenoid valve.

The propellants of each ring were drained into separate holding containers. Then each system was flushed. While flushing the fuel manifold of B ring, it was noted that fuel solenoid valves of thrusters 3 and 4 did not open fully and allow contaminated freon-mf to flow as required. As the operation was continued, the thruster solenoid valves finally loosened enough to allow some flow out the thrusters. The last operation of the deactivation was that of providing a positive 30 psig nitrogen pad on the upstream side of the tank bladders and the pressurant system.

The cap on the TP 15A was found only finger tight. All torque values of the caps and valves of each package were recorded.

The following are the operations performed according to reference 10 and the duration of each:

~~UNCLASSIFIED~~

UNCLASSIFIED

6-23

<u>Paragraph of reference 10</u>	<u>Title</u>	<u>Elapsed time, hr</u>
1.4	Prepare spacecraft for deactivation	1.50
1.5.1	Deservice RCS pressurant	1.25
1.5.2.1	Deservice oxidizer: RCS A ring	2.50
1.5.2.2	Deservice oxidizer: RCS B ring	1.25
1.5.3.1	Deservice fuel: RCS B ring	1.50
1.5.3.2	Deservice fuel: RCS A ring	1.00
1.6	Post deactivation	<u>1.25</u>
	Total	10.25

The deactivation of the spacecraft RCS was performed satisfactorily except for the one deviation mentioned above (A and B ring pressure indication).

Subsequent examination of the four propellant containers at the Cape revealed that no liquid fuel or oxidizer was present.

UNCLASSIFIED

UNCLASSIFIED

TABLE 6-I.- TELEMETRY COVERAGE

Signal	Duration of signal		Frequency, mc	Actual coverage, sec	Nominal pre-mission coverage, sec
	Acquisition, LO+sec	Loss, LO+sec			
MCC	0	421	230.4	421	409
	0	421	259.7	421	409
Tel II	0	465	237.0	465	409
	0	465	244.3	465	409
	0	420	230.4	420	409
	0	420	259.7	420	409
Tel III	0	313	237.0	313	409
	0	313	244.3	313	409
	0	423	230.4	423	409
	0	423	259.7	423	409
GBI	53	477	237.0	424	366
	53	477	244.3	424	366
	53	447	230.4	394	366
	53	447	259.7	394	366
GTT	164	521	ALL	357	349
BDA	213	518	230.4	305	466
	213	518	259.7	305	466
RKV	215	548	230.4	353	361
	215	548	259.7	353	361
ANT	344	548	ALL	204	283
CSQ	702	1096	230.4	396	No estimate
LIMA	701	1096	259.7	397	No estimate
	704	833	230.4	129	No estimate
Aircraft 497	704	833	259.7	129	No estimate
	435	1646	230.4	1191	No estimate
Aircraft 129	435	1646	259.7	1191	No estimate
	497	1644	230.4	1147	No estimate
Aircraft 630	497	1644	259.7	1147	No estimate
	510	1644	230.4	1134	No estimate
Aircraft 491	510	1644	259.7	1134	No estimate
	424	1021	259.7	597	No estimate

UNCLASSIFIED

UNCLASSIFIED

6-25

TABLE 6-II.- RADAR COVERAGE

Station	Duration of signal		Tracking mode	Actual coverage, sec	Nominal pre-mission coverage, sec
	Acquisition, LO+sec	Loss, LO+sec			
CNV FPS-16	0	200	Beacon	200	160
MLA TPQ-18	1	358	Beacon	347	309
PAT FPQ-6	0	363	Beacon and skin	363	303
GBI FPS-16	63	429	Beacon	366	238
SSI FPS-16	140	492	Beacon	352	215
GTI TPQ-18	235	510	Beacon	275	265
ANT FPQ-6	410	634	Beacon and skin	224	180
CNV S-band	0	315	Beacon	315	295
GBI S-band	114	348	Beacon	234	220
GTI S-band ^a	360	418	Beacon	58	173

^aGTI S-band operation terminated by spacecraft equipment adapter jettison.

TABLE 6-III.- ACQUISITION AID COVERAGE
[CW beacon, 246.3 mc]

Station	Duration of signal	
	Acquisition, LO+sec	Loss, LO+sec
Tel II	353	418
Tel III	353	418
MCC	373	418
GBI	353	418
GTI	353	418
RKV	None	None

UNCLASSIFIED

UNCLASSIFIED

TABLE 6-IV.- RECOVERY SUPPORT

Landing area	Access time, hr		Support
	Aircraft	Ships	
Launch site	2	4	4 LARC - amphibious vehicle 3 M-113 - tracked land vehicle 2 boats (40 and 50 feet long) with underwater salvage teams 1 LCU - large landing craft with spacecraft retrieval capability 2 HH-3C - helicopters
Launch abort	2	12	2 HU-16 - amphibious aircraft 2 MSO - minesweepers with salvage capability 1 AFT - spacecraft retrieval and deep water salvage capability 3 destroyers 3 aircraft on station (A/C1, HC-54; A/C2, HC-54; A/C3, HC-54) 1 standby aircraft at Grand Turk (HU-16)
Primary	2	4	2 destroyers 1 aircraft carrier with SH-3A helicopters (4 used) 3 aircraft on station (A/C4, HC-54; A/C5, HC-54; A/C6, HC-97)
Overshoot	2	12	1 destroyer 1 aircraft on station (A/C7, HC-97) 3 standby aircraft at Trinidad for support in primary or overshoot area (1 HC-97, 2 HC-54)
Total			8 ships, 13 aircraft, 6 helicopters

UNCLASSIFIED

NASA-S-65-1601

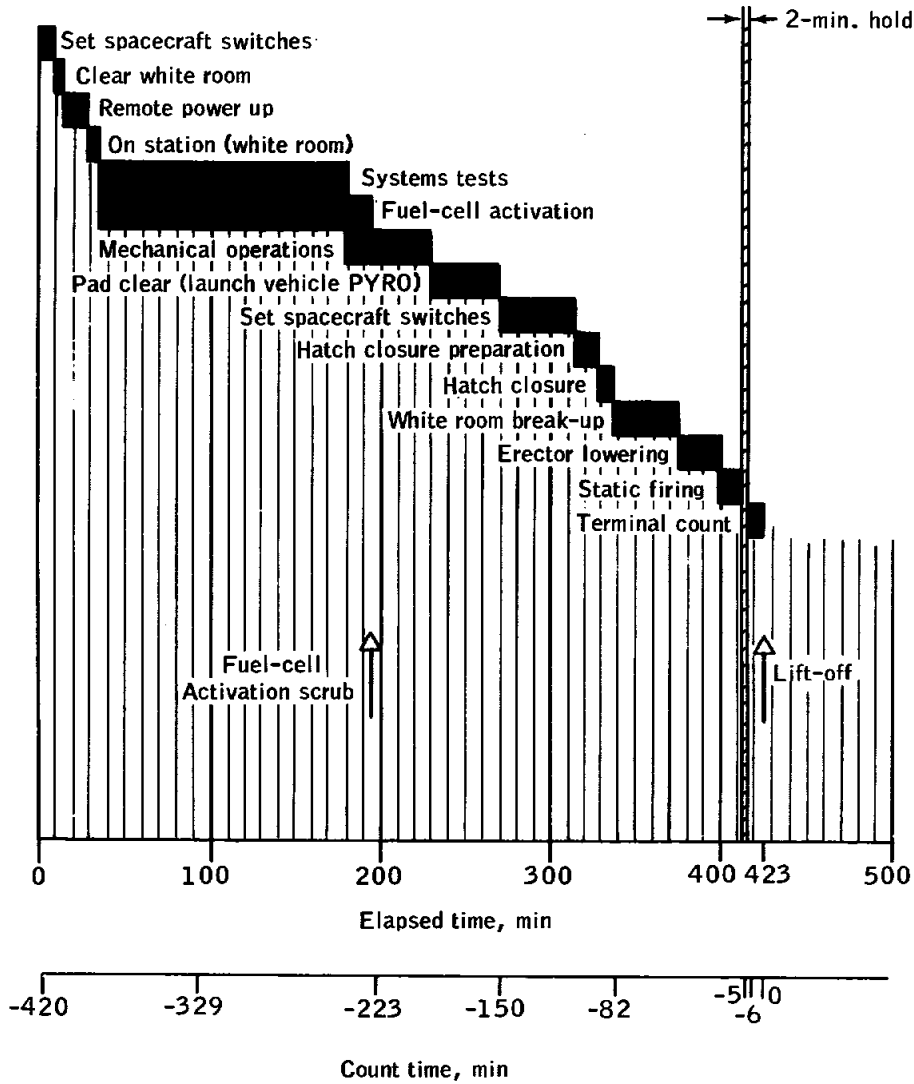


Figure 6-1. - Spacecraft 2 countdown sequence on January 19, 1965

NASA-S-65-1600

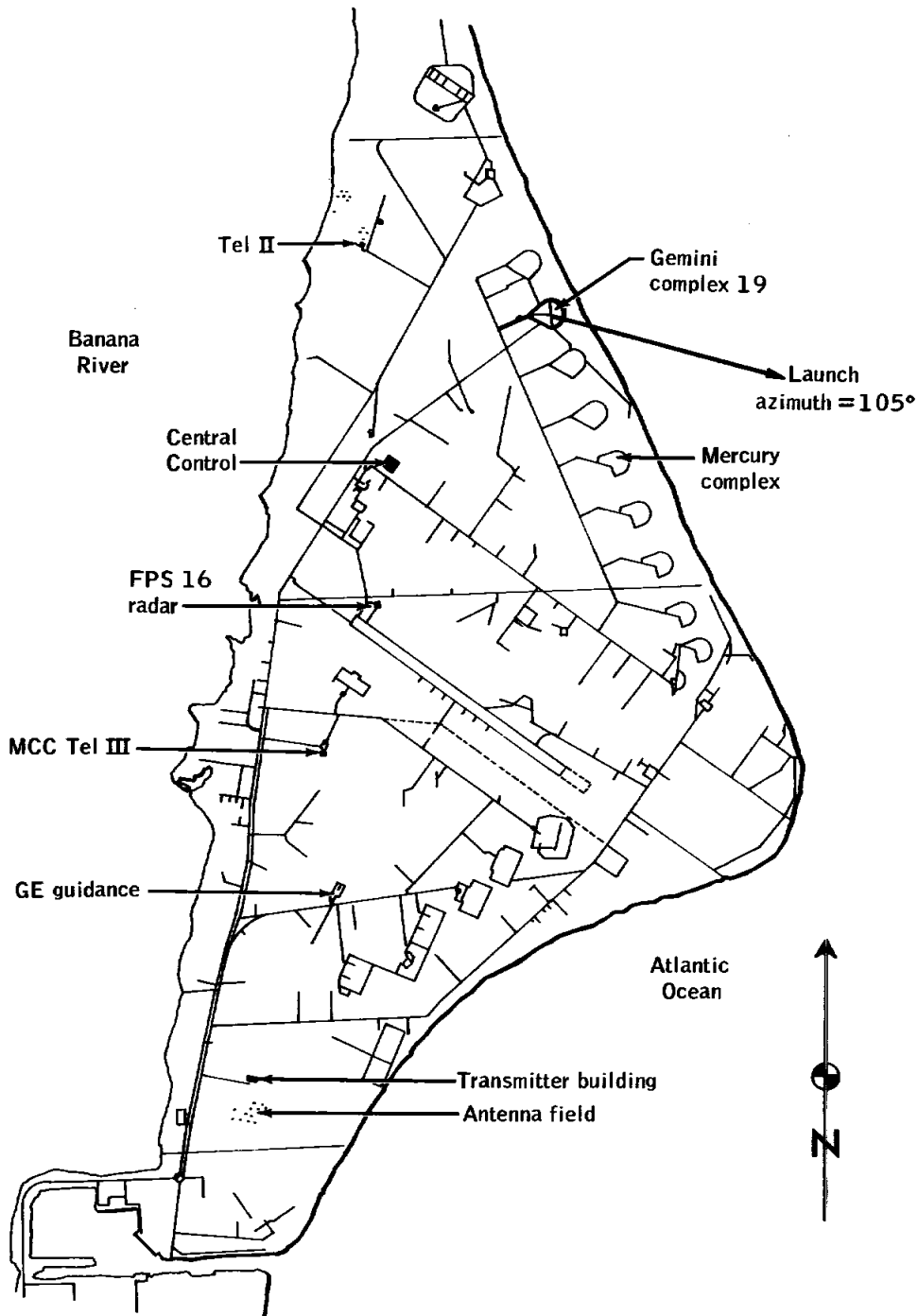


Figure 6-2. - Cape Kennedy Air Force eastern test range network stations

NASA-S-65-1598

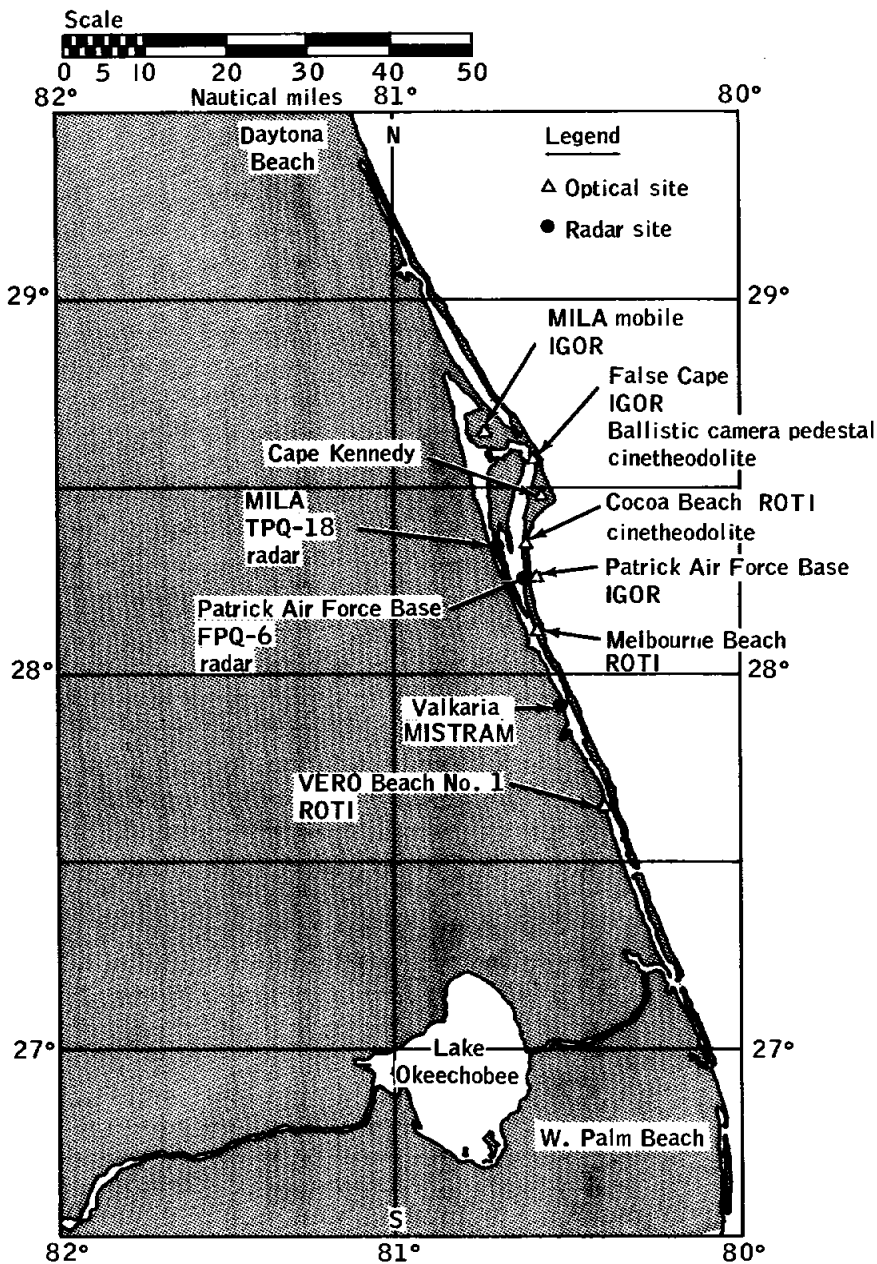


Figure 6-3. - Mainland Air Force eastern test range instrumentation facilities

UNCLASSIFIED

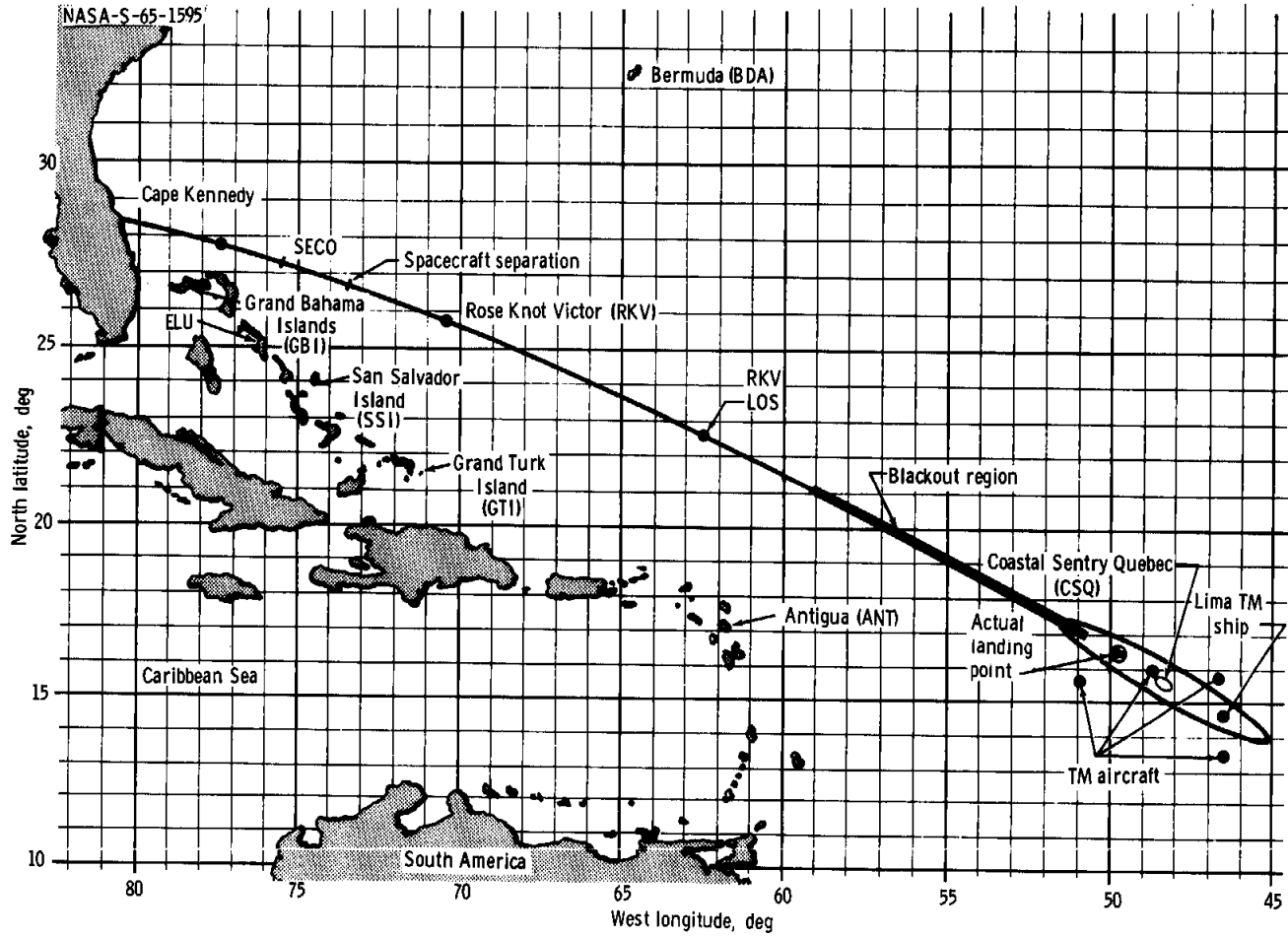


Figure 6-4. - Network remote stations

UNCLASSIFIED

UNCLASSIFIED

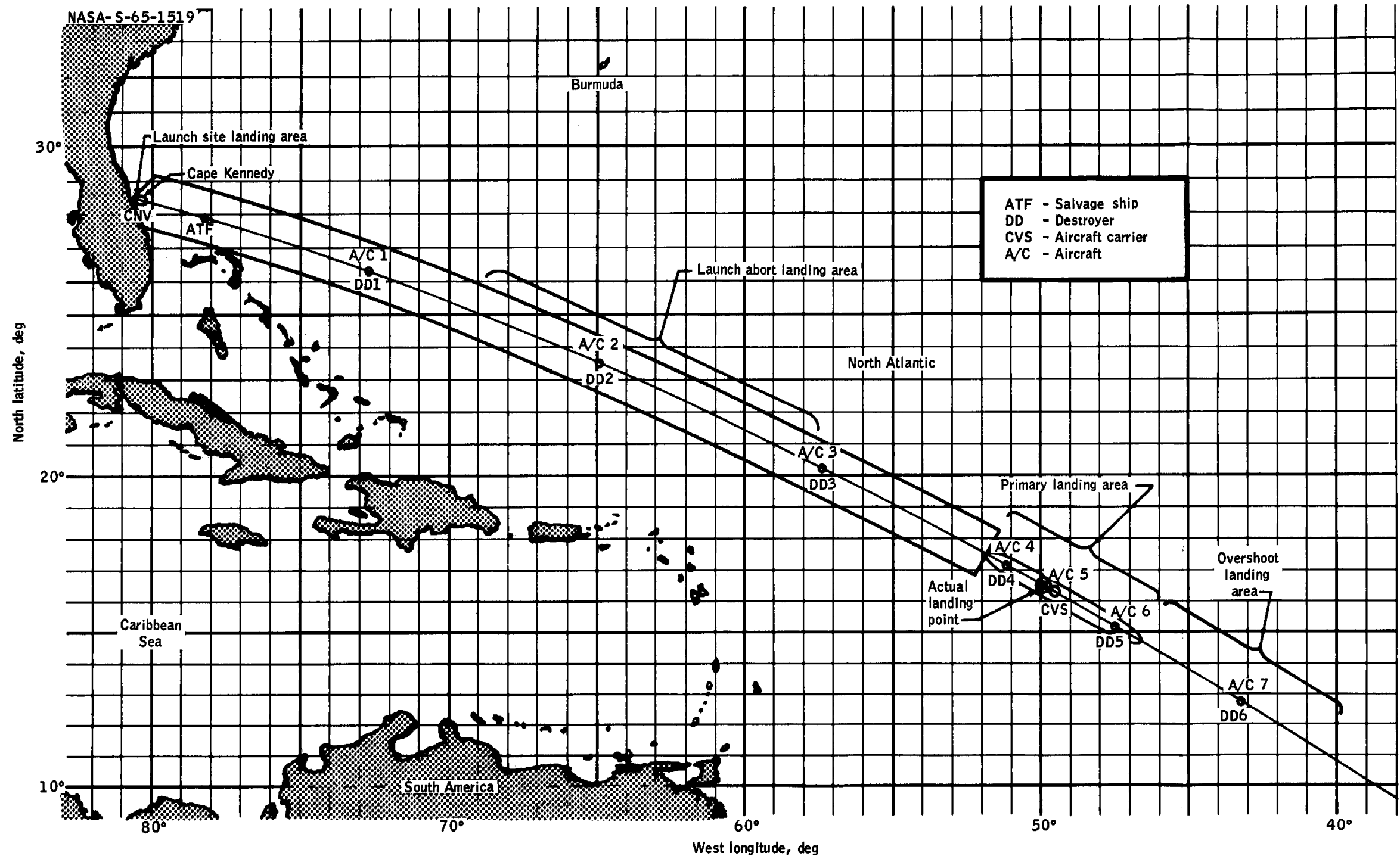
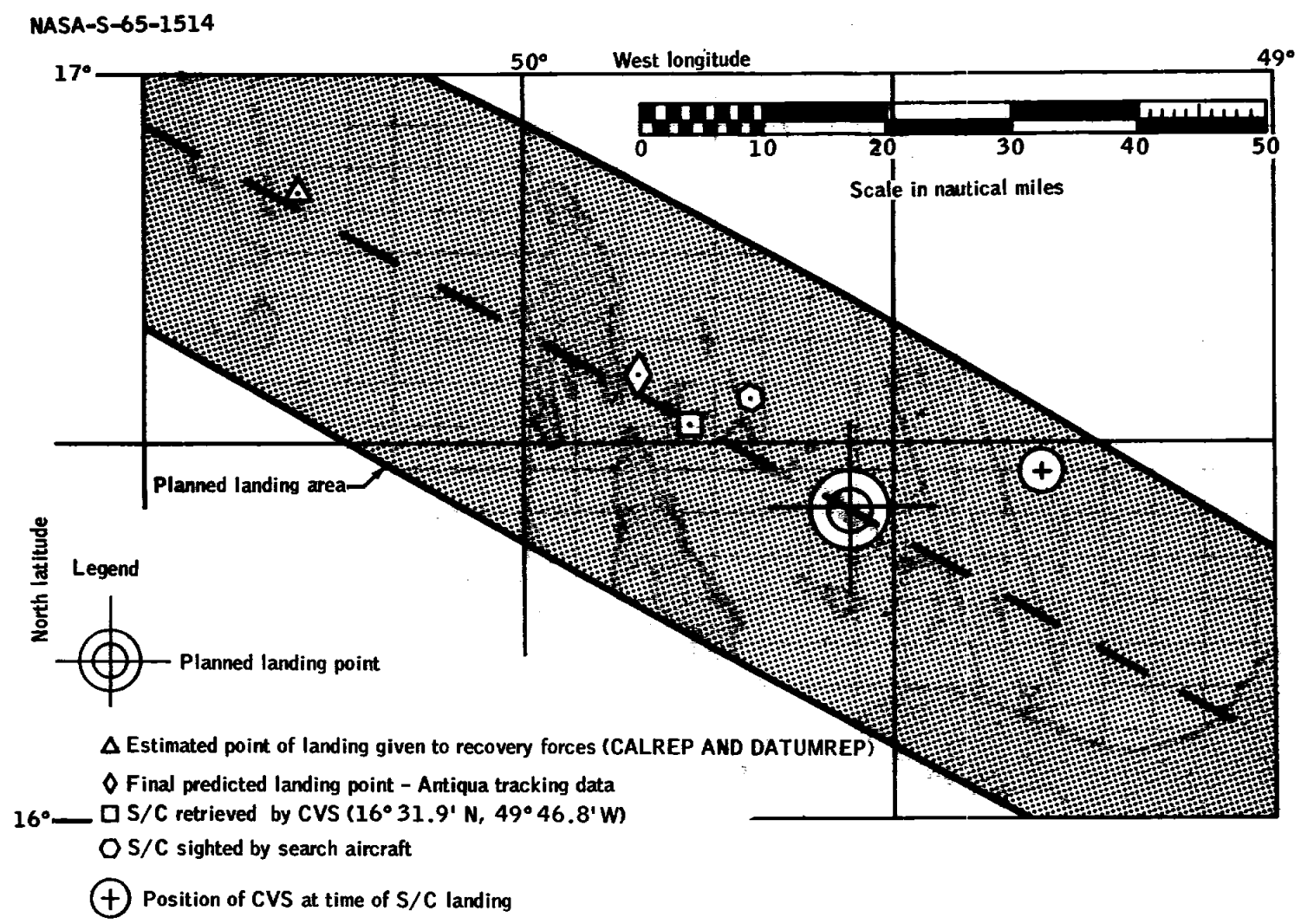


Figure 6-5. - Recovery force deployment

UNCLASSIFIED

UNCLASSIFIED

UNCLASSIFIED



6-32

Figure 6-6. - Detailed recovery area

NASA-S-65-1930



Figure 6-7. - Swimmers after installing flotation collar

NASA-S-65-1929



Figure 6-8. - R and R section being delivered to carrier

UNCLASSIFIED

6-35

NASA-S-65-1928

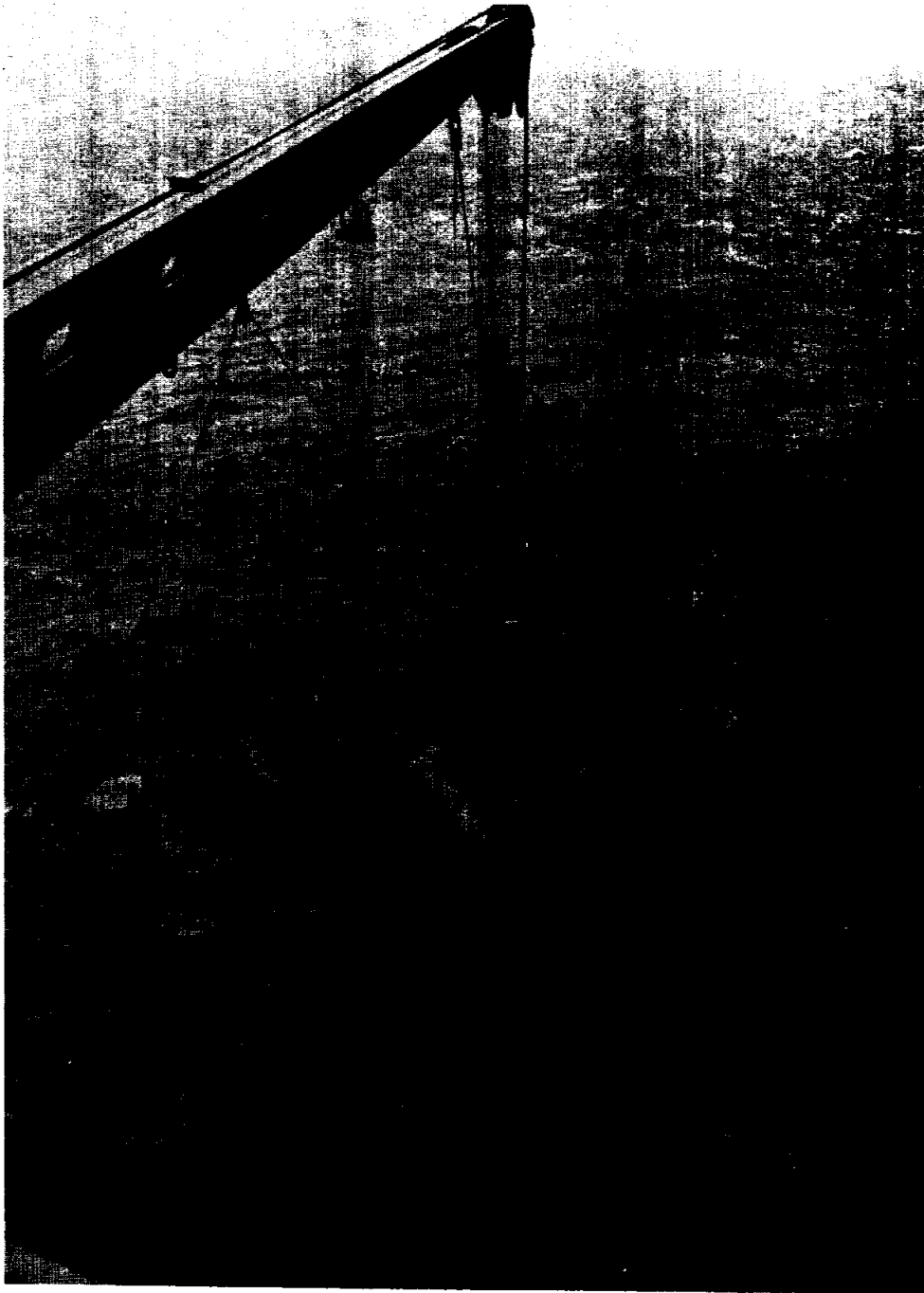


Figure 6-9. - Spacecraft being lifted from water

UNCLASSIFIED

NASA-S-65-1931

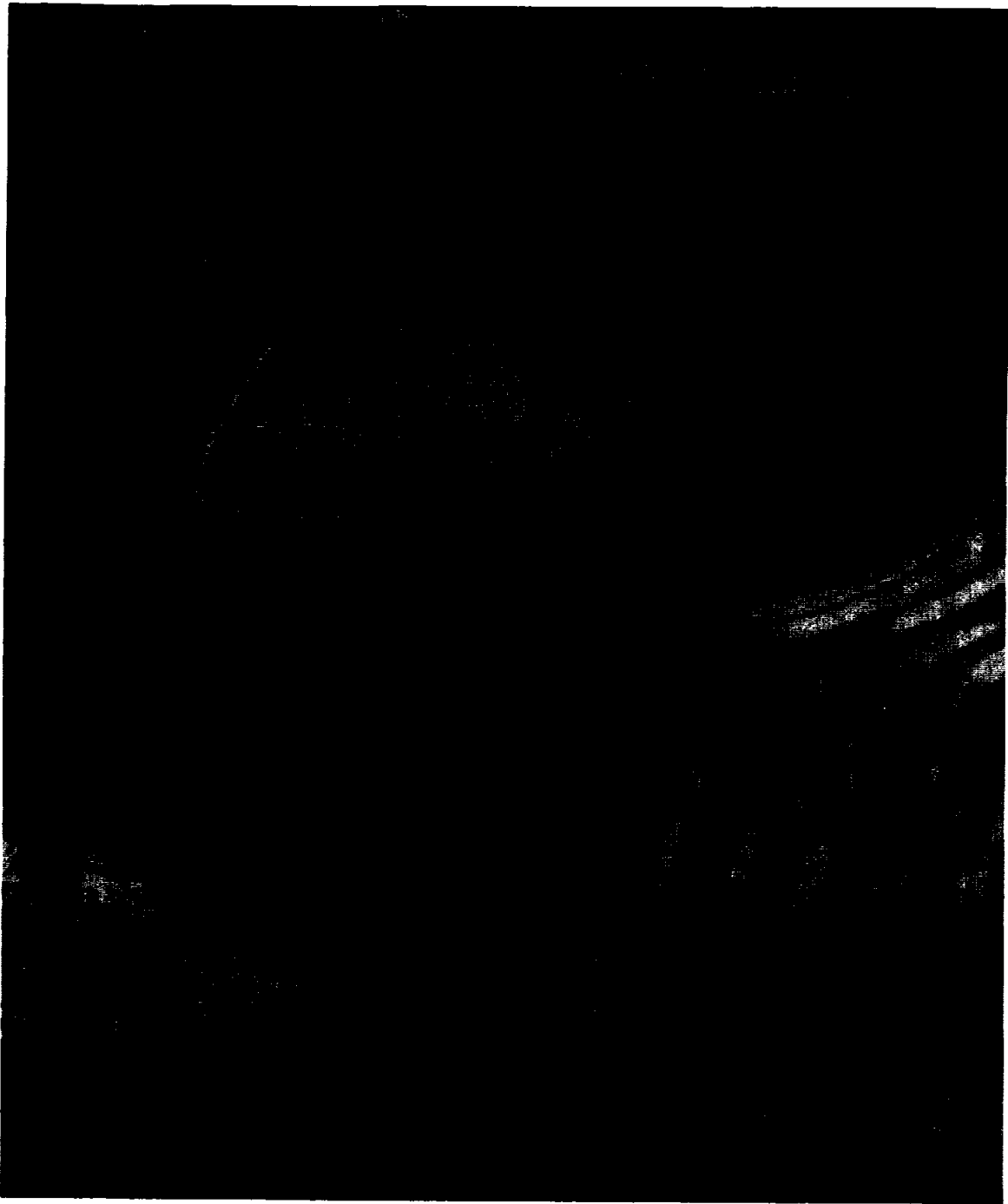


Figure 6-10. - Condensation on spacecraft window

UNCLASSIFIED

7-1

7.0

THIS SECTION IS NOT REQUIRED FOR THE REPORT

UNCLASSIFIED

UNCLASSIFIED

THIS PAGE LEFT BLANK INTENTIONALLY

UNCLASSIFIED

UNCLASSIFIED

8-1

8.0

THIS SECTION IS NOT REQUIRED FOR THE REPORT

UNCLASSIFIED

UNCLASSIFIED

THIS PAGE LEFT BLANK INTENTIONALLY

UNCLASSIFIED

UNCLASSIFIED

9-1

9.0 CONCLUSIONS

The second Gemini flight was successful and excellent data were obtained to evaluate the mission and derive the following conclusions.

(a) All primary and secondary mission objectives were attained except for the failure to flight test the activated fuel cell in the spacecraft. However, the reactant supply system was flown with the reactants in the supercritical state.

(b) The flight test reaffirmed the capability of the Gemini launch vehicle to place the spacecraft into a planned trajectory and provided the final verification of the readiness of the launch vehicle for manned flight.

(c) The spacecraft flight provided a validation test for those spacecraft systems essential for manned flight, but revealed minor areas which require correction prior to the GT-3 mission.

(d) The launch vehicle and spacecraft aerospace ground equipment and facilities performed satisfactorily. Minor propellant loading problems of the launch vehicle were associated with the propellant transfer and pressurization system.

(e) Launch operations including the countdown proceeded smoothly with no holds attributed to the launch vehicle and one two-minute hold attributed to the spacecraft.

(f) The two-element telemetry antenna array on the launch vehicle proved to be satisfactory.

(g) The engine hydraulic actuators performed satisfactorily as modified subsequent to their failure on the first launch attempt.

(h) The stage I primary-system turbine-driven hydraulic pump failed to supply normal pressure during the pad hold down time after engine start until just prior to lift-off. The pressure returned to normal at lift-off and remained there for the entire first stage flight.

(i) The spacecraft guidance and control system functioned adequately and would have guided the vehicle to a satisfactory insertion condition. However, the indicated velocity error at SECO was higher than predicted.

(j) Protuberance heating on the stage II forward oxidizer tank skirt was negligible.

UNCLASSIFIED

UNCLASSIFIED

(k) Vibrations, differential pressures, and other structural loads were within design limits.

(l) Oscillations on the combined spacecraft and launch vehicle after second stage engine cutoff were within acceptable limits.

(m) An indication of a reactant supply system hydrogen and oxygen pressure decay of 30 percent without a corresponding loss of quantity being indicated on the spacecraft panel gage occurred between the spacecraft - launch vehicle separation and equipment section jettison.

(n) The actuation mechanism for the spacecraft-to-adapter separation indication failed to function. This failure had no effect on the proper operation of the spacecraft sequencing system.

(o) The horizon definition which is evident in the out-of-the-window motion pictures appears adequate for backup attitude information during reentry.

(p) The René shingles successfully provided thermal protection to the spacecraft afterbody under the most critical reentry heating conditions to be encountered in the Gemini program.

(q) The temperatures of the beryllium shingles on the R and R section and the RCS section were well below predicted and design limit values. No problems are expected from the higher total heat inputs which will occur during reentry from the planned orbits for the Gemini spacecraft.

(r) Bondline temperatures of the GT-2 heat shield were well below predicted values. The heat shield maintained its structural integrity and the loss of ablative material was less than expected. It is considered to be fully qualified for maximum lift reentry from the planned Gemini orbits.

(s) A redundant guillotine failed to cut a wire bundle.

(t) The recovery flashing light failed to deploy because of structural interference.

(u) Exceptional overall telemetry coverage and data recording was obtained.

UNCLASSIFIED

10.0 RECOMMENDATIONS

As a result of the evaluation of the GT-2 mission, the following action is recommended:

(a) A detailed investigation and testing of the RSS should be conducted to determine the nature, source, and effects of the gradual pressure decay in the hydrogen and oxygen tanks at spacecraft - launch-vehicle separation.

(b) It is recommended that an analysis of the reentry heating factors be established. The following action is recommended: a detailed review of the lift-to-drag ratio evaluation including an analysis of the computation equations, refinement of the angle-of-attack estimates during reentry, refinement of the reentry temperature boundary, redefinition of after-body correlations between GT-2 mission data and wind-tunnel data, and the correlation of ground-test and GT-2 mission ablation shield data to improve the preflight prediction capability.

(c) It is recommended that the IGS evaluation be completed. Recommendations are that the IGS accuracy evaluation be continued to completion and that the spacecraft contractor conduct a thorough analysis of the IMU performance anomaly and provide corrective action for manned Gemini spacecraft. It is further recommended that the contractor provide the correction for reentry guidance initialization for manned flights.

(d) The reentry assembly-to-retrograde section separation sensing switches should be deleted for all subsequent spacecraft. In addition, there must be no sequential events which are dependent upon the successful operation of all other separation sensing switches.

(e) The RCS to R and R section guillotine malfunction investigation should be completed and corrective design changes should be made, if necessary.

(f) The poor reception of the HF transmitter in the DF mode should be investigated and corrective action taken which prevents water from shorting the antenna.

(g) It is recommended that certain small changes be made to increase the available margins of safety for reentry heating. Consideration should be given to reducing the angle of attack, increasing the thickness of the shingles in the affected area, and improving the aerodynamic shape of the spacecraft adapter interconnect fittings which caused the local disturbance. Wind-tunnel tests should be planned to substantiate any design changes.

UNCLASSIFIED

(h) A study should be made of the recovery flashing light malfunction to determine if present changes for subsequent spacecraft will preclude the problem encountered on spacecraft 2.

(i) Equipment and procedural changes should be incorporated within the propellant transfer and pressurization system of the launch vehicle to improve reliability and performance during the propellant loading operation.

(j) The insulation should be removed from the stage II forward oxidizer tank skirt to save weight and improve the payload capability.

(k) The launch vehicle contractor should perform a detailed analysis of the hydraulic pump design and provide corrective action if necessary. In addition, the contractor must provide procedures for checking the hydraulic pump compensator performance capability as late as possible prior to stage I engine ignition.

UNCLASSIFIED

UNCLASSIFIED

11-1

11.0 REFERENCES

1. Gemini Mission Evaluation Team: Gemini Program Mission Report for Gemini-Titan 1 (GT-1). MSC-R-G-64-1, NASA Manned Spacecraft Center, May 1964.
2. McDonnell Aircraft Corp.: NASA Project Gemini Familiarization Manual SEDR 300, March 15, 1964.
3. Mission Planning Office: GT-2 Mission Directive. NASA Program Gemini Working Paper no. 5013, NASA Manned Spacecraft Center. June 3, 1964.
4. McDonnell Aircraft Corp.: Gemini Spacecraft Instrumentation System Specification. Rep. 8640.
5. McDonnell Aircraft Corp.: Gemini Spacecraft Instrumentation System Specification - Spacecraft 2. Rep. 8640-2.
6. McDonnell Aircraft Corp.: Gemini Spacecraft Guidance and Control Specification. Rep. 8637, Feb. 20, 1962, (as revised).
7. McDonnell Aircraft Corp.: Gemini Spacecraft Propulsion System Specification. Rep. 8642. Feb. 20, 1962 (as revised).
8. Aerospace Corp.: System Test Objectives for GLV NASA Gemini Mission GT-2. TOR 269(4126)-23. July 21, 1964.
9. NASA Manned Spacecraft Center: Gemini Spacecraft/Launch Vehicle Interface Specification and Control Document Report ISCD-1, Nov. 22, 1963.
10. McDonnell Aircraft Corp.: Spacecraft Prelaunch Test Procedures. SEDR F399-2, Jan. 2, 1965.
11. McDonnell Aircraft Corp.: Project Gemini Postflight Inspection and Cleanup, Spacecraft 2. SEDR F498-2, Feb. 30, 1964.

UNCLASSIFIED

UNCLASSIFIED

THIS PAGE LEFT BLANK INTENTIONALLY

UNCLASSIFIED

12.0 APPENDIX A

This appendix contains the histories of the spacecraft and launch vehicle and a summary of weather conditions on launch day. It also contains a listing of all supplemental reports, a summary of data available for evaluation by the Mission Evaluation Team, and a discussion of the postflight spacecraft inspection.

12.1 VEHICLE HISTORIES

12.1.1 Spacecraft

12.1.1.1 Operations at St. Louis, Missouri.- Spacecraft systems testing (SST) at St. Louis, consisting of Phase I module tests and Phase II mated tests, began on January 13, 1964, and was completed on September 20, 1964, with the shipment of spacecraft 2. The spacecraft schedule at St. Louis is shown in figure 12-1.

Phase I module tests uncovered the following significant problems:

(a) X-ray examination of the brazed joints in the reentry control system (RCS) section revealed 22 instances of out-of-specification brazing. After rework, X-ray examination again indicated 12 out-of-specification joints. A review of qualification history on brazed joints was conducted by NASA and spacecraft contractor and resulted in the establishment of revised criteria for acceptance.

(b) The VSWR tests, beginning on January 16, 1964, disclosed that coaxial connectors were not acceptable for the following reasons: excessively short or braided shields, gaskets not cut through, excessive solder, voids in solder, and variation in disassembly torque from 0 to 100 pounds. The unacceptable quality of a large percentage of coaxial connectors resulted in rework to new specifications of all coaxial connectors on spacecraft 2.

(c) The Launch Preparations Group (LPG) accepted the pallets into SST on February 6, 1964. During pallet instrumentation, a playback of the onboard PAM tape recorder revealed excessive VCO noise on the 22 kc channel. The problem was determined to be in recorder design. A solution was obtained by wiring the 25-kc reference signal to the head which recorded the noisy 22-kc VCO output to facilitate adequate compensation during ground data reduction.

UNCLASSIFIED

(d) During preinstallation acceptance testing (PIA), the relief trip point of the secondary side of the ECS cabin regulator occurred at 5.9 psia instead of the specified 5.0 to 5.3 psia. The primary side operated within limits. A decision was made to deactivate the secondary side by removing the aneroid bellows and to go with only the primary side operational.

(e) The gas validation test on the reentry control system (RCS) B package began on February 24, 1964. Significant problems encountered were as follows:

(1) The initial package failed when a burst diaphragm and check valve began leaking on the fuel side.

(2) A replacement package failed during a PIA test.

(3) A third package failed when a check valve and a relief valve began leaking on the oxidizer side in the orbital attitude and maneuver system (OAMS). Failure analysis revealed that the discrepancies were attributed to contamination. As a result, the package was replaced with another unit which had a more rigid cleanliness requirement.

(f) Numerous problems were encountered during the testing of the reactant supply system and fuel cell. Typical of these problems are the following:

(1) Acidity of the product water leading to corrosion and rupture of water lines, contamination of product water, clogged filters, and failure of the product water regulator.

(2) Leaking cryogenic quick disconnects.

(3) General degradation of stack performance between tests. Corrective action taken during SST included replacement of aluminum lines with stainless steel, replacement of failed components, increasing the filter size, and a design reduction of side loads on quick disconnect fittings. Degradation of stack performance was accepted for flight, provided that stacks would be monitored for indication of imminent fuel-cell failure and an immediate shutdown effected as a result. Continuing problems with the fuel cell resulted in a decision not to use them as a source of spacecraft power. The fuel cells were retained in the vehicle for flight test utilizing a dummy load.

(g) During instrumentation system tests on the cabin section, the multiplexers experienced spurious resets which caused loss of data. Inductive coupling was identified as the cause and was corrected by re-design to desensitize the reset circuitry.

UNCLASSIFIED

(h) Difficulty was experienced in installing and aligning the horizon sensor head due to the mislocation of pins through the scanner platform base into the spacecraft structure. This resulted in an improper mating of an electrical connector and a misalignment of the sensor head. The former was corrected with shims, and the latter was accepted for GT-2 since precise angle readout was not required for the short duration flight. The misalignment was approximately 1° roll and 0.5° pitch.

After satisfactory completion of the module mate, Phase II (mated) SST began on July 3, 1964. Significant problems encountered were as follows:

(a) During the initial power-up sequence of the guidance and control system tests, a computer malfunction indication was noted. The malfunction light was resettable. Power was removed, and troubleshooting did not reveal the problem. The computer was again powered-up after being cooled by the coldplate for 2 hours, and again a malfunction resulted, but the malfunction light could not be reset. After the temperature had been elevated to 75° F for approximately 2 hours, the computer was energized without a malfunction light indication. It was agreed that controlled coolant to the inertial guidance system (IGS) coldplate could prevent a recurrence. Testing was successfully continued by maintaining the IGS coldplate at room temperature.

(b) During guidance and control systems tests, while torquing gibal no. 4, an intermittent output from the x- and z-accelerometer temperature-control amplifiers was observed. Further testing indicated that the intermittent condition existed over approximately 300° of total gibal travel. The platform was returned to the vendor and a new E-7 slip ring installed. The unit was retested and reinstalled in spacecraft 2. During simulated flight test (part II), an accelerometer malfunction light occurred during platform pre-lift-off checks. Dirty slip rings were a prime suspect. All gimbals were torqued through 360° , and the slip rings were thus successfully cleaned.

(c) During previbration simulated flight on August 18, 1964, the diplexer and UHF whip antenna failed to extend. The antenna covers were improperly installed, causing the pin assembly to bind and hang during the extend sequence. Because of suspected damage to the solenoids, both diplexer and antenna were replaced. On August 26, 1964, during vibration simulated flight, the diplexer and whip antenna again failed to extend. Investigation revealed that the antenna element was binding against the housing due to improper stowing procedures. The procedure was rewritten to resolve the problem.

UNCLASSIFIED

(d) During RCS-OAMS gas validation, several discrepant conditions were found:

(1) OAMS fuel-side solenoid-valve thrust chamber assembly (TCA) 1 would not actuate and was replaced.

(2) TCA 8 oxidizer valve had excessive leakage and was replaced.

(3) Several valves in the RCS B ring would not actuate at 28 V dc but did actuate at higher voltage. All eight of the fuel solenoid valves were sluggish in response to the firing command. Valves were flushed with de-ionized water, soaked and cycled, purged with gaseous nitrogen (GN_2), filled with methanol and purged at 10 cycles per minute for 20 minutes, and then purged with GN_2 after methanol drain. Simultaneity tests were rerun, and the valves found to be within specifications. Flow tests and leakage tests were also within specification. Preliminary analysis of initial flush of H_2O through the fuel valves indicated the sample contained Del-Chem 2302C flush fluid and MMH byproducts as constituents. These two fluids had possibly formed a resulting hydrazide compound which fortunately was water soluble.

During August and September, operations at St. Louis were characterized by receipt and installation of a number of flight items. The spacecraft and systems successfully passed the vibration tests conducted from August 20 to August 24, 1964.

A decision was made to eliminate the altitude chamber test since GT-2 was an unmanned mission. The simulated flight test was conducted on September 3 to September 15, 1964. The spacecraft acceptance review was held on September 17 and 18, 1964; the spacecraft was accepted for shipment, prepared, and flown to Cape Kennedy on September 21, 1964.

12.1.1.2 Cape Kennedy operations.- Gemini spacecraft 2 was received at the Merritt Island Launch area (MILA) on September 21, 1964. The spacecraft schedule at Cape Kennedy is shown in figure 12-2. The spacecraft was moved to the MILA cryogenic building on September 22. Following receiving inspection, the cryogenic and hypergolic AGE were connected to the spacecraft in preparation for LO_2 and LH_2 servicing and RCS and OAMS systems servicing.

Cryogenic servicing was started on October 3, 1964. Difficulties were encountered with the AGE cryogenic quick disconnects due to corrosion of the carbon steel bearings. The quick disconnects were returned to the vendor, repaired, and subsequently reinstalled on the cryogenic hoses.

UNCLASSIFIED

UNCLASSIFIED

12-5

Servicing of the RCS and OAMS systems was conducted from September 25, 1964, to October 2, 1964. A water flush of the OAMS and one of the RCS ring thrusters was required to obtain satisfactory simultaneity results. Also, the RCS TCA 4 was replaced on September 28 because of out-of-specification solenoid valve leakage.

RCS and OAMS static firing was accomplished on October 4 and 5. Two major problems were encountered. One was leaking aerospace ground equipment (AGE) which allowed the RCS pressurant tanks to bleed overboard, and the other was an excessive delay of the first OAMS engine firing.

RCS and OAMS system deservicing was accomplished on October 5 and October 9. Only one set of RCS disposal plugs was available at Cape Kennedy, and a change to the test procedure was required to obtain sequential flushing and purging of the RCS subsystem. Subsequently, an extensive flush and freon soak of the RCS A-ring and OAMS fuel subsystems were required to decontaminate the systems.

Prior to moving the spacecraft to the pyrotechnic installation building (PIB) on October 10, 1964, the following modifications were incorporated:

- (a) Additional pyroswitches to deactivate hot umbilical circuits.
- (b) Wiring modification for the addition of an electrically initiated igniter for the tubing cutter at the equipment-section to retrograde-section separation plane.
- (c) Wiring correction to instrumentation measurement DEOL.

The spacecraft was moved from the cryogenic building to the pyrotechnic installation building for buildup from October 10 to October 17, 1964. A nonflight horizon scanner was replaced with the flight article on October 10. A suit circuit leak check was performed on October 14 and 15. An excessive leak rate was isolated to a damaged disconnect assembly which was replaced on October 15. Upon completion of pyrotechnic buildup, the spacecraft was weighed and moved to Complex 19 on October 18, 1964.

Premate systems tests were run from October 21 to October 27. Significant problems were:

- (a) A bad test point on the S-band transponder, which necessitated replacement.
- (b) Replacement of OAMS TCA 2 because of excessive leakage.

UNCLASSIFIED

UNCLASSIFIED

The premate simulated flight was run on October 28 and 30. Twenty-one minor problems were recorded during the performance of the test, but none required a components change. Following Part I, data evaluation and the resolution of these problems took place over a 3-day period.

Part II of predated simulated flight was started November 2 and completed November 4. Eighteen problems were recorded. Two of these involved the horizon sensor and the UHF transmitter. The horizon sensor would not track properly. The sensor and its associated electronics package were removed on November 4 and shipped to the vendor for repair. The nonflight sensor was installed on November 8 to support testing, and the flight article was subsequently returned and reinstalled on November 17. The UHF transmitter was removed for a bench check November 3, and a nonflight unit was installed to support spacecraft testing. A new design UHF transmitter was subsequently installed because a new seal configuration had been incorporated as a result of qualification test failures.

The pallet tape recorder was replaced on November 10 because an analysis of the on-board tape recorded PAM-FM data had disclosed excessive "wow and flutter."

The joint guidance and control test was started on November 10 and was completed on November 11. Four problems were recorded as a result of system performance during this test. A rerun of the static gain portion of this test was required because of an improper flight-path setting in the computer. The flight-path angle was reset and system performance was satisfactory.

Propulsion simultaneity checks on November 14 revealed unsatisfactory operation of TCA 1, 3, 5, 6, 7, and 8 in the RCS B-ring fuel valves. Investigation and correction of the problem were completed on November 18.

An electrical-electronic interference (EEI) test was run on November 13. Six problems were recorded during the course of this test. One of these problems concerned glitches on the computer output steering signal; consequently, the IMU platform was replaced on November 15. Changing the platform necessitated a retest of the system on November 16 and 17.

The joint combined system test was accomplished November 18. Twelve problems were recorded from the test.

The flight configuration mode test was run November 20 and 21. A 1.8-ohm resistance reading between the GLV and complex ground was resolved, and a two-shift schedule delay was incurred as a result.

UNCLASSIFIED

UNCLASSIFIED

12-7

A wet mock simulated launch (WMSL) was conducted from November 22 to 24. The following portions of the test were not accomplished:

- (a) Pyrotechnic shield checks (completed in actual countdown).
- (b) Cryogenics loading - a tight LH₂ system could not be obtained; therefore, actual LH₂ flow was not accomplished. The problems were corrected by adding a teflon washer on the spacecraft side of the LH₂ fill lines on November 27. This problem prevented activation of the fuel cell as had been planned.
- (c) Propulsion pressure checks (performance in actual countdown).
- (d) Flight installation of shingles and access doors (considered untimely in view of other problems).

During the countdown portion of WMSL, a spacecraft hold had to be called at T-75 minutes for 25 minutes to complete the setting of spacecraft switches. As a result of the problems encountered with time during the WMSL, an additional 24 hours was added to the launch preparations in order to complete the pre-count tasks.

The R and R section was demated on November 25, and the main parachute was replaced with one that conformed to the proper blueprint configuration. The R and R pyrotechnics and the double bridgewire adapter for the single-point disconnect were installed, and the R and R was remated on November 28.

The window camera was replaced on November 27 with the backup camera which had less running time but better clearance between magazine cover and film spool.

The final systems test was accomplished on November 28 and 29. During the test, a low-level multiplexer failed to synchronize properly. The multiplexer was replaced on November 30. The low-level multiplexer was again replaced on December 2 since it displayed the same synchronization problem as the previous one.

An engineering change to cut and cap an OAMS fuel line to the forward thrusters was accomplished November 30 and December 1. This modification was incorporated to provide a safe separation of the OAMS propellant lines in case the tube cutter-sealer did not seal successfully when the tubes were cut at the separation of the equipment and retrograde sections.

UNCLASSIFIED

UNCLASSIFIED

A design change was incorporated during the period from December 1 to December 7 to assure that the molded plastic interconnect fairings would not pull away from the skin during firing of the adapter-to-reentry assembly separation charges.

From November 30 to December 2, the double bridgewire adapters were installed. This change was made to allow both bridgewires to receive firing current as a redundant measure.

A launch countdown was accomplished from December 5 to December 9. The precount operations were completed satisfactorily. Activation of the fuel cell was not accomplished because of AGE and procedural problems. The launch was aborted because of launch-vehicle problems, and the spacecraft was recycled and safetied on December 9 and 10.

The hypergolic isolation valves that were activated during the countdown static firing were replaced on December 12 and 13. From December 13 to December 17, the following propulsion checks were made:

- (a) Flush and purge of RCS and OAMS
- (b) Simultaneity checks
- (c) Leak check of isolation valves
- (d) Bleed OAMS oxidizer tank
- (e) X-ray of OAMS tanks
- (f) Top off OAMS and RCS oxidizer tanks

A change was incorporated December 16 on the fuel cell circuit wiring to insure proper operation of the fuel cell valves. Stack 1C of the fuel cell was activated on December 18 in less time than was allowed for this activity in the countdown.

A prelaunch retest activity was started January 4, 1965, and a final systems test was run January 4 and 5, 1965. During this test, the C-band transponder could not be interrogated and was replaced. One of the adapter separation sensor switches was broken while being tested and was replaced.

An abbreviated simulated flight was run January 12 to insure system readiness for the final simulated flight. Data evaluation disclosed a faulty high-level multiplexer, and this was replaced on January 13, 1965. A final simulated flight was accomplished January 14.

UNCLASSIFIED

The R and R-RCS separation bolts were replaced on January 15 as a result of a system qualification test which indicated the original bolts were unsatisfactory for separation with the firing of a single shaped charge.

F-4 day of the launch count was begun on January 15. During RCS pressure checks, a regulator in the RCS B-ring failed. This regulator was changed on January 15 and 16. A leak and functional check of the new regulator was performed on January 16. The precount activity was completed with no other problems on January 19, and the final count was started at 2:00 a.m. e.s.t.

12.1.2 Gemini Launch Vehicle

12.1.2.1 Operations at Denver, Colorado.- Major weld fabrication on the Gemini Launch Vehicle (GLV-2, Contractor Serial No. B002, Air Force Serial No. 6-12557) was begun at the contractor facility in Denver, Colorado, in September 1962. All tanks were subjected to the following manufacturing requirements: visual inspection, dye penetrant checks, radiographic inspection, weld eddy current checks, hydrostatic test, chemical cleaning, finish iridite, helium checks, nitrogen purge, and dew point checks. The hydrostatic test consisted of two pressure cycles at 1.10 times limit load and four cycles at limit load.

On February 14, 1963, an ultrasonic visual and metallurgical inspection revealed microcracking in one of the junction chords used to fabricate the stage II fuel tank. The tank was replaced. Load-limit hydrostatic pressure cycle tests and another complete X-ray examination in February 1963 revealed a crack in the stage I oxidizer-tank aft dome. A decision was made to fabricate a new tank since the X-rays on the forward dome could not be unconditionally guaranteed due to the masking effect of the ablative coating. During the "roll out" inspection on July 8, 1963, an investigation of a discrepancy revealed the presence of a tool mark in the leg of a "Y" chord in the stage II oxidizer tank which exceeded the stress concentration limits. As a result, the tank was replaced with a production line stage II oxidizer tank.

12.1.2.2 Operations at Baltimore, Maryland.- The replacement stage II fuel tank was received by the contractor's Baltimore facility on June 25, 1963. The stage II oxidizer tank and the stage I fuel and oxidizer tanks were received on July 12, 1963. A dew point check was made on all tanks, and where necessary, the tanks were purged with nitrogen in preparation for assembly and test operations.

Horizontal assembly and test of GLV-2 were accomplished during the period from July 1963 through January 1964. Significant events and problems during these operations were as follows:

UNCLASSIFIED

(a) Lock bolts, stage I fuel tanks: A discoloration was observed at the base of the collars attaching one of the fittings to the aft cone. The deposit was determined to be salts from the iridite solution. The faying surfaces were refinished, and the fitting was reinstalled.

(b) Welds, stage I fuel tank: A non-volatile white residue was found on the vinyl coating applied over the welds on the aft cone. Analysis showed that the residue corresponded to that obtained from Denver tap water. Therefore, the vinyl coating was stripped from the welds; the entire cone was cleaned with demineralized water; and the welds were revinylated.

(c) Skirt, stage II oxidizer tank: Pitting was observed in a localized area on the aft skirt. The probable cause was entrapment of water in minute surface irregularities. The entire area was burnished with aluminum wool, degreased, passivated, and reiridited.

(d) Panel, stage I fuel tank: Wires in a harness assembly were either too short or too long to permit proper connection. The locations of terminal boards and wiring runs were changed.

(e) Electrical connectors: On September 17, 1963, a metal sliver was found in an electrical connector on GLV-1. Further inspection revealed that a number of plugs contained burred key ways, crazed or cracked headers, bent pins, and contaminated O-rings. Subsequently, all connectors on GLV-2 were reinspected, and the results recorded in a special certification log. Bent pins, glass inserts, and O-rings were cleaned and reworked, or replaced, where applicable.

(f) Attenuator pads: The wires in a number of attenuator pads were found to be cut or nicked at points where the wires exit from the potted block. Nine installed modules were replaced. Teflon inserts were substituted for steel inserts during the molding process to eliminate the problem on future production units.

(g) Conduit: Screw holes in the aft cover of the external ladder did not align with the fasteners in the closing rib. The ladder had been mislocated $\frac{3}{16}$ -inch forward of its specified location. The closing rib was replaced and shimmed to provide proper alignment.

(h) Interstage rivets: The GLV-2 interstage assembly was checked for installation of rivets which had not been released for use in this application. The results of electrical conductivity checks indicated that the installed rivets were satisfactory for use.

UNCLASSIFIED

UNCLASSIFIED

12-11

(i) Truss assembly, stage I fuel tank: Cracked collars and fittings on the truss assembly were detected on N-series (Titan II) vehicles. The failures were attributed to stress corrosion. Prior to reinstallation of the truss assembly at Baltimore, Maryland, close-tolerance bolts and locknuts were installed.

(j) Skin panels, stage I fuel: Four 1-inch-diameter local areas on the chemically milled panels were found to be 0.003- to 0.006-inch below minimum design requirements. Analysis of these areas indicated an acceptable margin of safety.

(k) Wiring: Teflon coated wire used to fabricate harnesses for the vehicle was found to contain a number of faults. Investigation revealed that the wire was received from the vendors in this condition. The affected wiring was replaced on the GLV-2 interstage assembly, and a new contractor acceptance plan was instituted.

(l) Stage II engine: The stage II engine was received on December 10, 1963, and installed on December 31, 1963. Following installation of the engine, a check of the log books revealed that the bolts attaching the engine to the tank were overtorqued. The bolts were replaced and retorqued to specification. The structure was then dye penetrant inspected to assure that the skin was not cracked. Also, the pressure line to the tandem actuator required rerouting to eliminate interference with the electrical connector on the start cartridge. Four engineering changes were incorporated on the engine prior to vertical erection.

(m) Feed lines: On stage I and stage II, a flange type joint was substituted for the "alpin" joint. X-ray and helium leak inspection requirements were imposed on all welds. On stage I, a one-piece, extruded, and chemically milled tube with bonded retainer rings was substituted for a butt-welded segmented tube with spot welded retainer rings. Feed lines were modified to solve leakage problems.

(n) Bellows assembly, stage I feed line: The bellows assembly had to be reworked because the bellows flange specified in the drawing was too short.

(o) Truss assembly: Misalignment between the centerline of the feet on the truss assembly and that of the mounting pads on the aft cone was found to exceed tolerances. A "worst-case" analysis was made of the eccentric load condition by assuring that the maximum mismatch occurred in the stringer carrying the maximum load. The analysis showed an acceptable margin of safety.

UNCLASSIFIED

UNCLASSIFIED

(p) Stage I engine: The stage I engine was received on December 29, 1963. This engine was shipped for the purpose of supporting launch vehicle systems testing and acceptance testing, and was to be returned to the manufacturer at the completion of these phases. On December 31, 1963, a letter was submitted to the Air Force Space Systems Division (AFSSD) requesting direction to use the engine in accordance with the following approved plan:

(1) The engine was to be installed for the subsystems functional verification test (SSFVT) and the combined systems acceptance test (CSAT).

(2) A replacement engine was to be delivered to Baltimore on April 24, 1964.

(3) After the engines were exchanged, GLV-2 was to be delivered to the Eastern Test Range (ETR) and reverified during the SSFVT and the combined systems test (CST) at the ETR.

Nine engineering changes were incorporated in the engine prior to vertical erection.

Stage I and the interstage were erected in the vertical test facility (VTF) on February 5, 1964, and stage II was erected on February 7, 1964. Post-erection inspection was completed prior to "power-on" on February 20, 1964.

Subsystem functional verification test began on February 21, 1964. It should be noted that the contractor's in-plant operations are different from those conducted at Cape Kennedy. During the in-plant operation, each system is separately controlled with no automatic sequencing employed for combined systems testing. The systems evaluated during the SSFVT are as follows: Flight control, hydraulic, radio guidance, ordnance, command control, instrumentation, malfunction detection, electrical, propulsion, and MISTRAM. The propulsion system and the electrical system are not fully tested in-plant; however, these differences are not detrimental to satisfactory checkout for delivery to the launch site.

The SSFVT data were reviewed by AFSSD and Aerospace before beginning the instrumentation airborne marriage test on March 6, 1964. Seven anomalies were recorded and corrected during this test.

Electrical-electronic interference (EEI) formal testing was started on April 14, 1964. During the EEI test, oscillograph recorders were used to monitor 20 GLV and AGE circuits. Of these 20 circuits, 5 displayed anomalies. The SA₁ and SA₂ hydraulic switchover circuits displayed a voltage transient in excess of failure criteria. A special test

UNCLASSIFIED

UNCLASSIFIED

12-13

established that the voltage transient was caused by the AGE grounding systems, and that only a 0.4-volt level existed in the GLV. This level was well below the failure criteria level of 1.5 volts established for the airborne side of the isolation resistor.

The first dry-run CSAT was performed on April 17, 1964. This test attempt was invalidated because of out-of-specification switch operating time. From April 17 through April 20, CSAT runs 1, 1A, and 2 were completed, and 14 anomalies were reported and resolved. On April 22, 1964, the formal CSAT, consisting of test 02-022 (run 1) and test 02-023 (run 2) were completed satisfactorily. Momentary MISTRAM unlock occurred at T-12 minutes during transfer of the range safety system (RSS) to internal battery power in both runs. Investigation revealed that unlock at power transfer is characteristic of the transponder, and is not considered a problem, since transfer does not occur after lift-off.

Three additional nonscheduled tests were conducted after CSAT. A radio frequency susceptibility test was required to demonstrate the ability of GLV-2 ordnance to withstand an electromagnetic field strength up to 100 watts per square meter with live ordnance items connected in flight configuration. A GLV-spacecraft simulator EEI test was required to evaluate EEI on three attitude signal leads from the GLV to the spacecraft. Because the rate switch package was replaced after CSAT, partial SSFVT, data acquisition, and CSAT tests were required on this item.

The vehicle acceptance team (VAT) critique was held on April 27, 1964. The Baltimore Area Contract Monitor Office (BACMO) gave satisfactory reports on the delivery status of GLV-2. Contractor representatives met with the VAT to discuss the following major anomalies:

- (a) Disturbances on the oxygen inlet pressure measurement
- (b) Unlock of MISTRAM indication
- (c) Drop of chamber pressure
- (d) Oscillation of turbine inlet temperature
- (e) Disturbances on fuel-pump discharge pressure measurement
- (f) Erratic yaw "A" low rate switch

At the conclusion of all subsystem reviews, no de-erection constraints were reported. By May 1, 1964, all paper restraints to delivery had been cleared, and 11 non-flyable components for GLV-2 were identified. Non-flyable component categories were:

UNCLASSIFIED

UNCLASSIFIED

- (a) Modifications to be installed
- (b) Qualification tests to be completed
- (c) Ground test only (GTO) articles

De-erection of GLV-2 from the VIF was completed on May 2, 1964.

Between May 3, 1964, and June 16, 1964, GLV-2 was scheduled for stage I engine change, several engineering change incorporations, and scheduled testing in the GLV assembly area. Engine replacement was started May 11 and completed June 13. A stage II turbopump assembly (TPA) modification was completed on May 28. Non-scheduled testing consisted of stage I and stage II tank leak checks, hydraulic disconnect removal and installation retest, hydraulic functional flush and proof test, engine harness electrical test, telemetry instrumentation checkout, antenna pattern check, motor-driven switch cycle test, and instrumentation J-box retest.

Delivery of GLV-2 to ETR was rescheduled from June 22, 1964, to July 10, 1964. The available time was used to perform modifications which had been previously scheduled for Cape Kennedy.

To expedite ETR checkout, the following units were removed from the vehicle on June 26, 1964, and shipped to ETR for laboratory receiving tests:

- (a) Primary autopilot
- (b) Secondary autopilot
- (c) Primary rate gyro
- (d) Secondary rate gyro
- (e) Rate switch package
- (f) Three-axis reference system (TARS)

On June 29, 1964, the fuel accumulator potentiometer (POGO modification) was removed to correct for excessive friction in the dampener assembly. The piston and O-ring were replaced and the unit was retested. This work was completed on July 10, 1964.

On July 6, 1964, the gas generator and autogenous cooler were removed and returned to the manufacturer for cleaning. This action was

UNCLASSIFIED

directed because of component operating time and elimination of the sequential compatibility firing (SCF) test.

Examination of the thermal insulation had revealed a thickness which exceeded the blueprint tolerance by as much as 0.025-inch. Therefore, on July 2, 1964, the stage II forward skirt was sanded in the vicinity of the calorimeters to provide an accurate evaluation of the effects of protuberance heating.

GLV-2 was loaded on a C-133B aircraft on July 10, 1964, and flown to the ETR on July 11, 1964.

12.1.2.3 Gemini Launch Vehicle at the Eastern Test Range (ETR).- Subsequent to the arrival of GLV-2 at ETR on July 11, 1964, the vehicle was subjected to the effects of five natural phenomena, three of which resulted in a requirement for retest and rescheduling. These events were:

- (a) Electromagnetic damage caused by effects of nearby lightning on August 17, 1964
- (b) Hurricane Cleo on August 27, 1964
- (c) Hurricane Dora on September 8, 1964
- (d) The threat of Hurricane Ethel on September 11 and 12, 1964
- (e) The threat of Hurricane Isbell on October 14, 1964.

The testing milestones and phenomena are recorded on figure 12-3.

Stage I of the vehicle was erected at Complex 19 on July 13, followed by stage II on July 14, 1964. Prior to the erection of stage II, the stage II engine ablative skirt was rejected because of chipping and a questionably patched crack found during receiving inspection. After engineering acceptance by the agencies involved, the skirt was replaced with a Titan II ablative skirt which had been subjected to a dye penetrant check. (The Titan II skirt is identical to those fabricated for the Gemini program except for factory qualification test requirements.

Electrical power was applied to the GLV on July 20 to begin the SSFVT period. Testing had progressed to the point at which the combined systems test, pre-spacecraft mate verification test, was scheduled for August 19. However, during a severe electrical storm on the evening of August 17, 1964, at approximately 11:30 p.m., components were damaged at Complex 19, principally in the AGE area. A few semi-conductor failures were also discovered in airborne units. The subsequent investigation disclosed that the Complex had probably not received a direct

UNCLASSIFIED

lightning strike. The damage experienced was attributed to the electromagnetic effects of nearby lightning and/or the resultant induced static charges.

A recovery program was initiated to reestablish confidence in all launch-vehicle systems, aerospace ground equipment, ground instrumentation equipment, and facility systems to assure that all possibly degraded equipment was repaired or replaced and appropriate reverification tests successfully completed. It was decided after consulting with experts that too great a risk would be involved in retaining airborne units containing semiconductors which might have been degraded by the incident; therefore, all flight safety units were replaced.

During the finalization of these plans, the Cape Kennedy area was struck by Hurricane Cleo on August 27, 1964. Stage II was deerected and stored in the hangar; stage I remained on the launch pad during the extremely hard, driving rains associated with that disturbance.

Stage II was reerected on September 1, 1964. Following inspection, power was applied to the vehicle on September 2. Reverification was in the beginning stages when the Cape Kennedy area was struck by Hurricane Dora on September 8, 1964. Both stages were deerected and stored in the hangar. On September 10, weather forecasters advised that Hurricane Ethel was a threat to the area.

The GLV remained in the hangar until September 14 when both stages were reerected. The final series of tests and checkouts prior to launch were then initiated.

Total complex readiness was completed on September 17, and power was applied to the vehicle on September 18, 1964. Airborne units containing semi-conductors were replaced before the start of subsystems verification testing. The SSFVT, including the electrical-electronic interference marriage test, was completed on schedule on October 5, 1964. On October 6, the launch-vehicle pre-spacecraft mate verification test was performed. After this test was completed, the spacecraft simulator was connected to the GLV in preparation for the premate EEI tests. EEI 1 testing was completed on October 9. The spacecraft transient analyzer was installed at the complex at that time, and test EEI 1A, spacecraft guidance computer test, was completed on October 12.

On October 12, the spacecraft interface seal was installed, and final preparations to receive the spacecraft were in progress when Hurricane Isbell threatened on October 14 and 15. The hurricane path was sufficiently south of the Cape to make it unnecessary to deerect the vehicle; however, the testing was somewhat restricted as a result of inclement weather.

UNCLASSIFIED

UNCLASSIFIED

12-17

The spacecraft was erected on October 18, 1964.

Between October 16 and November 1, the stage I and stage II oxidizer tanks were inspected because burrs were discovered on internal tank structure fasteners during an inspection of GLV tanks in Baltimore. In addition to the deburring operation, all internal welds were dye checked for cracks and other weld imperfections.

The launch vehicle pre-mate simulated flight test was conducted on November 4, and the spacecraft was mechanically mated to the GLV on November 5, 1964.

The electrical interface integrated validation (ELIV) test was performed on November 9, followed by the joint guidance and control test and EEI 2 test on November 12 and 13, 1964. This testing thoroughly affirmed that the interface was valid and that no electrical interference problems would be encountered between launch vehicle systems and spacecraft systems.

A joint combined systems test (JCST) was run on November 18, followed by a flight configuration mode test on November 21, 1964, in preparation for the wet mock simulated launch (WMSL).

The WMSL was concluded satisfactorily on November 24, 1964. The scheduled launch date of December 9 was reaffirmed, and the final joint simulated flight test was completed on December 3, 1964.

The launch countdown began at 4:00 a.m. e.s.t. on December 9, 1964, and proceeded to T-0 at 11:40:57.00 a.m. e.s.t. with some minor holds. The beginning of the count had been delayed approximately 2 hours when the stage II oxidizer flowmeter failed to register properly, and it became necessary to load stage I and then stage II oxidizer tanks serially by using the stage I flowmeter.

The count proceeded in a normal fashion until approximately 1 second after engine ignition when a shutdown signal was initiated by the MOCS "hold-kill" monitoring circuitry. Shutdown was indirectly caused by loss of primary system hydraulic pressure and directly caused by the resultant automatic switchover to the secondary guidance system. This is monitored by the MOCS and constitutes a kill between T-0 and TCPS actuation plus 1.8 seconds. The malfunction was caused by high pressure in the actuator resulting from engine-start-transient side loads on the engine nozzle which reacted on the tandem actuator. A complete account of the attempted launch is given in appendix B of this report.

As a result of the subsequent malfunction investigation, all four stage I tandem actuators were replaced with redesigned actuators.

UNCLASSIFIED

UNCLASSIFIED

Although some retesting was done, most of the activity in preparing the GLV for launch was curtailed until new actuators were received and installed on January 6, 1965. Subsystems retesting then began, with concentration on the flight controls system. The final combined systems test, simulated flight test, was completed on January 14, 1965.

The GT-2 Mission Review Board assembled on January 16, followed by the Launch Vehicle Status Review Board and the Flight Safety Review Board on January 18, at which time the Board committed GLV to enter the final countdown.

12.2 WEATHER CONDITIONS

Weather conditions in the launch area were satisfactory for all operations for the several days of preparation and the day of launch. On launch day, there was only a thin surface haze. This weather prevailed in spite of the gloomy predictions presented at the Mission Review.

Weather observations in the launch area taken at 9:05 a.m. e.s.t. were as follows:

Cloud coverage	Clear skies
Wind direction, deg	320
Wind velocity, knots	7
Visibility, miles	8
Pressure, in. Hg	30.31
Temperature, °F	46
Dew point, °F	37
Relative humidity, percent	71

Weather observations taken onboard the U.S.S. Lake Champlain recovery ship located at 16.5° N, 49.5° W at 8:52 a.m. e.s.t. were as follows:

Cloud coverage $\frac{5}{10}$ covered, cumulus and cirrus; cloud base 2000 feet; high layer cloud at 10 000 feet; rain showers approximately 7 miles from recovery site.

UNCLASSIFIED

Wind direction, deg	80
Wind velocity, knots	23
Pressure, in. Hg	30.06
Humidity, percent	63
Visibility, miles	10
Wave height, feet	6 to 7 with 15-foot swells

Launch-area and recovery-area wind direction and velocity plotted against altitude are presented in figures 12-4 and 12-5.

Tables 12-I and 12-II list the atmospheric conditions measured in the launch area and recovery area for various altitudes.

12.3 FLIGHT SAFETY REVIEWS

Flight Safety and Mission Review meetings were conducted to determine the flightworthiness of the spacecraft and launch vehicle for the GT-2 mission and to ascertain the readiness of all supporting elements.

12.3.1 Spacecraft

12.3.1.1 Pre-Flight Readiness Review.- A Pre-Flight Readiness Review was held October 15, 1964, to review the testing and problems associated with each spacecraft system before moving the spacecraft to Complex 19. Major problems were those concerning the qualification status of the pyrotechnic system, reactant supply system, and propulsion system components. These and other relatively minor discrepancies were discussed, and were processed for correction.

12.3.1.2 Flight Readiness Reviews.- The Flight Readiness Review was held on November 27, 1964. The problem of sticking valves in the RCS "B" ring was discussed and operational procedures were initiated to insure functional valves. The spacecraft contractor was requested to submit a revised qualification parts list before launch since approximately 196 of the 383 items did not have the proper qualification designation. The contractor submitted a revised list to the board on December 5, 1964. All other system problems were minor, and the spacecraft was found ready for flight pending satisfactory completion of the

UNCLASSIFIED

final simulated flight test. This test was successfully conducted on December 3, 1964.

The second Flight Readiness Review meeting, required as a result of the aborted launch attempt on December 9, 1964, was held on January 13, 1965. The ability of the mild detonating fuse (MDF) ring to separate satisfactorily the rendezvous and recovery section from the spacecraft was discussed. Attaching bolts of lower strength were made available, and, based on further information received after the Flight Readiness Review, were substituted for the higher strength bolts. The receipt of a satisfactory explanation of a vendor failure analysis on the qualification test problems of the orbital attitude and maneuver system (OAMS) bladder was established as a constraint on the flight. A letter from the spacecraft contractor was received on January 14, 1965, which explained that the failure of the bladder was due to unrealistic temperature and testing procedures. The system was then declared to be satisfactory. All other systems were found to be ready for flight, pending the outcome of the simulated flight test. This test was completed satisfactorily on January 14, 1965.

12.3.2 Launch Vehicle

12.3.2.1 Flight Readiness Reviews.- The Launch Vehicle Review was held on November 28, 1964. The Air Force Space Systems Division (AFSSD) 6555th Aerospace Test Wing personnel summarized for the board all testing and operations conducted at the Eastern Test Range (ETR). All systems were found to be ready for flight, pending completion of the final propulsion leak checks and simulated flight test. These tests were satisfactorily completed.

The second Launch Vehicle Review was held on January 13, 1965. Hydraulic actuators with the modified servo valves were installed after the launch attempt on December 9, 1964. The three modifications that corrected the servo valve failure are discussed in appendix B.

All necessary component replacements and systems checkout were completed, and all systems were again ready for launch pending final tests. These tests were successfully completed.

12.3.3 Flight Safety Review Board

The Air Force Flight Safety Review Board met on December 8, 1964, and recommended to the Operations Director that the launch vehicle be committed to flight.

UNCLASSIFIED

At the second Air Force Flight Safety Review Board meeting on January 18, 1965, the board again recommended that the launch vehicle be committed for flight.

12.4 SUPPLEMENTAL REPORTS

Supplemental reports for the GT-2 mission will be prepared as shown in table 12-III. The format will conform to the external distribution format of the NASA or contractor organization preparing the report. Before publication, the supplemental reports will be reviewed by the cognizant Mission Evaluation Team (MET) Senior Editor, the Chief Editor, and the MET Manager and will be approved by the Gemini Program Manager.

The same distribution will be made on the supplemental reports as that made on the Mission Report.

12.5 DATA AVAILABILITY

Figure 12-6 shows the instrumentation and trajectory data made available to the Evaluation Team. Tables 12-IV, 12-V, and 12-VI list the photographic data which were processed. The instrumentation and trajectory data will be on file at the Manned Spacecraft Center (MSC) Computation and Analysis Division, Central Metric Data File; and the photographic data will be on file at the MSC Photographic Division.

12.5.1 Telemetry Data

12.5.1.1 Magnetic tape reproduction and formatting.- The onboard PAM-FM recorder was removed from the spacecraft in the landing area and returned to Cape Kennedy within LO + 15 hours. The tape was inadvertently broken during the rewind process on end of mission (EOM) +1 day. When the tape was spliced at the Cape Kennedy Mission Control Center (MCC) a 2-second data loss at LO + 279.2 seconds resulted. Copies of the tape were made available by LO + 30 hours. The splice in the tape introduced a 0.11-second error in the data-time correlation after LO + 281.2 seconds. Time was not recorded on the PAM recorder, but it was reconstructed by ground-time recording and data correlation. After final correction, the maximum time error introduced was less than 0.5 second.

UNCLASSIFIED

The onboard PCM recorder was removed from the spacecraft at Cape Kennedy on EOM + 4 days. The tape was removed from the recorder, and a playback copy was made at the Cape Kennedy MCC. This tape copy could not be formatted by the Kennedy Space Center (KSC). This procedure had been successfully checked prior to the mission using a test tape generated by the spacecraft contractor. The test tape was prepared with simulated data comprising an unrealistic bit transition density. The bit transition density of the flight tape precluded satisfactory reproduction on standard equipment at the MCC.

An attempt to reinstall the flight tape in the onboard recorder on the evening of EOM + 4 days failed because of inability to adjust for the proper tape tension. The recorder subcontractor personnel were summoned, and the installation was completed on EOM + 7 days. A tape was then made at the MCC, and a computer compatible tape was formatted at KSC on the evening of EOM + 7 days. MSC Computation and Analysis Division (CAAD) was unable to reduce the data from the tape on EOM + 8 days. KSC was informed of the problem, and upon investigation it was reported that a malfunction in a counting circuit and a timing delay circuit had caused the data to be formatted incorrectly even though synchronization was attained. The malfunctions were corrected, and a computer compatible tape was produced on EOM + 11 days and shipped to MSC Houston on EOM + 12 days. On EOM + 10 days, Tel II was requested to format a second tape copy. This copy was reduced at Houston on EOM + 12 days.

12.5.2 Trajectory Data

12.5.2.1 Air Force Eastern Test Range (AFEIR).- The impact predictor data reduced at AFEIR were made available on EOM + 3 days. The corrected but unsmoothed MISTRAM and C-band radar data which were requested within EOM + 3 days were made available on EOM + 8 days. Final reduced MISTRAM data which were also requested within EOM + 3 days were delivered on EOM + 17 days. The best estimate of trajectory was scheduled to be completed by EOM + 22 days. The preliminary signature analysis report was received on EOM + 13 days; however, the final report will be delayed until EOM + 30 days.

12.5.2.2 Kennedy Space Center.- The impact predictor data reduced by KSC were made available within 10 + 6 hours. KSC was not able to complete the program change requested to correct the trajectory for winds aloft. This correction will be completed for GT-3.

12.5.2.3 Goddard Space Flight Center (GSFC).- The Mod III radio guidance system data reduced by GSFC were made available on EOM + 1 day, as requested. GSFC also made available data points (position and velocity) for that portion of the trajectory after separation.

UNCLASSIFIED

12.5.3 Reduced Telemetry Data

12.5.3.1 Aerospace Corporation.- Gemini Launch Vehicle (GLV) telemetry data were reduced at Aerospace and made available in plotted form (engineering units versus time) 1 day ahead of schedule on EOM + 4 days.

12.5.3.2 Eastern Test Range.- GLV telemetry data which were to have been reduced to engineering units by the Quick Look Analysis Program (QLAP) within LO + 24 hours were not available until EOM + 6 days because of nonavailability of computer time at ETR.

12.5.3.3 Kennedy Space Center.- Quick-look tabulations and plots of selected spacecraft telemetry data were made available within LO + 4 to LO + 30 hours as requested.

12.5.3.4 Goddard Space Flight Center.- Goddard reduced the spacecraft digital command system transmission and made these data available on EOM + 17 days.

12.5.3.5 Spacecraft contractor.- The reduced vibration data (g_{rms} versus time and power spectral density plots) were made available between EOM + 6 and EOM + 9 days as requested. The analysis of onboard film to compute spacecraft pitch and roll attitudes is expected to be completed by EOM + 24 days. These data have been delayed because of an inconsistency in camera speed and the time required for data qualification. The computation of the ascent and reentry guidance equation simulations has been delayed because of the data gaps in the initial data, program deficiencies, and the time required to determine initial conditions. It is expected that the simulation will be completed by EOM + 24 days. The spacecraft contractor also made available time-history tabulations and plots of the available telemetry data in engineering units on EOM + 6 days.

12.5.3.6 Computation and Analysis Division - MSC.- CAAD reduced to engineering units and made available on EOM + 6 days the onboard PAM-FM data and all spacecraft telemetry data which had been delivered. Tabulations and plots of the onboard PCM data were distributed on EOM + 13 days, and tabulations of the final composite trajectory were made available on EOM + 15 days. Figure 12-7 shows the compilation of station recordings which were used in preparing the preliminary and final composite data books.

Instrumentation and Electronics System Division (IESD) prepared vibration analysis plots (g_{rms} versus time and power spectral density) using analog techniques as did CAAD using the digital computer.

UNCLASSIFIED

Heat-transfer rates through various sections of the spacecraft were calculated from data derived from the onboard PAM-FM recorder and the PCM instrumentation system. The PAM-FM data were available on EOM + 7 days; however, the heating rates derived from the PCM data were not available until EOM + 15 days because of program difficulties in filling the gaps in the preliminary composite and the late availability of the PCM data recorded on the onboard tape.

The lift-to-drag ratio and reentry angle-of-attack calculations were delayed by the late availability of the onboard PCM data. After several preliminary computations, the lift-to-drag ratio and reentry angle-of-attack calculations were completed on EOM + 15 days. These data are considered preliminary, and further review of the reduction techniques will be pursued.

The propellant weight and reentry control system pressurant leakage calculation was completed on EOM + 16 days. The inertial guidance system (IGS) actual versus nominal presentation was delayed until EOM + 8 days because of incorrect data inputs. The onboard film of the three instrument panels were analyzed, and the instrument readings were correlated with telemetry and tape recorded data. Time correlation of the right-hand panel camera proved to be very difficult since none of the parameters displayed on the panel provided an adequate correlation, and a number of time correlation errors were made. The final plots of these data were available on EOM + 22 days.

Fifty-four special requests for additional or expanded presentations of GT-2 data were processed during the evaluation period. The special requests included requirements for oscillograph recordings and special programing (i.e., computation of first and second differences of selected IGS parameters). It was not possible to complete all of these requests by EOM + 15 days, which was the planned time to complete the spacecraft performance analysis.

Reduction of GT-2 data was delayed due to many reasons. The primary reason was the nonavailability of a complete composite telemetry tape comprising recordings at MCC, Tel II, Grand Bahama Island (GBI), Antigua, Coastal Sentry Quebec (CSQ), aircraft 497, and the onboard recorder tapes.

12.5.4 Photographic Coverage

Photographic data were successfully obtained for each phase of the mission. Coverage consisted of metric, engineering sequential, and documentary photography. Metric photography was limited to the launch phase, while engineering sequential photography covered the launch, flight, recovery, and postflight inspection phases. Documentary film

UNCLASSIFIED

is incidental in its engineering value and will not be discussed. All photographic data discussed and listed were available to the Mission Evaluation Team during the period between 5 and 15 days after launch. Table 12-IV lists the photographic coverage comprising still and motion picture films provided to the Mission Evaluation Team.

12.5.4.1 Metric film.- Metric photographic coverage provided data for the initial (visual) trajectory and attitude calculations and served as additional engineering sequential data coverage. Seventeen cameras were committed for metric coverage. Film from 16 of these cameras was processed; the 17th camera jammed at launch.

12.5.4.2 Engineering sequential film.- Engineering sequential film provided an engineering surveillance of the events of the mission. Sequential film provided for each of the phases of the mission is described in the following paragraphs.

12.5.4.2.1 Launch film: The launch engineering sequential coverage film was obtained from fixed and tracking cameras as noted in table 12-V. Locations of the cameras are shown in figures 12-8 and 12-9. The duration of photographic coverage from respective cameras is shown in figure 12-10 and is defined as the period during which the spacecraft, launch vehicle, and/or exhaust flame was visible to the tracking cameras.

The coverage by 12 of the 13 tracking cameras committed was generally of good quality. Tracking camera coverage was obtained from lift-off through launch-vehicle staging. Quality and resolution of all tracking cameras were partially degraded by an atmospheric haze condition. One camera appeared slightly out of focus, one had a grainy film, and two cameras indicated poor tracking. Another camera failed to operate due to a short circuit in the power supply.

Three specially configured aircraft attempted to provide additional coverage of the spacecraft-launch vehicle as it passed through the region of maximum dynamic pressure between an altitude of 35 000 and 50 000 feet. Of these three aircraft, two obtained good coverage during the period noted. The third aircraft was out of position. The camera coverage obtained from the aircraft was not degraded by the atmospheric haze condition.

Twenty-nine fixed cameras were committed for coverage, five of which were for emergency use and were not required. In general, exposure and focus were good; however, two cameras were underexposed; and two were out of focus. Launch vibration affected two cameras and a timing image reflected into the picture of one camera film. Seven cameras experienced film breakage. Seventeen fixed cameras, however,

UNCLASSIFIED

provided adequate coverage for data evaluation. A detailed listing of cameras is contained in table 12-V, and the locations are depicted in figures 12-8 and 12-9.

12.5.4.2.2 Onboard spacecraft film: Engineering sequential film was taken of the right, center, and left instrument panels. This film was time correlated with a sync light placed in the field of view of each camera. The sync light was illuminated by the spacecraft telemetry system reset pulse which occurred every 2.4 seconds. Additional time correlation was provided on the left instrument panel by the event timer. Data were tabulated from the instruments listed in table 12-VI.

Engineering sequential film was also provided by a camera, mounted on the left pallet, which photographed the view out of the left window. The camera provided photographic coverage of the following:

- (a) Ionized gas due to reentry heating
- (b) Surface heating of the R and R and RCS sections
- (c) RCS thruster firing
- (d) Reentry roll program
- (e) Spacecraft attitudes
- (f) Parachute deployment sequence

12.5.4.2.3 Recovery film: Engineering photographic coverage in the recovery area was accomplished with the use of ten movie cameras and five fixed cameras. Reentry, descent, and touchdown were not photographed because the spacecraft flight was not visible from the recovery vessels. Table 12-VII identifies the coverage obtained and the cameras used during recovery operations.

The recovery helicopters carried fixed cameras which were designed for the Mercury program. As helicopters approached the spacecraft, pictures were taken as indicated in figure 12-11. The somewhat erratic movement of helicopter 2 from position 2-1 to 2-3 prevented helicopter 3 from moving to its planned position. Therefore, helicopter 3 was too far away from the spacecraft to provide adequate photographic coverage.

The lens on an experimental camera in helicopter 1 became overheated and had to be changed. The heat waves from the jet engines caused the film from this camera to look soft or out of focus. At times, vibration from all helicopter cameras became excessive. The original film in camera 2 on helicopter 1 was quite blue which indicates that

UNCLASSIFIED

the necessary filter required for Ektachrome commercial type film may not have been used. All other motion picture film was satisfactory.

Still coverage comprised most of the photography while the spacecraft was on the aircraft carrier. One fixed motion-picture camera onboard the aircraft carrier covered the operations from the time the spacecraft reached the carrier until it was placed in the dolly. All film, onboard cameras, and tapes were flown off the carrier 10 hours after recovery.

Complete photographic coverage (both still and motion picture) was obtained of the off-loading of the spacecraft at Roosevelt Roads. The entire deactivation operation was photographed.

12.5.4.2.4 Postflight inspection photography: The postflight inspection of spacecraft 2 required extensive photographic coverage to satisfy the requirements of engineering evaluation and documentation of procedures. Approximately 200 color still photographs and 500 to 700 feet of colored motion picture film were taken. All of the discrepancies detected during the postflight inspection were carefully documented in the still photographs.

12.6 POSTFLIGHT INSPECTION

The postflight inspection of the spacecraft 2 reentry assembly was conducted at the Kennedy Space Center from January 22 to February 19, 1965, according to the test procedures of reference 11.

The reentry assembly was received in relatively good condition. Approximately 200 photographs were taken to document the inspection and test. The following is a list of the discrepancies noted during the detailed inspection of the reentry assembly:

- (a) Holes were burned in the right-hand equipment bay shingles.
- (b) The right-hand wire bundle guillotine at station Z192 failed to cut the wire bundle.
- (c) A cracked shingle was found on upper centerline of the rendezvous and recovery (R and R) section.
- (d) Two cracked shingles were found on lower centerline of reentry control system (RCS) section.

UNCLASSIFIED

(e) The stub antenna on forward face of the R and R section was bent at approximately 45°.

(f) The radar fairing dome on the forward face of R and R section was dented inward.

(g) Two of the three retrograde section separation switches in the station Z10⁴ area were unactuated.

(h) Pilot parachute deployed signal switch in the forward part of the R and R section was unactuated.

(i) Pieces of the char layer on the surface of the heat shield had been scraped off in localized areas.

(j) A small piece was missing from phenolic ring in area of R and R section docking latch receptacle.

(k) Water was in electrical fuse blocks.

(l) Corrosion was around elapsed time meter on exterior of computer.

(m) Coaxial adapter (AGE) was found as a loose piece in the compartment forward of the left-hand landing gear door.

(n) Wiring pulled from potted connectors on RCS section by release of R and R section.

(o) Corrosion was found on the battery straps, landing-gear door fillers, environmental control system (ECS) door seal, and mild detonating fuse (MDF) ring.

(p) Water was found in one AGE receptacle of the attitude control maneuver electronics (ACME) package.

(q) RCS thrusters had peripheral cracks and several were nicked and gouged.

(r) Condensation was noted between the outer and center panes of both crew windows.

(s) The primary horizon-sensor electrical receptacle housing had a slight burn area and corrosion.

(t) The phenolic ring aft of the hoist loop at station Z10⁴ was crushed.

UNCLASSIFIED

UNCLASSIFIED

12-29

12.6.1 Chronology

The following is a chronological listing of the postflight inspection events beginning with spacecraft arrival at Cape Kennedy on January 22, 1965, and ending with spacecraft shipment to Houston on February 19, 1965.

January 22: The spacecraft arrived on schedule at 7:15 a.m. e.s.t. at the Cape Kennedy skid strip. After external washing, ejection seat pyrotechnics were safetied where possible. The reentry section was taken to the inspection area, and the pallets were removed. The remaining ejection seat pyrotechnics were safetied, and the data acquisition system (DAS) tape recorder was removed. Crew-station switch positions and instrument readings were recorded.

January 25: The detailed inspection of the external surface of the reentry assembly and R and R section was completed.

January 26: Shingle removal began, and pyrotechnic resistance checks were completed.

January 27: The heat shield was removed, weighed, and placed in the vacuum chamber for drying. The main, squib, and pallet batteries were removed and discharged to determine the remaining life.

January 28: The equipment bays were washed, and the fuse blocks were checked. The ECS door was removed and the ECS unit visually inspected. The 18-foot pilot parachute was charted for damage.

January 29: The heat shield drying was completed. The resistance check to determine the current leakage due to salt water immersion was completed. The ejection seats and hatch actuators were removed. The pyrotechnics were removed from the ejection seats and washing of the equipment bays completed.

February 1: The heat shield was removed from the vacuum chamber and weighed. The heat shield core samples were removed. The RCS section was demated from spacecraft. The hatch actuators were removed and dummy actuators installed. The wire bundle guillotines were removed. A functional check of crew station controls was performed.

February 2: The RCS section was prepared for the flushing operation. The flushing operation was delayed until AGE used in the operation was modified. Heat-shield coring was continued. Cores, $2\frac{1}{2}$ inches in diameter, were taken at the 42-inch radius to avoid cutting the

UNCLASSIFIED

UNCLASSIFIED

titanium ring on the shield. Discharging the batteries was completed. Reassembling the R and R section was begun.

February 3: Flushing of the RCS section was begun. The ACPU batteries were removed for discharging. The retrograde section separation switch was removed. The batteries were reinstalled in the spacecraft. The abort controller was removed from the spacecraft.

February 4: Heat-shield coring was continued. Removal of the ECS began. Flushing and purging of the RCS section was completed. The attitude controller was removed from the spacecraft. Pyrotechnic switches were removed from the spacecraft. The guidance and control components were removed.

February 5: RCS simultaneity and pressure tests were completed. The section was placed in the altitude chamber. The attitude controller was checked and reinstalled in the spacecraft. The HF transceiver and antenna were removed from the spacecraft.

February 6: RCS section was delivered to the malfunction analysis laboratory. Removal of components was started.

February 8: Four additional plugs from the heat shield to be used in evaluating temperature data were requested, and thirty-one heat-shield plugs were shipped to NASA-MSC Houston. The heat-shield coring continued. Reinstallation of access doors and shingles began. The preinstallation acceptance test was made on the abort controller. Seven of the ten pyrotechnic switches were reinstalled. The right-hand seat was reinstalled.

The following is the planned schedule of postflight inspection from February 9 to February 19:

February 9: The heat shield, access doors, and abort handle will be reinstalled.

February 10: The RCS section will be remated to the spacecraft, and the doors and shingles will be reinstalled.

February 11 to February 17: The seat and pallet will be reinstalled, and the reinstallation of the doors and shingles will be completed.

February 18 and 19: The spacecraft will be prepared and shipped to NASA-MSC at Houston, Texas.

UNCLASSIFIED

12.6.2 Spacecraft Systems

12.6.2.1 Structure.- In general, the cabin section exterior surfaces appeared as expected. There were varying degrees of heat damage ranging from slight discoloration to holes in the Rene' shingles on the right-hand equipment bay. The most significant heat damage occurred on the lower right-hand side on an angle of approximately 20° from the longitudinal axis of the vehicle. This heat-affected zone begins at the adapter interconnect fairing and extends to the RCS section in a fan shape. Within this zone, in a straight line from the most windward adapter interconnect fairing, there is a series of malformations which terminate with two holes, 3 feet from the edge of the heat shield. These holes, which are the most evident damage, are large enough to verify that the local temperature had reached the melting temperature of the material. (See fig. 12-12.)

Close examination of the area revealed a $\frac{1}{2}$ -inch-diameter half-moon burn at the leading edge (reentry) and a longitudinal buckle in the connecting strap located $6\frac{1}{2}$ inches upstream (reentry) from the previously mentioned holes. Again, the melting temperature had been attained. Plastic flow of the material was evidenced at $1\frac{1}{2}$, $2\frac{3}{4}$, $8\frac{1}{2}$, 10, and 11 inches from the strap, and there were varying degrees of crystalline structure change. A hole located 4 inches from the strap may have been the result of plastic flow rather than the melting temperature. The Rene' washer located 7 inches from the strap had undergone melting. The insulation blankets under this area exhibited discoloration similar to the insulation on the most windward side which had no protrusions. On this most windward side, a strap had two melted areas, although the melting was less pronounced than on the strap in the wake of the most windward adapter interconnect fairing. The other two adapter interconnect fairings produced similar fan-shaped discolorations; however, there was no evidence of plastic flow or melting in these areas.

The char layer of the heat shield had been damaged in several local areas. The recovery personnel explained that the damage was incurred when the divers' SCUBA gear contacted the shield during recovery operations.

Excessive corrosion was noted on the left-hand and right-hand landing-gear door fillers.

The left-hand hatch required a torque of 400 inch-pounds to open, and the right-hand hatch required 300 inch-pounds.

UNCLASSIFIED

Moisture condensation was noted between the outer and center panes of the crew windows.

All of the load-carrying structure was in good condition with no apparent deformations. The only discoloration was due to local deposits of foreign matter.

There was no significant damage to the RCS and R and R sections. The forward end of the RCS section had a slight gap which allowed hot gas to scorch slightly the insulation blanket around the thermocouple wires. Two shingles on the lower side of the RCS section were cracked, and the upper centerline shingle of the R and R section was cracked. All the cracks had sharp edges with no sign of plastic flow or melting, and the insulation blankets were not scorched, indicating the damage occurred after peak temperatures were experienced. There were corroded holes through the shingles on the cylindrical portion of the R and R section. An analysis of the corrosive material in this area indicated that beryllium, salt water, and gold were present. The mating bulkheads of the R and R section and RCS section at station Z192 were slightly deformed in the area of the MDF ring, as would be expected. A small piece was missing from the phenolic ring in the area of the R and R section docking latch receptacle.

12.6.2.2 Environmental control system.- External appearance of this system was normal. The magnesium access door seal was severely corroded. There was no water in the ECS cavity.

12.6.2.3 Communications.- The external appearance of the HF transceiver, UHF transceiver, UHF recovery beacon, and the two telemetry transmitters was normal. Small amounts of corrosion were noted on the external surfaces of the coaxial connectors and electrical connectors. The HF whip antenna was received in a bent-over condition and had to be cut off to facilitate working on the vehicle. The plug at the end of the HF whip antenna appeared to be normal and had a small amount of heat discoloration on the outer surface.

The stub antenna on the forward face of the R and R section was bent at a 45° angle, and the outer insulator was split at the top end. The end plug and nose fairing ejector spring were missing. (See fig. 12-13.) A coaxial adapter, normally used for checkout, was found in the compartment forward of the left-hand landing-gear door.

12.6.2.4 Guidance and control.- The computer case was penetrated by corrosion around the elapsed time meter. Water was draining from the computer case vent hole. Corrosion pitting of the end fittings of the computer package was evident. The inertial measuring unit (IMU) electronics package, the gimbal control electronics package, and the IMU

UNCLASSIFIED

appeared to be in a normal condition. (See fig. 12-14.) Water was found in the AGE receptacle 24 of the ACME package.

12.6.2.5 Pyrotechnics.- The right-hand wire bundle guillotine on the RCS section at station Z192 had failed to cut the wire bundle. The wire bundles to the guillotine on the right-hand side at station Z192 had been broken from the potted connectors in the RCS section. Corrosion was noted between the MDF ring and the R and R closure bulkhead at station Z192. Electrical resistance checks indicated that all returned pyrotechnics had detonated.

12.6.2.6 Instrumentation and recording.- The 2 and 3 retrograde section separation sensor toggle switches on the right-hand side of the reentry assembly had not been actuated.

The pilot parachute deployed indication toggle switch in the forward part of the R and R section had not been actuated.

Two ground wires were broken at the terminal lugs on the center pedestal in the cabin. (These wires may have been broken during pallet removal at Cape Kennedy.)

12.6.2.7 Electrical.- The batteries and their terminals appeared unaffected by corrosion; however, the battery retainer straps were badly corroded. Several other terminal strips were so corroded that they may have caused a power drain after landing. Water and corroded fuse holders were noted in several of the fuse blocks. The main, squib, and special pallet batteries were drained into a dummy load. The remaining battery life is given in table 12-VIII.

The fuse block check showed that no fuses had been blown. The exterior umbilical seal was torn and burned. (See fig. 12-15.) The primary horizon sensor electrical receptacle housing had a slight burn area and corrosion.

12.6.2.8 Crew station furnishings and equipment.- The general appearance of the crew station was normal, and the only water found was in the altimeter. The check of the cabin switch positions indicated that 62 switch positions were different from those recorded by the recovery team. Some of these differences were undoubtedly caused by necessary work performed in the cabin area.

12.6.2.9 Propulsion.- The appearance of the RCS system was as expected. Two of the thrust chamber nozzles were damaged by handling, as reported by the recovery team. Some delamination cracks and erosion were noted in the nozzles. No propellants were returned from the down-range deactivation area for analysis because the tanks were empty.

UNCLASSIFIED

12.6.2.10 Landing.- The 18-foot pilot parachute was charted for damage. The only damage found was some very slight weave separation and loose stitching in localized areas. The suspension lines were undamaged. The main parachute was not recovered.

12.6.2.11 Postlanding recovery aids.- The top edge of the station Z104 ring immediately aft of the hoist loop was crushed. The recovery flashing light door and bulb were received as loose pieces. The battery life in the recovery flashing light power supply was exhausted.

12.6.3 Continuing Evaluation

The following is a list of the approved Spacecraft Test Requests (STR's) for the postflight evaluation:

<u>System</u>	<u>Purpose</u>
ECS	To verify satisfactory operation of the ECS after exposure to the mission environment.
Ejection seat	To verify the capability of the ejection seat pyrotechnics after exposure to mission environment.
Crew station	To verify satisfactory operation of the abort and attitude controllers after exposure to mission environment.
RCS	To evaluate the RCS components after use on the mission.
RCS	To analyze the RCS components after exposure to the mission environment.
Electrical	To determine the cause of the stage II fuel pressure gage malfunction which occurred at about 1 second after lift-off.
HF transceiver, antenna, and associated wiring	To investigate the HF system for possible transceiver shorting, wiring failure, and antenna shorting which may have caused low transmitter power.
IMU, Guidance and control	To investigate failure of the accelerometer and the possible failure of the platform stiffeners.

UNCLASSIFIED

UNCLASSIFIED

12-35

<u>System</u>	<u>Purpose</u>
Pyrotechnic wire bundle guillotines	To run a failure analysis on the wire bundle guillotine which failed to cut the wire bundle and to inspect the remaining three wire bundle guillotines at the Z191 separation joint between the RCS section and R and R section and to compare them with the one which failed to cut.
Telemetry	To investigate retrograde section separation switches to determine why two of the three switches did not actuate on separation.
Electrical	To determine if the main bus was shorted after touchdown as a result of water reaching the underside of the terminal blocks.
Electrical and sequential	To determine if all the pyroswitches worked since the onboard camera showed about 15-amp excursions on the ammeter while the spacecraft was on the water because these excursions appeared to be in phase with the waves.
ECS	To verify switching of the ECS to the postlanding mode.

UNCLASSIFIED

UNCLASSIFIED

TABLE 12-I.- LAUNCH-AREA ATMOSPHERIC CONDITIONS AT 9:21 a.m. e.s.t.

Altitude, ft	Temperature, °F	Pressure, lb/sq ft	Density, slugs/cu ft
0 × 10 ³	46.9	2142.0	2456.0 × 10 ⁻⁶
5	47.3	1782.4	2046.4
10	29.8	1477.2	1757.3
15	19.8	1217.8	1479.7
20	1.8	997.9	1259.8
25	-18.2	811.6	1071.2
30	-38.2	653.3	903.0
35	-54.6	520.5	709.8
40	-71.3	411.4	617.4
45	-72.9	322.9	486.6
50	-81.9	252.9	390.0
55	-85.5	196.9	306.8
60	-83.2	153.3	237.3
65	-80.0	119.7	183.7
70	-71.1	93.8	140.7
75	-67.0	73.9	109.6
80	-65.2	58.3	86.1
85	-62.3	46.2	67.5
90	-55.5	36.5	52.8
95	-44.9	29.0	40.9
100	-42.5	23.4	32.6
105	-39.4	18.6	25.8
110	-40.9	14.8	20.8
115	-38.9	11.9	16.5
120	-26.1	9.6	12.8

UNCLASSIFIED

UNCLASSIFIED

12-37

TABLE 12-II.- RECOVERY-AREA ATMOSPHERIC CONDITIONS AT 1:37 p.m. e.s.t.

Altitude, ft	Temperature, °F	Pressure, lb/sq ft	Density, slugs/cu ft
0×10^3	76.6	2119.9	2283.5×10^{-6}
5	55.6	1777.1	1999.7
10	45.3	1479.1	1704.0
15	31.6	1227.0	1454.3
20	19.7	1011.5	1231.5
25	-.8	828.5	1051.6
30	-20.7	673.6	893.9
35	-44.0	540.9	758.1
40	-64.8	429.6	633.9
45	-81.0	337.7	519.8
50	-96.7	262.5	421.6
55	-106.6	202.0	333.5
60	-111.6	154.8	259.2
65	-91.8	119.3	189.0
70	-77.4	92.9	141.6
75	-68.8	72.9	108.9
80	-61.8	57.6	84.4
85	-58.9	45.7	66.4
90	-53.5	36.1	52.0
95	-48.6	28.8	40.9
100	-23.8	23.0	32.2
105	-36.9	18.4	25.4
110	-37.7	14.8	20.4

UNCLASSIFIED

TABLE 12-III. - SUPPLEMENTAL REPORTS

Number	Report title	Responsible organization	Completion date	Text reference section and/or remarks
1	GLV Engineering Evaluation Report (GT-2)	SSD and contractor (Aerospace)	Apr. 19, 1965	Section 5.2 Standing requirement
2	Burroughs Supplemental Data Report, GT-2	SSD and contractor (Burroughs)	Mar. 5, 1965	Section 5.2.5 Standing requirement
3	GE Supplemental Report, GT-2	SSD and contractor (GE)	Mar. 5, 1965	Section 5.2.5 Standing requirement
4	Launch Vehicle No. 2 Flight Evaluation	SSD and contractor (Martin)	Mar. 5, 1965	Section 5.2 Standing requirement
5	Manned Space Flight Network Performance for the Second Gemini Mission	Goddard Space Flight Center	Feb. 17, 1965	Section 6.3 Standing requirement
6	GT-2 Spacecraft Inertial Guidance System Evaluation	Space Technology Laboratory	Mar. 5, 1965	Section 5.1.6 Standing requirement
7	Aerothermodynamic Evaluation of Spacecraft 2	NASA-MSC (E and D)	Mar. 19, 1965	Section 5.1.1.2.2
8	Failure Analysis of the RCS to R and R Section Guillotine	Spacecraft contractor (MAC)	Mar. 5, 1965	Section 5.1.10
9	Failure Analysis of Retrograde Section Separation Sensor	Spacecraft contractor (MAC)	Mar. 5, 1965	Sections 10.0 and 12.6
10	Evaluation of Reactant Supply System Pressure Drop at Separation	Spacecraft contractor (MAC)	Mar. 5, 1965	Section 5.1.8.3
11	Spacecraft Inertial Platform Evaluation	Spacecraft contractor (Minneapolis Honeywell)	Mar. 5, 1965	Section 5.1.6
12	Hydraulic Pump Anomaly of GT-2 Flight	SSD and contractor (Martin)	Mar. 5, 1965	Section 5.2.4.1

UNCLASSIFIED

UNCLASSIFIED

UNCLASSIFIED

12-39

TABLE 12-IV.- STILL AND MOTION PICTURE CAMERA COVERAGE

	Still photographs, number	Motion-picture film, footage
Launch	5	8500
Recovery		4000
Swimmer deployment	19	
Underwater spacecraft flotation	6	
R and R inspection on aircraft carrier	3	
Spacecraft retrieval onboard carrier	24	
Flotation ring inspection	5	
Aircraft carrier inspection		293
General postflight inspection	18	
Hatch inspection	13	
RCS inspection	8	
Interior of spacecraft	6	
Roosevelt Roads		2000
Unloading	49	
Loading onto truck	12	
RCS deactivation	46	
Loading onto aircraft for Cape Kennedy	11	
Cape Kennedy postflight inspection		
Transportation to inspection area	10	
General preliminary inspection	7	
R and R can preliminary inspection	6	
Interior views of heat shield removal	10	
Heat-shield inspection	28	
Outer skin	38	
Other damaged areas	14	
RCS inspection	10	
Interior inspection	14	
R and R inspection	6	
ECS compartment	8	
Miscellaneous	5	
Onboard spacecraft		
Instrument panel	3	1200
Window	11	120

UNCLASSIFIED

TABLE 12-V.- ENGINEERING SEQUENTIAL CAMERA DATA

Operations Requirements Document - 3600		Sequential film coverage item (a)	Camera					Comments
Page	Item		Type	Lens	Speed, frames/sec	Location (b)	Presentation	
71	1	1.2-30 1.2-31 1.2-32	Tracking	40 in.	96	Cape Kennedy	Spacecraft centered in frame from lift-off to loss of vehicle. Maintained constant surveillance of spacecraft for possible track in event of abort.	
71	2	1.2-27 1.2-28	Fixed	40mm	400	Launch Complex 19	Spacecraft upper and lower umbilical plugs showing disconnect.	
71	3	1.2-12 1.2-13	Fixed	100mm	200	Launch Complex 19	Spacecraft centered in bottom of frame to evaluate spacecraft during launch sequence.	
72	1	1.2-7 1.2-8	Fixed	15mm	24	Launch Complex 19	Fuel-storage tanks to show possible leakage or spillage in the area.	Not required.
72	4	1.2-30 1.2-32	Tracking	40 in.	96	Cape Kennedy	Spacecraft centered in frame from lift-off to loss of vehicle. Maintained constant surveillance of spacecraft for possible track in event of abort.	Item 1.2-30: appeared grainy. Item 1.2-32: appeared slightly out of focus.
73	2	1.2-4 1.2-5 1.2-6	Fixed	25mm	24	Launch Complex 19	General surveillance of space vehicle, launcher and launcher stand.	Item 1.2-4: no coverage; short run due to film breakage
73	3	1.2-1 1.2-2 1.2-3	Fixed	25mm	24	Launch Complex 19	Space vehicle, launcher, and launcher stand centered in frame. Cameras remotely operated by Test Conductor in case of an emergency.	Not required.
74	4	1.2-20 1.2-21 1.2-22 1.2-23 1.2-24	Fixed	10mm	400	Launch Complex 19	3D1E and 3D2E umbilical plugs to show disconnect. 2DFVT umbilical plug to show disconnect. 1DOVT umbilical plug to show disconnect. 3B1E and associated umbilical plugs to show disconnect. 3B1E and associated umbilical plugs to show disconnect.	Slight camera movement. No coverage due to film breakage in camera. No coverage due to film breakage in camera.
74	4	1.2-25	Fixed	10mm	400	Launch Complex 19	Cable cutters to show cable cutters action.	
74	5	1.2-26 1.2-29	Fixed	10mm 152mm	400 400	Launch Complex 19	End of umbilical boom 3 to observe J-Bars and lanyards during launch. Umbilical booms 3 and 4 to show umbilical and lanyard action following umbilical release.	No coverage due to film breakage in camera. Slight camera movement.

^aData listed by item number in Operations Directive 3600.

^bSee figures 12-8 and 12-9.

UNCLASSIFIED

12-40

UNCLASSIFIED

TABLE 12-V. - ENGINEERING SEQUENTIAL CAMERA DATA - Concluded

Operations Requirements Document - 3600		Sequential film coverage item (a)	Camera					Comments
Page	Item		Type	Lens	Speed, frames/sec	Location (b)	Presentation	
75	6	1.2-14 1.2-15	Fixed	15mm 152mm	400 400	Launch Complex 19	Lower portion of space vehicle and "A" frames to observe explosive bolt action and space vehicle first motion.	Item 1.2-18: no coverage, camera jammed. Items 1.2-9 and 1.2-10: no coverage due to film breakage in camera. Item 1.2-11: timing bleeding into picture. Did not have smooth tracking.
75	7	1.2-18 1.2-19	Fixed	10mm	400	Launch Complex 19	Engine bells to be centered laterally to show the thrust chamber.	
75	8	1.2-16	Fixed	10mm	400	Launch Complex 19	Engine area to show possible leakage or spillage. Launcher lights used for illumination of the area.	
76	9	1.2-9 1.2-10 1.2-11	Fixed	25mm	400		Space vehicle centered in frame to show movement and vibration at launch.	
76	10	1.2-33	Tracking	20 in.	64	Cape Kennedy	Track from lift-off to loss of vehicle with space vehicle centered in frame throughout track.	
		1.2-34	Tracking	40 in.	64	Cape Kennedy	Track from lift-off to loss of vehicle with space vehicle centered in frame throughout track; if any components fall from the vehicle during powered flight, track the falling debris.	
		1.2-35 1.2-36	Tracking Tracking	120 in. 80 in.	64	Cape Kennedy	Track from first acquisition to loss of vehicle; engine section centered until I/F ratio allows full space vehicle to be centered.	
77	11	1.2-37	Tracking (IGOR)	180 in.	30	False Cape	Track from first acquisition to loss of vehicle. Engine section centered in frame until I/F ratio allows full space vehicle to be centered to show staging if event is recordable.	
		1.2-38	Tracking (ROTI)	400 in.	30	Cocoa Beach		
		1.2-39	Tracking (IGOR)	360 in.	32	Patrick Air Force Base		
		1.2-40	Tracking (ROTI)	500 in.	20	Melbourne Beach		
		1.2-41	Tracking (ROTI)	500 in.	32	Vero Beach		
89.2	5		Tracking (Airborne)			Cape Kennedy Area	Airborne photographic coverage of the launch sequence from specially configured aircraft.	
133	3	1.2-42	Tracking (IGOR)	50mm	30	Patrick Air Force Base	Track first acquisition to loss of vehicle. Photograph BX-7 video monitor.	

^aData listed by item number in Operations Directive 3600.

^bSee figures 12-8 and 12-9.

UNCLASSIFIED

UNCLASSIFIED

12-41

UNCLASSIFIED

TABLE 12-VI. - INSTRUMENTS FOR WHICH PANEL FILM WAS TABULATED

Left instrument panel
Flight director and altitude indicator Incremental velocity indicator (IVI) Stage I oxidizer and fuel pressure Stage II oxidizer and fuel pressure Event timer (no tabulation - reference only)
Center instrument panel
Cabin temperature Cabin pressure Right secondary O ₂ pressure ECS Cryo O ₂ quantity and pressure Fuel cell O ₂ quantity and pressure Fuel cell H ₂ quantity and pressure Propellant temperature and pressure
Right instrument panel
Flight director and altitude indicator dc voltmeter Bus 1 and bus 2 ammeter

UNCLASSIFIED

TABLE 12-VII. - CAMERAS USED DURING RECOVERY OPERATIONS

Camera positions	Type of camera	Frame rate, frames/sec	Size	Type film	Comments
Fixed	Milliken	24 - 36° shutter	16	Color	Camera overheated
Fixed	Milliken	24 - 36° shutter	16	Black and white	
Fixed	Milliken	24 - 36° shutter	16	Color	
Fixed	Milliken	24 - 36° shutter	16	Black and white	Covered R and R section retrieval
Fixed	Milliken	24 - 36° shutter	16	Color	Covered R and R section retrieval
Fixed	Arriflex	24	16	Color	Covered entire elevator
Portable	Milliken	48 - 72° shutter	16	Color	Covered entire collar installation
Portable	Speed Graphic Mamiyaflex		4x5	Color negatives	
Portable	Arriflex	32	16	Color ECO	Helicopter 3 - image small
Portable	Arriflex	24	16	Color ECO	
Portable	Mamiyaflex		$2\frac{1}{4} \times 2\frac{1}{4}$	Color negatives	
Portable	Bell and Howell	24	16	Color ECO	Film too blue
Portable	Speed Graphic		4x5	Color negatives	
Portable	Speed Graphic		4x5	Color negatives	Shot closeup technical stills
Portable	Bell and Howell	24	16	Color ECO	
Portable	Bell and Howell	24	16	Color ECO	

UNCLASSIFIED

UNCLASSIFIED

UNCLASSIFIED

TABLE 12-VIII.- SPACECRAFT BATTERY LIFE

Number	Estimated battery life prior to launch, A-hr	Battery life remaining after the flight, A-hr	Estimated battery life expended during flight, A-hr
Main battery			
1	45.0	35.0	10.0
2	45.0	45.0	0.0
3	45.0	35.0	10.0
4	45.0	35.0	10.0
Special pallet battery			
1	45.0	35.0	10.0
2	45.0	37.5	7.5
3	45.0	42.5	2.5
4	45.0	35.0	10.0
Squib battery			
1	15.0	12.0	3.0
2	15.0	12.0	3.0
3	15.0	12.0	3.0

UNCLASSIFIED

UNCLASSIFIED

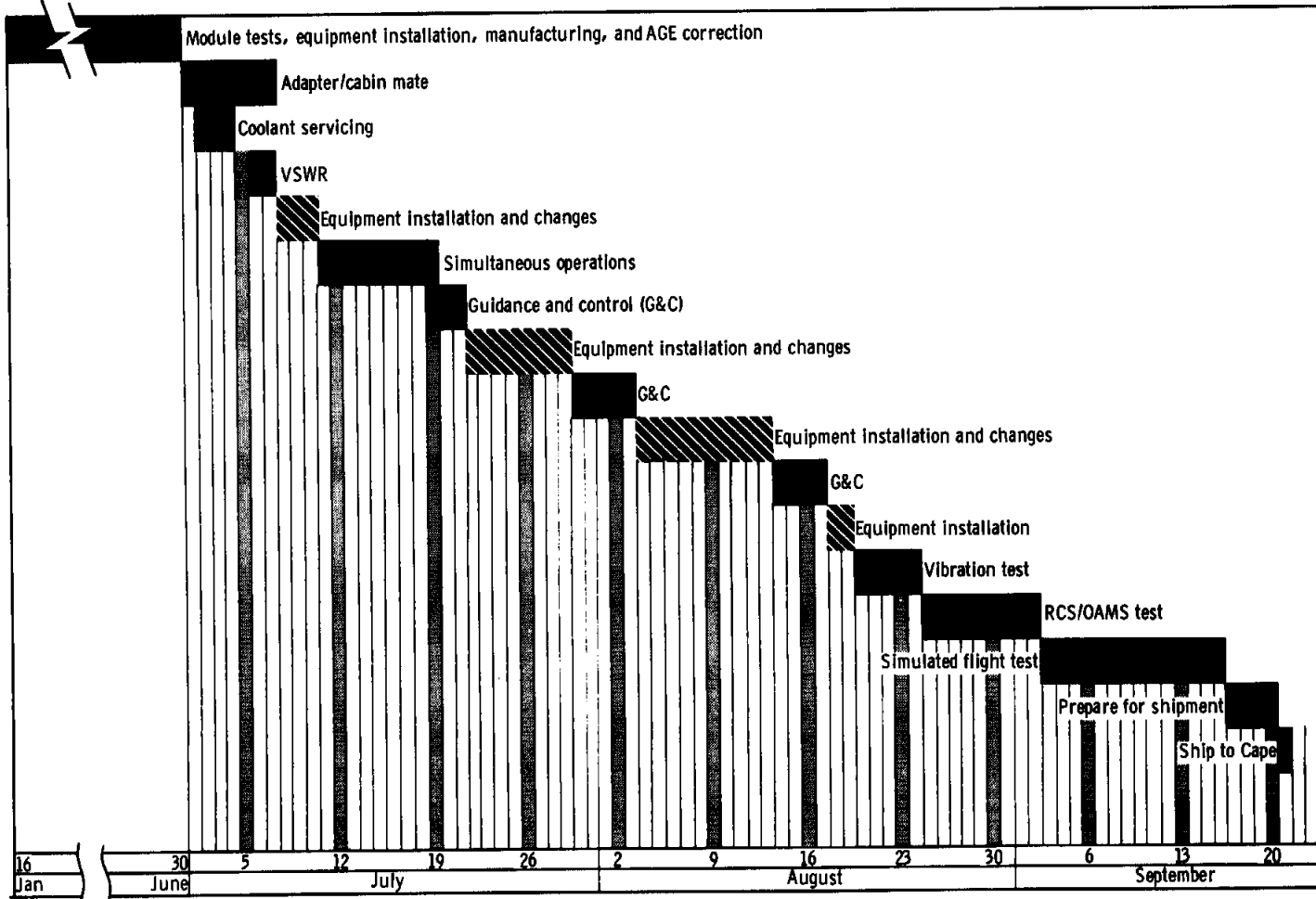


Figure 12-1. -Spacecraft 2 test history at contractor facility

UNCLASSIFIED

UNCLASSIFIED

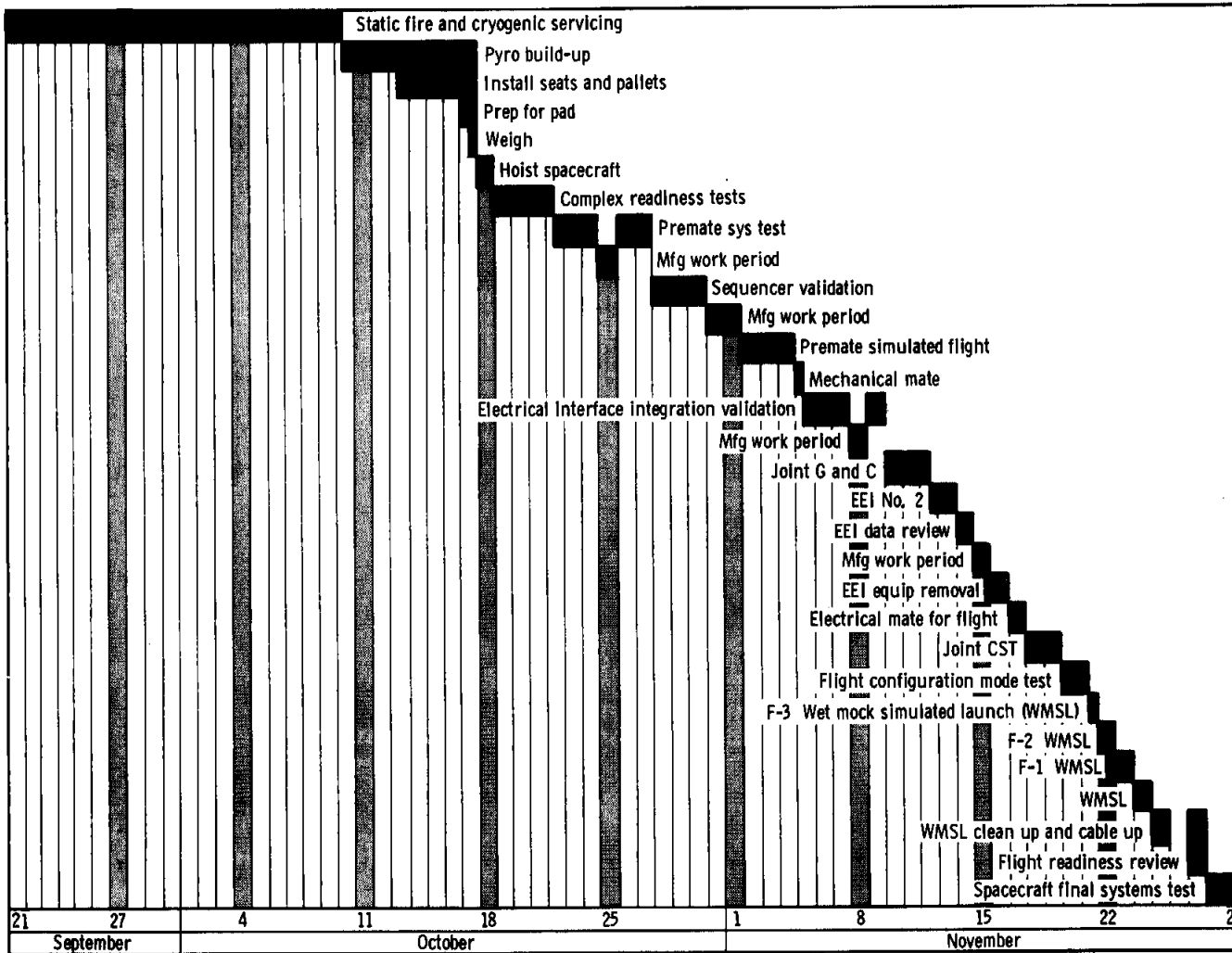


Figure 12-2. - Spacecraft 2 test history at Cape Kennedy

UNCLASSIFIED

UNCLASSIFIED

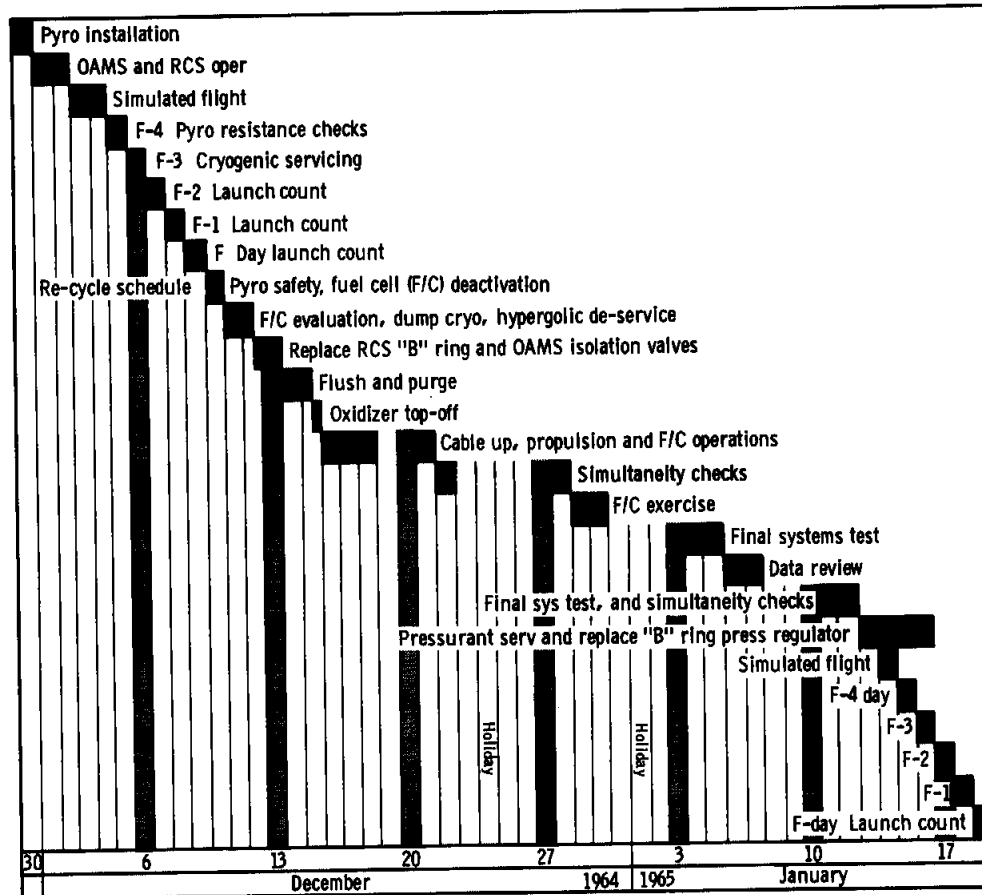


Figure 12-2. - Concluded

UNCLASSIFIED

UNCLASSIFIED

UNCLASSIFIED

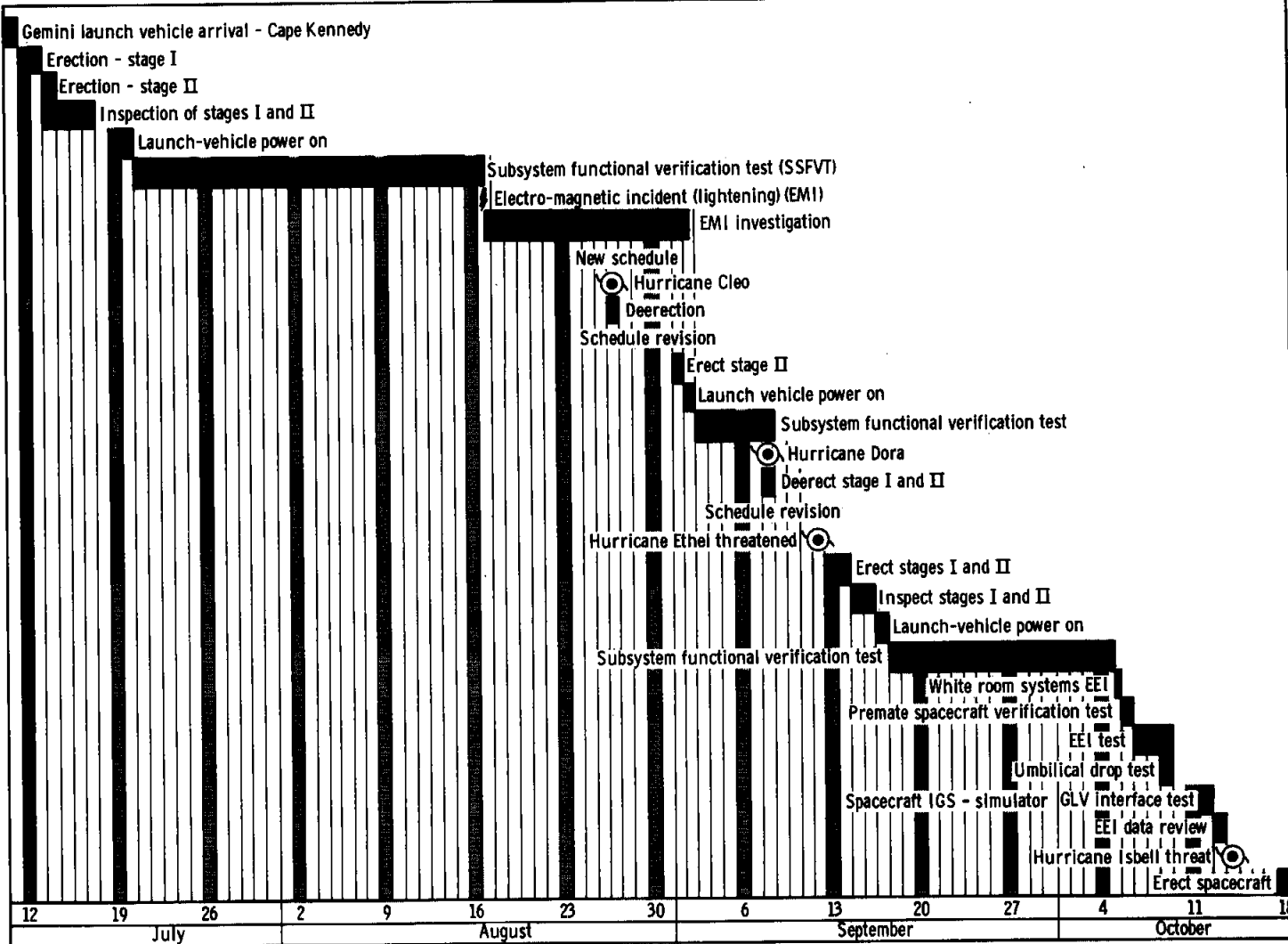


Figure 12-3. - GLV-2 test history at Cape Kennedy

UNCLASSIFIED

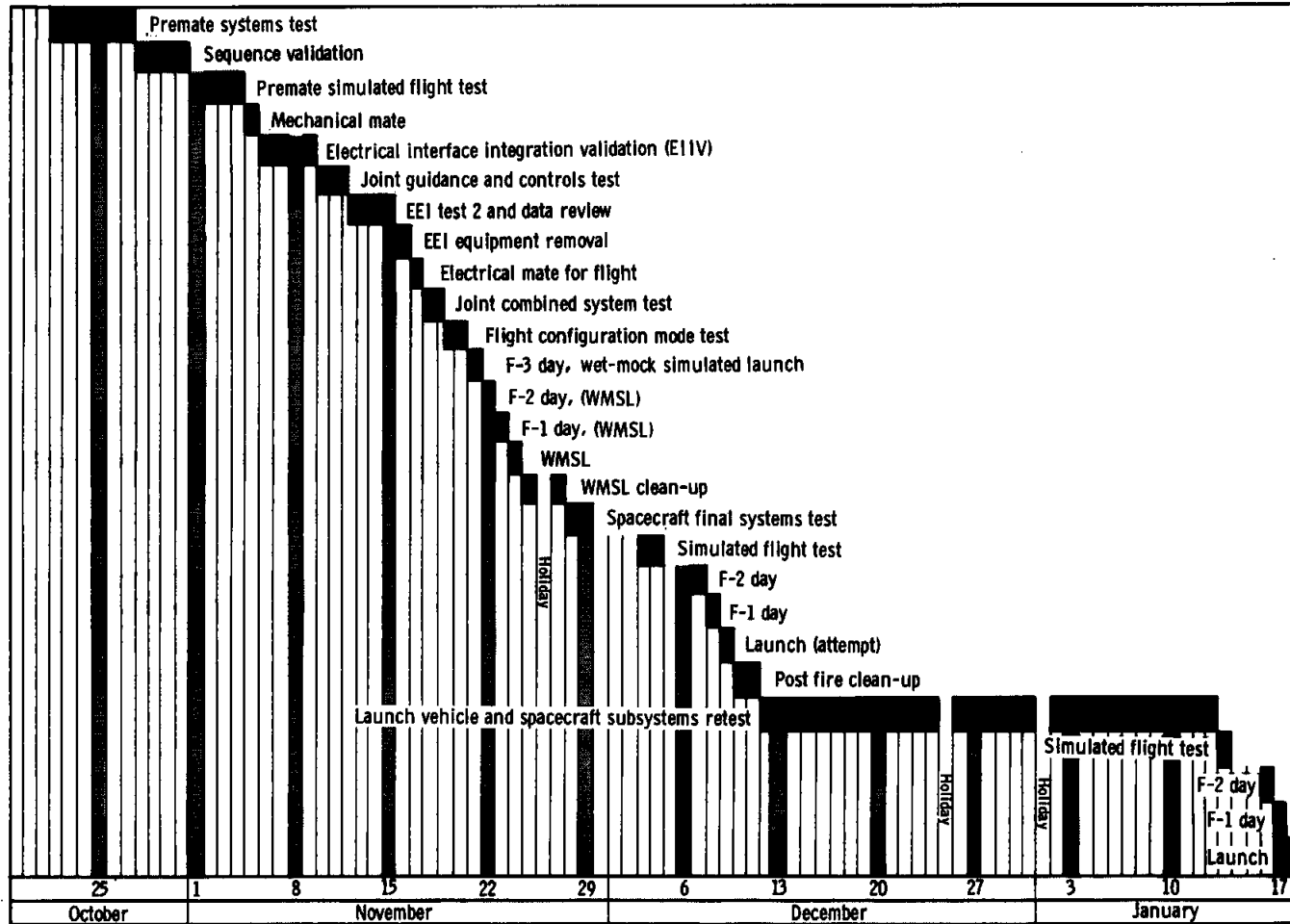


Figure 12-3. - Concluded

UNCLASSIFIED

UNCLASSIFIED

NASA-S-65-1517

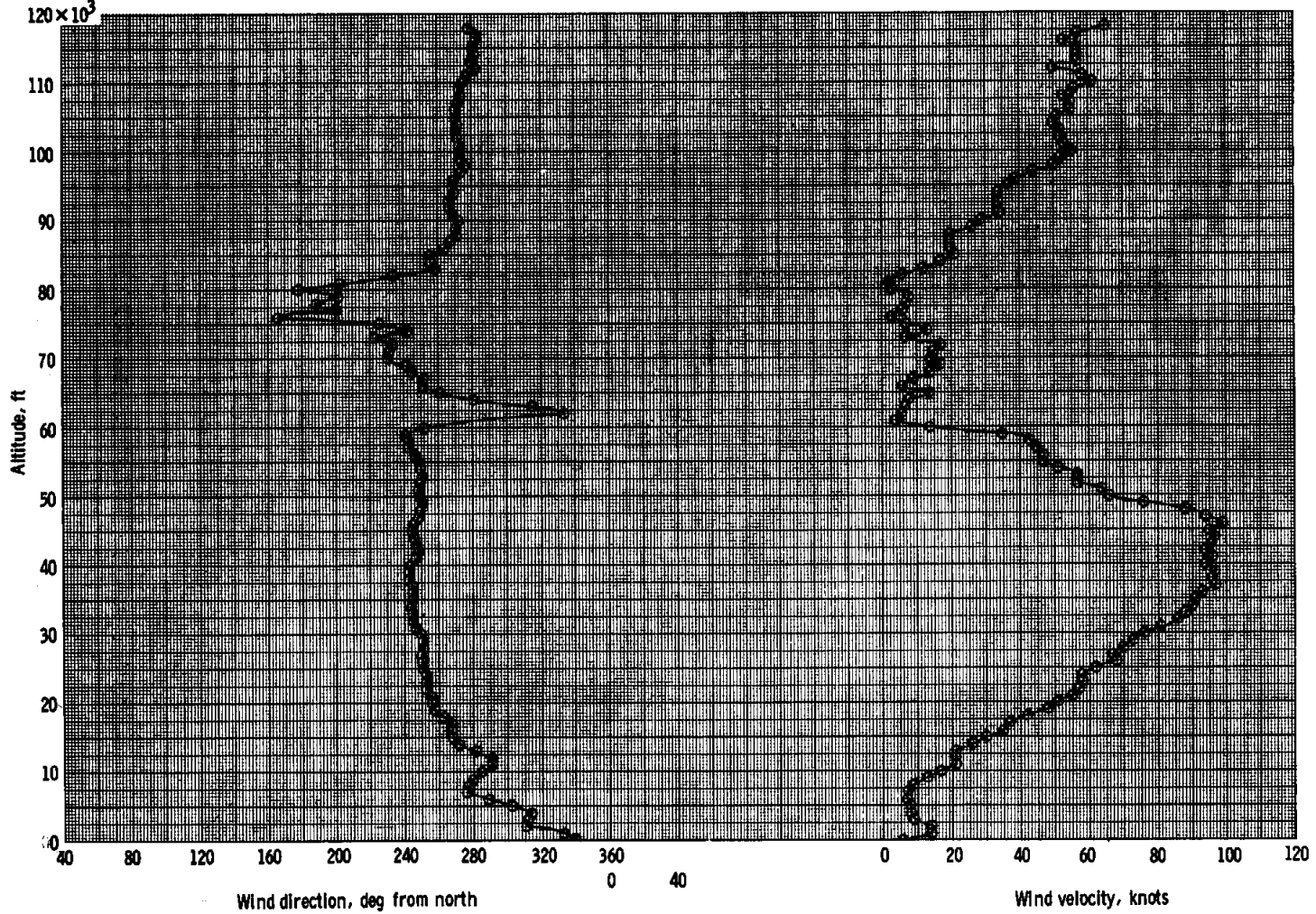
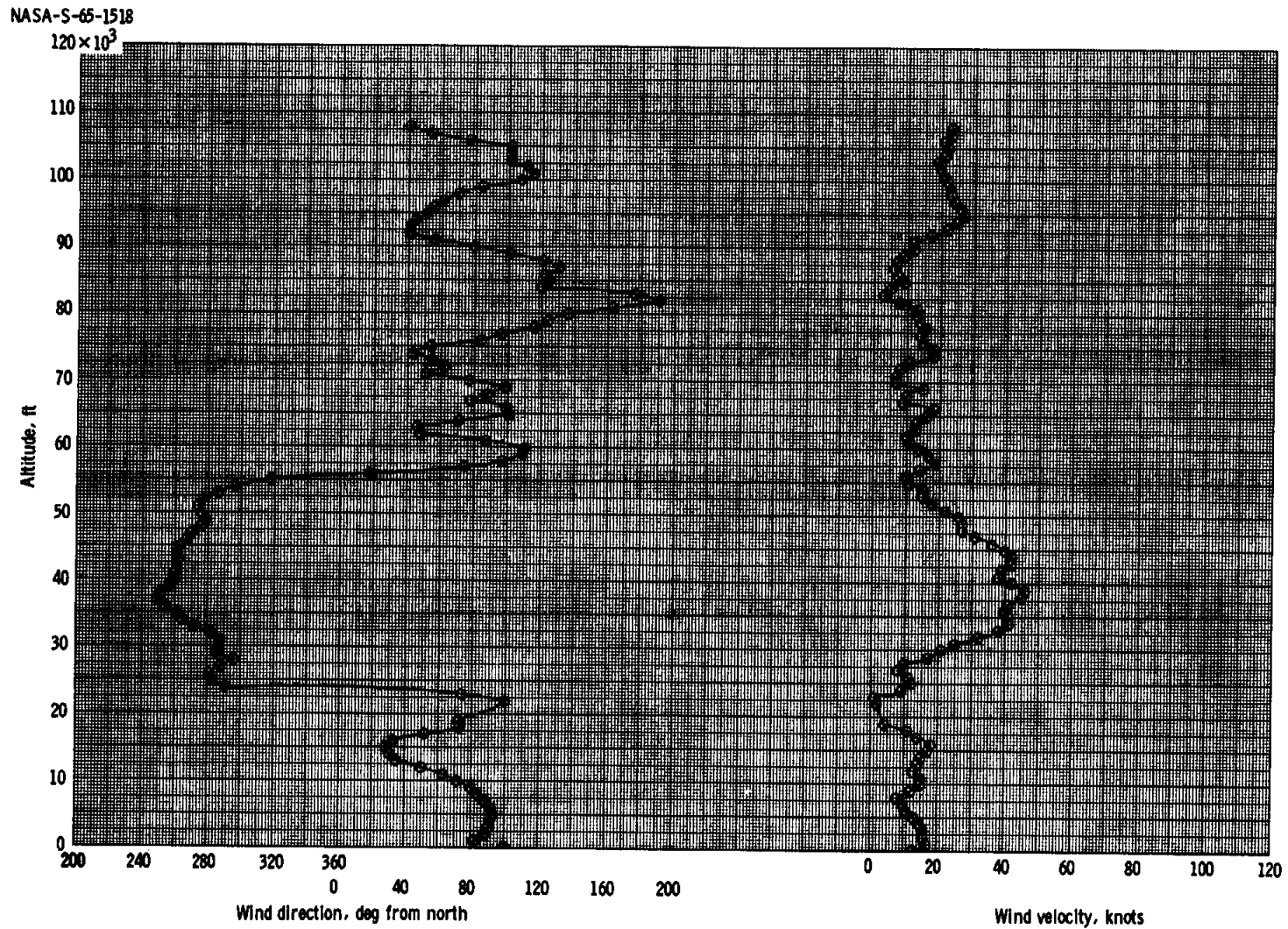


Figure 12-4. -Variation of wind direction and velocity with altitude for launch area.

12-50

UNCLASSIFIED

UNCLASSIFIED



UNCLASSIFIED

Figure 12-5. - Variation of wind direction and velocity with altitude for recovery area.

UNCLASSIFIED

UNCLASSIFIED

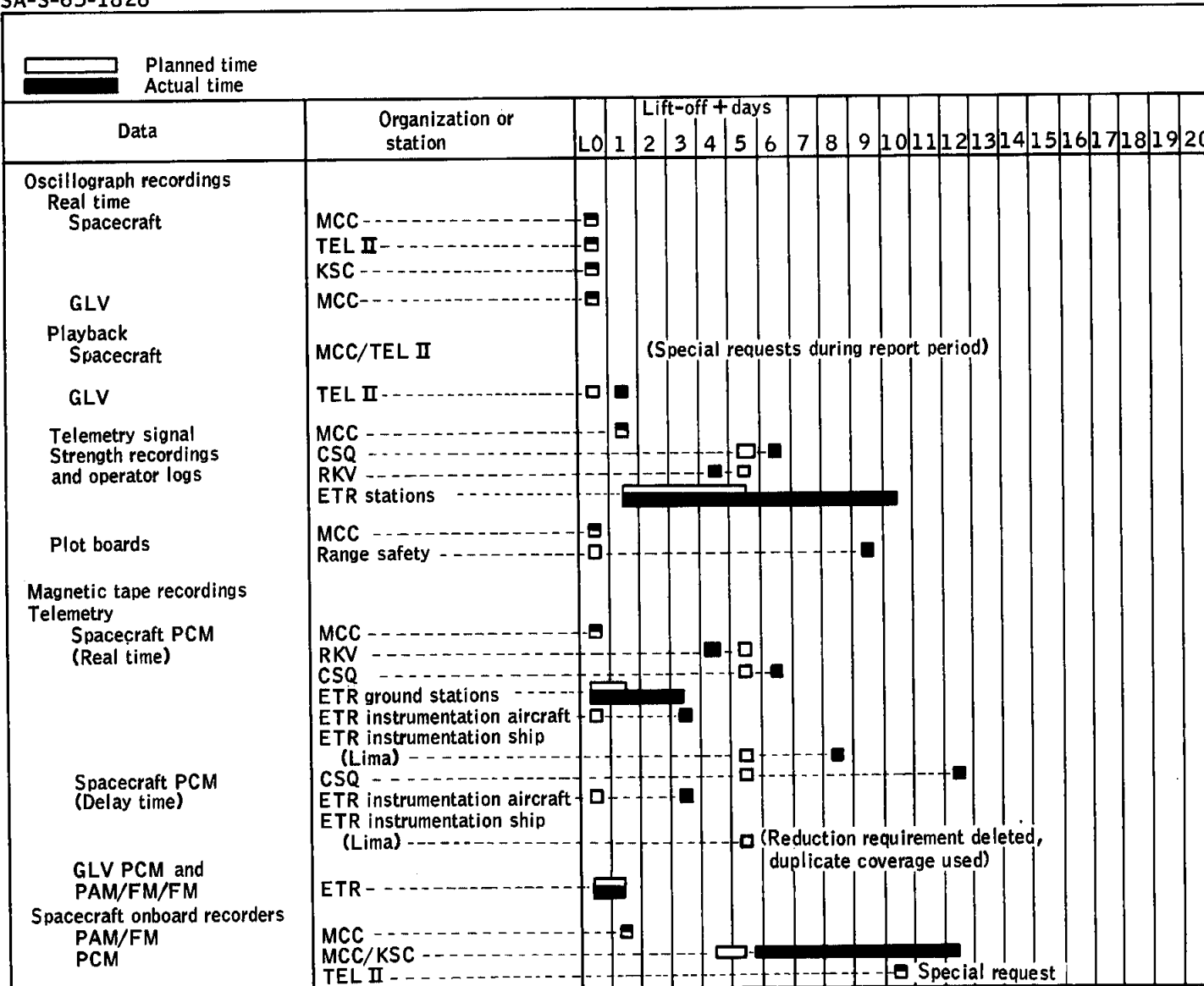


Figure 12-6. - Data availability

■ Special request

NASA-S-65-1802

Planned time
Actual time

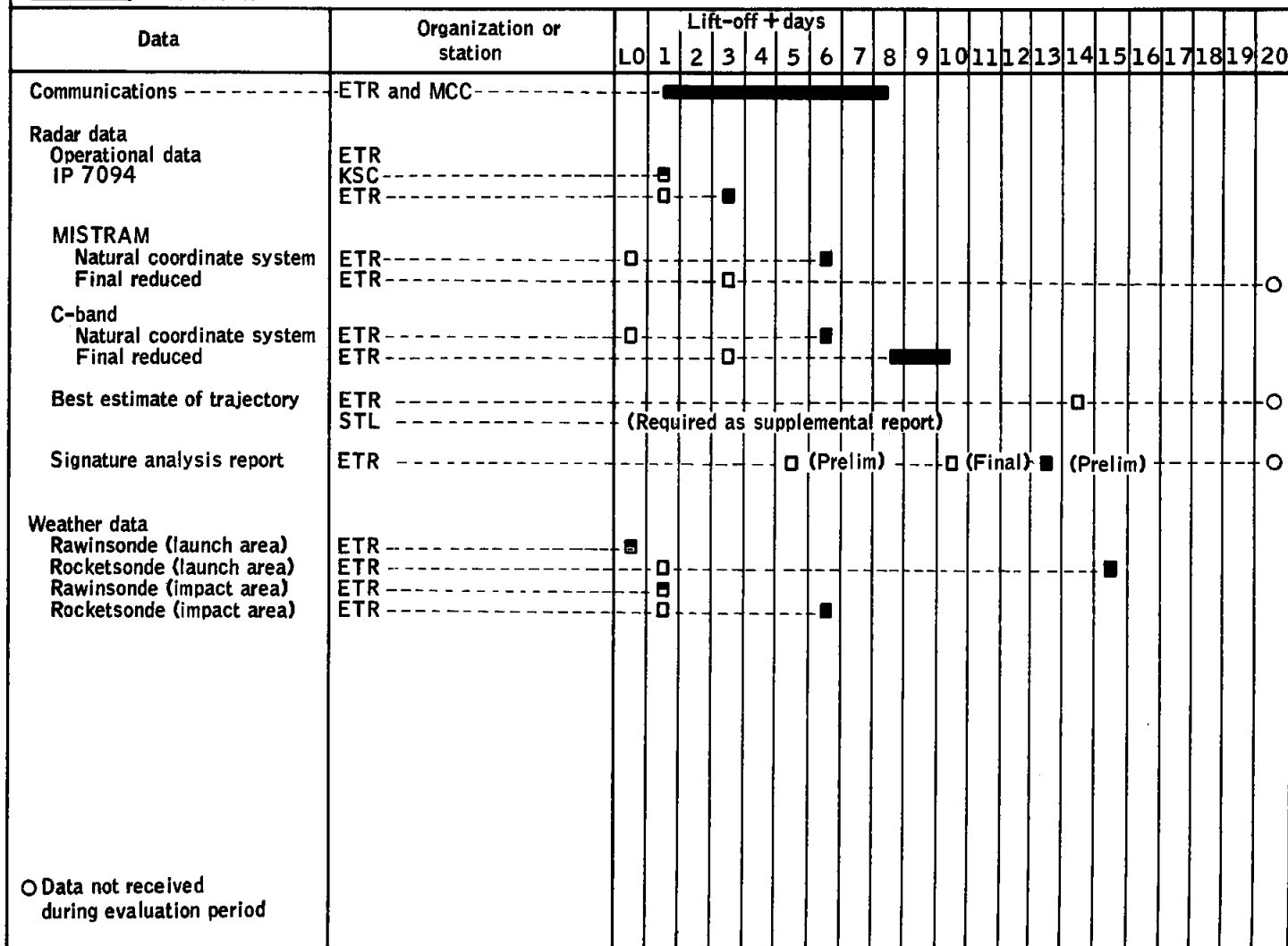


Figure 12-6. - Data availability (cont)

UNCLASSIFIED

UNCLASSIFIED

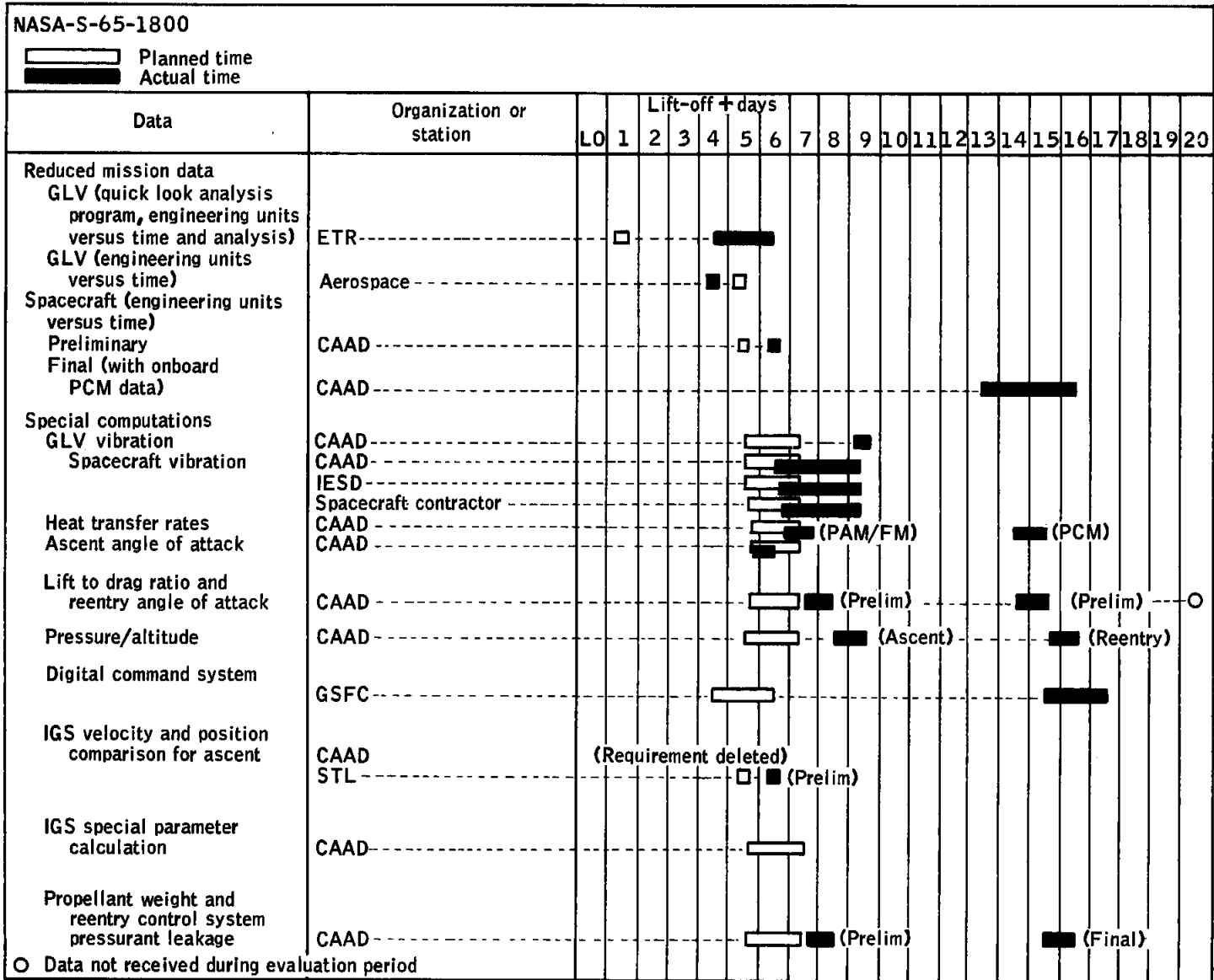


Figure 12-6. - Data availability (cont)

UNCLASSIFIED

UNCLASSIFIED

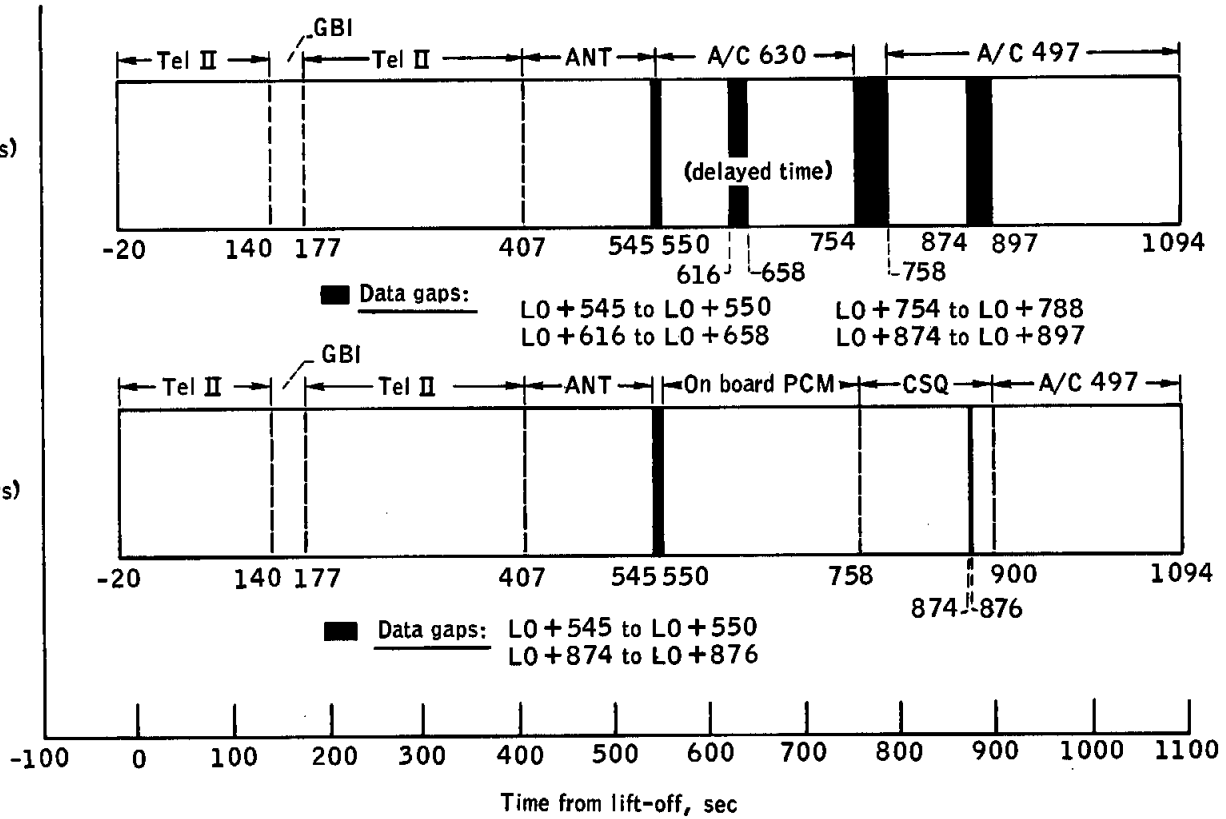


Figure 12-7. - Data selection for composite spacecraft instrumentation coverage

NASA-S-65-1601

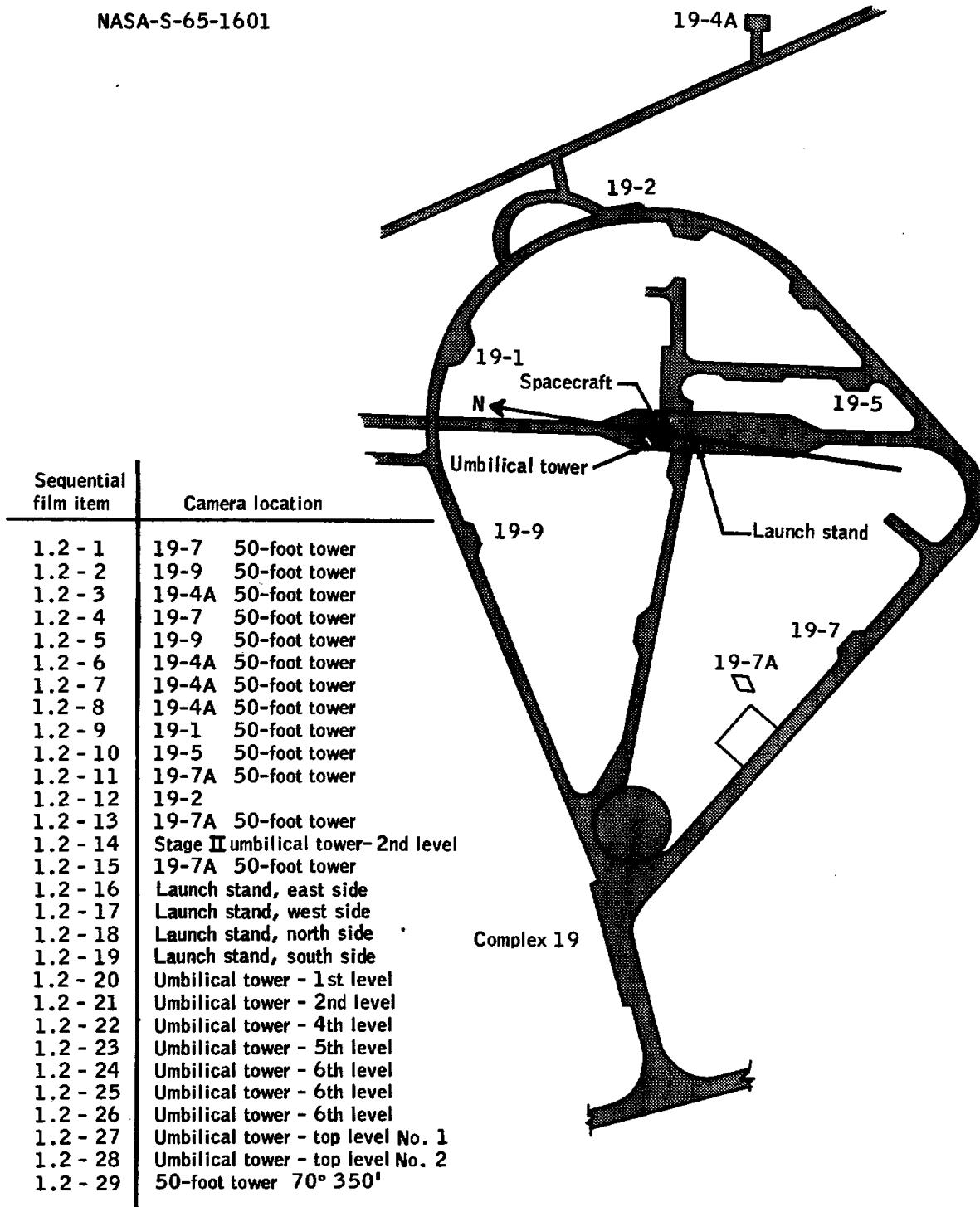


Figure 12-8. - Engineering sequential fixed camera locations

NASA-S-65-1604

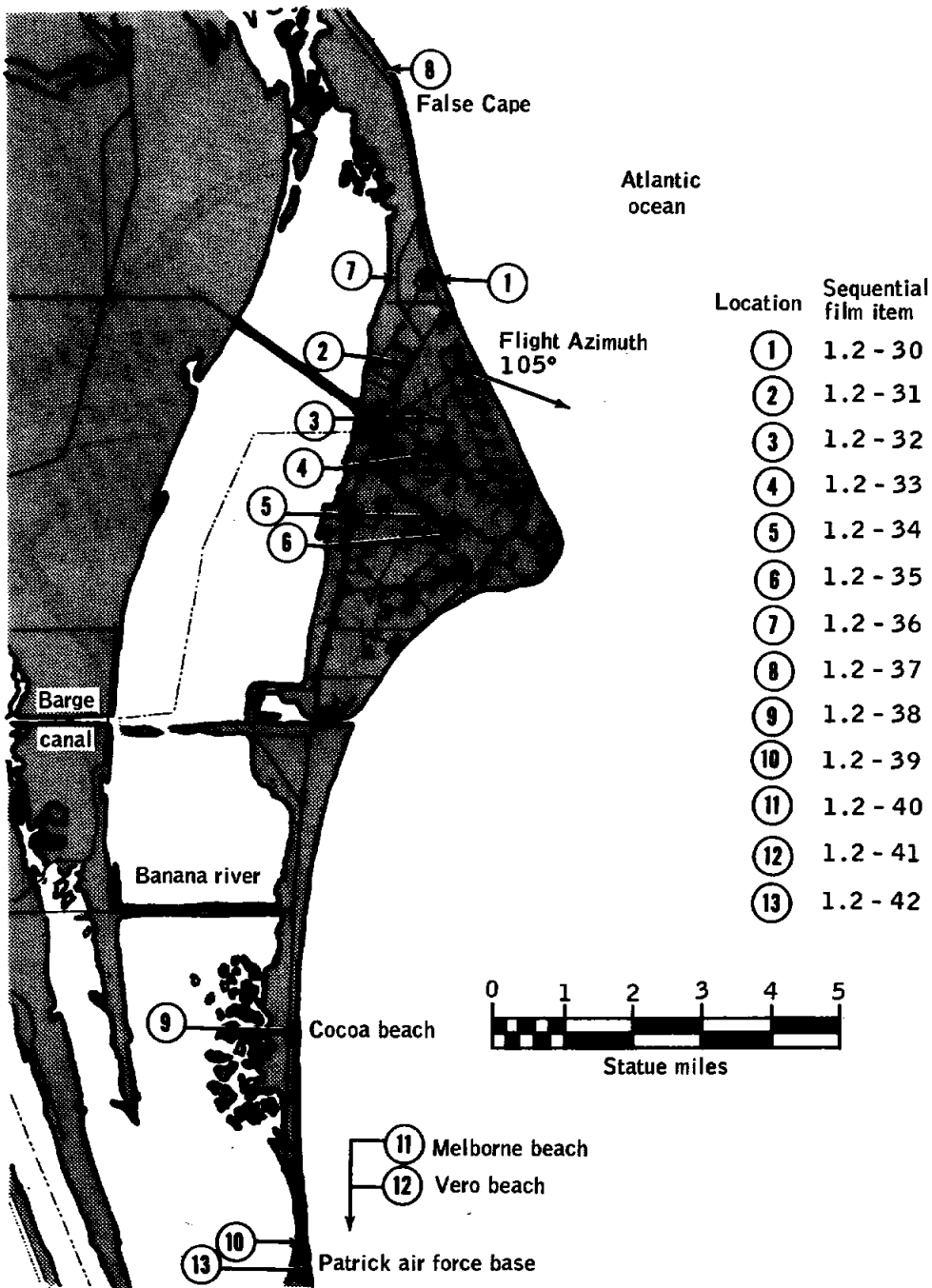


Figure 12-9. - Engineering sequential tracking camera locations

UNCLASSIFIED

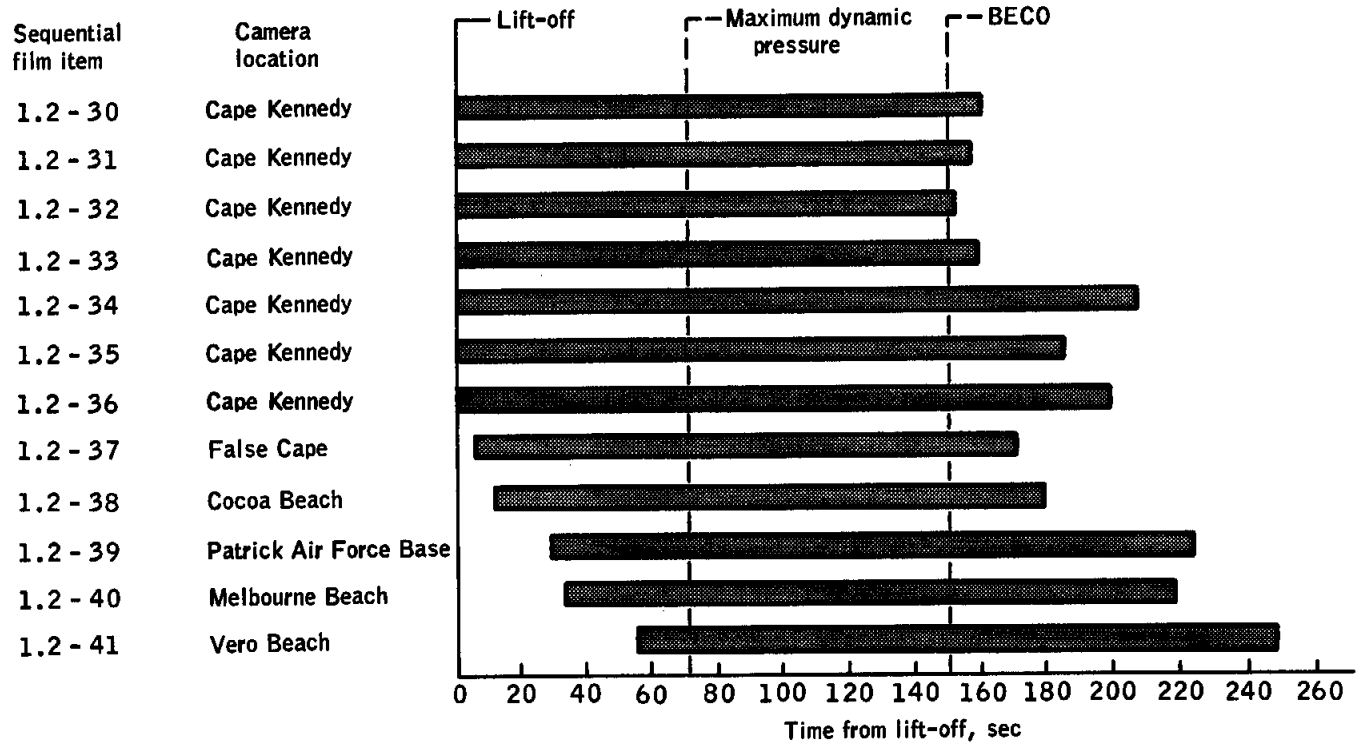


Figure 12-10. - Engineering sequential tracking camera coverage

UNCLASSIFIED

UNCLASSIFIED

NASA-S-65-1746

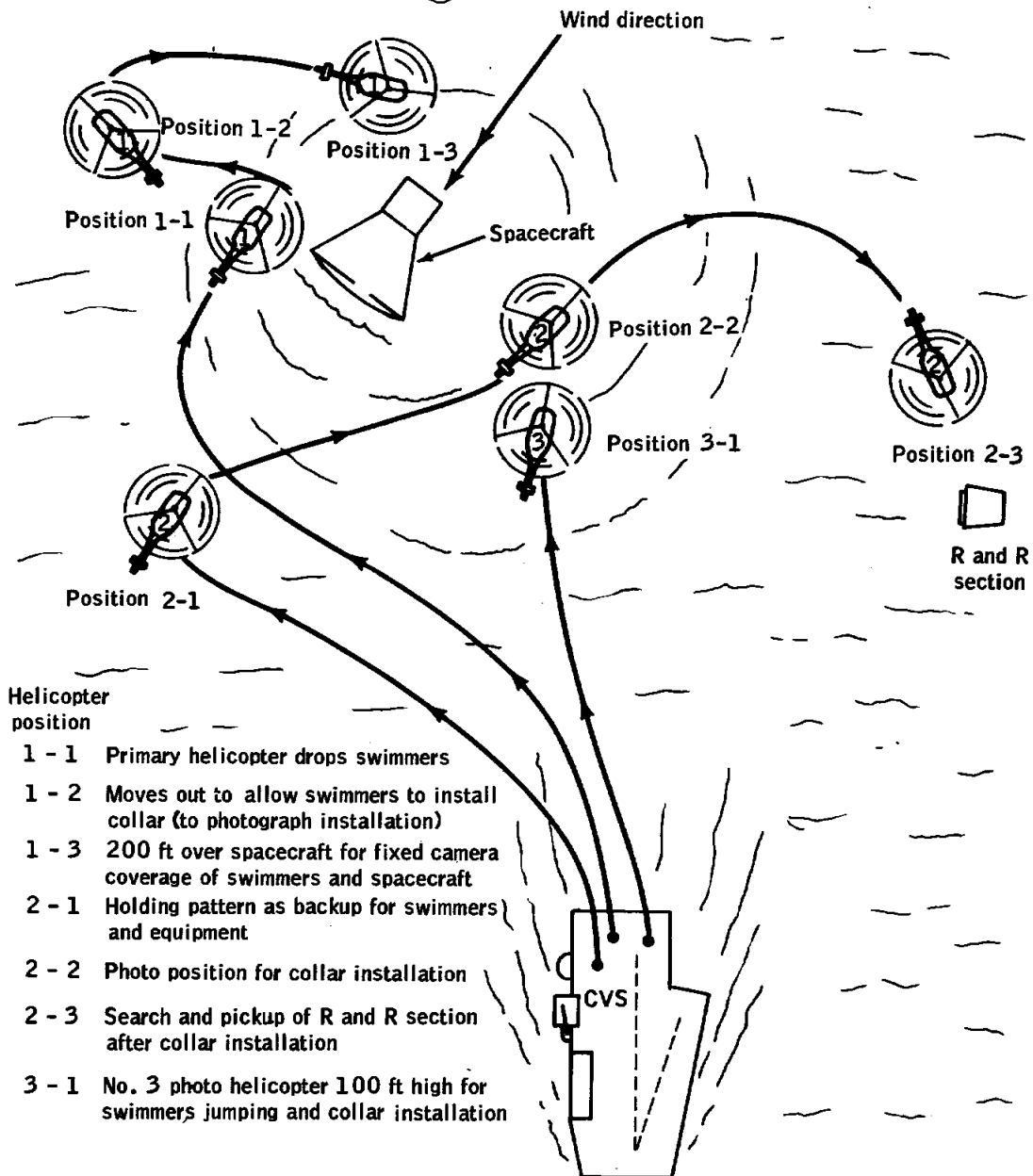


Figure 12-11. - Helicopter camera coverage

UNCLASSIFIED

NASA-S-65-1927



UNCLASSIFIED

UNCLASSIFIED

Figure 12-12. - Holes in shingles of reentry assembly

UNCLASSIFIED



UNCLASSIFIED

Figure 12-12. - Concluded

UNCLASSIFIED

12-63

NASA-S-65-1914



Figure 12-13. - R and R section and bent stub antenna

UNCLASSIFIED

UNCLASSIFIED

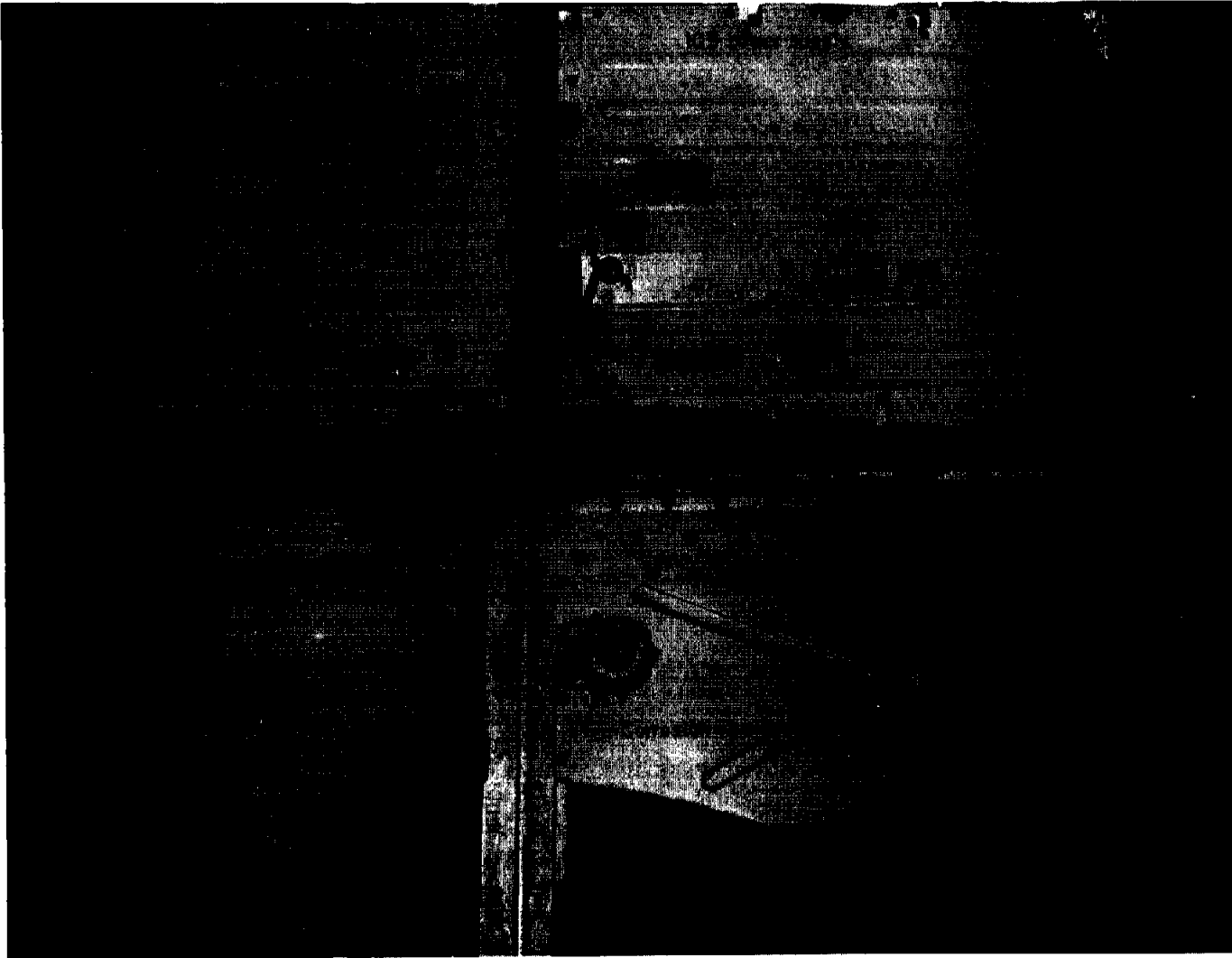
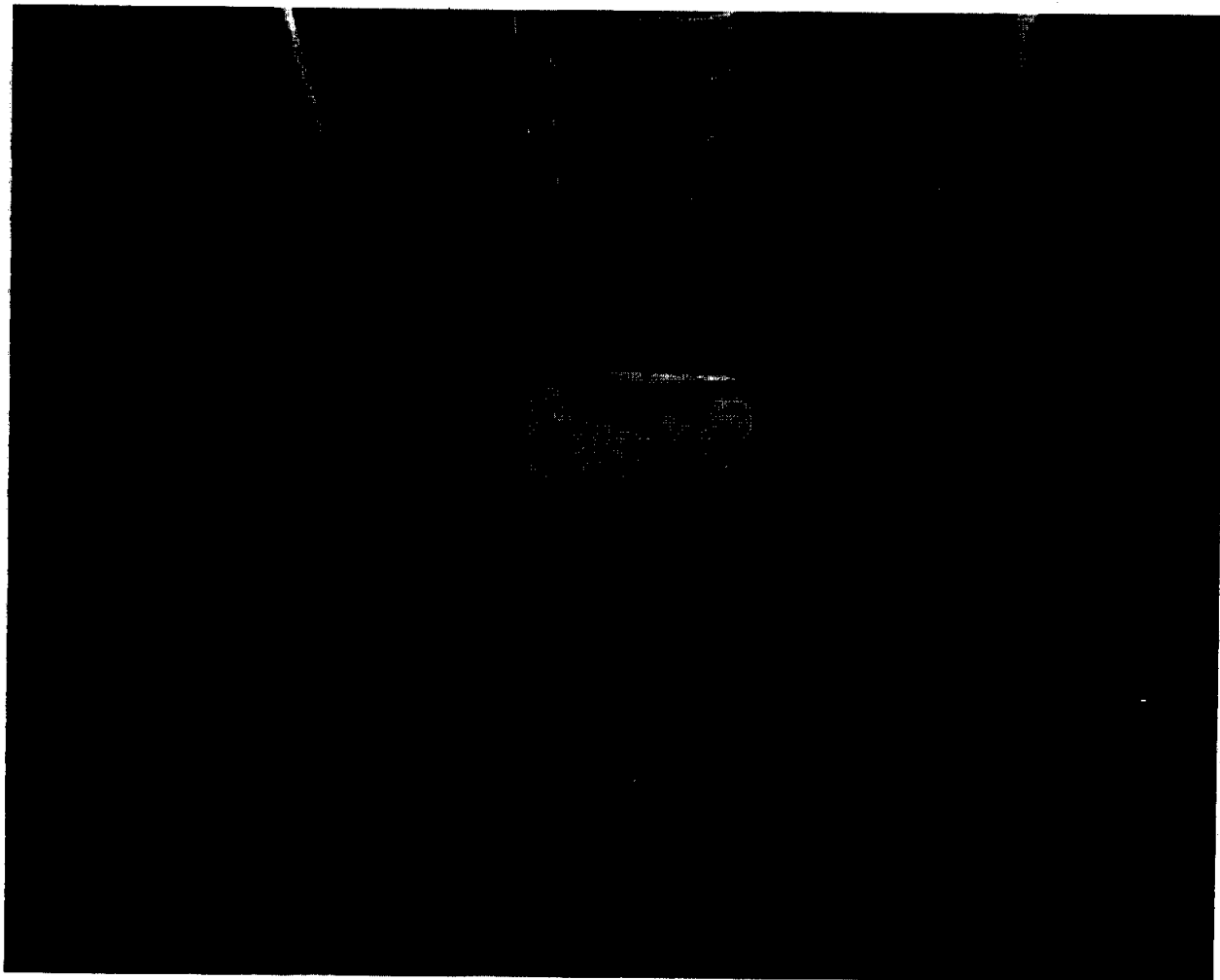


Figure 12-14. - Inertial guidance system components after flight

UNCLASSIFIED

NASA-S-65-1933



UNCLASSIFIED

UNCLASSIFIED

Figure 12 -15. - Damaged umbilical seal

12-65

12-66

UNCLASSIFIED

THIS PAGE LEFT BLANK INTENTIONALLY

UNCLASSIFIED

UNCLASSIFIED

13-1

13.0 APPENDIX B - GT-2 LAUNCH ATTEMPT

13.1 SUMMARY

The attempt to launch the second Gemini-Titan vehicle (GT-2) from Complex 19, Cape Kennedy, on December 9, 1964, was terminated 1.02 seconds after T-0 by the master operations control set (MOCS). Shutdown was initiated by the malfunction detection system (MDS) monitor when a switchover from the primary to the secondary control system occurred as a result of a failure of the primary servovalve in the yaw-roll actuator 2₁.

Other pertinent events concerning the GT-2 launch attempt were as follows: the attempt to actuate the fuel cell was unsuccessful and the fuel cell was deactivated for launch. An unexplainable loss of OAMS fuel occurred sometime before or after the launch attempt. The start of the final count was delayed for 2 hours due to difficulties encountered in loading the launch-vehicle propellants.

13.2 GLV PERFORMANCE

Except for the hydraulic anomaly resulting in switchover and shutdown, all GLV systems performed in a normal manner. The MDS correctly sensed the drop in primary pressure and effected a switchover to the secondary flight control system. Since the switchover was made during the 3.2-second holddown period and switchover during this time period is instrumented as a shutdown command, the master operation control set (MOCS) effected a shutdown 1.02 seconds after start command.

13.2.1 Hydraulic System Operation

The prelaunch operations on the hydraulic system were accomplished in a normal manner. At T-3 minutes, the stage I secondary system was pressurized using the stage I electric-motor-driven pump to verify proper operation. At T-2 minutes, the secondary system was dropped off the electric-motor-driven pump supply, and the primary system was pressurized with this pump. At T-0 the ignition command (87FS1) was sent, and the electric-motor-driven pump was shut off. Engine ignition followed 0.8 second later, and almost simultaneously a failure occurred in the primary hydraulic system, causing loss of system pressure.

UNCLASSIFIED

UNCLASSIFIED

Table 13-I lists a chronology of events during the period from engine command (87FS1) to shutdown command (87FS2). Figure 13-1 is a time history of pertinent parameters during the start and shutdown period. In this figure the near coincidence of the ignition spike with the beginning of the drop in hydraulic pressure can be seen. Also shown is the observed motion of the 2₁ actuator. A data review indicated an erroneous hardover in one direction (retract) and then a hardover in the opposite direction (extend) as shown. This was later proved to be a malfunction of the position transducer.

13.2.1.1 Hydraulic system postflight inspection. - After safing operations on the launch stand were complete, inspection revealed a defective 2₁ servoactuator. The outside of the actuator was covered with hydraulic fluid, indicating a loss of hydraulic fluid from within the actuator. The actuator was then removed and shipped to the manufacturer where inspection revealed an internal leak. An acceptance test performed on the secondary system of the actuator indicated satisfactory operation. The primary system was then tested to confirm the internal leak.

At this point disassembly of the actuator was begun. After removing the tailstock, it was found that both mounting feet on the torque motor end of the servovalve body had been fractured (see fig. 13-2) and the actuator-servovalve interface O-rings extruded from the grooves. Figure 13-3 shows a typical actuator with part of the case removed to reveal the assembly to a servovalve on the body of the actuator. Figure 13-3 shows the failed servovalve body and the fractures of the mounting lug. Note that one fracture passed through a small drilled hole; this hole (port) was for bench checking purposes. The larger ports with O-ring grooves are those for pressure supply, return, extend, and retract.

When the position transducer was removed, traces of hydraulic fluid were found in the probe bore and in other areas of the transducer. A small chip of potting compound was found inside the transducer case which had broken away from the potted cavity exposing a capacitor.

13.2.1.2 Servovalve failure analysis. - A routine metallurgical analysis of the servovalve housing disclosed some embrittlement of the 2014-T6 aluminum alloy. A structural analysis revealed that the mounting lug thickness should have been adequate for the design pressures. The bulk of the failure analysis effort was then directed toward systems analyses and systems tests. As a result of an extensive investigation by the contractor, involving the above mentioned analyses and tests, the following explanation of the failure was derived. Figure 13-4 shows a schematic of the hydraulic system. If an external

UNCLASSIFIED

force, such as the suddenly applied start transient of the engine bell at startup, were applied to the actuator shaft, an impulse pressure would result in the cylinder of the actuator. The force limiter would attempt to damp this impulse by passing hydraulic fluid to the system return line and relieve the overpressure. However, this fluid was dumped upstream of the flow limiter. The flow limiter was designed to pass only flow rates commensurate with established engine gimbal rates so that the added flow would choke the flow limiter. High pressure in the retract side of the actuator cylinder would thus not be relieved, and this pressure would be transmitted to the servovalve, causing higher than design pressures in the control and system return ports.

These pressures were shown to be high enough to fail the servovalve mounting lugs, and, in fact, impulse tests were conducted by the launch vehicle contractor in which failures identical to that which occurred during the GT-2 attempted launch were produced in two servovalves.

Failure analysis further showed that the apparent hardover indication was false, and that it was caused by the escape of hydraulic fluid from the servovalve housing into the tailstock causing the position transducer plunger to lift off the position cam of the actuator.

13.2.1.3 Modifications. - The basic modification made to the servoactuator as a result of the foregoing analyses and tests was to re-port the actuator so that the force limiter discharge would be downstream from the flow limiter. Improved action of the force limiter was also obtained by increasing the fluid orifice size. This change increased the flow capacity of the force limiter. In addition, the mounting lugs on the servovalve were increased in thickness from $\frac{3}{16}$ inch to $\frac{3}{8}$ inch and strengthened with webs. The bench check port was also moved to avoid stress concentrations.

The modified actuators were subjected to impulse tests in which it was shown that their impulse energy absorption characteristics were increased over those of the original actuator. The improvement achieved with the modified actuator is shown in figure 13-5. This figure shows the capability of the unmodified and modified actuator to absorb impulse energy. For example, for an impulse of 9000 in.-lb, a load of 39 000 pounds was produced across the unmodified actuator. For the same impulse loading, the modified actuator load is reduced to 29 300 pounds. The basic capability of the actuator to take impulse loading before failure was increased by a factor of 2. Further, it

UNCLASSIFIED

can be shown that the stress in the servovalve mounting lugs caused by external actuator loads has been reduced by a factor of 5 for the same impulse.

These tests, together with statistical studies of Titan II firings from which start transient impulse energy loadings were derived, demonstrated that the modified actuator had a strength capability to withstand the 3σ start transient impulse loading and was acceptable for flight.

13.2.2 Other Systems

13.2.2.1 Airframe. - In general, the overall loads experienced by the vehicle during the launch attempt were low relative to its structural capability. This is with reference to the preignition, ignition, shutdown, and post-shutdown periods.

One point of interest concerning the launch attempt is the indicated output of the lateral vibration sensor located on the actuator which failed (yaw-roll actuator 2_1 on subassembly 2). The peculiar waveform generated by this transducer, shown in figure 13-6, is typical of an output caused by a high-g shock input and has been confirmed by laboratory tests on an identical airborne system. Since this pickup was located very near the region of failure on the 2_1 actuator, its output behavior very strongly suggests that it was caused by the impact of the servovalve housing of the inside of the actuator tailstock housing at the exact time of failure.

13.2.2.2 Propulsion. - Analyses of the subassembly 1 and subassembly 2 thrust buildup transients indicate that both subassemblies had faster than average start transients approaching the high limits of Titan II experience. The ignition spikes (89 percent of subassembly 1, 84 percent on subassembly 2) are in excess of the engine model specification limit of 75 percent of rated thrust. However, the true magnitude of the ignition spikes cannot be established due to limitations in the pressure transducers.

Stage I engine steady-state performance was not achieved prior to shutdown. The engine shutdown was normal for a command shutdown.

The GT-2 engines were restored to flight readiness by performing the following major refurbishments and hardware replacements:

(a) One pin hole leak in a thrust chamber coolant tube was repaired in place.

UNCLASSIFIED

(b) Both of the stage I turbopump assemblies and gas generators were cleaned.

(c) Stage I autogenous pressurization system heat exchangers and burst discs were replaced.

(d) Stage I TCPS and MDS switches were replaced.

(e) Stage I start cartridge assemblies were replaced.

(f) Stage I pre-valves were replaced.

(g) Stage II gas generator injector resistance was verified.

13.3 SPACECRAFT PERFORMANCE

At T-6 minutes in the countdown, a check of all systems on the spacecraft was made as required in the countdown procedure. All systems were reported to be satisfactory for launch except for the fuel cell which had been previously deactivated for reasons which will be described in detail. An examination of the countdown records and telemetry data from spacecraft instrumentation up to the point of power shutdown shows no reason to suspect that any of the spacecraft systems were not capable of performing as planned throughout the mission, although verification of the OAMS static firing required more than the anticipated number of attempts. There was, however, an event which occurred 2 days after the aborted flight which, because of its uncertain nature, must be considered pertinent to the launch attempt itself. During the deservicing of the OAMS propellant system in preparation for extended storage, it was discovered that no fuel could be withdrawn from the tank. These incidents will also be discussed in later paragraphs of this section.

13.3.1 Fuel Cell

At approximately T-385 minutes during the countdown, fuel-cell activation was started in accordance with normal procedures. Delays in this attempted activation were encountered due to leakages in the AGE module used to control the gas supplies to the fuel cell. Efforts to rectify the problems continued until the decision was made to clear the erector and, therefore, to stop the fuel-cell activation attempt in order to allow launch vehicle operations to continue. Shortly prior to this time, the reactant supply system - fuel cell module water pressure rose and exceeded the limits of the water pressure transducer (22 psia).

UNCLASSIFIED

After the failure to launch GT-2, pressure and flow checks of the oxygen-to-hydrogen differential pressure regulator indicated a leak between the fuel, water, and hydrogen compartments. This leak had been caused by corrosion due to the acidity of the fuel-cell water. The oxygen-to-hydrogen differential pressure maintained by the regulator had resulted in a water pressure rise through the water separator, further hydrogen-pressure rise, and thus continued system-pressure rise. Further tests indicated an excessive (24 cc/hr) leakage rate in the section 2 water separator. The following table shows the stack leakage rates at that time:

Stack	Leakage, cc/hr
1B	213
1C	37
2A	680
2C	540

After examining these results it was decided to activate only stack 1C during further operations of the fuel-cell module.

Stack 1C was activated on December 18, 1964, and the following results were obtained:

Configuration	Load, A	volts dc
90-percent helium, 10-percent hydrogen	Open circuit	26.9
100 percent hydrogen	Open circuit	27.8
AGE load	2.2	21.8
Spacecraft load	3.0	20.4

Deactivation was satisfactorily completed in 1 hour. During this test it was determined that the fuel-cell differential-pressure indicators were inoperative. It was decided to ignore these indicators in further section operations. All other operations in this test were completed

UNCLASSIFIED

without major difficulty in much less time than was allotted in the GT-2 countdown.

No further operations were performed on the GT-2 fuel cell until the January 19, 1965, countdown.

In relating the experience with these fuel cell sections to future Gemini fuel cell operations, it should be noted that they were of the P2B configuration. Current production which is intended for all future Gemini fuel cells is the P-3 configuration, which has the improved hydrogen flow design and other minor modifications. In addition, the P2B sections in spacecraft 2 received coolant at 103° F; whereas future operations will be conducted with a coolant inlet temperature of 75° F which has been proven to extend the life of the fuel cell.

13.3.2 Propulsion

Between T-20 and T-6 minutes during the count, thrust chamber assemblies (TCA) 1 and 2 on the reentry control system (RCS) ring B and OAMS were test fired to 0.5-second pulse durations. The RCS TCA 1 did not fire on the first pulse but appeared satisfactory on the second. Both pulses of the RCS TCA 2 gave satisfactory visual indications. During the first three pulses of the OAMS TCA 1 and 2, only an oxidizer cloud was noted. Oxidizer-rich combustion was noted during the next three pulses, and then the seventh pulse appeared normal. The number of pulses required of the OAMS to obtain satisfactory combustion does not correlate with either theoretical calculations or tests conducted on a test spacecraft which indicated that satisfactory visual firings should be observed no later than the third pulse. Available data do not permit isolation of the cause, but it can be attributed to excessive helium gas in the fuel manifold and bladder, and/or valves which failed to open fully.

Two days after the attempted launch, OAMS deservicing was initiated. After replacement of the OAMS squib-operated isolation valve was completed, an absence of fuel within the system was discovered when it was attempted to obtain a sample from the fuel tank. The exact time and cause of loss of fuel has not been established. There are two possible leak paths: externally through the system or through flex line connections. System leakage can be excluded on the basis of the satisfactory results of the subsequent leak checks of the fuel circuit and bladder permeation rates.

Flexlines were connected to the system at two basic locations, the C and D packages and the TCA nozzles. The connections to the C and D packages provided an emergency propellant dump capability before

UNCLASSIFIED

and after the attempted launch. If a manual valve were opened inadvertently with pressure on the tanks, the propellant would be removed from the system and into the flush and purge trailer. The propellant could have taken two possible paths in the trailer: into the drain tank or into the aspirator. Since only 1 pound of fuel could be accounted for in the drain tank, it is assumed that most of the fuel was lost through the aspirator.

The quantity of propellant loaded had been verified by X-rays on October 22, 1964, while the spacecraft was on the pad. Since no further X-ray checks of the tanks were performed until December 15, 1964, the only definite conclusion is that fuel expulsion could have occurred any time within this period. Since the resolution of the instrumentation masks the amount of fuel loaded, propellant quantity calculations which are based on the magnitude of the helium pressure-temperature drop after system activation cannot provide any indication whether or not the fuel was expelled prior to launch. The remaining source of information, the static firing, only provides evidence that there was a sufficient quantity of fuel available for the firing.

As a consequence of the loss of fuel, the dump lines will not be connected to future spacecraft unless a dump is actually required. Other changes may be incorporated pending further investigation of this problem.

13.4 OPERATIONS

13.4.1 Countdown

Propellant loading of the launch vehicle prior to the beginning of the countdown began at 10:54 a.m. e.s.t. on December 8, 1964.

Delays, totaling 2 hours, were caused by incorrect readings from the stage II oxidizer flowmeter, the subsequent problems encountered in connecting to and using the stage I oxidizer flowmeter to complete stage II topping, and the faulty stage II oxidizer pump discharge pressure gage. Propellant loading operations were completed at 3:13 a.m. e.s.t., December 9, 1964. Sniffer checks and start cartridge hook-up were completed at 3:52 a.m. e.s.t.

The countdown was thus delayed in starting from 2:00 a.m. until 4:00 a.m. e.s.t. by the difficulties encountered in launch-vehicle propellant loading. Remote power-up and systems checks of the spacecraft were completed according to schedule with the exception of the telemetry calibration checks at T-313 minutes. Parameters BA01 (oxygen

UNCLASSIFIED

mass quantity) and BAO3 (hydrogen mass quantity) did not indicate the proper calibrate readouts. Since the uncalibrated readings were normal, this problem was considered to be a failure of the calibrate control circuit, and the count continued without a hold.

At T-280 minutes, the Mod III ASCO signal was not received. The MCC and RSO signals were received at this time. Investigation disclosed a patch error at Central Control which was then corrected. At T-255 minutes, verification of the three ASCO signals was confirmed.

At 7:54 a.m. e.s.t. (T-186 minutes), the decision was made to discontinue activation of the fuel cell. A hold was called at 8:05 a.m. e.s.t. (T-175 minutes) in order to complete launch-vehicle tank pressurization and initiate safe-arm checks. These checks had been delayed due to fuel-cell servicing operations. The countdown was resumed at 8:16 a.m. e.s.t. and continued until 10:34 a.m. (T-37 minutes) when a 19-minute hold was called to complete white room disassembly and erector clearing. Spacecraft hatch closure was delayed for 13 minutes due to the last-minute switch positioning required to complete securing of the fuel cells, thus delaying the disassembly and clearing of the white room. The countdown was resumed at 10:53 a.m. e.s.t.

Shortly after hatch closure, telemetry parameter DE05 (IGS 10.2 V dc bias voltage) dropped out. Since this parameter had a history of being intermittent with the hatches closed and the cause of the problem was never determined, the countdown was continued with this discrepancy noted. Parameter DE05 came back in shortly after the count was resumed at T-6 minutes.

Seven attempts were required to obtain a satisfactory firing of the OAMS thrusters, resulting in another hold at 11:24 a.m. e.s.t. (T-6 minutes). A good firing was obtained on the seventy try at 11:29 a.m. e.s.t., but the hold was continued until 11:35 a.m. e.s.t. at MCC request due to weather (inadequate camera coverage). After holding for a total of 11 minutes, the countdown was resumed at T-6 minutes.

T-0 occurred at approximately 11:41 a.m. e.s.t. The shutdown signal was sent approximately 2 seconds later, and the launch vehicle remained bolted to the launch stand.

The spacecraft was then remotely powered down from the blockhouse so that post-shutdown operations could proceed.

Figure 13-7 illustrates the sequential events of the countdown.

UNCLASSIFIED

13.4.2 Mission Control Operations

The network stations for this mission were Cape Kennedy (CNV), Patrick Air Force Base (PAT), Merritt Island Launch Area (MILA), Grand Bahama Island (GBI), Grand Turk Island (GTI), Antigua (ANT), Bermuda (BDA), Coastal Sentry Quebec (CSQ), Rose Knot Victor (RKV), Timber Hitch, and American Mariner. Commander Task Force 140 provided surface recovery forces, and the Air Rescue Service provided search and recovery aircraft. AFETR aircraft support consisted of four telemetry C-130 aircraft, a frequency control and analysis C-131 aircraft, and a weather reconnaissance T-33 aircraft. Associated tests were to be performed by two refractometer C-131 aircraft, a C-54 photography aircraft, and a Wright-Patterson Air Force Base C-121 aircraft.

13.4.2.1 Problem areas. - The following is a summary of the problems encountered during the mission:

(a) Down-range up-link (DRUL): Prior to the mission day, the operational status of the Cape, GBI, and GTI DRUL equipment in support of GT-2 was questionable because of deficiencies in the following areas: spare parts, qualified operators, and completion of engineering changes. Also, final acceptance of the system had not been completed by Goddard Space Flight Center (GSFC) engineering.

(b) RKV operational support position (OSP): The RKV was 12 hours away from its assigned OSP at approximately T-24 hours and was not scheduled to depart for the OSP until T-12 hours. The network controller contacted Range Scheduling and DDMS, and new sailing orders were issued. It has been resolved that the network controller is the point of contact for any ship movements while the network is in mission status.

(c) The aircraft controller console: The appropriate communications circuits on the aircraft controller's console were not completely identified. This delayed declaring the position as fully operational until late in the count. Procedures have been established by the controller to assure operational status the day prior to the mission.

(d) CSQ RF interference: The CSQ experienced interference on 230.4 mc (the real-time telemetry link) beginning at T-110 minutes and continuing until T-0. The interference lessened at T-45 minutes, although it was believed to be strong enough to cause intermittent unlocks in the received telemetry. At T-0 the interference was present but not significant enough to degrade the data.

13.4.2.2. Countdown summary. - The countdown started at 4:00 a.m. e.s.t (T-420 minutes). The first radar CADFISS tests (data flow) were

UNCLASSIFIED

UNCLASSIFIED

13-11

completed by 5:18 a.m. e.s.t. Goddard computers reported that all AFETR radars except MILA and SSI had successfully passed the CADFISS. SSI had failed the counterclockwise slew tests because of insufficient testing time.

At 7:18 a.m. e.s.t., the CSQ and RKV completed the CADFISS tests. CADFISS tests conducted at 7:33 a.m. e.s.t. were not long enough to complete BDA and SSI reruns.

At 8:04 a.m. e.s.t., radar 19.18, which was not available at the beginning of the count, was still not operational, with an estimated time of operation (ETO) of 8:15 a.m. e.s.t. At 8:05 a.m. e.s.t., a hold was called; the count was resumed at 8:16 a.m. e.s.t. (T-175 minutes). The hold was caused by a delay in clearing the white room which resulted in a pyrotechnic electrical installation delay.

At 8:22 a.m. e.s.t., radar 19.18 was declared operational, but it was desired that the radar not support the mission until T-45 minutes because of a hydraulic pump problem. CADFISS tests would not be run with this radar because it was desired not to use the hydraulic pump any more than necessary.

At 8:38 a.m. e.s.t., it was reported that the last aircraft had departed and was due at OSP at 10:51 a.m. e.s.t.

RKV reported a complete power failure at 9:46 a.m. e.s.t.; however, power was back on at 9:48 a.m. e.s.t. The number 4 generator had failed and caused the remaining generators to go out.

At 9:55 a.m. e.s.t., CSQ verbally reported RF interference on telemetry link at 230.4 mc. This interference had been reported at 9:20 a.m. e.s.t.

CADFISS reruns were completed at 10:04 a.m. e.s.t., and at 10:05 a.m. e.s.t. the SRO reported that the AFETR was operational without reservation.

At 10:11 a.m. e.s.t. Task force 140 reported ready to support the mission. FCA reported that the Intrepid had put its search radar to the low end of the frequency band (215 mc) at 10:23 a.m. e.s.t.

Silver 3, one of the telemetry aircraft, reported negative RF interference at 10:26 a.m. e.s.t. The CSQ reported interference with a pulse frequency repetition of 3 μ sec and one sweep every 9 seconds.

At 10:34 a.m. e.s.t., a hold was called at T-37 minutes for white room disassembly.

UNCLASSIFIED

UNCLASSIFIED

Silvers 1, 2, and 3 aircraft reported operational status at 10:42 a.m. e.s.t. Silver 1 reported that it had 6 seconds of interference on 230.4 mc at 10:37 a.m. e.s.t. CSQ was still reporting interference, but it was weakening and the source was apparently moving away.

The count was resumed at 10:37 a.m. e.s.t. All DOD support was reported ready at 11:09 a.m. e.s.t. At 11:24 a.m. e.s.t. (T-6 minutes) a hold was called to complete OAMS testing, and at 11:27 a.m. e.s.t. this hold was continued for camera coverage in the launch area. The count was resumed at 11:35 a.m. e.s.t.

Lift-off did not occur because of automatic shutdown, and the test was canceled at 11:57 a.m. e.s.t. A guidance switchover indication and loss of GLV primary hydraulic pressure were observed in the MCC at approximately T + 2.0 seconds.

UNCLASSIFIED

TABLE 13-I.- EVENT SUMMARY

Event	Actual time, a.m. e.s.t.
Engine ignition signal (87FS1) (T-0)	11:40:57.000
Ignition of subassembly 2	11:40:57.80
Ignition of subassembly 1	11:40:57.84
Pressure decay start (primary hydraulic system)	11:40:57.813
Switchover command	11:40:57.89 (+0 -0.05)
Command transfer to secondary control system	11:40:57.87 (+0 -0.01)
Transfer to secondary control system complete	11:40:57.88 (+0 -0.01)
MDTCPS make (subassembly 2)	11:40:57.96
MDTCPS make (subassembly 1)	11:40:57.99
Engine shutdown signal (87FS2)	11:40:58.021

UNCLASSIFIED

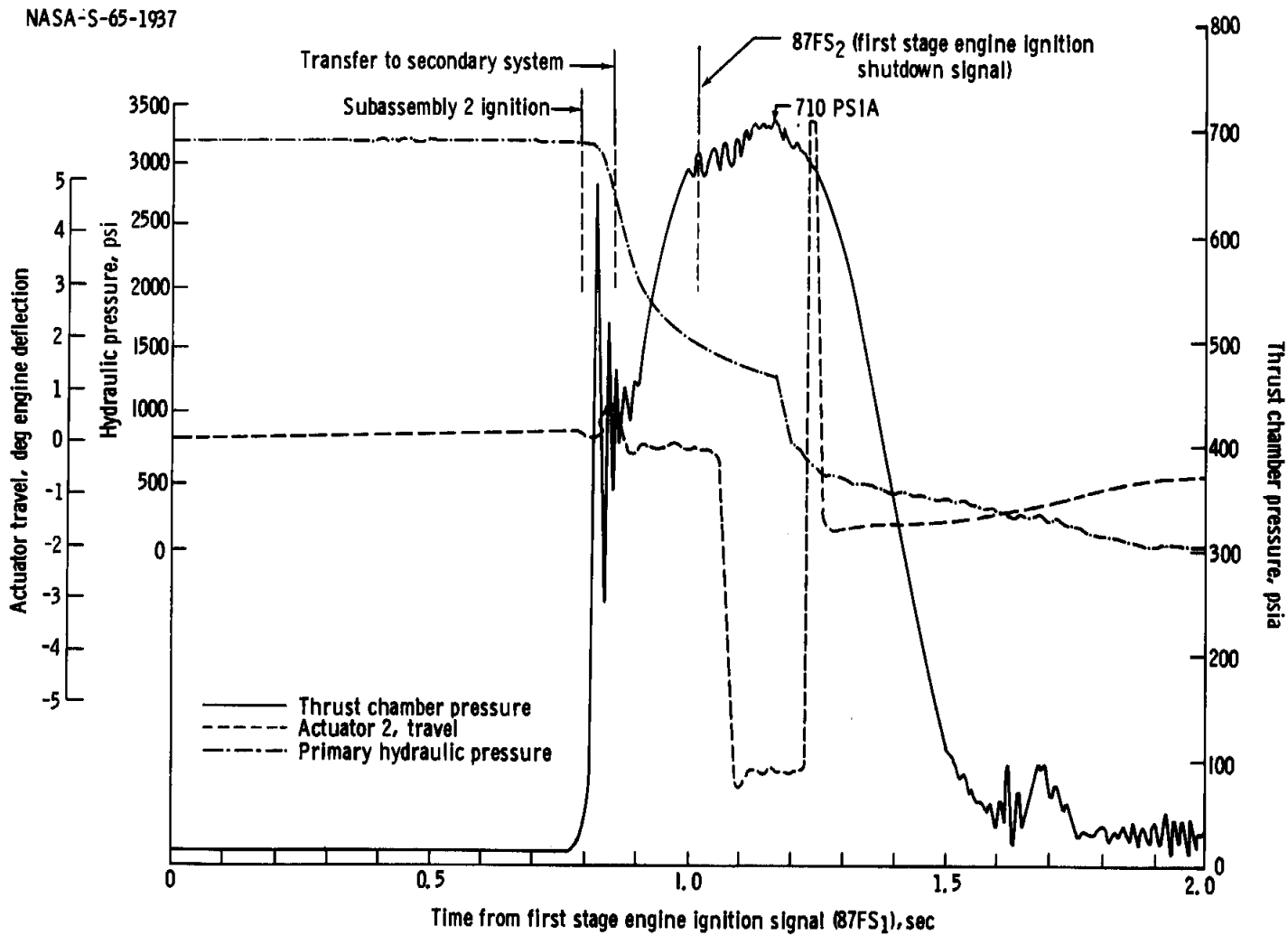


Figure 13-1. - GLV start transient

13-14

UNCLASSIFIED

NASA-S-65-1935

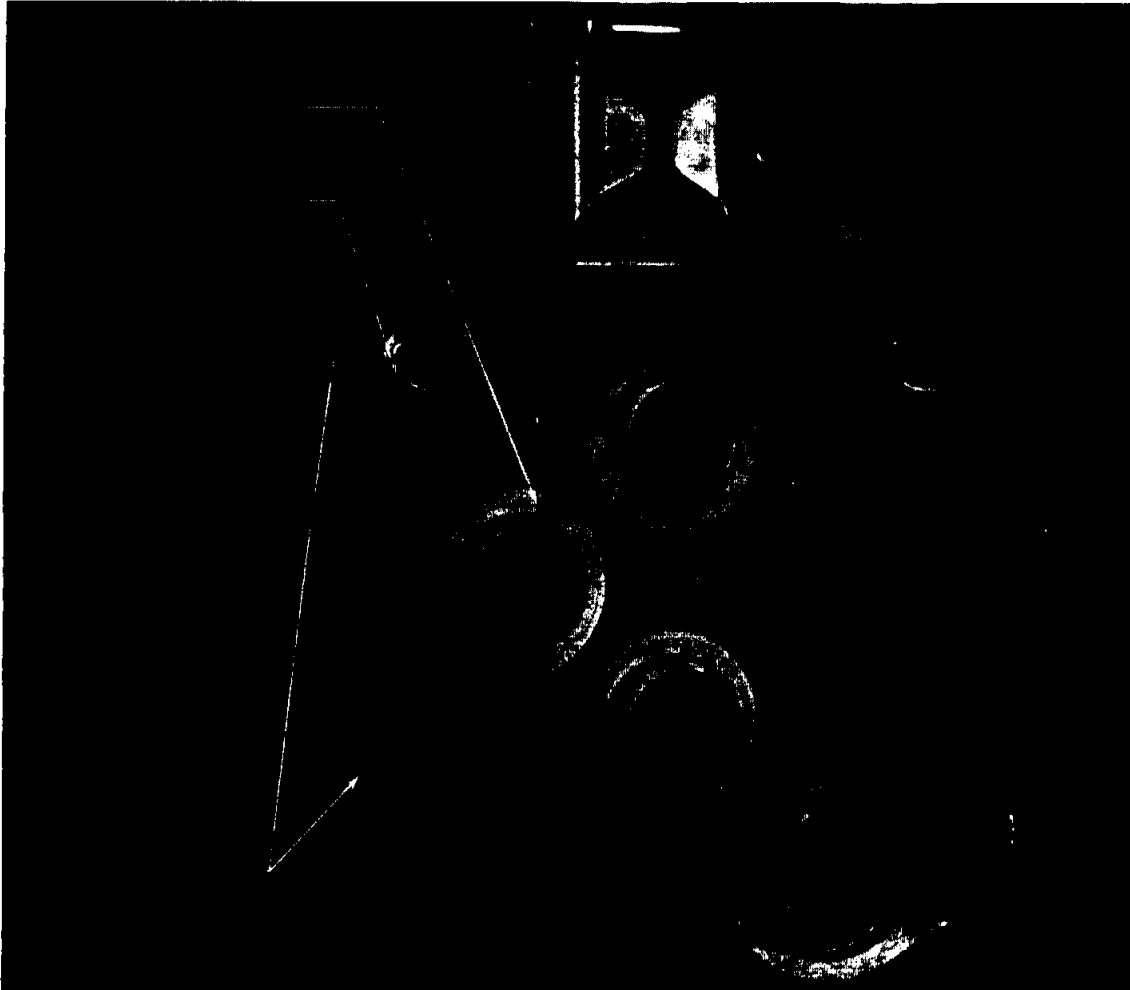


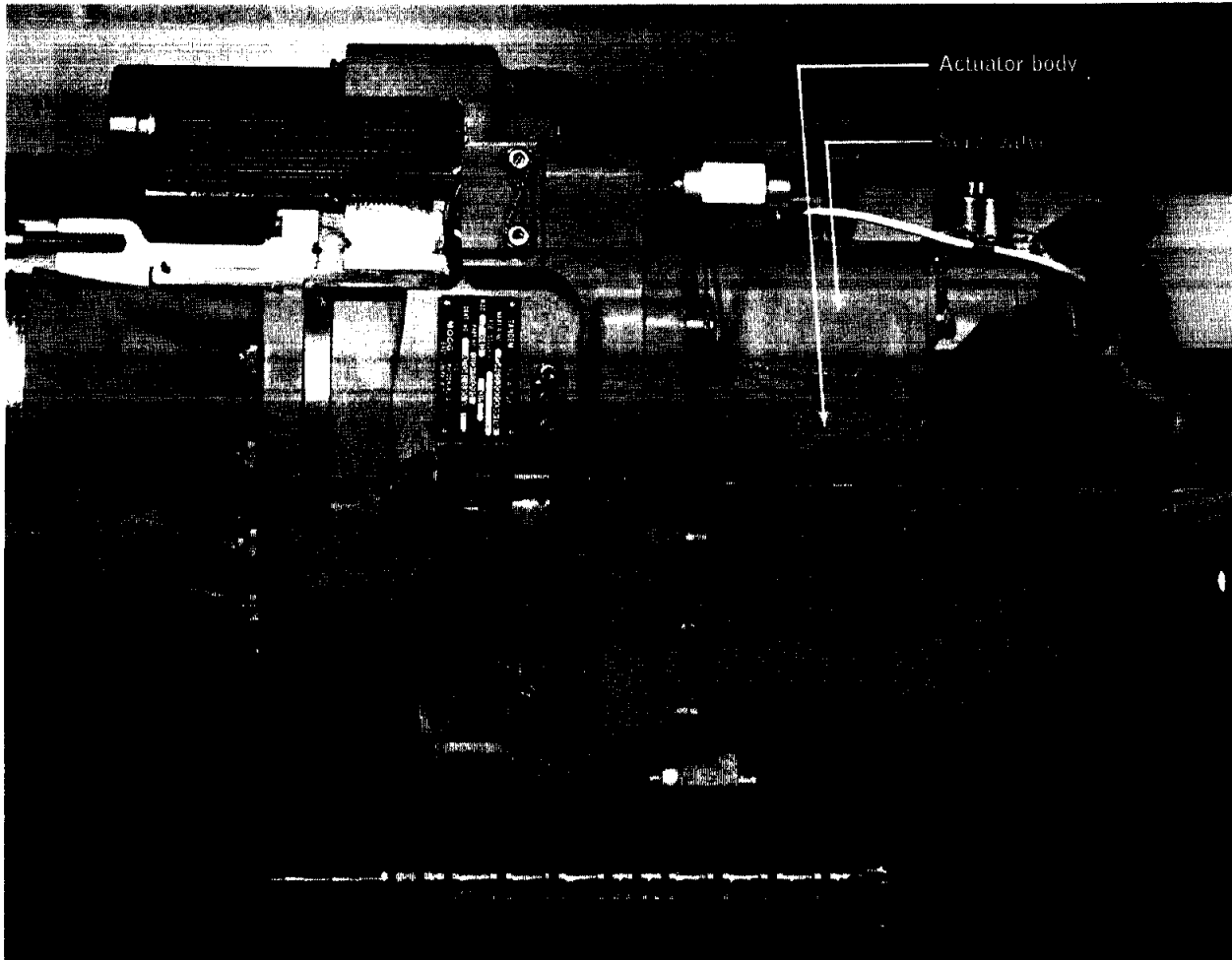
Figure 13-2. - Failed servovalve body showing fractures of the mounting lugs

UNCLASSIFIED

UNCLASSIFIED

13-15

UNCLASSIFIED



UNCLASSIFIED

Figure 13-3. -GLV Tandem actuator with part of the case removed

UNCLASSIFIED

NASA-S-65-1910

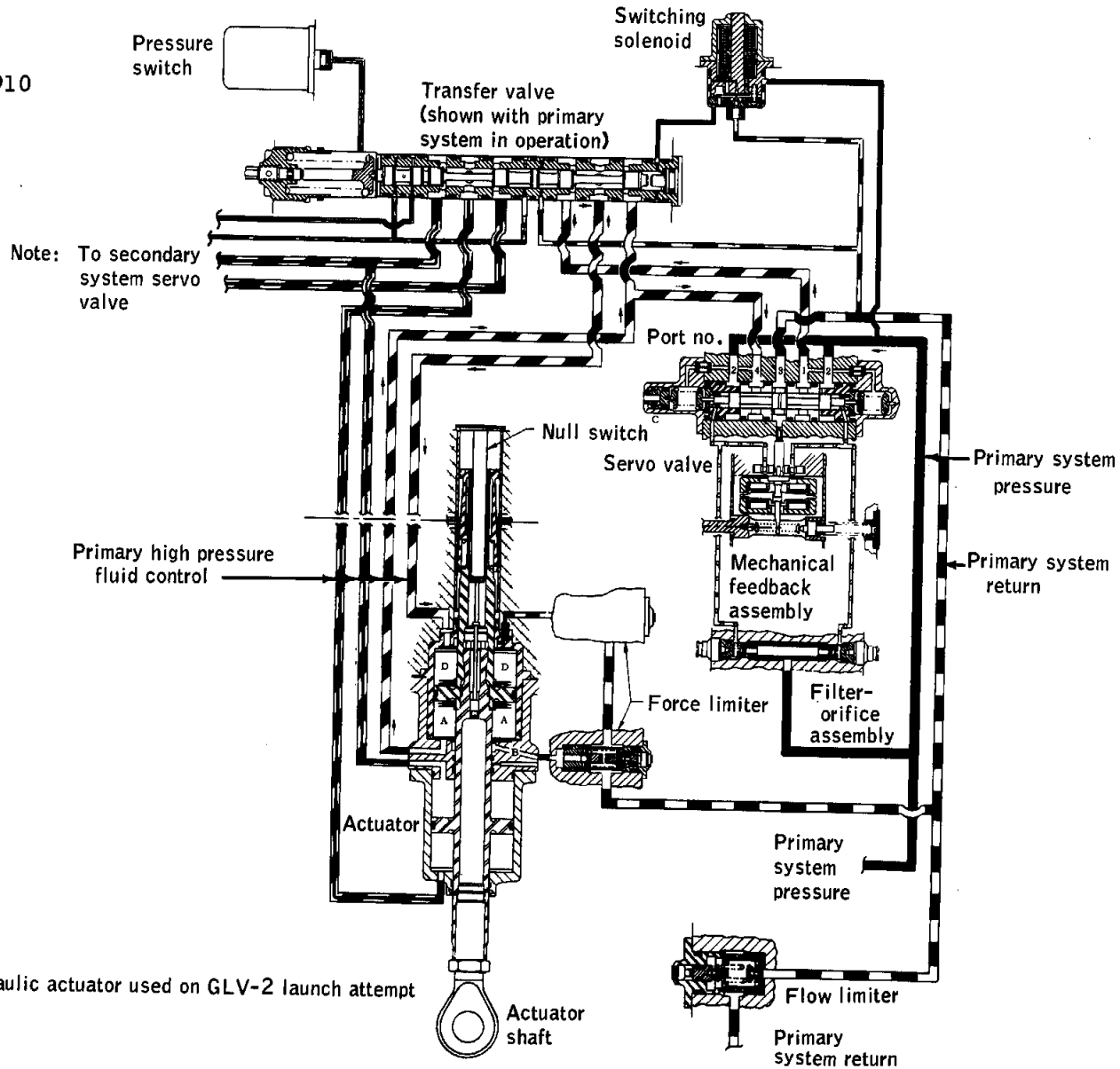


Figure 13-4. - Hydraulic actuator used on GLV-2 launch attempt

UNCLASSIFIED

UNCLASSIFIED

UNCLASSIFIED

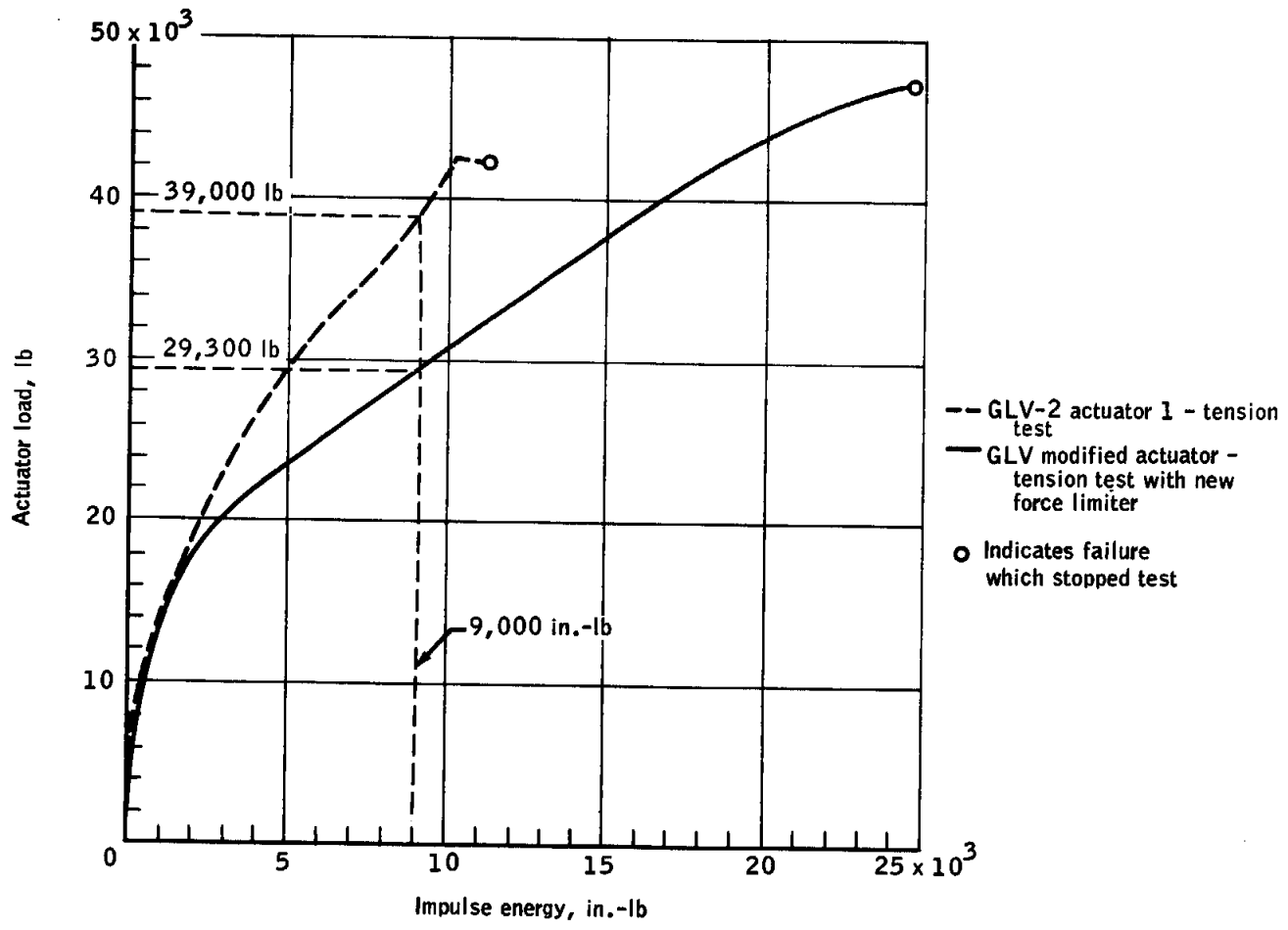


Figure 13-5. - Impulse energy capability of modified and unmodified actuators

NASA-S-65-1907

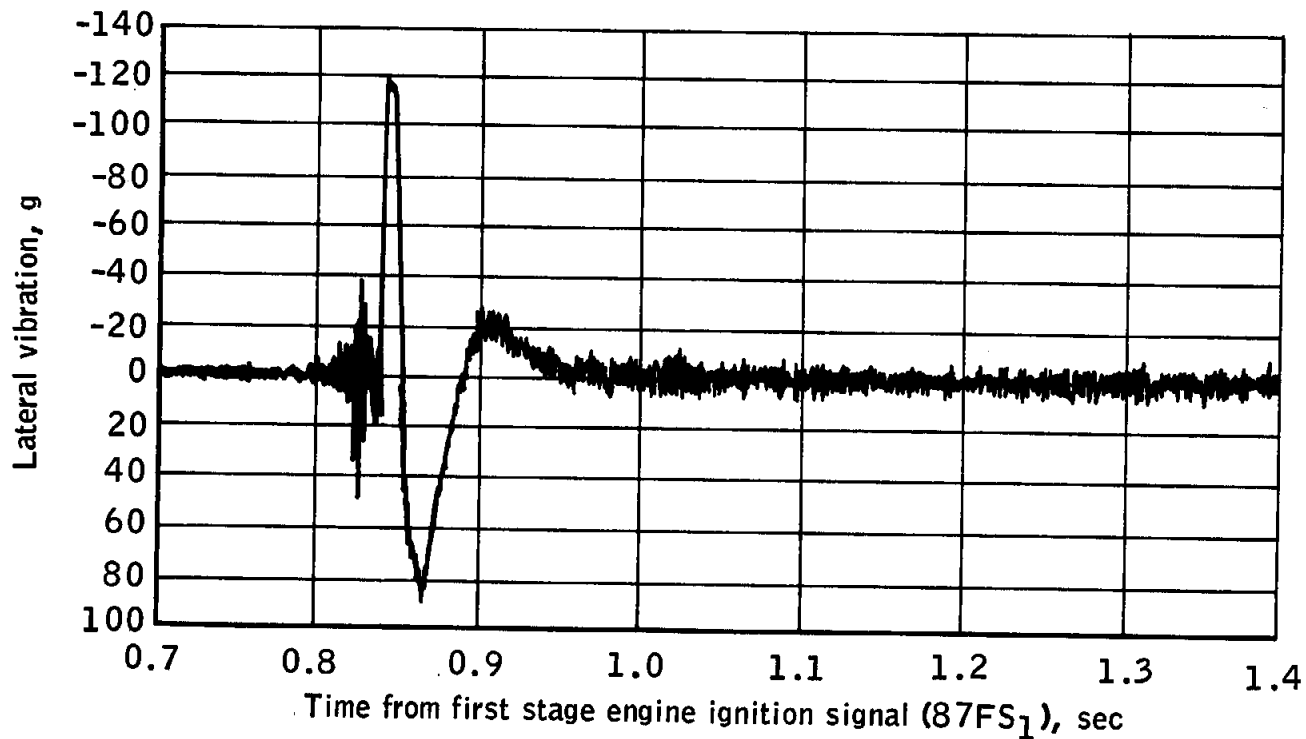


Figure 13-6. - Stage I tandem actuator vibration

UNCLASSIFIED

UNCLASSIFIED

UNCLASSIFIED

UNCLASSIFIED

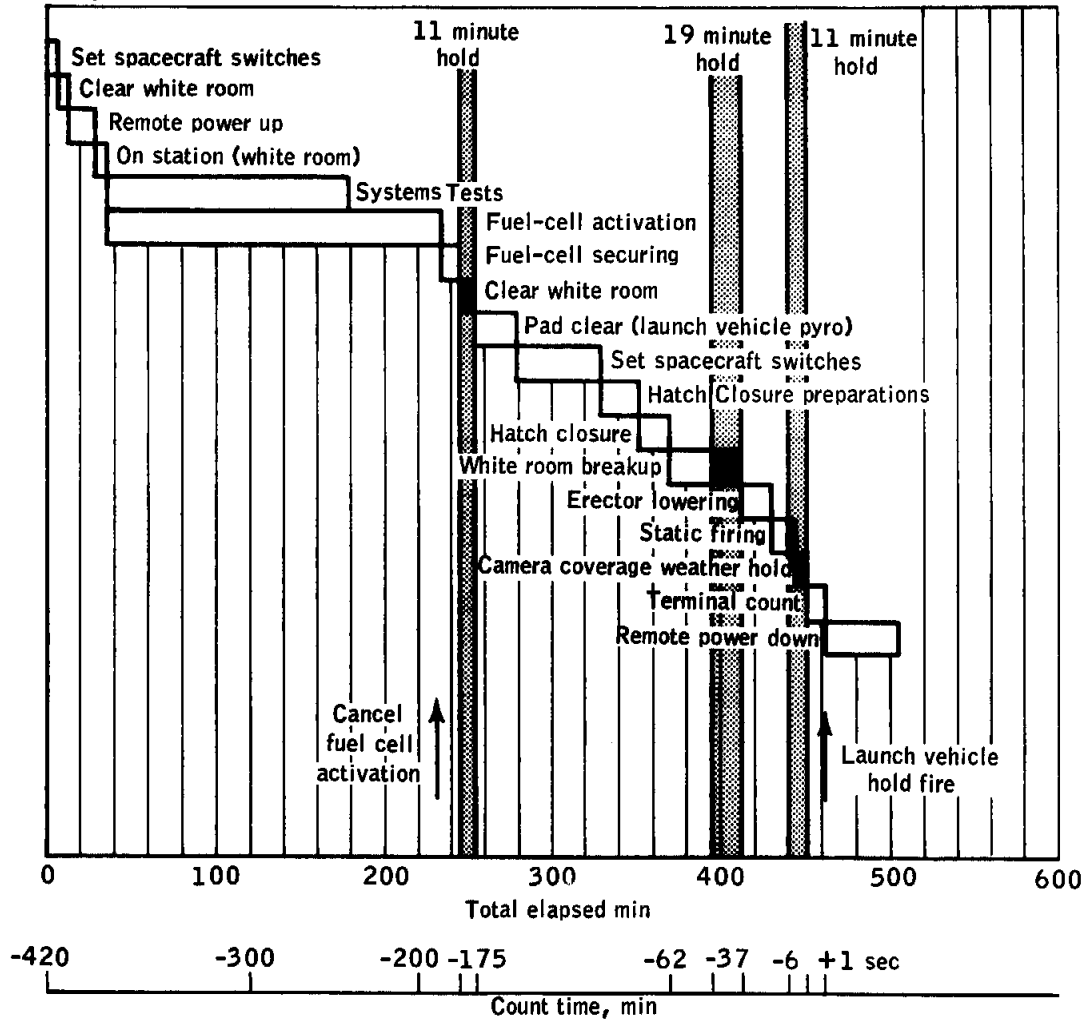


Figure 13-7. - GT-2 countdown sequence on attempted launch on Dec 9, 1964

UNCLASSIFIED

14-1

14.0 DISTRIBUTION

<u>Addressee</u>	<u>Number of Copies</u>
National Aeronautics and Space Administration Attention: Director, Gemini Program, MG Washington, D.C.	40
NASA Headquarters Library, ATSS-6	6
National Aeronautics and Space Administration Manned Spacecraft Center Houston, Texas 77058	
Director, AA	1
Deputy Director, AB	1
Special Assistant to the Director, AC	1
Executive Assistant to the Director, AF	1
Chief of Center Medical Programs, AH	2
Center Medical Office, AM	1
Flight Medicine Branch, AM2	1
Public Affairs Office, AP	1
Office of Chief at EAFB, AP12	1
Reliability and Quality Assurance Office, AR	4
Assistant Director for Administration, BA	1
Paperwork Management Office, BF13	25
Publications and Forms Distribution Branch, BF132	60
Technical Reports Branch, BF32	3
Technical Information Division Records, BF324	2
Technical Library Branch, BF33	6

UNCLASSIFIED

UNCLASSIFIED

<u>Addressee</u>	<u>Number of Copies</u>
Document Distribution, BF333	10
Security Division, BS	1
Assistant Director for Flight Crew Operations, CA	1
Astronaut Office, CB	5
Flight Crew Support Division, CF	11
Assistant Director for Engineering and Development, EA	8
Information Systems Division, EB	3
Crew Systems Division, EC	3
Computation and Analysis Division, ED	3
Instrumentation and Electronic Systems Division, EE	5
Guidance and Control Division, EG	5
Propulsion and Power Division, EP	3
Structures and Mechanics Division, ES	6
Advanced Spacecraft Technology Division, ET	5
Assistant Director for Flight Operations, FA	6
Flight Control Division, FF	7
Landing and Recovery Division, FL	4
Mission Planning and Analysis Division, FM	10
Flight Support Division, FS	4
Gemini Program Office, GA	10
National Aeronautics and Space Administration John F. Kennedy Space Center Cocoa Beach, Florida 32931 Attention: Gemini Program Office Resident Manager, HS	1

UNCLASSIFIED

UNCLASSIFIED

14-3

<u>Addressee</u>	<u>Number of Copies</u>
Resident Manager, GM Manned Spacecraft Center National Aeronautics and Space Administration c/o McDonnell Aircraft Corporation Post Office Box 516 St. Louis, Missouri 63166	5
Program Control, GP	5
Spacecraft, GS	8
Test Operations, GT	8
Vehicles and Missions, GV	8
Gemini Program Office Representative, GV2 Manned Spacecraft Center National Aeronautics and Space Administration c/o Martin Company Mail Code 388 Baltimore, Maryland 21203	1
Gemini Program Office Representative, GV3 Manned Spacecraft Center National Aeronautics and Space Administration c/o Lockheed Missiles and Space Company Sunnyvale, California 94086	1
Apollo Spacecraft Program Office, PA	6
Test Division, PT	1
National Aeronautics and Space Administration Manned Spacecraft Center White Sands Operations Post Office Drawer MM Las Cruces, New Mexico 88001 Attention: Manager, RA	1
National Aeronautics and Space Administration Ames Research Center Moffett Field, California 94035 Attention: Director	1

UNCLASSIFIED

UNCLASSIFIED

<u>Addressee</u>	<u>Number of Copies</u>
National Aeronautics and Space Administration Ames Research Center Moffett Field, California 94035 Attention: Library	5
National Aeronautics and Space Administration Ames Research Center Moffett Field, California 94035 Attention: Project Biosatellite	1
National Aeronautics and Space Administration Electronics Research Center 575 Technology Square Cambridge, Massachusetts 02139 Attention: Director	1
National Aeronautics and Space Administration Flight Research Center Post Office Box 273 Edwards, California 93523 Attention: Director	1
National Aeronautics and Space Administration Flight Research Center Post Office Box 273 Edwards, California 93523 Attention: Library	5
National Aeronautics and Space Administration Goddard Space Flight Center Greenbelt, Maryland 20771 Attention: Director, 100	1
National Aeronautics and Space Administration Goddard Space Flight Center Greenbelt, Maryland 20771 Attention: Library, 252	5
National Aeronautics and Space Administration Goddard Space Flight Center Greenbelt, Maryland 20771 Attention: Chief, Manned Flight Operations Division, 550	1

UNCLASSIFIED

UNCLASSIFIED

14-5

<u>Addressee</u>	<u>Number of Copies</u>
National Aeronautics and Space Administration Goddard Space Flight Center Liaison Representative, GSF-L c/o Manned Spacecraft Center Houston, Texas 77058	1
National Aeronautics and Space Administration Goddard Space Flight Center Eastern Test Range Post Office Box 186 Cape Canaveral, Florida 32920 Attention: Goddard Launch Operations	2
Jet Propulsion Laboratory 4800 Oak Grove Drive Pasadena, California 91103 Attention: Director, 180-905	1
Jet Propulsion Laboratory 4800 Oak Grove Drive Pasadena, California 91103 Attention: Technical Information, 111-122	1
National Aeronautics and Space Administration John F. Kennedy Space Center Cocoa Beach, Florida 32931	
Director, DIR	1
Library, GA72	5
Deputy Director, Launch Operations, HA	1
External Affairs, HA112	1
John F. Kennedy Space Center Representative, HA113 c/o Manned Spacecraft Center Houston, Texas 77058	1
Technical Document Control, HB23	3
Operations Support Plans and Programs Office, HC	4
Inspection and Quality Control, HD	1
Test Conductors, HE	1

UNCLASSIFIED

UNCLASSIFIED

<u>Addressee</u>	<u>Number of Copies</u>
Assistant Manager for Gemini, HG	1
Assistant Manager for Engineering, HJ	5
Launch Site Medical Support Branch, HU	1
Cape Simulator Operations Section, HW	1
Reliability and Flight Safety Office, HY	1
National Aeronautics and Space Administration Langley Research Center Langley Station Hampton, Virginia 23365 Attention: Director, 106	1
National Aeronautics and Space Administration Langley Research Center Langley Station Hampton, Virginia 23365 Attention: Library, 185	5
National Aeronautics and Space Administration Langley Research Center Representative, RAA c/o Manned Spacecraft Center Houston, Texas 77058	1
National Aeronautics and Space Administration Lewis Research Center 21000 Brookpark Road Cleveland, Ohio 44135 Attention: Director, 3-2	1
National Aeronautics and Space Administration Lewis Research Center 21000 Brookpark Road Cleveland, Ohio 44135 Attention: Library, 3-7	5
National Aeronautics and Space Administration George C. Marshall Space Flight Center Huntsville, Alabama 35812 Attention: Director, DIR	1

UNCLASSIFIED

UNCLASSIFIED

14-7

<u>Addressee</u>	<u>Number of Copies</u>
National Aeronautics and Space Administration George C. Marshall Space Flight Center Huntsville, Alabama 35812 Attention: Library	5
National Aeronautics and Space Administration George C. Marshall Space Flight Center Liaison Representative, RL c/o Manned Spacecraft Center Houston, Texas 77058	1
National Aeronautics and Space Administration Pacific Launch Operations Office P. O. Box 425 Lompoc, California 93438 Attention: Director	1
National Aeronautics and Space Administration Wallops Station Wallops Island, Virginia 23337 Attention: Director	1
National Aeronautics and Space Administration Western Operations Office 150 Pico Boulevard Santa Monica, California 90406 Attention: Director	1
Department of Defense Department of Defense Manager for Manned Space Flight Support Operations, DDMS Patrick Air Force Base, Florida 32925	3
Department of Defense Representative Liaison Officer, ZR2 c/o Manned Spacecraft Center Houston, Texas 77058	1
Commander, SSG Headquarters, Space Systems Division Air Force Systems Command Los Angeles Air Force Station Air Force Unit Post Office Los Angeles, California 90045	1

UNCLASSIFIED

UNCLASSIFIED

<u>Addressee</u>	<u>Number of Copies</u>
Director, Gemini Launch Vehicles, SSVL Headquarters, Space Systems Division Air Force Systems Command Los Angeles Air Force Station Air Force Unit Post Office Los Angeles, California 90045	5
Headquarters, Space Systems Division Air Force Systems Command Los Angeles Air Force Station Air Force Unit Post Office Los Angeles, California 90045 Attention: Lt. Col. T. E. Mahoney, SSTIR	1
System Program Director for Manned Orbital Laboratory, SSM Headquarters, Space Systems Division Air Force Systems Command Los Angeles Air Force Station Air Force Unit Post Office Los Angeles, California 90045	1
Deputy for Launch Vehicles, SSV Headquarters, Space Systems Division Air Force Systems Command Los Angeles Air Force Station Air Force Unit Post Office Los Angeles, California 90045 Attention: Colonel J. B. Hudson	2
Chief, Gemini Agena Division Agena Directorate Headquarters, Space Systems Division Air Force Systems Command Los Angeles Air Force Station Air Force Unit Post Office Los Angeles, California 90045 Attention: Lt. Col. Mark E. Rivers, SSVAT	1
Commander, SGR Headquarters, National Range Division Air Force Systems Command Andrews Air Force Base Washington 25, D. C.	1

UNCLASSIFIED

UNCLASSIFIED

14-9

<u>Addressee</u>	<u>Number of Copies</u>
Commander, Detachment 2, ZRL Headquarters, Space Systems Division Air Force Systems Command c/o NASA-Manned Spacecraft Center Houston, Texas 77058	3
Chief of Naval Operations The Pentagon Room 4E636 Washington, D. C. 20330	1
Commander-In-Chief, Atlantic Fleet Norfolk Naval Base Norfolk, Virginia	1
Assistant for Manned Space Flight, AFRMO Headquarters, U. S. Air Force The Pentagon Room 4D330 Washington, D. C. 20330 Attention: Colonel Kenneth W. Schultz	1
Commander, ETG Air Force Eastern Test Range Air Force Systems Command Patrick Air Force Base, Florida 32925	2
6555th Aerospace Test Wing	
Commander, 6555th Aerospace Test Wing, DWG Space Systems Division Air Force Systems Command Patrick Air Force Base, Florida 32925	1
Gemini Launch Vehicle Division, DWD Space Systems Division Air Force Systems Command Patrick Air Force Base, Florida 32925	5
Commander, NRGV National Range Division (Patrick) Air Force Systems Command Patrick Air Force Base, Florida 32925	3

UNCLASSIFIED

UNCLASSIFIED

<u>Addressee</u>	<u>Number of Copies</u>
Patrick Test Site Office Quality Assurance Division Gemini Program, RETPQC Post Office Box 4507 Patrick Air Force Base, Florida 32925	1
Mr. Paul D. Stroop Program Manager, Gemini, ETVPD Mail Unit 802 Pan American Airways Building 423 Patrick Air Force Base, Florida 32925	2
Air Force Systems Command Air Training Command Liaison Office, ZR3 c/o NASA-Manned Spacecraft Center Houston, Texas 77058	1
Commander, SCG Headquarters, Air Force Systems Command Andrews Air Force Base Washington 25, D. C. Attention: Office of Directorate of Plans and Programs, MSF-1	1
Commander, Cruiser-Destroyer Flotilla 4 Fleet Post Office New York, New York 09501	3
Commander, Hawaiian Sea Frontier Code 34 Box 110 Fleet Post Office San Francisco, California 96610	3
Commander Headquarters, Air Rescue Service Military Air Transport Service United States Air Force Orlando Air Force Base, Florida 32813	3

UNCLASSIFIED

UNCLASSIFIED

14-11

<u>Addressee</u>	<u>Number of Copies</u>
U. S. Weather Bureau	
U. S. Weather Bureau Chief, Spaceflight Meteorological Group Washington, D.C. 20235	1
U.S. Weather Bureau Spaceflight Meteorology Group c/o National Aeronautics and Space Administration Manned Spacecraft Center Houston, Texas 77058	1
U.S. Weather Bureau Spaceflight Meteorology Group c/o National Aeronautics and Space Administration John F. Kennedy Space Center Cocoa Beach, Florida 32931	1
Aerojet-General Corporation	
Mr. W. K. Nakasora Office of Gemini Product Support Aerojet-General Corporation Post Office Box 1947 Sacramento, California 95809	2
Mr. R. M. Groo Aerojet-General Corporation Hangar U Post Office Box 4425 Patrick Air Force Base, Florida 32925	1
Aerospace Corporation	
Dr. Ivan A. Getting President Aerospace Corporation Post Office Box 95085 Los Angeles, California 90045	3
Dr. Walter C. Williams Vice President and General Manager of Manned Systems Division Aerospace Corporation Post Office Box 95085 Los Angeles, California 90045	1

UNCLASSIFIED

UNCLASSIFIED

<u>Addressee</u>	<u>Number of Copies</u>
Mr. Bernhard A. Hohmann Group Director, Gemini Launch Systems Directorate Aerospace Corporation Post Office Box 95085 Los Angeles, California 90045	10
Mr. C. E. Agajanian Systems and Control Analysis Gemini Launch Systems Directorate Aerospace Corporation Post Office Box 95085 Los Angeles, California 90045	1
Mr. Newton A. Mas Manager, Gemini Program Aerospace Corporation Post Office Box 4007 Patrick Air Force Base, Florida 32925	6
Burroughs Corporation	
Mr. A. A. Holeczy Burroughs Corporation Box 873 Paoli, Pennsylvania	2
Mr. W. H. Caldwell Burroughs Corporation Post Office Box 4317 Patrick Air Force Base, Florida 32925	1
General Electric Company	
Mr. R. H. Dickinson General Electric Company Northern Lights Building Syracuse, New York 13202	1
Mr. A. G. Griffin General Electric Company Radio Guidance Operations Post Office Box 4247 Patrick Air Force Base, Florida 32925	1

UNCLASSIFIED

UNCLASSIFIED

14-13

<u>Addressee</u>	<u>Number of Copies</u>
Mr. H. C. Page General Electric Company Radio Guidance Operations Post Office Box 4247 Patrick Air Force Base, Florida 32925	1
Mr. M. J. Swing General Electric Company Radio Guidance Operations Post Office Box 4247 Patrick Air Force Base, Florida 32925	1
Mr. C. S. Whitting General Electric Company Radio Guidance Operations Post Office Box 4247 Patrick Air Force Base, Florida 32925	1
Lockheed Missiles and Space Company	
Mr. J. L. Shoenhair Manager, Medium Space Vehicles Programs Space Systems Division Lockheed Missiles and Space Company Sunnyvale, California 94086	1
Martin Company	
Mr. V. R. Rawlings, Vice President Martin-Marietta Corporation Mail No. 14 Baltimore, Maryland 21203	10
Mr. W. D. Smith Technical Director Martin-Marietta Corporation Mail No. 3134 Baltimore, Maryland 21203	1
Mr. J. M. Verlander Gemini Program Director Martin-Marietta Corporation Canaveral Division Cocoa Beach, Florida 32931	5

UNCLASSIFIED

UNCLASSIFIED

<u>Addressee</u>	<u>Number of Copies</u>
Mr. Colin A. Harrison Martin Company 1730 Farm Market 528 Suite 106 Houston, Texas 77058	1
McDonnell Aircraft Corporation	
Mr. Walter F. Burke Vice President and General Manager Spacecraft and Missiles McDonnell Aircraft Corporation Post Office Box 516 St. Louis, Missouri 63166	10
Mr. R. D. Hill, Jr. Base Manager McDonnell Aircraft Corporation Post Office Box M Cocoa Beach, Florida 32931	5
Mr. Frank G. Morgan McDonnell Aircraft Corporation 1730 Farm Market 528, Suite 101 Houston, Texas 77058	1

UNCLASSIFIED

CONFIDENTIAL

C

2-1-60

C

2-1-60

C

CONFIDENTIAL